

AD-A244 250



AGARD-AR-280

AGARD-AR-280

AGARD

ADVISORY GROUP FOR AEROSPACE RESEARCH & DEVELOPMENT

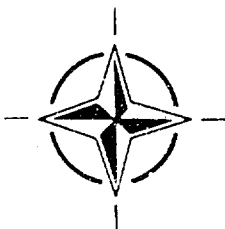
7 RUE ANCELLE 92200 NEUILLY SUR SEINE FRANCE

AGARD ADVISORY REPORT 280

Rotorcraft System Identification

(L'Identification des Systèmes de Voilures Tournantes)

Reproduced From
Best Available Copy



NORTH ATLANTIC TREATY ORGANIZATION

AGARD

ADVISORY GROUP FOR AEROSPACE RESEARCH & DEVELOPMENT

7 RUE ANCELLE 92200 NEUILLY SUR SEINE FRANCE

AGARD ADVISORY REPORT 280

Rotorcraft System Identification

(L'Identification des Systèmes de Voilures Tournantes)

Acquisition For	
NTIS	<input checked="" type="checkbox"/>
DTIC	<input type="checkbox"/>
Unpublished	<input type="checkbox"/>
Justification	
By	
Distribution	
Availability	
Dist	Special
A-1	

91-18294



This Advisory Report was prepared at the request of the
AGARD Flight Mechanics Panel.



North Atlantic Treaty Organization
Organisation du Traité de l'Atlantique Nord

91 1218 002

The Mission of AGARD

According to its Charter, the mission of AGARD is to bring together the leading personalities of the NATO nations in the fields of science and technology relating to aerospace for the following purposes:

- Recommending effective ways for the member nations to use their research and development capabilities for the common benefit of the NATO community;
- Providing scientific and technical advice and assistance to the Military Committee in the field of aerospace research and development (with particular regard to its military application);
- Continuously stimulating advances in the aerospace sciences relevant to strengthening the common defence posture;
- Improving the co-operation among member nations in aerospace research and development;
- Exchange of scientific and technical information;
- Providing assistance to member nations for the purpose of increasing their scientific and technical potential;
- Rendering scientific and technical assistance, as requested, to other NATO bodies and to member nations in connection with research and development problems in the aerospace field.

The highest authority within AGARD is the National Delegates Board consisting of officially appointed senior representatives from each member nation. The mission of AGARD is carried out through the Panels which are composed of experts appointed by the National Delegates, the Consultant and Exchange Programme and the Aerospace Applications Studies Programme. The results of AGARD work are reported to the member nations and the NATO Authorities through the AGARD series of publications of which this is one.

Participation in AGARD activities is by invitation only and is normally limited to citizens of the NATO nations.

The content of this publication has been reproduced directly from material supplied by AGARD or the authors.

Published September 1991

Copyright © AGARD 1991
All Rights Reserved

ISBN 92-835-0632-4



Printed by Specialised Printing Services Limited
40 Chigwell Lane, Loughton, Essex IG10 3TZ

Preface

The field of aircraft stability and control provides many examples of successful applications of system identification technology. For fixed wing aircraft, this approach to determine stability and control derivatives is used with confidence. The application of the same techniques to helicopters is not so far advanced mainly because the aeromechanical complexity of the helicopter requires more complicated mathematical models, and the generally much higher noise levels of helicopter flight data. Only a few specialists, mostly in research organisations, have concentrated on rotorcraft system identification. The considerable investment required to start up an in-house identification capability causes a major impedence to a widespread adoption of these techniques in the industry community. As there is no formal arrangement to coordinate these activities within the ACARD nations, it was deemed appropriate for the Flight Mechanics Panel (FMP) of the Advisory Group for Aerospace Research and Development to sponsor a Working Group to focus on the applicational aspects of the various individual approaches and to evaluate the strengths and weaknesses of the different methods.

In the established Working Group WG 18 on *Rotorcraft System Identification* the full range of available individual system identification approaches was exercised on three common flight test data sets (AH-64 of MDHC, BO 105 of DLR, and SA-330 of RAe). The scope of the work for each of the data bases was to

1. evaluate the kinematic consistency of the measured data,
2. conduct the identification of 6-degrees-of-freedom rigid body derivative models,
3. verify the identification results using flight test data other than those applied for identification,
4. examine selected special topics of concern in application rotorcraft system identification results: model robustness, simulation, handling-qualities, flight control.

Six Meetings of the Working Group were held at:

1. the European Rotorcraft Forum, Arles, France, 7–11 September, 1987,
2. STPA, Paris, France, 15–16 March 1988,
3. AFDI, Moffet Field, 13–14 October 1988,
4. RAe Bedford, United Kingdom, 11–13 April 1989,
5. NLR, Amsterdam, Netherlands, 11–15 September 1989,
6. DLR, Braunschweig, Germany, 19–20 March 1990.

Each meeting provided the opportunity for valuable information exchange about the individual technical approaches and for comparisons of the obtained results and ideas for further improvements. The fact that the Group almost simultaneously evaluated flight test data from three quite different helicopters provided a unique framework for detailed discussions and for a significant increase in experience. Another important aspect was the participation by helicopter industry scientists as WG members which allowed a more in depth appreciation of the potential present status, views, and needs for industry application of rotorcraft identification techniques. However, the bulk of the work was done by the Working Group Members back at their home offices, mostly in their spare time. Their motivation and efforts should not be underestimated and are highly appreciated.

Some WG Members were charged with the preparation of the various parts of this report, using the material provided by the Group. To acknowledge their additional effort, the principal authors of the individual Chapters or Sections are given in the form of footnotes to the headings.

All contributions were assembled at the DLR Institute for Flight Mechanics. Here, special recognition is made to Mr J. Kaletka and Mr G. Rosenau for the editorial work and the final layout of the individual contributions.

Peter G. Hamel
Chairman, FMP WG-18 *Rotorcraft System Identification*
Member, Flight Mechanics Panel

Préface

Le domaine de la stabilité et du contrôle des aéronefs fournit plusieurs exemples d'applications réussies de technologies d'identification des systèmes. Dans le cas des aéronefs à voilure fixe, la technique qui consiste à déterminer les dérivées de la stabilité et du contrôle peut-être employée avec confiance. Or, l'application des mêmes techniques aux hélicoptères n'est pas au même stade d'avancement, principalement parce que la complexité aéromécanique de l'hélicoptère exige des modèles mathématiques plus compliqués et parce que les niveaux de bruit des éléments du vol des hélicoptères sont plus élevés.

Seuls quelques spécialistes, pour la plupart employés auprès d'organisations de recherche, ont su concentrer leurs efforts sur l'identification des systèmes de voilures tournantes. L'investissement considérable que représente la création d'une installation d'identification dans l'usine même est l'un des empêchements majeurs à l'emploi banalisé des ces techniques dans l'industrie aéronautique.

Etant donné qu'il n'existe aucun accord officiel en ce qui concerne la coordination de ces activités au sein des pays membres de l'OTAN, il a été jugé opportun que le Panel de la Mécanique du Vol de l'AGARD (FMP) crée un groupe de travail pour examiner en particulier les possibilités d'applications des différentes initiatives individuelles qui ont été prises et pour évaluer les points forts et les points faibles des différentes méthodes.

Une fois créé, le groupe de travail No. 18 sur "L'identification des systèmes de voilures tournantes" a procédé à l'application de toute la gamme de méthodes individuelles d'identification des systèmes pour trois ensembles de données d'essais en vol communs (AH64 du MDHC, BO 105 du DLR et SA-330 du RAE). Les tâches imposées, pour chaque base de données furent les suivantes:

1. Evaluer la cohérence cinématique des données enregistrées.
2. Procéder à l'identification de modèles dérivés de corps rigides à six degrés de liberté
3. Vérifier les résultats de l'identification en se servant de données d'essais en vol autres que celles utilisées pour l'identification
4. Examiner des questions sélectionnées, ayant un intérêt particulier, en ce qui concerne les résultats de l'identification de systèmes pour applications.

Le groupe de travail s'est réuni six fois:

1. A l'European Rotorcraft Forum, à Arles, en France, du 7 au 11 septembre 1987
2. Au STPA, à Paris, en France, du 15 au 16 mars 1988.
3. Au AFDD à Moffet Field, du 13 au 14 octobre 1988
4. Au RAE, à Bedford, au Royaume-Uni, du 11 au 13 avril 1988.
5. Au NLR, à Amsterdam, au Pays-Bas, du 11 au 15 septembre 1988.
6. Au DLR, à Braunschweig, en Allemagne, du 19 au 20 mars 1990.

Chaque réunion a fourni l'occasion d'échanger des informations sur des méthodes techniques individuelles, de comparer les résultats obtenus et de formuler des idées sur d'éventuelles améliorations. Le fait que le groupe a évalué presque simultanément des données d'essais en vol obtenues sur trois hélicoptères tout à fait différents a créé un forum unique, qui a permis aux participants d'entamer des discussions approfondies et d'enrichir leurs connaissances dans ce domaine.

Un autre aspect important a été la participation au groupe de travail de scientifiques employés auprès de fabricants d'hélicoptères. Ceci a permis une appréciation plus approfondie de l'état de l'art actuel et potentiel, des avis des intéressés, et des besoins qui existent dans le domaine des applications industrielles des techniques d'identification des aéronefs à voilures tournantes. Toujours est-il que la majorité du travail a été effectué sur les lieux de travail des différents membres du groupe, souvent pendant leur temps libre. Leur degré de motivation et les efforts qu'ils ont bien voulu y consacrer ne sont pas à sous-estimer, car ils sont très appréciés.

Certain membres du groupe de travail ont été chargés de la préparation des différentes sections de ce rapport, à partir des éléments fournis par le groupe. Afin de reconnaître leurs contributions supplémentaires, les noms des principaux auteurs des sections ou des chapitres en question sont indiqués sous forme de postscripti aux titres.

L'ensemble des contributions a été mis en forme à l'Institut de la Mécanique du Vol au DLR. Ici, encore, il y a lieu de remercier en particulier M. Kaletka et M. Rosenau pour les travaux d'édition et de mise en page définitive des contributions individuelles.

Membership of AGARD Flight Mechanics Panel Working Group 18

Chairman: Dr Peter Hamel
DLR Institut für Flugmechanik
Germany

MEMBERS

Dr Dev Banerjee
McDonnell Douglas Helicopter Comp.
United States

M. Bernhard Gimonet
CERT/ONERA
France

Charles E.G.M. Hofman
NLR
Netherlands

Konstantin Kampa
MBB
Germany

Prof. David Murray-Smith
The University of Glasgow
United Kingdom

Anselmo Russo
Costruzioni Aeronautiche
Giovanni Agusta S.P.A.
Italy

Dr Mark B. Tischler
AFDD Ames Research Center
United States

André M. Dequin
Aérospatiale, Division Hélicoptères
France

Jürgen Kaletka
DLR Institut für Flugmechanik
Germany

Prof. Jaap H. de Leeuw
University of Toronto
Canada

Dr Gareth D. Padfield
RAF
United Kingdom

Prof. Daniel P. Schrage
Georgia Institute of Technology
United States

Robert A. Feik, Aeronautical Research Laboratories (ARL), Australia,
Jan H. Breeman, NLR, Netherlands, and
Anna Maria Reccelato, Costruzioni Aeronautiche Giovanni Agusta S.P.A.
participated in WG Meetings as invited guests.

Summary

For fixed wing aircraft, system identification methods to determine stability and control derivatives from flight test data are used with confidence. The application of the same techniques to helicopters is not so far advanced mainly because the aeromechanical complexity of the helicopter requires more complicated mathematical models, and the generally much higher noise levels of helicopter flight data. Only a few specialists, mostly in research organisations, have concentrated on this field and the application in industry is still sporadic.

To coordinate these activities within the NATO nations, a Working Group was constituted by the AGARD Flight Mechanics Panel to focus on the applicational aspects of the various individual approaches and to evaluate the strengths and weaknesses of the different methods. The Members of this Working Group (WG-18) on *Rotorcraft System Identification* applied their individual identification approaches to three common flight test data bases (AH-64, BO 105, and SA-330) that were provided to the Working Group by McDonnell Douglas Helicopter Comp. (MDHC), Deutsche Forschungsanstalt für Luft- und Raumfahrt (DLR), and Royal Aerospace Establishment (RAE).

This Report contains the findings of the Working Group. A review of the recent rotorcraft system identification activities is given. Comments obtained from a questionnaire that was distributed to the rotorcraft industry are summarized to document the role, interests, and needs of industry. The flight test data bases provided to the Working Group are described in detail. In the chapter on identification methodologies the major steps required for the identification are presented: flight test procedures, instrumentation, data processing and evaluation, and identification techniques. For each of the three helicopters, comparisons of the obtained results are discussed in the form of case studies, covering data quality evaluations, identification, and verification of the obtained models. Robustness issues for system identification are addressed. Finally three major application areas of identification results are emphasized: simulation validation, handling qualities, and control system design.

Contents

	Page
Preface	iii
Préface	iv
Membership of AGARD Flight Mechanics Panel Working Group 18	v
Summary	vi
List of Tables	x
List of Figures	xii
Notations	xv
Basic Symbols	xv
Other Symbols	xvi
Indices and Marks	xvi
List of Abbreviations	xvii
1. Introduction and Overview	1
1.1 Background	1
1.2 Basics of System Identification	1
1.3 Benefits of System Identification	1
1.4 Requirement for Multidisciplinary Collaboration	2
2. Working Group Objectives	6
3. Review of Recent System Identification Activities	7
3.1 System Identification Roadmap	7
3.2 Recent Helicopter System Identification Activities	14
3.2.1 Introduction	14
3.2.2 Activity Reviews	14
3.2.3 General Remarks	17
3.2.4 References	17
3.3 The Role of Industry	21
3.3.1 Introduction	21
3.3.2 Industry Response	22
3.3.3 Concluding Remarks and Recommendations	28
3.4 AGARD-Related System Identification Activities	30
4. AGARD Working Group Data Base	33
4.1 Introduction	33
4.2 System Identification Data Base	33
4.2.1 Requirements	33
4.2.2 Measured Quantities and Conventions Used	34
4.3 AH-64 Apache	34
4.3.1 Introduction	34
4.3.2 Manoeuvres	34
4.3.3 Measurements	34
4.3.4 Processing/Consistency Checks	35
4.4 BO 105	35
4.4.1 Introduction	35
4.4.2 Manoeuvres	36
4.4.3 Measurements	36
4.4.4 Processing/Consistency Checks	37
4.5 SA-330 Puma	37
4.5.1 Introduction	37

	Page
4.5.2 Manoeuvres	37
4.5.3 Measurement	38
4.5.4 Processing Consistency Checks	38
4.6 Summary and Concluding Remarks	39
5. Identification Methodologies	51
5.1 Introduction	51
5.2 Flight Test Procedures	51
5.2.1 Introduction	51
5.2.2 Planning of Flight Tests	51
5.2.3 Selection of Test Inputs	52
5.2.4 Conduct of Flight Experiments	54
5.2.5 Procedures Following Flight Experiments	55
5.3 Instrumentation and Data Processing	58
5.3.1 Introduction	58
5.3.2 Required Measurements	58
5.3.3 On-board Data Processing	59
5.3.4 Problem Areas	60
5.3.5 Off-line Data Processing	62
5.3.6 Summary	64
5.4 Data Evaluation and Reconstruction	68
5.4.1 Introduction	68
5.4.2 Techniques	68
5.4.3 Use of Error Corrections	72
5.4.4 Data Compatibility Tools in Use at the Institutes	72
5.4.5 Conclusions	74
5.4.6 References	74
5.5 Identification Techniques	77
5.5.1 Introduction	77
5.5.2 Model Structure	77
5.5.3 Time-Domain Identification Methods	83
5.5.4 Frequency-Domain Identification Methods	88
5.5.5 Time-Domain Verification of Identified Models	92
6. Identification Results	94
6.1 Case Study I: AH-64	95
6.1.1 Introduction	95
6.1.2 Helicopter and Instrumentation	95
6.1.3 Flight Testing and Data Evaluation	96
6.1.4 Identification Methods	100
6.1.5 Identification Results	102
6.1.6 Verification	103
6.1.7 Problem Areas	104
6.1.8 Conclusions	105
6.2 Case Study II: BO 105	133
6.2.1 Introduction	133
6.2.2 General Description of BO 105	133
6.2.3 Flight Testing and Data Evaluation	133
6.2.4 BO 105 Identification	139
6.2.5 Verification of the Identified Models	143
6.2.6 Discussion of Results	143
6.2.7 Conclusions	144
6.3 Case Study III: SA-330 PUMA	176
6.3.1 Introduction	176
6.3.2 Helicopter and Instrumentation	176
6.3.3 Flight Test Data Evaluation	176
6.3.4 Identification Methods	181
6.3.5 Identification and Verification Results	182
6.3.6 Discussion of Results	182
6.3.7 Conclusions	186

	Page
7. Robustness Issues	213
7.1 Introduction	213
7.2 A-Priori Information: Experimental Design and Data Consistency	213
7.2.1 Experimental Design	213
7.2.2 Kinematic (Measurement) Consistency	215
7.3 Identification Techniques	215
7.4 Model Structure	216
7.5 Parameter Estimates	217
7.6 Overall Robustness of the Model	217
7.7 Conclusions and Recommendations	218
8. Application of Identification	223
8.1 Simulation Model Validation	223
8.1.1 Introduction	223
8.1.2 Validation Criteria -- Model Accuracy and Range	223
8.1.3 Model Development and Upgrading	228
8.1.4 Example	229
8.1.5 Conclusions and Recommendations	232
8.2 Handling Qualities	243
8.2.1 Introduction	243
8.2.2 Basic Handling-Qualities Concepts	243
8.2.3 Non-parametric Model Identification for Handling-Qualities Studies	245
8.2.4 Parametric Model Identification for Handling-Qualities Analyses	246
8.2.5 Summary	249
8.3 System Identification Requirements for High-Bandwidth Rotorcraft Flight Control System Design	257
8.3.1 Introduction	257
8.3.2 Simple Model-Following Control System	257
8.3.3 Identification Models for Control System Design	258
8.3.4 A High-Order Model for Roll Response	259
8.3.5 Lower-Order Models for Broad-Band Roll Response	260
8.3.6 Quasi-Steady Models for Low-Frequency Roll Response	261
8.3.7 Conclusions	261

List of Tables

	Page
4.1 Conventions for Positive Signs of Control Displacements	39
4.2 Conventions for Positive Signs of Response Variables	40
4.3 List of runs (AH-64)	41
4.4 AH-64 Control Variables	42
4.5 AH-64 Response Variables	43
4.6 List of runs (BO 105)	44
4.7 BO 105 Control Variables	45
4.8 BO 105 Response Variables	45
4.9 List of runs (SA-330)	46
4.10 SA-330 Control Variables	47
4.11 SA-330 Response Variables	48
5.4.1 Six-degree-of-freedom kinematic equations for compatibility checking	75
6.1.1 List of physical characteristics of the AH-64	107
6.1.2 AH-64 Control Variables	107
6.1.3 AH-64 Response Variables	108
6.1.4 AH-64: List of runs	109
6.1.5 AH-64 Identification Results: Mean values of scale factors	110
6.1.6 AH-64 Identification Results: Mean values of biases	110
6.1.7 AH-64: AFDD results for mean values of frequency sweep biases	110
6.1.8 AH-64 Identification Results: List of specific force derivatives with respect to flight variables	111
6.1.9 AH-64 Identification Results: List of specific moment derivatives with respect to flight variables	112
6.1.10 AH-64 Identification Results: List of specific force derivatives with respect to control deflections	113
6.1.11 AH-64 Identification Results: List of specific moment derivatives with respect to control deflections	114
6.1.12 AH-64 Identification Results: Equivalent control time delays	115
6.1.13 AH-64 Identification Results: Time constants, damping ratios and undamped natural frequencies	116
6.2.1 List of physical characteristics of the BO 105	145
6.2.2 List of runs (BO 105)	146
6.2.3 BO 105 Control Variables	147
6.2.4 BO 105 Response Variables	147
6.2.5 BO 105 Data consistency analysis: Mean values of identified scale factors	148
6.2.6 BO 105 Data Consistency Analysis: Mean values of identified biases	148
6.2.7 Set-up for AFDD frequency domain identification	149
6.2.8 BO 105 Identification Results: List of specific force derivatives with respect to flight variables	150
6.2.9 BO 105 Identification Results: List of specific moment derivatives with respect to flight variables	151
6.2.10 BO 105 Identification Results: List of specific force derivatives with respect to control variables	152
6.2.11 BO 105 Identification Results: List of specific moment derivatives with respect to control variables	153
6.2.12 BO 105 Identification Results: Equivalent control time delays	154
6.2.13 BO 105 Identification Results: Time constants, damping ratios and undamped natural frequencies	154
6.3.1 Physical characteristics of the RAE Research SA-330	187
6.3.2 SA-330 Manoeuvres flown	188
6.3.3 SA-330 Control Variables	189
6.3.4 SA-330 Response Variables	190
6.3.5 Initial condition, bias, and calibration factor estimates with free optimisation	191
6.3.6 SA-330 data consistency analysis with constrained optimisation: Scale factors	192
6.3.7 SA-330 data consistency analysis with constrained optimisation: Biases	192
6.3.8 SA-330 data consistency analysis with constrained optimisation: Initial conditions	192

	Page
6.3.9 SA-330 Identification Results: List of specific force derivatives with respect to flight variables	193
6.3.10 SA-330 Identification Results: List of specific moment derivatives with respect to flight variables	194
6.3.11 SA-330 Identification Results: List of specific force derivatives with respect to control variables	195
6.3.12 SA-330 Identification Results: List of specific moment derivatives with respect to control variables	196
6.3.13 SA-330 Identification Results: Equivalent control time delays	197
6.3.14 SA-330 Identification Results: Time constants, damping ratios and undamped natural frequencies	197
6.3.15 SA-330 characteristics of short period mode	198
6.3.16 SA-330 comparison of phugoid characteristics	199
6.3.17 SA-330 comparison of roll rate sensitivity	199
6.3.18 SA-330 characteristics of Dutch roll mode	199
7.1 Robustness Aspect of the Experimental Design	219
7.2 Robustness Aspect of the Identification Technique	220
7.3 Robustness Aspect of the Identified Model Structure	220
7.4 Robustness Aspect of the Estimated Parameters	220
7.5 Robustness Aspect of the Resulting Mathematical Model	220
8.1.1 Helistab Data	235
8.1.2 Comparison of SA-330 lateral/directional characteristics	236
8.1.3 Dutch roll mode eigenvalues ~ Comparison of flight estimates (DLR) with theory	236
8.2.1 ADS-33C Specifications for Height Response Handling-Qualities	250
8.3.1 Roll response models, Φ/δ_r	263
8.3.2 Comparison of performance estimates	263

List of Figures

	Page
1.1 The "Quad M" basics of rotorcraft system identification	3
1.2 Rotorcraft system identification	3
1.3 System identification for rotorcraft flying qualities evaluation	4
1.4 System identification for rotorcraft flight control optimization	4
1.5 System identification for rotorcraft simulation validation	5
3.1.1 Roadmap for the evolution of system identification	10
3.1.2 System identification as guide for mathematical modeling	11
3.1.3 12 DoF helicopter simulation model structure	11
3.1.4 A systems approach to rotorcraft stability and control research	12
3.1.5 Helicopter linear handling qualities model	12
3.1.6 Methodology validation	13
3.1.7 Flight data processing	13
4.1 Characteristic helicopter responses to longitudinal control inputs	49
4.2 Characteristic helicopter responses to lateral control inputs	49
4.3 Characteristic helicopter responses to pedal control inputs	50
4.4 Characteristic helicopter responses to collective control inputs	50
5.2.1 Comparison of autospectrum and roll rate due to lateral stick frequency responses from three control input signals	57
5.2.2 Verification of identified model obtained from frequency sweep data signals	57
5.3.1 BO-105 distortions in airspeed measurement	65
5.3.2 BO-105 data: comparison of unfiltered and filtered linear accelerations and rates	65
5.3.3 Measured AH-64 unfiltered and filtered rotational accelerations and comparison with differentiated rates	66
5.3.4 Comparison of linear acceleration measurements obtained from an "agility" package and individual accelerometers (SA-330)	66
5.3.5 Resolution of the pitch and roll attitude measurements (AH-64)	67
5.3.6 CG correction of linear accelerometer measurements (AH-64)	67
5.4.1 The linearized error model for state estimation	76
5.4.2 Block diagram of wind modeling	76
6.1.1 AH-64 Apache in flight	117
6.1.2 Three-view drawing of AH-64	117
6.1.3 Control time histories for data group 1	118
6.1.4 Angular acceleration consistency for file 3 (MDHC)	119
6.1.5 Comparison of measured and reconstructed time histories: linear velocities (MDHC)	120
6.1.6 Comparison of measured and reconstructed time histories: linear accelerations (MDHC)	121
6.1.7 Comparison of measured and reconstructed time histories: angular rates (MDHC)	122
6.1.8 Comparison of measured and reconstructed time histories: Euler angles (MDHC)	123
6.1.9 Identification result: Time history comparison of measured data and the response of the identified model: linear velocities (DLR1)	124
6.1.10 Identification result: Time history comparison of measured data and the response of the identified model: linear accelerations (DLR1)	125
6.1.11 Identification result: Time history comparison of measured data and the response of the identified model: angular rates (DLR1)	126
6.1.12 Identification result: Time history comparison of measured data and the response of the identified model: Euler angles (DLR1)	127
6.1.13 Control time histories for data group 2	128
6.1.14 Verification result: Time history comparison of measured data and the response of the identified model: linear velocities, (DLR1)	129
6.1.15 Verification result: Time history comparison of measured data and the response of the identified model: linear accelerations, (DLR1)	130
6.1.16 Verification result: Time history comparison of measured data and the response of the identified model: angular rates, (DLR1)	131

	Page
6.1.17 Verification result: Time history comparison of measured data and the response of the identified model, Euler angles, (DLR)	132
6.2.1 DLR research helicopter BO 105	155
6.2.2 Three view drawing of BO 105	155
6.2.3 Pilot's display for input signal generation (BO 105)	156
6.2.4 Representative BO 105 flight test data: control input types and rate responses	156
6.2.5 Comparison of measured and reconstructed BO 105 data without scale factor corrections	157
6.2.6 Comparison of measured and reconstructed BO 105 speed data with scale factor corrections	157
6.2.7 Influence of equivalent time delays on BO 105 identification results	157
6.2.8 Control input signals of BO 105 flight test data used for identification (modified '3211' signals)	158
6.2.9 Comparison of BO 105 flight data and response of the identified model for linear accelerations (DLR result)	159
6.2.10 Comparison of BO 105 flight data and response of the identified model for linear speeds (DLR result)	160
6.2.11 Comparison of BO 105 flight data and response of the identified model for angular rates (DLR result)	161
6.2.12 Comparison of BO 105 flight data and response of the identified model for Euler angles (DLR result)	162
6.2.13 Comparison of measured rates and the response of identified BO 105 models (CERT and Glasgow University results)	163
6.2.14 Comparison of measured rates and the response of the identified BO 105 models (NAE results)	164
6.2.15 Comparison of BO 105 flight data and identified model frequency responses (roll and pitch rate, representative AFDD results)	165
6.2.16 Comparison of BO 105 flight data and identified model frequency responses (linear speeds and yaw rate, representative AFDD results)	166
6.2.17 Control input signals of BO 105 flight test data used for verification (doublet signals)	167
6.2.18 Verification of the identified model (linear accelerations, DLR result)	168
6.2.19 Verification of the identified model (linear speeds, DLR result)	169
6.2.20 Verification of the identified model (angular rates, DLR result)	170
6.2.21 Verification of the identified model (Euler angles, DLR result)	171
6.2.22 Verification of the identified BO 105 models (AFDD and CERT results)	172
6.2.23 Verification of the identified BO 105 models (DLR and Glasgow University results)	173
6.2.24 Verification of the identified BO 105 models (NAE and NLR results)	174
6.2.25 Comparison of BO 105 flight data and results from a computational nonlinear simulation (DLR SIMH)	175
6.3.1 RAE Research SA-330	200
6.3.2 3 view drawing of RAE Research SA-330	200
6.3.3 SA-330 database — response to 3211 longitudinal inputs	201
6.3.4 SA-330 database — response to 3211 lateral inputs	202
6.3.5 SA-330 database — response to 3211 collective inputs	203
6.3.6 SA-330 database — response to 3211 pedal inputs	204
6.3.7 Comparison of measured attitudes and air data with reconstructed inertial measurements — SA-330 F568FAC.FWD	205
6.3.8 Comparison of measured attitudes and air data with free optimisation of reconstructed inertial measurements — SA-330 F568FAC.FWD	205
6.3.9 Components of velocity derivatives — F568FAC.FWD	206
6.3.10 Comparison of measured attitudes and air data with constrained optimisation of reconstructed inertial measurements — SA-330	207
6.3.11 Comparison of flight and estimated times histories — Glasgow — Identification	208
6.3.12 Comparison of flight and estimated times histories — Glasgow — Verification	209
6.3.13 Comparison of flight and estimated times histories — DLR — Identification	210
6.3.14 Comparison of flight and estimated times histories — DLR — Verification	211
6.3.15 Helistab cyclic responses for varying M_a and M_u — SA-330 — 80 kn	212
7.1 Effect of upper frequency limit on identification	221
7.2 Comparison of identification and verification results	222
8.1.1 System identification	237
8.1.2 Derivative changes with design parameters (Helistab SA-330 — 80 kn)	237
8.1.3 Comparison of flight and Helistab control response (pedal and lateral cyclic input)	238
8.1.4 Comparison of flight and Helistab control response (collective and longitudinal cyclic input)	239
8.1.5 Comparison of flight and 3 DoF simulation (DLR estimates)	240

	Page
8.1.6 Comparison of flight and 6 DoF simulation (DLR estimates)	241
8.1.7 Comparison of flight and simulation estimates of Dutch roll stability characteristics with ADS 33C criteria	242
8.2.1 Pilot/vehicle system block diagram	250
8.2.2 Determination of bandwidth and phase delay criteria	251
8.2.3 Requirements for roll response to lateral stick inputs	251
8.2.4 Roll attitude response to lateral stick (ϕ/δ_{lat}) identified from BO 105 frequency-sweep data	252
8.2.5 Determination of phase delay using least squares fitting procedure	253
8.2.6 Flight data and handling-qualities model identification, equation (8.2.8), for vertical rate response	254
8.2.7 Pitch attitude response to longitudinal cyclic identified from AH-64 frequency-sweep data	255
8.2.8 Time-domain verification of first-order pitch model, equation (8.2.16), of the AH-64	256
8.3.1 BO 105 case study helicopter	264
8.3.2 Simple explicit model-following control system	264
8.3.3 Flight data of roll axis frequency-sweep	265
8.3.4 Frequency-response identification	265
8.3.5 Comparison of baseline model (7th order) and flight data	266
8.3.6 Short-term eigenvalue locations as a function of flapping stiffness	266
8.3.7 Stabilization loop root locus, varying roll attitude feedback gain K_ϕ	267
8.3.8 Comparison of closed loop response, Φ/Φ_m of baseline model vs data	267
8.3.9 Stabilization-loop root locus, varying roll-rate gain K_p	268
8.3.10 Lower-order broad-band models	268
8.3.11 Closed loop responses of lower-order broad-band models	269
8.3.12 Stabilization-loop root locus for 5th order (quasi-steady) model varying attitude gain	269
8.3.13 Effect of upper frequency limit ω_1 on quasi-steady identification	270
8.3.14 Band-limited and broad-band quasi-steady models	270

Notations

Basic symbols

a_x	Acceleration component along the longitudinal body axis	\tilde{X}	Component of the specific Resultant Aerodynamic Force along the longitudinal body axis
a_y	Acceleration component along the lateral body axis	Y	Component of the Resultant Aerodynamic Force along the lateral body axis <i>In derivatives:</i> Derivative of Y
a_z	Acceleration component along the normal body axis	\tilde{Y}	Component of the specific Resultant Aerodynamic Force along the lateral body axis
b	Bias	Z	Component of the Resultant Aerodynamic Force along the normal body axis <i>In derivatives:</i> Derivative of Z
f	Frequency, inverse of the period length T , $f = 1/T$	\tilde{Z}	Component of the specific Resultant Aerodynamic Force along the normal body axis
GM	Gain margin (of open-loop response)	α	Angle of attack
h	Altitude	β	Angle of sideslip
H	Altitude	$\gamma_{\delta \text{ lat } p}^2$	Coherence from lateral control inputs to roll rate outputs
K_p	Roll rate feedback gain	δ	Control deflection
K_ϕ	Roll angle feedback gain	Δ	Finite variation
L	Component of the Resultant Aerodynamic Moment about the longitudinal body axis <i>In derivatives:</i> Derivative of L	δ_{lat}	Lateral control input
\tilde{L}	Component of the specific Resultant Aerodynamic Moment about the longitudinal body axis	ζ	Damping ratio
L_p	Roll damping derivative	Θ	Pitch angle
M	Component of the Resultant Aerodynamic Moment about the lateral body axis <i>In derivatives:</i> Derivative of M	λ	Eigenvalue
\tilde{M}	Component of the specific Resultant Aerodynamic Moment about the lateral body axis	λ	Scale factor
N	Component of the Resultant Aerodynamic Moment about the normal body axis <i>In derivatives:</i> Derivative of N	σ	Modal damping
\tilde{N}	Component of the specific Resultant Aerodynamic Moment about the normal body axis	τ	Time delay
p	Roll rate	τ_p	Phase delay (of closed-loop response)
s	Laplace variable	Φ	Roll angle
T	Period length	Φ_c	Roll angle command input to command model
T	Time constant	Φ_e	Roll angle error signal $\Phi - \Phi_m$
u	Component of the air velocity along the longitudinal body axis	Φ_m	Roll angle command input to stability loop
v	Component of the air velocity along the lateral body axis	$\Phi_{2\omega_{180}}$	Phase angle of closed-loop system when the angular frequency $\omega = 2\omega_{180}$
w	Component of the air velocity along the normal body axis	Ψ	Yaw angle
X	Component of the Resultant Aerodynamic Force along the longitudinal body axis <i>In derivatives:</i> Derivative of X	ω	Angular frequency $= 2\pi f$
		ω_{bw}	Bandwidth angular frequency (of closed-loop response) For attitude command systems, the bandwidth is defined as the angular frequency at which the phase angle is -135°
		ω_c	Design crossover-frequency (of open-loop response) to give 45° phase margin

ω_u Angular frequency at which instability occurs due to increasing feedback gain (value of the angular frequency at which the root locus branch crosses the imaginary axis)

ω_0 Undamped natural angular frequency

ω_1 Lower limit for angular frequency of transfer function fitting range

ω_2 Upper limit for angular frequency of transfer function fitting range

ω_{180} Angular frequency where the phase angle of the closed-loop system = -180°

Other symbols

∇ Hamilton symbol for a differential operator, c.g. gradient of a scalar field ϕ :
 $\nabla \phi = \text{gradient } \phi$

Indices and marks

Latin letters

ag Quantities from the agility package

bw Bandwidth

cg In measured quantities: Quantity with respect to centre of gravity (centre of mass)

col Collective

est Estimated quantities

g Component in earth-fixed axes

GM Gain margin (of open-loop response)

lat Lateral

lon Longitudinal

m Measured quantity

p In measured quantities: Quantity with respect to pilot's seat

p In derivatives: Specific derivative with respect to p

ped Pedal

q In derivatives: Specific derivative with respect to q

r In derivatives: Specific derivative with respect to r

T Upper index: Transposed vector or matrix

tr Tail rotor

u In derivatives: Specific derivative with respect to u

v In derivatives: Specific derivative with respect to v

w In derivatives: Specific derivative

W Wind in earth-fixed axes

x Component with respect to an x-axis

y Component with respect to a y-axis

z Component with respect to a z-axis

Other

-- Overmark: Mean value

* Upper mark: Quantities corrected for scale factor and bias

Greek letters

α In derivatives: Specific derivative with respect to α

β In derivatives: Specific derivative with respect to β

δ_{col} In derivatives: Specific derivative with respect to δ_{col}

δ_{lat} In derivatives: Specific derivative with respect to δ_{lat}

δ_{lon} In derivatives: Specific derivative with respect to δ_{lon}

δ_{ped} In derivatives: Specific derivative with respect to δ_{ped}

ρ Air density

Digits

0 Natural frequencies

(1) Upper index: Fully coupled model

(2) Upper index: Lateral subset

(3) Upper index: Second order roll/yaw approximation

List of Abbreviations

ACT	Active Control Technology	GOB	Gold Oscillator Box
AD	Analogue-Digital	GPS	Global Positioning System
ADS	Aeronautical Design Standard	HADS	Helicopter Air Data System
AFC	Automatic Flight Control System	HARS	Heading Attitude Reference System
AFDD	Aeroflightdynamics Directorate (US Army)	IMSL	International Mathematical and Statistical Library
AGARD	Advisory Group for Aerospace Research and Development	INS	Inertial Navigation System
AHS	American Helicopter Society	MDHC	McDonnell Douglas Helicopter Corporation
ARL	Aeronautical Research Laboratory (Australia)	MilSpec	Military specification
ASE	Automatic Stabilisation Equipment	MIMO	Multi-Input/Multi-Output
ATHeS	Advanced Technology Testing Helicopter System	ML	Maximum Likelihood
BHII	Bell Helicopter Textron Inc.	MLE	Maximum Likelihood Estimator
BUCS	Backup Control System	MTE	Mission Task Element
CACTUS	Criterion rule (Complete, Appropriate, Correct, Testable, Unambiguous, Substantiated)	NAE	National Aeronautical Establishment (Canada)
CERT	Centre d'Études et de Recherches de Toulouse (France)	NASA	National Aeronautics and Space Administration (US)
CG	Centre of Gravity, centre of mass	NATO	North Atlantic Treaty Organization
CPU	Central Processing Unit	NLR	Nationaal Lucht- en Ruimtevaartlaboratorium (Netherlands)
CRT	Cathode Ray Tube	ONERA	Office National d'Études et de Recherches Aérospatiales (France)
DASE	Digital Automatic Stabilization Equipment	OE	Output Error
DEKFIS	Discrete Extended Kalman Filter/Smoothing	PCM	Pulse Code Modulation
DFVLR	Deutsche Forschungs- und Versuchsanstalt für Luft- und Raumfahrt (since 1989: DLR)	PEP	Parameter Estimation Package
DLR	Deutsche Forschungsanstalt für Luft- und Raumfahrt (until 1989: DFVLR)	PSD	Power Spectral Density
DoF	Degrees-Of-Freedom	RAE	Royal Aerospace Establishment
EKF	Extended Kalman Filter	RPM	Revolutions Per Minute
EKFS	Extended Kalman Filter/Smoothing	SAS	Stability Augmentation System
FE	Filter Error	SCAS	Stability and Command Augmentation System
FFT	Algorithm for the computation of the coefficients of a finite trigonometric interpolation polynomial (<i>so-called Fast Fourier Transform</i>)	SCU	Stabilizer Control Unit
FMP	Flight Mechanics Panel	SISO	Single-Input/Single-Output
		SI	System Identification
		SI	International Unit System (Système International)
		SMACK	Smoothing for Aircraft Kinematics program
		WG	Working Group
		WLS	Weighted Least-Squares

1. Introduction and Overview¹⁾

1.1 Background

Over the last two decades helicopters entering service and required to meet increased operational performance have with few exceptions, experienced prolonged flight test development to achieve full certification. In many cases the original requirement has, at a late stage, been reduced to enable release to service. The impact on the customer and manufacturer has been considerable and amounts to increased costs and employment of highly skilled resources and reductions in operational capability. These costly experiences are largely a result of the rotorcraft not behaving as designed (in terms of flying qualities and performance). The ensuing re-design effort requires improved and more accurate modeling at the design stage, utilizing advanced wind tunnel rotor model test data. However, it is indispensable to check wind tunnel predictions with results from actual flight tests. In this sense the evaluation of flight test data can be used as a tool for validating wind tunnel results, improving the confidence in rotorcraft mathematical models and, finally, reducing the uncertainty levels of important aerodynamic stability and control parameters of the model.

The methodology of system identification, i.e. the derivation from flight test results of a rotorcraft mathematical model in terms of both model structure and model parameters using the relationship between measured control inputs and system responses, is a key way of overcoming some of these problems (Häff, 1989, [1.1]; Klein, 1989, [1.2]; Padfield (editor), 1989, [1.3]).

1.2 Basics of System Identification

The system identification (S.I.) framework can be divided into three major parts (Hamel, 1987, [1.4]):

- **Instrumentation and Filters** which cover the entire flight data acquisition process including adequate instrumentation and airborne or ground-based digital recording equipment. Effects of all kinds of data quality have to be accounted for.
- **Flight Test Techniques** which are related to selected rotorcraft maneuvering procedures in order to optimize control inputs. The input signals have to be optimized in their spectral composition in order to excite all rotorcraft response modes from which parameters are to be estimated.
- **Analysis of Flight Test Data** which includes the identification of the mathematical model of the rotorcraft. An estimation criterion with an iterative computational algorithm is used to adjust starting values or a-priori estimates of the unknown parameters until a set of parameter estimates is obtained which minimizes the response error.

Corresponding to these strongly interdependent topics, four important aspects of the art and science of system identification have to be carefully treated (Figure 1.1).

- Importance of the control input shape in order to excite all modes of the vehicle dynamics motions.
- Type of rotorcraft under investigation in order to define the structure of the mathematical models,
- Selection of instrumentation and filters for high accuracy measurements,
- Quality of data analysis by selecting most suitable time or frequency domain identification methods.

These "Quad-M"-requirements must be carefully investigated from a physical standpoint in order to define and execute a successful experiment for system identification.

1.3 Benefits of System Identification

The objective to validate mathematical models from the knowledge of control inputs and system responses via flight test data collection and analysis will improve the confidence and reduce the uncertainty of important aerodynamic stability and control parameters describing rotorcraft flight mechanics (Figure 1.2).

¹⁾ Principal Author: P. G. Häff, DLR

Seen from the aspect of cost effectiveness important benefits of rotorcraft system identification are related to the potential to reduce the amount of costly and time-consuming rotorcraft flight testing with respect to specification and certification requirements. Improved assessment and evaluation of flying qualities becomes possible (Figure 1.3).

An additional important factor is emerging from the area of implementation of active-control-technology (ACT) concepts offering the promise of significantly increased rotorcraft performance and operational capabilities. It is well-known, that this approach extends the traditional trade-offs between aerodynamics, structures and propulsion to include the capabilities of a fulltime, full-authority digital fly-by-wire/light control system. It is imperative that the actual aerodynamic stability and control parameters turn out as predicted, since the inherent stability margins may be lower and the flight control system must compensate these deficiencies to provide required handling qualities. In cases of high bandwidth model-following flight control system designs, accurate mathematical models improve feed-forward control and, consequently, lower feedback gains for model deficiency compensation (Figure 1.4).

Still more important, system identification techniques are likely to become in the future mandatory for model validation purposes of ground-based rotorcraft system simulators. Such simulators require extremely accurate mathematical models in order to be accepted by pilots and government organizations for realistic complementary rotorcraft mission training (Figure 1.5).

1.4 Requirement for Multidisciplinary Collaboration

Due to the highly complex aeromechanical and coupled flight dynamic behaviour of helicopter and other rotorcraft configurations, long term interdisciplinary scientific knowledge combined with practical research expertise is required in order to use identification and mathematical modeling tools in a most efficient way. It is also important to establish an improved dialogue between research institutions and industry.

This is one of the reasons that these techniques are mostly concentrated in research organizations like US Army/ARTA, NASA, DLR, NLR, RAE and CERT/ONERA.

One efficient way of developing this knowledge and providing the research expertise is by using the combined strengths and complementary facilities of the relevant NATO nations in a collaborative programme. This is an area ideally suited to the mission of AGARD (Hamel, 1990, [1.5]).

References

- [1.1] Iltis, K. W.
Parameter Estimation Analysis for Flight Vehicles
Journal of Guidance, Control, and Dynamics, Vol. 12, No. 5, 1989
- [1.2] Klein, V.
Estimation of Aircraft Aerodynamic Parameters from Flight Data
Prog. Aerospace Sci., Vol. 26, pp. 1 - 77, 1989
- [1.3] Padfield, G. D. (Editor)
Applications of System Identification in Rotorcraft Flight Dynamics
Vertica 'Special Edition', Vol. 13, No. 3, 1989
- [1.4] Hamel, P. G.
Flight Vehicle System Identification - Status and Prospects
DFVLR-Mitt. 87-22, pp. 52 - 90, 1987
- [1.5] Hamel, P. G.
The Collaborative Role of AGARD in Recent Advances in Rotorcraft System Identification
AGARD Highlights 90/1, 1990

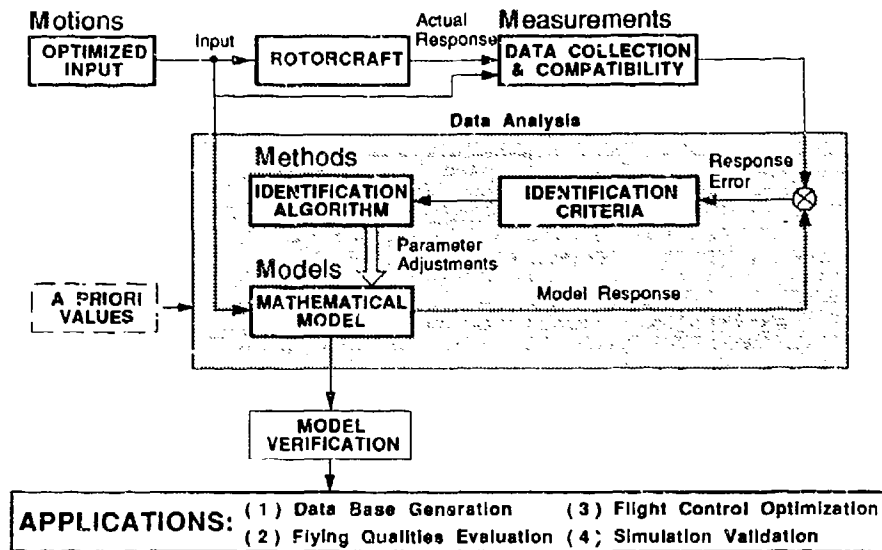


Figure 1.1. The "Quad-M" basics of rotorcraft system identification

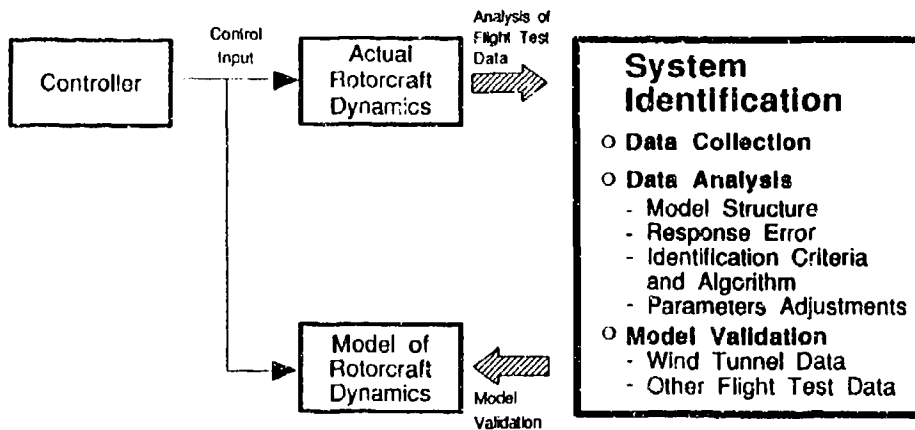


Figure 1.2. Rotorcraft system identification

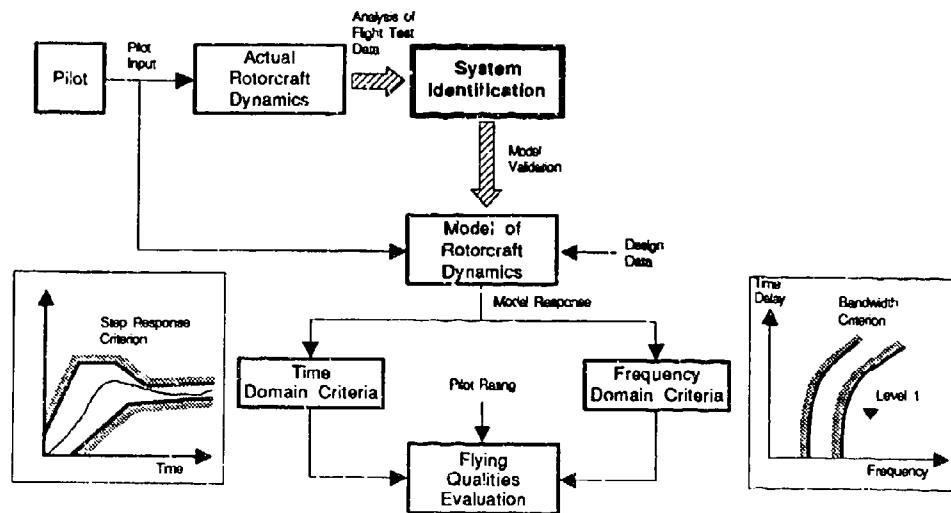


Figure 1.3. System identification for rotorcraft flying qualities evaluation

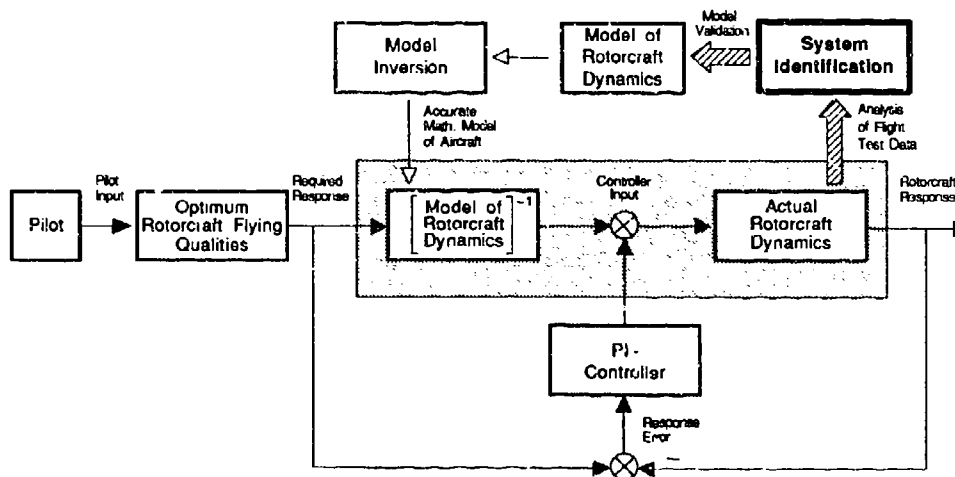


Figure 1.4. System identification for rotorcraft flight control optimization

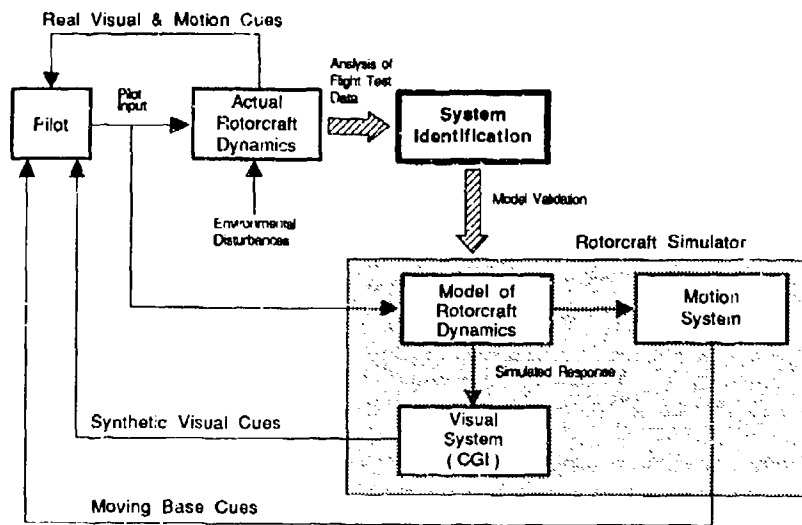


Figure 1.5. System identification for rotorcraft simulation validation

2. Working Group Objectives²⁾

The AGARD Flight Mechanics Panel (FMP) which for the last fifteen years has sponsored activities in the field of flight vehicle parameter and system identification, decided in 1987 that the optimum way in which AGARD could contribute to this area was to set up a Working Group 18 comprising a wide range of research specialists and industry representatives, tasked with exploring and reporting on the topic of Rotorcraft System Identification.

The first two objectives of the Working Group are

1. to evaluate the strengths and weaknesses of the different approaches and to develop guidelines for the application of identification techniques to be used more routinely in design and development,
2. to define an integrated and coordinated methodology for application of system identification based on the strengths of each method.

These objectives have been pursued in a time frame of about two and a half years (1988-1990), through the exercising of the full range of available individual system identification methods on three common data sets (AH-64 of MDHC, BO-105 of DLR, and SA-330 of RAE) and conducting a critical review of accomplishments.

Based on the work on the first two objectives the final objective of AGARD FMP Working Group 18 is

3. to provide an overview and expertise to Industry for
 - better understanding of the underlying scientific, technical and operational methodologies involved in rotorcraft system identification, and
 - increased utilization of this modern flight test support toolin cooperation with research centers of excellence in this field.

To be as effective as possible in achieving the declared objectives and making sensible recommendations, the Group has requested Industry to provide information with respect to any experience of using system identification tools and to indicate techniques currently used to validate simulation models (see chapter 3.3).

²⁾ Principal Author: P. G. Hamel, DLR

3. Review of Recent System Identification Activities

This chapter first gives some ideas of the use of system identification during the design, development, certification, production, and product improvement processes in form of a *System Identification Roadmap* (3.1). Then, recent helicopter identification activities of the Working Group Members are reviewed. Based on the evaluation of the answers to a questionnaire that was distributed to the rotorcraft industry, a discussion of industry's view and requirements is presented in the section on *The Role of Industry* (3.3). Finally, previous *AGARD-Related Identification Activities* (3.4) are summarized.

3.1 System Identification Roadmap³⁾

Rotorcraft System Identification is envisioned as a set analytical tools that can be used throughout the design, development, certification/qualification, production and product improvement process. Its objective is to provide for development, selection, improvement, and verification/validation of engineering and training mathematical simulation models. Such models are needed for both real time and non real time applications. While it is realized that rotorcraft system identification does not currently provide this set of tools an envisioned flow of how system identification *could* evolve is illustrated in Figure 3.1.1. The flow is initiated by a set of rotorcraft design requirements which then evolve through the life cycle phases and result in a full mission simulation capability which can be used for training and other uses which could greatly reduce the life cycle cost of rotorcraft. While not specifically illustrated in Figure 3.1.1 the approach taken is to try and utilize system identification techniques at the appropriate life cycle phase to gain maximum leverage during design and development. With this introduction of the roadmap, system identification will be addressed first in its broadest sense and then with respect to the intricacies of rotorcraft system identification.

System identification in its most general form could be defined as the deduction of system characteristics from measured data. Obviously, the solution of this postulated "black box" problem is impossible without further specification. A more realistic representation would be viewing system identification as a guide for mathematical modeling as illustrated in Figure 3.1.2. The application of system identification techniques is strongly dependent on the purpose for which the results are intended; radically different system models and identification techniques may be appropriate for different purposes related to the same system (Hiff et al., 1986, [3.1.1]). In this perspective, system identification techniques are applied to experimental data and depending on the intended purpose, a model is selected from a set of candidate models. The purpose intended is the key to the complexity of the desired model and the mathematical techniques used in the identification process. In actuality, it is seldom possible to identify a comprehensive model of the system except for simple systems and a subfield of system identification called parameter identification is often used. Parameter identification is the process of determining the coefficients or parameters in the equations of the system with a given structure using measured output data for known test inputs. In reality, on anything but for fairly simple systems, the parameters are really estimates that result in an adequate model of the system for the purpose intended.

For aerospace systems, the purpose intended could be associated with estimating the coefficients or parameters in a set of rigid body equations of motion or a set of elastic body equations of motion. For fixed wing applications, the majority of experience has been with the parameter estimation of stability and control derivatives for obtaining the linearized rigid body equations of motion involving six or less degrees of freedom. These stability and control derivatives can be used to assess handling and flying qualities compliance and for flight control system design. Often, for conventional fixed wing aircraft, decoupled 3 DoF longitudinal and lateral/directional models have been utilized.

Parameter estimation of fixed wing structural characteristics is a less mature field and has not been used routinely. Though all aircraft have observable structural modes, these structural modes could or could not affect the estimation of aerodynamic stability and control derivatives depending on the separation between the structural modes and the rigid body modes. In general, if the structural frequencies are higher than the highest rigid body modal frequency by more than a factor of 5 to 10, the effect of structural modes in the estimation of aerodynamic stability and control derivatives can be neglected unless the amplitudes of structural deflections are so large as to mask measurements desired for the aerodynamic analysis. However, if one or more structural modes are found to affect the rigid body modes, as may occur in large aircraft and spacecraft, those structural modes must be included in the mathematical model being analyzed (Hiff et al., 1984, [3.1.2]).

³⁾ Principal Author: D. Schrage, Georgia Institute of Technology

Thus far, the discussion has been concerned with identification of linear models from flight test data. When engineering simulation validation is the intended purpose of parameter estimation, it is often essential to include nonlinear models and techniques. This is especially true as simulations are being used to investigate the full and expanded flight envelopes.

Unlike the flight dynamics of most fixed wing aircraft, the dynamics of rotary wing aircraft are characteristically those of a high order system. The large number of degrees of freedom (DoF) associated with the coupled rotor-body dynamics leads to a large number of unknown parameters that have to be estimated, making it extremely difficult to achieve success in the application of parameter identification techniques. A 12 DoF helicopter simulation model structure, as illustrated in Figure 3.1.3, is about the minimum required for engineering simulation validation and flight control system design. However, for handling qualities evaluation, a 6 DoF model may be adequate. In view of the immaturity of rotorcraft parameter estimation, the WG 18 approach is to start at this model structure.

Central to virtually all aspects of helicopter design and evaluation is an appropriate mathematical model. Most of the recent efforts in this area have concentrated on the development of nonlinear simulation models. Though essential for establishing ground based simulators and for pilot training, these nonlinear models do not give clear insight into the vehicle characteristics under various flight conditions. Thus there is a need for the development of linear models of the vehicle about various operating points or trim conditions. These linear models can be used in establishing the stability and control characteristics of the vehicle and they are very useful for a systematic development and design of the vehicle flight control system. In addition, the linear models are easy to comprehend and they usually form the basis for flying qualities evaluation.

Thus system identification efforts can be viewed in two contexts. The first context is developmental in nature and consists of validation and update of a complex engineering simulation model using flight test data. The second and the most fundamental context of system identification is to determine the adequacy of rotorcraft modeling for flight control system design and handling qualities evaluation. In this case, the rotorcraft mathematical model should be such that it represents the physical situation as realistically as possible and at the same time it is sufficiently simple and mathematically tractable. As depicted in Figure 3.1.4, development of an accurate mathematical model with sufficient degrees of freedom is a prerequisite for effective flight control system design and hence an expanded flight envelope.

Since a simple, minimal-order model is a key to physically realizable control system design, it is important to determine the lowest order that would best fit the flight test data. In order to accomplish this, linear models of different order need to be used in the identification process. These different-order models may include body as well as rotor degrees of freedom depending on the order of the model:

1. Body longitudinal dynamics alone - 4th order model (3 DoF)
2. Body lateral dynamics alone - 4th order model (3 DoF)
3. Body coupled dynamics - 8th order model (6 DoF)
4. Body dynamics with first order flapping dynamics and engine response (longitudinal and lateral tip path plane tilts) - 11th order model (9 DoF)
5. Body dynamics with rotor flapping dynamics - 15th order model (10 DoF)
6. Body dynamics with rotor flapping and lead-lag dynamics - 21st order model (13 DoF)
7. Body dynamics with rotor flapping and lead-lag dynamics and with inflow dynamics - 24th order model (16 DoF)

Also, identification of different order models will give insight into the coupling present in body degrees of freedom (coupling between longitudinal and lateral dynamics), rotor degrees of freedom (effect of flapping and lead-lag dynamics on body dynamics), and inflow dynamics.

The need for system identification in the development of helicopter linear handling qualities models becomes apparent when one looks at the alternatives available. In general, there are three different methods available for developing the helicopter linear model about a given operating point (see Figure 3.1.5).

The most commonly used method is to obtain the linear model from a global nonlinear simulation model through a numerical perturbation scheme. In this method, using a nonlinear flight simulation model, the helicopter is first trimmed at a given flight condition. From their equilibrium values, the states and controls are perturbed one at a time to obtain the changes in body forces and moments. Then the stability and control derivatives are obtained as the ratio of change in corresponding force or moment and the perturbation size of the state or control. Though simple and straightforward the method can be very sensitive to the perturbation size which itself may be dependent on the flight condition. In order for successful implementation of the numerical perturbation scheme, it is often necessary to establish first the perturbation sizes that will result in appropriate stability and control derivative values at various flight conditions.

The second method is to obtain the stability and control derivatives through analytical differentiation of the force and moment equations. Due to the complexity of the helicopter force and moment equations, analytical differentiation by manual means may become formidable. However, the task involved gets simplified somewhat by the use of symbolic processing programs. The advantage of this method is that once an analytical linear model is obtained, it can be used for parametric studies on a routine basis.

The third method is to obtain the linear model from simulated nonlinear response data through system identification. Using the global nonlinear simulation program, the helicopter is trimmed at a particular flight condition. From this trim condition, the helicopter response data is obtained for wide band excitation in various control channels and measurement noise can be included. From the input-output data, linear models are obtained that best fit the response data. The advantage of this method is that once the methodology is established, the same may be used to obtain linear models from actual flight test data.

All the three methods described above assume that a very good nonlinear model of the helicopter is available for linear model extraction. In the nonlinear model development, often there are many assumptions and approximations made to represent the complicated aerodynamic effects such as rotor-body aerodynamic interference effects, body aerodynamics, etc. Thus it is required to develop a very good nonlinear model before any of the linear model extraction methods can be applied. Hence, the only way of circumventing the problem of the nonavailability of a good nonlinear model for linear model extraction is to obtain the linear models directly from flight test data using system identification as illustrated in Figure 3.1.5. Thus, in principle, this method complements the linear model extraction from simulated response data. The vehicle is flight tested and input-output data is recorded about a trim condition. The type of input selected is such that it has enough frequency content to excite all the dynamic modes and degrees of freedom of interest and the magnitude of the input is limited to keep the magnitude of the vehicle response from trim in the linear range. Using the vehicle input-output data from the trim flight condition, linear models are extracted through system identification.

For a new vehicle under development, the linear model extraction from flight test data is feasible only after the prototype of the vehicle is available. Thus, considerable insight into the problems associated with the model extraction peculiar to the vehicle under development can be gained by using the simulated response data. Also, experience gained through model extraction from simulated response data may be fruitfully used in the planning and execution of subsequent flight testing and the model extraction from flight test data.

Based on the above discussion, a unified approach to rotorcraft system identification can be summarized by the following five part approach (DuVal et al., 1983 [3.1.3]; see also Figure 3.1.6 and Figure 3.1.7):

1. Generate assumed linear model from simulation.
2. Develop methodology for identification from flight test data.
3. Validate methodology using simulation.
4. Process flight test data.
5. Upgrade simulation to match flight test results.

This approach could be incorporated in the envisioned flow diagram of Figure 3.1.1. The remainder of this report will provide a status report on rotorcraft system identification and what must be done.

References

- [3.1.1] Iliff, K. W.; Klein, V.; Maine, R. E.; Murray, J.
Parameter Estimation Analysis for Aircraft
AIAA Professional Study Series, Williamsburg, VA, 1986
- [3.1.2] Iliff, K. W.; Maine, R. E.
Maximum Likelihood Estimation with Emphasis on Aircraft Flight Data
Workshop on Identification and Control of Flexible Space Structures, Jet Propulsion Laboratory, 1984
- [3.1.3] Du Val, R. W.; Wang, J. C.; Demiroz, M. W.
A Practical Approach to Rotorcraft Systems Identification
Proceedings of the 39th Annual AHS Forum, St. Louis, MO, 1983

Roadmap for the Evolution of System Identification

during the

design, development, certification/qualification, production, and product improvement process

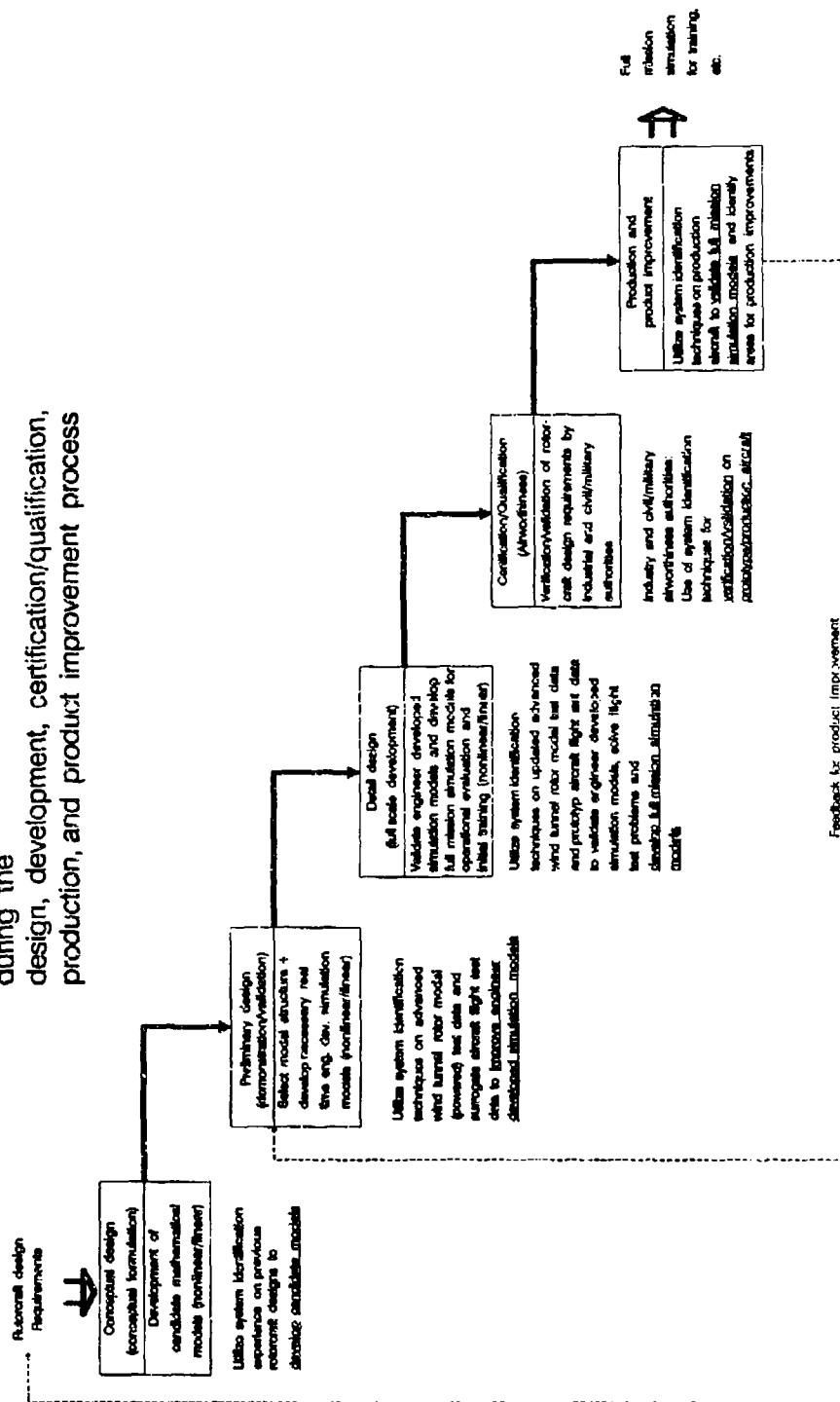


Figure 3.1.1. Roadmap for the evolution of system identification

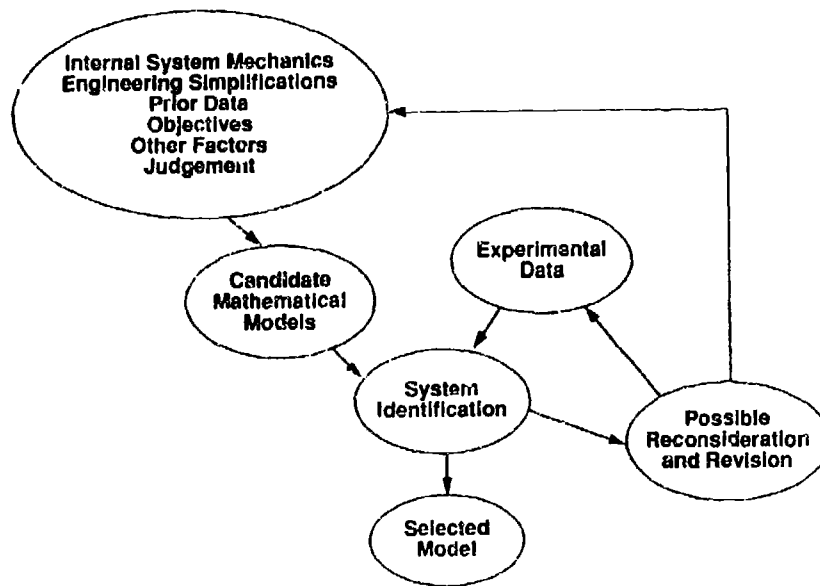


Figure 3.1.2. System identification as guide for mathematical modeling

6 DOF Fuselage Dynamics	Rotor/Fuselage Coupling	Inflow/Fuselage Coupling	U W Q P V P R Y
Fuselage/Rotor Coupling	3 DOF Rotor Flapping Dynamics	Inflow/Rotor Coupling	β_0 β_{1C} β_{1S}
Fuselage/Inflow Coupling	Rotor/Inflow Coupling	3 DOF Inflow Dynamics	λ_0 λ_{1C} λ_{1S}

Figure 3.1.3. 12 DoF helicopter simulation model structure

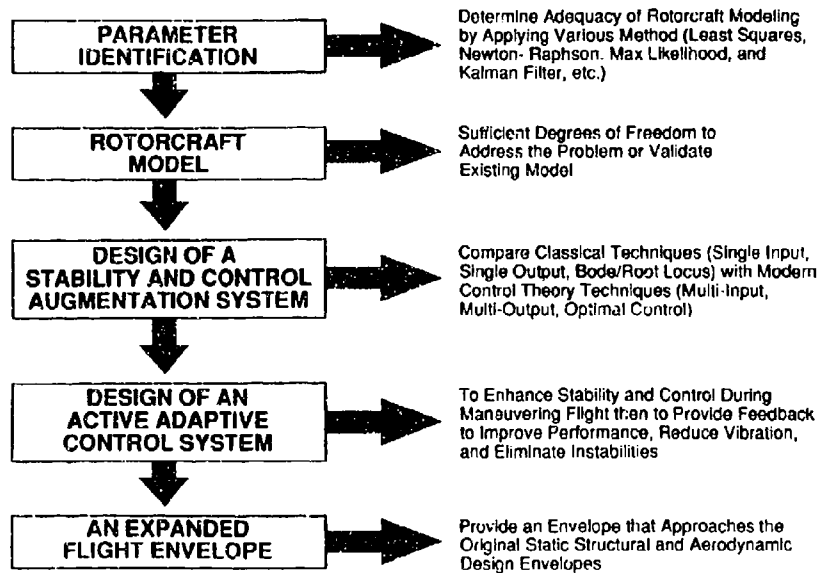


Figure 3.1.4. A systems approach to rotorcraft stability and control research

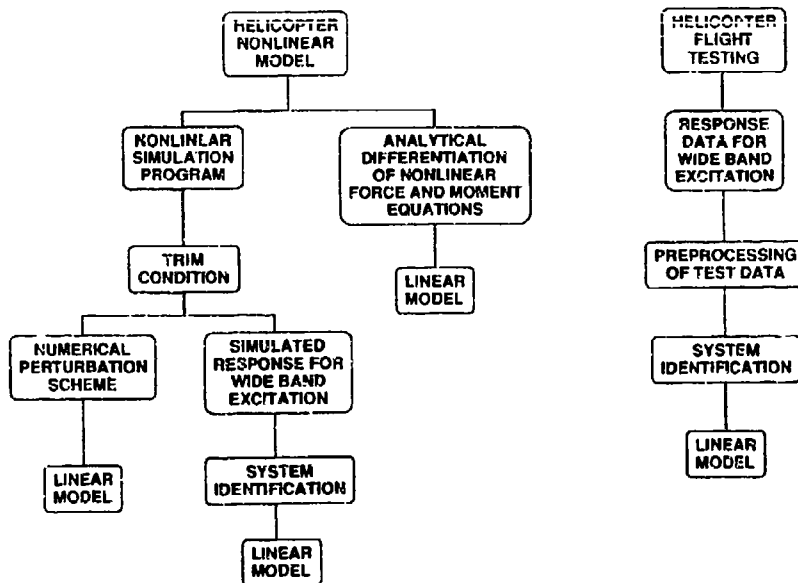


Figure 3.1.5. Helicopter linear handling qualities model

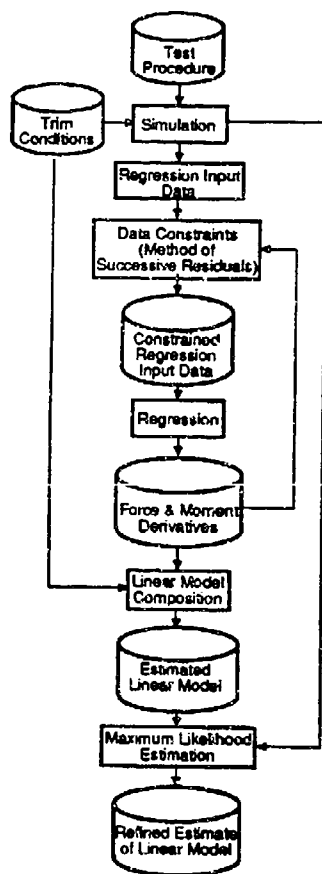


Figure 3.1.6. Methodology validation

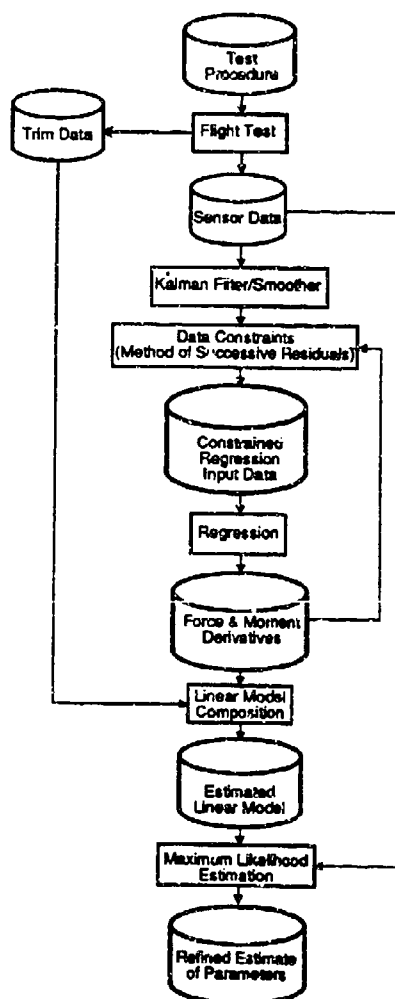


Figure 3.1.7. Flight data processing

3.2 Recent Helicopter System Identification Activities⁴⁾

3.2.1 Introduction

The last 10 years and 5 years in particular, has seen an increase in the number of organisations developing and applying the methods of system identification in rotorcraft flight dynamics. The Special Edition of *Vertica* (Padfield (editor), 1989, [3.2.1]) presents the most up-to-date snapshot of activities from most of the practising agencies; all present results of identification performed on flight test data gathered over the last few years at four of the principal flight research labs of the NATO countries, DLR, AFDD, NAE and RAE, together with the ARI, Melbourne. The availability of a wide range of quality test data, gathered for the purposes of flight dynamics analysis, has been the stimulant to this rejuvenation of interest. The early work of Molusis (1972 - 1974, [3.2.2]; [3.2.3], and [3.2.4]) and Gould and Hindson (1973, [3.2.5], 1974, [3.2.6]) highlighted the complexity of the rotorcraft identification problems compared with conventional aeroplanes but it was not until improved methods could be applied to quality test data in the early 1980s that the insight provided by this early work could be exploited fully. The applications presented in (Padfield (editor), 1989, [3.2.1]) reflect a strong investment of basic research into theoretical methods and test techniques. This Chapter presents the contributions made by the research agencies to this work, summarising the accomplishments, problem areas and future thrusts. The coverage is not exhaustive and omits the work of some non-participants to WG-18, notably Advanced Rotorcraft Technology Inc, University of York, and NASA Ames. The embryonic Industry activities in rotorcraft system identification are covered in chapter 3.3.

3.2.2 Activity Reviews

3.2.2.1 DLR, Braunschweig Research Center

DLR system identification activities are concentrated on both fixed wing and rotary wing aircraft. The close contact between the analysts and the common development and improvement of approaches and methods has proved to be very beneficial. For example, the 3211 input signal, which has become one of the standard input signals for identification, was originally designed for fixed wing aircraft flight testing by Marchand et al., (1974, [3.2.7]).

The first rotorcraft experience was gained in the late 1970s in collaboration with MB3 using a least square/instrumental variable approach (Rix et al., 1977, [3.2.8]; Kaletka et al., 1977, [3.2.9]; Kloster et al., 1980, [3.2.10]). The, now classical, helicopter identification problems were revealed - need for accurate measurements with sufficient data information content in the response, model structure aspects and careful test conduct (Kaletka, 1979, [3.2.11]). It was also demonstrated that the information content of only one maneuver with a single control input is not sufficient for the identification of a coupled six degrees of freedom model. An approach was developed that allowed the combination of independently flown maneuvers to increase the data information content and to extract one common model. This so called concatenated run evaluation has shown its effectiveness and is now used routinely in aircraft identification. With the acquisition of a dedicated BO 105 by the DLR in 1977 and, consequently, an easy access to appropriate flight test data, a standard approach to identification evolved, covering instrumentation and sensor calibration, data processing and state estimation, identification and verification of rotorcraft models (Kaletka, 1984, [3.2.12]; Holland, 1987, [3.2.13]). Significant progress could be made after three major software developments:

1. the Maximum Likelihood method was extended for concatenated run evaluation,
2. a Maximum Likelihood method for the identification of nonlinear systems was developed by Jategaonkar et al., (1983 and 1985, [3.2.14]; [3.2.15]),
3. a frequency-domain Maximum Likelihood technique was developed (Fu et al., 1983, [3.2.16]; Marchand et al., 1985, [3.2.17]).

Until recently, coupled 6 DoF rigid body models were used with an equivalent time delay to approximate the main rotor influence. Such models have been satisfactory for describing flight behaviour below about 13 rad/s. A principal application area at the DLR is modelling to support the BO 105 in-flight simulator, ATTHes. Here, however, research has shown that higher order models are required for the control system design and that 6 DoF models with equivalent time delays are inappropriate for the BO 105 (Pausder et al., 1988, [3.2.18]; Kaletka et al., 1989, [3.2.19]). Therefore, extended model formulations were developed. The present ATTHes control system design is based on a model that approximates rotor characteristics by using the roll and pitch

⁴⁾ Principal author: G. D. Padfield, RAE

accelerations as state variables. The identification of this model needs no rotor measurements and the result showed a significant improvement in bandwidth validity (Kaletka et al., 1989, [3.2.20]). The present work is concentrated on the extraction of higher order models with explicit rotor degrees of freedom. Here, rotor blade flapping measurements were required. First results are discussed by Fu et al., (1990, [3.2.21]).

As part of a Memorandum of Understanding (MOU) on *Helicopter Flight Control* between the United States and Germany, DLR and AFDD have worked in a close cooperation on identification research. The joint evaluation of XV-15 and BO 105 flight test data by applying the individual techniques have led to a deeper understanding of the approaches and a significant improvement of the methodologies of both research centers (Tischler et al., 1987, [3.2.22]; Kaletka et al., 1989, [3.2.19]).

3.2.2.2 AFDD, Ames Research Center

AFDD activities in rotorcraft system identification have focussed on the development of nonparametric and parametric frequency-domain techniques since 1983 (Tischler et al., 1983, [3.2.23]). The primary applications of these tools have been to

1. validate comprehensive simulation models (Tischler, 1987, [3.2.24]; Ballin et al., 1990, [3.2.25]).
2. document response characteristics of rotorcraft with advanced flight control systems (Hilbert et al., 1986, [3.2.26]; Tischler, 1987 [3.2.27]; Tischler et al., 1988 [3.2.28]).
3. demonstrate required compliance testing procedures contained in the specification for military rotorcraft (Tischler et al., 1987, [3.2.29]).

Research, begun in 1988 (Tischler, 1988, [3.2.30]), has led to the development of a comprehensive frequency-response approach for identification of rotorcraft stability and control derivative models. Applications of this approach to the XV-15 and BO 105 helicopters (Tischler et al., 1987, [3.2.22]; Tischler et al., 1990, [3.2.31]), has shown its benefits specially in model structure determination for an accurate multivariable frequency-domain characterization, such as is needed in modern Multi-Input Multi-Output (MIMO) design. Fletcher of the AFDD has developed a procedure for measurement system error identification and state reconstruction using Kalman filter/smoothing techniques (Fletcher, 1990, [3.2.32]). AFDD has worked in close cooperation with the DLR in joint identification research activities as part of the Memorandum of Understanding (MOU) between the United States and Germany on *Helicopter Flight Control*. Comparisons of AFDD frequency-domain results and DLR time-domain results for the XV-15 and BO 105 aircraft (Tischler et al., 1987, [3.2.22]; Kaletka et al., 1989, [3.2.19]) has significantly improved the methods and tools used by both research centres.

The AFDD tools are integrated into a software facility for system identification CIDER (Comprehensive Identification from Frequency Responses), which is described in the literature (Tischler et al., 1990, [3.2.31]). This facility is an interactive user-oriented package for the identification and verification of high-order coupled linear models. Recent applications of CIDER to the BO 105 WG data base has yielded a high-order model of the coupled body/rotor flap-lag dynamics (Tischler et al., 1990, [3.2.31]) that is accurate to frequencies of up to 30 rad/s, making it suitable for application to high-bandwidth flight control system design.

A key problem that is being addressed by AFDD is the formulation of higher-order models that represent the coupled body/rotor/inflow dynamics in a form suitable for system identification research. Flights are being conducted on the NASA/AFDD UH-60 BlackHawk to collect data useful for this research goal. Also, analytical methods are being used in parallel to formulate parametric model structures suitable for identification.

3.2.2.3 ARL, Melbourne

The principal driving force has been the development and validation of adequate simulation models for rotorcraft flight dynamics. The application has benefitted from a wide experience gained with fixed-wing aircraft e.g. ability to analyse flight records not previously amenable to analysis, improved and quantifiable accuracy, the provision of a large amount of information from a relatively small amount of testing. In addition, a range of methodology techniques in state and parameter identification developed for fixed wing applications are proving useful for helicopters e.g. least-squares equation and output error methods, maximum likelihood and extended Kalman filter. Current activities centre around the analysis of flight data gathered on a Sea King Mk50 (Guy et al., 1985, [3.2.33]; Williams et al., 1987, [3.2.34]). A study of the aircraft's vertical response in hover indicates the need to include inflow and flapping dynamics in the model structure and also to take account of blade flapping dynamics (Padfield (editor), 1989, [3.2.1]). The work is being extended to cyclic and pedal responses and forward flight. The approach being taken is to study each channel separately in limited flight regimes, thereby building up a complete representation step by step. Another activity involves identifying landing gear dynamics from drop test data.

Two problems are identified. Firstly, the lack of a well established model structure and the identification of manoeuvres which provide sufficient information for the accurate extraction of all the parameters of interest within a defined model structure. Secondly, the application of data compatibility checking procedures appears more difficult with helicopters arising from the coupled motions and generally noisier environment.

3.2.2.4 NAE, Ottawa

Pioneering work in the earlier 70s was motivated by the design requirements for a full-authority, multi-channel autopilot for the Bell 205 airborne simulator. Stability and control derivatives were estimated, using a modified Newton-Raphson method for uncoupled longitudinal and lateral/directional motions (Gould et al., 1973 and 1974, [3.2.5], [3.2.6]). Following this early work, and to support the establishment of a helicopter industry in Canada, a new effort was made in 1985 based on the use of the NASA MMLE3 (time-domain) program at the University of Toronto, and a new series of flight tests on the Bell 205 and 206 helicopters. The initial results were promising, but indicated the need for performing the flight tests under near ideal turbulence free conditions. Preliminary analysis with this test data and a 6 DoF linear model structure has been published (Padfield (editor), 1989, [3.2.1]).

Current activities involve a further series of tests with the Bell 205 with an emphasis on hover and slow flight conditions. A joint project with Bell Helicopter Textron of Montreal is underway, in which parameter estimation techniques will be studied by comparing flight test data obtained with the Bell 206 with computer simulations performed with the C-81 program. At the University of Toronto work is in progress to study ground based helicopter simulation, involving the comparison of flight test results with the prediction of candidate real-time simulation programs.

A major problem area is the selection of model structures that are as simple as possible under the circumstances, together with the determination of suitable control inputs and measurements to evaluate, in a meaningful way, the parameters defining that particular level of model.

3.2.2.5 RAE Farnborough / University of Glasgow

The principal aim of UK research in this field is to support the development and validation of predictive simulation models showing qualities and dynamic performance. In a collaborative activity between RAE and NASA, techniques developed for the RSRA flight programme were applied to RAE SA-330 data to investigate adequate model structures for low frequency dynamic motions (4 rad/s) (Padfield et al., 1982, [3.2.35]). Based on this initial experience, UK efforts were channelled towards the development of an integrated methodology encompassing state estimation, model structure estimation and parameter estimation (Padfield et al., 1987, [3.2.36]; Padfield, 1988, [3.2.37]; Black et al., 1986, [3.2.38]), including a frequency domain (state-space) maximum likelihood estimator (Black, 1988, [3.2.39]). Analysis in the frequency domain was considered essential to isolate specific modes of interest. A parallel activity focussed on equivalent system transfer function modelling (Padfield (editor), 1989, [3.2.1]; Houston, 1988, [3.2.40]). Applications of the UK tools have highlighted a number of issues,

1. great care needs to be taken when model building with equation-error techniques; singular value decomposition techniques can increase confidence in identified parameters (Black et al., 1986, [3.2.38]; Black, 1987, [3.2.41]).
2. including equivalent time delays in model structures can usefully extend identified frequency range; the method is particularly successful for low-offset articulated rotor helicopters (Padfield (editor), 1989, [3.2.1]; Black et al., 1986, [3.2.38]).
3. including cross-coupled effects as pseudo-controls has proved successful for helicopters without strong couplings (Padfield (editor), 1989, [3.2.1]).
4. a 3-degree-of-freedom model is required for vertical axis dynamic behaviour up to about 18 rad/s, including inflow and coning dynamics (Padfield (editor), 1989, [3.2.1]).

A central problem area being tackled is the design of efficient and robust control inputs to enable the identification of a large number of parameters with confidence. Current and future efforts are focussing on the use of system identification in validating non-linear simulation models including blade element rotor formulations. Flight tests with the RAE Lynx in 1990 will provide the test database for this new work.

3.2.2.6 CERT/ONERA Toulouse

A variety of different techniques have been developed over the years, principally for application to fixed-wing aircraft e.g. Airbus, and a range of industrial processes. Recent involvement with rotorcraft has been conducted in collaboration with Aérospatiale (see chapter 3.3). Current concerns include the optimal sequencing of tests to enable fully coupled models to be identified and the correct use of flight path reconstruction results.

3.2.2.7 Georgia Institute of Technology

The motivation behind rotorcraft parameter identification research at Georgia Institute of Technology, which started in 1986, is the development of an accurate mathematical model for effective control system design and flight envelope expansion. Both stochastic linear filter and extended Kalman filter identification algorithms are in use. Results have been obtained using simulated data (Fitzsimons et al., 1986, [3.2.42]) and UH-60 flight test data (Fitzsimons et al., 1988, [3.2.43]; Padfield (editor), 1989, [3.2.1]) highlighting consideration of record length, input frequency content and the need for multi-axis inputs. Current activities involve the application of the NASA Langley 'regression' package to AH-64 and BO 105 data.

3.2.3 General Remarks

More than 10 organisations in the NATO countries are now practising rotorcraft system identification and have access to quality flight test data. A common application area is simulation model validation, in support of control system design work. Analysis methods and test techniques have been developed over the last decade that are particularly suited to the rotorcraft identification problem - highly coupled dynamics with rotor modes, nonlinearities and often significant measurement and process noise. Particular areas of concern gleaned from a review of current activities include:

1. defining an adequate model structure for particular applications,
2. the high level of resource/expertise required to design experiments, gather data and conduct identification analysis,
3. the uncertainties in data compatibility checking in the presence of unknown levels of measurement and process noise,
4. the extension of linear parameter identification to the nonlinear case,
5. the extension of the presently often used 6 degrees of freedom models to higher order models with rotor degrees of freedom.

3.2.4 References

- [3.2.1] Padfield, G. D. (Editor)
Applications of System Identification in Rotorcraft Flight Dynamics
Vertica 'Special Edition', Vol. 13, No. 3, 1989
- [3.2.2] Molusis, J. A.
Helicopter Stability Derivative Extraction and Data Processing Using Kalman Filtering Techniques
28th AHS National Forum, Washington, DC, 1972
- [3.2.3] Molusis, J. A.
Helicopter Stability Derivative Extraction from Flight Data Using the Bayesian Approach to Estimation
Journal of the American Helicopter Society, Vol. 18, No. 2, 1973
- [3.2.4] Molusis, J. A.
Rotorcraft Derivative Identification from Analytical Models and Flight Test Data
In 'Methods for Aircraft State and Parameter Identification', AGARD CP 172, 1974
- [3.2.5] Gould, D. G.; Hindson, W. S.
Estimates of the Lateral-Directional Stability Derivatives of a Helicopter from Flight Measurements
NAE Aero Report LR-572, NRC-13882, 1973
- [3.2.6] Gould, D. G.; Hindson, W. S.
Estimation of the Stability Derivatives of a Helicopter and a V/STOL Aircraft from Flight Data
In 'Methods for Aircraft State and Parameter Identification', AGARD CP 172, 1974
- [3.2.7] Marchand, M.; Koehler, R.
Determination of Aircraft Derivatives by Automatic Parameter Adjustment and Frequency Response Methods
AGARD CP 172, 1974

- [3.2.8] Rix, O.; Huber, H.; Kaletka, J.
Parameter Identification of a Hingeless Rotor Helicopter
33rd Annual AHS Forum, Washington, DC, 1977
- [3.2.9] Kaletka, J.; Rix, O.
Aspects of System Identification of Helicopters
3rd European Rotorcraft and Powered Lift Aircraft Forum, Aix-En-Provence, Marseille, France, 1977
- [3.2.10] Kloster, M.; Kaletka, J.; Schaufele, H.
Parameter Identification of a Hingeless Rotor Helicopter in Flight Conditions with Increasing Instability
6th European Rotorcraft and Powered Lift Aircraft Forum, Bristol, UK, 1980
- [3.2.11] Kaletka, J.
Rotorcraft Identification Experience
AGARD LS 104, 1979
- [3.2.12] Kaletka, J.
Practical Aspects of Helicopter Parameter Identification
AIAA CP-849, 1984
- [3.2.13] Holland, R.
Digital Processing of Flight Test Data of a Helicopter without Using Anti-Aliasing Filters
ESA Translation from DFVLR-Mit. 87-12, ESA-TT-1094, 1987
- [3.2.14] Jategaonkar, R.; Plaetschke, E.
Maximum Likelihood Parameter Estimation from Flight Test Data for General Non-Linear Systems
DLR-FB 83-14, 1983
- [3.2.15] Jategaonkar, R.; Plaetschke, E.
Maximum Likelihood Estimation of Parameters in nonlinear Flight Mechanics Systems
7th IFAC Symposium on Identification and System Parameter Estimation, York, UK, 1985
- [3.2.16] Fu, K.H.; Marchand, M.
Helicopter System Identification in the Frequency Domain
9th European Rotorcraft Forum, Stresa, Italy, 1983
- [3.2.17] Marchand, M.; Fu, K.H.
Frequency-Domain parameter estimation of aeronautical systems without and with time delay
7th IFAC Symposium on Identification and System Parameter Estimation, York, UK, 1985
- [3.2.18] Pausder, H.-J.; von Grünhagen, W.; Henschel, F.; Zöllner, M.
Realization Aspects of Digital Control Systems for Helicopter
Conference on Helicopter Handling Qualities and Control, London, UK, 1988
- [3.2.19] Kaletka, J.; Tischler, M. B.; von Grünhagen, W.; Fletcher, J.
Time and Frequency-Domain Identification and Verification of BO 105 Dynamic Models
15th European Rotorcraft Forum, Amsterdam, NL, 1989
- [3.2.20] Kaletka, J.; von Grünhagen, W.
Identification of Mathematical Derivative Models for the Design of a Model Following Control System
Veruca, Vol. 13, No. 3, 1989
- [3.2.21] Fu, K.H.; Kaletka, J.
Frequency-Domain Identification of BO 105 Derivative Models with Rotor Degrees of Freedom
16th European Rotorcraft Forum, Glasgow, UK, 1990
- [3.2.22] Tischler, M. B.; Kaletka, J.
Modeling XV-15 Tilt-Rotor Aircraft Dynamics Using Frequency and Time-Domain Identification Techniques
AGARD-CP-423, 1987
- [3.2.23] Tischler, M. B.; Leung, J. G. M.; Dugan, D. C.
Frequency-Domain Identification of XV-15 Tilt-Rotor Aircraft Dynamics in Hovering Flight
AIAA Paper 83-2695, AIAA/AHS 2nd Flight Testing Conference, Las Vegas, NV, 1983. (Also published in condensed version in the Journal of the American Helicopter Society, Vol. 30, No. 2, 1985)
- [3.2.24] Tischler, M. B.
Frequency-Response Identification of XV-15 Tilt-Rotor Aircraft Dynamics
NASA TM-89428, 1987

- [3.2.25] Ballin, M. B.; Delang, A.
Validation of the Dynamic Response of a Blade-element UH-60 Simulation Model in Hovering Flight
Proceedings of the 46th Annual Forum of the American Helicopter Society, Washington DC, 1990
- [3.2.26] Hilbert, K. B.; Lebacqz, J. V.; Hindson, W. S.
Flight Investigation of a Multivariable Model-Following Control System for Rotorcraft
AIAA Flight Testing Conference, Las Vegas, NV, 1986
- [3.2.27] Tischler, M. B.
Digital Control of Highly Augmented Combat Rotorcraft
NASA TM-88346, 1987
- [3.2.28] Tischler, M. B.; Fletcher, J. W.; Morris, P. M.; Tucker, G. E.
Application of Flight Control System Methods on an Advanced Combat Rotorcraft
Royal Aeronautical Society International Conference on Helicopter Handling Qualities and Control, London, UK, 1988
- [3.2.29] Tischler, M. B.; Fletcher, J. W.; Diekmann, V. L.; Williams, R. A.; Cason, R. W.
Demonstration of Frequency-Sweep Testing Technique Using a Bell 214-ST Helicopter
NASA TM-89422, 1987
- [3.2.30] Tischler, M. B.
Advancements in Frequency-Domain Methods for Rotorcraft System Identification
2nd International Conference on Rotorcraft Basic Research, University of Maryland, College Park, MD, 1988
(also published in VERTICA, Vol 13, No. 3, 1989)
- [3.2.31] Tischler, M. B.; Cauffman, M. G.
Frequency-Response Method for Rotorcraft System Identification with Applications to the BO-105 Helicopter
Proceedings of the 46th Annual Forum of the American Helicopter Society, Washington DC, 1990
- [3.2.32] Fletcher, J. W.
Obtaining Consistent Models of Helicopter Flight-Data Measurement Errors Using Kinematic-Compatibility and State-Reconstruction Methods
Proceedings of the 46th Annual Forum of the American Helicopter Society, Washington DC, 1990
- [3.2.33] Guy, C. R.; Williams, M. J.
Flight Testing of an ASW Helicopter
Vertica, Vol. 9, No. 4, 1985
- [3.2.34] Williams, M. J.; Arney, A. M.; Perrin, R. H.; Feik, R. A.
Validation of a Mathematical Model of the Sea King Mk50 Helicopter Using Flight Trials Data
13th European Rotorcraft Forum, Arles, France, 1987
- [3.2.35] Padfield, G. D.; Du Val, R. W.
Application of System Identification to the Prediction of Helicopter Stability, Control, and Handling Characteristics: Helicopter Handling Qualities
NASA CP-2219, 1982
- [3.2.36] Padfield, G. D.; Thorne, R.; Murray-Smith, D.; Black, C.; Caldwell, A. E.
UK Research into System Identification for Helicopter Flight Mechanics
Vertica Vol. 11, No. 4, 1987
- [3.2.37] Padfield, G. D.
Integrated System Identification Methodology for Helicopter Flight Dynamics
Proceedings of the 42nd Annual Forum of the American Helicopter Society, Washington, DC, 1986
- [3.2.38] Black, C. G.; Murray-Smith, D. J.; Padfield, G. D.
Experience with Frequency-Domain Methods in Helicopter System Identification
Proceedings of the 12th European Rotorcraft Forum (Paper No. 76), Garmisch-Partenkirchen, FRG, 1986
- [3.2.39] Black, C. G.
A Methodology for the Identification of Helicopter Mathematical Models from Flight Data Based on the Frequency Domain
Ph.D. Thesis, University of Glasgow, 1988
- [3.2.40] Houston, S. S.
The Identification of Reduced Order Models of Helicopter Behaviour for Handling Qualities Studies
RAE TM FS(B) 682, 1988

- [3.2.41] Black, C. G.
Consideration of Trends in Stability and Control Derivatives from Helicopter System Identification
Proceedings of the 13th European Rotorcraft Forum (Paper No 7.8), Arles, France, 1987
- [3.2.42] Fitzsimons, P. M.; Prasad, J. V. R.; Tongue, B. H.; Schrage, D. P.
Non Iterative Parameter Identification Techniques
42nd Annual Forum of the American Helicopter Society, Washington, DC, 1986
- [3.2.43] Fitzsimons, P. M.; Teare, D.; Prasad, J. V. R.; Schrage, D. P.; Tongue, B. H.
Some Basic Issues in Helicopter System Identification
2nd International Conference on Rotorcraft Basic Research, University of Maryland, College Park, MD, 1988

3.3 The Role of Industry⁵⁾

3.3.1 Introduction

The AGARD Working Group 18 was tasked to review the maturity level of system identification for application in the Rotorcraft Industry and to make recommendations in three areas.

1. Expertise required to integrate methodology into design - development - certification life cycle.
2. Measurement and analysis techniques that offer efficiency, reliability and robustness.
3. Identification and alleviation of limiting factors from an Industry viewpoint.

Although the membership of WG 18 includes Industry representative from both Europe (Aérospatiale, Agusta, Messerschmidt-Bölkow-Blohm) and the US (McDonnell Douglas Helicopter Company), it was considered important that an opportunity be given to other manufacturers to comment on the utility of system identification, and particularly to draw attention to current methods that system identification may augment or even replace. A *Note and Questionnaire* was produced soliciting Industry's views under seven headings.

1. Any experience of using system identification methods? If so, please give reference and summarise main conclusions. If not, please comment on your perception of the methodology.
2. What techniques are currently used to validate simulation models used in design for performance and flying qualities?
3. What techniques are currently used to determine cause of problems and correct deficiencies during flight test development?
4. Are improvements required in the techniques outlined in (2) and (3)? If so, please quantify if possible.
5. Provide example(s) of case(s) where the behaviour during flight test development was unexpected and required design changes. How was the design solution arrived at (technique rather than engineering aspects) and what part did flight test data and the engineering simulation model play in the activity?
6. Are there any examples of unresolved flight behaviour anomalies that system identification may be able to shed light on and that your organisation would be prepared to release the relevant test data?
7. Are there any other comments that Industry wish to make?

Responses were received from all eight major manufacturers in Europe and the US:

1. Aérospatiale,
2. Agusta,
3. Bell Helicopter Textron Inc. (BHTI),
4. Boeing
5. Messerschmidt-Bölkow-Blohm (MBB),
6. McDonnell Douglas Helicopter Corporation (MDHC),
7. Sikorsky,
8. Westland.

It is clear that there is considerable interest in the techniques in Industry, balanced by a cautious scepticism. The experience level is varied but many common concerns and problem areas have, not unexpectedly, been identified. This section reviews the responses in more detail and draws conclusions where possible and makes recommendations for next steps.

Direct quotations from the Industry responses are included in *italics*.

⁵⁾ Principal author: G. D. Padfield, RAE

3.3.2 Industry Response

3.3.2.1 Question 1 - Experience and Perception

This question was aimed at establishing the experience level within the manufacturing industry and their perception of the maturity and potential of the techniques. The responses are summarised as follows.

1. *Aérospatiale*

Early, limited experience on SA3210 (1973), but more recently a joint activity has been conducted with CERT/ONERA, with Aérospatiale responsible for the flight test data and CERT/ONERA for the development and validation of time domain identification tools. Aérospatiale have drawn some early conclusions:

- high quality measurements, careful testing and test time durations in opposition with the requirement for short flight test development,
- identified linear models not as useful for validating and improving simulation models as expected,
- identified linear models good in mid speed range (70-110 kn), but, at higher or lower speeds, tests are far more difficult and results of poorer quality.

2. *Agusta*

Currently use time domain least-squares technique to minimise error between flight test and simulation, computed by nonlinear ARMCOP model. A constrained subset of effective configuration parameters are derived for each flight condition e.g. geometric and aerodynamic characteristics of vehicle components. Method has been applied to A109 and SA-330 (WG-18) flight test data.

3. *Bell Helicopter Textron Inc. (BHTI)*

Force determination methods are used by structural dynamics groups e.g. 206 LM pylon loads, AH-1W tail rotor gearbox loads. No formal System Identification methods used in handling qualities groups. The System Identification field has not, in our judgement, reached the same level of maturity as force determination as evidenced by the lack of validated software. The helicopter industry lacks evidence of the capability of the methods when used in design guidance or flight test problem correction.

4. *Boeing*

Currently two activities:

- 1) Use of FRESPID (US Army frequency domain) technique on ADOCS to document the closed loop command/response (conducted July 1988) at hover and 80 kn. Close correlation between flight test and analytical predictions of gain and phase.
- 2) Development of time domain maximum likelihood estimation (MLE) and Orthogonalised Projection Estimation (OPE) algorithms for stability and control derivative identification. The MLE approach is proving more robust.

Boeing currently perceive a trade-off with the two approaches:

- 1) does not require a defined model structure and is tailored for single input systems while
- 2) requires a pre-determined model structure and can handle multiple input/output systems.

5. *Messerschmidt-Bölkow-Blohm (MBB)*

A joint activity between MBB and DLR (Braunschweig) began in 1977. Two phases, both with a fly-by-wire BO 105, covered 70 kn and extended flight envelope conditions respectively (Rix et al., 1977, [3.3.1]; Kloster et al., 1980, [3.3.2]). Flight data problems included vibration, speed signal drift and poor accuracy of linear accelerations. Data were filtered to suppress rotor system dynamics. Time history comparisons between flight and theory were good but derivatives were sometimes poor.

6. *McDonnell Douglas Helicopter Company (MDHC)*

Currently utilise both MLE and basic Output Error (OE) methods with trade-off that OE is poor when process noise excessive and MLE more difficult to implement and converge to a solution. Application area is flight simulation model validation. MDHC have a very positive approach to the methodology: *System identification techniques are the most logical and systematic means for validation and upgrade of our modelling software. It is planned to extend their application to linear handling qualities models and aerodynamic performance models.*

7. Sikorsky

Sikorsky invested significant effort in helicopter parameter identification in the early 70's during the period of time that John Molusis and Ray Hansen were employed here. Parameter identification techniques provide the possibility of extracting physically meaningful parameters from flight test data. The premise is that these flight-test-derived parameters may provide insight toward a better understanding of helicopter flight dynamics, provide a means of validating existing simulations in both the time and frequency domains, and provide a validated model for use in design and development (e.g. AFCS development).

Much of the work done by Molusis and Hansen during that time is in the public domain. After a significant expenditure of time and effort however, it became obvious that the derived parameters, while able to reproduce time histories accurately, were physically meaningless (had the wrong signs, for example). This led to a period of disenchantment with parameter identification methods at Sikorsky.

More recently, Sikorsky has utilized frequency domain methods (nonparametric identification) with some success. The Technical Evaluation Program (TEP) on the CH-53E helicopter involved approximately 100 hours of flight testing to validate the stability characteristics of the aircraft when flying with external loads. These data have been used to validate the GENHEL model in the frequency domain. The result of this work is proprietary at this time, but a description of the program and some results were presented by Steve Hong at the 1989 AHS Annual Forum in Boston (Kapita et al., 1989, [3.3.3]). At this time we feel comfortable in applying frequency domain methods and now use it routinely with simulation. The new Handling Qualities Specifications, of course, make its use mandatory in order to show compliance with some parts of the specification.

There was an attempt at applying the modified 'pEst' parameter estimation code (Murray, 1987, [3.3.5]) to flight test data, but it did not give satisfactory results and has been discontinued. At this time, based on our experience, no parameter identification code is available that is robust and mature enough for industry use.

8. Westland

No specific experience identified that has been consciously thought of as system identification, as promulgated in learned publications. Westland do, however, offer a shrewd perception on the merits of system identification:

The methodology is perceived as providing a mechanism for reproducing a particular phenomenon under a particular set of circumstances but without necessarily advancing the understanding of the phenomenon ... Such an understanding forms the basis of any sound solution to real life engineering problems. In most instances, the more intractable problems either involve a large number of variables or are highly nonlinear or, more often, both. Under these circumstances, spurious values are possibly attributed to those parameters which are included in the model as compensation for any shortcomings in the postulated structure of the model. A good fit obtained for one condition may not be valid for other conditions. The Westland view here perhaps echoes the concerns of many in Industry who feel that, in the extreme, the tools are inappropriate. Westland go further and underscore their scepticism,

Any success is related to engineering experience, flair, judgement and understanding of the physical factors involved and which underlie the proposed model structure rather than any sophisticated system identification methodology.

3.3.2.2 Question 2 - Techniques For Simulation Model Validation In Design

The validation of simulation models used during the design of a new type is seen by WG 18 as a critical application area for system identification. Techniques currently used by Industry need to be understood to provide the foundations on which the new methodology could be built.

1. Aerospatiale

Principal method is through comparison of measured and calculated data for trim and dynamic response. For the latter, the method only applies to short runs because any trim errors soon integrate to significant attitude differences in the simulation. For similar reasons, the response to high frequency inputs are dif-

difficult to analyse. Aérospatiale stress that they consider these methods insufficient: *The direct comparison method used for model validation is not sufficient, especially when the range of frequencies used by the pilot are considered. Frequency domain identification seems to be a more interesting tool in this area.*

2. **Agusta**

Model validation is derived from comparison between flight test and simulator time histories; improvements are achieved through parameter modification, constrained by a physical understanding of the problem.

3. **Bell Helicopter Textron Inc. (BHTI)**

No input

4. **Boeing**

Both time and frequency domain methods are used to conduct validation of 6 DOF models against higher order, non-real-time models and flight test data. In the time domain, dominant mode frequencies and dampings are derived from step responses. The ADOCS activity was an exception, where gain and phase of the frequency responses were matched.

5. **Messerschmidt-Bölkow-Blohm (MBB)**

Comparison of simulator and flight test data for trim, loads, performance, stability of aircraft and rotor modes and vibrations throughout the flight envelope forms the principal method. Linearised stability and control derivatives have been more difficult to obtain with confidence. The most significant damping, control and cross coupling derivatives are obtained by matching low order equivalent systems and the test data.

6. **McDonnell Douglas Helicopter Company (MDHC)**

Three techniques currently in use,

- adjustment of preselected model parameters to satisfy pilot perception of differences between simulator and representative aircraft response e.g. time constants in dynamic inflow model.
- comparison of trims and response to control inputs.
- flight measurements together with (Kalman filter) estimated aircraft states are used to drive the simulation model in a *wind tunnel* mode to determine the aerodynamic loads. System identification method used to model the aerodynamic loads on various components e.g. main rotor, horizontal tail etc..

7. **Sikorsky**

Comparisons of steady state trims, time and frequency domain control responses.

8. **Westland**

Comparison with flight test data for trim, transient response to control and gain and phase relationships across various components of the total system loop. Engineering judgement is used to assess acceptability of comparisons.

Comments

The emphasis in the question was on the validation of models used in design. Industry responded, without exception, by referring to comparison with flight test data which, of course, is generally not available during the design process. It has to be assumed therefore that Industry consider that a simulation model can only be validated once test data becomes available i.e. after the aircraft has been built and flown.

3.3.2.3 Question 3 - Techniques For Problem Solving During Flight Test Development

Achieving performance and flying qualities standards and requirements early in the flight test programme is rare and has probably never been realised in practice. Highly skilled resources are often required to resolve problems and the resulting re-design and repair work can be time consuming. Both the manufacturer and potential customer will press for efficient resolution. Again, it was important that WG 18 pay cognizance to the established successful methods; it is assumed that problems have not been predicted at the design stage.

1. **Aérospatiale**

Currently, dynamic stability of the bare airframe presents the major handling qualities problem to be solved during flight test development, to ensure an acceptable safety level in the case of autopilot failure: *It (dynamic stability) is the more acute, as simulation is only valid to compare configurations but does not provide an accurate estimation in this field.* Aérospatiale search for solutions to stability deficiencies by modifying the fuselage/empennage design and initially rely on the experience of previous cases. When this is insufficient the phenomena are explored at model scale in the Marignane wind tunnel; eventually, solutions found in the wind tunnel are tested in flight.

2. **Agusta**

Personal experience is currently used to solve problems.

3. **Bell Helicopter Textron Inc. (BHTI)**

No input

4. **Boeing**

Typically, when problems occur at flight test, simulation models with increasing degrees-of-freedom are used until the problem is predicted. If still unresolved, the situation is re-examined with respect to modelling adequacy and missing elements.

5. **Messerschmidt-Bölkow-Blohm (MBB)**

Similar techniques used as for question 2. *The substantiation of flying qualities and flight performance at critical loading, atmospheric, and flight conditions has to be proved. Modern analytical methods are able to cover a majority of these aspects, but in extreme conditions at the boundary of the flight envelope, tests are still necessary.* Included in the list of test conditions provided by MBB are role related flying tasks. The information provided reflects a systematic approach to establishing substantiation and the identification of problems but says nothing concerning methods for cause and correction.

6. **McDonnell Douglas Helicopter Company (MDHC)**

Principal method used to determine problem areas is close scrutiny of flight test data. More basic research is required in the area of control input design to support this process.

7. **Sikorsky**

More flight testing combined with simulation.

8. **Westland**

A central and significant activity in the Westland approach is examination of flight data for conformation of the flight crew's qualitative reporting of the handling issue and hence a definition of the problem. Possible explanations are formulated but: *a major difficulty is being able to incorporate the various pieces of information into a form which is compatible with the mathematical model, e.g. non-linearities in the power servo, and 'engineering intuition' is required to devise an appropriate model structure. Once a physical understanding is achieved, design modifications are modelled and assessed leading to a preferred solution.* The approach highlights the craft-like nature of modelling to solve flight dynamic problems and emphasises the fact that problems stem from unexpected situations and are always absent in the design model.

3.3.2.4 Question 4 - Improvements Required

A particular concern to WG 18 was whether Industry could clearly perceive what improvements in the techniques addressed were required.

1. **Aérospatiale**

Systematic approach to modifying fuselage/empennage, outlined in the answer to question 3 breaks down when a reference aircraft case does not exist and then the objectives of the tunnel tests are more difficult to define. *Simulation could help to establish the minimum aerodynamic characteristics of the fuselage/empennage leading to acceptable stability, but this would need improved simulation models.*

2. **Agusta**

A quantitative method is called for to improve both model validation and flight test activities. *Identification methods can give an estimate of the quality of the mathematical model through the cost function value.*

3. **Bell Helicopter Textron Inc. (BHTI)**

No input

4. **Boeing**

Three areas are addressed

- need for a practical method of directly mapping transfer function models to state space form and hence derivatives,
- improved and dedicated flight experiments,
- methods which incorporate Kalman filters/observers should be expanded (improved) to bridge the gap between required signals and sensor availability.

5. **Messerschmidt-Bölkow-Blohm (MBB)**

A standardised identification procedure for the complete set of stability and control derivatives is necessary. *Most applications for these results are validation of linearised, flight mechanical computer codes and support in the design of electronic augmentation.*

6. **McDonnell Douglas Helicopter Company (MDHC)**

The Company considers that its approach is a correct and adequate one and that *fully exercising the methods outlined in (the response to) Question 2 should lead to a valid simulation model.* For flight test development, it is recognised that *more work needs to be done.*

7. **Sikorsky**

Reductions in flight time will be directly proportional to confidence in the validated model. Ideally, a dependable parameter identification procedure for rotorcraft should be one of the procedures used routinely for validating simulation models.

8. **Westland**

Following areas are cited as examples where current practice could be improved.

- improved occurrence reporting,
- enhanced data gathering, particularly in rotating system
- improved information about amplitude-conscious non-linearities,
- extension of frequency domain methods to multi-input/multi output,
- improved information about choice of frequency domain inputs e.g. manual or auto sweeps, Schroeder phased signals,
- extension of frequency domain methods to higher frequencies.

3.3.2.5 Question 5 - Examples Of Unexpected Behaviour Requiring Design Changes

1. **Aérospatiale**

see (Roesch et al., 1981, [3.3.4]).

2. **Agusta**

No input

3. **Bell Helicopter Textron Inc. (BHTI)**

No input

4. **Boeing**

Experience reported regarding the ADOCS development - *Flight test data from step disturbance inputs were examined and compared to both 6 DOF and 20 DOF model predictions. Some of the problems relating to unexpected time delays were identified with the lower order model; other responses*

due to coupled rotor/fuselage effects were identified with the higher order model. In addition, both models were used to design lead compensation to further improve stability, gain and phase margin characteristics.

5. **Messerschmidt-Bölkow-Blohm (MBB)**

For the BK117 prototype, deficiencies occurred:

- tail shake in descending flight - eliminated by fitting of hub cap and removal of aft fuselage spoilers
- early tests showed weak directional stability at high speeds and climb rates. A refined analytical study and dynamic pressure measurements in the tail area region showed that an improvement of the static lateral stability and dihedral stability could solve the problem; the end plate configuration was changed by increasing the area and shape.

In general it is difficult to model interference effects and also the nonlinear aerodynamic/dynamic effects on a blade (flutter, dynamic stall, 3-dimensional effects on future blade tips).

6. **McDonnell Douglas Helicopter Company (MDHC)**

Flight tests on YAH-64 with T-tail configuration revealed unexpected problems e.g. nose-up attitude at low speed/climb, sudden forward trim changes when accelerating from hover to high speed. The simulation model played a key role in redefining the tail with a scheduled stabilator and increased capacity tail rotor. Powered wind tunnel data were made available to model the main rotor to tail surface aerodynamic interference.

7. **Sikorsky**

No input

8. **Westland**

Three areas have been identified:

- The accurate retrimming of a helicopter to a desired airspeed with an attitude hold term within the ASE. This was addressed by applying reasoned changes to the ASE in the flight development programme and by education of the long time constant nature of the airspeed response. The inability to reproduce the original extent of the problem in the simulator was attributed in part to the 'clinical' simulator environment.
- A persistent poorly damped small oscillation in roll on a hingeless rotor under development was investigated by the in-flight testing of AFCS modifications leading to an operating technique which reduced the effect without entirely eliminating it. Although a number of relevant design parameter changes were simulated, the variation in this phenomenon over the speed range could not be satisfactorily reproduced to form a basis for recommending design modification.
- Pitch up in the low speed flight envelope due to wake impingement on the tail cone/tailplane which was significantly greater than prediction. This was addressed by flight testing mechanical modifications to the helicopter.

3.3.2.6 Question 6 - Unresolved Flight Behaviour

This question was intended to give Industry the opportunity to identify any outstanding handling problems which might be tackled (by a future WG?) using system identification methods. No specific examples were identified but two areas where identification may prove useful were highlighted - the determination of main and tail rotor thrust (Agusta) and the estimation of wake (effects) parameters in main rotor flapping models.

3.3.2.7 Question 7 - Comments

This question provided an opportunity to address issues or concerns not covered by the specific questions. Three of the US manufacturers responded with positive and optimistic comments. The main comments were:

1. **Aérospatiale**

(No comments).

2. **Agusta**

(No comments).

3. **Bell Helicopter Textron Inc. (BHTI)**

We encourage both the development of algorithms and validation of the technique.

BHTI went further and recommended a sequenced evaluation of emerging algorithms in estimating stability derivatives from time history data. Credibility in the methods could be established by a step-by-step demonstration using linear simulation data, nonlinear simulation data and corrupted simulation data.

4. **Boeing**

As system identification techniques improve, they will become an integral part of handling quality, optimisation and flight testing

5. **Messerschmidt-Bölkow-Blohm (MBB)**

In their response to the question, MBB re-iterated the range of potential application areas addressed by the questionnaire, but also suggested that the methodology could raise the confidence of certification authorities to theoretical results (certification phase) to allow acceptance of larger theoretical extrapolation with respect to the whole weight, atmosphere and temperature regime and a reduction of dangerous flight tests (e.g. engine failure). MBB completed their response by stating that the methodology would be used if it has advantages to the currently practised flight test procedures with respect to costs, accuracy, test time and handling and that it was important that companies understand the limitations of the methods in terms of frequencies, stability levels and flight conditions.

6. **McDonnell Douglas Helicopter Company (MDHC)**

MDHC is moving aggressively to implement system identification techniques in linear handling qualities and nonlinear flight simulation models and also in other applications where modelling parameters are not adequately quantified.

7. **Sikorsky**

Improvements are necessary which account for the inherently more complex nature of the rotorcraft system. The rotorcraft community has recently made large advances in parameter identification methods as applied to helicopter flight dynamics. (Kaletka et al., 1989, [3.3.6]). This research and development work needs to be matured and transferred to industry. Sikorsky intends to pursue this area of investigation, using its experience based on the CH-53E flight test program.

8. **Westland**

(No comments).

3.3.3 Concluding Remarks and Recommendations

This section has presented in condensed form the response by helicopter manufacturers to a questionnaire relating to the work of AGARD WG 18 - rotorcraft system identification. The questionnaire called for information on Industry's experience with, and perception of, the methodology and a description (and limitations) of current methods used to identify and cure (handling and control) problems in design, development and certification.

The eight major manufacturers in Europe and the US responded and the following general points can be made:

1. Current experience with system identification in Industry is limited but will increase when maturity levels grow and limitations are clearly defined.
2. It is vital to appreciate that system identification methods are no substitute for understanding physics of flight behaviour.
3. In the areas of model validation and trouble shooting during flight test development a strong reliance is placed on experience and engineering judgement in the interpretation of anomalies between simulation

and test time histories. Time history comparison stands out as the most common practice for information gathering.

4. Complete sets of stability and control derivatives (for AFCS design) are not obtainable from test data with confidence.
5. The Industry responses have emphasised the craft-like nature of modelling rotorcraft flight dynamics and the need for system identification tools to be compatible with this approach.
6. Within the framework of system identification, the concept of model structure adequacy would appear to be the most familiar and important in Industry. Methods that provide clear insight into this area should be given priority.
7. Many of the flight dynamics examples provided by Industry could, potentially, have been explained using system identification techniques.

The generally positive response from Industry has provided additional impetus and urgency to the work of WG 18. The fact that Industry appear to have got by without system identification so far does not reduce the scale of the effort required to increase the efficiency and robustness of the methods. Projects of the future, entirely reliant on active control for safe flight, will require that handling and control be the foremost design driver. Design simulation models will need to be considerably more accurate than is normally the case today; flight test techniques for handling qualities will need to be carefully designed for efficiency. System identification methods will need to play a key role in supporting the design - certification life cycle of these new types.

References

- [3.3.1] Rix, O.; Huber, H.; Kaletka, J.
Parameter Identification of a Hingeless Rotor Helicopter
33rd Annual Forum of the AHS, 1977
- [3.3.2] Kloster, M.; Kaletka, J.; Schäufele, H.
Parameter Identification of a Hingeless Rotor Helicopter in Flight Conditions with Increasing Instability
6th European Rotorcraft Forum, Bristol, UK, 1980
- [3.3.3] Kaplitz, T. T. et al.
Helicopter Simulation Development by Correlation with Frequency Sweep Flight Test Data
45th Annual Forum of the AHS, 1989
- [3.3.4] Roesch, P.; Vuillet, A.
New Designs for Improved Aerodynamic Stability on Recent Aérospatiale Helicopters
37th Annual Forum of the AHS, 1981
- [3.3.5] Murray, J. E.
The pEst Version 2.1 User's Manual
NASA TM-88280, 1987
- [3.3.6] Kaletka, J.; Tischler, M. B.; von Grünhagen, W.; Fletcher, J.
Time and Frequency-Domain Identification and Verification of BO 105 Dynamic Models
15th European Rotorcraft Forum, Amsterdam, NL, 1989

3.4 AGARD-Related System Identification Activities⁶⁾

The AGARD Flight Mechanics Panel (FMP) is one of the four original Panels established in 1952. As originally conceived, the Panel's primary focus was on flight test problems. One of the very first activities was related to flight test problems and future test requirements of primary interest to the member nations, leading to the publication of the AGARD Flight Test Manual (1952 - 1959, [3.4.1]). The importance of extracting flight vehicle stability and control parameters from flight tests has been discussed at a Flight Mechanics Panel meeting in Paris as early as 1958 (Leblanc, [3.4.2]; Zbrozek, [3.4.3]; Huff, [3.4.4]; Lenigk, [3.4.5]). Classical methods of parameter estimation had already been integrated in the second Volume of the AGARD Flight Test Manual. Additional general considerations including practical aspects have been published in an AGARD report (Wolowicz, 1966, [3.4.6]; Péré, 1966, [3.4.7] Burns, 1966, [3.4.8]) and in conference proceedings (1966, [3.4.9]).

Special reference should be made to the Conference Proceedings of a FMP Specialist's Meeting on *Methods of Aircraft State and Parameter Estimation* held at NASA Langley Research Center in November 1975 [3.4.10]. This was the first Flight Mechanics Panel interdisciplinary meeting of its kind to be organized for flight test engineers and pilots, handling qualities and simulation experts plus aircraft and control system designers to share their understanding, knowledge and experience in the area of aircraft system identification. It was demonstrated that conventional (e.g. fixed-wing) aircraft system identification methods have been successfully applied. But it became also apparent from special helicopter contributions (Gould, 1975, [3.4.11]; Molusis, 1975, [3.4.12]) that rotorcraft parameter identification is a much more complicated task mainly due to strong rigid-body and rotor coupling, rotor-induced measurement noise and the inherent instability of these vehicles (Hamel, 1976, [3.4.13]). As a direct outcome from this Specialist's Meeting a Lecture Series (LS-104) on Parameter Identification was organized by the FMP at two locations (Delft and London) in 1979 (Hamel (editor), [3.4.14]). A first critical assessment of international experience in rotorcraft identification so far was given (Kaletka, 1979, [3.4.15]).

In the mean-time the Flight Mechanics Panel sponsored major revisions and additions to the AGARD Flight Test Manual since 1968 leading to the current series of volumes in the two AGARDographs *Flight Test Instrumentation* (AG-160, 1972 - 1978, [3.4.16]) and *Flight Test Techniques* (AG-300, 1983 - 1988, [3.4.17]).

Within the AG-300 series a special volume on *Identification of Dynamic Systems* was prepared in 1985 on request of the FMP which addresses the parameter identification methodology in a more systematic and generic way (Maine, Iliff [3.4.18]). Related practical aspects are documented in another volume *Application to Aircraft. Part I: The Output Error Approach* by the same authors (Maine, Iliff, 1986, [3.4.19]).

Only extremely limited further rotorcraft system identification related AGARD publications became available (Kaletka et al., 1983, [3.4.20]; Padfield, 1985, [3.4.21]; Tischler et al., 1986, [3.4.22]) since the AGARD Working Group WG18 on *Rotorcraft System Identification* has been set up by the Flight Mechanics Panel.

References

- [3.4.1] Anon.
AGARD Flight Test Manual
AGARD, 4 volumes, 1952 - 1959
- [3.4.2] Leblanc, G.
Un Exemple de la Détermination des Principaux Coefficients Aérodynamiques à Partir des Essais en Vol
AGARD Report R-189, 1958
- [3.4.3] Zbrozek, J. K.
On the Extraction of Stability Derivatives from Full-Scale Flight Data
AGARD Report R-190, 1958
- [3.4.4] Huff, W. W. jun.
Application of Dynamic Testing Procedures to Stability and Control Flight Test Programs
AGARD Report R-191, 1958

⁶⁾ Principal Author: P. G. Hamel, DLR

- [3.4.5] Lenigk, S.
On the Structural Stability of a Certain Class of Linear Motions
AGARD Report R-194, 1958
- [3.4.6] Wolowicz, H.
Considerations in the Determination of Stability Derivatives and Dynamic Characteristics from Flight Data
AGARD Report R-549, Part I, 1966
- [3.4.7] Pérè, J.
Un Nouveau Type de Fonctions Modulatrices pour la Méthode de Shinbrot
AGARD Report R-549, Part II, 1966
- [3.4.8] Burns, B. R. A.
Experience with Shinbrot's Method of Transient Response. Analysis for the Extraction of Stability and Control Derivatives
AGARD Report R-549, Part II, 1966
- [3.4.9] Anon.
Stability and Control
AGARD Conference Proceedings CP-17, Part I and II, 1966
- [3.4.10] Anon.
Methods of Aircraft State and Parameter Estimation
AGARD Conference Proceedings CP-172, 1975
- [3.4.11] Gould, D. G. et al.
Estimates of the Stability Derivatives of a Helicopter and a V/STOL Aircraft from Flight Data
[3.4.10], Paper 23, 1975
- [3.4.12] Molusis, J. A.
Rotorcraft Derivative Identification from Analytical Models and Flight Test Data
[3.4.10], Paper 24, 1975
- [3.4.13] Hamel, P. G.
Status of Methods for Aircraft State and Parameter Identification
AGARD Conference Proceedings CP-187, Paper 8, 1976
- [3.4.14] Hamel, P. G. (editor)
Parameter Identification
AGARD Lecture Series LS-104, 1979
- [3.4.15] Kaletka, J.
Rotorcraft Identification Experience
[3.4.14], Paper 7
- [3.4.16] Anon.
AGARD Flight Test Instrumentation Series
AGARDograph AG-160, 18 Volumes, 1972 - 1987
- [3.4.17] Anon.
AGARD Flight Test Techniques Series
AGARDograph AG-300, 8 volumes, 1983 - 1988
- [3.4.18] Maine, R. E.; Iliff, K. W.
Identification of Dynamic Systems
[3.4.17], Vol. 2, 1985
- [3.4.19] Maine, R. E.; Iliff, K. W.
Identification of Dynamic Systems - Applications to Aircraft. Part I: The Output Error Approach
[3.4.17], Vol. 3, Part I, 1986
- [3.4.20] Kaletka, J.; Langer, H.-J.
Correlation Aspects of Analytical, Wind Tunnel, and Flight Test Results for a Hingeless Rotor Helicopter
AGARD Conference Proceedings CP-339, Paper 16, 1983

- [3.4.21] Padfield, G. D.
Flight Testing for Performance and Flying Qualities
AGARD Lecture Series LS-139, Paper 7, 1985
- [3.4.22] Tischler, M. B.; Kafelka, J.
Modeling XV-15 Tilt-Rotor Aircraft Dynamics by Frequency and Time Domain Identification Techniques
AGARD Conference Proceedings CP-423, Paper 9, 1986

4. AGARD Working Group Data Base⁷⁾

4.1 Introduction

A prerequisite to perform the work on helicopter parameter identification in the Working Group so that the obtained results can be compared is the selection of a common data base. From the flight test data offered by WG Members, data sets from three different helicopters were chosen for parameter identification purposes:

- McDonnell Douglas Helicopter Company (MDHC) provided data from an AH-64 (Apache), an attack helicopter with an articulated rotor.
- The Deutsche Forschungsanstalt für Luft- und Raumfahrt (DLR) provided data from a BO 105, a light transport helicopter with a high equivalent hinge offset rigid rotor.
- The Royal Aerospace Establishment (RAE) provided data from a SA-330, a transport helicopter with an articulated rotor.

In this chapter, the measurements and the flight test manoeuvres given in the data bases are characterized. It should be noted that the BO 105 and the SA-330 are operated by research organizations (DLR and RAE) which have been working in the field of system identification since several years. In consequence, the definition and development of the aircraft instrumentation was influenced by system identification requirements and the provided flight test data were generated particularly for identification purposes. The AH-64 data base was generated by MDHC, a company not yet involved in system identification work. The installed instrumentation and the flown manoeuvres were defined for other test objectives.

Some characteristic responses of the three helicopters on one-axis input signals are shown in Figure 4.1 through Figure 4.4.

4.2 System Identification Data Base

4.2.1 Requirements

An 'ideal' data base for system identification should mainly provide:

1. Data runs flown at practically the same conditions to allow concatenated run evaluations. This is true not only for helicopter characteristics like mass and CG location, but also for the environmental conditions, e.g. airspeed and altitude, and test conduction with respect to trim condition and input signal generation.
2. Control inputs particularly defined for system identification purposes, response amplitudes within small perturbation assumptions, and long enough time duration of the run to also provide sufficient low frequency information.
3. Redundant tests to show the repeatability and give the possibility to select the 'best suited' data.
4. Test runs with different input amplitudes to reveal nonlinearities.
5. Test runs with sign converted input signals to reveal asymmetries.
6. Different input signals to be used for the identification and the verification of the obtained models. Here, the basic idea is to extract a model from flight test data with one input signal type (e.g. 3211 signals). Then the model reliability is evaluated by comparing model prediction to measurements using flight test data with dissimilar control inputs (eg. doublets or frequency sweeps).
7. Measurements of at least all state and control variables of the model to be identified. As an example, for the identification of a 6 DoF rigid body model, measurements of the speed components, rates, attitude angles, and controls should be considered as the absolute minimum of required data.

To meet all these requirements generally leads to a flight test program specifically conducted for identification purposes. However, depending on the individual application of the identified model, some of them can be reduced or neglected. Then, the consequences must be quite clear. For example, a short data run may give a

⁷⁾ Principal Author: C. P. G. M. Hoffman, NLR

reliable model for the higher frequency range, low frequency characteristics however cannot be determined. Or, a verification of the identified model is only possible and meaningful when data are available that are significantly different from those used for the identification itself but are still within the same frequency range.

4.2.2 Measured Quantities and Conventions Used

Table 4.1 lists the measured control displacement and the sign conventions used for them on the different helicopters. On the BO 105 and the SA-330 these displacements were measured on the pilot's controls as on these two helicopters autostabilisation was not available or disengaged, respectively. On the AH-64, however, measurements were taken at the actuators, some runs having autostabilisation engaged.

The sign conventions for the measured response variables are listed in Table 4.2.

4.3 AH-64 Apache

4.3.1 Introduction

The flight test data for the MDHC AH-64 helicopter have been gathered for doublet and frequency sweep manoeuvres with control inputs in all axes at a 130 knots flight condition. Flights with pulse control inputs were made available for longitudinal and lateral cyclic inputs. All flight tests were selected from an existing data base with emphasis on practically the same helicopter state (mass, CG position, etc) and flight condition.

4.3.2 Manoeuvres

Table 4.3 lists the manoeuvres provided.

The data base included

- Two doublet runs for each control axis, each starting in opposite direction.
- One pulse run for each, forward and aft longitudinal control, and right lateral control.
- Sinusoidal frequency sweeps ranging from 0.1 Hz to 3 Hz for all controls (three sweeps for the longitudinal control, two for the lateral and the pedal and one for the collective control).
- One sinusoidal frequency sweep ranging from 0.3 Hz to 13 Hz for each, the lateral and the collective control.

All doublet and pulse inputs were pilot generated. The stability augmentation system was disengaged. The inputs for the frequency sweep control manoeuvres, however, were produced by a specially designed Gold Oscillator Box (GOB) unit. To maintain off-axis stability during the test, the stability augmentation system provided low gain feedback on the off-axis responses. The primary axes were in open loop configuration.

The data runs with doublet or pulse inputs were only about 13 seconds long. Data with frequency sweep had a time duration between 118 and 158 seconds consisting of a sweep up to the high frequency and then back down to the starting frequency. In total, 21 manoeuvres were provided (8 doublets, 3 pulses, 10 frequency sweeps).

4.3.3 Measurements

The AH-64 flight test data were mainly obtained from six different subsystems:

1. A noseboom with pressure sensors and vanes.
A boom is used to measure the air data: total velocity, angle of attack, and sideslip (V , α , β). The boom is mounted out in front of the aircraft to avoid main rotor wake interactions. From the measurements, the speed components u , v , w can be calculated.
2. A sensor package with gyros and linear accelerometers.
A sensor package installed close to the CG position is used to measure
 - roll, pitch, and yaw rates (\dot{p} , \dot{q} , \dot{r}),
 - roll, pitch, and yaw angular accelerations (\ddot{p} , \ddot{q} , \ddot{r}),
 - longitudinal, lateral, and vertical accelerations (a_x , a_y , a_z).

3. 'Pilot seat accelerometers'.
A package of linear accelerometers was installed at a position close to the pilot's seat. It provided the pilot's seat longitudinal, lateral, and vertical accelerations (a_{xp} , a_{yp} , a_{zp}).
4. Heading attitude reference system (HARS).
An inertial system (HARS) gave roll, pitch and yaw attitude (Φ , Θ , Ψ) and the vertical velocity w . Based on the attitude measurements, the Euler rates ($\dot{\Phi}$, $\dot{\Theta}$, $\dot{\Psi}$) were computed.
5. A Doppler system provided the forward and lateral ground speed components.
6. Control input generation and measurement.
Three types of input signals were flown. Doublets and pulses were generated by the pilot, frequency sweeps signals were produced electronically. To eliminate uncertainties in control linkage and actuator dynamics, control positions were not taken at the pilot's stick or pedals but at the actuators: pitch, roll, and yaw actuator, collective (δ_{lon} , δ_{lat} , δ_{ped} , δ_{col}).

Table 4.4 lists the measured control variables and Table 4.5 the measured response variables provided for all manoeuvres with some exceptions:

- Runs with doublet or pulse inputs and the collective sweeps had no HARS vertical speed and Doppler data (for the identification these data are not necessarily needed).
- The collective sweeps had no pitch attitude information which is in general needed for the identification.
- Two of the longitudinal sweeps, the two lateral sweeps (0.1 to 3 Hz) and the pedal sweeps had no boom data (making identification very difficult) and no pilot's seat acceleration measurements.

4.3.4 Processing/Consistency Checks

No filtering or smoothing has been performed on the data. Changes have been made to the sample rate. The sample rate of the original flight test data varied from sensor to sensor. To eliminate excessive data and to provide a uniform sampling rate, the raw data were sampled at 100 Hz. A zero order hold was applied to the measurements originally sampled at 59 Hz (attitude angles and heading).

Before delivery of the flight test data to the WG members a number of consistency checks have been performed on the raw data to determine the fidelity of the measurements.

1. Accelerometer measurements from different locations on the aircraft (including the pilot's seat and the CG accelerations provided) were found to agree within a 1° alignment error.
2. Rate measurements including both body rates and Euler rates from each test were integrated and compared to the attitudes to determine if any bias existed. Some small biases were found and consequently removed from the data.
3. Measured angular accelerations were also integrated and compared to the body angular rates. Despite the significant process noise, the integrated accelerations showed the same general shape as the rate signals.

4.4 BO 105

4.4.1 Introduction

Flight tests, especially designed for system identification purposes, were conducted with the DLR BO 105-S123 helicopter at DLR in Braunschweig. The tests were defined to meet three main objectives:

1. Investigate the influence of different input signals.
2. Allow identification with time-domain and frequency-domain techniques.
3. Generate measurements of blade motions for the identification of extended models with explicit rotor degrees of freedom.

The trim configuration for the BO 105 (total mass between 2250 kg and 2400 kg) flight tests was steady state horizontal flight at 80 knots and at a density altitude of about 3000 ft standard atmosphere. (Depending on the outside temperature the actually flown indicated pressure altitude was iteratively adjusted). Main emphasis was placed on calm air flight conditions.

4.4.2 Manoeuvres

The BO 105 manoeuvres provided to the WG are summarized in Table 4.6. Three different types of control input signals were flown:

1. Doublets (2 seconds total time length) for each control input and each control direction (positive/negative).
2. Modified 3211-signals (time length 7 seconds) for each control input and each control direction (positive/negative).
3. Frequency sweeps for each control input. The frequency sweeps ranged from about 0.08 Hz up to the highest frequency the pilot could generate (5 Hz to 8 Hz, depending on the control).

For redundancy reasons the doublet manoeuvres were flown twice and both the 3211-signals and frequency sweep manoeuvres three times. Within one test run only one control was used to excite the on-axis response and to avoid correlation with other controls. Because of the long time duration of the frequency sweeps, these tests required some stabilization by the pilot to keep the aircraft response within the limits of small perturbation assumptions for linear mathematical models. At the end of the 3211-signals and doublet input signals, the controls were kept constant and the recording of the helicopter response was continued until the pilot started to retrim the aircraft.

At the beginning of each run the main pilot carefully trimmed the aircraft to the defined steady state condition of 80 knots horizontal flight. He then flew hands-off while the second pilot generated the prescribed single-control input signal without touching the remaining controls to avoid correlations. A CRT was used as input signal indicator showing the desired input signal shape and the actual control position versus time. During the first test flights the input amplitudes were determined so that the aircraft response within a 30 seconds test was in agreement with linear model small perturbation assumptions. Here, it was primarily tried to limit the deviations in pitch and roll attitude angles to about 25 degrees.

To avoid larger changes in mass and CG location the helicopter was refueled after a total flying time of about one hour.

4.4.3 Measurements

The development of the instrumentation followed the concept of using individual sensors that are independent from each other. The instrumentation used for system identification purposes was:

1. Three rate gyros for roll, pitch, and yaw rates (p , q , r).
2. A vertical gyro for the roll and pitch attitude (Φ , Θ) and a gyro for heading (Ψ).
3. Three linear accelerometers, installed close to the aircraft CG to measure the longitudinal, lateral, and vertical accelerations (a_x , a_y , a_z).
4. Potentiometers at each pilot's control (stick, pedals, collective lever) to measure the control inputs (δ_{lon} , δ_{lat} , δ_{ped} , δ_{col}).
5. A tachometer at the main rotor shaft for RPM.
6. A HADS (helicopter air data system) was used that is designed for speed measurements in the total speed range of the helicopter including hover. The sensor is a swivelling probe installed under the rotor. It is designed to operate in two different flow conditions: for hover and low airspeed it is working within the downwash of the rotor and it aligns with the resulting flow (downwash and helicopter speed). For speeds higher than about 35 knots the sensor is out of the downwash. Then it aligns with the actual speed vector of the helicopter. Based on the pressure and probe angle signals the forward and sideward aircraft speed is derived (u , v). For the out-of-downwash condition the vertical speed (w) is obtained in addition.

All data were digitized and recorded on board of the helicopter. The standard sampling rates were 100 Hz or 50 Hz, depending on the signal frequency content; due to the high vibration level, linear accelerations were sampled with 300 Hz.

Table 4.7 summarizes the measured control variables and Table 4.8 the measured response variables provided to the Working Group.

4.4.4 Processing/Consistency Checks

During the flight tests, the measured signals were sent by telemetry to a ground station where time histories from selected variables were presented on both a monitor and plotter for on-line quick looks. A first computer supported data compatibility check was conducted to isolate data inconsistencies. Using these on-line data checks together with pilot's comments it was relatively easy

1. to control the tests,
2. to detect major data errors (e.g. sensor malfunction, signal saturation, etc.), test inaccuracies, disturbances (e.g. drifts, large coupling in the controls, turbulence, etc), and
3. to decide if the test was a "good" one or if it had to be repeated.

Ground-based data processing included a.o.:

- Data conversion to a unit system with meter, radian, second, Newton and percent,
- Calculation of the speed components along the helicopter axes,
- Digital filtering of linear accelerations and rates to reduce vibrations (zero-phase-shift filter with 12.5 Hz cut-off frequency),
- Digital differentiation of the rates to obtain angular accelerations,
- Correction of speed components and linear accelerations with respect to the center of gravity.
- Conversion of all data to a unique sampling rate of 100 Hz.

Time histories of all measured and derived data were plotted and visually checked for significant errors (e.g. sign, amplitude, dynamic characteristics, noise, drop outs). Before delivery of the flight test data to the WCG members, data compatibility calculations, using the non-linear kinematic equations, were done for calculated rotational accelerations/rates, rates/attitude angles, and linear accelerations/speed components. It can be concluded:

- Rates and angular measurements agree almost perfectly, but the agreement between integrated yaw rate and measured heading shows some differences because the directional gyro is of lower quality (heading is not used for the identification).
- Concerning the comparison of integrated linear accelerations and measured speed components it can be stated that in general a satisfactory agreement was found.

4.5 SA-330 Puma

4.5.1 Introduction

A flight test database for system identification research was gathered on the RAE Puma XW241 during the period 1981-87. Flight conditions flown included hover and forward flight trims at 60, 80, 100, 120 knots. Test points were generally flown at a high enough altitude to establish calm (i.e. low turbulence) and steady conditions which in practice were found between 3000 ft and 4000 ft pressure altitude. Aircraft configuration could be varied in terms of mass and CG position but the datum configuration with full fuel and 2 crew members was about 5800 kg and neutral. Typically, at each trimmed flight condition the pilot would hold the controls fixed for about five seconds, apply the required control input and continue to hold fixed controls until the disturbed response had decayed or a sufficiently long manoeuvre duration had been recorded or the excursions became large enough to warrant intervention. Following a control response the aircraft would be retrimmed in the initial condition and two repeat manoeuvres performed giving 3 records in all, enabling repeatability to be checked. This procedure would be repeated for the opposite control direction. (e.g. left/right, up/down) and for all four axes, amounting to 24 events per input type and size, per flight condition. The duration of the recorded manoeuvres varied with input type and size, and varied from a few seconds for a single-step input in, say, longitudinal or lateral cycle to about 20-30 seconds for a return-to-trim, multi-step e.g. doublet, 3211-signal, to more than 100 seconds for a frequency sweep. Repeat runs at different control amplitudes were sometimes recorded to check for linearity in the response.

4.5.2 Manoeuvres

The manoeuvre cases provided to WCG 18 are listed in Table 4.9. Two different data sets were given:

1. The primary set was flown at 80 kn and included 3211 multi-step in both initial directions of all four control axes.

2. A secondary set included multi-step and frequency sweeps for longitudinal cyclic only at the three speeds, 60, 80 and 100 knots.

Control amplitudes are typically $\pm 2\%$ (longitudinal cyclic) and $\pm 5\%$ (lateral cyclic, collective, pedal) of full range. Response amplitudes varied with different inputs of course but maximum excursions were about ± 15 kn airspeed, $\pm 6^\circ$ (incidence), $\pm 10^\circ$ (sideslip) and $\pm 10^\circ/\text{s}$ (roll-, pitch-, yaw rate).

The data were selected from various flights. This explains the flight condition differences in altitude.

4.5.3 Measurements

For the SA-330 the largest number of measured variables were provided although several measurements, not needed for the Working Group, were either not engaged or not yet transformed to engineering units. The following is, therefore, only concerned with those measurements that were of interest for the WG objectives. The measured control variables are given in Table 4.10, the measured response variables are given in Table 4.11. Basically, signals are obtained from individual sensors, an 'agility package', a noseboom, and control measurements.

1. Redundant data from individual sensors and the agility package.
The SA-330 provides redundant data obtained from two different sources: Individual sensors are accelerometers, rate and attitude gyros. The 'agility package' is an inertial system integrated in one box so that it can easily be installed for flight test measurements in an aircraft. Both systems provide:
 - roll, pitch, and yaw rates (p , q , r and p_{ag} , q_{ag} , r_{ag}),
 - roll and pitch attitudes (Φ , Θ and Φ_{ag} , Θ_{ag}).
2. Additional individual sensors.
 - heading (Ψ) is measured by a directional gyro.
 - longitudinal, lateral, and vertical accelerations (a_x , a_y , a_z and a_{xag} , a_{yag} , a_{zag}) are obtained from linear accelerometers.
3. Noseboom
A pressure transducer and two vanes are installed at a boom to give total airspeed, angle of attack, and sideslip (V , α , β). The boom is installed at the nose of the helicopter to avoid disturbances in the measurements due to rotor downwash and fuselage influences.
4. Controls
Potentiometers are used at the pilot's stick, pedals and collective lever (δ_{lon} , δ_{lat} , δ_{ped} , δ_{col}).

The data were recorded at a variety of sampling rates. All channels were passed through anti-aliasing filters at 72 Hz before digitising; in addition, the agility package data was further filtered by a 2-pole Butterworth at 10.6 Hz. The measurements were recorded in digital PCM form (12 bit numbers) on-board on magnetic tape. No de-skewing techniques were adopted, resulting in a maximum data skew of about 10 ms. For the AGARD WG data base, all measurements were transformed to a uniform sampling rate of 64 Hz.

4.5.4 Processing/Consistency Checks

The only pre-processing carried out on the data before dispatch to WG 18 members was a conversion to engineering units and a sorting into binary files. No referencing of data to the CG location was carried out. Time history traces were examined visually for obvious anomalies and observable errors. In addition, a direct comparison of air data velocities with integrated accelerations, and fuselage attitude with integrated angular rates was made. From these visual comparisons a number of observations can be made concerning data quality.

1. The angle of attack vane measurement and the normal acceleration require a reversal of scale factor signs.
2. Signal to noise ratios in the longitudinal and lateral accelerations are typically of the order unity, except for the larger yaw manoeuvres when the latter is of the order 10.
3. Departure of velocity and attitudes indicate possibility of small calibration errors on inertial and vane data.
4. Airspeed data contain process noise, possibly caused by rotor wake/fuselage interference at the boom.

Assuming that each organisation would be conducting their own kinematic consistency and state estimation checks, the recorded measurements were considered to be of high enough quality for system identification work.

4.6 Summary and Concluding Remarks

When the three data bases (AH-64, BO 105, SA-330) provided to the WG are compared to an 'ideal' system identification data base as characterized in section 4.2 it can be stated:

- The minimum requirement for the available measurements is easily met by all three data bases. All data bases provide even more data like linear accelerations and, in particular the AH-64 and SA-330 give a high level of measurement redundancies from additional sensors.
- Considering requirements like uniform flight test conditions, redundant runs, sign converted inputs, and different input types for all controls, the BO 105 data base takes its advantage out of the fact that all provided data were flown within one flight test program. It was conducted only for system identification purposes right after the first WG Meeting and, therefore, included most of the WG requirements. Currently, it is certainly one of the most comprehensive data bases available for system identification, the more so as it also includes flapping measurements for all blades (not provided to the Group). However, data were only generated for one flight condition and the data base still has to extended into other flight regimes.
- The AH-64 data base was not produced for system identification purposes and, therefore, no input signals were used that are felt to be most suited for the identification. In addition, most data runs are very short so that the low frequency information content is probably too small. Nevertheless, the Group decided to also work on these data in order to demonstrate what system identification can achieve with a typical industry generated data base.

Group	Variables	Helicopter		
	Quantity	AH-64	BO 105	SA-330
Control displacements (at input device)	Forward/Aft Cyclic	n.m.	stick aft	stick forward
	Lateral Cyclic	n.m.	stick right	stick left
	Collective	n.m.	up	up
	Pedals	n.m.	right pedal forward	left pedal forward
Control displacements (at actuators)	Forward/Aft Cyclic	stick aft	n.m.	n.m.
	Lateral Cyclic	stick right	n.m.	n.m.
	Collective	up	n.m.	n.m.
	Tail Rotor Collective	right pedal forward	n.m.	n.m.
Table 4.1. Conventions for Positive Signs of Control Displacements				

Group	Variables Quantity	All studied helicopters (AH-64, BO 105, SA-330)
Air data	Angle of attack	flow from below (nose up)
	Angle of sideslip	flow from starboard (nose left)
	Airspeed	forward
	Longitudinal speed	forward
	Lateral speed	right
	Normal speed	down
	Rate of climb	up
Flight path data	Longitudinal speed	forward
	Lateral speed	right
	Normal speed	down
Linear accelerations	Longitudinal acceleration	forward
	Lateral acceleration	right
	Normal acceleration	down
Attitude angles (Euler angles)	Bank angle (Roll angle)	Right side down
	Inclination angle (Pitch angle)	Nose up
	Azimuth angle (Yaw angle)	Nose right
Angular rates	Rate of roll	Right side down
	Rate of pitch	Nose up
	Rate of yaw	Nose right
Table 4.2. Conventions for Positive Signs of Response Variables		

Control	Control Input			Duration t_i or Frequency content f_i	Number of runs	Recording time per run in s	Flight Conditions	
	Type	Initial displacement					Airspeed	Altitude
Longitudinal	Doublet	Forward		$t_i \approx 6s$	1	13	130 kn	$H_p \approx 3500$ ft
Longitudinal	Doublet	Aft		$t_i \approx 7s$	1	13	130 kn	$H_p \approx 35000$ ft
Lateral	Doublet	Left		$t_i \approx 7s$	1	13	130 kn	$H_p \approx 35000$ ft
Lateral	Doublet	Right		$t_i \approx 7s$	1	13	130 kn	$H_p \approx 3500$ ft
Pedal	Doublet	Left		$t_i \approx 7s$	1	13	130 kn	$H_p \approx 3500$ ft
Pedal	Doublet	Right		$t_i \approx 7s$	1	13	130 kn	$H_p \approx 3500$ ft
Collective	Doublet	Up		$t_i \approx 8s$	1	13	130 kn	$H_p \approx 3500$ ft
Collective	Doublet	Down		$t_i \approx 8s$	1	13	130 kn	$H_p \approx 3500$ ft
Longitudinal	Pulse	Forward		...	1	13	130 kn	$H_p \approx 3500$ ft
Longitudinal	Pulse	Aft		...	1	13	130 kn	$H_p \approx 3500$ ft
Lateral	Pulse	Right		...	1	13	130 kn	$H_p \approx 3500$ ft
Longitudinal	Frequency sweep	...		$0.1Hz \leq f_i \leq 3Hz$	3	114 ... 158	130 kn	$H_p \approx 3500$ ft
Lateral	Frequency sweep	...		$0.1Hz \leq f_i \leq 3Hz$	2	127 ... 138	130 kn	$H_p \approx 3500$ ft
Lateral	Frequency sweep	...		$0.3Hz \leq f_i \leq 13Hz$	1	138	130 kn	$H_p \approx 3500$ ft
Pedal	Frequency sweep	...		$0.1Hz \leq f_i \leq 3Hz$	2	118 ... 141	130 kn	$H_p \approx 3500$ ft
Collective	Frequency sweep	...		$0.1Hz \leq f_i \leq 3Hz$	1	140	130 kn	$H_p \approx 3500$ ft
Collective	Frequency sweep	...		$0.3Hz \leq f_i \leq 13Hz$	1	131	130 kn	$H_p \approx 3500$ ft

Mass inertia: Aircraft inertias based on a mass of 6650 kg and referred to body axes with origin in CG appropriate to tests flown:

$I_x \approx 8300 \text{ kg m}^2$, $I_y \approx 53000 \text{ kg m}^2$, $I_z \approx 50200 \text{ kg m}^2$, $I_{xz} \approx 4850 \text{ kg m}^2$.

Airspeed: Airspeed given is conventional airspeed V_C .

Altitude: The altitude given is the pressure altitude H_p .

Temperature: Average outside temperature during the tests was 21°C.

Table 4.3. List of runs (AH-64)

Group	Variables	Source	Original Sampling Rate (in Hz)
	Quantity		
Control displacements	Forward/Aft Cyclic	Actuator	470
	Lateral Cyclic	Actuator	470
	Collective	Actuator	941
	Tail Rotor Collective	Actuator	470
Table 4.4. AH-64 Control Variables			

Group	Variables Quantity	Source	Original Sampling Rate (In Hz)
Air data	Angle of attack	Boom System	941
	Angle of sideslip	Boom System	470
	Airspeed	Boom System	59
Flight path data	Longitudinal speed	Doppler radar	941
	Lateral speed	Doppler radar	941
	Normal speed	HARS	470
Linear accelerations	Longitudinal acceleration	Accelerometer at CG	470
	Lateral acceleration	Accelerometer at CG	470
	Normal acceleration	Accelerometer at CG	470
Linear accelerations	Longitudinal acceleration	Accelerometer at pilot's seat	470
	Lateral acceleration	Accelerometer at pilot's seat	470
	Normal acceleration	Accelerometer at pilot's seat	941
Attitude angles (Euler angles)	Roll angle	HARS	59
	Pitch angle	HARS	59
	Yaw angle	HARS	59
Angular rates	Roll rate	Rate gyro	941
	Pitch rate	Rate gyro	941
	Yaw rate	Rate gyro	941
Angular rates	Euler roll rate	Calculated from roll angle	470
	Euler pitch rate	Calculated from pitch angle	941
	Euler yaw rate	Calculated from yaw angle	470
Angular accelerations	Roll acceleration	Angular accelerometer	941
	Pitch acceleration	Angular accelerometer	941
	Yaw acceleration	Angular accelerometer	941

Table 4.5. AH-64 Response Variables
Data provided at a uniform sampling rate of 100 Hz.

Control	Control input			Duration t_i or Frequency content f_i	Number of runs	Recording time per run in s	Flight Conditions	
	Type	Initial displacement					Airspeed	Altitude
Longitudinal	Doublet	Aft		$t_i \approx 2s$	2	29 ... 32	80 km	$H_0 \approx 3000 \text{ ft}$
Longitudinal	Doublet	Forward		$t_i \approx 2s$	2	26 ... 28	80 km	$H_0 \approx 3000 \text{ ft}$
Lateral	Doublet	Right		$t_i \approx 2s$	2	20 ... 26	80 km	$H_0 \approx 3000 \text{ ft}$
Lateral	Doublet	Left		$t_i \approx 2s$	2	19 ... 26	80 km	$H_0 \approx 3000 \text{ ft}$
Pedal	Doublet	Right		$t_i \approx 2s$	2	15 ... 27	80 km	$H_0 \approx 3000 \text{ ft}$
Pedal	Doublet	Left		$t_i \approx 2s$	2	17 ... 18	80 km	$H_0 \approx 3000 \text{ ft}$
Collective	Doublet	Up		$t_i \approx 2s$	2	19 ... 32	80 km	$H_0 \approx 3000 \text{ ft}$
Collective	Doublet	Down		$t_i \approx 2s$	2	20 ... 32	80 km	$H_0 \approx 3000 \text{ ft}$
Longitudinal	Modified 3211	Aft		$t_i \approx 7s$	3	12 ... 24	80 km	$H_0 \approx 3000 \text{ ft}$
Longitudinal	Modified 3211	Forward		$t_i \approx 7s$	3	25 ... 32	80 km	$H_0 \approx 3000 \text{ ft}$
Lateral	Modified 3211	Right		$t_i \approx 7s$	3	27 ... 37	80 km	$H_0 \approx 3000 \text{ ft}$
Lateral	Modified 3211	Left		$t_i \approx 7s$	3	19 ... 31	80 km	$H_0 \approx 3000 \text{ ft}$
Pedal	Modified 3211	Right		$t_i \approx 7s$	3	25 ... 28	80 km	$H_0 \approx 3000 \text{ ft}$
Pedal	Modified 3211	Left		$t_i \approx 7s$	3	26 ... 34	80 km	$H_0 \approx 3000 \text{ ft}$
Collective	Modified 3211	Up		$t_i \approx 7s$	3	24 ... 29	80 km	$H_0 \approx 3000 \text{ ft}$
Collective	Modified 3211	Down		$t_i \approx 7s$	3	23 ... 36	80 km	$H_0 \approx 3000 \text{ ft}$
Longitudinal	Frequency sweep	...		$0.08 \text{ Hz} \leq f_i \leq 8 \text{ Hz}$	3	68	80 km	$H_0 \approx 3000 \text{ ft}$
Lateral	Frequency sweep	...		$0.08 \text{ Hz} \leq f_i \leq 7 \text{ Hz}$	3	68	80 km	$H_0 \approx 3000 \text{ ft}$
Pedal	Frequency sweep	...		$0.08 \text{ Hz} \leq f_i \leq 5.5 \text{ Hz}$	3	68	80 km	$H_0 \approx 3000 \text{ ft}$
Collective	Frequency sweep	...		$0.08 \text{ Hz} \leq f_i \leq 7 \text{ Hz}$	3	68	80 km	$H_0 \approx 3000 \text{ ft}$

Aircraft mass: $\approx 2200 \text{ kg}$.

Aircraft inertias (manufacturer's estimates) based on 2200 kg and referred to body axes with origin in CG appropriate to tests flown:

$I_x \approx 1700 \text{ kg m}^2$, $I_y \approx 4200 \text{ kg m}^2$, $I_z \approx 4200 \text{ kg m}^2$, $I_{xz} \approx 0 \text{ kg m}^2$.

The altitude given is the density altitude. H_0 . The actually flown pressure altitude was 4400 ft (at -5°C) $\leq H_0 \leq 5200 \text{ ft}$ (at -13°C).

Table 4.6. List of runs (BO 105)

Group	Variables Quantity	Source	Original Sampling Rate (in Hz)
Control displacements	Forward/Aft Cyclic	Potentiometer	50
	Lateral Cyclic	Potentiometer	50
	Pedal	Potentiometer	50
	Collective	Potentiometer	50
Table 4.7. BO 105 Control Variables			

Group	Variables Quantity	Source	Original Sampling Rate (in Hz)
Air data	Longitudinal airspeed	HADS	50
	Lateral airspeed	HADS	50
	Normal airspeed	HADS	50
Linear accelerations	Longitudinal acceleration	Accelerometer at CG	300
	Lateral acceleration	Accelerometer at CG	300
	Normal acceleration	Accelerometer at CG	300
Attitude angles (Euler angles)	Roll angle	Vertical gyro	50
	Pitch angle	Vertical gyro	50
	Yaw angle	Directional gyro	50
Angular rates	Roll rate	Rate gyro	100
	Pitch rate	Rate gyro	100
	Yaw rate	Rate gyro	100
Rotor	RPM	Tachometer	50
Table 4.8. BO 105 Response Variables			
Data provided at a uniform sampling rate of 100 Hz.			

Control	Control Input			Duration t_i or Frequency content f_i	Number of runs	Recording time per run in s	Flight Conditions	
	Type	Initial displacement					Airspeed	Altitude
Longitudinal	3211	Aft		$t_i \approx 7s$	1	30	80 kn	$H_0 \approx 3800$ ft
Longitudinal	3211	Forward		$t_i \approx 7s$	1	30	80 kn	$H_0 \approx 3800$ ft
Longitudinal	3211	Aft		$t_i \approx 7s$	1	30	80 kn	$H_0 \approx 3800$ ft
Longitudinal	3211	Forward		$t_i \approx 7s$	1	30	80 kn	$H_0 \approx 3800$ ft
Longitudinal	3211	Aft		$t_i \approx 7s$	1	25	100 kn	$H_0 \approx 2000$ ft
Longitudinal	3211	Forward		$t_i \approx 7s$	1	40	100 kn	$H_0 \approx 2000$ ft
Lateral	3211	Right		$t_i \approx 7s$	1	30	80 kn	$H_0 \approx 3800$ ft
Lateral	3211	Left		$t_i \approx 7s$	1	40	80 kn	$H_0 \approx 1850$ ft
Pedal	3211	Right		$t_i \approx 7s$	1	30	80 kn	$H_0 \approx 3150$ ft
Pedal	3211	Left		$t_i \approx 7s$	1	30	80 kn	$H_0 \approx 3200$ ft
Collective	3211	Up		$t_i \approx 7s$	1	30	80 kn	$H_0 \approx 4150$ ft
Collective	3211	Down		$t_i \approx 7s$	1	20	80 kn	$H_0 \approx 4100$ ft
Longitudinal	2121	Aft		$t_i \approx 8s$	1	30	60 kn	$H_0 \approx 1800$ ft
Longitudinal	2121	Forward		$t_i \approx 8s$	1	30	60 kn	$H_0 \approx 1900$ ft
Longitudinal	Frequency sweep	---		$0.05Hz \leq f_i \leq 5Hz$	1	120	60 kn	$H_0 \approx 3000$ ft
Longitudinal	Frequency sweep	---		$0.05Hz \leq f_i \leq 5Hz$	1	120	80 kn	$H_0 \approx 3000$ ft
Longitudinal	Frequency sweep	---		$0.05Hz \leq f_i \leq 5Hz$	1	120	100 kn	$H_0 \approx 3000$ ft

Mass, inertia

Aircraft mass $m \approx 5800$ kg.

Aircraft inertias (manufacturer's estimates) based on this mass and referred to body axes with origin in CG appropriate to tests flown:

$I_x \approx 9640$ kg m², $I_y \approx 33240$ kg m², $I_z \approx 25890$ kg m², $I_{xz} \approx 2230$ kg m².

Table 4.9. List of runs (SA-330)

Group	Variables Quantity	Source	Original Sampling Rate (in Hz)
Control displacements	Forward/aft cyclic	Potentiometer	128
	Lateral cyclic	Potentiometer	128
	Pedal	Potentiometer	128
	Collective	Potentiometer	128
Table 4.10. SA-330 Control Variables Data provided at a uniform sampling rate of 64 Hz.			

Group	Variables Quantity	Source	Original Sampling Rate (In Hz)
Air data	Angle of attack	Noseboom vane	128
	Angle of sideslip	Noseboom vane	128
	Airspeed	Noseboom Pitot probe	128
	Climb rate	Static pressure probe	128
Linear accelerations	Longitudinal acceleration	Accelerometer at CG and agility package	256
	Lateral acceleration	Accelerometer at CG and agility package	256
	Normal acceleration	Accelerometer at CG and agility package	256
Attitude angles (Euler angles)	Roll angle	Vertical gyro and agility package	128
	Pitch angle	Vertical gyro and agility package	128
	Yaw angle	Directional gyro	128
Angular rates	Roll rate	Rate gyro and agility package	256
	Pitch rate	Rate gyro and agility package	256
	Yaw rate	Rate gyro and agility package	256
Rotor	RPM	Tachometer	256
Table 4.11. SA-330 Response Variables Data provided at a uniform sampling rate of 64 Hz.			

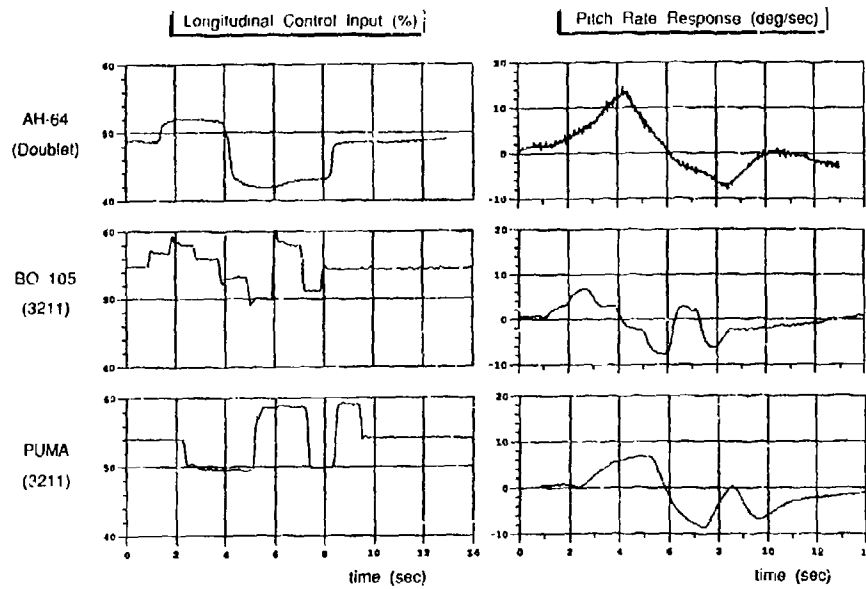


Figure 4.1. Characteristic helicopter responses to longitudinal control inputs

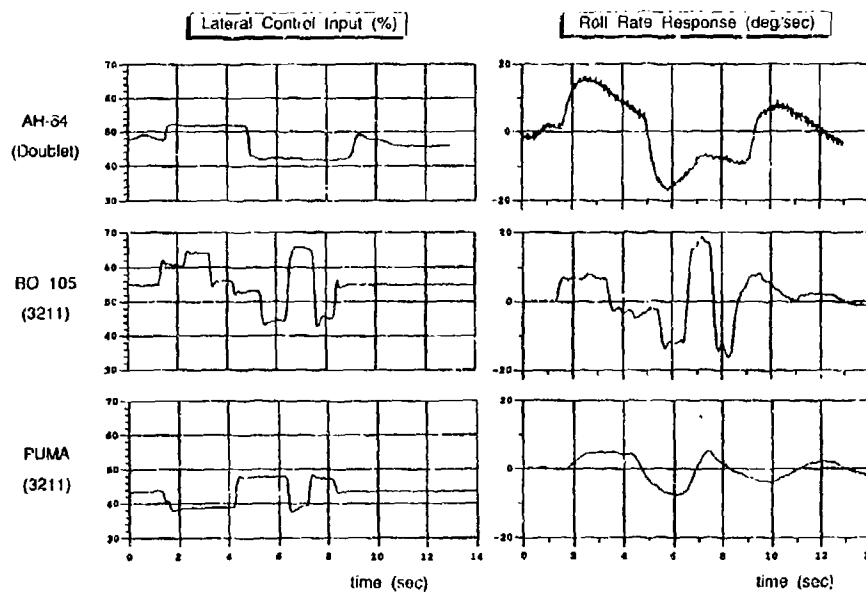


Figure 4.2. Characteristic helicopter responses to lateral control inputs

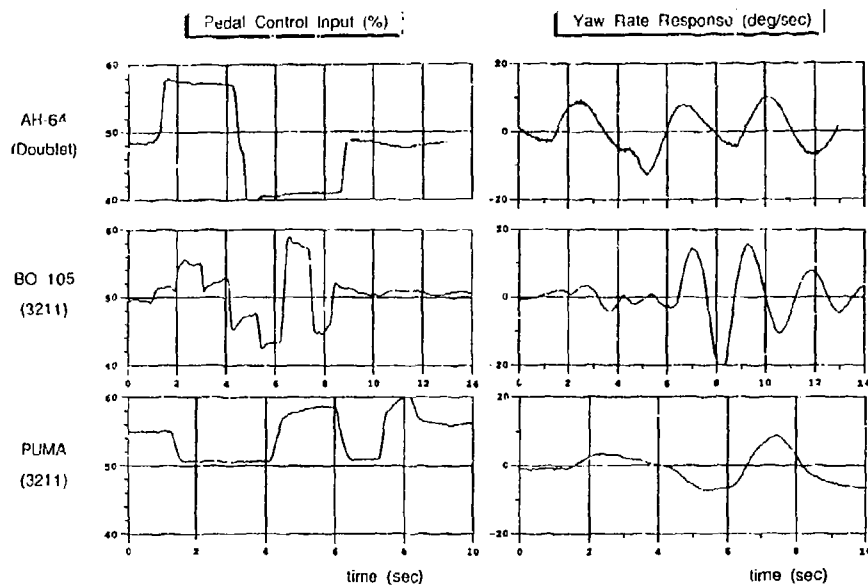


Figure 4.3. Characteristic helicopter responses to pedal control inputs

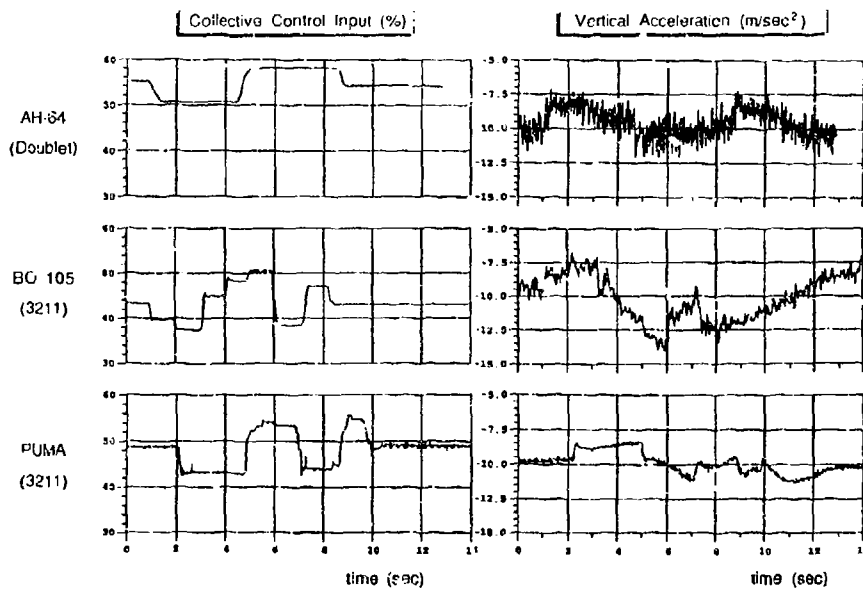


Figure 4.4. Characteristic helicopter responses to collective control inputs

5. Identification Methodologies

5.1 Introduction

Reliable identification results can only be obtained when all individual steps in the identification approach are carefully conducted. Therefore, this chapter concentrates on each of these steps. The section on *Flight Test Procedures* (5.2) includes a discussion on input signals and the planning and conduction of appropriate flight tests. Then, instrumentation requirements, data processing and evaluation are addressed (5.3 and 5.4). Finally, *Identification Techniques* applied in the Working Group are characterized (section 5.5).

5.2 Flight Test Procedures⁸⁾

5.2.1 Introduction

The success of aircraft system identification techniques depends, to a considerable extent, on the design and conduct of flight experiments. It is important to recognize that such flight experiments should be designed and performed specifically for the purposes of system identification and that satisfactory parameter estimates are seldom obtained from flight experiments which had some other primary objective. It must also be recognized that safety is of paramount importance at all times.

5.2.2 Planning of Flight Tests

The preparation of a complete matrix of flight experiments in advance is essential. This must cover factors such as the forms of test input to be used, the amplitude and duration of test signals, together with the precise set of trimmed flight conditions for which test inputs are to be applied. Experiments are usually repeated several times since replication provides valuable insight concerning robustness and allows averaging of the residual effects of turbulence. Test signals are also normally repeated in both directions for each control input.

Decisions must be made in advance, on the basis of previous flight experience, concerning the use of any form of stability augmentation during the flight experiments. At an early stage it is also necessary to establish whether signals are to be applied manually by the pilot or through some special form of input device such as that described by de Leeuw et al. (1989, [5.2.1]).

For test signals which involve a long sequence of control movements, such as a frequency sweep, it may be necessary for the pilot to take corrective action to ensure that the aircraft response is kept within specified limits. A clear policy must be established regarding such intervention. Policies must also be established concerning recovery action by the pilot at the end of each test and clear guidelines must be provided concerning acceptable excursions from the nominal trimmed flight condition.

It is essential that all the flight crew and others concerned with the conduct of the flight experiments are fully briefed and have detailed knowledge of the purpose of the tests. Every potential risk must be assessed carefully. In the planning of a sequence of tests for a range of points within the flight envelope it is important to ensure that experience is built up incrementally from a known (or low risk) condition towards an unknown (or high risk) condition. For example for tests involving hover conditions it is appropriate to start the test sequence at high altitudes and work down into ground effect, if required, in a series of well-defined steps.

Decisions must be made in planning flight experiments about the possible need for additional cockpit instrumentation. One example is a CRT showing both the desired test input signal and the actual control movement (section 6.2).

Arrangements must be made to provide test pilots with practice in achieving trimmed flight for specified flight conditions and in applying the required test input signals. It is also important to ensure that ground-based staff are fully conversant with the equipment used for monitoring the flight and for on-line detection of errors in the measurements.

⁸⁾ Principal Author: D. J. Murray Smith, Glasgow University

5.2.3 Selection of Test Inputs

Many factors should be taken into account in the design of practical test input signals but there are two aspects of the test input selection process which are of critical importance. Firstly the frequency content of test signals must be chosen to ensure that modes are excited sufficiently. Model responses to simulated test signals must show some sensitivity to variations of chosen model parameters if parameter estimation is to be achieved from flight data for those quantities and the accuracy of estimates can be highly dependent on frequency content. Appropriate allowance must, of course, be made for actuator dynamics in considering the frequency content of the inputs. Secondly, for the identification of linearised derivative models, the form of test input selected must ensure that the motion remains within a specified flight region. In addition, the form of input must ensure that the correlation between measured states and between separate control inputs is sufficiently low to give well-conditioned sets of equations at the identification stage. Ill-conditioning is often associated with near linear-dependence of the measured variables and this can be detected using measures based upon the information matrix or dispersion matrix (Beck et al., 1977, [5.2.2]).

Plaetschke et al., 1979, [5.2.4] have provided a useful review of practical input signal design methods with particular emphasis on multistep signal design by frequency-domain methods. Leith et al. (1989, [5.2.5]) have also applied frequency-domain methods to the design of multi-step signals and have provided details of experience gained in the application of such test inputs to a Lynx helicopter.

One form of multi-step test input signal which is traditionally used for the identification of fixed-wing aircraft is the doublet. Doublet inputs can be applied very effectively to excite the short period mode in longitudinal motion and the Dutch roll. Pilots can use such inputs to search for natural frequencies of the aircraft responses. As has been pointed out by Plaetschke et al. (1979, [5.2.4]) many derivatives are readily identifiable in the vicinity of natural frequencies, although some can only be found as ratios. In the case of the helicopter, doublet inputs are of limited value, although these inputs are capable of exciting modes in either axis very well. The highly coupled form of model structure presents difficulties using simple test signals of this kind and it is generally accepted that doublets are not ideal as test signals for helicopter identification although they are of value when used in conjunction with other types of input.

A second form of multi-step signal which has been used widely for rotorcraft and aircraft system identification is the so-called "3-2-1-1" band-optimized signal (Marchand et al., 1974, [5.2.3]; Plaetschke et al., 1979, [5.2.4]; Kaletka, 1979, [5.2.6]). The numbers used in the designation of this input refer to the time units between control reversals. Such inputs can, in principle, provide broader-band excitation than the doublet but, for cases in which stability margins are small, use of such signals may not allow an adequate length of data record without the use of stability augmentation or pilot intervention during the unforced part of the response. (Kaletka, 1979, [5.2.6]; Leith et al., 1989, [5.2.5]).

The Cramer-Rao bound, which relates the variance of parameter estimates to elements of the dispersion matrix, has led to algorithms for the design of inputs which minimize some appropriate function of the dispersion matrix or information matrix. The use of such design methods is based upon the assumption that an efficient estimator exists. Optimal test inputs designed in this way are therefore most useful in situations where test records are available which are long compared with the time constants of the system under test so that the asymptotic properties of appropriate estimators (e.g. maximum likelihood estimators) apply. This approach to test input design has been found to be useful for the selection of simple multi-step signals for manual application in rotorcraft identification (Leith et al., 1989, [5.2.5]).

Robustness of test inputs is an important but often neglected aspect of the input design process. As already discussed, only an approximate model of the vehicle is available prior to testing and the inputs used should be as insensitive as possible to errors in the model. For manual application, responses must also be insensitive to errors in timing and amplitude of the inputs.

A second important point is that inputs should not contain a d.c. component (non-zero mean value) since this will tend to change the operating condition of the aircraft away from the initial trim state unless this is specifically required (e.g. classical speed-stability tests).

Typically, the transfer function between a given control input and a given state variable will contain resonant peaks. If an input excites such a resonance the response will tend to be large and may become non-linear thus leading to a short test record. Hence by designing inputs which avoid exciting these resonances it is possible to obtain longer test records.

The requirements that the dispersion matrix is reasonably "small" can be satisfied in terms of the frequency-domain if the autospectrum of the input is chosen to avoid frequencies around the resonances but to excite the remaining frequencies over the frequency range of interest. Leith et al. (1989, [5.2.5]) have found that, by using

frequency-domain methods to tailor multi-step signals to avoid excitation at resonant frequencies while giving a satisfactory dispersion matrix, it is possible to obtain practical broad-band multi-step inputs. In the case of the Lynx helicopter a double-doublet form of input, designed in this way, provided useful test records, without stability augmentation, of more than thirty seconds duration before pilot intervention became necessary. Using 3211 inputs with the same helicopter useful test records could not be obtained since corrective pilot actions were required very early in each test and resulting records were of very short duration. It should be noted that a modified form of 3211 signal involving a reduced amplitude of the initial step has been used by de Leeuw et al. (1989, [5.2.1]) to reduce the magnitude of the initial excursion and to balance the total perturbation about the trim.

A different form of broad-band test signal which has been used increasingly in recent years is the 'frequency sweep' (Tischler et al., 1985, [5.2.7]). Such signals are generally initiated by applying two low frequency sinusoidal cycles having a period which corresponds to the lower bound of the frequency range required. The frequency is then increased gradually until the control is being driven at a relatively high frequency but with a smaller amplitude of motion. The control is then returned to trim. The overall period of this test sequence is chosen ideally to allow good identification of the low frequency modes and to give an even excitation of the vehicle dynamics over the frequency range of interest (Tischler, 1987, [5.2.8]).

In designing a test signal for identification a three-stage process may be adopted. The first stage involves initial simulation and analysis, based on the best currently available mathematical model, to obtain a first estimate of the dynamic range for testing. This provides a basis for the second stage which involves the design of a preliminary experiment using broad-band test signals such as frequency sweeps. Analysis of results from this initial characterisation is of considerable value for the design of the flight experiments from which parameter estimates are to be obtained. For example, assumptions of overall linearity can be checked by examining the coherence for selected pairs of input and output variables and the tests provide opportunities to characterize the linear and nonlinear dynamic characteristics of the actuation system. Preliminary tests of this type should be monitored in real time with particular reference to the assessment of the loading of critical components. Test signal amplitudes should be small initially and should be increased gradually until it becomes clear that all modes of significance have been captured while avoiding problems of nonlinearity and excessive loading.

Requirements in terms of test signal frequency range are determined by the most demanding application of the identified model. Examples of demanding applications include flight control system design, the development of research flight simulations and their application in handling qualities studies at the limit of the envelope. Typical requirements involve upper frequency limits of at least 20 rad/s in order to capture regressing lead-lag and flap models in helicopters such as the BO 105. With lower order models and less demanding applications it is appropriate to use test inputs conditioned to avoid high frequencies which could excite higher order rotor and engine modes.

It is important to note that in the application of any form of test input design process initial estimates must be available for the parameters to be determined by system identification. The design of truly optimal inputs is thus impossible and the process of selecting the most appropriate form of test input is thus an iterative one. An experienced test pilot can provide valuable assistance in the process of searching for the best input for a particular application. It should be noted that since the response following the application of the test input is dominated by the natural modes the run length required for estimation of stability derivatives is generally greater than that needed if only control derivatives are to be estimated. The AH-64, BO 105, and SA-330 flight data used by the Working Group contained three different types of control input waveforms: doublets, 3211's, and frequency sweeps. Each of these types of inputs were used to perform system identification by at least some of the Working Group members. The purpose of this study is to examine, in the frequency domain, the effects of control input design on the identification results. Since all three input types were available in the BO 105 data base, the comparison will make use of this data source.

Figure 5.2.1 shows

- the input autospectrum of each of the three input types,
- the identified roll rate due to lateral stick frequency responses for each of the three types of inputs. Magnitude, phase, and coherence are given.

The input autospectrum indicates the frequency distribution of the input excitation. Broad band excitation, as indicated by a fairly flat input autospectrum, is a goal of input design for system identification. The coherence function may be interpreted as that fraction of the output autospectrum which may be accounted for by linear relation with the input autospectrum (Otne et al., 1978, [5.2.9]) and is therefore a good measure of successful excitation as a function of frequency (Tischler, 1987, [5.2.8]). Factors which may cause the coherence function

to drop below the ideal value of unity are: non-linearities in the system to be identified, process noise, and lack of input power and/or lack of response power (Bendat et al., 1980, [5.2.10]; 1986, [5.2.11]).

Examination of Figure 5.2.1 reveals larger values of coherence over a wider frequency range for the sweep data compared to the other two input types. This is particularly true at very low frequencies (< 1 rad/s) and high frequencies (> 10 rad/s). Comparison of the input autospectrum curves shows that the drops in coherence for the doublet and 3211 inputs correspond in frequency to drops in input power. This lack of input power causes the frequency response curves for the doublet and 3211 inputs to appear less smooth than the sweep results for frequencies between 5 and 7 rad/s and to diverge from the sweep results at low frequency. Generally, larger and less variable coherence, as well as relatively smooth and strong input power over a wide range of frequencies, makes the frequency-sweep results more favourable for use in system identification. The primary drawback of such inputs is their longer duration.

It is interesting and somewhat surprising to note that, despite its larger input power at most frequencies, the 3211 input yields a frequency response with generally lower coherence values than that produced with the doublets. This is particularly true for frequencies less than 1 rad/s and can also be seen at frequencies greater than 10 rad/s.

Comparing the frequency response results in the 2 to 3 rad/s range we see distinct differences in the response characteristics despite high coherence values for all three input types. The resulting dutch-roll mode for the 3211 result appears to be more heavily damped than that for the doublet result but less damped than that for the sweep result. Since the doublet and frequency sweep input autospectra are practically of the same magnitude in this frequency range this result cannot be explained simply as a non-linear dependence on input magnitude, but perhaps there is a dependence on input shape.

What can be said, however, is that a model derived from frequency sweep data and then verified with doublet data will appear to be overdamped. Indeed this was the experience of the AFDD during its identification and verification work with the BO 105 data. This is illustrated in Figure 5.2.2.

Another interesting result of this study is that the identified response characteristics of the flapping modes for the doublet and 3211 type inputs are very similar damping and natural frequencies (approximately 14 rad/s) while the frequency sweep result is slightly less damped and has a natural frequency closer to 15 rad/s. Again, the discrepancy may reflect dependence on the input shape.

Comparison of the frequency-response identification results for different input types shows that significant differences in the identified results may occur when input characteristics are changed. These differences must be kept in mind when conducting identification and verification and when comparing results.

5.2.4 Conduct of Flight Experiments

Calm air is essential for accurate system identification. Gust or turbulence influences usually cause significant problems during the data evaluation. In principle, techniques like the Maximum Likelihood method (incorporating a state estimator like a Kalman filter) are able to account for process and measurement noise, assuming certain statistical characteristics. For fixed wing aircraft, such approaches have demonstrated their utility for the identification of 3 DoF models from flights in turbulent air (Jategaonkar et al., 1987 [5.2.12]). For helicopter models, however, with a higher number of unknowns to be determined, such successes have not yet been obtained. As rotorcraft identification is already complicate in itself, it is advisable to avoid problems due to atmospheric disturbances. But what is considered as 'calm' air? Usually the flight test engineer has to rely on pilot's comments and judgement. So, if possible, the best way to conduct the tests is for the pilot to be asked to find an area with favourable conditions and to apply some test inputs. Then, telemetry data are additionally recorded on the ground to check the data for any turbulence effects.

During the first flight, some time is needed:

1. To familiarize the pilot with the specific tests.
This includes the aircraft trim at the desired flight condition, the generation of the control input signal either manually or by any control input device, and the retrim of the aircraft.
2. To train regarding the shape and timing of the control input signal, if it is generated manually by the pilot.
3. To determine appropriate control input amplitudes.
For the identification usually locally linearized models are applied that are only valid for small perturbation maneuvers. Large response amplitudes violate this assumption and lead to the problem of suitable nonlinear model formulations and their more complicated identification.
4. To check the instrumentation system and to detect and eliminate any measurement errors using (for example) quick-look evaluations and first consistency analyses.

For a reliable system identification it is necessary to apply control inputs that sufficiently excite the aircraft modes of interest. Input signals like doublets, 3211, or sweeps have become standard. There are arguments whether these signals should be generated by the pilot or, if possible, by an electronic device (Tischler et al., 1987, [5.2.13]). When the signal shape is not too complicated, pilot involvement seems to have some advantages. It was shown that after a training phase a pilot can fly such signals with the required accuracy. His expertise and possible suggestions for alternatives (eg. in the sequence of the controls, when more than one is used) are valuable. Pilots also prefer to be actively involved as they have a better control of the test and are more prepared to react to unexpected situations. Tests in more unstable flight conditions or longer lasting tests also often require some additional control inputs to stabilize the aircraft and to keep the amplitudes within the small perturbation range. This can easily be accomplished by a pilot using pulse type control inputs. A SAS would work with a continuous feedback and consequently can cause unwanted high input/output correlations.

A practical way for pilots to generate control inputs might involve the following procedure as exercised in the BO 105 flight tests:

1. the main pilot trims the aircraft in the prescribed flight condition.
2. the copilot generates the input signal for the desired control with hands-off for the other controls. During this phase, the main pilot flies practically hands-off but is prepared to react to any unexpected situation.
3. at the end of the test, the main pilot retracts the aircraft.

Such an approach is helpful in ensuring that, as far as possible, correlation between the control inputs is avoided (except for the stick with some coupling between longitudinal and lateral stick). Although described in terms of a situation involving a pilot and a copilot the procedure can easily be modified for a single pilot.

During the test, the engineer on the ground carefully observes the flight test data provided via telemetry. At the end of each test he has to decide whether the test was a 'good' one or has to be repeated. Criteria are the accuracy of the trim, the quality of the input generation, the excursions from the trim condition, the data run length, disturbances (turbulence) during the test, and others. Although it highly depends on the specific test and the considered aircraft, a useful guideline may be that the run duration should at least be about 25 to 30 seconds when lower frequency modes have to be identified, and that the pitch and roll attitude angles should not exceed about 20 to 25 degrees from trim to stay within small perturbations. After each test, pilot and ground engineer briefly exchange their comments before the next test is defined. In any case, each test should be repeated (if possible twice, but at least once) to provide some data redundancy for the evaluation. Usually, a large part of the total flight test costs occur when the aircraft is still on the ground (instrumentation, calibration, trouble shooting, adverse weather). Savings obtained from reducing flying hours are only small in comparison to the total costs. Therefore, in order to obtain a comprehensive data base, every effort should be made, while in the air, to collect as much usable data as possible.

5.2.5 Procedures Following Flight Experiments

Activities immediately after a flight test can be divided into operational aspects for preparing the next flight and the checking of the measured data.

As with other forms of flight tests, careful de-briefing must be carried out to assess any problems encountered. Here, pilots' more detailed comments about the flight and suggestions for modifications are taken into account in the planning of the following flights. In addition, the aircraft must be prepared for the next tests. This includes a routine safety check, refueling, or any modifications (like additional weights) to meet weight and CG location requirements.

It is extremely important to do as much evaluation as possible with the latest measured data to make sure that they can be used for identification. Often, the data are recorded on-board. Right after the aircraft landing these data must be checked for their suitability and measurement quality. This is not an easy task and it is often neglected or not done carefully enough under the time pressure for the next scheduled flight. In consequence, measurements later turn out to be useless or they require much effort for defining meaningful corrections and reconstructions.

The data quality check should at least include a thorough visual inspection of time history quicklook plots of all data needed for the identification. Data errors like dropouts, saturation, large offsets, non-realistic noise level, or the absence of a signal can easily be seen. If possible, a first data consistency analysis should be used as it helps in finding more 'hidden' errors, like sign inversions, scale factors, and biases. Sources for such errors are mostly in the instrumentation or data processing units and must be eliminated before the next flight test can be conducted. In addition, a detailed data inspection should confirm which data runs seem to be suitable

for the identification. Then, the next flight test program can be defined with new test conditions and, if necessary, repeats of previous runs.

References

- [5.2.1] de Leeuw, J.H.; Hui, K.
The application of linear maximum likelihood estimation of aerodynamic derivatives for the Bell-205 and Bell-206
Vertica, Vol. 13, Number 3, 1989.
- [5.2.2] Beck, J.V.; Arnold, K.J.
Parameter Estimation in Engineering and Science
John Wiley & Sons, Inc., New York, 1977.
- [5.2.3] Marchand, M.; Koehler, R.
Determination of Aircraft Derivatives by Automatic Parameter Adjustment and Frequency Response Methods
AGARD-CP 172, 1974
- [5.2.4] Plaetschke, E.; Schulz, G.
Practical Input Signal Design
AGARD-LS-104, Paper 3, 1979.
- [5.2.5] Leith, D.; Murray Smith, D. J.
Experience with Multi-step Test Inputs for Helicopter Parameter Identification
Vertica, Vol. 13, 1989.
- [5.2.6] Kaleska, J.
Rotorcraft Identification Experience
AGARD-LS-104, Paper 7, 1979
- [5.2.7] Tischler, M. B.; Leung, J. G. M.; Dugan, D. C.
Frequency-Domain Identification of XV-15 Tilt-Rotor Aircraft Dynamics in Hovering Flight
J. American Helicopter Society, Vol. 30, 1985.
- [5.2.8] Tischler, M. B.
Frequency Response Identification of XV-15 Tilt-Rotor Aircraft Dynamics
NASA TM-89428, 1987.
- [5.2.9] Otnes, R. K.; Enochson, L.
Applied Time Series Analysis
John Wiley and Sons, Inc., New York, 1978.
- [5.2.10] Bendat, Julius S.; Piersol, Allan G.
Engineering Applications of Correlation and Spectral Analysis
John Wiley & Sons, Inc., New York, 1980.
- [5.2.11] Bendat, Julius S.; Piersol, Allan G.
Random Data: Analysis and Measurement Procedures
Second Edition. John Wiley & Sons, Inc., New York, 1986.
- [5.2.12] Jategaonkar, R.; Plaetschke, E.
Maximum Likelihood Estimation of Parameters in Linear Systems with Process and Measurement Noise
DFVLR-FB 87-20, 1987
- [5.2.13] Tischler, M. B.; Fletcher, J. W.; Dickmann, V. L.; Williams, R. A.; Cason, R. W.
Demonstration of Frequency-Sweep Testing Technique Using a Bell 214-ST Helicopter
NASA TM-89422, 1987

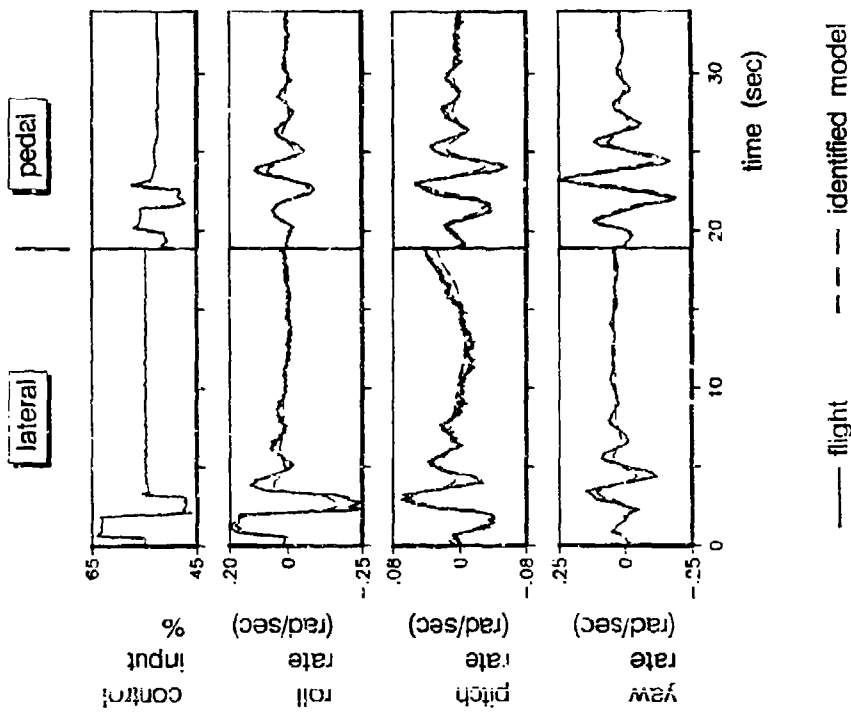


Figure 5.2.2. Verification of identified model obtained from frequency sweep data signals

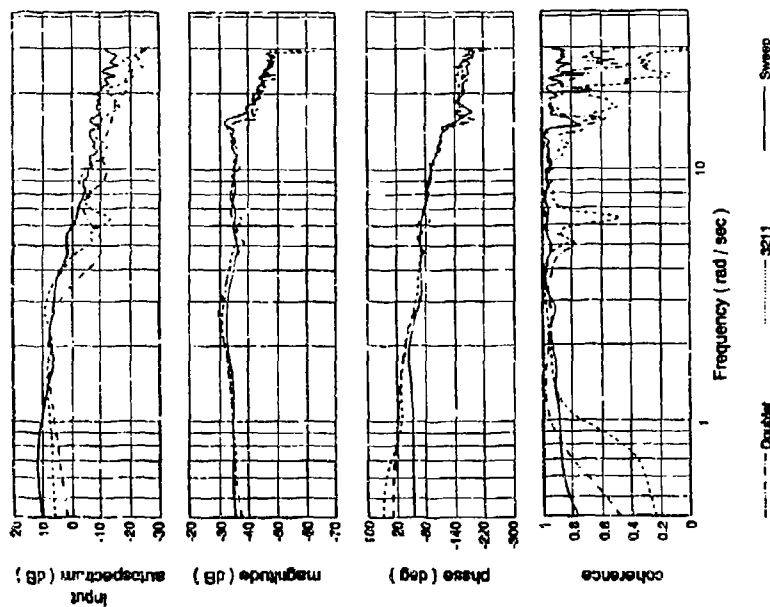


Figure 5.2.1. Comparison of autospectrum and roll rate due to lateral stick frequency responses from three control input signals

5.3 Instrumentation and Data Processing⁹⁾

5.3.1 Introduction

Independent from the actually applied method, the general system identification approach is always based on the same principle: the measured inputs and outputs of a system are used to extract the unknown system characteristics. There are many differences in the complexity of identification techniques and their requirements: 'parametric' methods need an a priori knowledge of the model structure and often parameter starting values, whereas 'nonparametric' methods (e.g. spectra analysis) work without model structure. But all methods rely on the information provided by the amplitude and phase relationship between

- the measured control inputs and
- the measured system response.

Consequently, errors in the measurements must also cause errors in the identification and it is evident that an appropriate instrumentation is necessary. Although methods to detect errors and to correct or even completely reconstruct unreliable measurements have been developed and are successfully applied, they cannot avoid that information is lost that could have been provided by accurately measured data.

In the following it is concentrated on the system identification carried out in the Working Group. The required measurements are briefly summarized, some typical problem areas and sensor characteristics are discussed in more detail, and the main data processing steps are addressed.

5.3.2 Required Measurements

In the Working Group it was decided to concentrate on the identification of a linear rigid body helicopter model with six degrees of freedom. It is given by a system of eight coupled first order differential equations:

$$\dot{\mathbf{x}} = \mathbf{Ax} + \mathbf{Bu} \quad (5.3.1)$$

with the state vector

$$\mathbf{x}^T = (u, v, w, p, q, r, \Phi, \Theta), \quad (5.3.2)$$

and the control vector

$$\mathbf{u}^T = (\delta_{ion}, \delta_{lat}, \delta_{col}, \delta_{peu}). \quad (5.3.3)$$

The measurement (or observation) vector \mathbf{y} defines the measured variables to be compared to the calculated model response. Or from an identification point of view: the parameters of the model will be modified to obtain the best possible agreement between the model response and the measurement vector. The measurement vector is

$$\mathbf{y} = \mathbf{Cx} + \mathbf{Du} \quad (5.3.4)$$

The variables to be included in the measurement vector can to a certain extent be chosen by the analyst. In general, the measured state variables are used or equivalent data like dynamic pressure, angle of attack, and sideslip angle instead of the speed components. In addition (or eventually in replacement) however, measurements like linear and rotational accelerations, or helicopter position data, etc. can also be included. There are close relationships between instrumentation, observed variables, and parameter identification:

1. In any case, the measurement vector and the helicopter instrumentation are directly dependent from each other. Usually, the instrumentation is given and the observed variables can only be selected from the available measurements. The request for additional measurements often leads to an extension of the instrumentation.
2. The selection of the considered measurements can have a significant effect on the identified parameters and the model validity. When only measurements dominated by the low frequency helicopter characteristics are chosen, like speed components and attitude angles, the model will give a good representation of the lower frequency range but it can be less accurate for higher frequencies. The opposite result will be obtained by the use of mainly higher frequency data like accelerations and rates. Although it depends on

⁹⁾ Principal Author: J. Kaletka, DLR

the intended application of the model, it is in general advisable to use both data groups in the observation equations.

For the six degrees of freedom models like they were used in the Working Group, a 'standard' set of suitable variables to be measured can be recommended:

1. controls
2. airspeed data
 - speed components in longitudinal, lateral, and normal direction (u , v , w),
or
 - airspeed, angle of attack, and angle of sideslip (V , α , β).
3. angular information,
 - rates (\dot{p} , \dot{q} , \dot{r}),
and
 - roll and pitch attitude (Φ , Θ).
4. acceleration information
 - linear accelerations (a_x , a_y , a_z),
and optionally
 - rotational accelerations (\dot{p} , \dot{q} , \dot{r}).

The measurement of helicopter rotational accelerations is difficult and often not available. Therefore, differentiation of the measured rates is probably more appropriate.

Usually, helicopter instrumentation systems can easily provide these measurements (see documentation in the chapter 4 on *AGARD Working Group Data Base*). There is no specific preference for an instrumentation concept, like inertial system packages or individual sensors. In any case it is absolutely necessary to know the sensor characteristics and, probably even more important, the data processing like filtering and sampling rates, that is done along the data flow from the sensor to the data recording. For commercially available instrumentation packages it is often difficult to obtain more detailed information. From this point of view some advantages are seen in the use of individually installed sensors. They can also provide more redundancies in the measurements which can be used for data quality investigations.

A high measurement accuracy is the dominant requirement for system identification. The transducers used for the measurements of control positions, linear accelerations, rates, and attitudes are usually potentiometers or synchros, linear accelerometers, and gyros. The today available sensors generally provide high accuracies and are appropriate for identification purposes. However, when transducers are selected and installed, emphasis should be placed on two aspects:

- the measuring range has to be chosen to, on one hand, provide a high signal resolution and accuracy and, on the other hand, avoid signal saturation for the planned flight test experiments.
- cross axis sensitivities can generate significant problems and must be kept as small as possible. They can be caused by both, sensor characteristics and installation misalignments.

In contrast to the measurements of accelerations, rates, attitude angles, and control positions, it is problematic to obtain reliable airspeed data. This subject will be discussed in more detail in the following section on *problem areas* (section 5.3.4).

5.3.3 On-board Data Processing

Extensive on-board data processing is needed for all processes that are based on the immediate availability of measurements. Such on-line data processing is for example a prerequisite for control systems, ranging from mode stabilization up to in-flight simulation. As rotorcraft system identification still is an off-line procedure, no specific on-board data processing is required except for the standard signal conditioning steps converting sensor signals to the appropriate format for data recording. They include all modifying operations applied to signals like the adaption of transducer outputs to the input requirements of the data handling system (e.g. synchro to analogue conversion), signal amplification, filtering, multiplexing, digitization, and data recording (often on board of the aircraft to avoid disturbances from the telemetry). The data conditioning is certainly necessary and helps to maintain the data quality. However, some of the procedures can significantly modify the original sensor output data.

For system identification, care must be taken with analogue (anti-aliasing) filters, causing phase shifts, and with data sampling where data are scanned sequentially with time delays between the individual channels. These effects can be corrected during the further data processing. However, it is evident, that the analyst must know exactly what has 'happened' to the data. Only then, appropriate corrections can be made. In practise, here is quite often the main gap: the instrumentation engineers are not informed of the data requirements for a specific evaluation and the analysts are not aware of the data conditioning steps that can already have deteriorated the data for their applications. Therefore, a close cooperation and a detailed information exchange between these two groups is absolute necessary. It can be more important than increasing a sensor accuracy by another tenth of a percent in order to generate more reliable data.

5.3.4 Problem Areas

Some of the typical problem areas in helicopter flight data measurement were also seen in the data provided to the Working Group. They are mainly due to helicopter and sensor characteristics but also can occur during the signal conditioning. Some examples are illustrated in more detail:

1. Airspeed measurement

The conventional sources for air data measurement are vanes and pressure probes. They were originally developed for fixed wing aircraft and are also used for helicopters. Rotorcraft, however pose special problems in accurate sensing of air data: The sensors have to be installed on a relatively long boom to keep them away from main rotor wakes. The boom must be quite stiff to avoid oscillations excited by the helicopter vibration. With decreasing speed, pressure measurements become more and more inaccurate and near hover both, pressure tubes and vanes cannot be used at all. Although these deficiencies are obvious and well known, only a few air data systems are available that were designed to also operate in the low speed regime of helicopters.

The AH-64 and the SA-330 use a boom to provide air data. For the flight conditions considered in the Working Group (120 kn for the AH-64 and 80 kn for the SA-330) the systems gave good measurements. (The AH-64 is additionally equipped with a low range airspeed system. These data however were not provided to the Working Group).

The BO 105 uses a helicopter air data system. It consists of a swivelling pitot static probe installed at the fuselage close to the rotor. For low speed it is designed to work within the rotor downwash. Measurements are dynamic pressure and probe angle of attack and sideslip. For the flight condition considered in the Working Group (80 kn) the sensor is out of the rotor downwash and aligns with the total flow. The measurements however show that rotor wake interferences cannot be avoided in dynamic flight manoeuvres. Figure 5.3.1 shows the helicopter response due to a longitudinal stick doublet input. In the speed data, and particularly in the lateral speed, significant disturbances are seen. They are caused by rotor wakes that 'hit' the sensor when the helicopter pitches nose-down. Then, the sensor rotates to the left and indicates a high sideslip angle and consequently a high sideward speed. In the signals this effect is seen like a data drop-out. It can last for even a few seconds until the sensor is in undisturbed flow again.

2. Measurement of linear accelerations and rates

In general, all measurements of the helicopter motion are influenced by a high vibration level. This is particularly true for the linear accelerations and the rates. For BO 105 data obtained from a longitudinal stick control input Figure 5.3.2 first presents the actually measured unfiltered data. Then, on the same scale, it shows the data after being filtered by a digital low-pass filter with a cut-off frequency of 12.5 Hz. From the comparison it can be seen

- the high frequency noise (mainly blade harmonics) can easily be removed by low-pass filters. As system identification results are very sensitive to phase errors, zero-phase shift digital filters should be used.
- for the linear accelerations (and in particular the forward and sideward accelerations) there is a very low signal-to-noise ratio. In this test, the helicopter forward and sideward accelerations are less than 0.5 m/s^2 . (In general, helicopters cannot produce large linear accelerations, except for the vertical axis). The vibration level on the data is more than 5 m/s^2 and reaches even higher values in other flight conditions (flare and hover). Consequently, the measuring range of the accelerometers is practically defined by the vibration levels. Therefore, the BO 105 was equipped with sensors of a $\pm 12 \text{ m/s}^2$ range for a_x and a_y . Although the 'useful' part of the signal is less than 5 % of the total sensor range a high accuracy is required for system identification.

Fortunately, linear accelerometers belong to the best sensors in an aircraft instrumentation. They have a high linearity and resolution with only small hysteresis and work in a wide bandwidth without significant phase errors. Nevertheless, the sensor range should carefully be selected to avoid saturation and still to provide a high signal resolution.

Helicopter responses due to control inputs are primarily rates (not linear accelerations). Therefore, the 'useful' signal in the rate measurements is still dominant although it is also highly deteriorated by the helicopter vibration. Together with linear accelerometers, rate gyros have reached a high quality and, for the identification, rates certainly belong to the most accurate and important measurements.

3. Measurement of rotational accelerations

Rotational accelerations were only measured in the AH-64. For the identification they are useful as they provide more high frequency information for the determination of the moment equations. Figure 5.3.3 first shows the measured roll and pitch accelerations due to a longitudinal control input. The high vibration level is obvious. Then, the filtered data (digital filter, 12.5 Hz cut-off frequency) are plotted together with data that were obtained by differentiating the measured rates. The agreement is very good and proves a high consistency although the measurements still show a higher noise level. It cannot yet finally be answered how helpful measured rotational accelerations can be for the identification in comparison to differentiated signals obtained from accurately measured rates.

4. Measurement of the control inputs

The influence of data errors on the identification results also depends on the applied identification technique. Least Squares equation error methods assume that all variables are accurate whereas more complex output error techniques allow measurement errors on the response variables. All techniques, however, fully rely on accurately measured control inputs and, at best, can compensate for noise on the measurements. Although it is relatively easy to measure the control positions, there are two main error sources: signal resolution and sensor position.

The control inputs for system identification purposes are usually small to allow a linearised model formulation, whereas the sensors, e.g. potentiometers, normally measure the full range of the controls. For the identification data, it must be made sure that the range of interest is sufficiently resolved.

Control positions are often measured at the pilot controls. When they are used in the identification the characteristics of the (mechanical) linkage and of the hydraulic system have often to be neglected. Attempts to model and identify effects like backlash, flexibility, hydraulic characteristics lead to highly non-linear models and significantly complicate the identification. Therefore, it should be tried to measure the control inputs as close to the rotor as possible. In any case, the measurement must be related to the control input at the blades. When feedback systems are engaged, the sum of both, the pilot inputs and the control system activity, must be measured unless both inputs are provided separately.

For the AH-64, measurements of the hydraulic actuator positions at the main rotor (or tail rotor) swashplate were given. These locations have the advantage of being close to the rotor but still in the non-rotating system.

For the BO 105, stick deflections, collective lever, and pedal positions were used. Control linkage effects were assumed to be negligible and the hydraulic system was supposed to be represented by a time delay or time constant on the control measurements. Specific measurements have shown that these assumptions can be justified.

The SA-330 data base gave control positions obtained from three different locations. However, except from pilot controls (similar to the BO 105) the other data were obtained in the rotating system at only one control rod and one blade root. A transformation into the fixed axis system was not given. For dynamic tests, it also seems to be necessary to include at least three blade control angles to derive three controls in the non-rotating system. Therefore, the inputs measured at the pilot position were used for the identification.

5. Signal filtering

As some measurements of the helicopter motion are very noisy, low-pass filtering is usually applied before the data are used for system identification. It must be taken into account that analogue filters not only reduce the high frequency amplitudes but also influence the phase characteristics of the measured signal. In particular with higher order filters, the phase shifts can already be significant at frequencies far below

the filter cut-off frequency. Considering that the identification is based on the amplitude and phase relationship between the individual measurements it is quite obvious that filters can strongly deteriorate identification results and even render them unusable. Therefore, it is absolutely necessary that all measurements are passed through identical filters. This requirement is often neglected as it is not so important for most data evaluation other than system identification. Only when zero-phase shift filters with a constant gain of 1.0 in the frequency range of interest are applied, it is possible to filter selected measurements. Here, digital off-line filters are applied.

When sensors with integrated (analogue) filters or sensor packages (e.g. inertial systems) are used, it is essential to know the built-in signal processing. As an example Figure 5.3.4 compares linear acceleration measurements obtained from an 'agility' sensor package and from individual accelerometers. The package signals do not follow the more dynamic manoeuvre part in the data when the control input is given. A closer view also showed that there is a phase lag between the accelerometer and the package data. It indicates that some strong damping or filtering was done in the agility package although the data are still very noisy.

For the identification it was decided to use the individually measured linear accelerations.

6. Signal resolution

For system identification usually only small amplitude control inputs are applied to keep the helicopter response so small that linear models can be used. When the amplification or scaling of the data is based on the maximum helicopter response capability, the small amplitudes can probably not be resolved satisfactorily by the data recording system. For the pitch and roll attitude response due to lateral and collective control inputs Figure 5.3.5 demonstrates that the digitization of the vertical gyro signal could only resolve about 0.3 degrees per bit. As the tests with controls other than collective (e.g. the shown lateral control input) produced attitude angles between 20° and 30° the resolution errors probably do not affect the identification results significantly. However, such problems can usually be avoided when signal amplification is based on the expected maximum amplitudes of the specific tests.

7. Control input generation

It is widely agreed that for system identification specific control inputs should be used to properly excite the aircraft modes. Some of the designed input signals are quite complex so that they cannot be generated by the pilot but require electronic devices. Only the AH-64 was equipped with a specially designed Gold Oscillator Box (GOB) unit. It commanded sinusoidal frequency sweeps in two ranges from 0.1 Hz to 3 Hz and 0.3 Hz to 13 Hz. For the BO 105 and the SA-330 only pilot generated inputs were used. (In the BO 105 a relatively simple display was installed. It showed the prescribed signal and the actual control position.) The input signals used in the Working Group, doublet, multistep, and frequency sweep could be generated by the pilot without any real difficulties. It proved that system identification does not require an electronic control input device when rigid body models have to be identified. It is only needed when frequencies exceeding the human capability (more than 2 Hz to 5 Hz) are required.

5.3.5 Off-line Data Processing

The off-line data processing for system identification purposes mainly includes:

- conversion to a consistent unit system,
- detection and removal of data drop outs,
- low-pass filtering,
- corrections for the centre of gravity, and
- the calculation of additional variables.

These procedures are standard for flight testing and therefore this section will briefly document the off-line data processing conducted within the Working Group and, for completeness, give the applied equations.

A more detailed data analysis for detecting and correcting data deficiencies is considered as a first essential task in data evaluation and system identification. It will be described in the chapter 5.4 on *Data evaluation and reconstruction*.

1. Unit system

The measurements needed for system identification were converted to the International Unit System (SI) based on meter, second, kilogram and radian. Control displacements were given in percent with 100 percent as full travel.

2. Data drop outs

When data drop outs are restricted to only a few samples it can be justified to eliminate these samples and reconstruct a new value by interpolation between the neighbouring data. Of course, this technique cannot reproduce the lost data. However, it gives a more realistic value for the sample instead of keeping the drop out data. It is also the only possibility to avoid even more data distortion which occurs when the uncorrected measurement is filtered. For the data in the Working Group only minor work had to be done to eliminate drop-outs.

3. Digital low-pass filtering

Problems associated with analogue filtering have already been addressed. Analogue filters significantly influence the phase where this effect increases with higher filter order. As identification results are very sensitive to phase errors it should be tried to reduce analogue filtering as much as possible. Here, high sampling rates make it possible to use anti-aliasing filters with a high cut-off frequency. When, in addition, these filters have almost identical characteristics their influence in the frequency range of interest is small and similar. Then, zero-phase shift digital filtering can be applied to

- eliminate the unwanted higher frequency effects and noise, and
- to reduce the sampling rate.

This approach was consequently used for the measurement of the BO 105 data, where almost all analogue filters were removed. Comparisons of the obtained data to previous flight test measurements with strong analogue low-pass filtering clearly showed the data quality improvements.

The efficiency of digital filters has already been shown in Figure 5.3.2.

4. Calculation of speed components at the sensor position

Using the measured airspeed, angle of attack and angle of sideslip (V , α , β) the longitudinal, lateral, and normal speed components at the sensor position (boom) were calculated by

$$\begin{aligned} u_b &= V \cdot \cos \alpha \cdot \cos \beta \\ v_b &= V \cdot \sin \beta \\ w_b &= V \cdot \sin \alpha \cdot \cos \beta \end{aligned} \quad (5.3.5)$$

5. Correction for CG Position

In contrast to data obtained from rate and attitude gyros, the measurements of linear accelerations and aerodynamic data are influenced by the distance between the sensor position and the helicopter centre of gravity (CG). Ideally, these sensors should be installed at the CG. Linear accelerometer locations can at least be close to the CG. Air data sensors, however, are usually installed far in front of the aircraft. During dynamic flight tests the measured signals also contain acceleration or speed components due to the helicopter angular motion. Mathematical models as used for system identification always describe the forces and moments with respect to the CG. There are two different approaches to handle the influence of the CG location on the measurements:

- the measurements are corrected for CG position, or
- in the measurement equations the model response is transformed to the individual sensor location.

In the Working Group the first approach was chosen.

With the sensor locations in

x-direction (positive forward):	x_m
y-direction (positive to the right):	y_m
z-direction (positive downward):	z_m

the speed components at the CG (u_{cg} , v_{cg} , w_{cg}) are obtained as

$$\begin{aligned} u_{cg} &= u_b - z_m \cdot q + y_m \cdot r \\ v_{cg} &= v_b - x_m \cdot r + z_m \cdot p \\ w_{cg} &= w_b - y_m \cdot p + x_m \cdot q \end{aligned} \quad (5.3.6)$$

For the corrections of the linear acceleration measurements the rotational accelerations (\dot{p} , \dot{q} , \dot{r}) are needed. When no measurements are available, differentiated rates are used. Then, the linear accelerations at the CG (a_{xcg} , a_{ycg} , a_{zcg}) are:

$$\begin{aligned} a_{xcg} &= a_x - z_m \dot{q} + y_m \dot{r} - (y_m \dot{p} - x_m \dot{q}) q + (x_m \dot{r} - z_m \dot{p}) r \\ a_{ycg} &= a_y - x_m \dot{r} + z_m \dot{p} - (z_m \dot{q} - y_m \dot{r}) r + (y_m \dot{p} - x_m \dot{q}) p \\ a_{zcg} &= a_z - y_m \dot{p} + x_m \dot{q} - (x_m \dot{r} - z_m \dot{p}) p + (z_m \dot{q} - y_m \dot{r}) q \end{aligned} \quad (5.3.7)$$

For the helicopters studied by the Working Group, the linear accelerometers were located close to the CG. The AH-64, however, was equipped with a second accelerometer package installed at the pilot seat position with a distance of about 1.50 meters from the CG. To demonstrate the influence of the (still relatively small) off-CG location, Figure 5.3.6 shows for a tail rotor input

- the uncorrected and the CG corrected longitudinal accelerations obtained from the pilot seat sensor,
- the uncorrected and the CG corrected lateral accelerations obtained from the pilot seat sensor,
- the CG corrected lateral acceleration obtained from the pilot seat sensor and the lateral acceleration obtained from the CG accelerometer package.

Considering that the helicopter response to a pedal input is primarily a yaw motion, it makes sense that the longitudinal acceleration is not much influenced by the CG distance. The lateral acceleration however clearly shows differences. The improvement obtained from the signal correction becomes evident in the last part of the figure where the signals obtained from the different sensors are in good agreement.

5.3.6 Summary

As far as the availability of measurements is concerned it is seen that the instrumentation systems of the three helicopters provide more signals than usually needed for system identification. The flight tests have also shown that no specific instrumentation, like electronic control input boxes, is required. To generate reliable and useful data seems to be more a task of properly defined measurement ranges, careful data processing, and of course the flight testing itself. In conclusion some main guidelines can be given:

- Control inputs can be generated by the pilot. Some training and if possible a display type device are helpful. Electronically generated inputs with a direct link to the control are not necessary unless high frequencies are needed,
- If possible, the sensors should have a measuring range that is suitable for the expected signal amplitudes,
- If analogue filtering of signals is applied it is important that all signals used for the identification are filtered and the filters have identical characteristics,
- The signal digitization range should be defined by the maximum signal amplitudes in the tests to obtain a good signal resolution,
- Standard data processing steps, like removal of drop outs, digital-low pass filtering, CG correction, etc., are applicable and adequate.

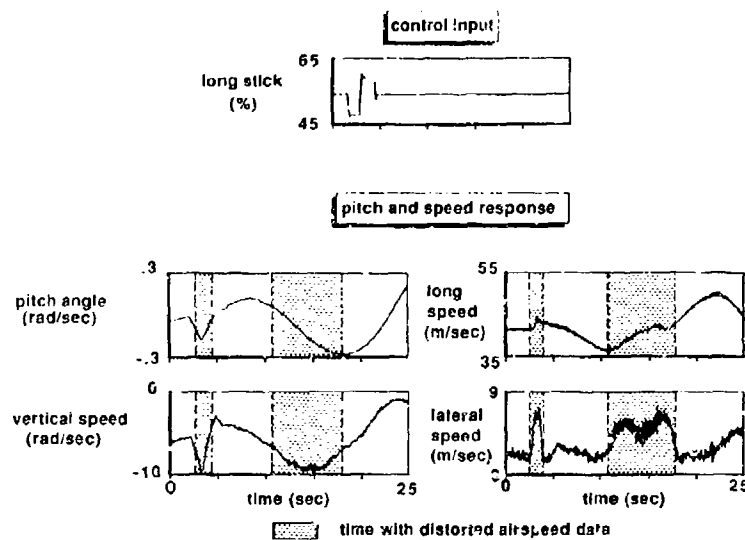


Figure 5.3.1. BO 105 distortions in airspeed measurement

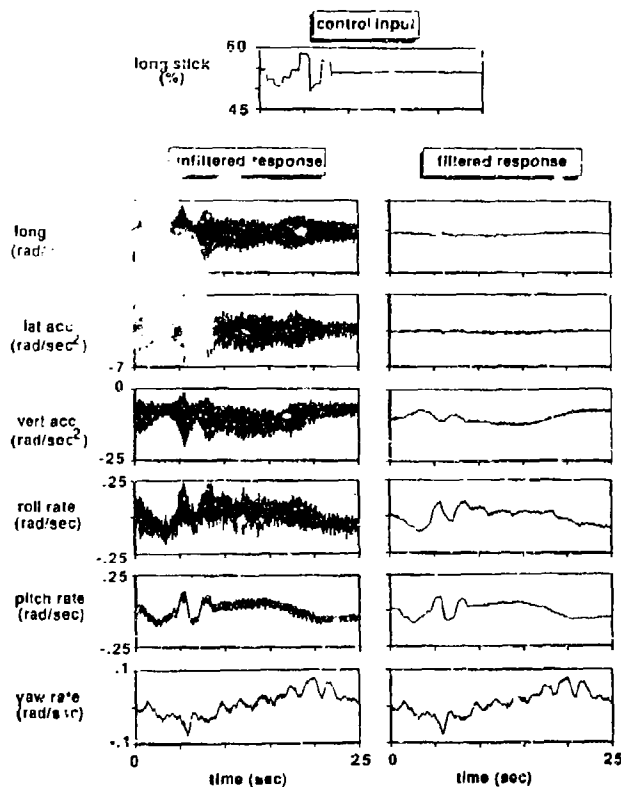


Figure 5.3.2. BO 105 data: comparison of unfiltered and filtered linear accelerations and rates

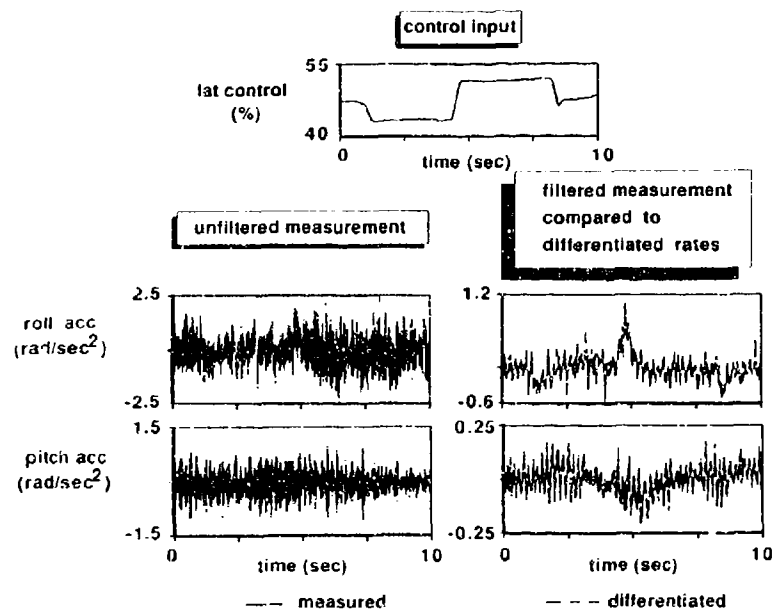


Figure 5.3.3. Measured AH-64 unfiltered and filtered rotational accelerations and comparison with differentiated rates

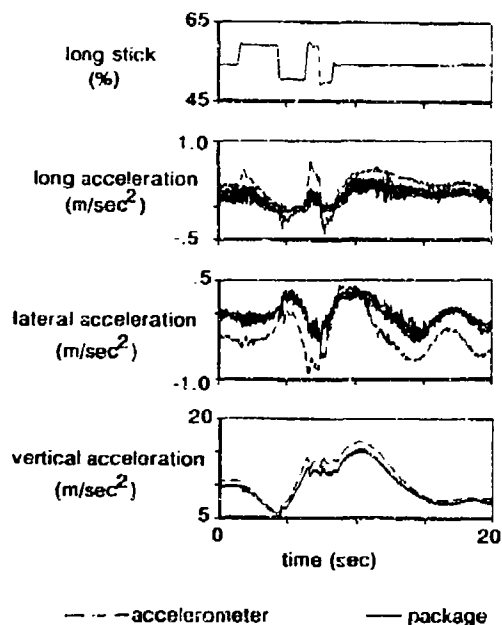


Figure 5.3.4. Comparison of linear acceleration measurements obtained from an 'agility' package and individual accelerometers (SA-330)

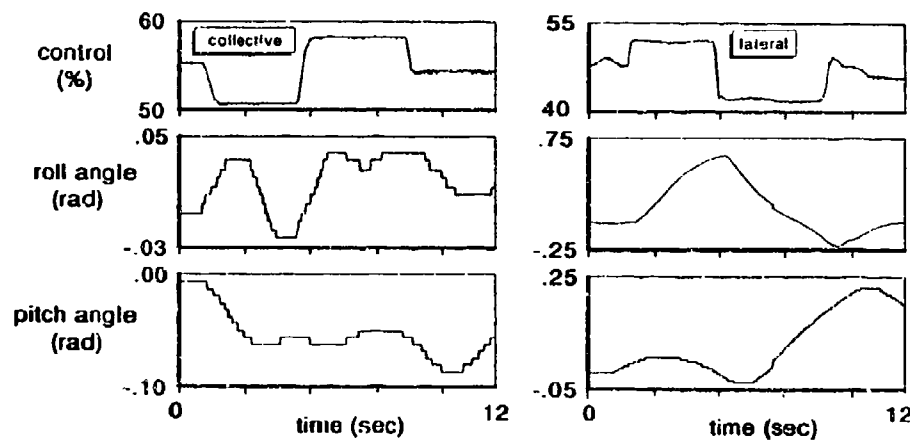


Figure 5.3.5. Resolution of the pitch and roll attitude measurements (AH-64)

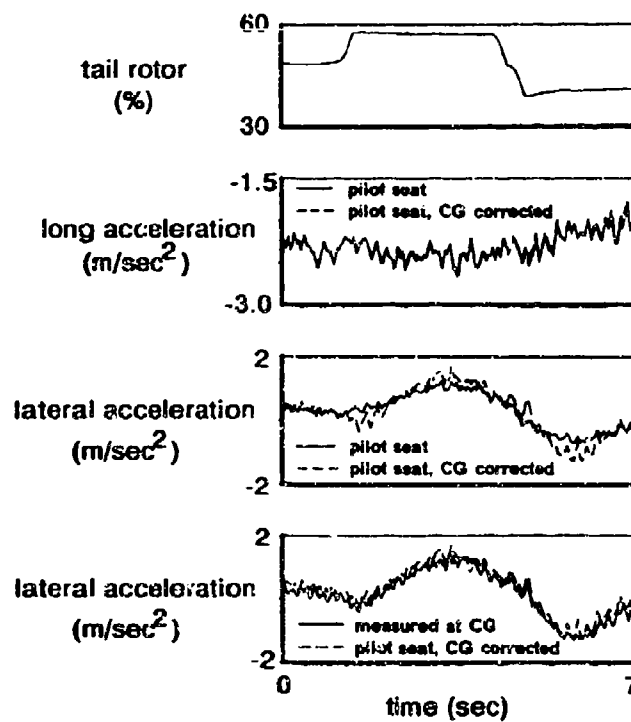


Figure 5.3.6. CG correction of linear accelerometer measurements (AH-64)

5.4 Data Evaluation and Reconstruction¹⁰⁾

5.4.1 Introduction

The quality of the measurement data determines the quality of the parameter identification results. Therefore it is of the utmost importance to ensure the data quality before any attempt at identification is made. In principle the best time to perform data quality checks is in dedicated tests before or during the actual flight tests: in the instrumentation laboratory, on the flight line and during instrumentation check-out flights. Accurate determination of each individual error effect can also be done best in a dedicated test. These tests are ideally performed with a computer in the aircraft to reduce the loss of time and the cost of flight tests with inaccurate measurements.

The evaluation of the data quality from existing flight test data, as was the case for the Working Group, is generally much more difficult. But it is still very important to do this evaluation for the following reasons:

1. A particular measurement channel may deteriorate or fail during the course of a flight test program.
2. A specific error effect may only be present during actual flight tests, such as static pressure distortions in dynamic flight conditions. These effects can only be determined from the flight tests.

For the members of the Working Group there were two extra reasons to spend a considerable amount of time on the data quality. The first reason is that the data recordings were made by another institute. Within one institute, one is familiar with the verification procedures in use by the instrumentation department and one knows how far they can be relied on and when caution is needed.

A more important reason is the fact that the evaluation of the data quality also gives a good feel for the data content. It gives a first indication of the actual accuracy of the measurements and it can clear up misunderstandings in the definition of measured variables (e.g. sign conventions).

Apart from complete failure, which is often (but not always) easy to spot there are a number of errors that can occur:

1. Sensing: the transducer may not sense the desired quantity directly, for example a static pressure may be distorted by the flow around the aircraft.
2. Transducer: change in bias, sensitivity, range. Change in sensitive axis (misalignment), hysteresis, output noise, spikes.
3. Data acquisition system: changes in offset, gain and range in the analog components, such as amplifiers, pre-sample filters and AD converters. Change in filter characteristics of the pre-sample filters. Bit errors in the recording chain (dropouts). Time shifts and other phase errors.

Because of the large number of possible error sources, an intimate knowledge with the characteristics of the instrumentation system is absolutely necessary for successful correction of data errors.

5.4.2 Techniques

5.4.2.1 Data inspection

Visual inspection of dataplots is an important first step in the evaluation of data quality. The measurements can be scrutinized for obvious errors such as wrong signs, excessive measurement noise, data dropouts, spikes and missing (or even switched) data channels.

In addition, frequency domain techniques can be very useful for data quality evaluation. Examples are:

1. Time shift of a signal can be determined by examining the slope of the phase response with respect to a reference. This method is very sensitive, but it is most useful in ground checks, because it may be difficult to find a suitable reference measurement in flight. Time domain modelling can also be used to determine time shift.

¹⁰⁾ Principal Author: J. H. Breeman, NLR

2. Initial checks of compatibility between variables may be quickly performed in the frequency domain. For instance it can be verified that q/θ has a $1/\omega$ frequency response characteristic. Sign errors are also easily detected by inspecting the phase response.
3. The coherence function can be used to ensure that both input and output signals have low noise contents and are well correlated with each other.
4. Noise spectrum can give an indication of the correct functioning of a transducer (channel). Excessive noise (perhaps in part of the frequency spectrum) can give an indication of malfunction in sensing, transducer or data acquisition. For example discrete frequencies in a gyroscope signal could indicate a bearing failure, noise spikes could be a vibration problem or a faulty wiring or connectors.

The noise analysis also gives vital information for the design of data processing filters, which remove the measurement noise and allow the sampling rate to be reduced.

This may also be a good place to warn for the effect of pre-sample filtering. If a failing transducer has high-frequency noise or sudden steps in its output, the pre-sample filters will transform the signals in smooth signals, thus masking the problem. In normal operation pre-sample filters are essential to prevent aliasing errors, but it may be a good idea to record the unfiltered signals as an instrumentation test. Another important point is the negative effect of phase errors in the analogue filters on the parameter identification. Some authors even recommend dispensing with anti-aliasing filters altogether.

If the recording techniques permit it, it is therefore recommended to use the highest possible sampling rates (and pre-sample filter bandwidths) and to reduce the sample rate in the analysis by digital filtering in the ground processing. This has the added advantage of allowing a more considered choice of sampling rate in the data analysis.

5.4.2.2 Compatibility checking

5.4.2.2.1 Introduction

Any redundancy in the measured variables can be exploited to verify the data quality. There are a large number of techniques in use for the purpose of data quality evaluation. In fact everyone has his own private tricks.

The measurement of a single variable by two different transducers is a simple example:

1. If the transducers are of the same type, the outputs of the two measurement channels can be compared to find discrepancies in sensing, transducer or data acquisition.
2. If the two transducers are of a different type, the characteristic errors will be different. This difference can be used to determine if one of the signals is wrong.
3. Even if one transducer is much better than the other, a comparison is still very useful, if only to show that the "better" transducer has failed completely.

In practice it is rare that two redundant transducers are used, but it is not uncommon to have a standard aircraft instrument as well as a flight test instrumentation sensor. In this case it is strongly recommended to record the aircraft instrument output as well. The disadvantage is not so much the extra data channel to be wired in the aircraft, but rather the extra effort needed to calibrate and evaluate the aircraft instrument, which is necessary to allow its use for data quality checks.

Redundant information can also be used in a complementary filter approach, e.g. rate gyro data is used for the low frequency range and angular accelerometer data is used for the higher frequency range (this is just a special case of the state estimation techniques described below). It is very important that undesirable error characteristics, such as hysteresis, nonlinearities or spurious responses, do not destroy the quality of the result. In the example given, rate accelerometers tend to have these undesirable error characteristics.

5.4.2.2.2 Kinematic compatibility checking

A special case of compatibility checking is Kinematic Compatibility checking. Here the kinematic relationships that exist between the different measured variables are used. The procedure can be applied in many forms: from the simple comparison between two signals to the complete 6 DoF flight path reconstruction. The procedure is also called Kinematic Consistency Checking or Flight Path Reconstruction. The chosen name reflects whether the procedure is seen as an independent check or as an integral part of the processing. Descriptions can be found in (Gerlach, 1970, [5.4.1]) and (Wingrove, 1972, [5.4.2]). Klein et al. (1977, [5.4.3]) seem to have introduced the term *compatibility checking*.

Table 5.4.1 shows the 6 DoF kinematic equations. Linearizing these equations leads to the basic error model as shown in Figure 5.4.1. The errors in the velocity components u , v , w , the attitude angles Φ , Θ , Ψ and the position in earth axes are the components of the state. The errors in the inertial measurements a_x , a_y , a_z , p , q , r are treated as inputs to the state equation. In addition, the wind speed components u_w , v_w , and w_w are included as inputs to the model. The idea is that the errors in the input signals drive the errors in the state.

In principle any measurement which depends on the state vector can appear in the observation equation, for example air speed or doppler velocity, pressure or radio altitude, angle of attack or angle of sideslip, latitude and longitude from Inertial Navigation Systems, VOR/DME or the Global Positioning System. The error in the measurements, whether in the input or in the observation vector, can be modelled as bias, scale factor, time shift and white, gaussian random noise. If the random noise is not white and gaussian it may be necessary to extend the state with a model of the noise characteristics.

With modern inertial sensors the measurement errors are very small. As a consequence the variations in the wind components during a recording become the dominant error source. This makes it possible as well as desirable to estimate these wind variations. The estimation of the absolute wind components requires the presence of absolute position or velocity references of reasonable accuracy, e.g. from an Inertial Navigation System, Global Positioning System or radio beacons. However, it should be noted that in general only the variations in the wind speed components are of interest for flight mechanics, because constant wind components only affect the error in the absolute velocities in earth-fixed coordinates. This means that absolute position references are not strictly required, although they can be of great use.

One simple way of modelling the wind variations that works very well in practice describes the wind variation as a linear trend in time and/or as proportional to altitude. A more sophisticated description is a colored gaussian noise model, e.g. integrators driven by white noise.

An interesting variation in the problem formulation is presented in a block diagram form in Figure 5.4.2. Here, the position in earth axes x_g , y_g , and z_g , the Euler angles Φ , Θ and Ψ and (optionally) the wind velocities in earth coordinates u_{wg} , v_{wg} , and w_{wg} at the right hand of the figure can be treated as measurements or estimates or both.

The estimation of wind components is an example of the use of estimation procedures to reconstruct an unmeasured state component. Another practical example is the estimation of the angle of attack in the case that no direct measurement is available or the direct measurement is unusable. See section 5.4.3 for further discussion on how the reconstructed state should be used.

It is in general not possible to identify this large number of error components. If too many error components are included the standard deviations of the estimates and the correlation coefficients increase rapidly. The degree of correlation is also dependent on the type of and shape of the manoeuvre, so it is feasible to perform specially designed manoeuvres for the purpose of identifying the error components, but these manoeuvres will not necessarily be optimal for parameter identification. It may be more fruitful to combine several different manoeuvres in a multi-manoeuve analysis and then estimate an error model which is valid for all the recordings (see section 5.4.3).

A simple example is the comparison of a rate gyroscope and an attitude gyroscope. The rate signal is integrated and compared with the attitude signal. Error models for each of the two types of gyroscopes can be defined, e.g. bias and time shift for the rate gyroscope and linear drift and time shift for the attitude gyroscope. The difference signal can then be attributed to various errors sources and the parameters of the error model can be estimated using parameter identification.

Even this simple example already points out a common problem, e.g. the bias of the rate gyroscope has exactly the same effect as the linear drift of the attitude gyroscope and the same is true for the time shifts. This means that the errors in the different measurements must have different characteristics in order to be useful for compatibility checking. If it could be assumed that the attitude gyroscope has negligible drift and the rate gyroscope has a negligible (or perhaps known) time shift, then rate gyro bias and the time shift of the attitude gyro can be put in the error model and values for these parameters can be found. But in general these assumptions are difficult to make and need the advice of the instrumentation department.

The bias in the rate gyro will always have the same effect, a linear increase of the error with time. But a scale factor error, e.g. in the attitude measurement, will only be noticeable if larger excursions are present. Even in the case of large excursions, the estimate of bias and scale factor may be highly correlated, e.g. when the attitude angle also increases linearly with time. This demonstrates the dependence of identifiability on the manoeuvre shape.

In the more complicated cases all these problems are also present at the same time and are even more difficult to detect. For example, in manoeuvres that do not deviate too much from level flight the following simplified equation is valid:

$$\dot{w} = qu + a_z$$

This shows that the effect of a bias in the normal acceleration a_z is equivalent to the effect of a bias in the pitch rate signal q . In the estimation procedure this will show up as a high correlation between the estimates of the two error parameters.

5.4.2.2.3 Solution techniques

The formulated problem can be solved by a number of different methods. For more detailed descriptions see (Maine et al., 1985, [5.4.4]) or (Moulder et al., 1979, [5.4.5]). In principle no one method is theoretically superior, because all estimators can be shown to be Maximum Likelihood estimators for a specific choice of error model. In other words the assumed error model determines which solution method applies. The techniques used by the Working Group are:

1. Weighted Least-Squares (WLS)

This method solves the case where the random error is in the inputs (so-called state noise). It is a very simple and efficient procedure.

2. Extended Kalman Filter/Smoothen (EKSF)

A standard Kalman filter estimates the state of a linear system with an error model which allows noise in the inputs (state noise) as well noise in the observations. The Kalman algorithm is a recursive formula, which proceeds sequentially (filters) through the data. For a fixed time interval a substantial improvement in accuracy can be obtained by adding a smoothing step in the reverse time direction.

Nonlinear state equations are handled by linearizing around a nominal trajectory (usually the current best estimate of the state is used) and bias and scale factors can be estimated by including them as undriven states with unknown initial condition (Jonkers, 1976, [5.4.6]). The EKSF is more expensive than the WLS method, but much cheaper than the OE or FE methods discussed below. Because of the recursive formulation the computer memory requirements are also modest. The disadvantage is that it is not easy to include other error components into the error model.

3. Output Error (OE)

This method applies in the case where all errors are in the observations, i.e. there is no state noise. In principle the method compares a simulation of the actual system with the measurements, while integrating the sensitivities, which describe the influence of the model parameters on the state. After one simulation run, a Gauss-Newton optimization is used to find new estimates of the model parameters. In practice this process has to be repeated for several iterations, which makes this method expensive in computer time. In addition the sensitivity matrix can be of large dimension, which adds to the computer memory requirements. The advantage of the OE method is that it is very easy to incorporate parameters in the error model. The incorporation of nonlinear models in the OE method can be handled by deriving the sensitivity equations analytically by hand, but this makes it difficult to change the error models quickly. Numerical calculation of the sensitivities is a better solution here and results in very flexible programs.

4. Filter Error (FE)

This method solves the most general problem formulation, i.e. with state noise and observation noise. In principle it is a combination of a Kalman Filter in an Output Error parameter identification iteration. The FE method is the most expensive in computer time and the most complex to use and, therefore, is seldom used.

Of course it is not always possible or even necessary to use the complete error model. Omitting error components or observations which are not important can reduce the problem formulation considerably, but the same solution techniques apply. For example it can be assumed that the air data measurements do not give enough information on the estimation of the attitude errors. This allows the separate estimation of attitude and velocity equations.

5.4.3 Use of Error Corrections

After all error corrections have been determined as far as possible, the question remains what to do with this information. There are two extreme philosophies:

1. The identified error components are put in an error model, which is added to the aerodynamic model. The parameter identification procedure is then performed on the combined model, using the original measured variables as observations. The determined values of the error components are sometimes used as initial conditions.
2. All error corrections are applied to the measured variables and the parameter identification procedure is performed on the corrected variables.

The first procedure has the advantage that the parameter identification results are a true Maximum Likelihood estimate of the complete problem, in other words the solution is theoretically optimal. In the second procedure the parameter identification is much simpler due to the smaller model. In fact if all measurement errors are corrected (and the complete state can be reconstructed), the Maximum Likelihood estimator reduces to Equation Error.

In practice a compromise between the two approaches is always made: for some error components it cannot be expected that better values can be found by including these in the parameter identification model and the corrected instead of the original measurements are used. For other error components it can be expected that the combined parameter identification will yield the best values. It is not possible to give a clearcut recommendation which error component should be included and which one not and the actual choice will have to depend on the judgement of the analyst.

Finally the instrumentation department should always be asked to verify the estimated instrument errors. It may turn out that an error which is successfully modelled in one way, should be attributed to another cause which has the same effect (for an example see below).

When a large number of manoeuvres are conducted in a particular flight condition, the error model identified for each of the manoeuvres should be the same. This makes good physical sense since the calibration of the instrumentation will change very little during one particular flight. Failure of a sensor or other instrumentation components during the flight would, of course, be an exception.

The same logic suggests that when a sufficient number of events exist, mean values of the biases and scale factors should be used as corrections for the whole flight. Simple statistical analysis can be performed to establish if the sample is large enough so that statistically significant values can be determined. If only some of the estimated error components are significant, it may be necessary to reduce the size of the error model until only significant parameters remain.

5.4.4 Data Compatibility Tools in Use at the Institutes

1. Aeronautical Research Laboratory (ARL)

Compatibility checking of helicopter flight data at ARL is based on the full nonlinear 6 DoF kinematic equations, supplemented if necessary by the three equations describing the aircraft position in earth axes. The accelerometer and gyro measurements are regarded as inputs and are assumed to be subject to systematic bias and scale factor errors. For more details see (Evans, 1985, [5.4.7]) and (Feik, 1984, [5.4.8]).

Two solution methods are in use. The first method is a Maximum Likelihood estimator (ML), which is a very flexible program that easily allows different combinations of observed outputs, alternative problem formulations and error models. The sensitivity matrix is calculated numerically, which makes the estimation of parameters in general non-linear systems possible, including systems with discontinuities and time shifts (Blackwell, 1988, [5.4.9]). The second method is an Extended Kalman Filter (EKF) which models random errors in the inertial instruments, but allows a more restricted set of outputs.

2. Aeroflightdynamics Directorate (AFDD)

The AFDD uses the program *Smoothing for Aircraft Kinematics (SMACK)* for consistency analysis (Bach, 1985, [5.4.10]; [5.4.11]). This program solves the full nonlinear, six-degree of freedom aircraft kinematic equations and estimates time-varying winds, states and measurements. In the process measurement biases and scale factors are identified. The program is based on a zero-phase-shift backward information filter and forward smoother algorithm which produces a zero phase shifted output estimates with a cutoff frequency which is one tenth of the sample rate. The solution is iterative, providing improved state and measurement estimates until a minimum squared-error is achieved.

A 3-DOF angular check is conducted first. Then, the angular error parameters and their covariances are used as start up values in an overall 6-DOF check. The error model is then refined by iteration until only statistically significant biases and scale factors remain (Kalecka et al., 1989, [5.4.12]).

3. **Deutsche Forschungsanstalt für Luft- und Raumfahrt (DLR)**

DLR uses a Maximum Likelihood program for the purpose of flight path reconstruction. The full nonlinear six-degrees of freedom kinematic equations are used. The sensitivity matrix is also calculated numerically, see (Jategaonkar et al., 1983, [5.4.13]).

4. **Georgia Institute of Technology**

The integrated rate signals were compared with the attitude angles.

5. **McDonnell Douglas Helicopter Corporation (MDHC)**

The biases and scale factors of the angular accelerations were determined using a Least-Squares procedure, which minimized the difference between the integrated angular accelerations and the body rates. A Kalman filter/smoothen was also applied to ensure data consistency, to reduce the effect of measurement noise on the state estimates and to estimate unmeasured states.

6. **Nationaal Lucht- en Ruimtevaartlaboratorium (NLR)**

In the past the standard identification procedure at NLR used an extended Kalman filter/smoothen to reconstruct the complete state of the aircraft based on an optimal combination of inertial and air data measurements. The accelerometer and gyro errors were modelled as state noise, the bias in these instruments were modelled as extra states, and pressure altitude, airspeed and sideslip angle errors were modelled as observation noise (Breeman, 1978, [5.4.14]).

In recent years NLR employs highly accurate inertial systems for all its flight tests. Therefore the current state estimation program is based on a model that includes complex variations in the wind components and errors in the air data sensors, but no errors at all in the inertial sensors. In the parameter identification step the smoothed time histories are used in a linear regression program. Because the helicopter data provided did not include either of the above combinations of measurements, NLR used its output error program for compatibility checking. This program uses nonlinear kinematic equations and allows estimating biases in accelerometers and gyros.

7. **University of Glasgow**

No tools were reported.

8. **NAE/University of Toronto**

The compatibility check uses the full set of kinematic equations of motion. As a first step a least-square fit procedure is used to determine gyro and attitude offsets and then the reconstructed attitudes and rates are used to determine accelerometer and velocity biases. The reconstructed state is normally used in the following parameter identification.

9. **Royal Aerospace Establishment (RAE)**

Data compatibility checking is a standard procedure at RAE, where it is a part of the Parameter Estimation Package (PEP). In the preliminary data interpretation phase the KINECON program performs this task. The aim is to find likely calibration errors, such as bias errors. Bias estimates can be derived using a weighted Least Squares output-error algorithm.

In a later stage of the processing filtered or smoothed estimates from the measurements and reconstructions of unmeasured states are computed using an extended Kalman filter algorithm. The program DEKFIS (Discrete Extended Kalman Filter/Smoothen) typically uses measurements from rate and attitude gyros, accelerometers and airspeed probe and incidence vanes and has the option to revise calibration factors.

10. **CERT**

For flight path reconstruction CERT applies the same Output Error program as used for identification. The full 6 DoF nonlinear kinematic equations are used and the locations of the sensors are taken into account. Nonlinear kinematic terms are dealt with in the calculation of the sensitivities. Inertial sensors are treated as inputs and air data and attitude angles are the observations. Bias and scale factor of all

measurements are included in the error model, but time delays are estimated manually after the first identification results.

5.4.5 Conclusions

It can be concluded that data quality evaluation is a necessary step in the process leading to parameter identification. The final test of the validity of instrumentation error models is of course in the results of the parameter identification.

5.4.6 References

- [5.4.1] Gerlach, O. H.
Determination of Performance and Stability Parameters from Non-Steady Flight Test Manoeuvres
SAE Paper 700236, Kansas, 1970
- [5.4.2] Wingrove, R. C.
Applications of a Technique for Estimating Aircraft States from Recorded Flight Test Data
AIAA 72-965, 1972
- [5.4.3] Klein, V. et al.
Compatibility Check of Measured Aircraft Responses Using Kinematic Equations and Extended Kalman Filter
NASA TN D-8514, 1977
- [5.4.4] Maine, R. E. et al.
Identification of Dynamic Systems
AGARD AG-300-Vol.2, 1985
- [5.4.5] Moulder, J. A. et al.
Analysis of Aircraft Performance, Stability, and Control Measurements
AGARD Lecture Series LS-104, Paper 5, 1979
- [5.4.6] Jonkers, H. L.
Application of the Kalman Filter to Flight Path Reconstruction from Flight Test Data Including Estimation of Instrumental Bias Error Corrections
TUD Report VTH-162, Delft, 1976
- [5.4.7] Evans, R. J. et al.
Aircraft Flight Data Compatibility Checking Using Maximum Likelihood and Extended Kalman Filter Estimation
7th IFAC Symposium on Identification and System Parameter Identification, York, 1985
- [5.4.8] Feik, R. A.
On the Application of Compatibility Checking Techniques to Dynamic Flight Test Data
Aeronautical Research Laboratory, Melbourne, Australia, AR-003-931, 1984
- [5.4.9] Blackwell, J. A.
Maximum Likelihood Parameter Estimation Program for General Non-Linear Systems
ARI, Aero Tech Memo 392, 1988
- [5.4.10] Bach, R. E. Jr.; Wingrove, R. C.
Applications of State Estimation in Aircraft Flight-Data Analysis
Journal of Aircraft, Vol. 22, No. 7, 1985
- [5.4.11] Bach, R. E. Jr.
State Estimation Applications in Aircraft Flight-Data Analysis (A User's Manual for SMACK)
(pending NASA TR)
- [5.4.12] Kaletka, J.; Tischler, M. B.; von Grynhausen, W.; Fletcher, J.
Time and Frequency-Domain Identification and Verification of BO-105 Dynamic Models
15th European Rotorcraft Forum, Amsterdam, NL, 1989
- [5.4.13] Jategaonkar, R.; Plaetschke, E.
Maximum Likelihood Parameter Estimation from Flight Test Data for General Non-Linear Systems
DFVLR-FB 83-14, 1983

[5.4.14] Breeman, J. H. et al.

Evaluation of a Method to Extract Performance Data from Dynamic Manoeuvres for a Jet Transport Aircraft
11th ICAS Congress, Lisbon, 1978

Kinematic Equations

$$\dot{u} = -q \cdot w + r \cdot v + (a_x - g \cdot \sin \Theta)$$

$$\dot{v} = -r \cdot u + p \cdot w + (a_y + g \cdot \cos \Theta \cdot \sin \Phi)$$

$$\dot{w} = -p \cdot v + q \cdot u + (a_z + g \cdot \cos \Theta \cdot \cos \Phi)$$

$$\dot{\Phi} = p + (q \cdot \sin \Phi + r \cdot \cos \Phi) \cdot \tan \Theta$$

$$\dot{\Theta} = (q \cdot \cos \Phi - r \cdot \sin \Phi)$$

$$\dot{\Psi} = (q \cdot \sin \Phi + r \cdot \cos \Phi) / \cos \Theta$$

$$\dot{x}_q = u \cdot \cos \Theta \cdot \cos \Psi + v \cdot (-\cos \Phi \cdot \sin \Psi + \sin \Phi \cdot \sin \Theta \cdot \cos \Psi) \\ + w \cdot (\sin \Phi \cdot \sin \Psi + \cos \Phi \cdot \sin \Theta \cdot \cos \Psi) + u_w$$

$$\dot{y}_q = u \cdot \cos \Theta \cdot \sin \Psi + v \cdot (\cos \Phi \cdot \cos \Psi + \sin \Phi \cdot \sin \Theta \cdot \sin \Psi) \\ + w \cdot (-\sin \Phi \cdot \cos \Psi + \cos \Phi \cdot \sin \Theta \cdot \sin \Psi) + v_w$$

$$\dot{h} = u \cdot \sin \Theta - v \cdot \sin \Phi \cdot \cos \Theta - w \cdot \cos \Phi \cdot \cos \Theta - w_w$$

Inputs

$$a_x, a_y, a_z, p, q, r$$

Error Model for Inputs

$$a_x = (1.0 + \lambda_{a_x}) \cdot a_{x_{true}} + b_{a_x} + n_{a_x} - \tau_{a_x} \cdot \dot{a}_x$$

etc.

Outputs

$$\Phi, \Theta, \Psi, V, h, x_q, y_q$$

Error Model for Outputs

$$\Phi_{out} = (1.0 + \lambda_{\Phi}) \cdot \Phi + b_{\Phi} + n_{\Phi} - \tau_{\Phi} \cdot \dot{\Phi}$$

etc.

Table 5.4.1. Six-degree-of-freedom kinematic equations for compatibility checking

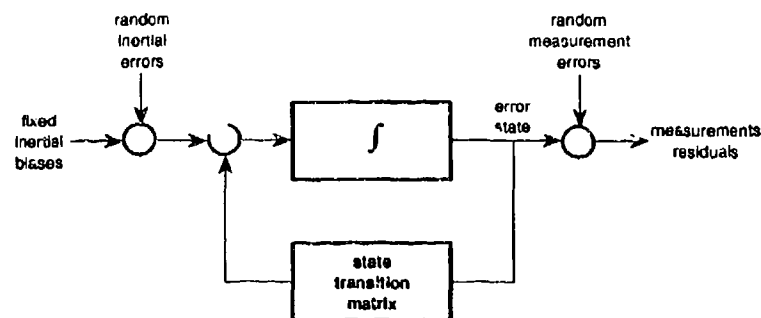


Figure 5.4.1. The linearized error model for state estimation

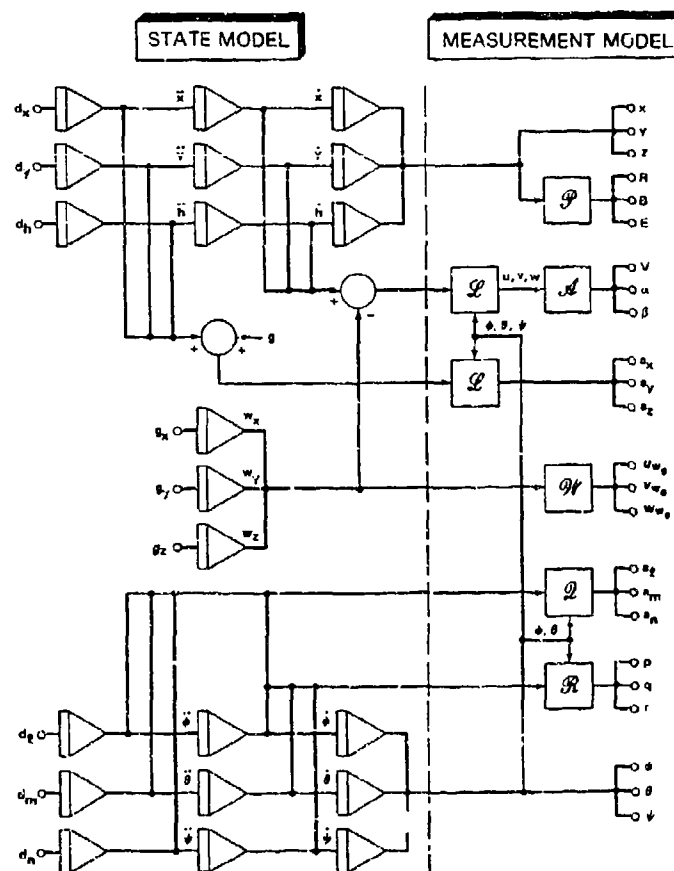


Figure 5.4.2. Block diagram of wind modeling

5.5 Identification Techniques¹⁾

5.5.1 Introduction

This section presents an overview of rotorcraft system identification techniques used by WG 18. More thorough coverage of the general system identification field, including extensive treatment of the theoretical basis of the various techniques, is found in a number of excellent textbooks (Ljung, 1987, [5.5.1]; Soderstrom et al., 1989, [5.5.2]; Bendat et al., 1986, [5.5.3]) and reference publications (Maine et al., 1986, [5.5.4]; Klein, 1980, [5.5.5]; Tischler, 1987, [5.5.6]).

This section first considers the selection of model structure. Here, special emphasis is given to ensuring that the model structure is appropriate to the intended model application. For example, simple decoupled first-order models that characterize the helicopter dynamics over a limited frequency range may be suitable for handling-qualities applications, while coupled 6-DoF models suitable for a broader range are needed for piloted simulation. At the other end of the complexity spectrum are models needed for use in advanced high-bandwidth rotorcraft control system design that must consider the coupled fuselage/rotor/airmass dynamics. Both non-parametric model structures (frequency-responses) and parametric model structures (transfer functions and state-space equations) are considered in this section.

The next step in the identification problem definition is the formulation of the criterion or "cost" function. The simplest formulation, referred to as "equation-error" is valid when the measurement noise is small relative to process noise. This assumption, while often not suitable for the high measurement noise environment of the rotorcraft, has the advantage of resulting in a cost function that is linear in the unknown parameters. This leads to the simple and rapidly-implemented least-squares (step-wise) regression techniques for identification. A more complex formulation, referred to as "output-error" is valid when process noise is small relative to measurement noise - a better assumption for rotorcraft data. Output-error techniques are more mathematically complex than equation-error techniques, and also require more sophisticated nonlinear search algorithms to determine the unknown parameters. Output-error techniques were extensively used by WG 18. A third approach to the cost function formulation is based on the use of frequency-responses. This approach requires much more preprocessing of the flight data, but has the advantage of being valid in the presence of both measurement and process noise. Also, the frequency-response formulation allows for the consideration of the differing frequency content of the state variables.

Once the model structure and cost function have been defined, the model is identified from the input/output time-history data using either time-domain or frequency-domain methods. Each method contains at its core a sophisticated search method to find the set of parameter values that provides the best fit according to the adopted cost function. Again, the choice of methods depends on the application, the formulation of the cost function (frequency-response methods are completed in the frequency-domain), the familiarity of the analyst with the methods, and finally the availability of computational tools. For example, the extraction of nonlinear models or identification from flight data with distinctly non-symmetric wave forms is best completed in the time-domain. On the other hand, when the model structure includes widely separated dynamic modes (such as low-frequency rigid body dynamics and high frequency rotor dynamics) or when highly unstable modes are presents, the identification in the frequency-domain has some distinct advantages. Both time-domain and frequency-domain methods were extensively used by WG 18.

The final step in system identification is referred to as "model verification." Here the extracted model is driven with flight data not used in the identification process to ensure the correctness of the identification procedure, and the utility of the model in predicting control responses rather than simply matching them. Model verification is completed in the time-domain in the WG 18 study, although frequency-domain verification techniques techniques have also been used (Kaletka et al., 1989, [5.5.7]).

5.5.2 Model Structure

5.5.2.1 General

Selection of model structure is a critical step in system identification, which will greatly affect both the degree of difficulty in extracting the unknown parameters, and the utility of the identified model in its intended application. For example, while a 1-DoF roll response model containing 3 unknown parameters (gain, roll mode, time delay) is fairly easy to obtain and is often quite sufficient to evaluate on-axis handling-qualities, it

¹⁾ Principal Authors: J. H. de Leeuw, Mark B. Tischler

is obviously unsuitable for investigations of cross-coupling effects. On the other hand, a flight control design model that considers coupled fuselage/rotor/airmass dynamics may contain nearly 100 parameters and will require rotor state measurements and significant computational capability. The simplest model structure that serves the intended application is the best choice.

Model structures can be broadly divided into two groups: nonparametric and parametric. A nonparametric model is one in which no model order or form of the differential equations-of-motion are assumed. Generally, nonparametric models are expressed as frequency-responses between key input/output variable pairs (eg. pitch-rate response to longitudinal stick), that are calculated using Fast Fourier Transform techniques. Non-parametric models are presented in Bode plot format of Log-magnitude and phase of the input-to-output ratio versus frequency. Typical applications of nonparametric identification results are handling-qualities analyses based on bandwidth and phase delay and simulation model validation. Non-parametric identification is a relatively fast and easy process, and has even been implemented in real time for control system performance validation on the X-29 (Chapter 8).

A parametric model requires the assumption of both system order and the structure of the system's dynamical equations. The simplest parametric model structure is a transfer-function, which is a (lumped) pole-zero representation of the input-to-output process. These models have relatively few unknown parameters. On the other end of the scale is a full 6-DoF (or higher) set of coupled linear differential multi-input/multi-output (MIMO) state-space equations, derived from Newton's Laws applied to the helicopter system. Such a rotorcraft model may contain as many as 50-100 unknown parameters - a formidable identification problem. Common applications of parametric models include control system design, wind-tunnel validation, and math model derivation and validation. Key aspects of model structure selection for transfer-function and MIMO state-space model formulation are discussed in the following paragraphs.

Transfer Function Model Structure Selection Transfer-function models are generally identified by direct fitting of the nonparametric frequency responses. Specific aspects of the model structure that must be considered are:

- Selection of input/output variable pairs,
- Frequency-range of model applicability,
- Physically meaningful order of the numerator and denominator polynomials,
- Inclusion of equivalent time delay, and
- Fixing, freeing, or constraining coefficients in the fitting process.

In order to illustrate some of these aspects, consider the selection of transfer function model structure for handling-qualities analyses. Such analyses are generally concerned with lumped low-order (equivalent systems) characterizations of on-axis input-to-output responses in terms of gain, natural frequency, damping ratio, and time delay that are representative of the helicopter's response in the pilot's "crossover frequency range" (eg. 0.1-10 rad/s). Results for the AH-64 show that the short-term pitch dynamics are very well characterized by such a simple model. However, transfer-function models for high-bandwidth flight control system design need to be of fairly high order (8th order for the BO 105) to adequately predict achievable gain levels as shown in section 8.3.

MIMO State-Space Model Structure Selection The MIMO state-space model structure problem is much more complicated than the transfer-function model problem. The analyst must make a host of a priori decisions that will profoundly affect the difficulty in extracting parameters, and the validity of the extracted parameters. As in transfer function model structure selection, the overall goal is to select a model structure that is consistent with the frequency range of interest. Some of the many important aspects of state-space model structure formulation for rotorcraft are:

- Degree of coupling between the longitudinal and lateral/directional motions
- Order of model needed to characterize the frequency range of interest
- Identifiability of the parameters as a function of the available measurements
- What parameters are known and should be fixed? (eg. gearing, gravity, filter dynamics)
- Physical constraints between the parameters (eg. common actuators, aerodynamic symmetry, geometry).

Since most of the WG 18 effort involved identification of 6-DoF MIMO state-space models, this model structure is presented in detail below

5.5.2.2 6-DoF State-Space Model Structure Used in WG 18

In the study undertaken by WG 18 the area of application was chosen to be that of helicopter flying qualities, i.e., the dynamic performance of the helicopter in response to its flight controls and as evidenced by the tradi-

tional flight mechanical variables. As a consequence, the basic dynamic equations selected for the aircraft model are the usual equations of flight mechanics as given in equations (5.5.1) through (5.5.4).

Force equations

$$\begin{aligned} m \dot{u} + m(qw - rv) &= X - mg \sin \Theta \\ m \dot{v} + m(ru - pw) &= Y + mg \cos \Theta \sin \Phi \\ m \dot{w} + m(pv - qu) &= Z + mg \cos \Theta \cos \Phi \end{aligned} \quad (5.5.1)$$

Moment equations

$$\begin{aligned} I_x \dot{p} - I_{zx} \dot{r} + (I_z - I_y)qr - I_{zx}pq &= L \\ I_y \dot{q} + (I_x - I_z)r p + I_{zx}(p^2 - r^2) &= M \\ I_z \dot{r} - I_{zx} \dot{p} + (I_y - I_x)pq + I_{zx}qr &= N \end{aligned} \quad (5.5.2)$$

Kinematic equations for Euler rates

$$\begin{aligned} \dot{\Phi} &= p + \sin \Phi \tan \Theta q + \cos \Phi \tan \Theta r \\ \dot{\Theta} &= \cos \Phi q - \sin \Phi r \\ \dot{\Psi} &= \frac{\sin \Phi}{\cos \Theta} q + \frac{\cos \Phi}{\cos \Theta} r \end{aligned} \quad (5.5.3)$$

Assumptions

$$\begin{aligned} I_{xy} &= 0 \\ I_{yz} &= 0 \end{aligned} \quad (5.5.4)$$

Gyroscopic reactions due to rotating elements of the helicopter neglected

These equations are non-linear in structure because of the gravitational and rotation related terms in the force equations and the appearance of products of angular rates in the moment equations. The model also has to adopt expressions for the aerodynamic forces X , Y , and Z and moments L , M , and N that are central in the equations.

In this regard a judgement has to be made which state variables are significant for the particular application. For conventional, fixed-wing aircraft 6 degrees-of-freedom models involving only the rigid body states u , v , w , p , q and r , and even the simpler longitudinal or lateral subsystems, have been remarkably successful. For dynamically more complex aircraft, and this certainly includes helicopters, additional states and auxiliary dynamic equations may be required to provide a satisfactory representation. In the case of the helicopter, the dynamics of the main rotor represents such a complication, introducing the potential need of adding state variables associated with blade flapping, flexible blade mode, airmass motion or combinations of these. Another source of complexity is that the rotor drive is governed to maintain constant rotational speed by a control system which may add states and equations to the model.

Fortunately, in many current helicopters, the eigenvalues associated with these additional states are sufficiently higher than those of the rigid body modes, such that by constraining the flight control inputs to relatively gradual excitations, the rotor modes approximately are not excited and a model based on the rigid body states can still give useful results. It should be pointed out, however, that especially in the highly manoeuvrable modern helicopter, this approximation to the model structure is likely to be marginal.

The model that has been adopted as the basis for the WG 18 study is the fully coupled, 6 degrees-of-freedom rigid body system of equations given in (5.5.1) through (5.5.4).

A simplified set of equations results under the assumption that products of angular rates are small and can be neglected in the moment equations.

Furthermore, by dividing the force equations by the mass and multiplying the simplified moment equations by the inverse inertia matrix, forces and moments are presented as "specific" quantities (equations (5.5.5) through (5.5.7)). This substitution, however, implies

- that for calculating the full values of the aerodynamic parameters the knowledge of these mass and inertia properties of the aircraft is required and
- that these properties are constants.

Specific forces

$$\begin{aligned}\tilde{X} &= X/m \\ \tilde{Y} &= Y/m \\ \tilde{Z} &= Z/m\end{aligned}\tag{5.5.5}$$

Specific moments

$$\begin{pmatrix} \tilde{L} \\ \tilde{M} \\ \tilde{N} \end{pmatrix} = \begin{pmatrix} I_x & 0 & -I_{zx} \\ 0 & I_y & 0 \\ -I_{zx} & 0 & I_z \end{pmatrix}^{-1} \begin{pmatrix} L \\ M \\ N \end{pmatrix}\tag{5.5.6}$$

$$\begin{aligned}\tilde{L} &= \frac{I_z L + I_{zx} N}{I_x I_z - I_{zx}^2} \\ \tilde{M} &= \frac{M}{I_y} \\ \tilde{N} &= \frac{I_{zx} L + I_x N}{I_x I_z - I_{zx}^2}\end{aligned}\tag{5.5.7}$$

This gives the following sets of equations for the accelerations (5.5.8) and (5.5.9), in which the mass and the moments of inertia no longer appear explicitly.

Equations for linear accelerations

$$\begin{aligned}\dot{u} &= \tilde{X} - q \sin \Theta & -q w & + r v \\ \dot{v} &= \tilde{Y} + q \cos \Theta \sin \Phi & -r u & + p w \\ \dot{w} &= \tilde{Z} + q \cos \Theta \cos \Phi & -p v & + q u\end{aligned}\tag{5.5.8}$$

Equations for angular accelerations

$$\begin{aligned}\dot{p} &= \tilde{L} \\ \dot{q} &= \tilde{M} \\ \dot{r} &= \tilde{N}\end{aligned}\tag{5.5.9}$$

The linear form that is assumed for the specific aerodynamic forces and moments is given in (5.5.10) and (5.5.11).

Equations for the specific aerodynamic forces

$$\begin{pmatrix} \tilde{X} \\ \tilde{Y} \\ \tilde{Z} \end{pmatrix} = \begin{pmatrix} \tilde{X}_0 \\ \tilde{Y}_0 \\ \tilde{Z}_0 \end{pmatrix} + \begin{pmatrix} \Delta \tilde{X} \\ \Delta \tilde{Y} \\ \Delta \tilde{Z} \end{pmatrix}\tag{5.5.10}$$

with

$$\begin{pmatrix} \Delta \tilde{x} \\ \Delta \tilde{y} \\ \Delta \tilde{z} \end{pmatrix} = \begin{pmatrix} X_u & X_v & X_w \\ Y_u & Y_v & Y_w \\ Z_u & Z_v & Z_w \end{pmatrix} \begin{pmatrix} \Delta u \\ \Delta v \\ \Delta w \end{pmatrix} + \begin{pmatrix} X_p & X_q & X_r \\ Y_p & Y_q & Y_r \\ Z_p & Z_q & Z_r \end{pmatrix} \begin{pmatrix} \Delta p \\ \Delta q \\ \Delta r \end{pmatrix} + \begin{pmatrix} X_{\delta_{lon}} & X_{\delta_{lat}} & X_{\delta_{ped}} & X_{\delta_{col}} \\ Y_{\delta_{lon}} & Y_{\delta_{lat}} & Y_{\delta_{ped}} & Y_{\delta_{col}} \\ Z_{\delta_{lon}} & Z_{\delta_{lat}} & Z_{\delta_{ped}} & Z_{\delta_{col}} \end{pmatrix} \begin{pmatrix} \Delta \delta_{lon} \\ \Delta \delta_{lat} \\ \Delta \delta_{ped} \\ \Delta \delta_{col} \end{pmatrix} \quad (5.5.11)$$

Equations for the specific aerodynamic moments

$$\begin{pmatrix} \tilde{L} \\ \tilde{M} \\ \tilde{N} \end{pmatrix} = \begin{pmatrix} \tilde{L}_0 \\ \tilde{M}_0 \\ \tilde{N}_0 \end{pmatrix} + \begin{pmatrix} \Delta \tilde{L} \\ \Delta \tilde{M} \\ \Delta \tilde{N} \end{pmatrix} \quad (5.5.12)$$

with

$$\begin{pmatrix} \Delta \tilde{L} \\ \Delta \tilde{M} \\ \Delta \tilde{N} \end{pmatrix} = \begin{pmatrix} L_u & L_v & L_w \\ M_u & M_v & M_w \\ N_u & N_v & N_w \end{pmatrix} \begin{pmatrix} \Delta u \\ \Delta v \\ \Delta w \end{pmatrix} + \begin{pmatrix} L_p & L_q & L_r \\ M_p & M_q & M_r \\ N_p & N_q & N_r \end{pmatrix} \begin{pmatrix} \Delta p \\ \Delta q \\ \Delta r \end{pmatrix} + \begin{pmatrix} L_{\delta_{lon}} & L_{\delta_{lat}} & L_{\delta_{ped}} & L_{\delta_{col}} \\ M_{\delta_{lon}} & M_{\delta_{lat}} & M_{\delta_{ped}} & M_{\delta_{col}} \\ N_{\delta_{lon}} & N_{\delta_{lat}} & N_{\delta_{ped}} & N_{\delta_{col}} \end{pmatrix} \begin{pmatrix} \Delta \delta_{lon} \\ \Delta \delta_{lat} \\ \Delta \delta_{ped} \\ \Delta \delta_{col} \end{pmatrix} \quad (5.5.13)$$

The derivatives used are the *specific derivatives* of the ISO-Standards [5.5.12].

As the aerodynamic forces are the only external forces in the equations (5.5.10), it is their effect that will be measured by accelerometers. We, therefore, write

$$\begin{pmatrix} \tilde{x} \\ \tilde{y} \\ \tilde{z} \end{pmatrix} = \begin{pmatrix} a_x \\ a_y \\ a_z \end{pmatrix} \quad (5.5.14)$$

According to (5.5.10) this is decomposed to give

$$\begin{pmatrix} \tilde{x} \\ \tilde{y} \\ \tilde{z} \end{pmatrix} = \begin{pmatrix} \tilde{x}_0 \\ \tilde{y}_0 \\ \tilde{z}_0 \end{pmatrix} + \begin{pmatrix} \Delta \tilde{x} \\ \Delta \tilde{y} \\ \Delta \tilde{z} \end{pmatrix} = \begin{pmatrix} a_{x0} \\ a_{y0} \\ a_{z0} \end{pmatrix} + \begin{pmatrix} \Delta a_x \\ \Delta a_y \\ \Delta a_z \end{pmatrix} \quad (5.5.15)$$

The remaining non-linear terms (products) in equation (5.5.15) can be approximated assuming

- small values of the angular speeds (p , q , and r),
- small variations of the Euler angles Φ and Θ ,
- small variations of the translational speeds (u , v , and w).

This leads to the fully linearized equations of the translational accelerations:

$$\begin{pmatrix} \dot{u} \\ \dot{v} \\ \dot{w} \end{pmatrix} = \begin{pmatrix} a_{x0} \\ a_{y0} \\ a_{z0} \end{pmatrix} + \begin{pmatrix} \Delta a_x \\ \Delta a_y \\ \Delta a_z \end{pmatrix} + \dot{\vartheta} \begin{pmatrix} -\sin \vartheta_0 - \Delta \Theta \cos \Theta_0 \\ \Delta \Phi \cos \Theta_0 \\ \cos \Theta_0 - \Delta \Theta \sin \Theta_0 \end{pmatrix} + \begin{pmatrix} -w_0 q + v_0 r \\ -u_0 r + w_0 p \\ -v_0 p + u_0 q \end{pmatrix} \quad (5.5.16)$$

In the estimation analysis the control inputs are assumed to be known accurately. In the helicopters for this study, the flight controls are actuated by hydraulic systems. The control deflection that is measured may represent the position of a control actuator rather than the immediate aerodynamic control input. In lieu of modelling this power control system, an effective time delay between the measured control motion and the actual rotor control input is assumed. In addition, although rotor state variables have been omitted explicitly, the rotor dynamics can be coarsely modelled as time delay between rotor control applications and the aerodynamic response. Although this delay has to be small, it may still affect the behaviour of the faster rigid body modes. To acknowledge these effects, the model formulation allows, as a compromise, the introduction of a single time delay for each of the four flight controls.

To complete the information necessary for the parameter estimation algorithms, the relationship between the observed variables and the state variables has to be specified.

This requires detailed calibration knowledge of the various sensors and their locations, so that corrected values to the centre of gravity of the aircraft can be determined. The data supplied by the experimental groups were largely preprocessed to supply data relative to the centre of gravity. It was further assumed that the calibration relationships were linear with unity scale factors, but allowing for unknown bias values.

In each experiment the available measured variables were assessed by several different data compatibility checks. It is noteworthy that incompatibilities were found that perhaps reflect the difficulty of interpreting helicopter air data measurements with certainty. In principle these air data sensors are to be calibrated in steady, rectilinear flight over a representative range of speeds and climb rates. This is a difficult task and still only defines the performance of the air data system under static conditions, leaving the dynamic response characteristics unknown to all intents and purposes. The measurements provided by the 'inertial' instruments, such as the accelerometers and angular rate gyros, also contain offsets which (although they should be small in good quality sensors) will vary between experiments. The model for the observation equations is shown in (5.5.17).

$$\begin{aligned}
 u_m &= u + b_u \\
 v_m &= v + b_v \\
 w_m &= w + b_w \\
 p_m &= p + b_p \\
 q_m &= q + b_q \\
 r_m &= r + b_r \\
 \Phi_m &= \Phi + b_\Phi \\
 \Theta_m &= \Theta + b_\Theta \\
 \theta_{xm} &= \theta_x + b_{\theta_x} \\
 \theta_{ym} &= \theta_y + b_{\theta_y} \\
 \theta_{zm} &= \theta_z + b_{\theta_z}
 \end{aligned} \tag{5.5.17}$$

5.5.2.3 General State and Observation Equations

The general state and observation equations are described in (5.5.18).

$$\begin{aligned}
 \dot{x}(t) &= f[x(t), u(t), \xi, t] + F n(t) \\
 y(t) &= g[x(t), u(t), \xi] + G \eta(t) \\
 x(0) &= x_0
 \end{aligned} \tag{5.5.18}$$

where

$$\begin{aligned}
 x &= \text{state vector} = (u, v, w, p, q, r, \Phi, \Theta)^T \\
 y &= \text{measurement vector} = (u_m, v_m, w_m, p_m, q_m, r_m, \Phi_m, \Theta_m, \theta_{xm}, \theta_{ym}, \theta_{zm})^T \\
 \xi &= \text{vector of unknown parameters, such as } X_u, L_{\delta_{lon}} \text{ etc.} \\
 F n(t) &= \text{state noise - ideally zero in output error method} \\
 \eta(t) &= \text{Gaussian, white random identity sequence} \\
 G \eta(t) &= \text{Measurement noise} \\
 u &= \text{control input vector} = (\delta_{lon}, \delta_{lat}, \delta_{col}, \delta_{ped})^T
 \end{aligned}$$

For our linear case, they take the special form of equation (5.5.19).

$$\begin{aligned}
 \dot{\mathbf{x}}(t) &= \mathbf{A} \mathbf{x}(t) + \mathbf{B} \mathbf{u}(t) + \mathbf{S} + \mathbf{V} + \mathbf{F} \mathbf{n}(t) \\
 \mathbf{y}(t_i) &= \mathbf{C} \mathbf{x}(t_i) + \mathbf{D} \mathbf{u}(t_i) + \mathbf{H} + \mathbf{G} \boldsymbol{\eta}(t_i) \\
 \mathbf{x}(0) &= \mathbf{x}_0
 \end{aligned}
 \tag{5.5.19}$$

In these equations

\mathbf{A} and \mathbf{B} are the matrices containing the stability and control derivatives.

\mathbf{S} represents vector of aerodynamic biases, which represent the reference state about which the manoeuvre is performed plus the effects of any deviations from perfect trim in the initial state for each manoeuvre.

The vector \mathbf{V} contains the gravity and rotation related terms in the force equation.

$\mathbf{n}(t)$ is the noise in the state equation.

The observation equation is in time discrete form, representing the sampled nature of the experiments and contains the matrices \mathbf{C} and \mathbf{D} which relate the observed variables to the state and control variables. No new unknown parameters appear in these matrices if the calibrations contain accurate scale factors.

The vector \mathbf{H} contains any measurement bias.

$\boldsymbol{\eta}(t_i)$ represents the noise sequence in the measurements.

With the system structure now laid down, the problem becomes primarily one of estimating the parameter values that describe the aerodynamic response to changes in the state variables (the stability derivatives) and the controls (the control derivatives). An important element of system identification remains in the deslection of those parameters that do not or only marginally contribute to the fidelity of the model response, a procedure referred to as *model structure determination*.

5.5.3 Time-Domain Identification Methods

There is a vast body of theoretical literature on the properties time-domain optimal estimation methods, when special forms are assumed for the noise that appears in equation (5.5.19).

One set of assumptions defines the so-called output error method, another leads to regression methods or the so-called equation error method. These will now be discussed in general terms.

5.5.3.1 Output Error Method

The idealized situation underlying this method is based on the absence of noise in the state equation and the assumption that the noise in the observation equation consists of a zero-mean sequence of independent random variables with a Gaussian distribution identity covariance. The objective is to adjust the values for the unknown parameters in the model to obtain the best possible fit between the measured data y_m and the calculated model response y_c . For aircraft identification the Maximum Likelihood Technique is mostly used: For each set of parameter values in the model, the probability of the response time histories taking values near the observed values can be defined and a maximum likelihood solution is obtained for that set of parametric values that maximizes this probability. With all unknown parameters collected in a vector $\boldsymbol{\xi}$, the Maximum Likelihood estimate of $\boldsymbol{\xi}$ is obtained by minimizing the negative log likelihood function given in (5.5.20).

$$J(\boldsymbol{\xi}) = \frac{1}{2} \sum_{i=1}^N [\mathbf{y}_m(t_i) - \mathbf{y}_c \boldsymbol{\xi}(t_i)]^T (\mathbf{G} \mathbf{G}^T)^{-1} [\mathbf{y}_m(t_i) - \mathbf{y}_c \boldsymbol{\xi}(t_i)] + \ln |\mathbf{G}(\boldsymbol{\xi}) \mathbf{G}^T(\boldsymbol{\xi})| \tag{5.5.20}$$

with

\mathbf{y}_m = measured

and

$\mathbf{y}_c \boldsymbol{\xi}$ = model output based on parameter vector $\boldsymbol{\xi}$.

The difference between the measured and model response time histories that appears in the cost function is the 'output' error of the model, so explaining the name of the method.

Both terms of the sum in this equation include the matrix \mathbf{G} which describes the magnitude information of the measurement noise. (The product $\mathbf{G} \mathbf{G}^T$ is the measurement noise covariance matrix). When the noise is known,

the second term in equation (5.5.20), is constant and can be neglected for the minimum search. The cost function then reduces to (5.5.21).

$$J(\xi) = \frac{1}{2} \sum_{i=1}^N [y_m(t_i) - y_{c\xi}(t_i)]^T (GG^T)^{-1} [y_m(t_i) - y_{c\xi}(t_i)] \quad (5.5.21)$$

In this case, there is a quadratic criterion, weighted by the measurement covariance matrix. So in principle, the technique is a weighted least squares output error method. In general, the Maximum Likelihood method also estimates noise statistics. This is not done in the techniques used in the Working Group.

If the matrix G is not known, the measurement noise covariance matrix must also be determined. It is obtained from (5.5.22).

$$GG^T = \frac{1}{N} \sum_{i=1}^N [y_m(t_i) - y_{c\xi}(t_i)] [y_m(t_i) - y_{c\xi}(t_i)]^T \quad (5.5.22)$$

As the off-diagonal terms in this matrix have no physical significance, it is in practice often restricted to be diagonal.

The set of parameter values that minimizes the Maximum Likelihood cost function has to be found by a search procedure. Several types of such procedures exist and depending on the circumstances one or another may prove to be more effective. However, the most widespread method is the Gauss-Newton or Newton-Raphson algorithm, which starts from a set of initial estimates for the parameters and then refines these estimates by an iterative method that stops when a desired level of convergence has been reached. The updating algorithm is given in (5.5.23).

$$\xi_{k+1} = \xi_k - [\nabla_{\xi}^2 J(\xi_k)]^{-1} [\nabla_{\xi} J(\xi_k)]^T \quad (5.5.23)$$

with

$$\nabla_{\xi} J(\xi_k) = - \sum_{i=1}^N ([y_m(t_i) - y_{c\xi_k}(t_i)]^T (GG^T)^{-1} [\nabla_{\xi} y_{c\xi_k}(t_i)]) \quad (5.5.24)$$

$$\begin{aligned} \nabla_{\xi}^2 J(\xi_k) = & \sum_{i=1}^N ([\nabla_{\xi} y_{c\xi_k}(t_i)]^T (GG^T)^{-1} [\nabla_{\xi} y_{c\xi_k}(t_i)]) \\ & + \sum_{i=1}^N ([y_m(t_i) - y_{c\xi_k}(t_i)]^T (GG^T)^{-1} [\nabla_{\xi}^2 y_{c\xi_k}(t_i)]) \end{aligned} \quad (5.5.25)$$

In the last equation, (5.5.25), the second gradient $\nabla_{\xi}^2 y_{c\xi_k}(t_i)$ is needed. Its computation requires a high effort. As this expression becomes zero when the optimum set of estimated parameters is reached, it can be justified to neglect this term at all, when the initial starting values for the unknown parameters are not too far away from the final 'true' values. This approach, known as Gauss-Newton or modified Newton-Raphson approximation, is computationally very efficient and sometimes results in superior convergence performance of the iterative search. Neglecting the second gradient does not affect the final optimal values of the parameters.

The Maximum Likelihood Technique is an iterative procedure. It minimizes the differences between measured data and the calculated response of the identified model by modifying the model parameters. The main steps in the procedure are:

1. calculation of the cost function value; (5.5.20),
2. determination of the measurement noise covariance matrix; (5.5.22),
3. update of the values of the unknown parameters; (5.5.23),
4. calculation of the time history response of the updated model,

5. calculation of the new value of the cost function.

This procedure is repeated until the change in the cost function is smaller than a prescribed value. The change in the cost function also indicates convergence of the estimation. To start the technique, a first guess for the unknowns, the apriori values, is needed. They should be as close as possible to the 'true' values to improve the convergence and to avoid that the estimation ends up in a local minimum. To obtain starting values, a least squares equation error technique is often applied.

The core of the computational effort lies in the calculation of the gradient of the cost function with respect to the parameter vector. This gradient can be computed by finite difference techniques or by analytic differentiation. In the finite difference technique the elements of the gradient are determined by perturbing each of the elements of the parameter vector in turn, reintegrating the model equations to determine the perturbed model response and then using these perturbations to form the approximate finite difference form of the desired partial derivative. The choice of the magnitude of the parameter perturbation has to be made with care when the model equations are non-linear. In the latter case the alternative of analytic differentiation is not attractive, but for the case of linear systems, such analytic differentiations often turn out to be much more efficient.

The Maximum Likelihood estimator also provides a measure of the reliability of each estimate. From (5.5.25) the Gauss-Newton Approximation (neglect of the second gradient) yields (5.5.26)

$$I(\xi) = \sum_{i=1}^N ([\nabla_{\xi} y_{c\xi}(t_i)]^T (GG^T)^{-1} [\nabla_{\xi} y_{c\xi}(t_i)]) \quad (5.5.26)$$

This is the so-called information matrix. For the idealized case of no state noise and 'simple' measurement error properties the Maximum Likelihood estimation leads to asymptotically efficient unbiased parameter estimates. Then, the inverse of the information matrix given in (5.5.27)

$$\text{covar}(\xi) = [I(\xi)]^{-1} \quad (5.5.27)$$

is the covariance matrix of the estimation errors, which is a measure for the accuracy of the estimated unknowns. This uncertainty level, called the Cramer-Rao bound, for the individual parameters is obtained from the diagonal terms by (5.5.28).

$$CR(\xi_m) = [\text{covar}(m,m)]^{1/2} \quad (5.5.28)$$

The obtained values are often referred to as standard deviations of the identified parameters. It should be mentioned, that these values indicate the lowest obtainable bound. They are very useful for the comparison to each other to develop a feeling about the reliability of the estimation. For a practical interpretation they are usually too small and it is often suggested to multiply these values by a factor of 5 to 10 to make the standard deviation physically more meaningful.

The covariance matrix (5.5.27) also provides information about the correlation between parameters to be identified. The correlation coefficients are obtained from (5.5.29)

$$\rho(\xi_m, \xi_n) = \frac{\text{covar}(m,n)}{[\text{covar}(nn)\text{covar}(mm)]^{1/2}} \quad (5.5.29)$$

Both, the standard deviations and the correlation coefficients are extremely helpful in the search for an appropriate model structure. Output error techniques make this information readily available as it is contained in the inverse of the information matrix, which has to be calculated anyhow for the estimation procedure.

It should be pointed out that the reality of the working model obviously represents a considerably more complex situation than that of the ideal assumptions in the observation equation of no state noise and random measurement noise of a simple statistical type. In the first place, the measurement errors are likely to contain modelling errors, largely because of the limited knowledge of the dynamic behaviour of the air data system. The magnitude of these modelling errors may be appreciated from the data compatibility studies. To the extent that such modelling errors exist, the measurement error will contain contributions that reflect the particulars of the manoeuvre. Secondly, the assumption of no-state-noise is equally, or perhaps even more strongly, violated. The flight tests may have experienced some residual turbulence which would then represent a random contribution to the state noise. More importantly, the model we have adopted for the helicopter is only an approximation to its real characteristics and will therefore contribute modelling error to the state noise. Under these non-ideal real circumstances it is not possible to state that the use of the output error algorithms will lead to unbiased estimated parameters. Nevertheless, use of the algorithm to estimate parameter values remains a

powerful and useful tool. Also the indicators of the 'quality' of parameter estimates embodied in the Cramer-Rao bounds and correlation matrix are still expected to indicate in a relative sense which parameters are finely determined and which parameters play a less important role in the model. This information provides then a guide to removing the marginal parameters from the parameter set to be used.

In the WG-18 project several computer programs based on the output error method are used. Some of these are confined to linear model equations. The use of these linear algorithms requires either the use of the linearized forms of the gravity and rotation related terms in the force equations or, as an alternative, the treatment of these non-linear terms as known functions calculated from measured values. If the model with its optimally estimated parameters provides small differences between the calculated model responses and measured variables, then this approach will be reasonable and computationally effective.

5.5.3.2 Equation Error Method

The theoretical ideal case leading to the output error method is based on no-state-noise so that only measurement noise is present and it is assumed to be of a simple random type. A converse ideal situation would occur when the measurements are without error and the state-noise present is assumed to be random with simple statistical properties. In this case the unknown parameters can be estimated with non-iterative methods in which the system model equations do not have to be integrated. As shown, the application of this method uses the methodology of regression analysis.

If we assume that a sufficient number of observed variables are available to determine the state variables from the observation equations, then, if the measured variables are measured without error, the state variables can also be determined without error. These are then completely deterministic. Now, the linear parametric representation of the specific aerodynamic forces and moments in terms of the perfectly known state variables can be confronted with the time histories of these forces and moments as determined from the accelerometer measurements and the angular accelerations provided by numerical differentiation of the angular rate measurements (or from angular accelerometers, if available):

$$y(t) = f_0 + f_1 x(t) + \dots + f_{n-1} x_{n-1}(t) + \epsilon(t)$$

or:

$$y = X\xi + \epsilon \quad (5.5.30)$$

The functions $x_1(t)$ through $x_{n-1}(t)$ represent the perfectly known state variables and control inputs and $y(t)$ represents one of the observed components of the specific force or angular acceleration. The function $\epsilon(t)$ is called the equation error. The following assumptions are made:

- The equation error ϵ is stationary with zero mean.
- ϵ is uncorrelated with the state variables.
- The state variables x_i are without error.
- ϵ is identically distributed, uncorrelated and has the variance σ^2 .

In vector form, the observation vector y represents the variables measured at N time intervals, one at a time. Similarly, the state variables and control inputs are each perfectly known at N intervals. The vector y is then $n \times 1$ and the matrix X is $N \times n$. Under these circumstances the parameter vector ξ associated with the particular observed variable is estimated to be

$$\xi_{\text{est}} = (X^T X)^{-1} X^T y \quad (5.5.31)$$

The covariance of the estimated parameter vector is given by (5.5.32).

$$E\{(\xi_{\text{est}} - \xi)(\xi_{\text{est}} - \xi)^T\} = \sigma^2 (X^T X)^{-1} \quad (5.5.32)$$

with σ^2 estimated by

$$s^2 = \frac{1}{N-n} \sum_{i=1}^N \epsilon_{\text{est}}(t_i)$$

and

$$\epsilon_{\text{est}}(t_i) = y(t_i) - y_{\text{est}}(t_i)$$

$$y_{\text{est}}(t_i) = (\xi_{\text{est}})_0 + (\xi_{\text{est}})_1 x_1(t_i) + \dots + (\xi_{\text{est}})_{n-1} x_{n-1}(t_i)$$

When in addition, the state noise is assumed to be normal, i.e., to have a Gaussian distribution, then the classical measures of significance of the regression, the F number, the partial F numbers and the squared multiple correlation coefficient, can be expressed as in (5.5.33).

$$\begin{aligned}
 F &= \frac{\xi_{\text{est}}^T \mathbf{x}^T \mathbf{y} - N \bar{y}^2}{(n-1)s^2} \\
 \bar{y} &= \frac{1}{N} \sum_{i=1}^N y(t_i) \\
 F_p &= \frac{(\xi_{\text{est}})_i^2}{s^2 (\xi_{\text{est}})_i} \\
 R^2 &= \frac{\xi_{\text{est}}^T \mathbf{x}^T \mathbf{y} - N \bar{y}^2}{\mathbf{y}^T \mathbf{y} - N \bar{y}^2}
 \end{aligned}
 \tag{5.5.33}$$

A deliberate selection of the significant parameters can be made by using a stepwise regression procedure. In such a procedure, the (regression) model increases its complexity by adding one new term at a time from the group of available state variables and control inputs to the model. The selection can be guided subjectively by the analyst or be under the control of a computer algorithm. Typically, the first regression variable selected is the one that exhibits the largest correlation with the dependent variable, y . Subsequent decisions are made on the basis of new, modified regression problems in which modified dependent variables are represented at each step by their residuals that result when the prediction by the model determined in the previous step is subtracted, e.g. after two steps,

$$y' = y - (\xi_{\text{est}})_0 - (\xi_{\text{est}})_1 x_1 - (\xi_{\text{est}})_2 x_2 \tag{5.5.34}$$

The next regressor to be added to the model will be that variable from amongst the remaining candidate regressor functions that shows the highest correlation with the modified dependent variable. At each step the partial F numbers are determined for each of the parameters that have been entered into the problem and only those that exceed a threshold for their partial F values stipulated by the analyst will be retained. The procedure will terminate when no further additions to the model can meet the threshold criterion.

Several implementations of the stepwise regression procedure are available in commercial statistics software packages, and a number of laboratories have developed their own programmes. The actual matrix arithmetic in these programmes is finely tuned to be as efficient as possible and to minimize the effects of poorly conditioned problems.

As mentioned previously, the rigorous theory for this method is based on the assumptions of perfectly known state variables and random noise. For the F values to be statistically meaningful this random noise has to be a white, Gaussian sequence. In reality these assumptions are violated. Even when state reconstructed values are used for the state variables, hopefully improving their accuracy, these will still not be perfectly known. Under such conditions, the estimates will no longer be unbiased. Also the noise statistics do not satisfy the assumed characteristics, partly because of modelling errors, and the information carried by the partial F values as determined by the application of the regression method is no longer closely related to the actual variance of the parameter estimates. This is clearly illustrated when the parameter variances calculated on the basis of applying the method to a number of different experimental time histories are analyzed. These turn out to be significantly larger than the variances inferred from the partial F values. As is the case in the application of the output error method under non-ideal circumstances, the use of the equation error method and the information about the relative importance of the various parameters, especially where augmented by practical judgement, nevertheless provides usable information.

5.5.3.3 Closing Comments on Time-Domain Methods

On theoretical grounds the application of both output-error and equation-error methods is flawed in that neither promises to deliver unbiased estimates of the parameters. Since in the WG 18 project we analyze flight test data of aircraft for which the model is not accurately known a priori, the preference for a particular method or combination of methods will depend on the ability of the identified model to predict aircraft performance in some sense. This ability is assessed via model verification discussed later in this section and model robustness discussed in section 7.

5.5.4 Frequency-Domain Identification Methods

The starting point in frequency-domain identification methods is the conversion of time-based data to frequency-based data. This conversion, which is batch and non-iterative process, involves a considerable amount of data conditioning not required for time-domain methods. However, once the frequency-domain data base is completed, the computational burden of the parameter nonlinear search is considerably reduced. Also, there are some important benefits of formulating the cost function in the frequency-domain. This section presents an overview of frequency-domain methods used by WG 18 members.

Overview of Frequency-Domain Methods. Discrete data are converted from time sequences to frequency sequences using the Fast Fourier Transform (FFT), in conjunction with data windowing and digital filtering. These resulting frequency sequences are estimates of the Fourier Series coefficients for continuous time-history signals. These Fourier coefficients are used to calculate the signal power spectral density (PSD) functions, which provide important information on the frequency content of excitation and response signals, as needed in test input design. The frequency-response function and associated accuracy metric, the coherence function, are determined directly from the PSD results; these are the "non-parametric" identification results that are very useful for handling-qualities analyses, simulation validation, and flight control. Frequency-response data obtained from flight responses containing multiple control inputs are post-processed to remove the effects of partially-correlated control inputs.

Parametric identification equations based on output-error and equation-error cost function formulations presented earlier for the time-domain techniques are essentially unchanged for the frequency-domain solution, once the time index is replaced by the frequency index. Transfer-function identification is completed by direct fitting of single-input/single-output (SISO) frequency-responses using an assumed transfer-function model structure. State-space model identification based on frequency-response cost functions is achieved by simultaneously fitting the MIMO set of frequency-responses.

Conversion to the Frequency-Domain. Continuous time-history signals are converted to the frequency-domain via the Fourier Transform. For example, the time-based signal $x(t)$ is converted to the frequency-based signal $X(f)$ by:

$$X(f) = \int_{-\infty}^{\infty} x(t) e^{-j2\pi ft} dt \quad (5.5.35)$$

The condition for existence of the Fourier Transform $X(f)$ is:

$$\int_{-\infty}^{\infty} |x(t)| dt < \infty \quad (5.5.36)$$

This condition for existence is satisfied provided that the time-history signal $x(t)$ is bounded (i.e., does not blow up). The piloted frequency-sweep technique requires that the test starts and ends in trim ($x(0) = x(t_0) = 0$), thereby ensuring that this condition is satisfied. It is important to emphasize here that the Fourier Transform is valid and can be determined without modification for flight data obtained from helicopters that exhibit either stable or unstable (most common) dynamic characteristics. Furthermore, the frequency-response function $H(f)$ which relates the input and output Fourier Transforms ($X(f)$ and $Y(f)$, respectively) will also exist and be completely valid for either stable or unstable systems:

$$Y(f) = H(f) X(f) \quad (5.5.37)$$

Flight test techniques and numerical examples of extracting unstable responses are presented by Tischler [5.5.7].

Real time-history data is of finite time duration T , so the Fourier Transform of equation (5.5.35) becomes the Finite Fourier Transform:

$$X(f, T) = \int_0^T x(t) e^{-j2\pi ft} dt \quad (5.5.38)$$

⁽¹⁾ Author: Mark E. Tischler

The record length T is the fundamental period of the signal, and defines the minimum frequency of identification:

$$\omega_{\min} = 2\pi/T \quad (5.5.39)$$

Frequencies $\omega < \omega_{\min}$ **do not exist** in the data and, so cannot be identified ["padding with zeroes" simply produces interpolation, and does not allow lower frequencies to be identified]

When the data is in digital form, as is the case here, the finite Fourier Transform is calculated digitally via the Discrete Fourier Transform (DFT):

$$X(f_k) = X(k \Delta f) = \Delta t \sum_{n=0}^{N-1} x_n \exp[-j2\pi(kn)/N]; \quad (5.5.40)$$

$$k = 0, 1, 2, \dots, N-1$$

where:

$X(f_k)$ = Fourier coefficients
 $x_n = x(n \Delta t)$ = data points
 Δt = time increment
 N = number of discrete frequency points

Finally, the Fast Fourier Transform ("FFT") is a numerically efficient algorithm for calculating the DFT. The quality (accuracy, resolution, random error content) of the achievable frequency-domain data and resulting model identification results is significantly enhanced by a number of relatively easy, but important data processing procedures (Bendat and Piercol, 1986, [5.5.3]; Tischler, 1987, [5.5.6]; Tischler and Cauffman, 1990, [5.5.8]):

- Digital prefiltering
- Overlapped / tapered windowing
- Chirp z-transform
- Composite window averaging

When the time-history does not end in trim (eg. 3211 test inputs), a correction term can be applied to the FFT to account for the conversion error introduced by the truncation effects in equation (5.5.38) (Fu et al., 1983, [5.5.9]). However, this correction term is not significant if tapered, overlapped windows are used, as is recommended.

Spectral Functions. The Fourier coefficients can be manipulated to determine the spectral distribution of the input, output, and cross-correlated signals -- the power spectral density ("PSD") functions:

Input autospectrum:

$$\tilde{G}_{xx}(f_k) = \frac{2}{TU} |X(f_k)|^2, U = 1.63 \text{ for Hanning window} \quad (5.5.41)$$

= distribution of xx as a function of frequency

Output autospectrum:

$$\tilde{G}_{yy}(f_k) = \frac{2}{TU} |Y(f_k)|^2 \quad (5.5.42)$$

= distribution of yy as a function of frequency

Cross spectrum:

$$\tilde{G}_{xy}(f_k) = \frac{2}{TU} [X^*(f_k) Y(f_k)] \quad (5.5.43)$$

= distribution of xy as a function of frequency

Examination of the input autospectrum provides the bandwidth of the excitation signal, the key characteristic for input signal design. Test inputs for system identification must have excitation bandwidths that cover the frequency range of the intended application. An example of input signal analysis based on autospectrum evaluation is presented in section 5.2.

Frequency-Response Calculation. The SISO frequency-response $H(f)$ is determined from the PSD functions:

9()

$$H(f) = \frac{G_{xy}(f)}{G_{xx}(f)} \quad (5.5.44)$$

The frequency-response as determined from equation (5.5.44) is unbiased in the presence of both output measurement noise (aircraft response sensors), and process noise (eg. turbulence). This is a key benefit of frequency-response based identification methods as compared to equation-error or output-error approaches.

The coherence function γ_{xy}^2 calculated at each frequency point indicates the accuracy of the identified frequency-response:

$$\gamma_{xy}^2 = \frac{|G_{xy}(f)|^2}{G_{xx}(f) G_{yy}(f)} \quad (5.5.45)$$

Coherence function values less than unity are due to nonlinearities in the input-to-output process, or the presence of measurement noise or process noise. A coherence function of greater than 0.6 generally indicates acceptable identification accuracy for that frequency point.

Frequency-Response Identification When Multiple Partially-Correlated Inputs are Present. Most test data generated by a pilot or with computer generated signals involve inputs to multiple controls. For example, in the frequency-sweep test technique, the pilot may apply inputs in the secondary channels to maintain aircraft motion near the reference flight condition. If dynamic coupling exists in the system being identified, the presence of correlated secondary inputs, if ignored, will bias frequency-responses obtained from the SISO relationship of equation (5.5.44) (Tischler, 1987, [5.5.6]). The correct responses are obtained from the multi-input/single-output MISO solution of the matrix frequency-response equation at each frequency point (Otnes et al., 1978, [5.5.10]):

$$T(f_k) = G_{xx}^{-1}(f_k) G_{xy}(f_k) \quad (5.5.46)$$

where

$G_{xx}(f_k) = n_c \times n_c$ matrix of auto and cross-spectra between the n_c inputs

$G_{xy}(f_k) = n_c \times 1$ matrix of SISO cross-spectra between each control input and the single input

The associated coherence function obtained from the MISO solution is referred to as the "partial coherence":

$$\gamma_{x_1 y \cdot (n_c - 1)}^2 = \frac{|G_{x_1 y \cdot (n_c - 1)}|^2}{G_{x_1 x_1 \cdot (n_c - 1)} G_{y y \cdot (n_c - 1)}} \quad (5.5.47)$$

This solution is repeated for each of the (n_o) outputs to obtain the ($n_c \times n_o$) MIMO set of "conditioned" frequency-responses.

Output-error and Equation-Error Formulations in the Frequency-Domain. The time-domain state equations ((5.5.19)) are converted to the frequency-domain by taking the Fourier Transform and dropping the initial conditions and bias terms:

$$\begin{aligned} j\omega X(\omega) &= A X(\omega) + B u(\omega) + G_{nn}(\omega) \\ Y(\omega) &= C X(\omega) + D u(\omega) + G_{\eta\eta}(\omega) \end{aligned} \quad (5.5.48)$$

where:

$u(\omega)$ and $Y(\omega)$ are the control (input) and output Fourier coefficients obtained from equation (5.5.49) with $\omega = 2\pi f$.

$G_{nn}(\omega)$ is the PSD of the process noise

$G_{\eta\eta}(\omega)$ is the PSD of the measurement noise

Including both process and measurement noise sources leads to the general frequency-domain Maximum-Likelihood problem (Klein, 1980, [5.5.5]). The frequency-domain output-error and equation-error solutions follow directly from the earlier time-domain solutions:

$$G_{nn}(\omega) = 0 \Rightarrow \text{Output-error}$$

$$C_{yy}(\omega) = 0 \rightarrow \text{Equation error}$$

At first look, it may appear that a great deal of computational effort has been expended to arrive right back at the same equation error and output-error solutions obtainable in the time domain. But, there are some important benefits of using the frequency domain formulation, especially for identifying higher-order models of helicopter dynamics that include widely spaced dynamic modes (eg. fuselage and rotor modes). This problem is discussed in detail by Lu et al. (1990, [5.5.11]). In the current application to the identification of 6-Dof-handling qualities models, the most significant benefits of the frequency-domain methods are:

- **Direct estimation of time delays.** This is very important for achieving a representative model. Time delays are directly and very accurately determined with frequency-domain methods, since such delays have a linear effect on the cost function. In contrast, time-domain methods can estimate these delays only in an indirect fashion.
- **Band limiting data and frequency weighting.** In the frequency-domain formulation, the cost function is calculated only in the frequency range selected by the user. This allows the analyst to closely match the data with the model structure. For example, the 6-Dof identification is conducted in the frequency range up to the first rotor regressing flapping mode. Within the identification range, the frequency-domain fitting errors are equally weighted at all frequencies. Unless specific explicit weighting is applied, the time-domain formulation provides higher weighting of the lower frequencies which can degrade the identification of the higher frequency modes. Also, the data must be digitally filtered to achieve time-domain band limiting for consistency with the model structure.

Frequency-Response Cost Function Formulation. The frequency-response cost function is formulated by taking the Laplace Transform of equation (5.5.41) and solving for the state-space model transfer-function T_m :

$$T_m(s) = C[sI - A]^{-1}B + D \quad (5.5.49)$$

A matrix of time delays τ is included in the model by noting that

$$T_d(s) = e^{-\tau s} \quad (5.5.50)$$

So, the frequency responses of the state-space model are obtained by substituting $s = j\omega$

$$T_m(j\omega) = (C[j\omega I - A]^{-1}B + D) e^{-j\omega\tau} \quad (5.5.51)$$

The unknown state space model parameters (Θ) in the matrices A , B , and τ are determined by minimizing J , a weighted cost function of the error e between the identified frequency responses $T(j\omega)$ [of equation (5.5.46)] and the model responses $T_m(j\omega)$ [of equation (5.5.51)] over a selected frequency range:

$$J(\Theta) = \sum_{n=1}^N e^T(\omega_n, \Theta) W e(\omega_n, \Theta) \quad (5.5.52)$$

The frequency ranges for the identification criterion ($\omega_1, \omega_2, \dots, \omega_N$) are selected individually for each input/output pair according to their individual ranges of good coherence. In this way, only valid data are used in the fitting process. Within these frequency ranges, the points are selected linearly across the logarithmic frequency range. The weighting matrix (W) is based on the values of coherence at each frequency point to emphasize the most accurate data. These features are key benefits of the frequency-response approach.

As in the time domain methods, the Cramer-Rao bounds and parameter correlation information are obtained from the numerical estimate of the Hessian matrix H . For the frequency-response method,

$$H = \nabla_{\Theta}^2 J = \frac{\partial^2 J}{\partial \Theta^2} \cong 2 D^T W D \quad (5.5.53)$$

where $D \equiv \partial e / \partial \Theta_j$ is obtained numerically from first differences

The Cramer-Rao lower bound for each parameter CR_i is obtained as before:

$$CR_i = \sqrt{(H^{-1})_{ii}} \quad (5.5.54)$$

A reasonable estimate of the parameter standard deviation usually requires a scale factor of 5 to 10 on the Cramer-Rao bound to account for modelling errors and non-Gaussian noise. The frequency-response ratio of

equation (5.5.44) eliminates the noise effects, which from experience lowers the appropriate scale factor to about 2. This factor is included in all tabulated Cramer-Rao bound results for the AFDD.

Concluding Remarks Regarding Frequency-Domain Methods. Frequency-domain methods provide some important benefits in rotorcraft system identification, especially in the identification of higher-order models with widely spaced dynamic modes. The tradeoff is in the considerable amount of data conditioning involved in the conversion of the time-domain data base to the frequency-domain data base. The proliferation of data in this conversion process makes a data-basing capability very important. Also, since frequency-domain methods tend graphics intensive (spectral curves, frequency-response, coherence, etc), user-friendly graphics-oriented software is important. The growing availability of frequency-domain identification software is a key factor in recent growth of interest in these techniques. Sophisticated software for output-error and equation-error formulations has been developed by DLR and University of Glasgow. The AFDD has developed an integrated package for the frequency-response based approach.

5.5.5 Time-Domain Verification of Identified Models

Time-domain verification is completed by driving the identified state-space model with flight data not used in the identification process. This is useful for assessing the differences between alternate model structures and for checking the model's predictive capability. A key concern is that the model, which was identified based on one input form, must be capable of predicting the response characteristics to other input forms.

The state-space equations are integrated in the time-domain, with the model stability and control parameters held constant at their identified values. Then, the output-error algorithm is used to solve for the unknown biases and reference shifts in the verification time-history records.

References

- [5.5.1] Ljung, L.
System Identification, Theory for the User
Prentice-Hall Inc., Englewood Cliffs (New Jersey), 1987
- [5.5.2] Soderstrom, T.; Stoica, P.
System Identification
Prentice-Hall Inc., Englewood Cliffs (New Jersey), 1989
- [5.5.3] Bendat, J. S.; Piersol, A. G.
Random Data, Analysis and Measurement Procedures
Second Edition, John Wiley & Sons, Inc., New York, 1986
- [5.5.4] Maine, R.; Hiff, K. W.
Identification of Dynamic Systems, Application to Aircraft
AGARD AG 390, 1986
- [5.5.5] Klein, V.
Maximum Likelihood Method for Estimating Airplane Stability and Control Parameters from Flight Data in the Frequency Domain
NASA TP-1637, 1980
- [5.5.6] Tischler, M. B.
Frequency Response Identification of XV-15 Tiltrotor Aircraft Dynamics
NASA TM 89428, ARMY TM-87 A-2, 1987
- [5.5.7] Kuletska, J.; von Grunhagen, W.
Identification of Mathematical Derivative Models for the Design of a Model Following Control System
45th Annual National Forum of the American Helicopter Society, Boston, MA, 1989
- [5.5.8] Tischler, M. B.; Cauffman, M. G.
Frequency-Response Method for Rotorcraft System Identification with Applications to the BO-105 Helicopter
46th Forum, American Helicopter Society, Dynamics I-Session, Washington, DC, 1990
- [5.5.9] Fu, K. H.; Marchand, M.
Helicopter System Identification in the Frequency-Domain
9th European Rotorcraft Forum, Sirena, Italy, 1983

- [5.5.10] Oates, R. K.; Enochson, L.
Applied Time Series Analysis
John Wiley and Sons Inc., New York, 1978
- [5.5.11] Fu, K. H.; Kaletka, J.
Frequency-Domain Identification of BO-105: Derivative Models with Rotor Degrees of Freedom
16th European Rotorcraft Forum, Glasgow, UK, 1990
- [5.5.12] Anon.
Flight dynamics - Concepts, quantities and symbols - Part 3: Derivatives of forces, moments and their coefficients
International Standard ISO 1151-3: 1989

6. Identification Results

In this chapter, identification results obtained from three helicopter data bases are presented in the form of case studies. For each of the three helicopters (AH-64, BO 105, SA-330) a brief characterization of the aircraft is first given. Then, the flight test data and results from data quality checks are presented. Both, identification and verification results generated by the Working Group Members are given in the format of tables and representative time history and frequency response plots, comparing the measured flight test data to the response of the identified models. A detailed discussion of the obtained results is given.

6.1 Case Study I: AH-64¹³⁾

6.1.1 Introduction

Flight test data from the U.S. Army/McDonnell Douglas AH-64 Apache attack helicopter was provided to the Flight Mechanics Panel Working Group 18 from an existing data base. Several of the members applied various system identification techniques to identify stability and control derivatives from the data. This case study presents results of the AH-64 identification efforts.

6.1.2 Helicopter and Instrumentation

The AH-64 Apache, shown in Figure 6.1.1, is an attack helicopter specifically designed for the U.S. Army for day, night, and adverse weather operation. It is a two-place, tandem seat, twin-engine helicopter with four-bladed main and tail rotors. The main rotor has a fully articulated retention system equipped with elastomeric lead-lag dampers. The tail rotor is a semi-rigid teetering design. The helicopter is powered by two horizontally-mounted turbo-shaft T700-GE-701 engines manufactured by General Electric. The physical characteristics of the AH-64 primary components are presented in Table 6.1.1. A three-view drawing of AH-64 is shown in Figure 6.1.2.

The flight controls consist of mechanical and electrical links from the pilot and co-pilot stations to the collective, longitudinal cyclic, lateral cyclic, and tail rotor actuators. Each actuator hydraulically sums the pilot/co-pilot mechanical inputs with those from the electrical link via electrohydraulic servo valves. In the lateral, longitudinal and directional axes, the electrical links provide authority limited Stability and Command Augmentation System (SCAS) functions for a variety of manually and/or automatically selectable modes. In the event of a mechanical link failure such as a jam or severance, the electrical link control path provides a full authority Back-Up Control System (BUCS) in all four control axes. The SCAS and BUCS control modes along with their associated monitoring and control logic are implemented in the Digital Automatic Stabilization Equipment (DASE) subsystem.

The flight control system also includes an electrically controlled horizontal stabilator which is used to adjust trim pitch attitude with airspeed. The stabilator actuators are driven by the Stabilator Control Units (SCUs). The Stabilator Control Units automatically position the stabilator as a function of airspeed, pitch rate, and collective pitch position. The Stabilator Control Units can be manually overridden by the pilot at airspeeds below 80 knots to increase visibility at the lower speeds.

Flight test measurements for the AH-64 were recorded on board the aircraft and telemetered to the ground station for backup recording/filtering and on-line monitoring. Table 6.1.2 lists the control variable measurements and Table 6.1.3 the output variable measurements provided for the AH-64 records. The filter cutoff frequencies (-3dB bandwidth frequencies) were

- 50 Hz for the measurements of the control deflections, the pilot seat accelerometers, and the Euler rates,
- 6 Hz for all other measurements.

Longitudinal and lateral velocity components (from Doppler) as well as the normal velocity component (from Heading Attitude Reference System HARS) were only available for the frequency sweeps and not the doublets and pulses. However, airspeed V , angle of attack α , and angle of sideslip β from the boom were given to allow reconstruction of u , v , and w . The boom is mounted out in front of the aircraft to avoid main rotor wake interactions.

A strap-down sensor package near the centre of gravity provides body angular rates, angular accelerations, and linear accelerations. Body angular accelerations (dp/dt , dq/dt , dr/dt) are measured independently from the angular rates (p , q , r). Euler angles (Φ , Θ , Ψ) and Euler rates ($d\Phi/dt$, $d\Theta/dt$, $d\Psi/dt$) are provided by the HARS. Euler rates are signals computed within HARS based on the Euler angles.

Control positions were taken at the actuators and not at the pilot's controls thus eliminating uncertainty in control linkage and actuator dynamics.

¹³⁾ Principal Authors: D. Banerjee, J.W. Harding, MDHC; D.P. Schrage, C.K. Gardner, Georgia Institute of Technology.

6.1.3 Flight Testing and Data Evaluation

The AH-64 aircraft was flown in 1984 in a series of tests for the purpose of transfer function evaluation. These tests were designed to obtain aircraft responses to

- doublet inputs,
- pulse inputs, and
- frequency sweep type inputs

to each control (longitudinal, lateral, directional, and collective) from level flight at 130 knots. Table 6.1.4 lists the AH-64 manoeuvres provided to the Working Group. Files 1 through 11 contain doublet and pulse runs suitable for time domain identification. Manoeuvres were performed open-loop. Two half-inch doublets starting in opposite directions are included for each control axis. Pulses for both forward and aft longitudinal control and right lateral control are also included.

Control inputs for the 130 knot frequency sweep manoeuvres in files 12 through 21 were produced by a specially designed Gold Oscillator Box (GOB). It commands sinusoidal frequency sweeps in two ranges from 0.1 Hz to 3 Hz and from 0.3 Hz to 13 Hz in one minute sweeps. A typical two minute run consists of a sweep up to the high frequency and then back down to the starting frequency. A modified Stability Augmentation System (SAS) was used to maintain a stable reference during input sweeps. The primary axes remain open-loop and are stabilized by pilot inputs.

System identification results are highly dependent on the quality of flight test data used. Prior to any identification, a thorough analysis of recorded measurements must be performed. WG members have spent considerable time evaluating the quality of the AH-64 data base. Although several undesirable characteristics exist, data consistency has been established and the data has been deemed acceptable for time domain identification. The shortcomings associated with the manoeuvres used for time domain identification (files 1 to 11 from Table 6.1.4) include

1. Short record length (12 seconds):
Parameters associated with long period aircraft modes such as the phugoid, which has a period of about 20 seconds for the AH-64, cannot be adequately identified from short duration records.
2. Large-amplitude response:
Linear models of rotorcraft are appropriate for predicting small-amplitude response only. The change in body attitudes were as large as 20° to 30° for both longitudinal and lateral doublets.
3. Noisy acceleration measurements:
Accelerations had low signal-to-noise ratios due to 4/rev vibrations (Figure 6.1.5 through Figure 6.1.8).
4. Quantization errors in Euler angles:
Quantization errors were introduced due to the large ranges used when recording Euler angle measurements.
5. Gust effects:
Wind conditions at the time of the test, although small, are unknown.

The frequency sweep data contained some of the same problems listed above but was not acceptable for frequency domain identification for the following reasons:

1. Limited SCAS activity:
Sweeps were flown open-loop in the primary axis and closed-loop in the off axes resulting in a high level of correlation among the control inputs, which precludes identification of off-axis responses.
2. Inadequate low frequency information:
Sweeps were conducted using computer-generated signals that began at a frequency of 0.63 rad/s, which precludes the identification of the low frequency (speed) derivatives.

In general, the angular measurements Φ , Θ , Ψ , $d\Phi/dt$, $d\Theta/dt$, $d\Psi/dt$, p , q , and r are consistent for all of the AH-64 data. Because of the large range used on the attitudes during the recording process, the Euler angles have small quantization errors. This problem has been overcome without too much difficulty either by data reconstruction techniques or simply replacing the Euler angles with integrated Euler rates.

Translational states are inherently difficult to measure, especially on a helicopter where high vibration levels lead to noise in the acceleration measurements and the main rotor wake interacts with air data systems. In the AH-64 data base, velocities u , v , and w were not directly available for the doublet and pulse manoeuvres but were calculated from V , α , and β from the boom system. Since the boom projects out in front of the aircraft, the calculated velocities did not contain wake interaction problems. The acceleration measurements had low signal-to-noise ratios, especially in the a_x and a_y measurements. This problem of small magnitude longitudinal

and lateral accelerations is not unique to the AH-64 data base. Helicopters generally have no means of producing large forces along the body longitudinal and lateral axes. Two noted inconsistencies in the longitudinal acceleration include the wrong sense and a bias of about 2.1 m/s^2 . The sign on a_x was corrected on the entire database and biases were identified by the members separately.

The Working Group concentrated on files 1 through 8 for time domain identification. These files were separated into two groups, one of which was used for identification and one for verification. Group 1 contained files 1, 3, 5, 7, and group 2 contained files 2, 4, 6, 8. The main difference between these two groups is a sign conversion in the control inputs. Control time histories for group 1 are shown in Figure 6.1.3.

This section describes the methods WG members used for consistency checks and data reconstruction of the AH-64 data. Results are presented as tables of biases and scale factors and as time histories of reconstructed states.

6.1.3.1 McDonnell Douglas Helicopter Company (MDHC)

MDHC used several methods to assess the quality of the AH-64 data including:

1. Simple comparisons between redundant sensors.

The limited data set available to the Working Group eliminates the availability of most redundant sensor checks except accelerations. However, multiple acceleration measurements were available. Accelerations from the centre of gravity (CG) and the pilot seat (which were transferred to the CG) were compared and found to be consistent for several manoeuvres. The only differences were small biases in the a_x and a_y signals. Since it could not be determined (at this stage in the consistency checks) which signal contained the bias, no action was taken.

2. Comparisons between kinematically redundant sensors

Several comparisons between kinematically redundant sensors were carried out:

- The body angular accelerations (dp/dt , dq/dt , dr/dt) were integrated and compared to body angular rates (p , q , r). Scale factors and biases were identified using Least Squares (Figure 6.1.4). To eliminate quantization errors, Euler angles (Θ , Φ , Ψ) were reconstructed from Euler rates $d\Theta/dt$, $d\Phi/dt$, $d\Psi/dt$ calculated within the HARS. Scale factors and biases were identified to match integrated Euler rates with measured Euler angles.
- The compatibility between body rates obtained from separate rate gyros and the rates and attitudes provided by HARS was checked using kinematic relations.

3. A Kalman Filter/Smoothing state estimation method.

The final phase in data consistency checks was the use of an Extended Kalman Filter/Smoothing (Bryson and Ho, 1975, [6.1.1]). The Extended Kalman Filter/Smoothing algorithm, as presented by DuVal et al. (1989, [6.1.2]), is derived by posing an optimization problem to find the time histories of the vehicle states, that are consistent with both a prescribed dynamic model and available measurements.

This approach was applied to the AH-64 time-domain database. The data was initially sampled at 25 Hz. Measurements used in the reconstruction include: Φ , Θ , Ψ , p , q , r , u , v , w , a_x , a_y , and a_z , where the body axis velocity components (u , v , w) were derived from the angle of attack α , angle of sideslip β , and airspeed V measurements. Further processing included a zero phase shift, lowpass filter with a cutoff frequency of 3 Hz after the Kalman filter.

Results from the Kalman filter state estimation for the doublet manoeuvres indicated the following

- The angular measurements Φ , Θ , Ψ , p , q , and r are generally very good.
- The pitch rate signal has a bias of about 0.01 rad/s .
- The longitudinal acceleration signal has a bias of roughly 2.1 m/s^2 . Part of this bias was apparently caused by the accelerometers being calibrated with the helicopter on the ground at a 5° nose-up attitude.

6.1.3.2 National Aeronautical Establishment (NAE)

Consistency checks were performed on all 8 doublet input files. The data was initially lowpass filtered with a Butterworth fourth-order zero phase shift filter with a cutoff frequency of 4 Hz. Spectral analysis had revealed considerable excitation at 19 Hz (blade passage frequency). After lowpass filtering, the data was sampled at 20 Hz, excluding the first and last 50 points.

Biases in the data were estimated with a Least Squares method. The measurements used were: $d\Phi/dt$, $d\Theta/dt$, $d\Psi/dt$, u , v , w , a_x , a_y , a_z , p , q , r , Φ , Θ , and Ψ . The Least Squares procedure is outlined below:

1. Integrate Euler rates with measured Euler angle initial conditions and use Least Squares to determine the 6 biases for the measured attitudes and rates.
2. The corrected Euler angles and rates are used in the angular kinematic equations to determine biases in the body angular rates.
3. The corrected body angular rates and attitudes enter the translational kinematic equations for determination of biases in the velocities and translational accelerations.

The obtained results are included in Table 6.1.6.

6.1.3.3 Deutsche Forschungsanstalt für Luft- und Raumfahrt (DLR)

Rate and linear acceleration were filtered using a zero phase shift digital filter with a cutoff frequency of 12.5 Hz to eliminate higher frequency noise. Air data (boom) and linear acceleration measurements were corrected with respect to the CG location. Then, DLR completed consistency checks on each of the doublet input manoeuvres, and also on the concatenation of all the manoeuvres. In the nonlinear kinematic equations, the attitude angles and speed components are treated as states whereas the linear accelerations and rates are considered as control inputs (driving functions). A nonlinear Maximum Likelihood program was used to estimate scale factors for u , v , w , Φ , Θ , Ψ and biases for a_x , a_y , a_z , p , q , and r . The obtained results are summarized in Table 6.1.5 and Table 6.1.6.

6.1.3.4 Nationaal Lucht- en Ruimtevaartlaboratorium (NLR)

Data preprocessing consisted of sampling the data at 20 Hz with no filtering.

NLR initially tried to perform compatibility checks using a linear output error program. However, the bias estimates from the linear program varied considerably between manoeuvre files. NLR believes the poor results were due to the large pitch and roll excursions, which cannot be adequately represented by the linear kinematics formulation.

NLR therefore adopted an output error program which uses the nonlinear kinematic equations to estimate measurement biases. This technique was applied separately to each manoeuvre file to estimate the biases in the acceleration measurements and in the body angular rate measurements. The bias estimates obtained from the nonlinear output error program proved to be relatively constant.

The agreement between measured and reconstructed records was found to be generally satisfactory. The bias estimate for a_x is consistently large and indicates the longitudinal accelerometer calibration error. NLR also notes that the a_x time history is very noisy, making it difficult to judge whether the signal is valid. The identified biases are given in Table 6.1.6.

6.1.3.5 U.S. Army Aeroflightdynamics Directorate (AFDD)

The AFDD performed consistency checks on all the files. The data was initially lowpass filtered with a four-pole, zero phase shift digital filter supplying a 6 dB attenuation at 3 Hz. Analysis was performed at the full sample rate of 100 Hz for the first 11 files, while files 12 through 21 were decimated to 20 Hz for analysis.

The AFDD used the state estimation program SMACK (Bach, 1988, [6.1.3]) to estimate biases and scale factors. Measurements used in the estimation were Φ , Θ , Ψ , p , q , r , V , α , β , a_x , a_y , and a_z . Euler angles and body angular rates were used as measurements in an initial check of angular consistency and were also estimated in this check. Errors on Euler angles were not estimated because of the high reliability of the HARS system from which Euler angle and rate measurements were obtained.

All the measurements were used in a final 6 DoF check. Biases and scale factors estimated in the angular check were used along with their program-estimated covariances as start-up values in the 6 DoF check. Measurements were also estimated as were angular accelerations in this final check. Biases were assumed to be on a_x and a_y rather than Φ and Θ because of high confidence in HARS data.

Scale factors were not estimated, except for files 12 and 13 where a sign error in the pitch rate measurement was deduced from visual inspection of the data and corrected. Table 6.1.6 lists the bias estimates obtained from the files with doublet and pulse for comparison to other WG results.

AFDD also evaluated the data consistency for the frequency sweep data except for file 14 because its a_{xco} channel was previously shown, through frequency response identification techniques, to be dynamically incorrect. Results are given in Table 6.1.7.

6.1.3.6 Results

Table 6.1.5 and Table 6.1.6 summarise the data consistency results for the AH-64 flight test data. AFDD, DLR, NAE, and NLR evaluated each of the doublet files separately, estimating biases and scale factors. From the results of the considered files, the mean values and the standard deviations were determined. They are presented in the tables. It has to be noted that the standard deviation is calculated using the mean values; it is not based on the Cramer-Rao lower bound given by the estimation programs. The identified biases and scale factors can be used to correct the measurements by

$$y_c = (y_m + b)/\lambda$$

where

y_m = measurement,

b = bias,

λ = scale factor.

Scale factors are only given in the DLR results. They are close to one with relatively small standard deviations and indicate that the measurements have no significant scale factor errors. All four WG Members provided bias estimates for the linear accelerations and rates. In addition, NAE identified biases for the speed components, attitude angles and heading. All results are in good agreement and show that most biases are very small. The standard deviations are roughly of the same magnitude as the bias values and indicate that the measurements are reliable and need not be corrected. However, larger values are seen for the pitch rate measurement (0.01 rad/s) and the longitudinal acceleration (about 2 m/s²). A part of the bias of the longitudinal acceleration was apparently caused by the accelerometers being calibrated with the helicopter on the ground at a 5° nose-up attitude. As for both measurements the standard deviation is only about 10% of the bias value, these results are consistent and justify correction of the measured data.

AFDD statistics for the frequency-sweep data are given in Table 6.1.7. In comparison to the results obtained from the doublet-input files, significantly larger values were determined for the biases of the linear accelerations. The change in magnitude and sign for the individual files also shows that no consistent result could be obtained.

WG Members also provided time history comparisons of the estimated and measured data. As representative example, results obtained from the MDHC Kalman state estimation are presented in Figure 6.1.5 through Figure 6.1.8. They show the time histories for speed components, linear accelerations, rates, and attitudes for the files 1, 3, 5, and 7. The reconstructed data is given without corrections for scale factors and biases. The general good agreement confirms the data quality. The previously mentioned two larger biases for the pitch rate and, in particular, for the longitudinal acceleration are clearly seen. Some larger deviations are only seen in the speed measurements. This indicates that air data measurement results still are significantly less accurate than data obtained from gyros and linear accelerometers.

6.1.3.7 Summary

Flight test data evaluation is essentially a parameter identification problem. The objective is to establish the compatibility of measured flight test data with known kinematic relations. The procedure is to assume a model for the measurement error and identify the error model parameters using state estimation techniques. A common error model used by most of the WG members is a simple scale factor and bias combination where even scale factor effects are often neglected. The differences in data evaluation approaches between the WG members lie in the choice of parameter estimation techniques. The methods used here include:

1. Least Squares,
2. non-linear output error,
3. non-linear Maximum Likelihood, and
4. extended Kalman filter.

Despite the range of identification methods applied to the AH-64 database, the data evaluations for files 1 through 11 showed consistent results. The identified mean values were close to one for the scale factors and small for most biases. It indicates that the measurements are accurate and require no corrections. However, significant biases were seen in the pitch rate and particularly in the longitudinal acceleration. As their standard

deviations are small, these biases are reliable and can be used for correcting the measured data. The statistics indicate that all error parameters identified for the sweep manoeuvres, with the exception of the bias on the roll rate for files 20 and 21, are significant.

In conclusion it can be stated that the data quality of the doublet-input and pulse-input files was acceptable for identification purposes. (Other limitations, e.g. short record length, large amplitudes, etc., were already addressed). For the frequency-sweep manoeuvres, however, significant measurement deficiencies were seen. As they were not consistent, a physically meaningful correction is problematic.

6.1.4 Identification Methods

6.1.4.1 Model Structure

The model which has been used by WG members investigating the AH-64 is a coupled six degree-of-freedom rigid body model with equivalent time delays for the control variables. All Working Group members used a linear model except for the nonlinear gravity and kinematic terms. These were either taken from the flight data or calculated from the simulated response data. The stability and control derivatives, aerodynamic biases and measurement biases are estimated.

Estimating the aerodynamic biases would not be necessary if the aircraft initiated each manoeuvre from an unaccelerated flight condition and the trim conditions of the aircraft were exactly known. In this case, the aerodynamic biases would be simply the steady state gravity force components (e.g. $a_{x0} = -g \sin \Theta_0$, etc.). In practice, however, the aircraft is not in steady flight at the beginning of the manoeuvre and the trim conditions are not exactly known. Therefore, the estimation of the aerodynamic biases is important in obtaining good results. In fact, MDHC attempted to identify a model in which the aerodynamic biases were not estimated but were calculated from the steady state gravity components. However, the results from this identification were not considered reasonable.

Additionally, a bias term can be added to the measurement equation and/or a bias identified for each measurement. Although estimation of both aerodynamic and measurement biases is a standard practice, care must be taken to ensure that the aerodynamic and measurement biases are independent or identifiability problems will result.

There are three different approaches to handle the nonlinear gravity and centrifugal force terms along with the Euler angle kinematics:

1. Linearising yields a complete eight state linear model. This approach is based on small-perturbation assumptions. It is acceptable with small-amplitude manoeuvres, in particular with respect to the pitch and roll angle (they should not exceed about 25°). A fully linearised model was used by MDHC.
2. The nonlinear terms are calculated using the measured data and then treated as known quasi control input (driving function). This approach was taken by NAE.
3. The nonlinear terms are calculated using the model states. The only control variables are the actual pilot controls. This model formulation was chosen by DLR.

With the first two methods, the identification can be conducted with a linear model formulation whereas in the third approach a nonlinear model has to be identified.

While both MDHC and NAE identified all derivatives in the stability and control matrices NLR and DLR used reduced parameter sets in which many of the derivatives were not estimated. The reduced parameter sets can be determined by several methods. DLR determined insignificant model parameters based on the parameter covariance estimates provided by their nonlinear Maximum Likelihood program. NLR employed a step-wise linear regression to determine insignificant parameters.

6.1.4.2 Parameter Estimation Algorithm

Several different parameter estimation procedures were applied to the AH-64 data. Most of the members used time domain techniques ranging from the relatively simple linear regression to the more sophisticated Maximum Likelihood (ML). The AFDD used a frequency domain approach. Because of problems with the frequency sweep data, AFDD was only able to estimate a few control derivatives and time delays. This section describes the estimation techniques applied to the AH-64 data by different WG members.

6.1.4.2.1 MDHC

MDHC used a time domain output error method to estimate a model from files 1, 3, 5, 7. The output error program iteratively adjusts the model parameter values to minimize the sum of squared weighted errors between measured and simulated responses. Minimization is based on a finite difference Levenberg-Marquardt algorithm (ZXSSQ from the IMSL, [6.1.4]) which solves a nonlinear Least Squares problem. This routine behaves as a first order method far from the minimum and a second order method near the minimum, and so generally has good convergence properties. The output error program can accommodate multiple manoeuvre time histories during a single run. Usually four manoeuvres (one for each control axis) are used simultaneously so that all derivatives can be estimated during a single run. In addition to estimating the aerodynamic derivatives, MDHC estimated the initial state derivatives (aerodynamic biases).

The outputs from the simulation which were compared with the measurements to form the error cost function were u , v , w , a_x , a_y , a_z , p , q , and r .

Because MDHC was unable to identify consistent control time delays from files 1 through 11, no time delays were used during the identification. However, the discrete-time simulation in the output error program introduces a delay in the simulated outputs of one-half the sample interval or 0.020 s.

6.1.4.2.2 NAE

NAE's model was estimated using the concatenated data files 1, 3, 5, 7, and verified using files 2, 4, 6, 8. Starting with the reconstructed data, NAE first applied stepwise regression to find values for the parameters in the aerodynamic model, as well as estimates of the parameter variances. The regression values of the parameters were then used as starting values for the Maximum Likelihood algorithm MMLE-3 (Maine et al., 1980, [6.1.5]; 1981, [6.1.6]). The full set of parameters was identified with a time delay of 0.100 s applied to all the controls.

The measurements compared with the ML output were: u , v , w , p , q , r , a_x , a_y , and a_z . In addition to the aerodynamic derivatives, aerodynamic biases were estimated for each state equation of each manoeuvre file. Measurement biases were also estimated for each measurement equation of each manoeuvre file.

6.1.4.2.3 DLR

Three models were identified by DLR: one from files 1, 3, 5, and 7 (DLR-1), one from files 2, 4, 6, and 8 (DLR-2), and one from all eight files (DLR-3). A nonlinear Maximum Likelihood program was used to estimate derivative values. The measurement vector included: a_x , a_y , a_z , p , q , r , Φ , Θ , u , v , w , dp/dt , dq/dt , and dr/dt . The parameter covariance matrix provided by the ML program was used to eliminate insignificant model parameters, giving the reduced model order. During the identification procedure, the nonlinear kinematic and gravity terms were calculated from the model response data.

DLR usually estimates equivalent control time delays using the cross-correlation between input and response signals. For the AH-64 data, time delays were not calculated but were assumed to be 0.100 s on all controls which are the average value as identified in the frequency domain by AFDD.

6.1.4.2.4 NLR

NLR identified two models from two separate groups of data. Each group of data consisted of four doublet manoeuvres representing inputs in each control axis. The first group included files 1, 3, 5, and 8 (NLR-1) and the second group files 2, 4, 6, and 7 (NLR-2). The following helicopter response measurements were used during the identification: Φ , Θ , Ψ , p , q , r , V , α , β , a_x , a_y , a_z . No filtering was performed on the flight data when the data sampling was reduced to 20 Hz.

NLR used a two step method. As a first step, all state variables are reconstructed as described in 6.1.3.4. In the second step, the reconstructed variables and the measured control variables are used in a stepwise linear regression procedure to estimate parameter values.

Time delays of 0.100 s were applied to the four controls during the identification and verification process to account for time lags in the actual response. These delays were assumed as representative delays, and were not actually calculated from the data.

6.1.4.2.5 AFDD

Because of the limitations of the AH-64 frequency-domain database, AFDD was only able to identify the high frequency control derivatives and time delays for the longitudinal and collective controls. The longitudinal cyclic parameters were obtained from multi-variable frequency response matching of the 3 DoF longitudinal dynamics: q/δ_{lon} , $\dot{\theta}_z/\delta_{lon}$, w/δ_{lon} , $\dot{\theta}_x/\delta_{lon}$, and u/δ_{lon} . The time delay associated with the longitudinal cyclic was estimated as 0.110 s.

The collective stick parameters were obtained from single-input/ single-output transfer function model fitting of the collective frequency responses: q/δ_{col} , r/δ_{col} , and $\dot{\theta}_z/\delta_{col}$. Collective stick time delay, which was taken as an average from the q , r , and $\dot{\theta}_z$ responses, was 0.089 s. The average of all time delays is approximately 0.100 s which is the value used by NAE, DLR, and NLR.

6.1.5 Identification Results

The identification results are presented in this section in the format of

1. identified derivatives,
2. model eigenvalues,
3. time history plots comparing the model response with the flight data used to generate the model.

6.1.5.1 Identified Derivatives

Stability and control derivative estimates and the variance of these estimates are listed in Table 6.1.8. Since it is not practical to discuss each derivative, a brief comparison of the primary derivatives associated with helicopter dynamics has been made.

Diagonal terms (X_u , Y_v , Z_w , L_p , M_q , and N_r) in the 6 DoF models characterising the damping derivatives were consistently identified by the members. Contrary to expectations, drag damping (X_u) is well identified despite the lack of significant speed data due to the short record length. The effects of time delays used in the identification process are evident in the pitch and roll damping terms L_p and M_q . Identified values of L_p and M_q are reduced when time delays associated with rotor dynamics are omitted from the model structure. MDHC did not include the 0.10 s time delay used by the other members. The MDHC values for L_p and M_q are subsequently smaller than those obtained by NAE and DLR which did include the time delay. The yaw damping derivative, N_r , is the least identifiable of the diagonal terms. Values from the DLR-1 and DLR-2 models using different records for identification vary from -0.607 1/s to -0.246 1/s unlike the other diagonal terms which are consistent between the two models. The verification time histories show good correlation for yaw response to directional inputs for all of the identified models. However, the yaw response to pitch inputs is poor on all the models leading to the possibility that airmass states associated with interactional aerodynamics are needed to uniquely model the yaw equation.

Dihedral effect (L_p) and directional stability (N_r) show good agreement between the various models. Coupling derivatives L_q and M_p are not easily identified since aircraft coupling is not strong. Less significant stability derivatives vary widely as might be expected.

Time delays were identified by AFDD during frequency-response identification with the longitudinal and collective sweep data. Results are given in Table 6.1.12 and discussed in more detail in section 6.1.7.2.2.

The identified on-axis control derivatives representing control power such as $M_{\delta lon}$, $L_{\delta lat}$, $N_{\delta ped}$ (see Table 6.1.11) and $Z_{\delta col}$ (see Table 6.1.10) show reasonable agreement.

6.1.5.2 Model Eigenvalues

The AH-64 eigenvalues were calculated from each of the identified models. For comparison, MDHC additionally has provided eigenvalue estimates for the phugoid and dutch roll modes. These estimates were arrived at through visual inspection of flight data designed to excite the oscillatory modes (these flight test data were provided to the Working Group):

- The time history of an AH-64 flying DASE-off at 130 knots exhibited an unstable phugoid response. The period of oscillation and time to double amplitude have been estimated resulting in the phugoid eigenvalues.
- The dutch roll mode was excited by a directional pulse. The period and time to half amplitude were estimated and used to compute the dutch roll eigenvalues.

In Table 6.1.13 the time constants, damping ratios and undamped natural frequencies derived from the eigenvalues obtained from both, the identified models and the visual inspection are given.

The phugoid eigenvalues of the identified models are not consistent and do not agree well with the phugoid mode estimated from flight test data. The speed derivatives Z_u and M_u directly affect the phugoid motion and are shown in Table 6.1.8 and Table 6.1.9 to vary greatly between the models. The 12 s record length limits the identification of these speed related derivatives and thus the phugoid mode which has a period of roughly 20 s. The limited data also affects the identifiability of the spiral mode which is a slow, lightly damped mode.

The roll convergence roots are close between the models as a result of the fairly consistent roll damping derivative L_p . The Dutch roll eigenvalues for most of the identified models agree with each other and with the MDHC values indicating that this motion is easily identified from the data. The important lateral stability derivatives associated with Dutch roll Y_v , N_v , and N_r are relatively consistent between the models.

6.1.5.3 Comparison of Time Histories

Time history plots of the measured data and the calculated response of the identified model were provided by the WG Members. Although the individual results showed some differences in the model responses and the agreement with the flight test data, the identifications were in general considered acceptable in characterizing the helicopter response. As representative example, the time histories of the DLR identification from the first data group (files 1, 3, 5, and 7) are given in Figure 6.1.9 through Figure 6.1.12. The model was only driven with the measured control inputs. The nonlinear gravity and kinematic force terms were calculated from the model response (no pseudo controls were used). Biases were estimated to compensate for offsets in the measurement of the control and observer variables.

The comparison of the time histories shows:

1. The agreement of the measured data and the response of the identified model is satisfactory.
2. The longitudinal motion is more accurately represented than the lateral-directional motion.
3. For the force equations, the fit in the linear accelerations is very good. The differences in the speed components show similar tendencies as the results from the data consistency checks. This indicates that these differences also reflect the inaccuracies in the speed measurements.
4. The time history fits of the rates demonstrate that the on-axis response of the model (u/δ_{lon} , p/δ_{lat} , r/δ_{ped}) follow the flight test data closer than the off-axis response.

6.1.6 Verification

Model verification is performed by comparing identified model response to flight test data not used to generate the model. For the identification the model parameters were modified to obtain the best curve fit. Now, for the verification, the model parameters are fixed to the identified values. The model is driven with the measured control inputs to calculate the model response. For comparison, both, the model output and the measured flight test data are plotted. The agreement of both time history plots is a measure of the predicting capability of the identified model.

On the whole, all the models identified in the Working Group do a good job of predicting primary axis response. However, larger deviations were seen in the coupled off-axis response. Figure 6.1.13 through Figure 6.1.17 contain verification plots of the files 2, 4, 6, and 8. The model response was calculated using the previously described DLR model which was identified from the files 1, 2, 3, and 4. (The difference between these two data groups is the control input sign conversion). All model parameters (derivatives) were fixed and only bias terms were estimated to compensate for offsets in the control and observer measurements. As the model response is now compared to data not used for the identification, some larger differences have to be expected. The verification time history plots confirm the above given conclusions from the identification time histories:

1. There is satisfactory agreement between the flight test data and the model prediction.
2. The match for the longitudinal motion variables is significantly better than for the variables of the lateral directional motion.
3. The on-axis responses are very close whereas larger differences are seen in the off-axis time histories.
4. The yaw rate fit is less accurate than the roll or pitch rate fit. Even the on-axis response shows some larger discrepancies. A similar tendency was seen on the BO 105 results. In the Working Group Meetings DLR

pointed out that previous work also revealed difficulties in the yaw rate match. In conclusion, the conventionally used yaw motion formulation in 6 DoF models seems to be not quite appropriate.

6.1.7 Problem Areas

6.1.7.1 Data Quality

The data evaluation is discussed in section 6.1.3. Although it is difficult to assess the degree to which data problems influence the identification results, it is clear that the AH-64 database has some notable problems. Some of these data problems include:

1. short record lengths,
2. large amplitude response,
3. noisy translational acceleration measurements,
4. quantization errors in Euler angle measurements, and
5. possible turbulent flight conditions.

Noise in the acceleration measurements and quantization errors in Euler angles can be minimized or corrected during the state estimation step. Other problems such as the short record length cannot be corrected. The process noise due to gusts in particular has been shown to have detrimental effects on output error identification results.

6.1.7.2 Time Delays

Six degree-of-freedom linear models cannot account for response lags between the control input and vehicle acceleration (linear and angular) which occur in the real helicopter as a result of higher-order dynamics (e.g. rotors and actuators). Additional higher-order dynamics are further introduced into the flight data as a result of instrumentation system response and filters. In the frequency range of interest for 6 DoF flight mechanics models (e.g. 0.1 rad/s to 10 rad/s), the high-order dynamics can be satisfactorily approximated by including an effective time delay on each control input. An accurate estimate of these effective time delays is important for obtaining physically reasonable values for primary angular damping derivatives of the 6 DoF models (i.e. L_p , M_q , N_r). Time domain identification results for the BO 105 obtained by the DLR (Kaletka et al., 1989, [6.1.7]) show, for example, that the identified value of L_p is reduced by 25 % when the time delays associated with the rotor and actuators are omitted from the model structure. This reduction in the value of damping derivatives occurs so that the 6 DoF model can match the extra phase lag associated with the higher-order dynamics. Thus, the resulting damping derivatives no longer retain their physical meaning. Clearly, time delays must be included in the 6 DoF model structure for rotorcraft identification.

6.1.7.2.1 Theoretical Estimate of AH-64 Time Delays

The control signals for the AH-64 database were measured at the output of the actuators. This eliminates the contribution of the control linkages and actuators to the higher-order dynamics. The remaining higher-order dynamics are those associated with the rotor response and the sensor filters. The measurement system dynamics (rate gyros, etc.) are neglected since their bandwidth is usually very large and thus contribute only a very small effective time delay. The dynamics of the rotor tip-path-plane flapping can be approximated by a first-order response, with a time constant $\tau = 16/(\gamma\Omega)$ (Heffley, et al., 1986, [6.1.8]). The equivalent time delay for this first-order pole has the same value $\tau = 16/(\gamma\Omega)$. For the AH-64, this equivalent time delay is 0.064 s.

Before data recording, the measurements were filtered by analogue filters. For most data channels, filters with a cutoff frequency of 6 Hz (-3dB bandwidth frequency) were used. However, for the controls, the pilot seat accelerometers, and the Euler rates, filters with a cutoff frequency of 50 Hz were applied. Assuming 2nd-order Butterworth filters, the time delays associated with the measurement system filters are determined from a transfer-function fit of the filter frequency-response (Tischler, 1987, [6.1.9])

- 6 Hz filter: 0.0390 s
- 50 Hz filter: 0.0046 s.

Thus, the effective time delay due to the angular response filters is the difference between the output sensor filter delay and the input sensor filter delay: $0.039 \text{ s} - 0.0046 \text{ s} = 0.0344 \text{ s}$. The estimated total effective delay for the angular responses is the combined delay of the rotor and measurement system: $0.064 \text{ s} + 0.0344 \text{ s} = 0.0984 \text{ s}$. The vertical response to collective will have a significantly smaller time delay associated predominantly with the filter effects (0.0344 s).

6.1.7.2.2 Identification of Time Delays

Frequency- and time-domain methods were used by WG members to identify equivalent time delays for use in the 6 DoF models. Frequency-domain methods are particularly well suited to time delay identification because the time delay causes a linear increase in phase shift with frequency and thus a linear effect in the identification cost function. Parameters that cause linear changes in the cost function are identified with the highest relative accuracy. The AFDD conducted frequency-response identification and transfer-function modelling on the longitudinal and collective sweep data. Time delays were included in these models. The following time delays and standard deviations were determined:

- For the longitudinal control

Transfer function	Time delay	
	Value	Standard deviation
q / δ_{lon}	0.110 s	13%
r / δ_{lon}	0.105 s	14%
\dot{a}_z / δ_{lon}	0.117 s	14%

- For the collective control

Transfer function	Time delay	
	Value	
η / δ_{col}	0.132	
r / δ_{col}	0.104	
\dot{a}_z / δ_{col}	0.031	

The average delay for the longitudinal cyclic input responses is 0.111 s. This corresponds well with the previous estimate of 0.0978 s. The vertical response to collective has a time delay of 0.031 s, which corresponds to the filter delay of 0.0335 s, also as expected. Note that the estimated variances for the time delays (available only for the longitudinal sweeps) are quite small, indicating a reliable identification result. The use of a single time delay for each control (4 delays in total), causes all the responses to a particular input to have the same effective time delay. Thus, the effective time delay for application to the longitudinal input should be about 0.111 s. As seen by the spread in the time delays for each response variable, this is a good approximation. For collective inputs, the angular responses have an average delay of about 0.118 s. However, the use of a single delay for collective inputs, will lead to a poor match of the \dot{a}_z response. This problem in the use of the delay approximation was also found in the BO 105 results. The adoption of a high-order model that includes explicitly the rotor response, eliminates this problem (Tischler et al., 1990, [6.1.10]; (Fu et al., 1990, [6.1.11]).

Time domain analyses of the equivalent time delays were conducted by DLR, NAE, and MDHC. Each member used time-domain correlation between the control (input) and measurement (output) signals. None of these analyses provided conclusive estimates of the time delays. Therefore, the Working Group adopted the control input delay of 0.1 s for subsequent identification studies, based on the average value obtained from the AFDD frequency-domain analysis.

6.1.8 Conclusions

The models identified by the members using several different techniques all predict the aircraft response with reasonable accuracy and are therefore useful for such tasks as flight control and flight simulation analysis. The identification techniques start with flight test data evaluation. Methods ranged from Least Squares identification of simple biases and scale factors to an extended Kalman filter for data reconstruction. Identification of the model involved choice of model structure and treatment of gravitational and kinematic force terms with a range of state estimation algorithms used from Least Squares to Maximum Likelihood. Considering the different aspects of the overall identification process, it is difficult to assess the impact of any one procedure on the final results. In the end, identification of helicopter models from flight test data can be achieved using a variety of the techniques shown here with acceptable accuracy.

References

- [6.1.1] Bryson, A. E. Jr.; Ho, Y. C.
Applied Optimal Control
 Hemisphere Publishing Corporation, 1975

- [6.1.2] Du Val, R. W.; Bruhis, O.; Harrison, J. M.; Harding, J. W.
Flight Simulation Model Validation Procedure. A Systematic Approach
Vertica, Vol. 13, No. 3, 1989
- [6.1.3] Bach, R. E. Jr.
State Estimation Applications in Aircraft Flight Data Analysis (A User's Manual for SMACK)
pending NASA TR
- [6.1.4] Anon.
IMSL - FORTRAN Subroutines for Mathematics and Statistics
IMSL, Inc., Houston (Texas)
- [6.1.5] Maine, R. E.; Hiff, K. W.
Users' Manual for MMLE3, a General Fortran Program for Maximum Likelihood Parameter Estimation
NASA TP-1563, 1980
- [6.1.6] Maine, R. E.; Hiff, K. W.
Programmers' Manual for MMLE3, a General Fortran Program for Maximum Likelihood Parameter Estimation
NASA TP-1690, 1981
- [6.1.7] Kaletka, J.; von Grynhausen, W.; Tischler, M. B.; Fletcher, J. W.
Time and Frequency-Domain Identification and Verification of BO 105 Dynamic Models
15th European Rotorcraft Forum, Amsterdam, NL, 1989
- [6.1.8] Hefley, R. K.; Bourne, S. M.; Curtiss, H. C. Jr.; Hindson, W. S.; Hess, R. A.
Study of Helicopter Roll Control Effectiveness Criteria
NASA CR-177404, 1986
- [6.1.9] Tischler, M. B.
Frequency-Response Identification of XV-15 Tiltrotor Aircraft Dynamics
NASA TM-89428, ARMY TM-87-A-2, 1987
- [6.1.10] Tischler, M. B.; Cauffman, M. G.
Frequency-Response Method for Rotorcraft System Identification with Applications to the BO 105 Helicopter
46th Annual Forum of the American Helicopter Society, Washington, DC, 1990
- [6.1.11] Fu, K.H.; Kaletka, J.
Frequency-Domain Identification of BO 105 Derivative Models with Rotor Degrees of Freedom
16th European Rotorcraft Forum, Glasgow, UK, 1990

Overall dimensions Overall Length 17.73 m Fuselage Length 14.97 m Overall Height 5.23 m	Main rotor		Wing	
	Diameter	14.83 m	Span	4.88 m
	Blades	4	Planform Area	5.75 m ²
	Chord	0.533 m	Aspect Ratio	4.31
Mass and moments of inertia Mass 6643 kg I_x 8294 kg m ² I_y 52994 kg m ² I_z 50187 kg m ² I_{zx} 4847 kg m ²	Profile	HH02	Incidence	6°
	Blade Area	15.6 m ²	Horizontal stabilator	
	Solidity (Thrust)	0.092	Span	3.92 m
	Tip Sweep	20°	Area	3.34 m ²
	Twist	-9°	Aspect Ratio	4.6
	Shaft Angle	5°	Profile	NACA 0018
			Incidence	0°
			Dihedral	0°
	Tail rotor		Vertical tail	
	Diameter	2.785 m	Span	2.73 m
	Blades	4	Area	2.99 m ²
	Chord	0.254 m	Aspect Ratio	2.50
	Profile	NACA 84A410	Profile	NACA 4415 root
	Solidity	0.2258		NACA 4418 tip
	Twist	-8.8°	Incidence	0°
			Dihedral	0°

Table 6.1.1. List of physical characteristics of the AH-64

Group	Variables	Source	Original Sampling Rate (in Hz)
	Quantity		
Control displacements	Forward/Aft Cyclic	Actuator	470
	Lateral Cyclic	Actuator	470
	Collective	Actuator	941
	Tail Rotor Collective	Actuator	470

Table 6.1.2. AH-64 Control Variables

Group	Variables	Source	Original Sampling Rate (in Hz)
	Quantity		
Air data	Angle of attack	Boom System	941
	Angle of sideslip	Boom System	470
	Airspeed	Boom System	59
Flight path data	Longitudinal speed	Doppler radar	941
	Lateral speed	Doppler radar	941
	Normal speed	HARS	470
Linear accelerations	Longitudinal acceleration	Accelerometer at CG	470
	Lateral acceleration	Accelerometer at CG	470
	Normal acceleration	Accelerometer at CG	470
Linear accelerations	Longitudinal acceleration	Accelerometer at pilot's seat	470
	Lateral acceleration	Accelerometer at pilot's seat	470
	Normal acceleration	Accelerometer at pilot's seat	941
Attitude angles (Euler angles)	Roll angle	HARS	59
	Pitch angle	HARS	59
	Yaw angle	HARS	59
Angular rates	Roll rate	Rate gyro	941
	Pitch rate	Rate gyro	941
	Yaw rate	Rate gyro	941
Angular rates	Euler roll rate	Calculated from roll angle	470
	Euler pitch rate	Calculated from pitch angle	941
	Euler yaw rate	Calculated from yaw angle	470
Angular accelerations	Roll acceleration	Angular accelerometer	941
	Pitch acceleration	Angular accelerometer	941
	Yaw acceleration	Angular accelerometer	941

Table 6.1.3. AH-64 Response Variables
 Data provided at a uniform sampling rate of 100 Hz.

File	Control Input			Number of runs	Recording time per run in s	Flight Conditions	
	Control	Type	Initial displacement	Duration t_i or Frequency content f_i		Airspeed	Altitude
1	Longitudinal	Doublet	Forward	$t_i \approx 6s$	1	13	$H_0 \approx 3500$ ft
2	Longitudinal	Doublet	Aft	$t_i \approx 7s$	1	13	$H_0 \approx 3500$ ft
3	Lateral	Doublet	Left	$t_i \approx 7s$	1	13	$H_0 \approx 3500$ ft
4	Lateral	Doublet	Right	$t_i \approx 7s$	1	13	$H_0 \approx 3500$ ft
5	Pedal	Doublet	Left	$t_i \approx 7s$	1	13	$H_0 \approx 3500$ ft
6	Pedal	Doublet	Right	$t_i \approx 7s$	1	13	$H_0 \approx 3500$ ft
7	Collective	Doublet	Up	$t_i \approx 8s$	1	13	$H_0 \approx 3500$ ft
8	Collective	Doublet	Down	$t_i \approx 8s$	1	13	$H_0 \approx 3500$ ft
9	Longitudinal	Pulse	Forward	---	1	13	$H_0 \approx 3500$ ft
10	Longitudinal	Pulse	Aft	---	1	13	$H_0 \approx 3500$ ft
11	Lateral	Pulse	Right	---	1	13	$H_0 \approx 3500$ ft
12 ... 14	Longitudinal	Frequency sweep	---	$0.1Hz \leq f_i \leq 3Hz$	3	114 ... 158	$H_0 \approx 3500$ ft
15, 16	Lateral	Frequency sweep	---	$0.1Hz \leq f_i \leq 3Hz$	2	127 ... 138	$H_0 \approx 3500$ ft
17	Lateral	Frequency sweep	---	$0.3Hz \leq f_i \leq 13Hz$	1	138	$H_0 \approx 3500$ ft
18, 19	Pedal	Frequency sweep	---	$0.1Hz \leq f_i \leq 3Hz$	2	118 ... 141	$H_0 \approx 3500$ ft
20	Collective	Frequency sweep	---	$0.1Hz \leq f_i \leq 3Hz$	1	140	$H_0 \approx 3500$ ft
21	Collective	Frequency sweep	---	$0.3Hz \leq f_i \leq 13Hz$	1	131	$H_0 \approx 3500$ ft

Table 6.1.4. AH-64: List of runs

Scale factor for		AFDD		DLR		DLR	NAE		NLR	
Symbol	Unit	Value	σ	Value	σ	Value	Value	σ	Value	σ
u	1	---	---	1.0987	0.1495	1.128	---	---	---	---
v	1	---	---	1.0834	0.1704	1.015	---	---	---	---
w	1	---	---	1.0154	0.1465	0.962	---	---	---	---
Φ	1	---	---	0.9591	0.0292	0.981	---	---	---	---
Θ	1	---	---	0.9488	0.0237	0.972	---	---	---	---
Ψ	1	---	---	0.8210	0.1651	1.002	---	---	---	---

* From doublet and pulse files ** From doublet files *** From concatenated doublet files
 σ = Standard deviation

Table 6.1.5. AH-64 Identification Results: Mean values of scale factors

Bias for		AFDD		DLR		DLR	NAE		NLR	
Symbol	Unit	Value	σ	Value	σ	Value	Value	σ	Value	σ
a_x	m/s ²	2.0228	0.2041	2.2731	0.1757	2.281	2.2100	0.335	2.1450	0.9286
a_y	m/s ²	0.0223	0.1678	-0.0137	0.2263	-0.080	-0.0170	0.163	0.0233	0.2077
a_z	m/s ²	-0.0888	0.1768	-0.2043	0.2511	-0.165	-0.144	0.202	0.0274	0.2210
p	rad/s	-0.0021	0.0007	-0.0025	0.0012	-0.0025	-0.0025	0.0014	-0.0032	0.0018
q	rad/s	-0.0115	0.0011	-0.0109	0.0019	-0.011	-0.0110	0.0017	-0.0111	0.0017
r	rad/s	-0.0015	0.0017	-0.0015	0.0033	-0.0021	-0.0013	0.0024	-0.0019	0.0028
u	m/s	---	---	---	---	---	0.085	1.29	---	---
v	m/s	---	---	---	---	---	0.301	0.864	---	---
w	m/s	---	---	---	---	---	0.492	1.09	---	---
Φ	rad	---	---	---	---	---	-0.0025	0.0089	---	---
Θ	rad	---	---	---	---	---	-0.006	0.005	---	---
Ψ	rad	---	---	---	---	---	0.0003	0.0105	---	---

* From doublet and pulse files ** From doublet files *** From concatenated doublet files

Table 6.1.6. AH-64 Identification Results: Mean values of biases

Quantity		Longitudinal control		Lateral control		Tail rotor		Collective control	
Symbol	Unit	Files 12 and 13		Files 15 through 17		Files 18 and 19		Files 20 and 21	
		Value	σ	Value	σ	Value	σ	Value	σ
a_x	m/s ²	-1.0720	0.1928	-1.1638	0.0657	-1.1900	0.2089	1.2695	0.0008
a_y	m/s ²	-1.4200	0.0284	1.2680	0.1630	1.1180	0.0361	0.7912	0.0445
a_z	m/s ²	-0.0600	0.0028	1.0994	0.2300	1.0184	0.0437	-0.2747	0.0608
p	rad/s	-0.0012	0.0008	-0.0013	0.0011	-0.0120	0.0023	0.0013	0.0019
q	rad/s	0.0244	0.0107	0.0864	0.0028	0.0927	0.0008	-0.0015	0.0002
r	rad/s	-0.0018	0.0012	-0.0955	0.0010	-0.0040	0.0020	-0.0053	0.0020

* From doublet and pulse files ** From doublet files *** From concatenated doublet files
 σ = Standard deviation

Table 6.1.7. AH-64: AFDD results for mean values of frequency sweep biases

Derivative		MDHC	NAE		DLR 1		DLR 2		DLR 3		NLR 1		NLR 2	
Symbol	Unit	Value	Value	σ	Value	σ	Value	σ	Value	σ	Value	σ	Value	σ
X_u	1/s	-0.0038	-0.0250	0.0007	-0.0224	0.0011	-0.0292	0.0006	-0.0272	0.0004	-0.0291	0.0041	-0.0335	0.0065
X_v	1/s	-0.011	0.0173	0.0013	0 *	—	0 *	—	0 *	—	0 *	—	0 *	—
X_w	1/s	0.034	0.0119	0.0009	0.0153	0.0009	0.0223	0.001	0.0200	0.0006	-0.0252	0.0022	-0.0337	0.0027
X_p	m/(rad s)	-0.524	0.332	0.039	0 *	—	0 *	—	0 *	—	0 *	—	0 *	—
X_q	m/(rad s)	-0.804	0.035	0.060	0 *	—	0 *	—	0 *	—	0 *	—	0 *	—
X_r	m/(rad s)	-0.332	-0.266	0.030	0 *	—	0 *	—	0 *	—	0 *	—	0 *	—
Y_u	1/s	-0.018	-0.0172	0.0011	0 *	—	0 *	—	0 *	—	0 *	—	0 *	—
Y_v	1/s	-0.059	-0.114	0.0021	-0.141	0.0042	-0.122	0.0026	-0.125	0.0022	-0.088	0.0141	-0.109	0.0098
Y_w	1/s	0.039	0.0241	0.0016	0 *	—	0 *	—	0 *	—	0 *	—	0 *	—
Y_p	m/(rad s)	-0.254	-0.548	0.065	-0.101	0.107	-0.195	0.068	-0.469	0.057	0 *	—	0 *	—
Y_q	m/(rad s)	-2.70	-1.005	0.109	0 *	—	0 *	—	0 *	—	0 *	—	0 *	—
Y_r	m/(rad s)	0.575	1.050	0.053	-0.010	0.093	-0.490	0.073	-0.410	0.056	0.268	0.62	0.321	0.40
Z_u	1/s	0.021	-0.0160	0.0062	0.0834	0.0069	0.0281	0.0025	0.0266	0.0018	0.0650	0.018	-0.2315	0.033
Z_v	1/s	0.06	0.017	0.010	0 *	—	0 *	—	0 *	—	0 *	—	0 *	—
Z_w	1/s	-0.416	-0.414	0.0081	-0.547	0.0056	-0.506	0.0056	-0.528	0.0041	-0.641	0.010	-0.396	0.013
Z_p	m/(rad s)	0.394	-1.192	0.30	0 *	—	0 *	—	0 *	—	0 *	—	0 *	—
Z_q	m/(rad s)	-15.2	-11.84	0.53	-7.01	0.40	-4.12	0.30	-5.60	0.25	0 *	—	0 *	—
Z_r	m/(rad s)	1.83	1.259	0.26	0 *	—	0 *	—	0 *	—	0 *	—	0 *	—
* Eliminated from model structure														
σ = Standard deviation														

Table 6.1.8. AH-64 Identification Results: List of specific force derivatives with respect to flight variables

Derivative Symbol	Unit	MDHC Value	NAE		DLR Value	DLR 2		DLR 3		NLR 1		NLR 2	
			Value	σ		Value	σ	Value	σ	Value	σ	Value	σ
L_u	rad/(s m)	-0.029	-0.24	0.0013	0.0010	-0.3298	0.0002	-0.0096	0.0003	-0.0161	0.0026	-0.0124	0.0045
L_v	rad/(s m)	-0.038	-0.05	0.0021	-0.123	0.0027	0.0013	-0.106	0.0013	-0.087	0.0045	-0.073	0.0030
L_w	rad/(s m)	0.034	0.0403	0.0017	0.0141	0.0016	0.0011	0.0297	0.0010	-0.0004	0.0039	0.0088	0.0026
L_p	1/s	-2.78	-3.189	0.065	-3.637	0.080	0.040	-3.216	0.041	-2.073	0.133	-1.956	0.111
L_q	1/s	-0.21	-0.366	0.11	0.719	0.11	0.040	-0.507	0.066	0.660	0.24	0.123	0.19
L_r	1/s	0.537	0.155	0.055	-0.013	0.047	-1.285	-0.598	0.030	0.423	0.122	0.325	0.086
M_u	rad/(s m)	0.010	0.0076	0.0003	0.0027	0.0002	-0.0002	0.00005	0.0008	-0.0016	0.0015	-0.0011	0.0026
M_v	rad/(s m)	0.017	0.0177	0.0007	0.0256	0.0004	0.0171	0.0002	0.0186	0.0133	0.0018	0.0120	0.0014
M_w	rad/(s m)	0.005	0.0068	0.0005	0.0130	0.0003	0.0107	0.0002	0.0120	0.0129	0.0022	0.0035	0.0013
M_p	1/s	0.088	0.0795	0.019	0.1142	0.014	-0.0539	0.005	-0.0387	-0.1536	0.060	-0.0436	0.056
M_q	1/s	-0.574	-0.757	0.032	-0.774	0.019	-0.723	0.012	-0.739	-0.648	0.13	-0.304	0.11
M_r	1/s	-0.082	-0.0244	0.015	0.0	0.0	0.0	0.0	0.0	0.0	0.0	0.0	0.0
N_u	rad/(s m)	-0.004	-0.00395	0.0006	0.0	0.0	0.0	0.0	0.0	0.0	0.0	0.0	0.0
N_v	rad/(s m)	0.028	0.0274	0.0012	0.0394	0.0005	0.0430	0.0003	0.0437	0.0371	0.0026	0.0328	0.0016
N_w	rad/(s m)	-0.0003	-0.0018	0.0008	0.0	0.0	0.0	0.0	0.0	0.0075	0.0013	-0.0004	0.0009
N_p	1/s	-0.122	-0.1351	0.037	-0.0562	0.014	-0.0731	0.008	-0.0804	0.0226	0.079	-0.0998	0.054
N_q	1/s	0.701	0.788	0.051	0.832	0.011	-0.025	0.010	0.316	0.092	0.084	0.283	0.061
N_r	1/s	-0.642	-0.723	0.027	-0.607	0.008	-0.246	0.027	-0.415	-0.329	0.069	-0.318	0.044

* Eliminated from model structure
 σ = Standard deviation

Table 6.1.9. AH-64 Identification Results: List of specific moment derivatives with respect to flight variables

Derivative		MDHC		NAE		DLR 1		DLR 2		DLR 3		NLR 1		NLR 2		AFDD **	
Symbol	Unit	Value	σ	Value	σ	Value	σ	Value	σ	Value	σ	Value	σ	Value	σ	Value	σ
$X_{\delta col}$	m/(s ² %)	0.008	0.0055	-0.0055	0.0007	0 *	—	0 *	—	0 *	—	0 *	—	0 *	—	—	—
$X_{\delta lon}$	m/(s ² %)	-0.025	-0.0391	-0.0391	0.0010	-0.0354	0.0011	-0.0351	0.0014	-0.0356	0.0009	-0.0443	0.0040	-0.0798	0.0051	-0.0317	0.0019
$X_{\delta lat}$	m/(s ² %)	0.005	-0.0202	0.0008	0.002	0 *	—	0 *	—	0 *	—	0 *	—	0 *	—	—	—
$X_{\delta ped}$	m/(s ² %)	-0.008	0.0101	0.0008	0.0008	0 *	—	0 *	—	0 *	—	0 *	—	0 *	—	—	—
$Y_{\delta col}$	m/(s ² %)	0.049	0.0257	0.0257	0.0012	0 *	—	0 *	—	0 *	—	0 *	—	0 *	—	—	—
$Y_{\delta lon}$	m/(s ² %)	0.046	0.0369	0.0369	0.0017	0 *	—	0 *	—	0 *	—	0 *	—	0 *	—	—	—
$Y_{\delta lat}$	m/(s ² %)	0.015	0.0288	0.0288	0.0028	0.0349	0.0035	0.0150	0.0029	0.0243	0.0022	0.0108	0.0130	0.0011	0.0109	—	—
$Y_{\delta ped}$	m/(s ² %)	-0.031	-0.0291	-0.0291	0.0012	-0.0004	0.0019	-0.0031	0.0016	-0.0039	0.0013	0.0132	0.0123	-0.0098	0.0098	—	—
$Z_{\delta col}$	m/(s ² %)	-0.153	-0.171	-0.171	0.001	-0.294	0.005	-0.227	0.005	-0.259	0.004	-0.259	0.023	-0.271	0.024	-0.314	—
$Z_{\delta lon}$	m/(s ² %)	-0.058	-0.051	-0.051	0.008	-0.141	0.006	-0.092	0.006	-0.104	0.005	-0.207	0.018	0.0512	0.025	-0.234	0.009
$Z_{\delta lat}$	m/(s ² %)	0.041	0.0862	0.0862	0.012	0 *	—	0 *	—	0 *	—	0 *	—	0 *	—	—	—
$Z_{\delta ped}$	m/(s ² %)	-0.018	-0.0531	-0.0531	0.006	0 *	—	0 *	—	0 *	—	0 *	—	0 *	—	—	—

* Eliminated from model structure
 ** Values determined from frequency domain calculations
 σ = Standard deviation

Table 6.1.10. AH-64 Identification Results: List of specific force derivatives with respect to control deflections

Derivative		MDHC	NAE		DLR 1		DLR 2		DLR 3		MLR 1		MLR 2		AFDD **	
Symbol	Unit	Value	Value	σ	Value	σ	Value	σ	Value	σ	Value	σ	Value	σ	Value	σ
$L_{\delta col}$	rad/(s ² %)	0.021	0.0303	0.001	0.0140	0.001	-0.0058	0.001	0.0185	0.0008	-0.0062	0.004	0.0138	0.003	—	—
$L_{\delta lon}$	rad/(s ² %)	0.01	0.0152	0.0018	-0.0295	0.0019	-0.0471	0.0015	-0.0209	0.0011	-0.0063	0.0044	-0.0170	0.0039	—	—
$L_{\delta lat}$	rad/(s ² %)	0.124	0.141	0.0027	0.140	0.0027	0.135	0.0014	0.139	0.0015	0.097	0.0054	0.093	0.0046	—	—
$L_{\delta ped}$	rad/(s ² %)	-0.045	-0.0480	0.0012	-0.0208	0.0013	-0.0216	0.0006	-0.0222	0.0006	-0.0434	0.0028	-0.0290	0.0023	—	—
$M_{\delta col}$	rad/(s ² %)	0.008	0.0077	0.0003	0.0112	0.0002	0.0127	0.0002	0.0118	0.0002	0.0125	0.0022	0.0085	0.0017	0.0169	—
$M_{\delta lon}$	rad/(s ² %)	0.017	0.0195	0.0005	0.0275	0.0003	0.0288	0.0003	0.0272	0.0002	0.0254	0.0023	0.0227	0.0019	0.0317	0.0010
$M_{\delta lat}$	rad/(s ² %)	-0.009	-0.0098	0.0008	-0.0081	0.0005	0.0000	0.0002	-0.0024	0.0003	-0.0008	0.0025	-0.0028	0.0023	—	—
$M_{\delta ped}$	rad/(s ² %)	0.002	0.0025	0.0004	0 *	—	0 *	—	0 *	—	0 *	—	0 *	—	—	—
$N_{\delta col}$	rad/(s ² %)	0.004	0.0004	0.0006	0.0028	0.0002	0.0091	0.0002	0.0084	0.0002	0 *	—	0 *	—	0.17	—
$N_{\delta lon}$	rad/(s ² %)	-0.015	-0.0195	0.0009	-0.0150	0.0003	-0.0014	0.0002	-0.0088	0.0002	0 *	—	0 *	—	—	—
$N_{\delta lat}$	rad/(s ² %)	0.010	0.0112	0.0016	0.0079	0.0004	0.0026	0.0003	0.0018	0.0003	0.0013	0.0032	0.0029	0.0022	—	—
$N_{\delta ped}$	rad/(s ² %)	0.028	0.0315	0.0007	0.0293	0.0002	0.0249	0.0002	0.0291	0.0002	0.0285	0.0016	0.0231	0.0011	—	—
* Eliminated from model structure																
** Values determined from frequency domain calculations																
σ = Standard deviation																

Table 6.1.11. AH-64 Identification Results: List of specific moment derivatives with respect to control deflections

Derivative		MDHC		NAE		DLR 1		DLR 2		DLR 3		NLR 1		NLR 2		AFDD **	
Symbol	Unit	Value	σ	Value	σ	Value	σ	Value	σ	Value	σ	Value	σ	Value	σ	Value	σ
$r_{\delta col}$	S	0	0.1 *	—	—	0.1 *	—	0.1 *	—	0.1 *	—	0.1 *	—	0.1 *	—	—	—
$r_{\delta lon}$	S	0	0.1 *	—	—	0.1 *	—	0.1 *	—	0.1 *	—	0.1 *	—	0.1 *	—	—	—
$r_{\delta lat}$	S	0	0.1 *	—	—	0.1 *	—	0.1 *	—	0.1 *	—	0.1 *	—	0.1 *	—	—	—
$r_{\delta ped}$	S	0	0.1 *	—	—	0.1 *	—	0.1 *	—	0.1 *	—	0.1 *	—	0.1 *	—	—	—
$r_{q/ \delta col}$	S	—	—	—	—	—	—	—	—	—	—	—	—	—	—	0.132	—
$r_{r/ \delta col}$	S	—	—	—	—	—	—	—	—	—	—	—	—	—	—	0.104	—
$r_{az/ \delta col}$	S	—	—	—	—	—	—	—	—	—	—	—	—	—	—	0.031	—
$r_{q/ \delta lon}$	S	—	—	—	—	—	—	—	—	—	—	—	—	—	—	0.110	0.0132
$r_{w/ \delta lon}$	S	—	—	—	—	—	—	—	—	—	—	—	—	—	—	0.105	0.0137
$r_{ax/ \delta lon}$	S	—	—	—	—	—	—	—	—	—	—	—	—	—	—	0.117	0.140
* Values taken from AFDD identification average ** Values determined from frequency domain calculations σ = Standard deviation																	

Table 6.1.12. AH-64 Identification Results: Equivalent control time delays

Mode of motion	MDHC *	MDHC	NAE	DLR 1	DLR 2	DLR 3	NLR 1	NLR 2
Phugoid oscillation	[-0.29, 0.3]	[-0.45, 0.32]	[-0.39, 0.28]	[-0.68, 0.206]	[-0.062, (-0.20)†]	[-0.84, 0.162]	[-0.023, 0.12]	[0.43, 0.23]
Dutch roll oscillation	[0.05, 1.65]	[0.077, 1.53]	[0.0, 3, 1.46]	[0.098, 1.74]	[0.043, 1.78]	[0.064, 1.80]	[0.089, 1.59]	[0.042, 1.61]
Aperiodic roll mode	—	(2.98)	(3.40)	(3.81)	(3.39)	(3.36)	(2.11)	(2.14)
Aperiodic pitch mode 1	—	(1.25)	(1.47)	(1.63)	(1.42)	(1.54)	(1.54)	(0.89)
Aperiodic pitch mode 2	—	(0.32)	(0.34)	(0.22)	(0.11)	(0.60)	(-0.22)	(-0.30)
Spiral mode	—	(0.020)	(0.0036)	(0.01)	(0.055)	(0.028)	(0.17)	(0.053)

* From visual inspection of other flight tests.

† In this case the phugoid oscillation degenerates into two aperiodic modes.

Shorthand notation:

s Laplace variable (in 1/s)

[ζ, ω_0] represents ($s^2 + 2\zeta\omega_0 s + \omega_0^2$)

with ζ = damping ratio and ω_0 = undamped natural frequency (in rad/s)

(1/T) represents ($s + 1/T$)

with T = time constant (in s)

Table 6.1.13. AH-64 Identification Results: Time constants, damping ratios and undamped natural frequencies



Figure 6.1.1. AH-64 Apache in flight

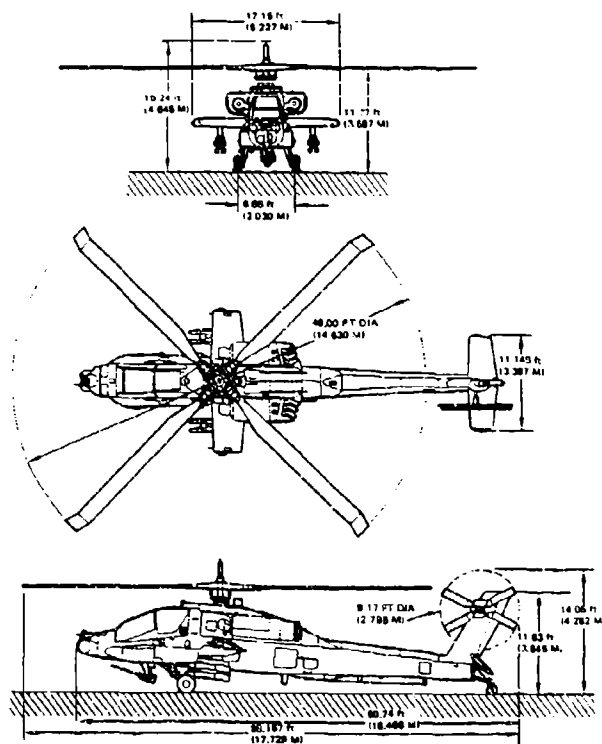


Figure 6.1.2. Three-view drawing of AH-64

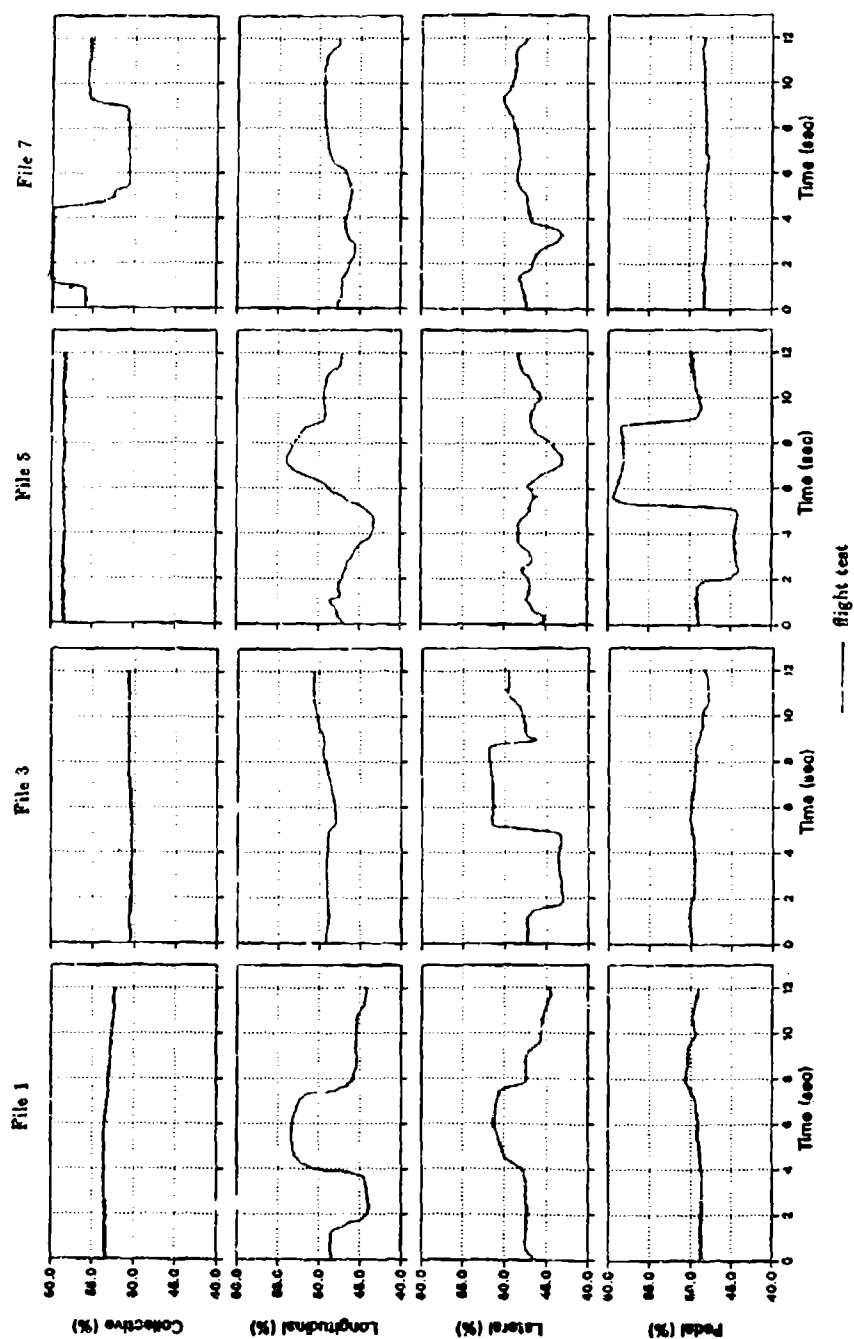


Figure 6.1.3. Control time histories for data group 1

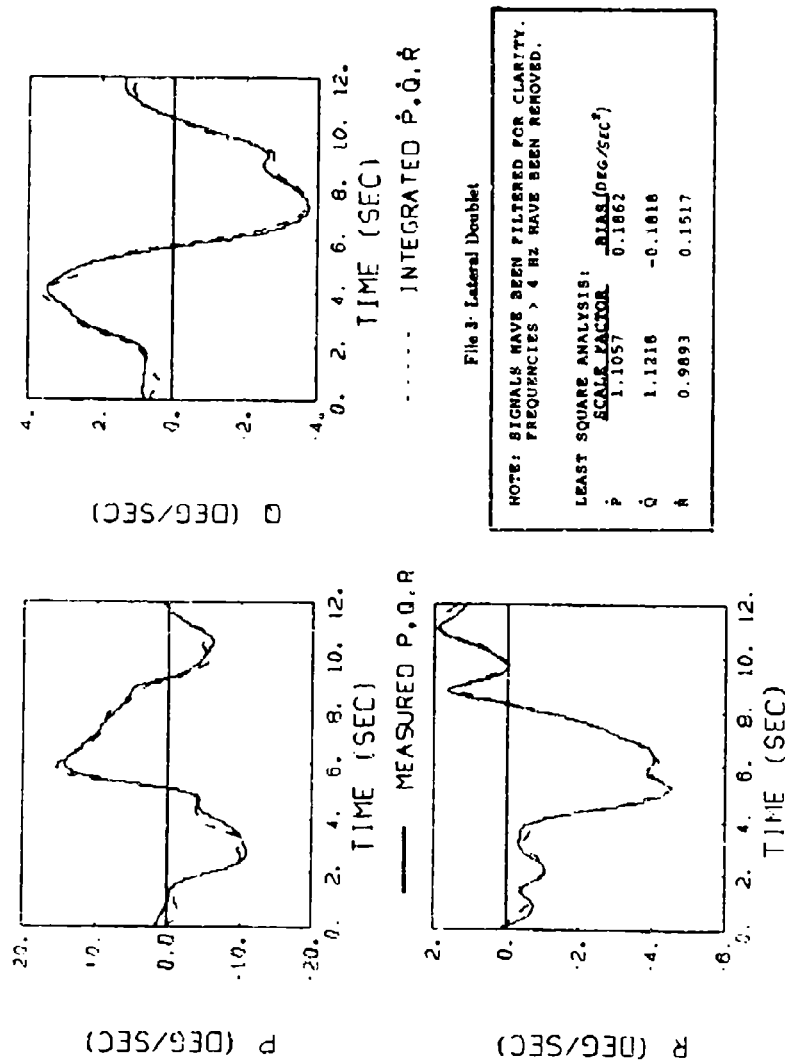


Figure 6.1.4. Angular acceleration consistency for file 3 (MDHC)

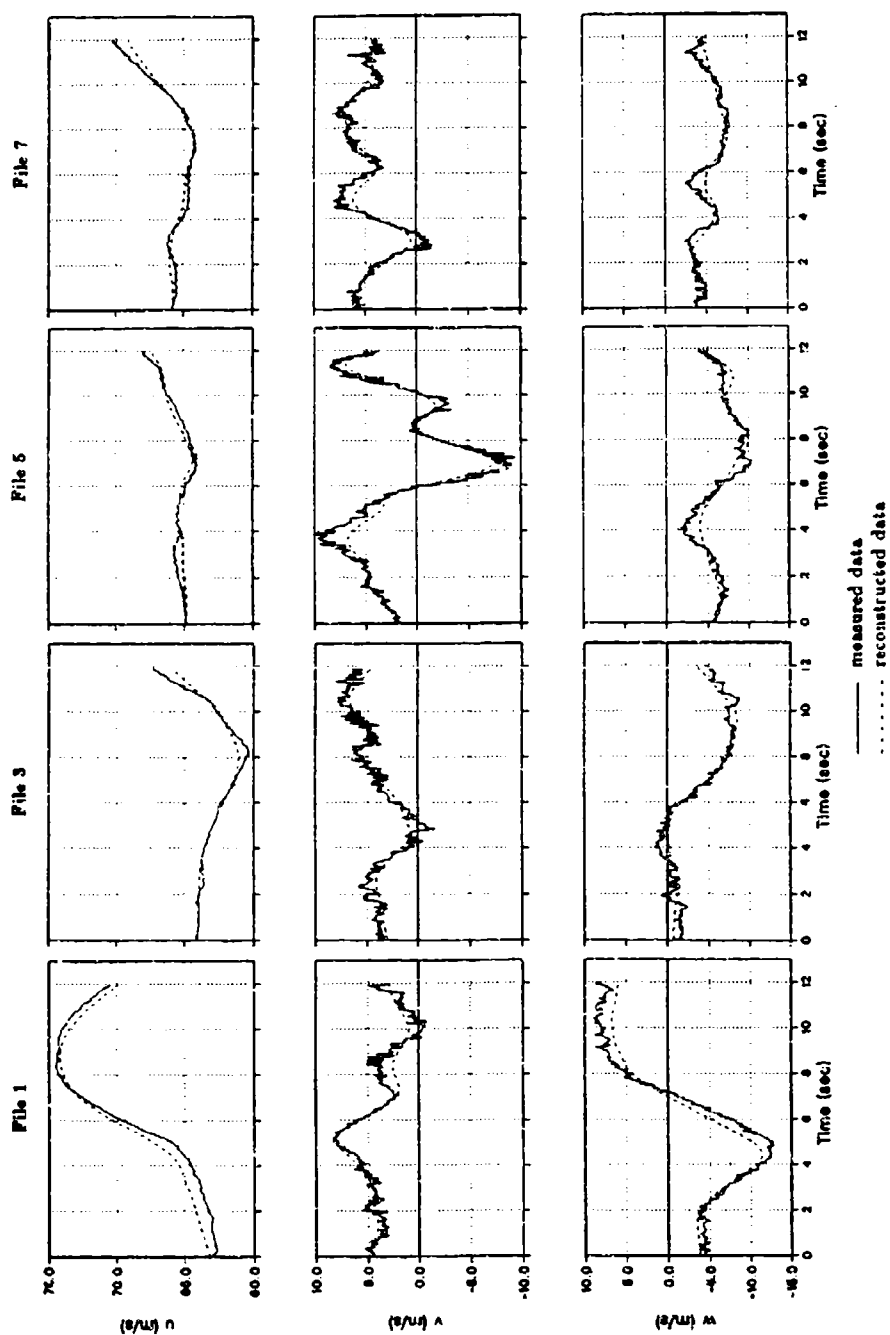


Figure 6.1.5. Comparison of measured and reconstructed time histories: linear velocities (MDHC)
(Result from Kalman Filter state estimation)

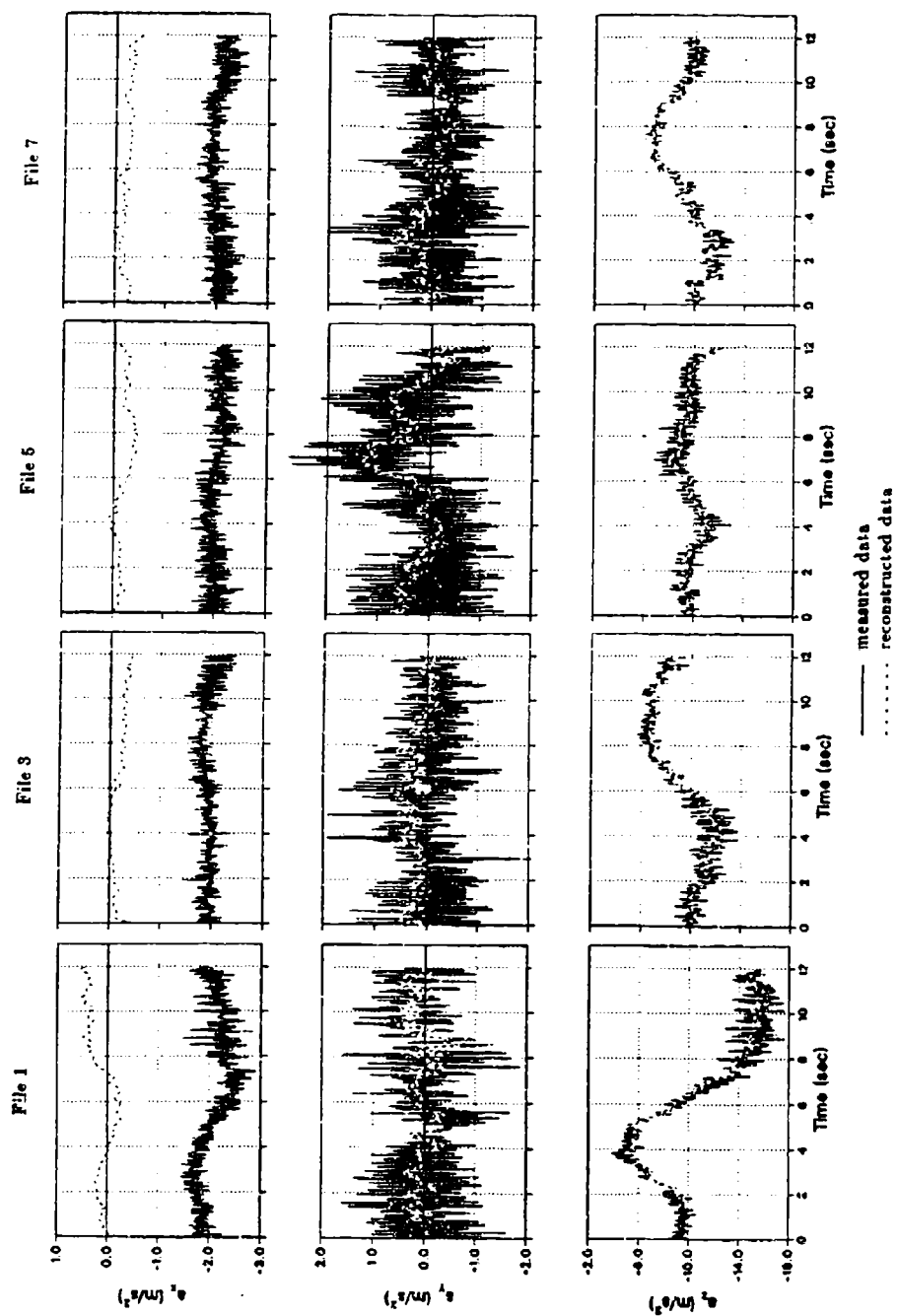


Figure 6.1.6. Comparison of measured and reconstructed time histories: linear accelerations (MDHC)
(Result from Kalman filter state estimation)

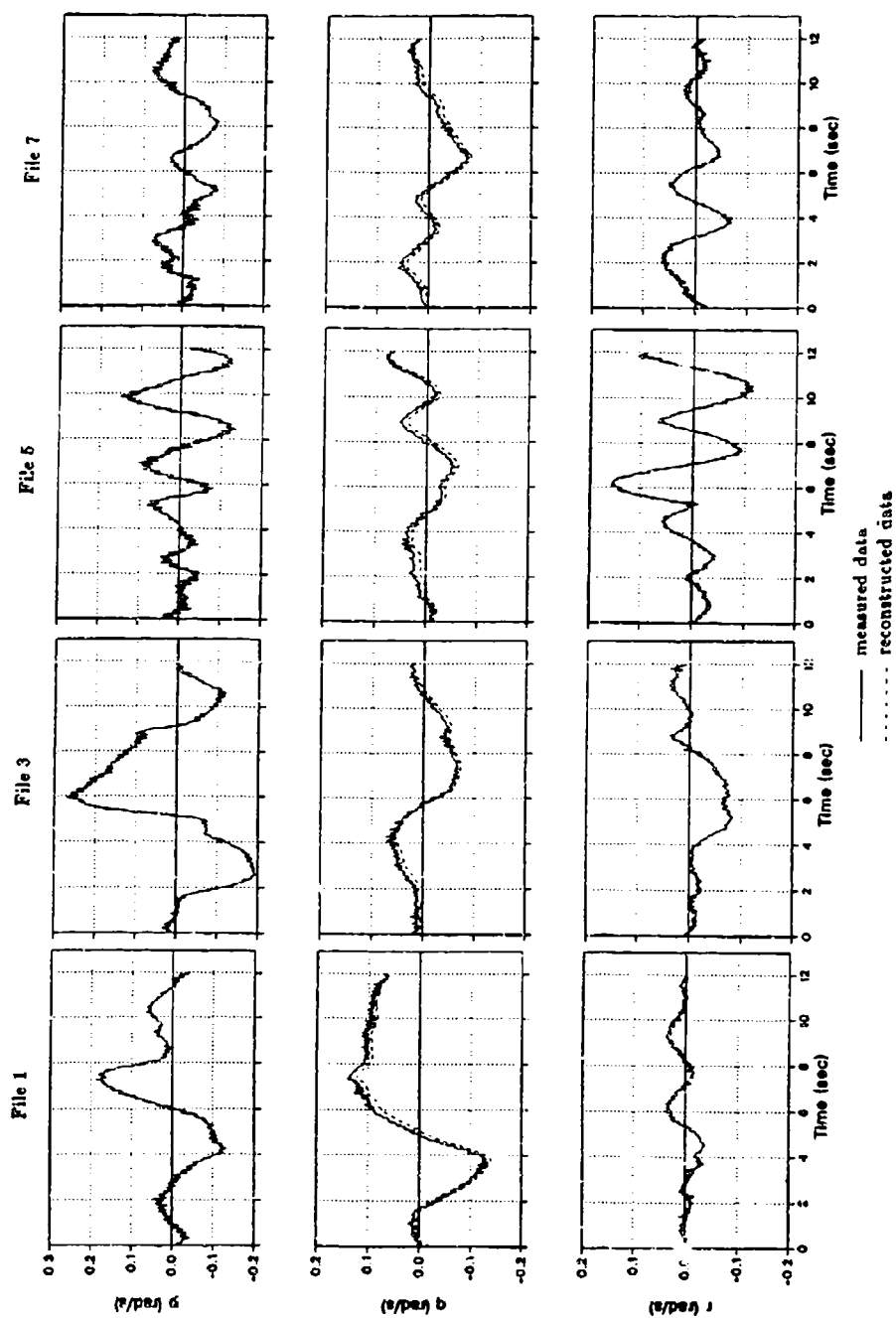


Figure 6.1.7. Comparison of measured and reconstructed time histories: angular rates (MDHC)
(Result from Kalman filter state estimation)

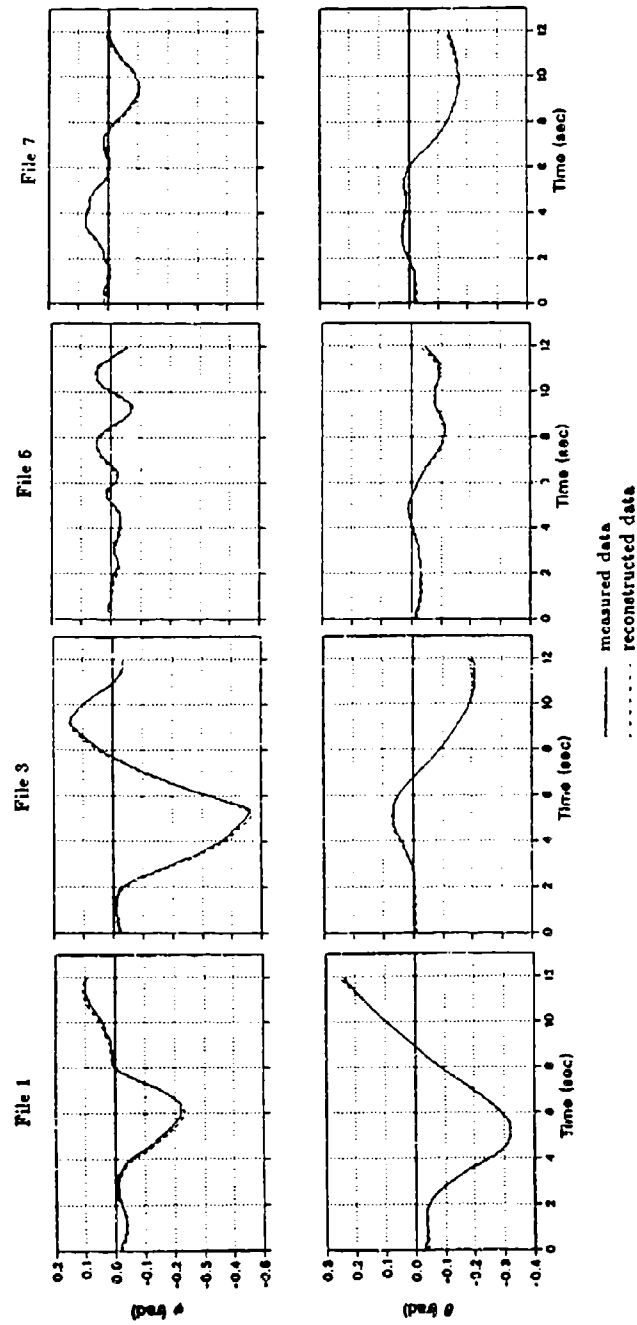


Figure 6.1.8. Comparison of measured and reconstructed time histories: Euler angles (MDHC)
(Result from Kalman filter state estimation)

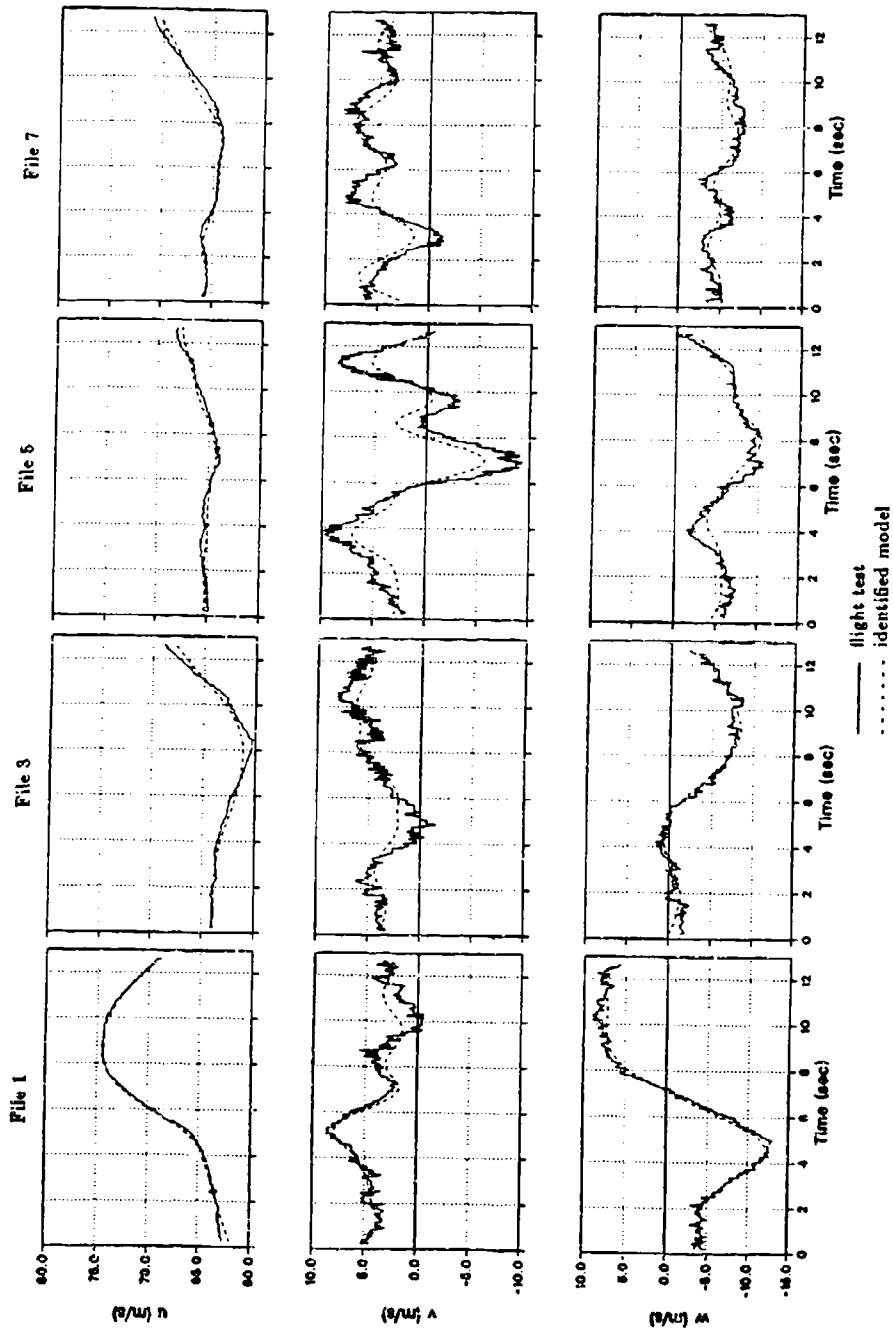


Figure 6.1.9. Identification result: Time history comparison of measured data and the response of the identified model, linear velocities (DLR I)

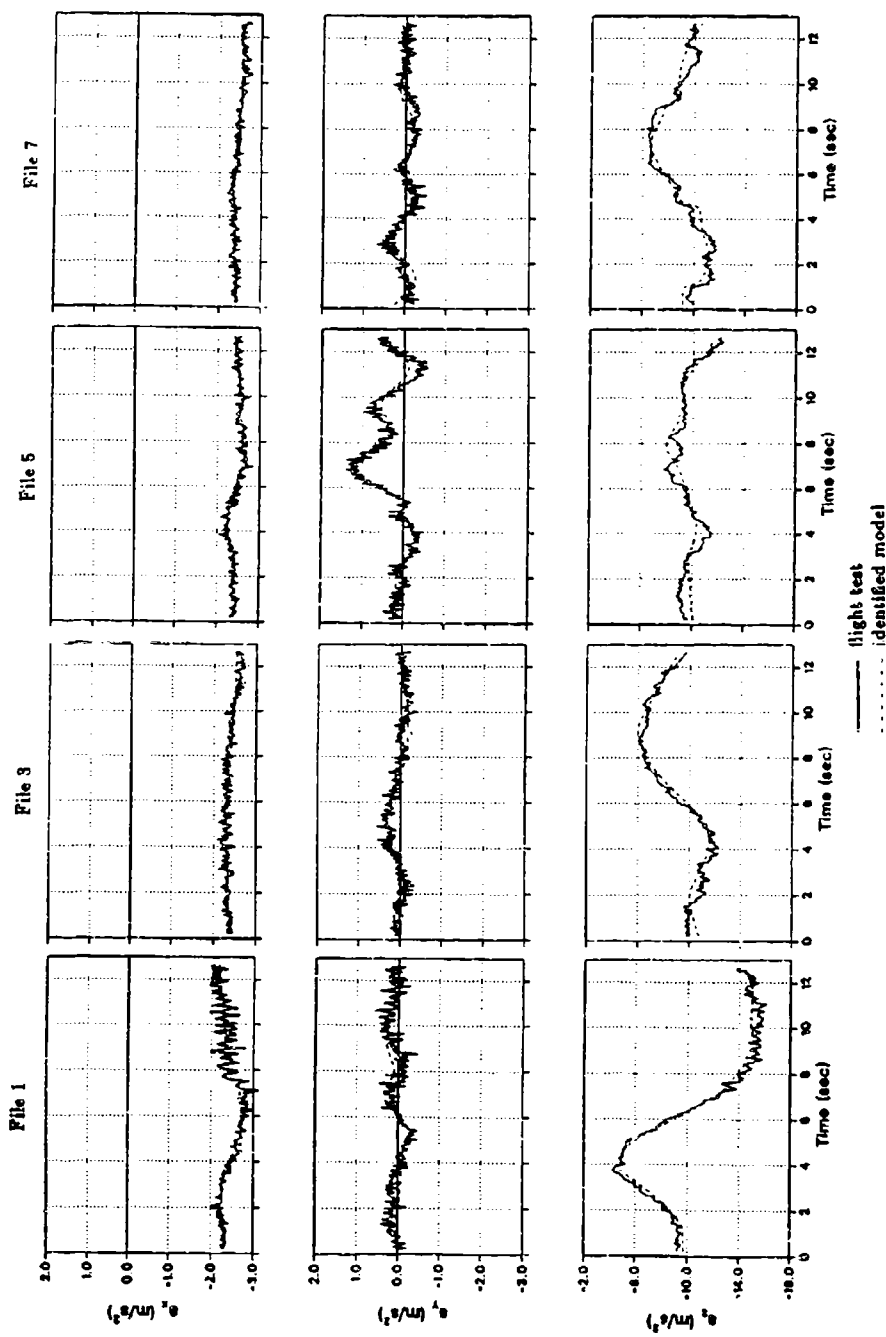


Figure 6.1.10. Identification result: Time history comparison of measured data and the response of the identified model, linear accelerations (DLR1)

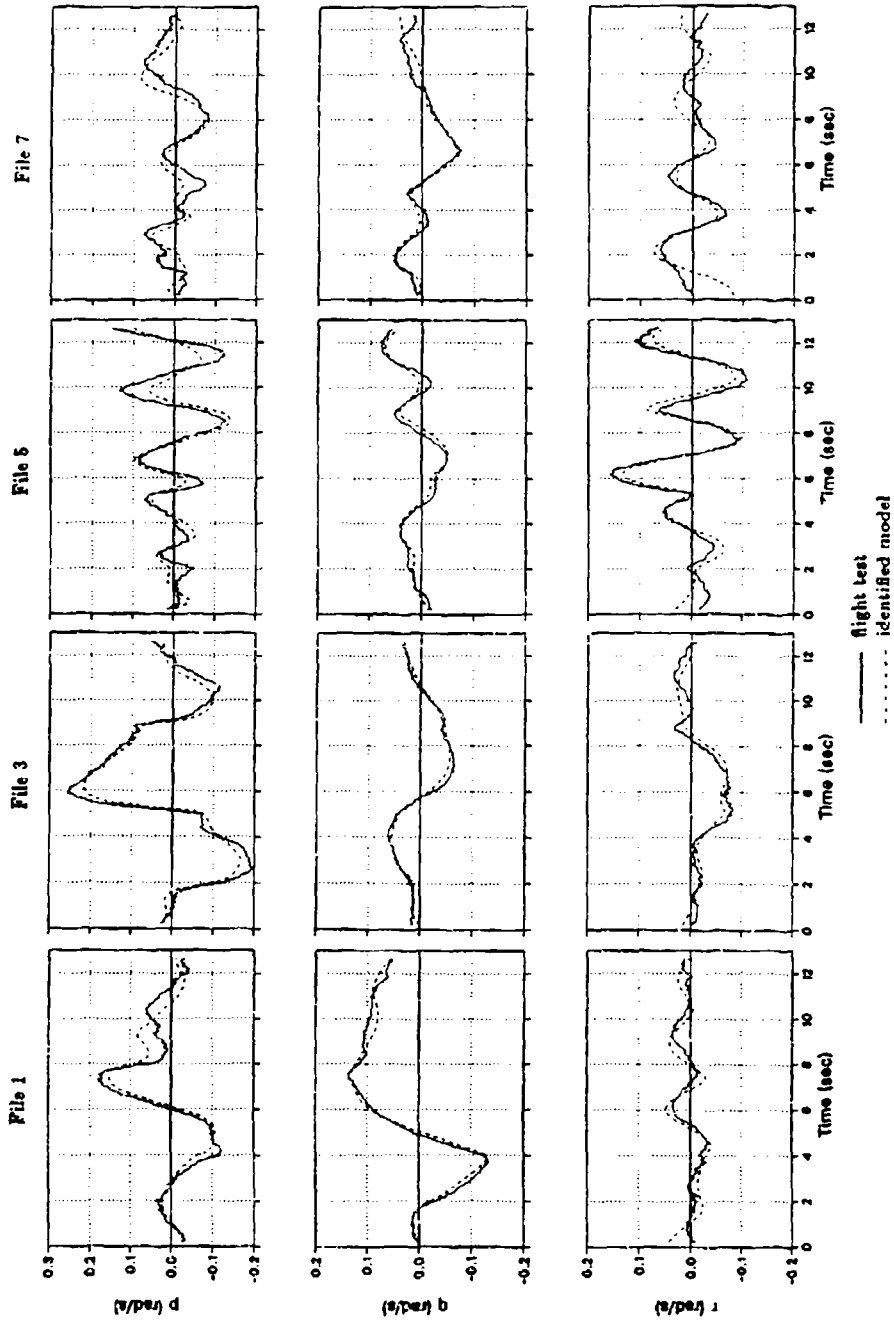


Figure 6.1.11. Identification result: Time history comparison of measured data and the response of the identified model, angular rates (DLR1)

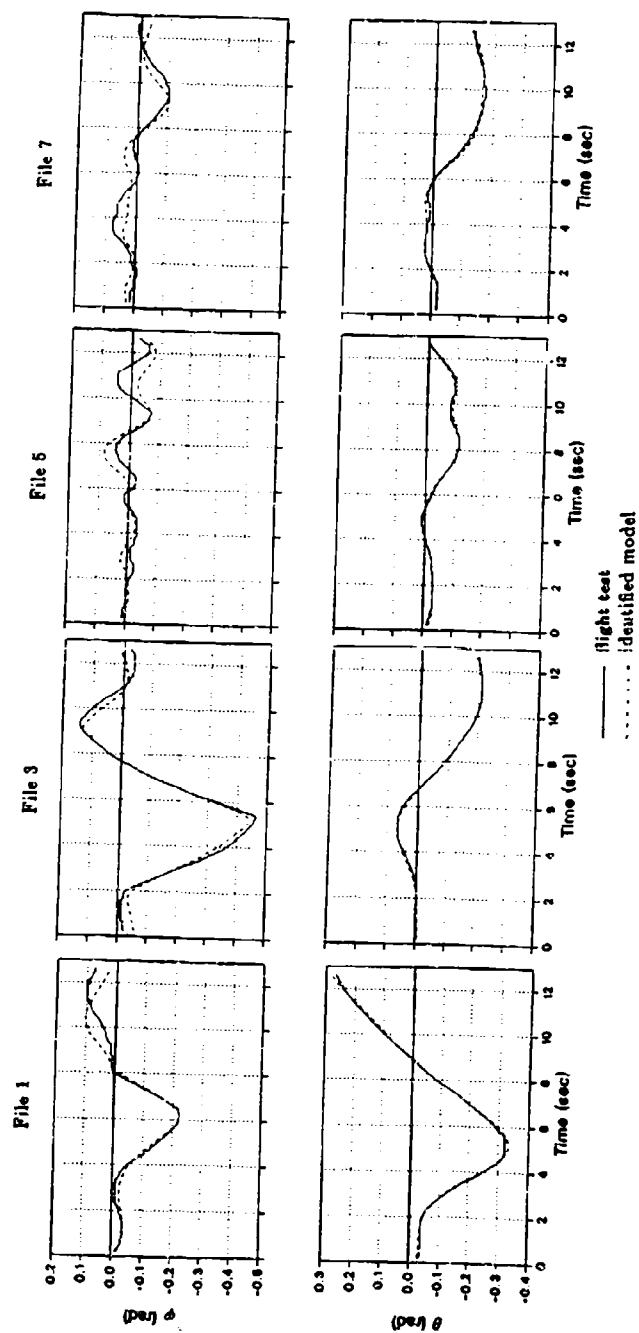


Figure 6.1.12. Identification result: Time history comparison of measured data and the response of the identified model, Euler angles (DLR1)

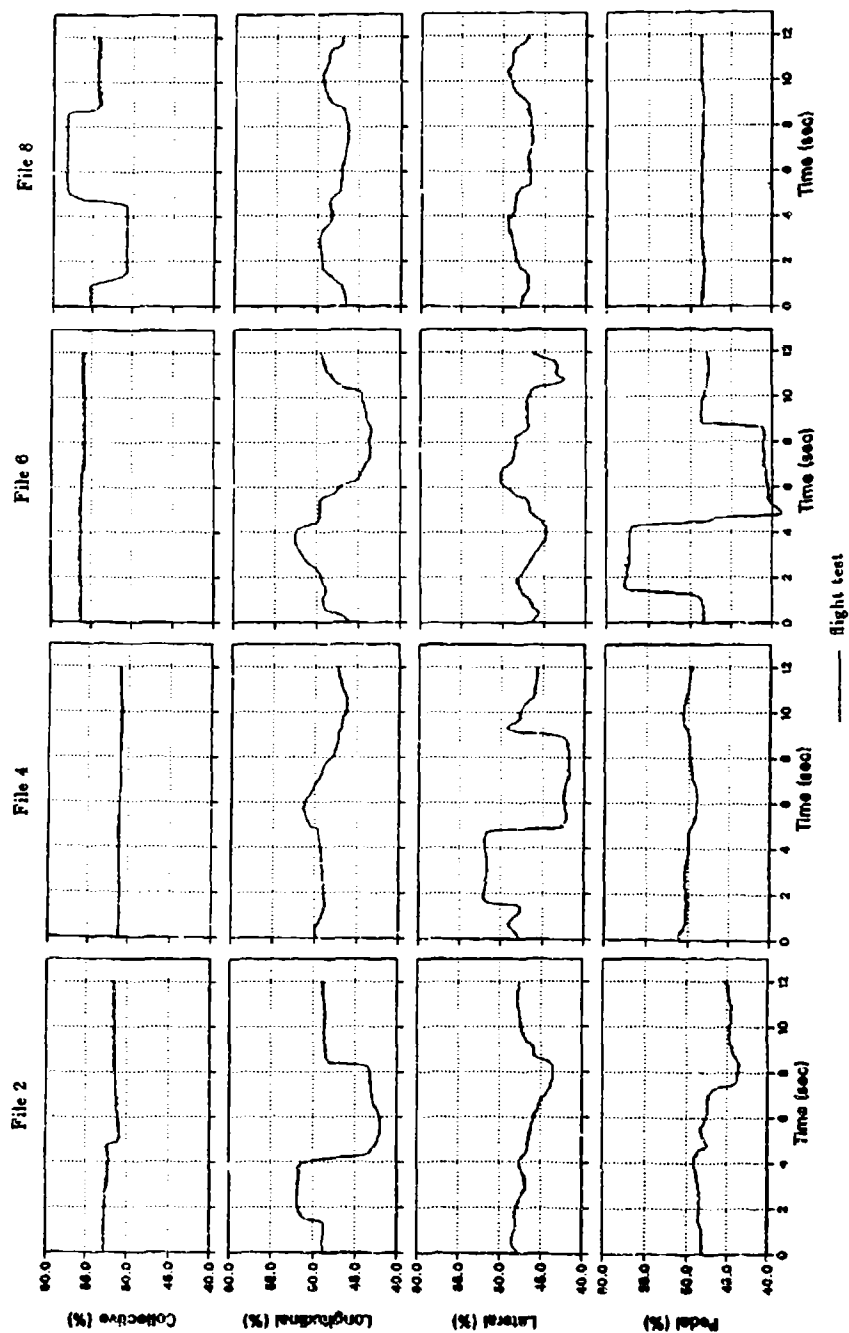


Figure 6.1.13. Control time histories for data group 2

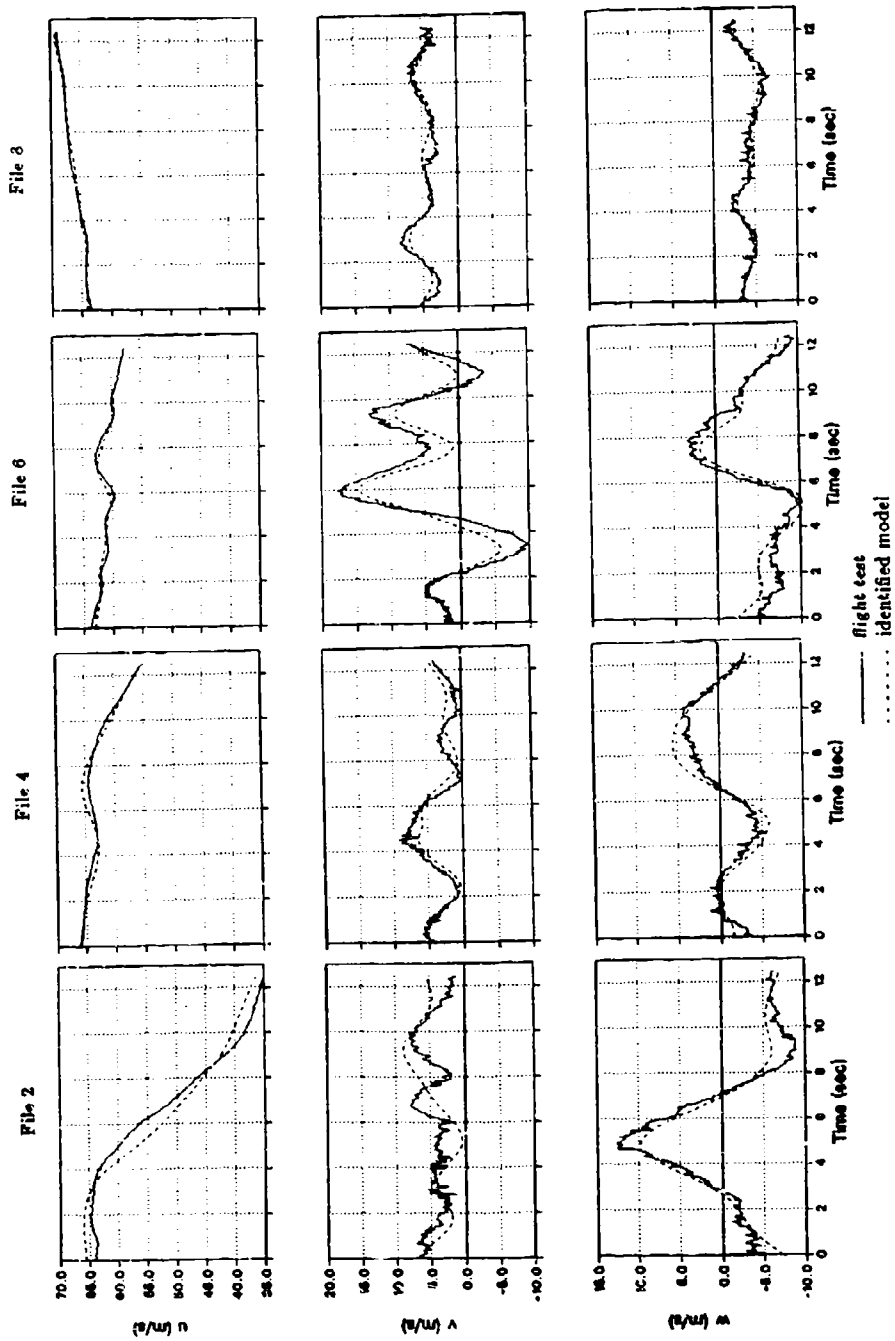


Figure 6.1.14. Verification result: Time history comparison of measured data and the response of the identified model, linear velocities, (DLR1)

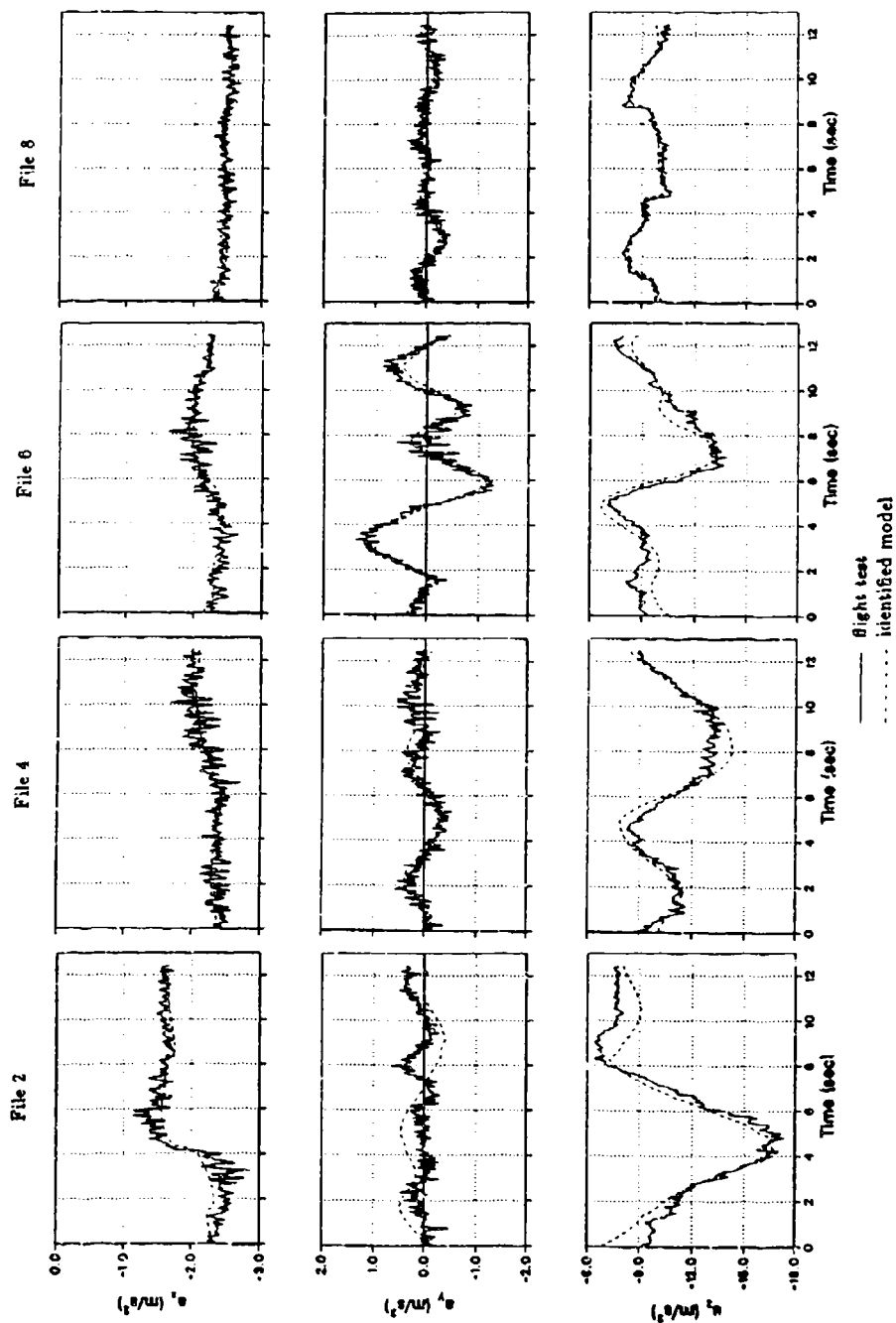


Figure 6.1.15. Verification result: Time history comparison of measured data and the response of the identified model, linear accelerations, (DLR1)

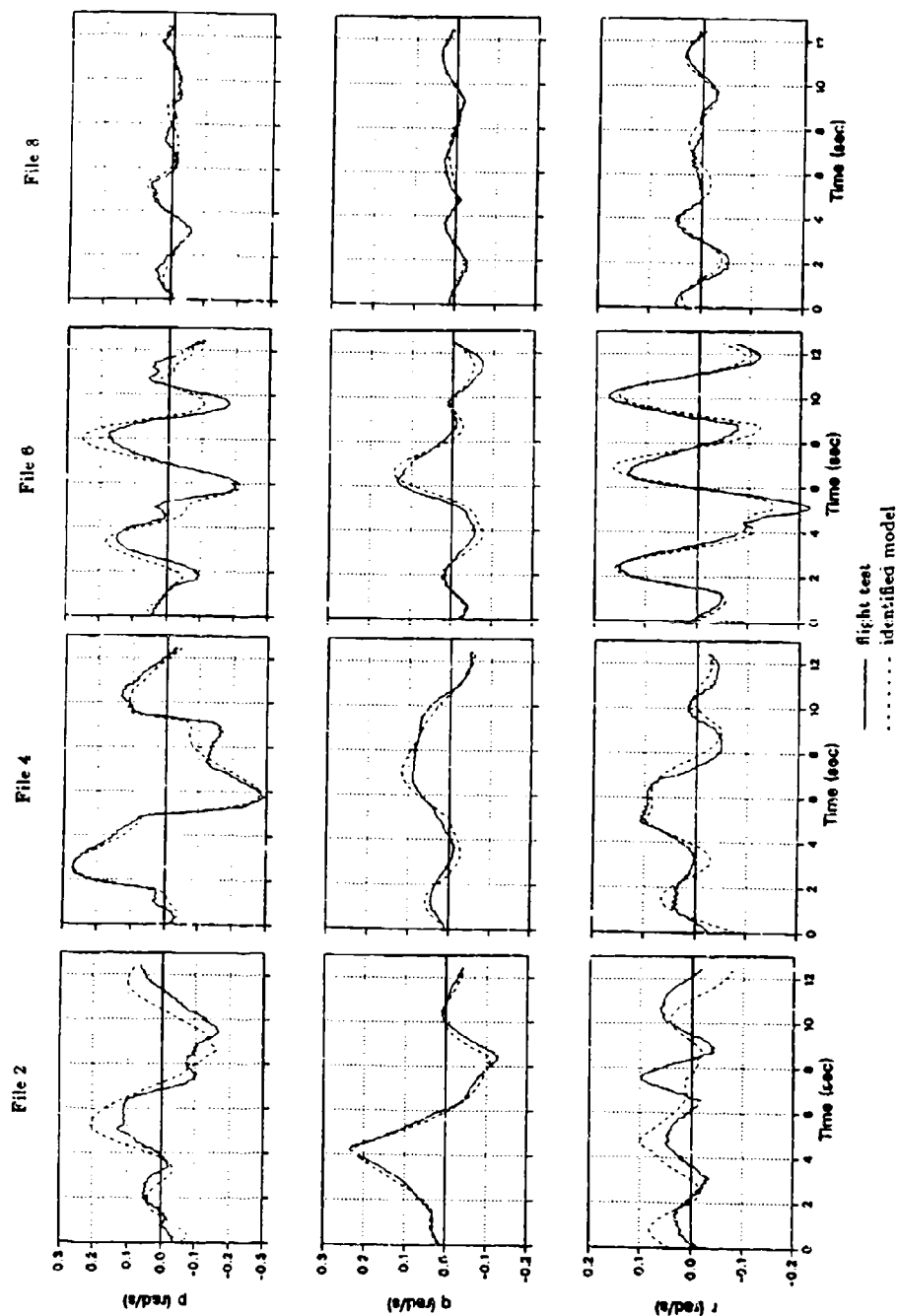


Figure 6.1.16. Verification result: Time history comparison of measured data and the response of the identified model, angular rates, (DLR1)

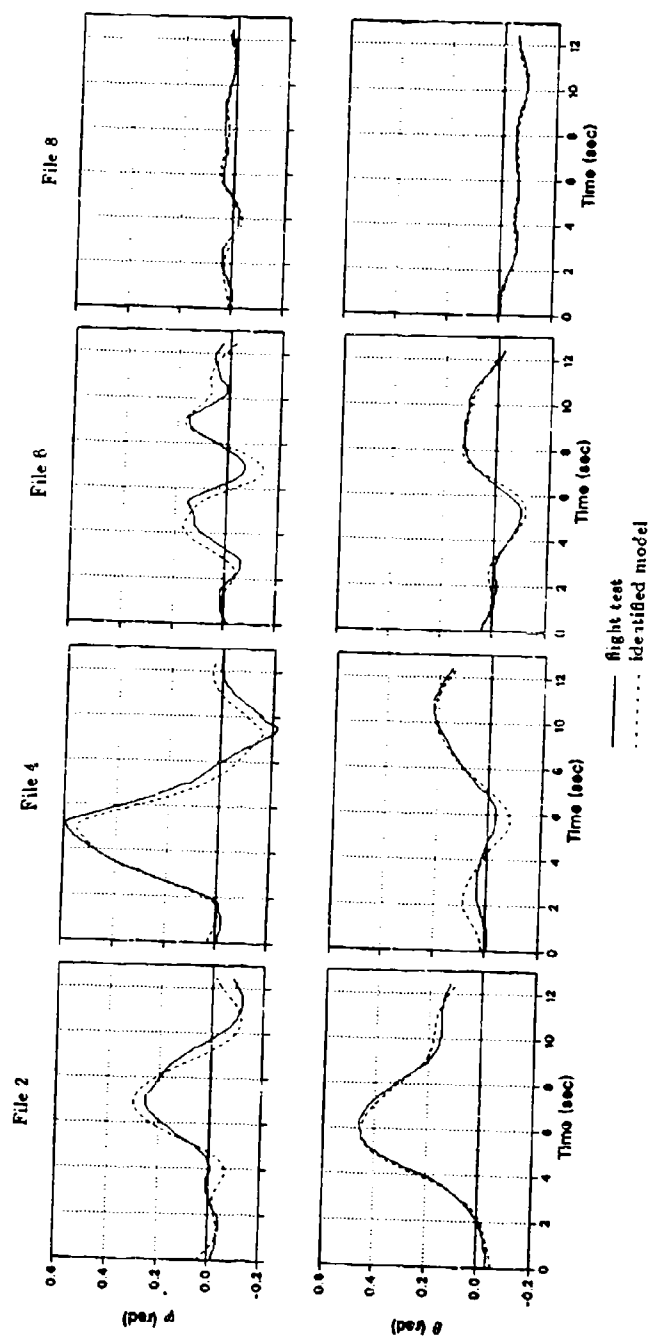


Figure 6.1.17. Verification result: Time history comparison of measured data and the response of the identified model, Euler angles, (DLR1)

6.2 Case Study II: BO 105¹⁴⁾

6.2.1 Introduction

BO 105 flight test data, generated particularly for system identification purposes, were provided to the Working Group by DLR. In the Working Group the data were used for three major steps:

- 1 data consistency analysis,
- 2 identification of 6-degrees-of-freedom models, and
- 3 verification of the identified models.

This case study mainly concentrates on the applied approaches and the obtained results. It also gives a short review of the flight tests and the data base. Here, however, more information is provided in section 4.

6.2.2 General Description of BO 105

The BO 105 is designed as a multiple purpose light helicopter. Typical use of the highly manoeuvrable twin engine vehicle are transport, offshore, police, and military missions. An important design feature is the hingeless rotor system with four fiber-reinforced composite rotorblades. There are no additional lead/lag dampers. The semi-rigid teetering tail rotor is on the left side of the helicopter, working as a pusher.

Pilot control inputs are augmented by two parallel hydraulic servo systems. There is no specific mixing unit, so that control inputs are only mixed at the swash plate. The BO 105 is equipped with two Allison 250 C20 engines located above the cargo compartment.

DLR operates two different BO 105 helicopters. The first one is the standard serial type (BO 105-S123) shown in Figure 6.2.1. Its instrumentation is designed to meet the requirements of two DLR institutes, the Institut for Flight Mechanics and the Institut for Flight Guidance and Control, both located in Braunschweig. This helicopter was used to generate the system-identification flight-test data provided to the Working Group. The second DLR helicopter (BO 105-S3) has been modified for the use as an in-flight simulator. For this ATHeS helicopter (Advanced Technology Testing Helicopter System) a model-following control system was developed at DLR and is presently improved. Here, highly accurate BO 105 mathematical models are required and the research work conducted at DLR has shown that system identification is the best suited tool to generate such models (Kaletka et al, 1989, [6.2.1]).

To give an impression on the helicopter size and basic characteristics, a three view drawing of the BO 105 is given in Figure 6.2.2 and some more details are provided in Table 6.2.1.

6.2.3 Flight Testing and Data Evaluation

6.2.3.1 General

The identification of dynamic systems is always based on the evaluation of the relationship between the measurements of the control inputs and the resulting system response. Therefore, accurate measurements are an indispensable prerequisite for a reliable identification. Usually results are obtained from one flight test run. However, when the time duration of the test is too short or when the system is rather complex, the information content of a single run can be insufficient. This is often the case for the identification of helicopters as a high number of unknowns must be determined and the data run length is limited due to helicopter instabilities. To still provide more information for the identification algorithm it is possible to simultaneously evaluate different test runs and generate one common model. This method, known as *multiple or concatenated run* evaluation has become a common approach in rotorcraft identification. However, it can only be applied when the concatenated runs have practically the same initial flight test conditions and helicopter and instrumentation status. Therefore, the DLR BO 105 flight test data provided to the AGARD Working Group were generated within one flight test program. The tests were especially designed for system identification purposes with particular input signals and carefully controlled initial conditions and conduct of the tests.

The flight test data evaluation with respect to the generation of appropriate data and the analysis of the data quality can be separated into three major steps.

¹⁴⁾ Principal Author: J. Kaletka, DLR

1. on-line data control during the flight tests,
2. first off-line data quality assessment immediately after each flight,
3. detailed data consistency analysis after the end of the flight test program.

The first two steps were done by DLR before the data were released to the Working Group. Then, the more thorough analysis was performed by the Working Group. In this chapter, the approaches and obtained results are presented.

6.2.3.2 On-line data control

During the flight tests the measured signals were sent by telemetry to a ground station. They were plotted in the form of quick-look plots and, in addition, selected variables were shown on a monitor. The objectives of the quick-look evaluation were

1. to control the conduct of the flight tests and give recommendations to the pilot,

Main emphasis was placed on the atmospheric conditions, the proper input signal and the aircraft response. The tests were flown in calm air to avoid gust disturbances. Here, pilot comments proved to be very helpful. Based on outside temperature measurements on board of the helicopter, the required pressure altitude was iteratively determined to make sure that all tests were flown at the same air density level.

The input signals were generated by the pilot. Within one test run only one control was used to excite the on-axis response and to avoid correlation with other controls. After an accurate trim configuration was reached, the on-line data evaluation concentrated on the shape of the input signal and possible control coupling. Then, it was checked if the resulting helicopter response met two main criteria:

- As the models to be identified are based on small perturbation assumptions, the response amplitudes should not be too large. As a certain guideline: the pitch and roll angles should not exceed 25 to 30 degrees.
- The total time length of the test should at least be about 25 seconds to provide sufficient information about the phugoid mode.

2. to detect data errors,

The on-line quick-look helped in detecting major and obvious data errors like sensor malfunctions, signal saturations, larger sensor drifts, data drop outs, noise disturbances, etc.. But it has to be considered that only some selected data channels can be observed on-line and therefore, a more detailed data analysis after the flight is necessary.

3. to decide if the test is acceptable.

Based on the quick-look evaluation and pilot comments it was decided after each test if the test was acceptable. When it had to be repeated, recommendations were given to the pilot, such as improvement of trim, adjustment of control input amplitudes, input signal generation, etc..

6.2.3.3 First off-line data quality assessment

Experience in working with measured data has shown that significant errors in the data can occur although great efforts were made to generate accurate data. Unfortunately, errors are often only detected during the evaluation phase, when all flight tests are completed and the instrumentation system has probably already been modified for other tests. Then, flight tests cannot be repeated and often it is difficult or impossible to find the physical error source and to correct the data.

To reduce this risk it is necessary to carefully check the data quality immediately after each test. Therefore, plots of all measured data from the BO 105 data tape were produced for a detailed visual inspection. Emphasis was placed on both, data suitability for identification and the detection of errors:

- physically meaningful data,

With some knowledge of the helicopter response due to a control input most of the measurements can easily be checked for

- correct sign,

- realistic magnitude,
- noise level.
- signal saturation and resolution,

In preliminary tests the expected maximum helicopter response for the specific tests was determined. Based on these measurements, sensors were selected with an appropriate measuring range. The digitization range was fitted to the expected response range. Both actions help to improve the data accuracy and resolution. However, they also increase the risk of data saturation due to a higher amplitude response or higher noise level as expected.

- data drop outs,

For the BO 105, unfiltered data were recorded. Therefore, data drop outs are seen as large spikes in time history plots and can easily be detected. If only a few drop outs occur it is relatively easy to correct the data by removing the erroneous samples and replace them by interpolated data. However, some inaccuracy must be accepted, which is particularly true in data parts with higher dynamics. The major 'danger' of data drop outs occurs when data are filtered. Then the errors are no longer obvious and can cause significant inaccuracies in the data.

- data recording errors,
- any other data irregularities.

In addition to the visual data check, a first data compatibility analysis was conducted. Using a fast Least Squares technique the consistency of the rotational measurements (rates and angular measurements) and the translational measurements (linear accelerations and speed components) was investigated. Scale factors, offsets and drifts can be determined. This technique is applied routinely in DLR flight tests and proved to be a very efficient approach.

Before the BO 105 flight test data were provided to the Working Group, first data quality checks and compatibility analyses were performed by DLR to ensure that the data did not contain significant deficiencies.

6.2.3.4 BO 105 Data Base provided to the Working Group

From all flight tests, 52 runs were selected by DLR and provided to the Working Group Members. They are listed in Table 6.2.2. Flight test data obtained from three different input signals were provided:

1. a modified multi-step 3211 input signal with a total time length of 7 seconds,
2. a frequency sweep from about 0.08 Hz up to the highest frequency the pilot could generate. Time length of the sweep was about 50 seconds followed by the retrim to the initial steady state condition (important for frequency domain evaluation).
3. a doublet with a total time length of 2 second.

Flight data with the input signal starting in opposite direction were generated for the 3211 and doublets. For redundancy reasons, one or two repeats of each test were provided (see Table 6.2.2). Within a run, only one control was used to excite the on-axis response. For the flights with 3211 and doublet inputs the controls were held constant after the end of the input for at least 20 seconds. Because of the long time duration of the frequency sweeps, these tests required stabilization by the pilot to keep the aircraft response within the limits of small perturbation assumptions for linear mathematical models. To help the pilot generate the inputs, a CRT was used that showed both, the desired input and the actual control movement (Figure 6.2.3). For the sweeps, the CRT showed the lowest frequency as a 'starting' help. Then, the pilot progressively increased the frequency on his own.

The measured variables provided to the Working Group are given in Table 6.2.3 and Table 6.2.4. As a representative example from the data base, Figure 6.2.4 gives the roll and pitch rate responses due to the three input signals in the same scales. It shows that the input amplitudes were adjusted to generate similar helicopter on-axis response magnitudes. It also demonstrates the highly coupled BO 105 characteristic: the (coupled) roll rate response due to a longitudinal stick input is as high as the primary pitch rate response. More time histories of the measurements will be given later in this chapter when identification results are discussed.

6.2.3.5 Detailed data consistency analysis in the Working Group

Based on the initial data check results from the 52 data files, DLR suggested a minimum data set of four runs with 3211 input signals to be used for the identification and another set of 4 data runs with doublet control inputs to be applied for the verification of the identified models. Each of these data groups included one run for each control. This proposal was made to reduce the amount of work for each Member and to make results comparable. For the AFDD frequency domain technique the sweep inputs were used for identification.

All Members used the same principle approach to check the data quality. It is based on the comparison of redundant measurement: rates and angular measurements are physically related by the equations

$$\begin{aligned}\dot{\Phi} &= p + \sin \Phi \tan \Theta q + \cos \Phi \tan \Theta r \\ \dot{\Theta} &= \cos \Phi q - \sin \Phi r \\ \dot{\Psi} &= \frac{\sin \Phi}{\cos \Theta} q + \frac{\cos \Phi}{\cos \Theta} r\end{aligned}\quad (6.2.1)$$

The relationship between linear accelerations and speed components is given by:

$$\begin{pmatrix} \dot{u} \\ \dot{v} \\ \dot{w} \end{pmatrix} = \begin{pmatrix} a_x \\ a_y \\ a_z \end{pmatrix} + g \begin{pmatrix} -\sin \Theta \\ \sin \Phi \cos \Theta \\ \cos \Phi \cos \Theta \end{pmatrix} + \begin{pmatrix} -wq + vr \\ -ur + wp \\ -vp + uq \end{pmatrix}\quad (6.2.2)$$

In these nonlinear equations, linear accelerations and rates are taken from measured data and used as 'control' inputs. The integration then yields calculated angles and speed components that can be compared to the measured ones. When differences are seen, a more detailed analysis is needed to isolate the error sources. In general it is tried to estimate scale factors or zero offsets (biases) for the measured data. Depending on the applied method, the estimation procedure is different in its power and complexity. When the technique does not allow the integration of nonlinear systems, all variables on the right hand side are taken from measurements. Then, all terms are known and the equation system can easily be integrated. When nonlinear systems can be handled, there is more flexibility with respect to the use of the attitude angles and speed components: each of these variables can either be treated as a known measured control or as a state variable obtained from the actual integration. This possibility is very useful to isolate erroneous data channels. However, independent from the applied method, some general statements can be made from the BO 105 data evaluation:

1. Due to parameter correlations it is not possible to estimate all scale factors and biases for all measurements. Based on the assumption that rate gyros and linear accelerometers are the more reliable sensors, the usual approach therefore is to estimate:
 - scale factors for attitude angles and speed components,
 - and/or biases for rates and linear accelerations.
2. The error estimation for the angular motion equations causes no major problems.
3. The determination of errors for the translational motion equations is more difficult because of some unique problems:
 - the equations are coupled with the rotational equations by the gravity terms. As they have a significant effect, errors in the attitude data also highly influence the comparison of the speed data.
 - the linear acceleration measurements have a high noise level due to vibrations. Helicopters, and in particular rigid rotor helicopters like the BO 105, generate only small accelerations in the longitudinal and lateral body-fixed axes as the acceleration components due to a speed change are practically compensated by the gravity components. The fact that, on the one side, sensors must have a high measuring range due to the noise level whereas, on the other side, the signal to noise ratio is small (about 0.1 for the BO 105) reduces the high measurement and resolution quality of the linear acceleration data. This is particularly the case for the longitudinal and lateral accelerations.
 - measurement of aircraft speed components is still a major problem and the obtained accuracies are significantly lower than those of the angular or linear acceleration data. This is also true for the helicopter air data system, which is installed on the BO 105. For the considered flight condition of about 80 knots it cannot improve the data quality in comparison to other data sources like nose-boom mounted vanes and pressure sensors.

In the Working Group, AFDD, CERT, DLR, NAE, and NLR performed data consistency checks for the BO 105 data. In the following, the individual approaches are characterized.

AFDD

Extensive work on data consistency for all provided BO 105 data runs was done by AFDD. First results, presented in Kaletka et al., 1989, [6.2.2], were obtained from the separate evaluation of each individual run. A more detailed study, including concatenated evaluations, is given by Fletcher, 1990, [6.2.3]. The Kalman Filter Smoother program SMACK (Smoothing for Air Craft Kinematics) developed at the Ames Research Center was employed. The algorithm is based on a variational solution of a six degrees of freedom linear state and non-linear measurement model and employs a forward smoother and zero-phase-shift backward information filter. The solution is iterative, providing improved state and measurement estimates until a minimum squared-error is achieved. Linearization is about a smoothed trajectory and convergence is quadratic (Bach, 1984, [6.2.4]).

Consistency checks were performed in two steps:

1. a preliminary three degrees of freedom check including only the Euler angle and body angular rate measurements,
2. a final six degrees of freedom check including the angular variable measurements and the air-data and linear specific force measurements.

This approach allowed initial estimation of the angular-variable error parameters to be performed unbiased by the noisier air-data and specific-force measurements. The values estimated in the angular solution and their variances were then used as start-up values in the final overall solution. This two-step procedure resulted in a final solution with smaller parameter Cramer-Rao bounds and quicker convergence than a one-step coupled solution. The obtained results are included in Table 6.2.5 and Table 6.2.6.

CERT

CERT has used an output error minimization technique to estimate scale factors, biases and initial conditions. From the obtained results it was concluded, that the measurement errors were not so significant to justify use of reconstructed data.

DLR

The airdata measurement problem has already been addressed. In the flight tests the measured lateral speed was about 4 m/sec and the vertical speed about -5 m/sec. It was felt that these values were not realistic and contained offsets. Therefore, for each run, the initial vertical trim speed was calculated from steady state horizontal flight using forward speed and pitch angle (this approach was also used by NAE). The lateral speed could not be determined from other measurements. As the pilots were asked to minimize the sideslip during trim, the initial lateral speed was assumed to be zero.

For the state estimation, DLR used the Maximum Likelihood program that is also applied for system identification. The nonlinear kinematic equations were integrated, where the measured rates and linear accelerations were treated as 'inputs' and all other variables were used as states. Calculated attitude angles, heading, and speed components were obtained. Comparing the derived time histories with the measured data two groups of unknowns were estimated:

- scale factors for the speed components, attitude angles and heading,
- biases (offsets) for the rates and linear accelerations.

Both, single and concatenated files were evaluated. The final results, obtained from all files as well as from the suggested files are given in Table 6.2.5 and Table 6.2.6.

NAE

Consistency checks were performed on all data files. The same method as already described in the AH 64 case study was used (section 6.1). Angular data were found to be of good quality and they were then used without any changes for the identification. Speed data, however, were felt to be not acceptable and therefore, for all three speed components, reconstructed data were generated.

NLR

The BO 105 data were originally provided with a sampling rate of 100 Hz. This sampling rate was reduced to 25 Hz. No filter was used for the data reduction. Then NLR applied an output error technique, which uses the nonlinear kinematic equations to estimate measurement biases. Various data runs were evaluated. The obtained results for the biases were comparable with the biases obtained from the combination of the four data runs that were suggested for identification. Visual inspection of the reconstructed time histories with the measured ones confirmed that the quality of the measured data is satisfactory and no significant errors were detected. The measured linear accelerations and rates were corrected by the identified biases and the reconstructed speed components were generated for the use in the identification.

The estimated bias terms for the linear accelerations and rates obtained from the data consistency checks of the four combined runs are given in Table 6.2.6.

6.2.3.6 Discussion of results

In the following, results obtained from the data consistency analysis are illustrated by representative plots and the estimated scale factors and biases are summarized in the form of tables.

In Figure 6.2.5 and Figure 6.2.6 measurements from two flight tests are shown. Modified 3211 input signals were used for the longitudinal stick (in the first run) and for the pedal (in the second run). Figure 6.2.5 compares the measured speed components, attitude angles and heading to reconstructed data. All scale factors were assumed to be one. It is clearly seen that angular variables are in good agreement, whereas the speed components show larger differences. In particular, in the lateral speed data two deficiencies are obvious:

1. In the first run there are two sections with 'data drop outs' where the sensor was affected by the rotor downwash when the helicopter is in climb and
2. a scale factor error, which is best seen during the time of the pedal input.

The longitudinal and vertical speed data show some smaller differences. In a second data consistency evaluation, scale factors were estimated. The factors for the angular data stayed at about one. For the speed components, however, scale factors of about 0.9 for the both, the longitudinal and vertical speed, and 0.7 for the lateral speed were identified. (Definition: Measurement = Scale factor * Reconstructed Data). Figure 6.2.6 compares the obtained reconstructed data with scale factor corrections and the measurements.

Table 6.2.5 and Table 6.2.6 summarize the results obtained from the data consistency analysis conducted by AFDD, DLR, and NLR. Two different cases must be distinguished:

1. When all data runs were evaluated separately, the mean values and the so called 'practical' standard deviations were calculated from all individual results.
2. When only the suggested four data runs were considered, they were concatenated so that one single result was obtained. Then, the standard deviation given in the table corresponds to the Cramer-Rao lower bound.

Scale factors and their standard deviations are given in Table 6.2.5. For the angular measurements they are close to one and indicated a high data consistency between the measurements of the rates and angles. The scale factors for the forward and vertical speed data are about 0.9 and may be acceptable. But for the lateral speed component there are larger deviations from one and a higher standard deviation. This result is in agreement with the visual inspection of Figure 6.2.5 and Figure 6.2.6.

Table 6.2.6 gives the identified biases for the linear accelerations and rates. The small values confirm the reliability of the measurements.

When deficiencies in measured data are detected, the analyst has to decide how to use this information. In the case of the BO 105 speed measurements, the choice could be made to either use the measured or the reconstructed data. On the one hand, the measured data can still provide useful speed information although they may not be fully compatible with the other measured signals (e.g. linear accelerations). On the other hand, compatible reconstructed data can be generated. However, they are derived from the linear accelerometer and vertical gyro signals and therefore transfer errors from these instruments into the calculated speed data.

Both approaches have their advantages and disadvantage. Consequently, different decisions were also made by the Working Group Members. CERT, DLR, and University of Glasgow used the measured data, whereas AFDD, NAE, and NLR replaced the measurements by reconstructed speed data.

6.2.4 BO 105 Identification

Based on the results from the data consistency analysis of all data files provided to the Working Group, DLR selected eight flight tests for a more detailed evaluation. Working Group Members then concentrated on this smaller common data base to make the obtained identification results better comparable. The eight files were divided into two different data sets with four files each:

1. one run with a longitudinal stick control input,
2. one run with a lateral stick control input,
3. one run with a pedal control input,
4. one run with a collective control input.

For the first data set, flight tests with 3211 control inputs were selected to be used for the identification. The second data set with doublet control inputs was suggested for the verification of the obtained identified models. For the 'identification data runs' it was proposed to use the first 27 seconds of each data run.

Identification results obtained from the suggested data runs with 3211 inputs were provided by CERT, DLR, NAE/University of Toronto, Glasgow University, and NLR. AFDD provided results obtained the flight tests with frequency sweep control inputs. In this section, the identification approaches are characterized. Then, the identification results are summarized in the format of tables of derivatives and eigenvalues. Representative time histories and frequency responses are presented for the comparison of measured data and the response of the identified models.

6.2.4.1 Identification approaches

All Working Group Members used a coupled six degrees of freedom rigid body model as derived in section 5.5 for the identification. Main differences in the model structures are: the treatment of the nonlinear kinematic and gravity terms, the number of derivatives to be identified, and the determination of equivalent time delays. In the following, these subjects are discussed in more detail:

1. Nonlinear kinematic and gravity terms,

Including nonlinear terms in the state equations requires that the actual model states are used in the nonlinear terms, like the state variable Θ in the gravity term $g \cdot \sin \Theta$. Consequently, an identification method is needed that can handle nonlinear state equations in both, the estimation of the unknown parameters and the calculation of the model responses. Such a 'nonlinear method' was only applied by DLR. As most computer codes for system identification are written for linear systems, nonlinear terms have also to be linearized or, as a compromise, so called 'forcing functions' are used. Here, the variables in the nonlinear expressions are taken from the measured data, e.g. the measured Θ in $g \cdot \sin \Theta$. Then the nonlinear terms can be calculated and are treated like known control inputs (pseudo controls) in the integration of the state equations. This 'forcing function' approach was applied by NAE. All other Working Group Members used fully linearized models.

2. Number of derivatives to be identified,

The definition of an appropriate model structure still is one of the basic and essential problems in system identification. It is present standard in rotorcraft identification to work with linear coupled six degrees of freedom rigid body models. They have proved to be suitable for various applications. The more difficult problem is to decide which parameters in the state equations can be identified or can be neglected or set to a fixed value. The determination of too many unknowns can lead to severe convergence problems in the identification and to high correlations between the individual parameters, causing inaccuracies and large variances in the estimates. When, on the other side, the number of unknowns is reduced and significant parameters are neglected, the model can no longer adequately describe the helicopter dynamics. There is not yet an unique solution to this model structure problem and consequently, the models used for the BO 105 identification in the Working Group ranged from models with almost all parameters included to highly reduced models. From totally 60 possible derivatives, NAE identified 58 parameters, whereas in the model of the Glasgow University the number of unknowns was reduced to 30 parameters. In such reduced models, the derivatives that are neglected and not identified are usually set equal to zero or, alternatively, they are fixed at values obtained from simulation or wind tunnel results. In the WG, neglected parameters were assumed to be zero.

3. Determination of equivalent time delays.

Six degrees of freedom rigid body models show an immediate on-axis (linear and rotational) acceleration response due to control inputs. The helicopter response however is delayed mainly due to the dynamics

of the rotor and the hydraulic actuators. To approximate their effects, equivalent time delays for the controls are usually used. This approach has proved to be suitable and can be considered as a reasonable compromise to extending the model order by additional degrees of freedom.

For the evaluation of the BO 105 data base, significantly different identification techniques were applied. Time- and frequency-domain approaches as well as Least Squares and Maximum Likelihood identification criteria were used.

In the following, the individual identification approaches are characterized.

1. Time-domain identification techniques

• CERT

CERT applied a Maximum Likelihood output error technique for the identification of linear models. The proposed four BO 105 data files were concatenated and evaluated without further modifications. The measurement vector (variables to be fitted by the model response) included 11 variables: linear accelerations, speed components, rates, attitude and roll angles. The structure of the linear model was reduced to 35 derivatives to be identified.

• DLR

As a first step, equivalent time delays between the control inputs and the on-axis acceleration responses were determined by a cross-correlation technique. The measured control time histories were then shifted by these time delays. For the identification, a Maximum Likelihood method was used that allows the estimation of nonlinear models. Therefore, the kinematic and gravity terms in the state equations were kept nonlinear and calculated from the model response data. The other terms were linear. Based on first identification results, the significant and identifiable derivatives were determined by evaluating the inverse of the information matrix which gives the standard deviations (Cramer-Rao lower bounds) and the correlation between individual parameters. In the final model structure, 38 derivatives were identified.

For the identification, the measured data were used without modifications except for the lateral and vertical speed. For the horizontal flight trim condition, the lateral speed was about 4 m/sec and the vertical speed about -6 m/sec. These values were felt to be unrealistic and therefore, the lateral speed measurements were corrected to a zero value in trim. The 'true' steady state for the vertical speed was reconstructed from forward speed and attitude angle measurements. Such corrections in the initial conditions are necessary for nonlinear models as they use total amplitude values, whereas for linear systems, the steady state is usually subtracted from the measurements so that the data represent only the deviations from trim.

The measurement vector included 14 variables: linear accelerations, speed components, rates, attitude and roll angles, and rotational accelerations. A concatenated run evaluation was used, however for each individual run the initial conditions were fixed at the mean value of the first data points, and offsets in the controls and most of the measurement variables were identified in form of bias terms.

• NAE

Based on the results from the data consistency evaluation, the measured speed data were felt to be inadequate to be used in the identification. Therefore, NAE concentrated on the reconstruction of more reliable speed variables. First, the initial trim conditions for the lateral and vertical speed were determined from forward speed, roll and pitch angles. Then the time histories obtained from the consistency analysis were used in the measurement vector and for the calculation of the forcing functions. A Maximum Likelihood identification method for linear systems was applied. However, the gravity and kinematic terms in the state equations were kept nonlinear. They were calculated using the measured angles and rates as well as the reconstructed speed components and considered as additionally generated time histories and treated like control variables in the control vector ('pseudo controls').

Equivalent time delay values, suggested by DLR, were used to time-shift the measured control variables before the identification was started. The measurement vector included 9 variables: linear accelerations, reconstructed speed components, and rates. A concatenated run evaluation was applied to identify an almost full set of 58 derivatives, where only N_u and $X_{\delta ped}$ were neglected. Offsets in the controls and measurements were taken into account by estimating bias terms for each

individual manoeuvre. These biases were used for the force and moment state equations as well as for the speed and linear acceleration measurement equations.

- **NLR**

NLR was the only Working Group Member who applied an equation error method or regression analysis. In this technique, each state equation is treated separately and independently. All state and control variables in the considered equation are taken from the measured data and the unknown parameters are determined by fitting the linear and rotational accelerations by a Least Squares criterion. As in principle all terms in the state equations are treated as pseudo controls, it is essential to work with highly accurate data. Therefore, NLR first concentrated on a data reliability analysis although the 'standard' quite complex NLR approach for flight path reconstruction could not fully be applied as some additionally required measurements were not available.

In the identification step, equivalent time delays for the controls were used and then concatenated manoeuvres were evaluated to identify a model with 36 unknown parameters.

Frequency-domain identification techniques

- **AFDD**

As the data consistency analysis revealed a low quality of the airspeed measurements, AFDD decided to use reconstructed speed data for the identification. A key step in the AFDD frequency-domain identification approach is the extraction of high-quality frequency responses between each input/output pair. AFDD experience has shown that flight test data obtained from frequency sweep control inputs are better suited for this approach than multi-step inputs. Consequently, it was concentrated on the evaluation of the BO 105 flight test data obtained from frequency sweep inputs. These manoeuvres could not be flown using only a single control but some activity in the other controls was required to keep the aircraft response within small perturbation assumptions. Therefore, conditioned frequency responses were determined. Making use of the redundant flight tests, the frequency-sweep manoeuvres were concatenated to increase the reliability of the frequency responses. Then, the unknown model parameters of a linear six degrees of freedom state space model and the equivalent time delays were identified by minimising the weighted Least-Squares error between measured and model frequency responses. The weighting was based on the values of the associated coherences at each frequency point.

A total of 26 frequency responses, with 19 frequencies in each, were matched in the identification process (Table 6.2.7). The frequency range of fit was selected individually for each response corresponding to its range of good partial coherence. However, the upper frequency was limited to a maximum of 13 rad/s since a 6 DoF model is not capable of matching lead/lag and body/rotor flapping dynamics. Without this restriction, physically meaningless derivatives can be obtained. A detailed model structure analysis was conducted based on parameter insensitivities, Cramer-Rao bounds, and cost function changes. The final model included 51 identified parameters (47 derivatives and 4 equivalent time delays).

- **Glasgow University**

Glasgow University applied a frequency-domain identification technique, where the time-domain state space model and the measurement equations

$$\dot{\mathbf{x}}(t) = \mathbf{A} \mathbf{x}(t) + \mathbf{B} \mathbf{u}(t)$$

$$\mathbf{y}(t) = \mathbf{C} \mathbf{x}(t) + \mathbf{D} \mathbf{u}(t)$$

are transferred to the frequency-domain format

$$j\omega \cdot \mathbf{x}(\omega) = \mathbf{A} \mathbf{x}(\omega) + \mathbf{B} \mathbf{u}(\omega)$$

$$\mathbf{y}(\omega) = \mathbf{C} \mathbf{x}(\omega) + \mathbf{D} \mathbf{u}(\omega)$$

where $\mathbf{x}(\omega)$, $\mathbf{u}(\omega)$, and $\mathbf{y}(\omega)$ are the Fourier transformed variables. The control vector $\mathbf{u}(\omega)$ and the matrices \mathbf{B} and \mathbf{D} were modified to compensate for non-periodic states (Fu et al., 1983, [6.2.5]).

The unknown parameters in the matrices \mathbf{A} , \mathbf{B} , \mathbf{C} , and \mathbf{D} are then estimated in the frequency domain, using a Maximum Likelihood criterion. For the BO 105 identification, the DLR suggested file, with modified 3211 control inputs were used as concatenated manoeuvres. The measurement vector included the Fourier transforms of 11 measured variables: linear accelerations, speed components,

rates, and attitude and roll angles. 30 derivatives and 4 equivalent time delays were identified. (In frequency-domain approaches it is not necessary to estimate bias terms).

6.2.4.2 Identification results

In this section, BO 105 identification results provided by the Working Group Members are presented and discussed in detail. Tables of the derivatives and eigenvalues of the identified models are given and representative plots of time histories and frequency responses are presented for the comparison of measured data and model responses.

Table 6.2.8 to Table 6.2.11 list the derivative values identified in the Working Group by AFDD, CERT, DLR, Glasgow University, NAE, and NLR. From the tables the detailed model structures can also be seen. In addition to the stability and control derivatives the associated standard deviations are given. These are the values provided by the identification techniques (Cramer-Rao lower bounds). They represent the theoretically lowest achievable standard deviation. It is well known that for practical use these values are usually too small. Therefore it is often recommended to multiply them by a factor of 5 to 10 to make the standard deviations physically more realistic. Depending on the identification approach, the standard deviations were defined slightly differently. Therefore this information is not intended for comparisons between the results from different Members but more as a help to relate the significance of parameters within one set of results to each other.

There are quite large differences between the identification results. Even for significant parameters, like the diagonal terms of the state matrix, which are related to system damping, some major differences are seen. $X_{\dot{u}}$ is between $-0.05/s$ and $-0.06/s$ for time-domain results, but $-0.03/s$ to $-0.04/s$ for the frequency-domain methods. Larger $Y_{\dot{u}}$ values in the AFDD and NAE results reflect the lateral speed measurement problem. These two Working Group Members used reconstructed data instead of the measurements. In the data consistency analysis, a scale factor of about 0.7 was determined between the reconstructed and measured lateral speed. Consequently, this factor is also seen in the identified $Y_{\dot{u}}$. The heave damping $Z_{\dot{w}}$ shows reasonable agreement.

The identification of the pitch and roll damping L_p and M_q is a major problem for the BO 105. The obtained values highly depend on

- the equivalent time delays.
- the bandwidth of the flight test data, and
- the high correlation with the control derivatives.

These dependencies have different influences in the individual estimation techniques, which explains the large variations within the Working Group results. The yaw damping N_r is in reasonable agreement. From the main (on-axis) control derivatives, $Z_{\delta_{ca}}$ and $N_{\delta_{ped}}$ agree fairly well. In the roll and pitch moment control derivatives $L_{\delta_{lat}}$ and $M_{\delta_{lon}}$ the larger differences are caused by the high correlation of these terms with L_p and M_q and the associated problems as discussed above. The coupled off-axis derivatives are not discussed in detail. It is seen that there are also some large differences. However, it should be noted that several of these terms also show larger standard deviations indicating less parameter significance.

The equivalent time delays used for the controls are listed in Table 6.2.12. These time delays approximate the effects of rotor and hydraulic dynamics. How important it is to include accurate equivalent time delays in six degrees of freedom models is demonstrated by Figure 6.2.7. For two major derivatives, the roll damping L_p and the roll control derivative due to lateral stick $L_{\delta_{lat}}$, the figure shows the high sensitivity of the identification results to time delays. It is obvious that special care must be taken to accurately determine equivalent time delay values. In the Working Group DLR extracted time delays by a cross-correlation of the acceleration responses from the measurements and the model response. The obtained values were also used by NLR and NAE. The frequency-domain method used by AFDD and University of Glasgow allow the direct estimation of equivalent time delays together with the unknown derivatives.

The eigenvalues of the identified models are given in Table 6.2.13. A comparison shows that the phugoid and dutch roll modes are in good agreement with slightly higher damping in the AFDD model. The increased Dutch roll damping for the AFDD results is consistent with the differences in the frequency response results for the sweep compared to the 3211 inputs (see section 5.2.3). The values for the lower frequency aperiodic pitch mode agree satisfactorily, and all Working Group Members identified the spiral mode to be close to the origin. Major differences, however, are seen in the roll and higher frequency pitch modes. They reflect the different values of the roll and pitch damping derivatives.

The comparison of the derivative and eigenvalue results shows that the values obtained by AFDD, DLR, and NAE (and probably University of Glasgow) are relatively close to each other.

As representative example Figure 6.2.8 through Figure 6.2.12 show a full set of time-history plots for the comparison of flight test measurements and the response of the DLR identified model for all four data runs used for the identification. It demonstrates that a good agreement was obtained for all variables. From the time histories provided by CERT, University of Glasgow, and NAE the pitch and roll rate responses for the flight tests with longitudinal or lateral stick control inputs are presented in Figure 6.2.13 and Figure 6.2.14. Some representative results obtained from the AFDD frequency-domain method are given in the format of frequency response fits in Figure 6.2.15 and Figure 6.2.16.

6.2.5 Verification of the Identified Models

The verification of the identified models is a key step in the identification process that assesses the predictive quality of the extracted model. Flight data not used in the identification are selected to ensure that the model is not tuned to specific data records or input forms. In the Working Group, identification results were generated from flight tests with multistep 3211 or frequency-sweep control inputs. Therefore, doublet inputs for each control were used for model verification and comparison.

All Members applied a very similar approach to calculate the responses of the identified models: All model coefficients were fixed and only biases were estimated to account for control and measurement offsets. In all cases, the model was only driven with the measured control variables and no pseudo controls were used. As DLR and NAE worked with a nonlinear model in the identification, the same model was also used for the verification (nonlinear terms were calculated from model states).

Corresponding to the presentation of time-history fits in the previous section on identification results, Figure 6.2.17 through Figure 6.2.21 compare the time history response predictions of the DLR identified model for all observation variables and for all four doublet control inputs. From the verification results provided by AFDD, CERT, Glasgow University, NAE, and NLR the pitch and roll rate responses due to longitudinal and lateral stick inputs are given in Figure 6.2.22 through Figure 6.2.24 (for completeness, the DLR result is repeated in the same format). From the complete set of results in Figure 6.2.17 through Figure 6.2.21 it is seen that the predictive capability of the identified model is very good in both the on- and off-axis response, especially considering the dynamically unstable and highly-coupled nature of the BO-105. The differences seen in the speed data, and here in particular in the lateral speed, are due to measurement problems. Although there are also some smaller differences in the other variables, the overall agreement is very satisfactory.

A first comparison of the verification plots in Figure 6.2.22 through Figure 6.2.24 demonstrates that basically all model responses match the measured data fairly well. The lower frequency modes (phugoid and pitch) are in good agreement for all models. A closer comparison reveals some larger differences for the time history sections where the doublet control inputs were given. Some models are more damped or the coupling between the pitch and roll motion is less accurate. The fact, however, that none of the models can fully reach the maximum peak amplitudes of the rates demonstrates that six degrees of freedom models cannot describe this higher frequency range completely. It is obvious that a further improvement of the model prediction can only be reached when the model order is extended by additional degrees of freedom, like rotor or inflow dynamics.

6.2.6 Discussion of Results

In the list of derivatives (Table 6.2.8 to Table 6.2.11) and eigenvalues (Table 6.2.13) it was seen that the identified values varied significantly. A decision for the more suitable model can only be made on the basis of a comparison between the model responses and the flight test data for both, the identification and the verification plots. Therefore, a more detailed evaluation was conducted. It also included all frequency-response and time-history fits, which, for space reasons, cannot all be given within this Report. It was concluded that the models obtained by AFDD, DLR, NAE, and, with some more deviations, the model from the University of Glasgow showed the more satisfactory overall agreement with the measurements.

The importance of accurate equivalent time delays has already been addressed. The identified values provided by AFDD and DLR (Table 6.2.12) are in good agreement, except for the value for the collective control, where larger differences are seen. The DLR time-domain approach for extracting time delays is based on evaluating the cross-correlation of the on-axis (linear or angular) accelerations. The frequency-domain method searches for a time delay in conjunction with the other model parameters that will produce the best match of all of the responses. The use of a single time delay for each input imposes the assumption that all input/output response pairs have the same high-frequency zeros, and thus the same high-frequency phase shift. This corresponds to modelling the rotor response as an actuator. When this assumption is valid, the two methods should produce essentially the same time delays, as they do for the lateral, longitudinal, and pedal inputs. However, this assumption is not acceptable for the collective inputs. Further frequency-domain analyses indicated an

effective time delay of about 93 ms for linear responses (u, w, θ_z) to collective, but a much larger effective time delay of about 255 ms for angular responses (p, q). The time-domain method reflects the vertical acceleration delay, while the frequency-domain result reflects an average delay. In conclusion, it can be stated that for the collective control a single time delay value is only a poor compromise in characterizing all of the responses. However, a better approach either requires the use of different time delays for each control and each response axis or a higher-order dynamic model is needed.

As a further help for the evaluations of the results, three additional sets of identified derivatives were considered. They were not produced within the Working Group but they were obtained from the same BO 105 data base. These models were extracted by DLR (frequency-domain technique, similar to the University of Glasgow approach; Fu et al, 1983, [6.2.5]), by Stanford University, USA (a newly developed identification algorithm based on smoothing; Idan, 1990, [6.2.6]), and by Technische Hochschule Darmstadt, Germany (equation error technique; Gerlach, 1991, [6.2.7]). Both, the DLR frequency-domain results and the results from Stanford University are in good agreement with the AFDD, DLR, and NAE identified derivatives and eigenvalues and confirm the reliability of the models. All these results have in common, that they were obtained by quite complex identification methods although the individual approaches are very different. Another link between AFDD, DLR, and NAE is their high involvement in rotorcraft system identification since a long time. It is well known and accepted that system identification still is a relatively difficult task and that a successful application requires the analyst's skill and experience. The previously gained experience in these organisations has also certainly been helpful for the BO 105 identification.

The results from the Technische Hochschule Darmstadt are in a very good agreement with the NLR identified values. Both approaches are based on less complicated equation error techniques. In comparison with the more complex iterative methods such techniques are computationally very efficient with respect to computing time and storage requirements. From the obtained results it can be stated that equation error methods are appropriate for the rotorcraft identification when models of lower accuracy can be accepted. Such models are certainly useful for various applications, which may not justify the significantly higher efforts and costs for the extraction of more accurate models by more sophisticated methods.

To give an impression of what system identification can do in comparison to a computational simulation, the measured 3211 control inputs for the longitudinal and lateral stick were used in the DLR simulation program SIMH (von Grünhagen, 1988, [6.2.8]). The obtained rate responses are compared to the measured time histories in Figure 6.2.25. In the figure, the same data section is given for the comparison of the identified (DLR) model response and the measurements.

6.2.7 Conclusions

BO 105 flight test data specifically generated for system identification purposes were provided to the Working Group. Flight test trim condition was horizontal flight at 80 knots forward speed.

Results obtained from data consistency analysis, identification, and verification were provided by AFDD, CERT, DLR, University of Glasgow, NAE, and NLR. The identification approaches included frequency- and time-domain techniques with identification criteria ranging from Least-Squares equation error to Maximum Likelihood output error. Data consistency results proved that the measurement quality was appropriate for system identification. Typical for all aircraft and particularly for helicopters, some inconsistencies were seen in the speed data. Therefore, some Members decided to work with reconstructed speed data instead of the measurements.

Six-degrees-of-freedom derivative models were identified. The comparison of the obtained identification results showed quite large differences in both, the identified derivatives and the eigenvalues. This is also true for significant derivatives like the diagonal terms in the state matrix associated to system damping. A more detailed evaluation of all identification and verification results showed that the more complex identification methods, like Maximum Likelihood and Frequency-Response Matching Techniques, gave similar results and provided a good time history agreement with the measurements. Still remaining deficiencies were seen for the higher frequency dynamics. Here, it is evident, that six-degrees-of-freedom models are well suited for the lower and mid-frequency range where rotor dynamics can be approximated by equivalent time delays. For the higher frequency range, however, the helicopter models must be extended by rotor degrees of freedom. For applications that need a suitable overall system characterization but do not require higher accuracies, less complex but computationally more efficient identification methods, like equation error techniques, are applicable and useful.

In conclusion, it can be stated that the BO 105 identification results demonstrate that system identification is a potential tool for extracting reliable helicopter models from flight test data. Depending on the applied evaluation techniques, different accuracy levels for the results are reached. Therefore, it is advisable to establish a

close contact between the analyst and the user of the results before system identification is conducted. Then, a reasonable compromise can be defined between the user's application oriented model accuracy needs and the efforts and costs of the identification analysis.

References

- [6.2.1] Kaletka, J.; von Grünhagen, W.
Identification of mathematical models for the design of a model following control system
45th Annual Forum of the American Helicopter Society, May 1989
- [6.2.2] Kaletka, J.; Tischler, M.B.; von Grünhagen, W.; Fletcher, J.W.
Time- and frequency identification and verification of BO 105 dynamic models
15th European Rotorcraft Forum, September 1989
- [6.2.3] Fletcher, J.W.
Obtaining Consistent Models of Helicopter Flight-data Measurement Errors Using Kinematic-compatibility and State-reconstruction methods
46th Annual Forum of the American Helicopter Society, May 1990
- [6.2.4] Bach, R. E. Jr.,
State Estimation Applications on Aircraft Flight-data Analysis (a User's Manual for SMACK),
NASA Ames Research Center, May, 1984
- [6.2.5] Fu, K.-H.; Marchand, M.,
Helicopter System Identification in the Frequency Domain
9th European Rotorcraft Forum, September 1983
- [6.2.6] Idan, M.
An Identification Algorithm Based on Smoothing
Dissertation, Department of Aeronautics and Astronautics, Stanford University, USA, 1990
- [6.2.7] Gerlach, R.
Parameterschätzung eines zeitkontinuierlichen Hubschraubermodells
Studienarbeit Nr. 1/1632, Institut für Regelungstechnik, TH Darmstadt, Germany, 1991, (in German)
- [6.2.8] von Grünhagen, W.,
Modellierung und Simulation von Hubschraubern
DLR Institute Report IB 111 88/06, 1988 (in German)

Overall dimensions		Main rotor	Tail rotor	
Overall Length	11.84 m		Diameter	1.9 m
Fuselage Length	8.45 m	Diameter	Blades	2
Overall Height	3.03 m	Blades	Chord	0.179 m
		Chord	Profile	NACA 0012
		Profile	Solidity	0.12
		Blade Area	Twist	0.0°
		Solidity (Thrust)	Horizontal stabilizer	
		Tip Sweep		
		Twist	Span	2.0 m
		Shaft Angle	Chord	0.4 m
			Area	0.8 m ²
			Profile	NACA 0010/C020
			Incidence	0°

Table 6.2.1. List of physical characteristics of the BO 105

Control	Control Input		Duration t_f or Frequency content f_f	Number of runs	Recording time per run in s		Flight Conditions	
	Type	initial displacement					Airspeed	Altitude
Longitudinal	Doublet	Aft	$t_f \approx 2s$	2	29 ... 32		80 kn	$H_0 \approx 3000$ ft
Longitudinal	Doublet	Forward	$t_f \approx 2s$	2	26 ... 28		80 kn	$H_0 \approx 3000$ ft
Lateral	Doublet	Right	$t_f \approx 2s$	2	20 ... 26		80 kn	$H_0 \approx 3000$ ft
Lateral	Doublet	Left	$t_f \approx 2s$	2	19 ... 26		80 kn	$H_0 \approx 3000$ ft
Ped 1	Doublet	Right	$t_f \approx 2s$	2	15 ... 27		80 kn	$H_0 \approx 3000$ ft
Pedal	Doublet	Left	$t_f \approx 2s$	2	17 ... 18		80 kn	$H_0 \approx 3000$ ft
Collective	Doublet	Up	$t_f \approx 2s$	2	19 ... 32		90 kn	$H_0 \approx 3000$ ft
Collective	Doublet	Down	$t_f \approx 2s$	2	20 ... 32		80 kn	$H_0 \approx 3000$ ft
Longitudinal	Modified 3211	Aft	$t_f \approx 7s$	3	12 ... 24		80 kn	$H_0 \approx 3000$ ft
Longitudinal	Modified 3211	Forward	$t_f \approx 7s$	3	25 ... 32		80 kn	$H_0 \approx 3000$ ft
Lateral	Modified 3211	Right	$t_f \approx 7s$	3	27 ... 37		80 kn	$H_0 \approx 3000$ ft
Lateral	Modified 3211	Left	$t_f \approx 7s$	3	19 ... 31		80 kn	$H_0 \approx 3000$ ft
Pedal	Modified 3211	Right	$t_f \approx 7s$	3	25 ... 28		80 kn	$H_0 \approx 3000$ ft
Pedal	Modified 3211	Left	$t_f \approx 7s$	3	26 ... 34		80 kn	$H_0 \approx 3000$ ft
Collective	Modified 3211	Up	$t_f \approx 7s$	3	24 ... 29		80 kn	$H_0 \approx 3000$ ft
Collective	Modified 3211	Down	$t_f \approx 7s$	3	23 ... 36		80 kn	$H_0 \approx 3000$ ft
Longitudinal	Frequency sweep	...	$0.08\text{Hz} \leq f_f \leq 8\text{Hz}$	3	68		80 kn	$H_0 \approx 3000$ ft
Lateral	Frequency sweep	...	$0.08\text{Hz} \leq f_f \leq 7\text{Hz}$	3	68		80 kn	$H_0 \approx 3000$ ft
Pedal	Frequency sweep	...	$0.08\text{Hz} \leq f_f \leq 5.5\text{Hz}$	3	68		80 kn	$H_0 \approx 3000$ ft
Collective	Frequency sweep	...	$0.08\text{Hz} \leq f_f \leq 7\text{Hz}$	3	68		80 kn	$H_0 \approx 3000$ ft

Table 6.2.2. List of runs (BO 105)

Aircraft mass: ≈ 2200 kg.

Aircraft inertias (manufacturer's estimates) based on 2400 kg and referred to body axes with origin in CG appropriate to tests flown:

 $I_x \approx 1700 \text{ kg m}^2$, $I_y \approx 4200 \text{ kg m}^2$, $I_z \approx 4200 \text{ kg m}^2$, $I_{xz} \approx 0 \text{ kg m}^2$.The altitude given is the density altitude H_0 . The actually flown pressure altitude was 4400 ft (at -5°C) $\leq H_0 \leq 5200$ ft (at -13°C).

Group	Variables Quantity	Source	Original Sampling Rate (in Hz)
Control displacements	Forward/Aft Cyclic	Potentiometer	50
	Lateral Cyclic	Potentiometer	50
	Pedal	Potentiometer	50
	Collective	Potentiometer	50
Table 6.2.3. BO 105 Control Variables			

Group	Variables Quantity	Source	Original Sampling Rate (in Hz)
Air data	Longitudinal airspeed	HADS	50
	Lateral airspeed	HADS	50
	Normal airspeed	HADS	50
Linear accelerations	Longitudinal acceleration	Accelerometer at CG	300
	Lateral acceleration	Accelerometer at CG	300
	Normal acceleration	Accelerometer at CG	300
Attitude angles (Euler angles)	Roll angle	Vertical gyro	50
	Pitch angle	Vertical gyro	50
	Yaw angle	Directional gyro	50
Angular rates	Roll rate	Rate gyro	100
	Pitch rate	Rate gyro	100
	Yaw rate	Rate gyro	100
Rotor	RPM	Tachometer	50
Table 6.2.4. BO 105 Response Variables			
Data provided at a uniform sampling rate of 100 Hz.			

Scale factor for		AFDD		DLR		DLR		NLR	
Symbol	Unit	Value	σ	Value	σ	Value	σ	Value	σ
u	1	0.9556	0.0272	0.9856	0.0104	0.9244	0.0027†	---	---
v	1	0.7043	0.0524	0.6723	0.0855	0.6932	0.0082†	---	---
w	1	0.8771	0.0378	0.9521	0.0813	0.9283	0.0039†	---	---
Φ	1	1.0199	0.0128	1.0144	0.0177	1.0168	0.0005†	---	---
Θ	1	1.0290	0.0352	1.0364	0.0281	1.0351	0.0004†	---	---
Ψ	1	---	---	1.0202	0.1371	1.0392	0.0016†	---	---

* From all files
 ** From 4 concatenated files proposed for identification
 *** From 4 files proposed for identification
 † Cramer Rao lower bound
 σ = Standard deviation

Table 6.2.5. BO 105 Data consistency analysis: Mean values of identified scale factors

Bias for		AFDD		DLR		DLR		NLR	
Symbol	Unit	Value	σ	Value	σ	Value	σ	Value	σ
a_x	m/a^2	---	---	0.0571	0.1130	0.0194	0.0027†	0.0243	0.0028†
a_y	m/s^2	---	---	0.0443	0.1096	0.0157	0.0047†	0.0016	0.0029†
a_z	m/s^2	---	---	0.0007	0.0458	0.0463	0.0023†	0.0145	0.0023†
p	rad/s	-0.0015	0.0002	-0.0015	0.0005	-0.0013	0.0002†	-0.0015	0.0001†
q	rad/s	-0.0017	0.0002	-0.0016	0.0005	-0.0014	0.0001†	-0.0019	0.0001†
r	rad/s	---	---	-0.0005	0.0019	-0.0002	0.0004†	-0.0011	0.0001†

* From all files
 ** From 4 concatenated files proposed for identification
 *** From 4 files proposed for identification
 † Cramer Rao lower bound
 σ = Standard deviation

Table 6.2.6. BO 105 Data Consistency Analysis: Mean values of identified biases

Components	Motivator deflections			
	δ_{lon}	δ_{lat}	δ_{ped}	δ_{col}
u	*	*	*	*
v		*	*	
w	*	*		*
p	*	*	*	*
q	*	*	*	*
r	*	*	*	
a_x	*			
a_y	*	*	*	
a_z	*			*

State vector:

$$[u \ v \ w \ p \ q \ r \ \Phi \ \Theta]^T$$

Measurement vector:

$$[u \ v \ w \ p \ q \ r \ a_x \ a_y \ a_z]^T$$

Number of frequencies: 19

Weight: 7.570 deg-error/dB-error

* indicates an input/output frequency response included in the identification cost function

Table 6.2.7. Set-up for AFDD frequency-domain identification

Derivative Symbol	Unit	AFDD		CERT		DLR		Glasgow Uni		NAE		NLR	
		Value	σ	Value	σ	Value	σ	Value	σ	Value	σ	Value	σ
X_u	1/s	-0.0385	0.0036	-0.058	0.0014	-0.059	0.0006	-0.032	0.0044	-0.050	0.0094	-0.050	0.0008
X_v	1/s	0*	—	0*	—	0*	—	0*	—	0.0043	0.0021	0*	—
X_w	1/s	-0.061	0.0094	0.025	0.0027	0.036	0.0013	-0.0422	0.0064	-0.017	0.002	0.015	0.0014
X_p	m/(rad s)	0.756	0.120	0*	—	0*	—	0*	—	0.479	0.058	0*	—
X_q	m/(rad s)	2.548	0.273	0*	—	0*	—	0*	—	1.206	0.072	0*	—
X_r	m/(rad s)	0*	—	0*	—	0*	—	0*	—	0.232	0.019	0*	—
Y_u	1/s	0*	—	0*	—	0*	—	0*	—	-0.061	0.0021	0*	—
Y_v	1/s	-0.221	0.011	-0.177	0.003	-0.170	0.003	-0.131	0.055	-0.279	0.005	-0.064	0.002
Y_w	1/s	-0.083	0.007	0*	—	0*	—	0*	—	-0.0307	0.0022	0*	—
Y_p	m/(rad s)	-2.030	0.251	0*	—	0*	—	0*	—	-2.993	0.138	0*	—
Y_q	m/(rad s)	4.823	0.263	0*	—	0*	—	0*	—	3.021	0.164	0*	—
Y_r	m/(rad s)	0.950	0.139	0*	—	1.332	0.045	0*	—	0.807	0.041	1.191	0.241
Z_u	1/s	0.2457	0.018	0.222	0.006	0.014	0.0034	-0.0833	0.0087	0.1016	0.0063	0.0204	0.0033
Z_v	1/s	0*	—	0*	—	0*	—	0*	—	-0.135	0.012	0*	—
Z_w	1/s	-1.187	0.0555	-1.171	0.012	-0.998	0.0072	-0.791	0.0178	-1.106	0.013	-0.875	0.0058
Z_p	m/(rad s)	2.622	0.359	0*	—	0*	—	0*	—	0.365	0.29	0*	—
Z_q	m/(rad s)	7.011	1.133	0*	—	5.012	0.28	0*	—	7.011	1.711	0*	—
Z_r	m/(rad s)	0*	—	0*	—	0*	—	0*	—	0.27	0.096	0*	—

* Eliminated from model structure

 σ = Standard deviation

Table 6.2.8. BO 105 Identification Results: List of specific force derivatives with respect to flight variables

Derivative Symbol	Unit	AFDD		CERT		DLR		Glasgow Uni		NAE		NIR	
		Value	σ	Value	σ	Value	σ	Value	σ	Value	σ	Value	σ
L_y	rad/(s m)	-0.061	0.0077	-0.014	0.0008	-0.081	0.0016	-0.027	0.0036	-0.099	0.0032	-0.012	0.0019
L_z	rad/(s m)	-0.207	0.021	-0.092	0.0019	-0.271	0.004	-0.096	0.0090	-0.270	0.0071	-0.038	0.0028
L_w	rad/(s m)	0.168	0.014	0.038	0.0028	0.116	0.0035	0.130	0.0095	0.116	0.007	0.028	0.0048
L_p	1/s	-8.779	0.641	-2.693	0.056	-8.501	0.110	-4.470	0.392	-7.048	0.201	-1.995	0.114
L_q	1/s	3.182	0.624	1.558	0.090	3.037	0.125	0*	—	4.454	0.222	0.558	0.171
L_r	1/s	0.991	0.187	1.321	0.029	0.410	0.036	1.318	0.14	0.434	0.055	1.221	0.057
$M_{\dot{u}}$	rad/(s m)	0*	—	0.0145	0.0002	0.029	0.0004	0.0203	0.0005	0.0078	0.001	0.0144	0.001
$M_{\dot{w}}$	rad/(s m)	0.050	0.0034	0.025	0.0006	0.048	0.0012	0*	—	0.0248	0.0024	0.0039	0.0015
$M_{\dot{p}}$	rad/(s m)	0.036	0.0064	0.356	0.0006	0.053	0.0011	0.0491	0.0011	0.0696	0.0022	0.0186	0.0026
$M_{\dot{q}}$	1/s	-0.998	0.056	-0.491	0.0152	-0.419	0.038	-1.367	0.032	-1.414	0.066	-0.878	0.062
$M_{\dot{r}}$	1/s	-4.493	0.235	-2.26	0.025	-3.496	0.047	-2.217	0.009	-2.992	0.074	-1.441	0.093
M_r	1/s	-0.438	0.052	0*	—	-0.117	0.013	0*	—	-0.584	0.019	0*	—
$N_{\dot{u}}$	rad/(s m)	0.082	0.0049	0.102	0.0009	0.117	0.0012	0.0784	0.0045	0.112	0.0017	0.051	0.0016
$N_{\dot{w}}$	rad/(s m)	-0.119	0.009	0.0025	0.001	0.034	0.006	0.0281	0.008	-0.0634	0.003	0.0195	0.002
$N_{\dot{p}}$	1/s	-0.466	0.15	-1.116	0.025	-1.057	0.025	-1.302	0.017	-0.692	0.061	-1.953	0.06
$N_{\dot{q}}$	1/s	5.432	0.292	0.491	0.029	0.809	0.016	0.959	0.231	3.254	0.107	1.227	0.071
N_r	1/s	-1.070	0.061	-1.116	0.0126	-0.858	0.0058	-0.756	0.0640	-1.017	0.0234	-0.699	0.0347

* Eliminated from model structure

 σ = Standard deviation

Table 6.2.9. BO 105 Identification Results: List of specific moment derivatives with respect to flight variables

Derivative Symbol	Unit	AFOD		CERT		DLR		Glasgow Uni		NAE		NLR	
		Value	σ	Value	σ	Value	σ	Value	σ	Value	σ	Value	σ
$X_{\delta col}$	m/(s ² %)	-0.046	0.004	0*	—	0*	—	0*	—	-0.022	0.001	0*	—
$X_{\delta lon}$	m/(s ² %)	-0.072	0.0045	-0.048	0.0029	-0.028	0.0015	-0.048	0.0016	-0.050	0.0014	-0.027	0.0019
$X_{\delta lat}$	m/(s ² %)	0*	—	0*	—	0*	—	0*	—	-0.00176	0.001	0*	—
$Y_{\delta col}$	m/(s ² %)	-0.032	0.0031	0*	—	0*	—	0*	—	-0.0152	0.0023	0*	—
$Y_{\delta lon}$	m/(s ² %)	0*	—	0*	—	0*	—	0*	—	-0.0253	0.0032	0*	—
$Y_{\delta lat}$	m/(s ² %)	0.066	0.0051	-0.001	0.0015	0.006	0.0013	0.0764	0.0094	0.0795	0.0024	-0.0006	0.0024
$Y_{\delta ped}$	m/(s ² %)	0.015	0.0039	-0.009	0.0018	-0.011	0.0017	-0.071	0.0425	-0.0274	0.0013	-0.014	0.0032
$Z_{\delta col}$	m/(s ² %)	-0.388	0.020	-0.273	0.003	-0.349	0.002	-0.259	0.021	-0.337	0.005	-0.242	0.003
$Z_{\delta lon}$	m/(s ² %)	-0.103	0.0288	-0.0078	0.0041	-0.300	0.008	-0.140	0.0492	-0.175	0.0073	-0.075	0.008
$Z_{\delta lat}$	m/(s ² %)	0*	—	0*	—	0*	—	0*	—	0.029	0.0052	0*	—
$Z_{\delta ped}$	m/(s ² %)	0*	—	0*	—	0*	—	0*	—	-0.0059	0.003	0*	—

* Eliminated from model structure

 σ = Standard deviation

Table 6.2.10. BO 105 Identification Results: List of specific force derivatives with respect to control variables

Derivative Symbol	Unit	AFDC		CERT		DLR		Glasgow Uni		NAE		NLR	
		Value	σ	Value	σ	Value	σ	Value	σ	Value	σ	Value	σ
$L_{\delta\text{col}}$	rad/(s ² %)	0.052	0.005	0.0044	0.0012	0.032	0.0011	0*	--	0.0142	0.003	0.022	0.007
$L_{\delta\text{lon}}$	rad/(s ² %)	0.073	0.0064	-0.0028	0.0016	0.024	0.0025	0*	--	-0.005	0.0044	0.0301	0.0045
$L_{\delta\text{lat}}$	rad/(s ² %)	0.179	0.0139	0.0551	0.0009	0.185	0.0023	0.0764	0.0094	0.1361	0.0036	0.0534	0.0024
$L_{\delta\text{ped}}$	rad/(s ² %)	-0.027	0.0045	-0.018	0.0009	-0.028	0.001	-0.0209	0.0046	-0.0172	0.0017	-0.0096	0.0021
$R_{\delta\text{col}}$	rad/(s ² %)	0.073	0.0034	0.034	0.0004	0.057	0.0006	0.039	0.0012	0.048	0.0010	0.032	0.0016
$M_{\delta\text{lon}}$	rad/(s ² %)	0.088	0.0043	0.050	0.0016	0.063	0.001	0.0565	0.0020	0.0787	0.0015	0.054	0.0025
$M_{\delta\text{lat}}$	rad/(s ² %)	0*	--	-0.0003	0.0003	-0.009	0.0008	0*	--	0.0106	0.0013	0.005	0.0013
$M_{\delta\text{ped}}$	rad/(s ² %)	0.013	0.0017	0*	--	0*	--	0*	--	0.005	0.0006	0*	--
$N_{\delta\text{col}}$	rad/(s ² %)	-0.051	0.0041	0*	--	0*	--	0*	--	-0.036	0.0016	0*	--
$N_{\delta\text{lon}}$	rad/(s ² %)	-0.075	0.005	0*	--	0*	--	0*	--	-0.051	0.002	0*	--
$N_{\delta\text{lat}}$	rad/(s ² %)	0.033	0.0023	0.0147	0.0004	0.026	0.0005	0*	--	0.047	0.001	0.045	0.0014
$N_{\delta\text{ped}}$	rad/(s ² %)	0.057	0.0023	0.043	0.0005	0.049	0.0003	0.443	0.0020	0.484	0.0008	0.044	0.0014

* Eliminated from model structure
 σ = Standard deviation

Table 6.2.11. BO 105 Identification Results: List of specific moment derivatives with respect to control variables

Delay		AFDD		CERT		DLR		Glasgow Uni		NAE		NLR	
Symbol	Unit	Value	σ	Value	σ	Value	σ	Value	σ	Value	σ	Value	σ
T_{dcl}	s	0.158	0.0056	0.0	—	0.040	—	0.102	—	0.040 *	—	0.040 *	—
T_{dln}	s	0.113	0.0059	0.0	—	0.100	—	0.044	—	0.100 *	—	0.100 *	—
T_{dlt}	s	0.062	0.0056	0.0	—	0.060	—	0.074	—	0.060 *	—	0.060 *	—
T_{dcd}	s	0.044	0.0065	0.0	—	0.040	—	0.0	—	0.040 *	—	0.040 *	—

* From DLR value
 σ = Standard deviation

Table 6.2.12. BO 105 Identification Results: Equivalent control time delays

Mode of motion	AFDD	CERT	DLR	Glasgow Uni	NAE	NLR
Phugoid oscillation	[-0.36, 0.30]	[-0.17, 0.32]	[-0.15, 0.33]	[-0.010, 0.35]	[-0.014, 0.33]	[-0.07, 0.33]
Dutch roll oscillation	[+0.22, 2.60]	[+0.13, 2.51]	[+0.14, 2.50]	[+0.16, 2.27]	[+0.13, 2.58]	[+0.17, 2.17]
Roll mode	(8.32)	[+0.99, 2.89]	(8.49)	(5.12)	(8.47)	(2.38)
Aperiodic pitch mode 1	(6.04)	—	(4.36)	(1.98)	(4.38)	(1.37)
Aperiodic pitch mode 2	(0.49)	(0.66)	(0.60)	(0.84)	(0.63)	(0.71)
Spiral mode	(0.03)	(-0.05)	(0.02)	(-0.007)	(0.03)	(0.04)

† In this case the aperiodic roll mode and the fast pitch mode combine into an oscillatory mode.

Shorthand notation:
 s Laplace variable (in 1/s)
 $[\zeta, \omega_0]$ represents $(s^2 + 2\zeta\omega_0s + \omega_0^2)$
 with ζ = damping ratio and ω_0 = undamped natural frequency (in rad/s)
 $(1/T)$ represents $(s + 1/T)$
 with T = time constant (in s)

Table 6.2.13. BO 105 Identification Results: Time constants, damping ratios and undamped natural frequencies

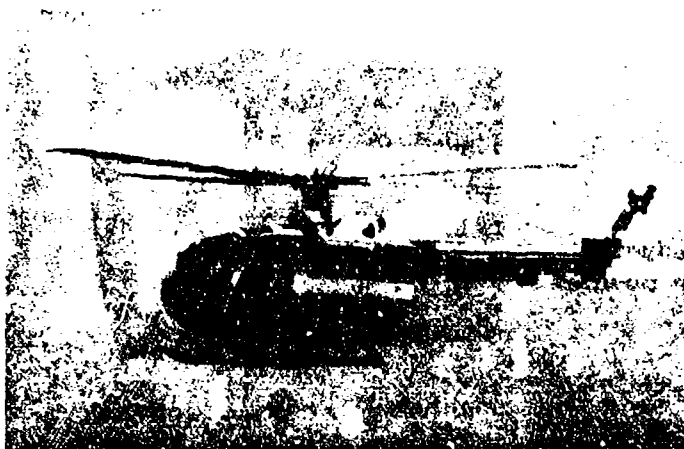


Figure 6.2.1. DLR research helicopter BO 105

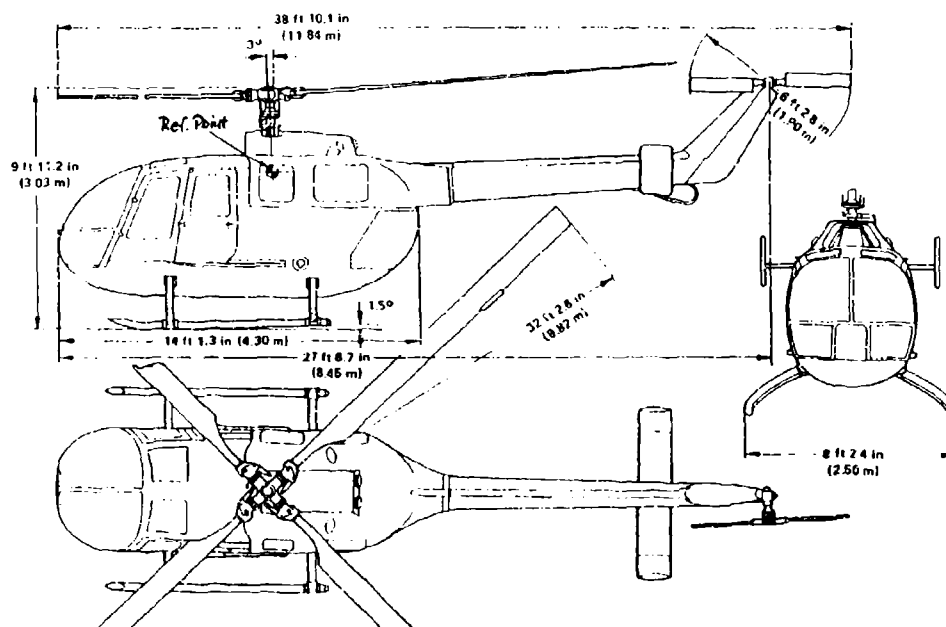


Figure 6.2.2. Three view drawing of BO 105

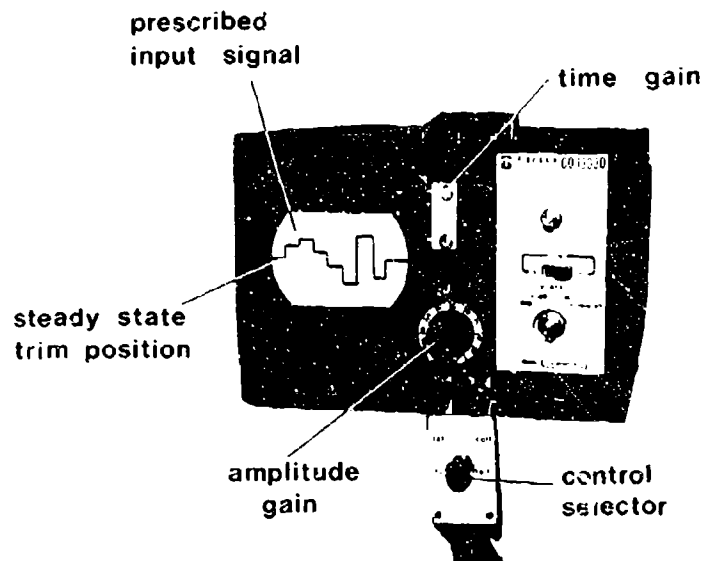


Figure 6.2.3. Pilot's display for input signal generation (BO 105)

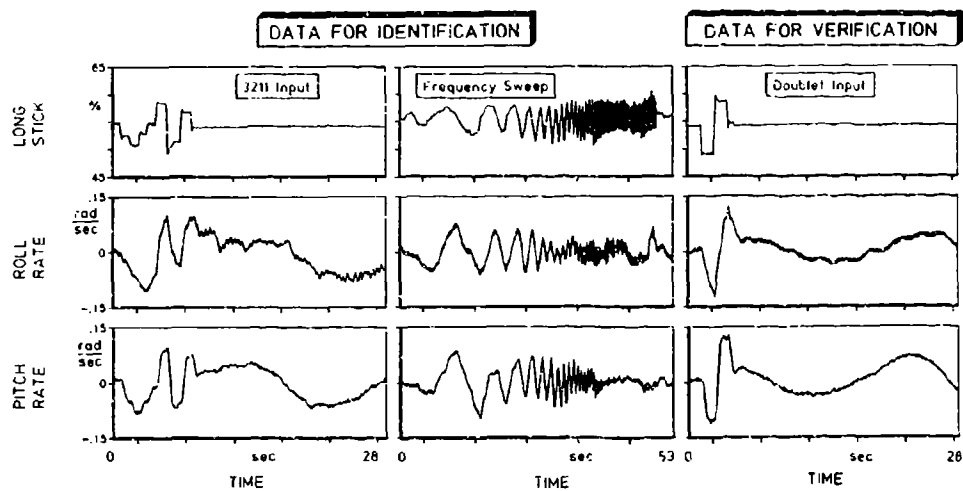


Figure 6.2.4. Representative BO 105 flight test data: control input types and rate responses

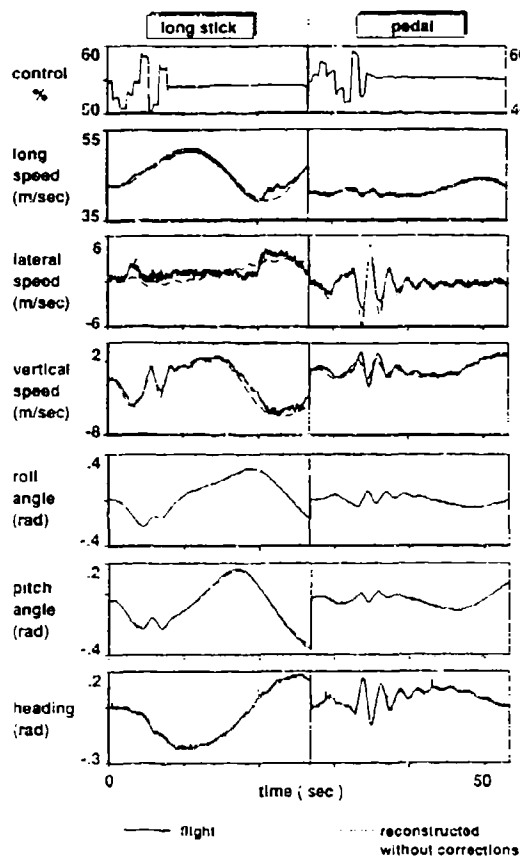


Figure 6.2.5. Comparison of measured and reconstructed BO 105 data without scale factor corrections

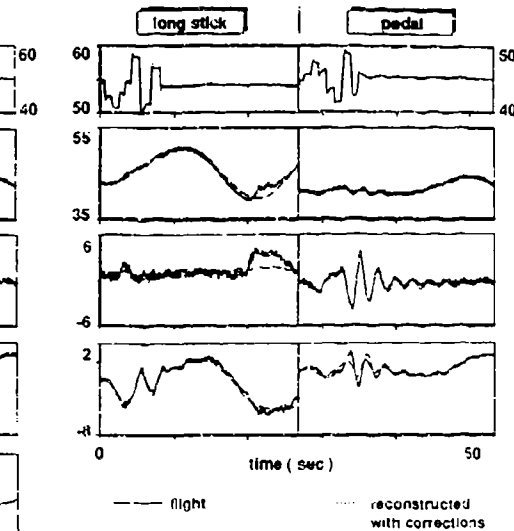


Figure 6.2.6. Comparison of measured and reconstructed BO 105 speed data with scale factor corrections

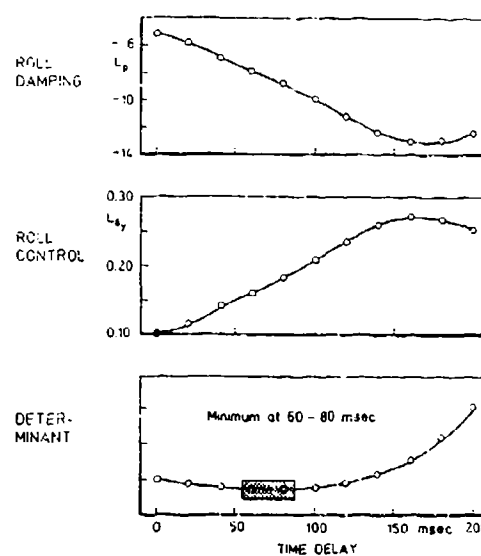


Figure 6.2.7. Influence of equivalent time delays on BO 105 identification results

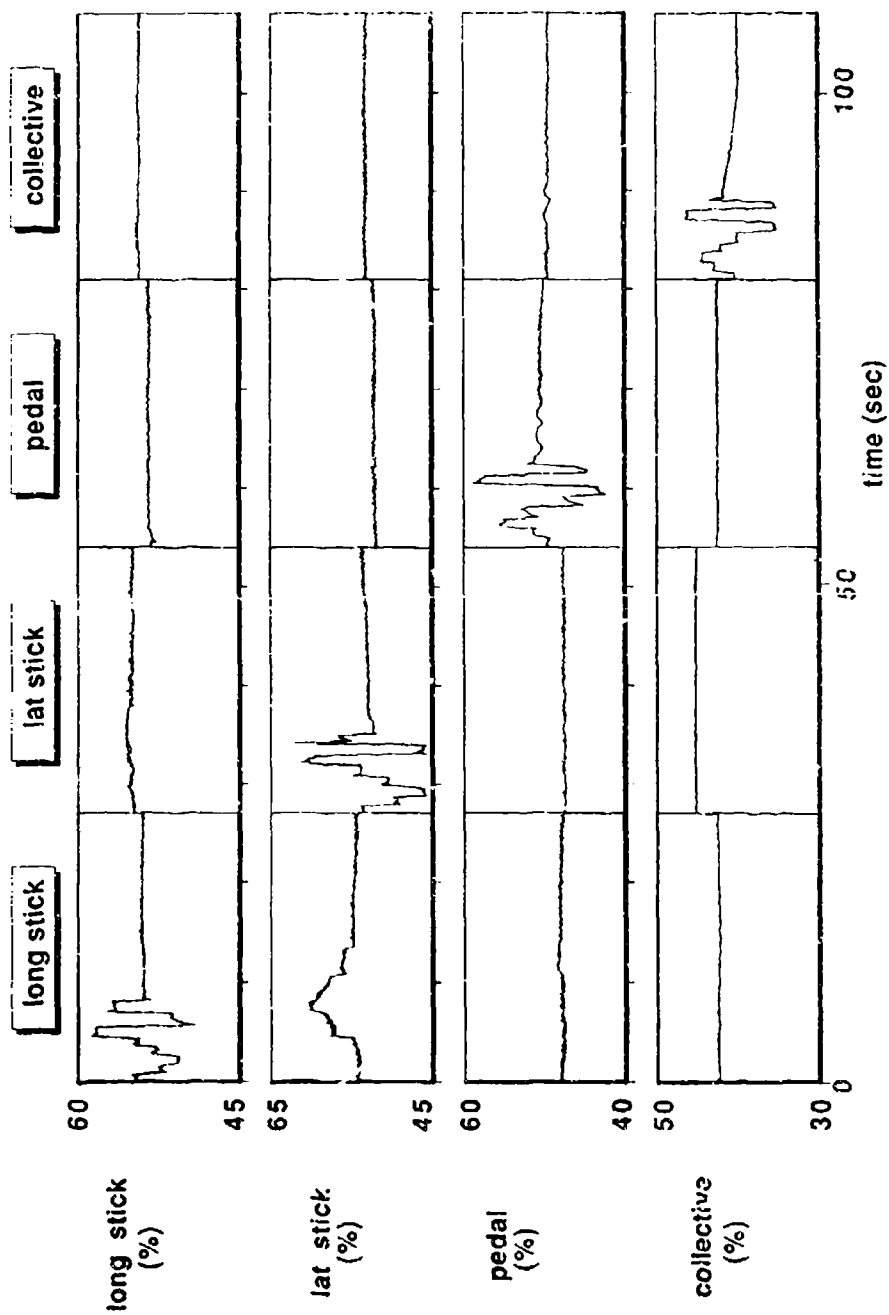


Figure 6.2.8. Control input signals of BO 105 flight test data used for identification (modified '3211' signals)

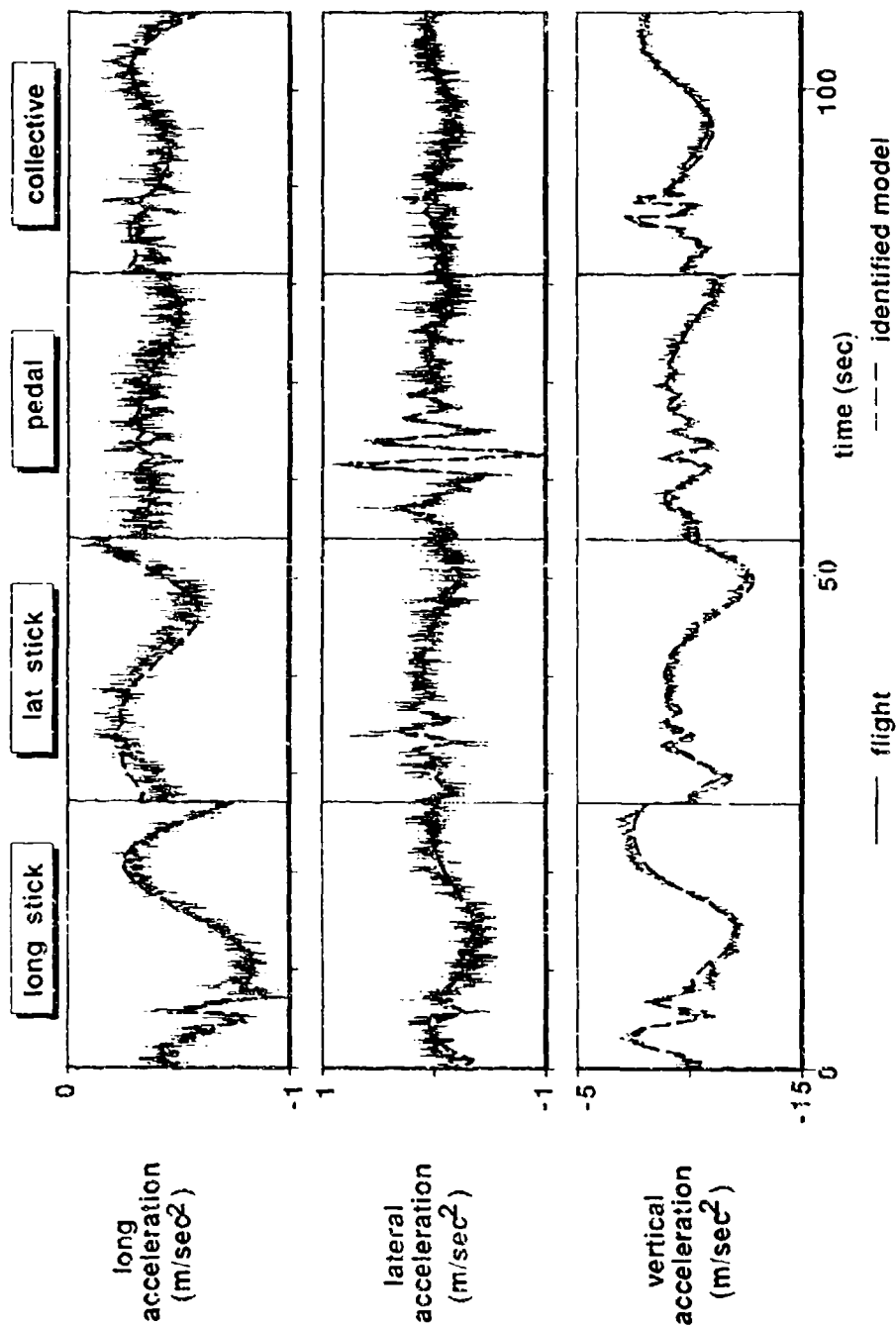


Figure 6.2.9. Comparison of BO 105 flight data and response of the identified model for linear accelerations (DLR result)

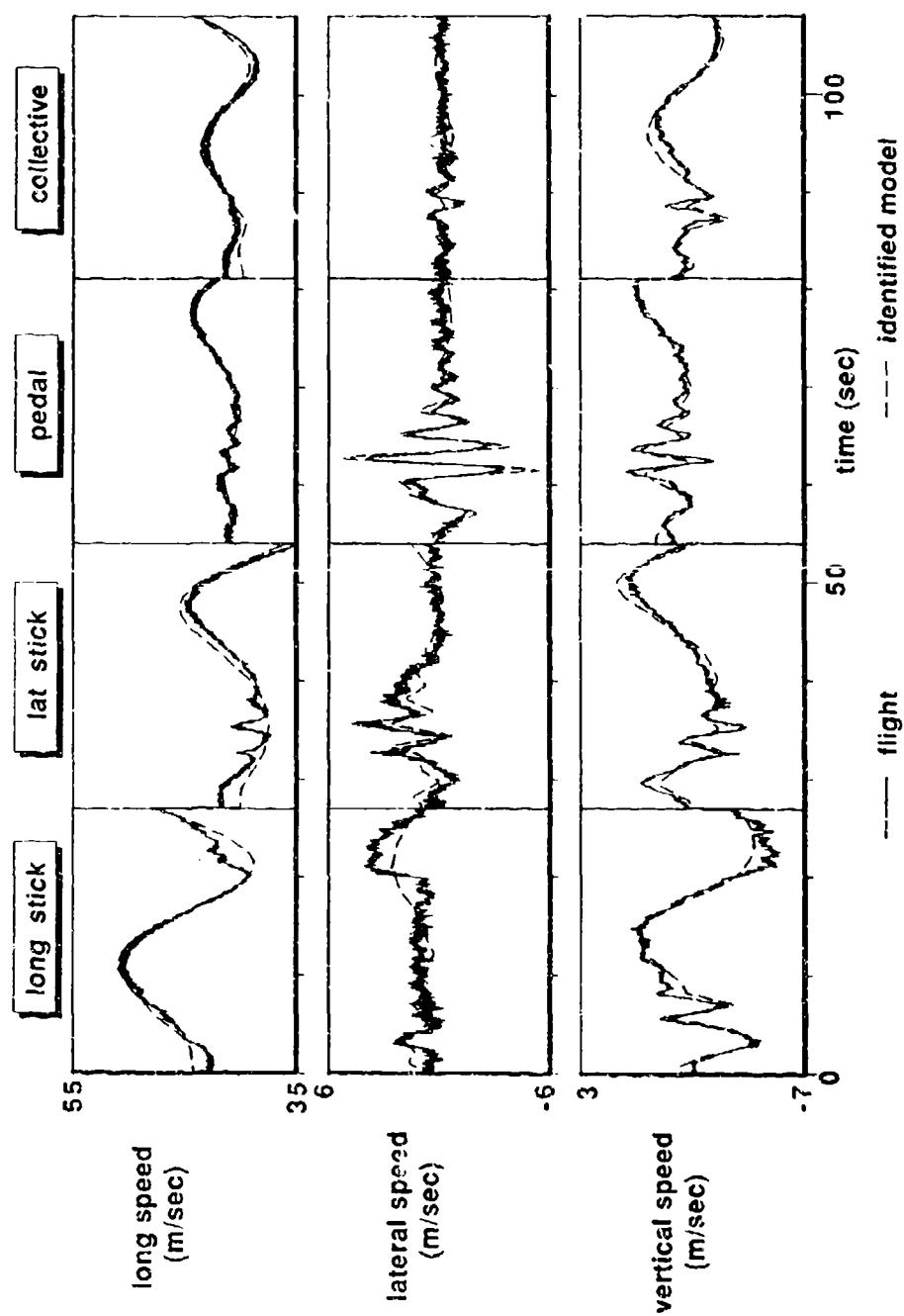


Figure 6.2.10. Comparison of BO 105 flight data and response of the identified model for linear speeds (DLR result)

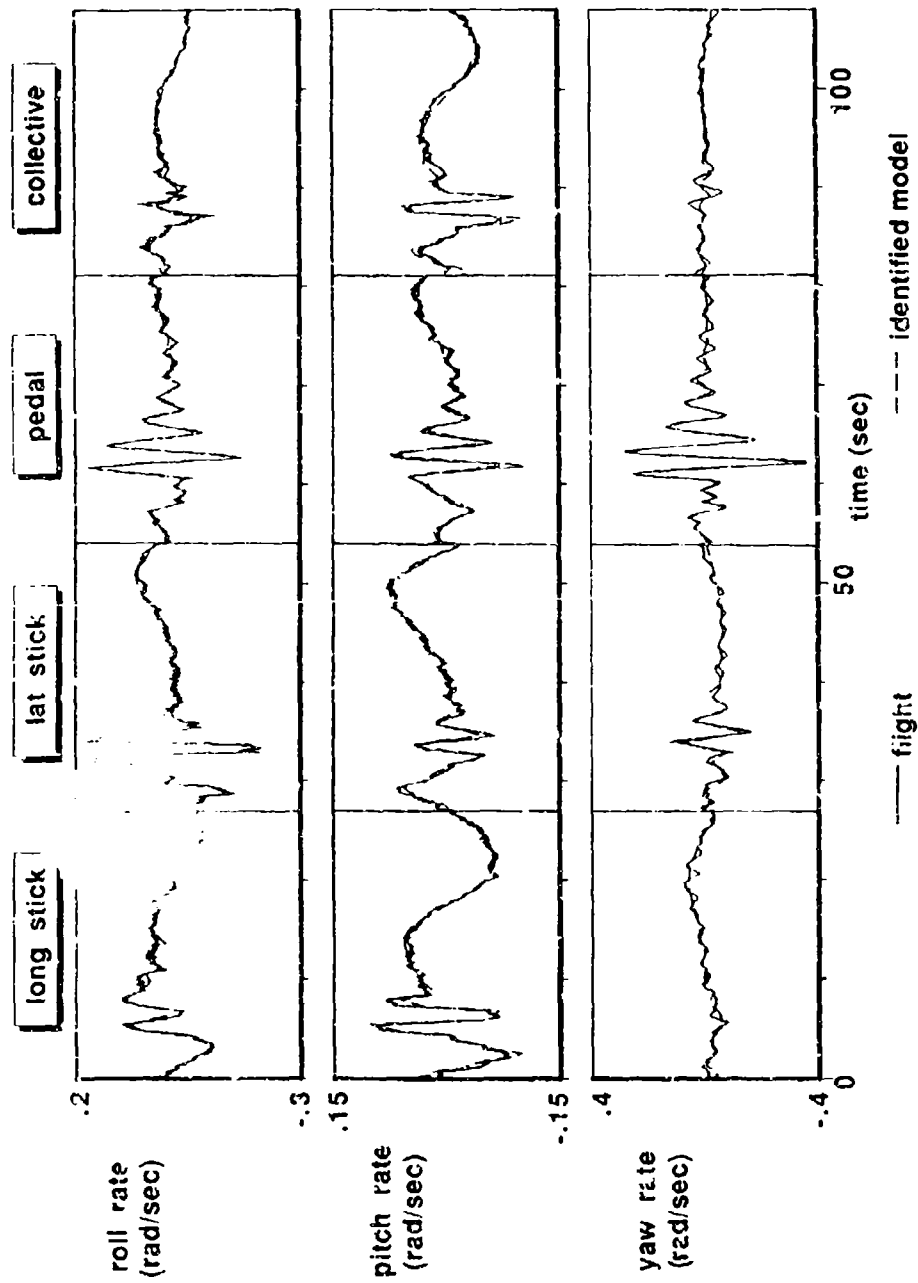


Figure 6.2.11. Comparison of 30 105 flight data and response of the identified model for angular rates (DLR result)

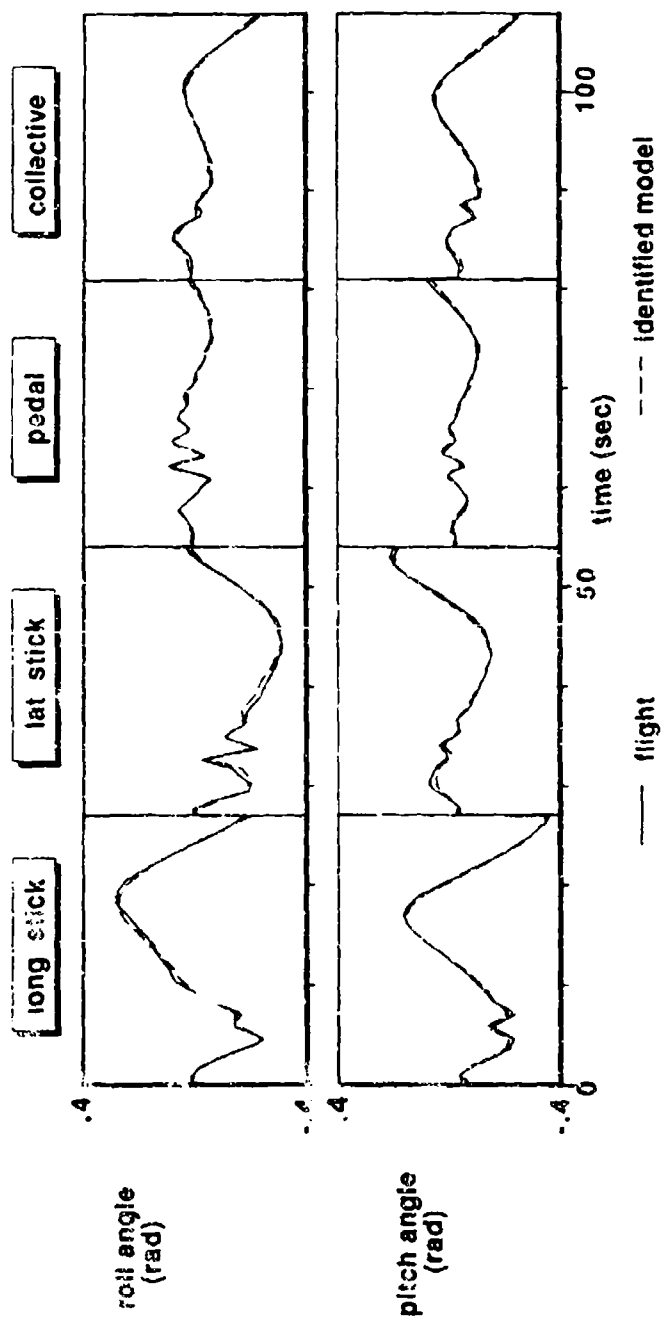


Figure 6.2.12. Comparison of BO 105 flight data and response of the identified model for Euler angles (DLR result)

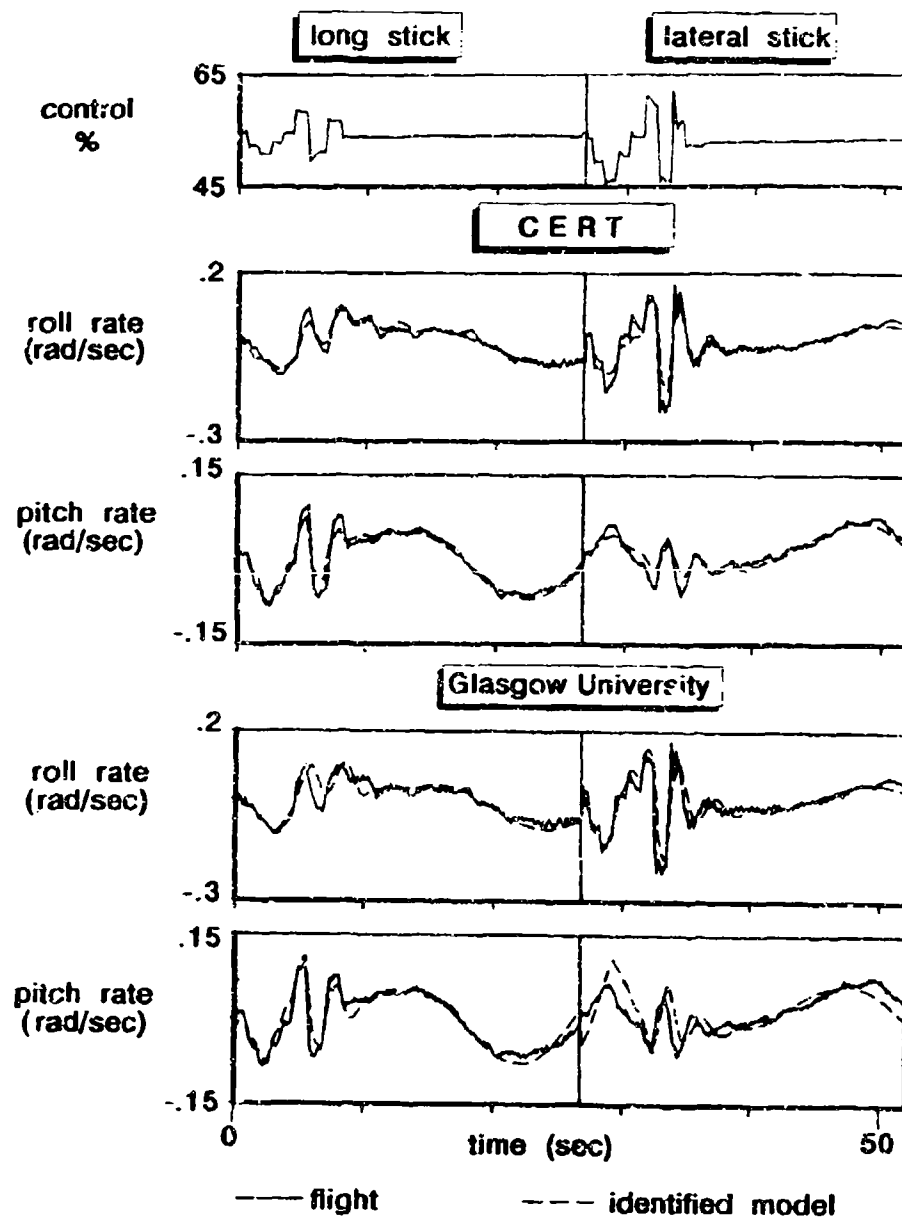


Figure 6.2.13. Comparison of measured rates and the response of identified BO 105 models (CERT and Glasgow University results)

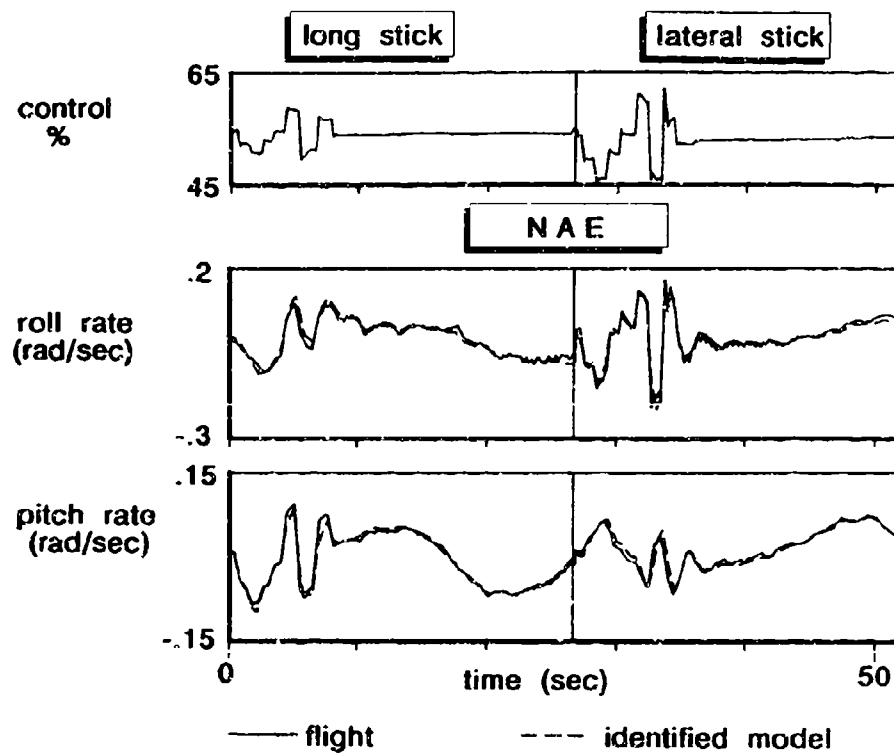


Figure 6.2.14. Comparison of measured rates and the response of the identified BO 105 models (NAE results)

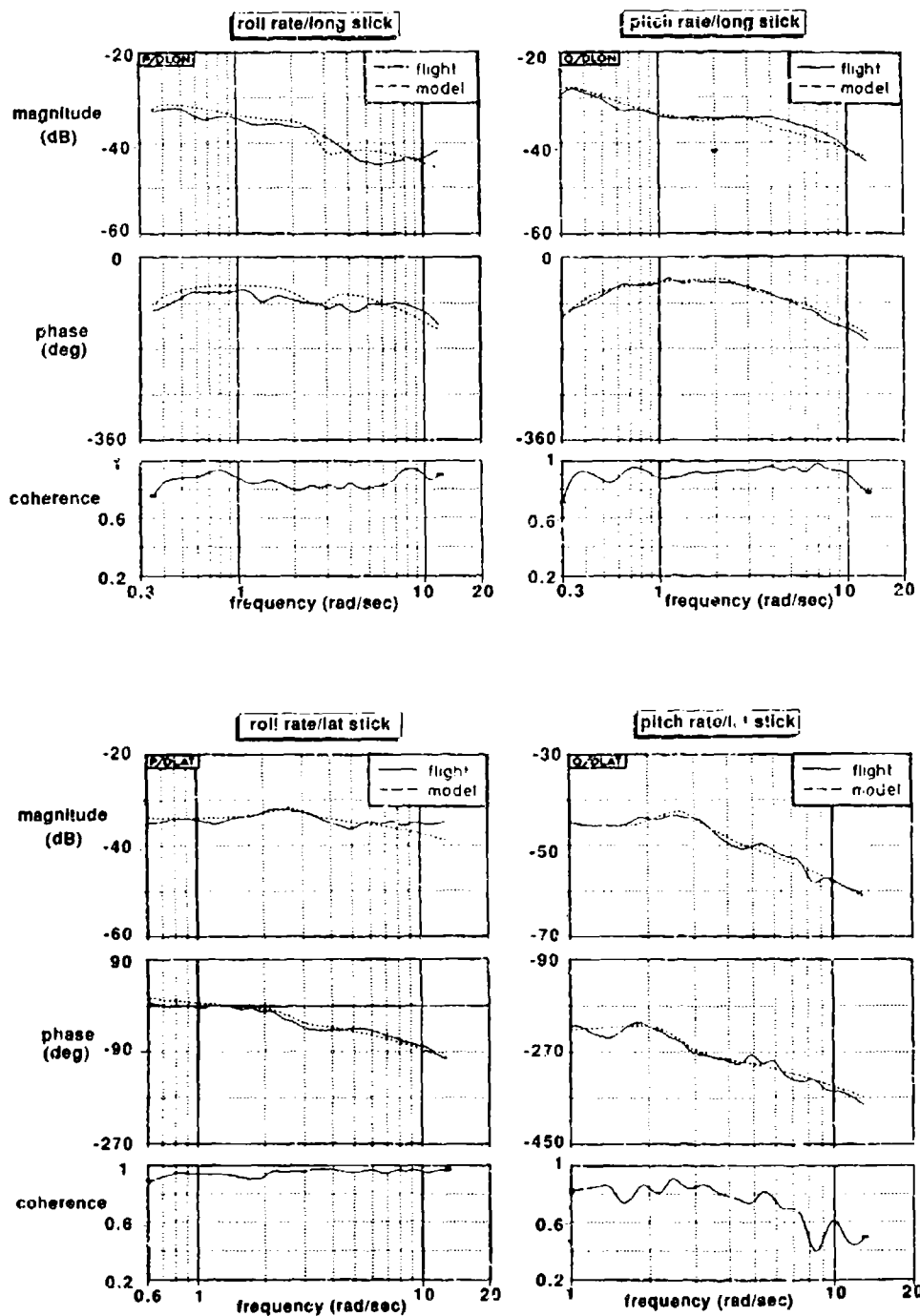


Figure 6.2.15. Comparison of BO 105 flight data and identified models frequency responses (roll and pitch rate, representative AFDD results)

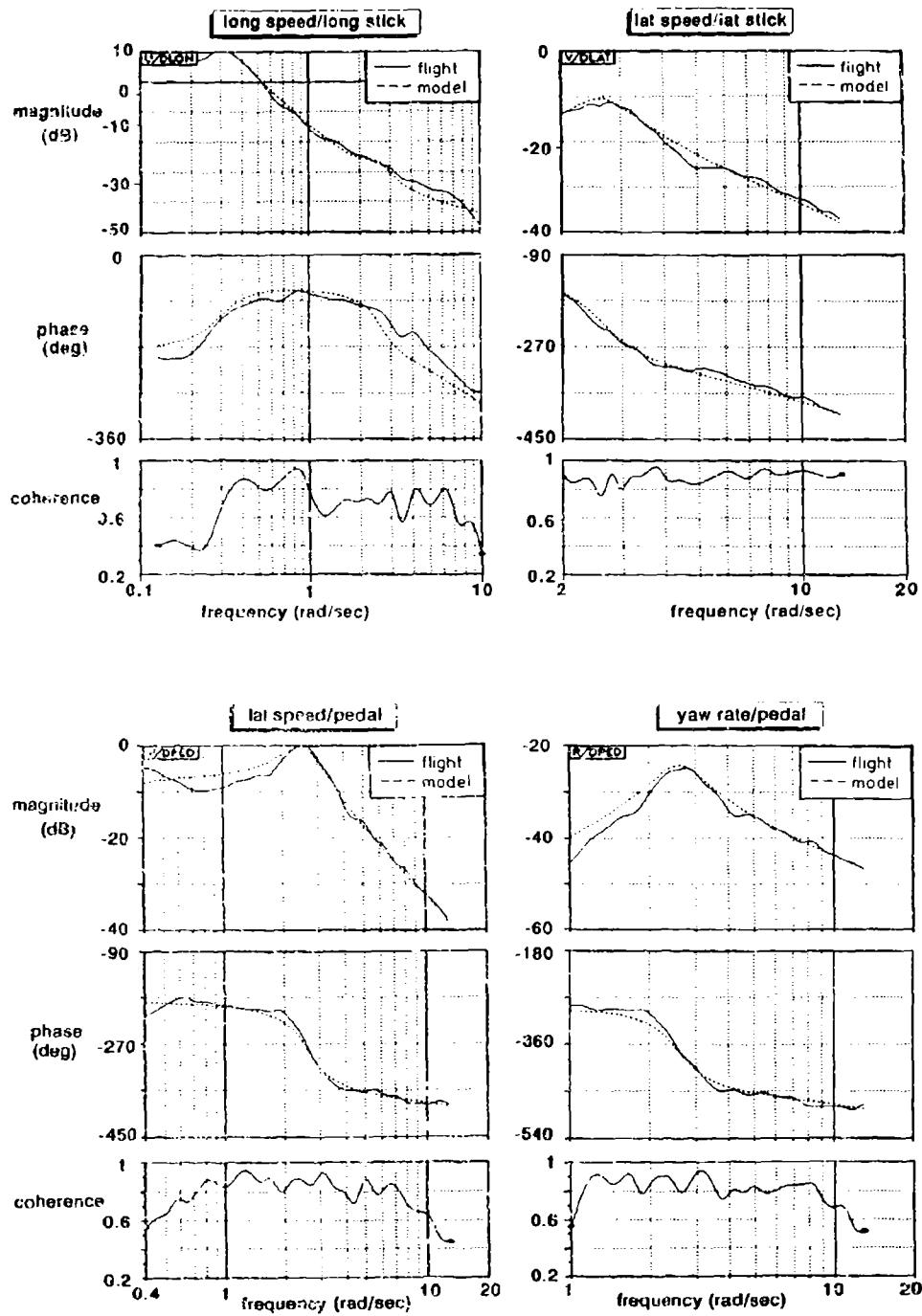


Figure 3.2.16. Comparison of BO 305 flight data and identified models frequency responses (linear speeds and yaw rate, representative AFDD results)

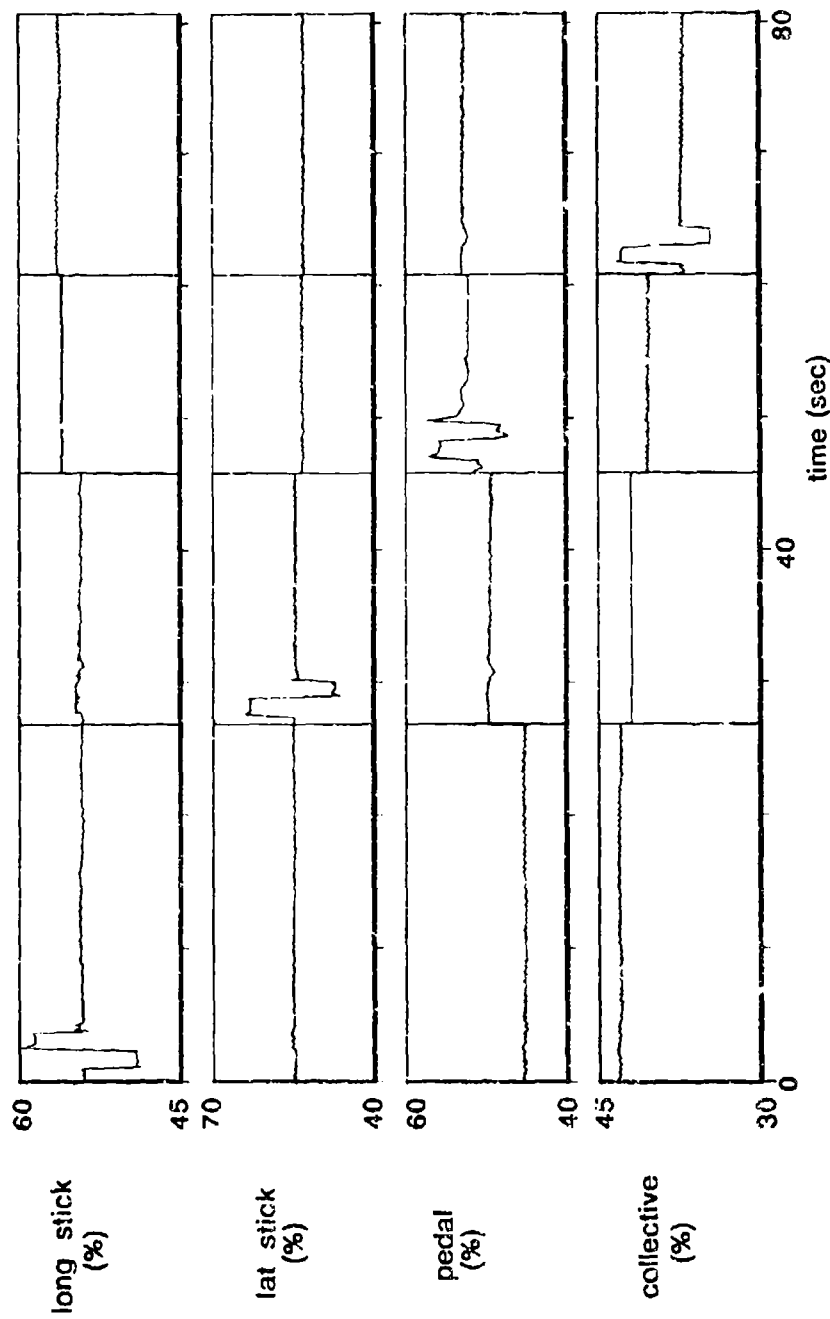


Figure 6.2.17. Control input signals of BO 105 flight test data used for verification (doublet signals)

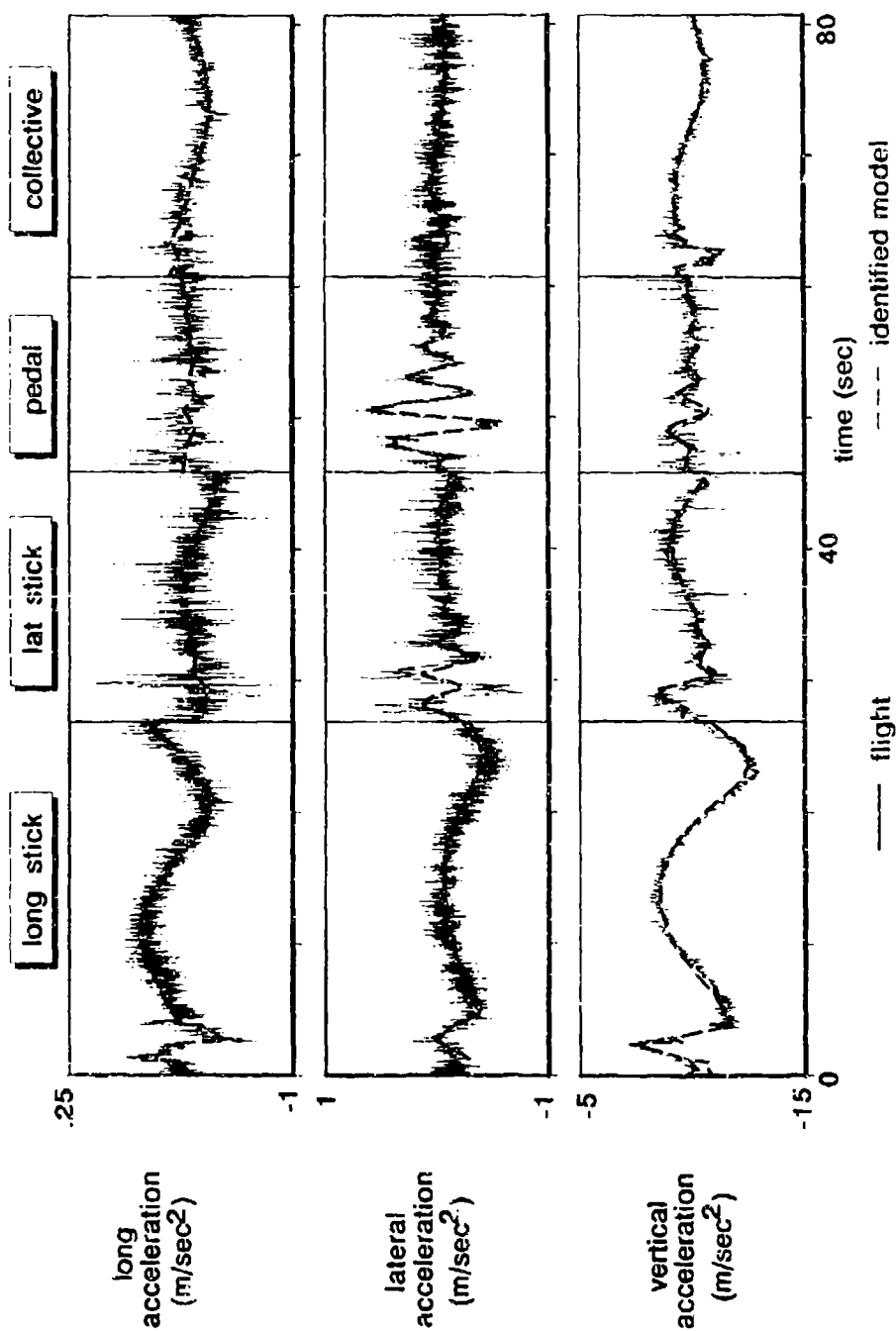


Figure 6.2.18. Verification of the identified model (linear accelerations, DLR result)

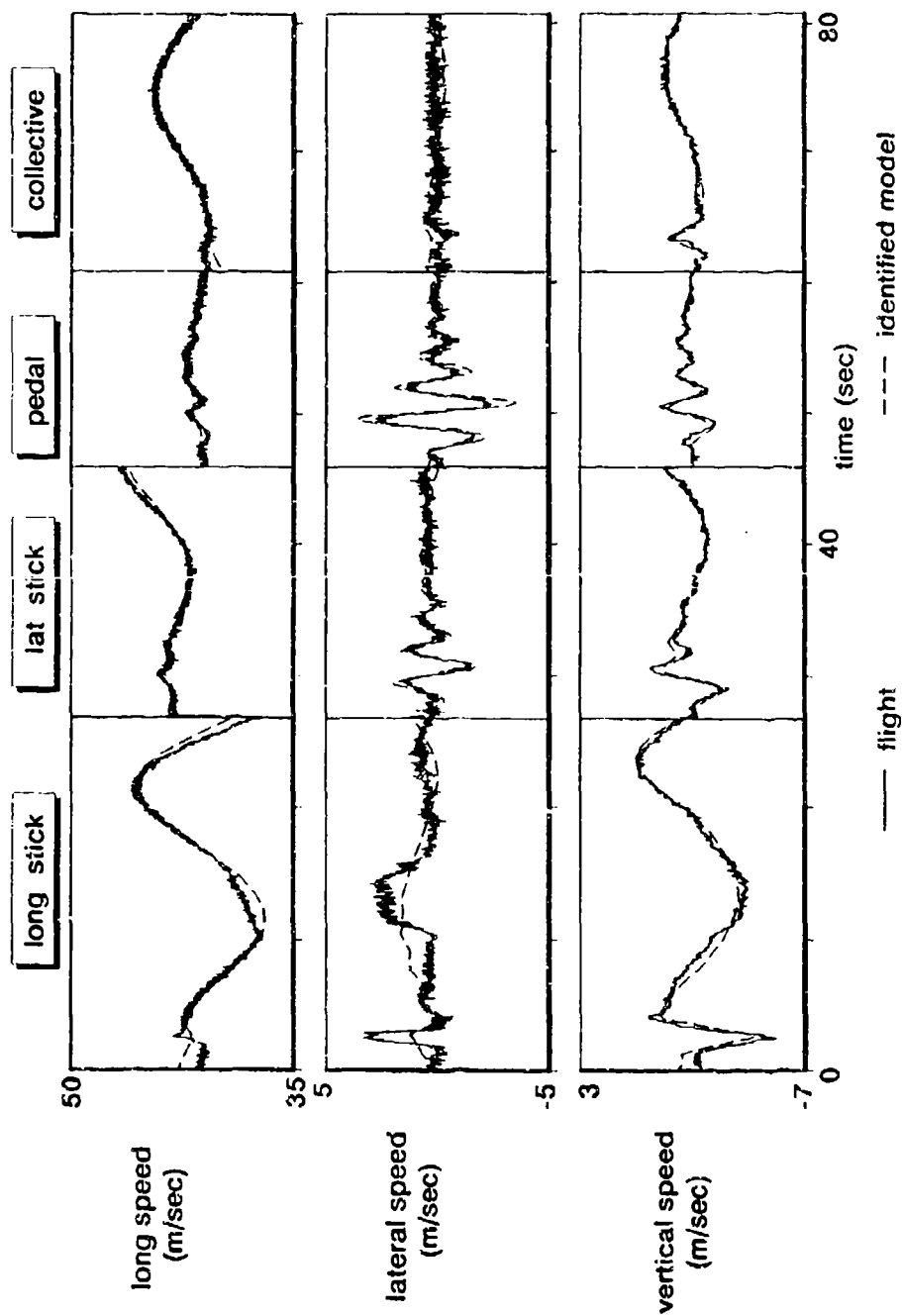


Figure 6.2.19. Verification of the identified model (linear speeds, DLR result)

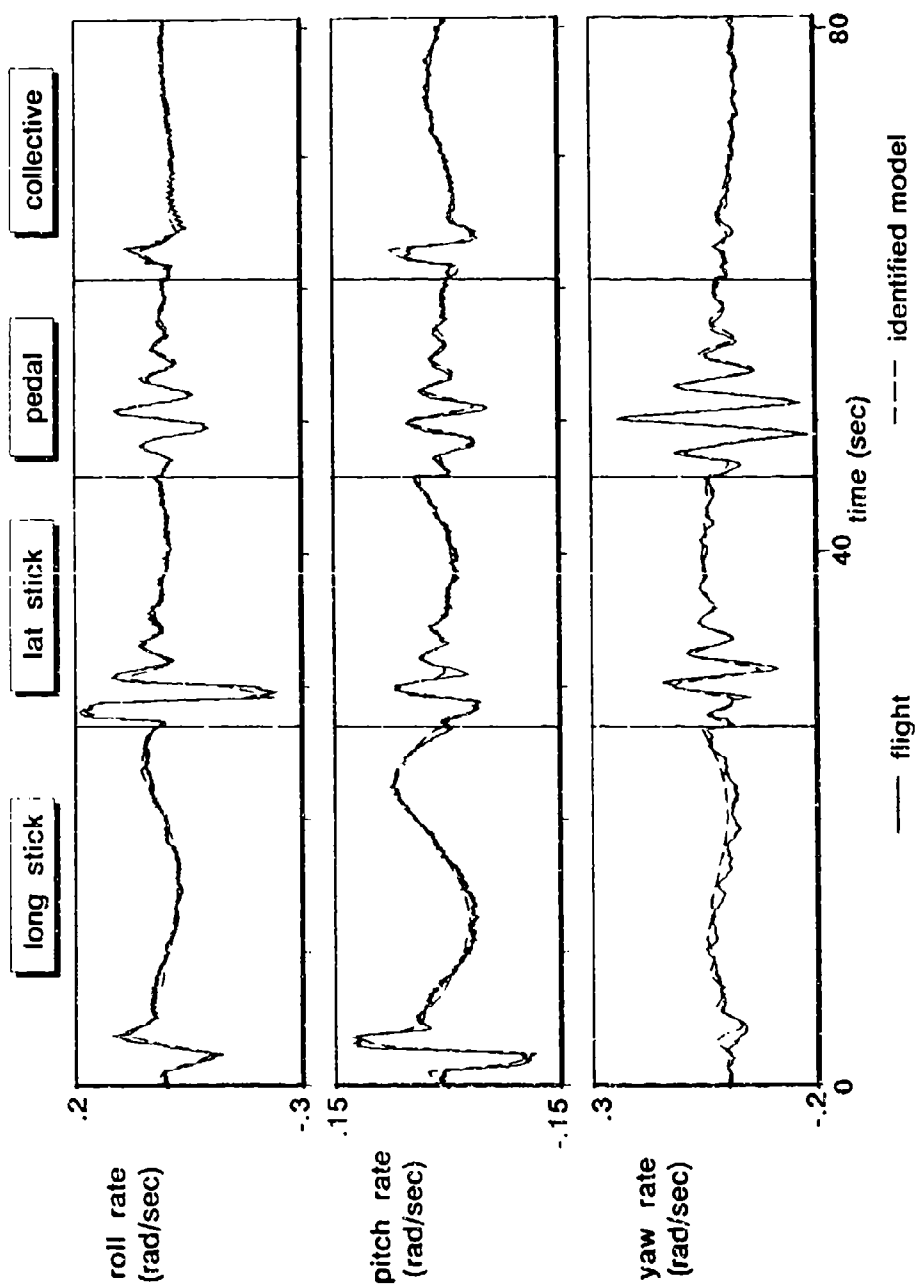


Figure 6.2.20. Verification of the identified model (angular rates, DLR result)

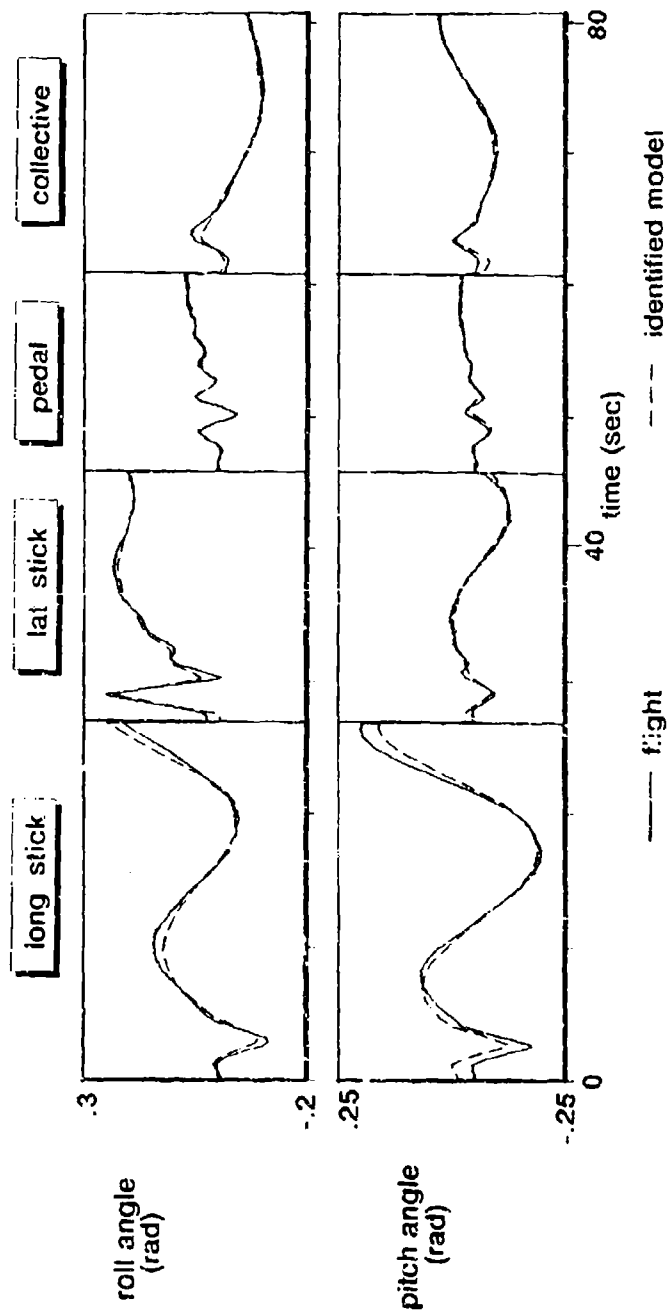


Figure 6.2.21. Verification of the identified model (Euler angles, DLR result)

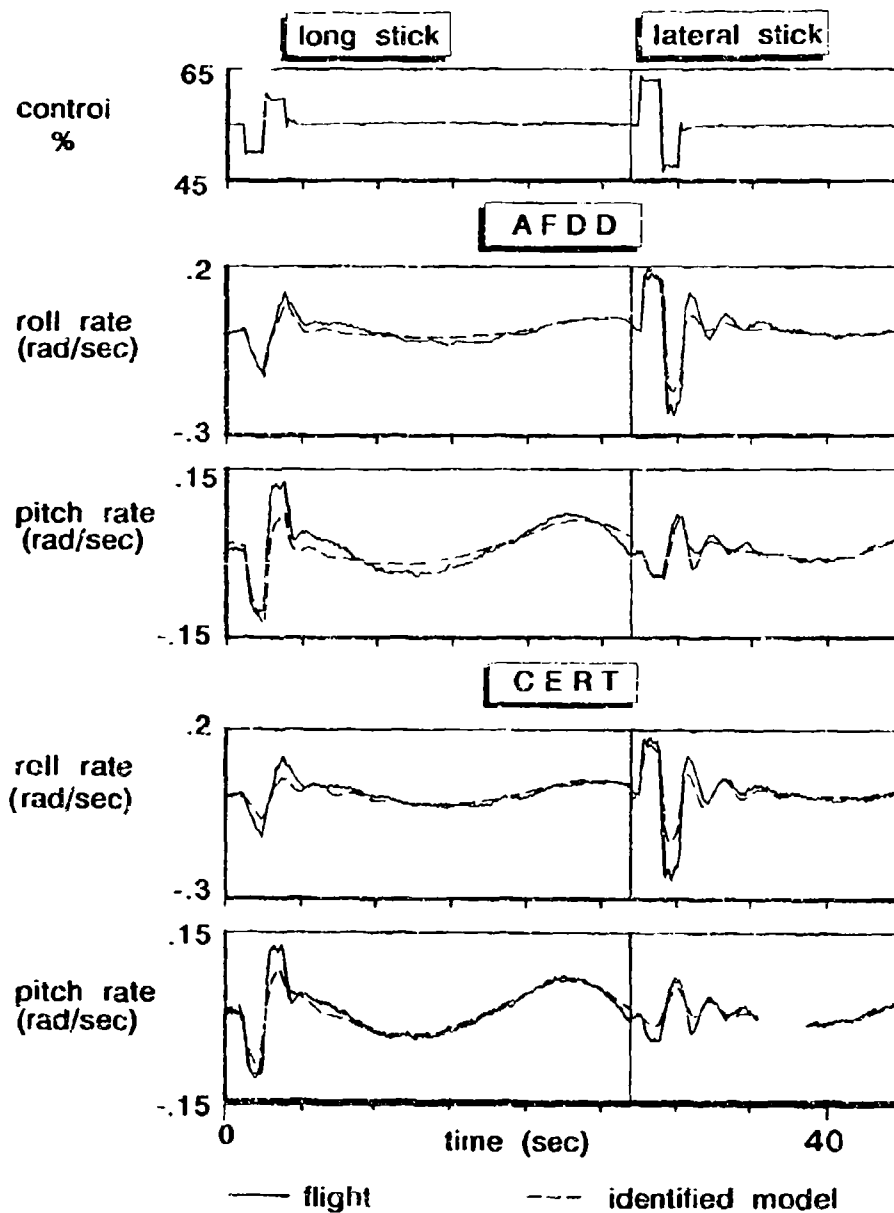


Figure 6.2.22. Verification of the identified BO 105 models (AFDD and CERT results)

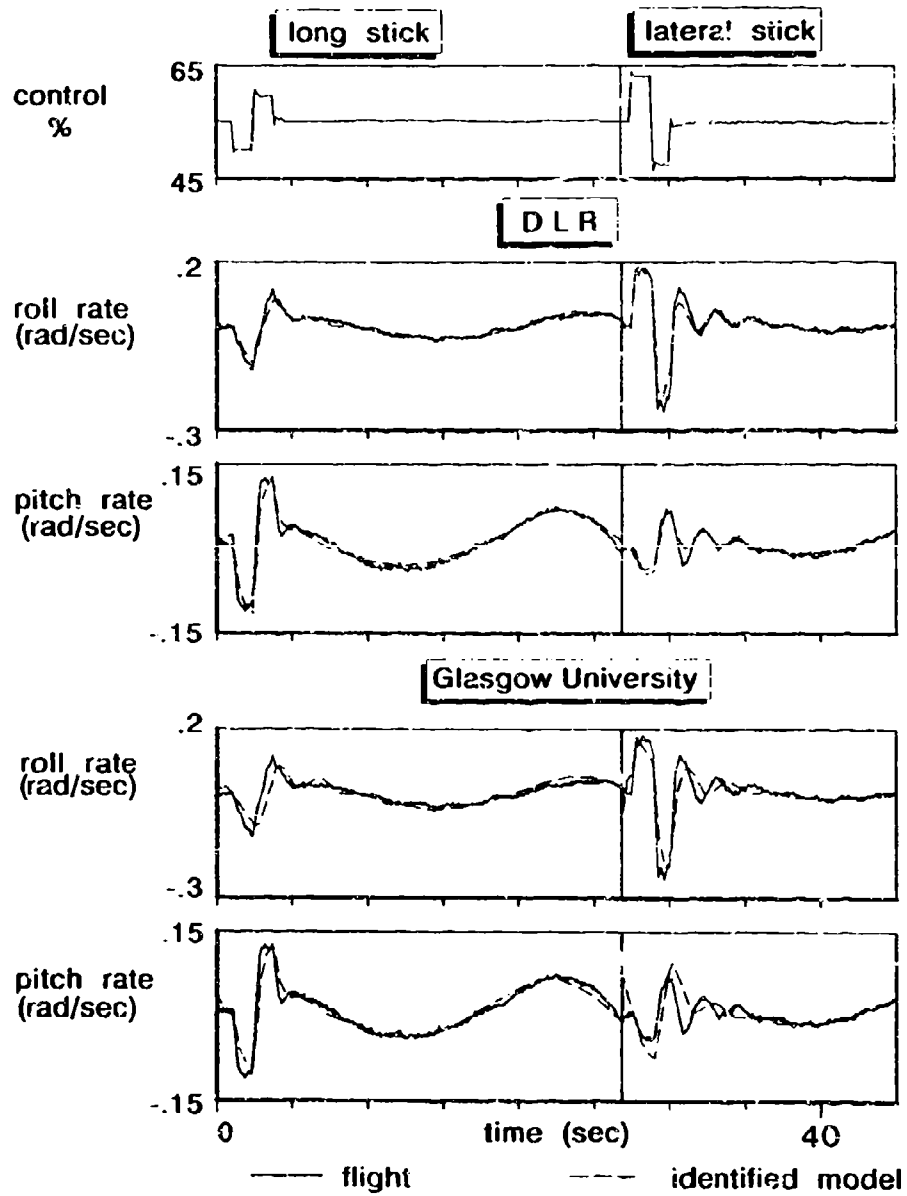


Figure 6.2.23. Verification of the identified BO 105 models (DLR and Glasgow University results)

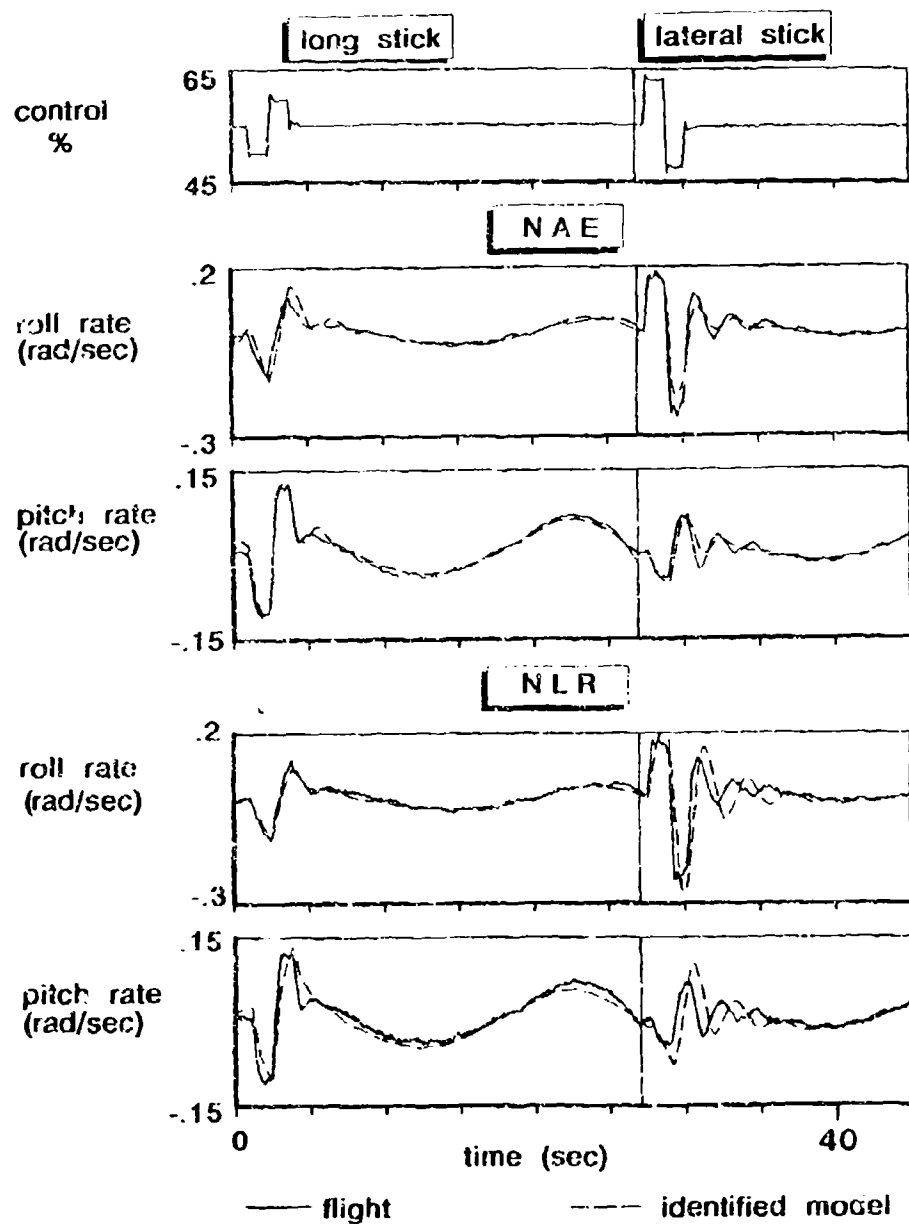


Figure 6.2.24. Verification of the identified EO 105 models (NAE and NLR results)

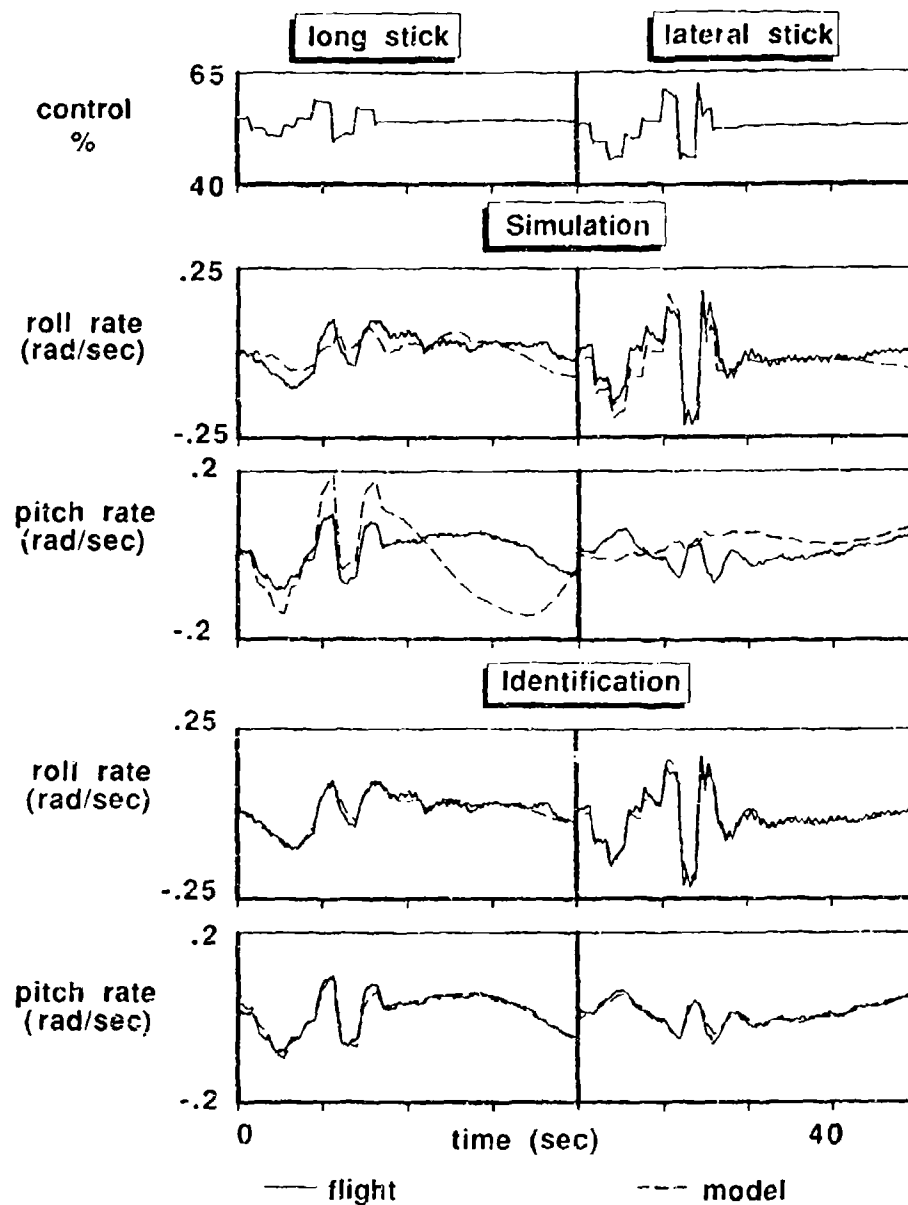


Figure 6.2.25. Comparison of BO 105 flight data and results from a computational nonlinear simulation (OLR SIMH)

6.3 Case Study III: SA-330 PUMA¹⁵⁾

6.3.1 Introduction

The Royal Aerospace Establishment provided flight test data from the Research SA-330 (Puma) to AGARD WG-18. This chapter describes the aircraft and the associated test database. The results of data consistency analysis, parameter identification and verification analysis are presented. A detailed kinematic consistency study conducted by RAE is included, followed by derivative identification conducted by six of the AGARD participating organisations. The discussion of results is approached from a modal perspective; each of the six degree of freedom modes and their approximations is examined in turn, the major contributing derivatives highlighted and the comparisons between methods discussed. Based on this analysis, some conclusions are drawn that reflect on the confidence in and maturity of system identification methods in helicopter flight mechanics.

6.3.2 Helicopter and Instrumentation

The SA-330 Puma is a twin engine, medium support helicopter in the six tonnes category, in service with a number of armed forces including the Royal Air Force to support battlefield operations.

The RAE Research SA-330 Puma XW 241 (Figure 6.3.1) is one of the early development aircraft acquired by RAE in 1974 and extensively instrumented for flight dynamics and rotor aerodynamics research. With its original analogue data acquisition system, the SA-330 provided direct support during the 1970s to the development of new rotor aerofoils through the measurement of surface pressures on modified blade profiles. In the early 1980s a digital PCM system was installed in the aircraft and a research programme to support simulation model validation and handling qualities was initiated. Over the period between 1981-1987, more than 100 hours of flight testing was carried out to gather basic flight mechanics data throughout the flight envelope of the aircraft.

A three-view drawing of the aircraft in its experimental configuration is shown in Figure 6.3.2. The aircraft has a four-metal-bladed articulated main rotor (modified NACA 0012 section, 3.8 % flapping hinge offset). Basic physical characteristics of the aircraft are provided in Table 6.3.1.

Full details of the manoeuvres flown and measurements recorded on the SA-330 and provided to WG-18 are included in Chapter 4 of this Report. Table 6.3.2 summarises all data files provided. The flight tests from the 80 kn trim condition were eventually selected as the set for primary analysis, comprising 3211 inputs on all controls.

All control inputs were applied by the pilot through the cockpit controls, using a controls fixture to guide the inputs. Manoeuvre times are typically 20 s to 30 s and the recovery was initiated at the test pilot's discretion or when the manoeuvre amplitude had either grown too large or subsided to very small amplitude. Control input amplitudes are typically less than 5 % of full range.

The measurements recommended for use by WG-18 are listed in Table 6.3.3 and Table 6.3.4 and were provided to the Working Group in unprocessed Imperial engineering units. No pre-distribution corrections were made to reference accelerations or nose-boom vane measurements to the centre of mass. It should be noted that all kinematic measurements are positive in the usual 'left hand' reference frame sense, except the normal acceleration which is positive up. Many of the measurements were sampled at 128 Hz and 256 Hz but a reduced rate of 64 Hz was provided to the Working Group. All channels were passed through anti-aliasing filters at 72 Hz before digitising; in addition, the agility pack data were further filtered by a 2-pole Butterworth at 10.6 Hz. The measurements were recorded in digital PCM (12 bit numbers, 4096 counts) form on magnetic tape on the aircraft. No de-skewing techniques were adopted, resulting in a maximum data skew of about 16 ms.

6.3.3 Flight Test Data Evaluation

6.3.3.1 General considerations

As noted in the previous section, the SA-330 datasets provided to WG-18 members had received very limited preprocessing, amounting to decimation down to 64 samples/s and conversion to Imperial engineering units. The relevant measurements from the 80 kn flight tests are reproduced in Figure 6.3.3 through Figure 6.3.6.

¹⁵⁾ Principal Authors: G. D. Padfield, RAE; D. J. Murray-Smith, University of Glasgow

The response range plotted in these figures is 25 s; in some cases the response continues beyond this, in others recovery is initiated within this range (see the collective *up*-input in Figure 6.3.5). Prior to model structure and parameter identification it is important to establish the consistency of the kinematic measurements used and, for some identification methods, to determine the properties of any process or measurement noise present in the data. In addition, referencing the measurements to the centre of mass to accord with the reference frame of the dynamic equations, is required. The state estimation procedures applied form part of the system identification methodology and different organisations approached this task in different ways. The following section addresses the RAE approach but some general observations on the raw data in Figure 6.3.3 through Figure 6.3.6 are worth making at this stage:

1. Longitudinal cyclic manoeuvres (Figure 6.3.3)
The initial response perturbations are all within the 'linear range'; however, during the free response phase, excursions in pitch and roll attitude rise above 0.3 and 0.4 rads respectively. The angular rates and incidence angles remain small however. Roll and yaw excursions during the forward cyclic manoeuvre are of the same order as the pitch excursions and considerably larger than for the aft cyclic manoeuvre. The signal to noise ratios on the x and y accelerations are very low and of the order unity, with a significant component of noise at higher frequency (actually 4/rev) than the frequency of the test manoeuvre. The normal acceleration channel is positive in the unconventional sense as noted but the incidence vane also appears to have an inverted scale factor, the excursions being clearly in the opposite sense to the pitch attitude. While the 'short period' pitch mode appears to be adequately excited, barely one period of the 'phugoid' is contained in the manoeuvre. The initial conditions for incidence and pitch appear inconsistent with steady level flight.
2. Lateral cyclic manoeuvres (Figure 6.3.4)
Throughout both manoeuvres, response perturbations appear to be within the 'linear range'. The Dutch roll mode is dominant in the free response with roll/yaw/pitch ratio of the order 1/1/0.5. The velocity measurement is supplied in uncalibrated form for the left cyclic manoeuvre (flown on a different occasion to the right cyclic manoeuvre).
3. Collective manoeuvres (Figure 6.3.5)
All response perturbations lie within the linear range for both manoeuvres; in particular, velocity excursions are very small (5 kn). Recovery action in the roll axis occurs within the 25s manoeuvre range.
4. Pedal manoeuvres (Figure 6.3.6)
The dominant mode of response is the lateral/directional Dutch roll with moderate excursions in sideslip (0.2 rad), lateral acceleration (0.1 g) and roll/yaw rate (0.25 rad/s). The phugoid mode appears to have been more strongly excited in the right manoeuvre resulting in greater speed and pitch angle excursions.

From these initial and tentative observations it is clear that some data inconsistencies and noise-related features are present that state estimation can potentially shed light on.

6.3.3.2 RAE Bedford Analysis

In previous applications RAE have used an extended Kalman filter (Padfield et al., 1987, [6.3.1]) to derive consistent state estimates for the SA-330 flight test data. Attempts to estimate noise statistics and calibration correction parameters simultaneously have not succeeded however. For the present activity it was felt that establishing good estimates for the scale factor and bias corrections was more important and hence a technique based on output-error estimation was developed (Turner et al., 1991, [6.3.2]). The state equations can be written in the usual way for attitudes and velocities.

Attitudes

$$\dot{\Phi} = p^* + q^* \sin \Phi \tan \Theta + r^* \cos \Phi \tan \Theta. \quad (6.3.1)$$

$$\dot{\Theta} = q^* \cos \Phi - r^* \sin \Phi. \quad (6.3.2)$$

$$\dot{\Psi} = q^* \sin \Phi \sec \Theta + r^* \cos \Phi \sec \Theta. \quad (6.3.3)$$

where

$$p^* = (1 + \lambda_p)p_m - b_p$$

etc., with

λ_p = scale factor correction
 b_p = bias correction
 p_m = measurement of roll rate.

Velocities

$$\dot{u} = -q^*w + r^*v + a_x^* - g \sin \Theta \quad (6.3.4)$$

$$\dot{v} = -r^*u + p^*w + a_y^* + g \cos \Theta \sin \Phi \quad (6.3.5)$$

$$\dot{w} = -p^*v + q^*u + a_z^* + g \cos \Theta \cos \Phi \quad (6.3.6)$$

where

$$a_x^* = (1 + \lambda_{ax})a_{xm} - b_{ax}$$

etc., with

$$\lambda_{ax} = \text{scale factor correction}$$

$$b_{ax} = \text{bias correction}$$

respectively to

$$a_{xm} = \text{measurement of longitudinal acceleration referred to the centre of mass}$$

The estimation procedure is configured to run in two sequential passes with the converged results of the attitude pass fixed for the velocity pass. The corresponding measurement equations can be written in the form:

Attitudes

$$\Phi_m = (1 + \lambda_\Phi)\Phi + b_\Phi + n_\Phi \quad (6.3.7)$$

$$\Theta_m = (1 + \lambda_\Theta)\Theta + b_\Theta + n_\Theta \quad (6.3.8)$$

$$\Psi_m = (1 + \lambda_\Psi)\Psi + b_\Psi + n_\Psi \quad (6.3.9)$$

where the measurement noise vector

$$[n_\Phi, n_\Theta, n_\Psi]^T$$

is assumed to have a Gaussian distribution with zero mean. The model output is obtained from:

$$\Phi_0 = (1 + \lambda_\Phi)\Phi + b_\Phi \quad (6.3.10)$$

$$\Theta_0 = (1 + \lambda_\Theta)\Theta + b_\Theta \quad (6.3.11)$$

$$\Psi_0 = (1 + \lambda_\Psi)\Psi + b_\Psi \quad (6.3.12)$$

Once again, λ and b represent scale factor and bias corrections respectively.

Velocities

$$V_m = (1 + \lambda_V)(u^{*2} + v^{*2} + w^{*2})^{1/2} + b_V + n_V \quad (6.3.13)$$

$$\beta_m = (1 + \lambda_\beta) \tan^{-1} \left(\frac{v^*}{u^*} \right) + b_\beta + n_\beta \quad (6.3.14)$$

$$\alpha_m = (1 + \lambda_\alpha) \tan^{-1} \left(\frac{w^*}{u^*} \right) + b_\alpha + n_\alpha \quad (6.3.15)$$

where the measurement noise vector

$$[n_v, n_\beta, n_\alpha]^T$$

is assumed to have a Gaussian distribution with zero mean. The model output follows as for the attitude pass. The velocities

$$u^*, v^*, w^*$$

refer to the velocity components of the boom tip where the vanes and pitot tube are located. Hence for example, if the point has coordinates

$$x_B, y_B, z_B$$

relative to the centre of mass, we can write:

$$\begin{aligned} u^* &= u + qz_B - ry_B, \\ v^* &= v + rx_B - pz_B, \\ \text{etc.} \end{aligned} \quad (6.3.16)$$

The vectors of parameters to be estimated in the two-pass-process are:

$$\mathbf{y}_a = [\Phi(0), \Theta(0), \Psi(0), b_p, b_q, b_r, \lambda_p, \lambda_q, \lambda_r, b_\phi, b_\theta, b_\psi, \lambda_\phi, \lambda_\theta, \lambda_\psi]^T \quad (6.3.17)$$

and

$$\mathbf{y}_v = [u(0), v(0), w(0), b_{ax}, b_{ay}, b_{az}, \lambda_{sx}, \lambda_{sy}, \lambda_{sz}, b_v, b_\beta, b_\alpha, \lambda_v, \lambda_\beta, \lambda_\alpha]^T \quad (6.3.18)$$

Where $\Phi(0)$, $u(0)$, etc, are the state initial values.

The cost function to be minimised in the output-error scheme can be written (Turner et al., 1991, [6.3.2]):

$$J = \frac{1}{2} \sum_t \mathbf{z}^T \mathbf{S}^{-1} \mathbf{z} + \frac{N}{2} \log_e |\mathbf{S}| + \frac{1}{2} \sum_p \Delta \mathbf{y}^T \mathbf{S}_p^{-1} \Delta \mathbf{y} \quad (6.3.19)$$

where, the residual vector \mathbf{z} represents the difference between the measured predicted model output vectors:

$$\mathbf{z} = \mathbf{z}_m - \mathbf{z}_0 \quad (6.3.20)$$

The residual vector $\Delta \mathbf{y}$ represents the difference between the current model parameter estimates and the initial guesses for these parameters:

$$\Delta \mathbf{y} = \mathbf{y} - \mathbf{y}_0 \quad (6.3.21)$$

\mathbf{S} is the measurement (noise) error-covariance matrix and \mathbf{S}_p is an input weighting matrix indicating confidence in the initial guesses provided for the parameter estimates.

The summations in (6.3.19) are carried out over all N time points (t) and parameters (p) respectively. The Bayesian component (third term in (6.3.19)) is included to allow some parameters to be held fairly constant during the iterations for cases where these are known with high confidence a-priori or over-parametrisation could cause solutions to converge to an obviously incorrect answer. This approach is discussed further by Maine et al. (1985, [6.3.3]). The need for this facility will be demonstrated in the following analysis.

The cost function J is minimised using a Gauss-Newton method, incorporating first and second order partial derivatives with respect to the vector \mathbf{y} .

The steady-state error covariance matrix \mathbf{S} is estimated using the definition:

$$\mathbf{S}_{\text{est}}^{k+1} = \text{Diag} \left[\frac{1}{N} \sum_t (\mathbf{z}_m - \mathbf{z}_0^k)(\mathbf{z}_m - \mathbf{z}_0^k)^T \right] \quad (6.3.22)$$

i.e. the expected value of the off-diagonal terms is zero. \mathbf{z}_0^k is the estimated model output obtained by using the model parameter estimates given at the k^{th} iteration.

The formulation given above assumes that process noise is absent and hence that the model equations (6.3.1) through (6.3.6) are correct. This is not the case in general but the uncertainties of most concern are associated with differences between inertial and local aerodynamic velocities in the velocity pass and vertical gyro anom-

alies in the attitude pass. These sources of error are often distinctly non-Gaussian and attempts to account for such noise using the usual Kalman-filter approach for estimating \mathbf{S} will themselves be faulted.

To give some indication of the quality of the unprocessed measurements, Figure 6.3.7 shows a comparison of measurements and model output without any calibration corrections. The case examined is the forward cyclic 3211, F568FAC.FWD. Some notable observations are:

- the reverse scale factor on the incidence vane,
- evidence of bias errors manifested in the roll angle and sideslip,
- process noise on the velocity measurement.

The output-error optimisation can first be run with the parameter constraint weighting set to very low values (unity) to disable this part of the cost function effectively. The optimised time history comparisons are shown in Figure 6.3.8 and corresponding calibration correction estimates in Table 6.3.5. The time histories show excellent agreement after 30 iterations. Some notable observations are:

1. the roll and pitch time histories have been scaled to about 50 % of their original values,
2. the initial yaw angle has been shifted by about 30°,
3. the process has been incapable of fitting the process noise on the speed measurement.

An examination of the calibration parameters in Table 6.3.5 provides evidence for some of these observations. The scaled attitudes are entirely a result of over-parametrisation with the rate and attitude gyro scale factors, strongly correlated, i.e.:

$$\begin{aligned} (1 + \lambda_r) &\approx \frac{1}{1 + \lambda_\phi} \\ (1 + \lambda_q) &\approx \frac{1}{1 + \lambda_\theta} \end{aligned} \quad (6.3.23)$$

The scale factor and bias on the yaw channel Ψ and the initial value $\Psi(0)$ appear also to be correlated such that

$$\lambda_\Psi \Psi(0) \approx b_\Psi$$

A quite distinct problem arises in the velocity pass, and is manifested in the magnitude of the accelerometer scale factor corrections λ_{ax} , λ_{ay} . These estimates are considered to be physically implausible even though the standard deviations are very small. The expected accuracy of these quality inertial sensors is high and the small amplitude of the excursions (see Figure 6.3.3 through Figure 6.3.6) in all but the pedal manoeuvres suggests that the effects should actually be very small in equations (6.3.4) and (6.3.5). In fact, these equations show that for small manoeuvres, du/dt and dv/dt are linearly related to Θ and Φ respectively and that the gravitational terms dominate. The acceleration a_x will however be strongly correlated with du/dt and Θ and the optimisation will try to use this signal to minimise errors. Figure 6.3.9 shows the individual components of the du/dt and dv/dt variations confirming qualitatively the above points. This is the source of the anomaly and for both the velocity and attitude pass, recourse to parameter constraints has to be sought to achieve realistic solutions.

The selection of the weighting elements of the matrix \mathbf{S}_p is not obvious and in general may need to be different for each run. For the present study a ratio of 1 to 10^0 was chosen between corresponding free and fixed parameters. On the basis of the previous arguments the 'fixed' parameters were selected as:

$$\lambda_p, \lambda_q, \lambda_r, \lambda_{ax}, \lambda_{ay}, \lambda_{az}, b_\Psi, \Psi(0)$$

The results for the constrained runs from the priority dataset are given in Figure 6.3.10 along with the optimized calibration corrections for all runs in Table 6.3.6 through Table 6.3.8. For the attitude pass the time history comparisons indicate that an excellent fit has been achieved. The attitude scale factor corrections are small with low standard deviations except for the pitch attitude in the left cyclic run where a 13 % change has been identified. The bias estimates are also in general small, typically of the order of 1°. Exceptions are the roll biases for the collective runs which are of the order of 3°. The initial values have been corrected accordingly as shown in Table 6.3.6 through Table 6.3.8. The results of the attitude pass lead to increased confidence in the measurements but there is sufficient scatter in the results from run to run to cause concern about the accuracy of any particular value.

Turning to the velocity pass results, a more interesting set of comparisons can be observed. In general, a good optimisation has been achieved for each run with one or two exceptions. The integrated velocity data typically exposes the need for bias corrections on the accelerometers and highlights the presence of process noise on the velocity channel. The aft cyclic run has converged with a high scale factor correction estimated for the sideslip velocity. Scale factor corrections are to be expected on the air data measurements on account of static cali-

bration inaccuracies and also the bias effects of process noise present due to local flowfield effects. In general these are less than 10 % and the estimates have fairly low standard deviations ($< 10\%$ parameter value). The aft cyclic run is a strong exception and attempts to stiffen other parameters to resolve the anomaly have not produced consistent results.

The kinematic consistency analysis described above was conducted by RAE after most of the identification work had been completed by participating organisations. This study is provided insight into some of the pitfalls of state estimation. Estimated calibration correction factors vary from run to run in an unexpected manner although in absolute terms most of the values are small. It is not possible to recommend a definitive set of corrections for these supposedly deterministic errors and therefore in most cases filtered measurements are, it could be argued, appropriate for use directly in the model structure and parameter identification stages.

6.3.4 Identification Methods

6.3.4.1 DLR

Files for the 80 kn flight condition with 3211 test inputs, which were concatenated for identification purposes, involved longitudinal cyclic (aft), lateral cyclic (right), pedal (left) and collective (up) control inputs. Files used for verification purposes involved longitudinal cyclic (forward), lateral cyclic (left), pedal (right) and collective (down) control inputs. In the model structure and parameter estimation stage of the identification process the chosen state vector was:

$$\mathbf{x} = (u, v, w, p, q, r, \Phi, \Theta)^T \quad (6.3.24)$$

and the measured vector was:

$$\mathbf{y} = (a_x, a_y, a_z, p, q, r, \Phi, \Theta, u, v, w)^T \quad (6.3.25)$$

Estimation was carried out using the DLR non-linear Maximum Likelihood program (see, e.g. Jategaonkar et al., 1983, [6.3.4]). Variables were used and no use was made of pseudo-controls. No elements of the system and control input matrices were fixed and all kinematic and gravity terms were included. Pure time delays were included for control inputs, except for the pedal input.

6.3.4.2 RAE/Glasgow University

Files principally used for parameter identification involved the 80 kn flight condition with 3211 inputs. Measurements used were speed, incidence, flank angle, pitch rate, pitch angle, roll rate, roll angle, yaw rate, longitudinal acceleration, lateral acceleration, normal acceleration, collective, longitudinal cyclic, lateral cyclic and pedal. The portion of each record used was not the same in all cases. The responses to the collective-down input were truncated after approximately 14 s and were thus significantly shorter than all other records which involved between 20 and 25 seconds of data. The sampling frequency used was 32 Hz. No filtering was carried out on the flight data.

Model structure and parameter estimation was carried out using a three stage approach involving frequency-domain equation-error and output-error techniques (Black et al., 1989, [6.3.5]; Black, 1989, [6.3.6]). Work was carried out using both single records and combinations of records. The analysis of combinations of records has involved the application of a technique, developed at the University of Glasgow, for multiple-run identification (Black et al., 1990, [6.3.7]). This approach retains the individuality of separate runs and avoids some of the known problems of concatenation. It involves the introduction of an additional summation loop in front of the individual cost functions associated with each separate data set. This gives a combined cost function

$$J_{\text{total}} = \sum_{i=1}^N J_i \quad (6.3.26)$$

for N data sets. Expressions have been derived which show that, under certain conditions (e.g. the cost surface is a close approximation to a quadratic in the vicinity of the minimum), the multiple-run estimates and corresponding standard deviations may be obtained a-priori using the individual results from the runs forming the basis of the multiple-run identification.

The individual cost functions for the frequency-domain output-error stage of the identification process were based upon a Maximum Likelihood form of criterion involving summation over a specified frequency range. Pseudo control inputs were used in this approach. In this application the range considered was 0.049 Hz to 0.492 Hz. The error-covariance matrix estimate was updated at each iteration on the basis of predicted model

outputs. Convergence is required in both the model parameter values and in diagonal elements of the error-covariance matrix. Minimisation involved a quasi-Newton method together with an optimal linear-search algorithm. Some parameters were fixed in the identification process but no other constraints were included.

A time-domain output-error identification stage was used, following the frequency-domain output-error identification, in order to estimate zero offsets and initial states.

Verification was carried out using data sets which were not used in identification.

6.3.5 Identification and Verification Results

The principal results of the studies are as follows:

- Table 6.3.9 through Table 6.3.13 contain the stability and control derivatives and equivalent time delays estimated by Glasgow, DLR, CERT (with and without time delays), NAE and NLR. All 36 stability and 24 control derivatives are included although in many cases (particularly Glasgow, DLR and NLR analyses), some are deleted a-priori on the assumption of the small contribution to an adequate model structure.
- Table 6.3.14 contains the eigenvalues corresponding to the assembled state matrices (with known gravitational and kinematic terms). Included are the US Army results derived from transfer function fitting of the roll rate, yaw rate and sideslip response to lateral cyclic and pedal.
- Figure 6.3.11 and Figure 6.3.12 and illustrate the Glasgow time history fits for translational and angular velocities corresponding to the identification and verification runs respectively. The concatenated runs for the identification are, from left to right, longitudinal cyclic (aft), lateral cyclic (right), pedal (left) and collective (up). Inputs for the verification runs correspond to the opposite control input directions.
- Figure 6.3.13 and Figure 6.3.14 illustrate similar results from the DLR.
- Figure 6.3.15 shows Helistab results for varying static stability derivatives (discussed in relation to longitudinal dynamics in section 6.3.6).

The derivatives in Table 6.3.9 through Table 6.3.12 are accompanied by their standard deviations. Values of the latter below 5 % of the associated parameters are deemed to be estimated with very high confidence. Nearly all the major derivatives (dampings, primary control, roll/yaw sideslip) fall into this category. Many of the cross coupling derivatives fall outside this category. The most disturbing feature is the variation of derivative estimates across the methods. Comparing results from Glasgow, DLR and CERT (with equivalent time delays) there is some consistency (< 20 %) across derivatives like L_v , $Z_{\dot{\delta}_{col}}$, Z_w and $N_{\delta_{ped}}$, while other, equally important, effects are estimated with variations of 50 % and higher, e.g. L_p , M_q , $L_{\delta_{lat}}$, $M_{\delta_{lon}}$.

In some cases, very small but important derivatives are estimated with striking consistency, e.g. γ_v , and others much less so, e.g. M_w , X_u . The total damping, computed either from the sum of diagonal elements or eigenvalue real parts varies from greater than 5 (Glasgow, DLR) to less than 3 (NAE, NLR). These anomalies are a source of concern and insufficient effort has been focused on resolving them to date. In most cases the same or very similar time histories were used in the identification, but the different cost functions, minimisation algorithms and parameter constraints used will all lead to particular solutions and exacerbate the non-uniqueness of system identification process. The variation of results across the methods cannot be fully accounted for without recourse to more detailed examination. The issue is raised however as to which, if any, of the approaches is the better. This is also difficult to resolve; the DLR and Glasgow multi-run results are classic examples. Roll and pitch damping are estimated to be greater than 2 and 1 respectively; the Helistab simulation predictions are -1.68 and -0.71 respectively and are considered to be reasonable theoretical estimates of these effects. Is the simple Helistab theory really 50 % in error or are the flight derived estimates in some sense biased? Such a question must have a validated answer before system identification methods can be used with strong confidence. In the next section, the results summarised above will be examined in more detail with respect to the dynamic modes of motion to support an improved understanding of the variations discussed.

6.3.6 Discussion of Results

From the compendium of results contained in Table 6.3.9 through Table 6.3.12 and Figure 6.3.11 through Figure 6.3.14, we can extract subsets that reflect the fundamental properties of the dynamic modes under suitable conditions. In the mid-speed range, articulated-rotor helicopters typically exhibit conventional flight modes, e.g. short period, roll subsidence, etc; while couplings can be moderate, e.g. roll/pitch, they manifest themselves as forced motions and tend not to have a strong effect on modal frequencies and dampings. Most of the dynamic excursions in the test manoeuvres can be considered to be within the normal linear range, at least as far as the aerodynamic loads are concerned. The estimated stability and control derivatives should

therefore be reasonably close to their physical counterparts. Assembling the approximating factors from these can provide insight into the corresponding fit errors and the overall confidence levels in the results.

1. Longitudinal short period mode

The approximate characteristic equation for this mode is very well documented in textbooks and has received detailed scrutiny by Padfield (1981, [6.3.8]).

$$\lambda^2 - (Z_w + M_q)\lambda + Z_w M_q - M_w(Z_q + V) = 0. \quad (6.3.27)$$

This approximation assumes that speed is constant during the pitch manoeuvre. Table 6.3.15 shows a comparison of the approximate results with the eigenvalue data from Table 6.3.14, included are the RAF Helistab simulation results. In most cases the agreement is within 20 %, some better than 5 %. Where the comparisons are good, attention can be focused on the simple components of the approximation. A comparison of results across the methods reveals stronger variations in damping and frequency. Why this should be so is difficult to explain without access to the details of the estimation algorithms and procedures. In order that these comparisons can be related to the short period time responses, the control effectiveness ratios need to be compared as shown in Table 6.3.15. Both cyclic and collective control sensitivity/damping ratios are included and these show a similar level of variation between methods. Another key parameter featuring in equation (6.3.27) is the static stability derivative M_w , which serves to couple pitch and heave and turn what would otherwise be a pair of subsidences (Z_w , M_q) into an oscillation. The variation across the results is again strong and reflects the variations in short period frequency ω_{sp} . The standard deviations for the parameter estimates discussed are typically quite small, indicating good confidence in the values.

The key time histories for pitch short period behaviour are pitch rate and incidence (q and w in Figure 6.3.11 through Figure 6.3.14) for the identification run in response to longitudinal cyclic control. Both the DLR and Glasgow analyses used air data measurements. An obvious question to address is how such distinct derivatives and associated modal characteristics can result in such similar time responses. A comparison of the Glasgow and DLR results illustrates the point adequately; using the Glasgow results as a reference, the DLR results indicate,

- a. 25 % difference in damping,
- b. 40 % difference in frequency,
- c. 300 % difference in static stability M_w .

The fits for the verification runs shown in Figure 6.3.11 and Figure 6.3.14 are poorer, particularly the Glasgow incidence comparison.

Overall the results are inconclusive regarding the relative merits of one technique over another, with regard to estimating short period characteristics.

2. Longitudinal phugoid

With only 25 s of response, the information content on the low frequency phugoid mode is low. In general however, the match of the u velocity component is quite good and reveals a complete cycle of the phugoid mode. The approximate formulae for damping and frequency set out in Padfield (1981, [6.3.8]) is based on an assumption that the phugoid is characterised by weakly damped vertical and horizontal motions. The damping is composed of a large number of small effects including the drag derivative X_u . It is shown by Padfield (1981, [6.3.8]) that this approximation is unlikely to be valid at 80 kn and, of course, with barely one oscillation cycle of data, such weak damping would not be easy to estimate. The frequency on the other hand is dominated by a particular combination of derivatives:

$$\omega_p^2 \sim g \cos \Theta_0 \frac{(Z_u M_w - Z_w M_u)}{(M_q Z_w - M_w(Z_q + V))} \quad (6.3.28)$$

$$\omega_p^2 \sim -g \cos \Theta_0 \frac{Z_w M_u}{(M_q Z_w - M_w(Z_q + V))} \quad (6.3.29)$$

Table 6.3.16 shows a comparison of ω_p^2 derived from equation (6.3.29) with the corresponding eigenvalues of the full system taken from Table 6.3.14. It is clear that the estimation methods agree very well on these parameters and that the approximation in equation (6.3.29) gives good agreement, with variations generally less than 10 %. It should be noticed that this correlation results from combining individual effects (i.e. ω_{sp}^2 , M_u) that typically vary by more than 100%. This result suggests that some cor-

relation exists between the identified parameters, e.g. the ratio of M_0 to ω_{sp} is roughly a constant. Both the static stability derivatives M_0 and M_w are small, poorly identified (based on the scatter between different methods) but at the same time play a key role in the form of the response history. Figure 6.3.15 shows Helistab results for the SA-330 at 80 kn in response to a 3211 input applied to the longitudinal cyclic. The short term response is strongly sensitive to M_w and the longer term to M_0 . The range of derivative values depicted cover those values estimated by the different organisations. These results confirm the classical importance of these derivatives to vehicle behaviour.

The results for the two longitudinal modes described above suggest some conflict in the estimation of physically meaningful characteristics for both modes simultaneously.

3. Roll subsidence

The roll damping L_p is the key derivative here and Table 6.3.10 indicates an estimation range between -0.7 1/s (NAL) and -2.5 1/s (DI.R). The standard deviations are very small for all estimates. It is interesting to note that the two examples cited above correspond to cases with effective time delays of zero and 175 ms respectively. It is well known (Padfield et al., 1987, [6.3.1]) that the roll damping can sometimes be grossly underestimated if no account is taken of the effective delay introduced by the actuation and rotor system. This could well have played a part here. The roll mode eigenvalues given in Table 6.3.14 correlate well with the damping in most cases. Table 6.3.17 compares the rate sensitivity ratio for the various cases revealing a spread from 0.015 rad/(s %) to 0.03 rad/(s %). Such a wide variation is not reflected in the short term roll response to lateral cyclic shown in identified responses, see e.g. Glasgow traces. As with the longitudinal modes, however, the quality of lateral mode estimation cannot be fully discussed in isolation.

4. Dutch roll

The approximating polynomial for the Dutch roll mode is more difficult to derive and will depend on the extent of coupling between roll, yaw and sideslip. The most general formulation has been derived by Padfield (1991, [6.3.9]) and assumes that sideslip and sideways velocity can be regarded as weakly coupled.

The quadratic then takes the form:

$$\lambda^2 + 2\zeta_r \omega_r \lambda + \omega_r^2 = 0, \quad (6.3.30)$$

where,

$$(2\zeta_r \omega_r)^* = - \frac{N_r + Y_v + \sigma \left(\frac{L_r}{V} - \frac{L_v}{L_p} \right)}{1 + \frac{\sigma L_r}{L_p V}} \quad (6.3.31)$$

$$\omega_r^{*2} = \frac{VN_v + \sigma L_v}{1 + \frac{\sigma L_r}{L_p V}} \quad (6.3.32)$$

$$\sigma = \frac{\rho - N_p V}{L_p}$$

A comparison of Dutch roll damping and frequency for the different methods is provided in Table 6.3.18. The frequency is generally predicted very well by the approximation, being dominated by the directional stability N_v . In most cases about 75 % of the damping is predicted by the approximation; the variation between methods is, however, quite large. Time history matches are good, particularly for yaw, but also roll and pitch. The quality of comparison in the verification runs is less good with even small mis-matches in frequency and damping clearly visible in some cases (e.g. Glasgow results). Equations (6.3.31) and (6.3.32) highlight the role of the yaw/roll coupling derivatives (L_r , N_p) in the Dutch roll dynamics. In general, these parameters are expected to be physically less dominant and smaller than their primary counterparts (L_p , N_r). The results shown in Table 6.3.10 suggest the contrary in some cases (e.g. NAL: L_r/L_p , DI.R, NI.R: N_p/N_r). To an extent these apparent distortions can be explained by the effects of inertial coupling between roll and yaw, but by no means entirely. The potential for parameter correlation in the Dutch roll analysis is believed to be very high, especially with such low damping and the almost anti-phase relationship between roll and yaw.

5. Spiral mode

The usual approximation for the slow spiral mode takes the form (Padfield et al., 1982, [6.3.10]):

$$\lambda_s \approx \frac{g}{V} \frac{L_v N_r - N_v L_r}{L_p N_v - N_p L_v + \frac{g}{V} L_v} \quad (6.3.33)$$

A cursory examination of the time histories indicates that there is little evidence of any spiral mode excitation at all in the dynamic response. A comparison of approximate and full model results for just the Glasgow and DLR data reveals the poor correlation particularly for the former, which is typical of results from all the different methods.

Glasgow $\lambda_s^* = -0.022$,
 $\lambda_s = -0.005$;

DLR $\lambda_s^* = -0.0673$,
 $\lambda_s = -0.048$.

Like the phugoid damping, the spiral mode is difficult to identify, being a residue of two quite strong effects (cf. numerator in equation (6.3.33)) and is probably better identified in part by conventional 'turns-on-one-control' manoeuvres (Padfield, 1985, [6.3.11]).

6. Cross coupling

The prediction and estimation of cross coupling effects on helicopters has presented serious hurdles and has been reported in much of the published identification work. An underlying concern has been that if the coupling effects are poorly estimated or distorted then this will reflect on the primary responses too and in many cases this has led to the neglecting of coupling effects or their relegation to pseudo controls. Regarding the current SA-330 analysis and the results in Figure 6.3.11 through Figure 6.3.14 and Table 6.3.9 and Table 6.3.10, the following observations can be made:

- Lateral velocity, roll and yaw response for the longitudinal cyclic inputs are poorly predicted in both identification and verification runs. The flight data indicates that the Dutch roll mode has been strongly excited while this mode is practically absent for the reconstructed responses. Most of the related derivatives, e.g. L_q , L_w , N_q , N_w are estimated with low confidence and often have unrealistic values (e.g. L_q). The analyses do not normally provide data on the sensitivity of individual time history fits to the overall cost functions. This kind of information could prove very useful in understanding some of the anomalies, e.g. the roll response to longitudinal cyclic is as pronounced as the pitch response and yet, in most cases, the optimisation appears to have ruled out roll as a contribution to the minimising process.
- In contrast, the pitch and heave responses during the lateral cyclic and pedal manoeuvres appear to be reasonably well modelled. This is particularly true for the DLR identification and verification results. Both the contributing derivatives M_p and M_v are estimated with high confidence although the former is of opposite sign to that predicted from purely aerodynamic considerations (Helistab value = -0.22). The relatively high value of M_v is surprising and almost certainly a major contribution to the pitch response in the Dutch roll.
- In general the collective responses provide the poorest comparisons. The Dutch roll mode is clearly excited yet few of the methods appear to capture the corresponding roll and yaw motions. The pitch/collective coupling is generally well represented, suggesting compatibility between the estimated character of the short period mode in response to cyclic and collective inputs.

7. Control derivatives

The control effectiveness is one of the few derivatives with a direct physical interpretation, following an application of control an aerodynamic force is generated that induces measurable fuselage accelerations. Control derivatives are by far the most important parameters for control law design and having accurate estimates across the required frequency range is vital for maximising robustness. The SA-330 estimates are contained in Table 6.3.11 and Table 6.3.12. Some notable features are:

- Primary cyclic derivatives are estimated with low standard deviations but vary across the methods by more than 50 % relative to the Glasgow reference value.
- Cross cyclic control derivatives are estimated with low confidence, sometimes not at all and sometimes with different signs.

- e. With the exception of the DFR value, the pitching moment from collective is estimated with strong consistency.
- d. The collective sensitivity $Z_{\delta_{col}}$ is estimated with confidence but again varies between methods; the heave sensitivity $Z_{\delta_{col}}/Z_w$ appears to be reasonably constant across the methods however.
- c. The yaw control derivative $N_{\delta_{ped}}$ varies by about 25 % of the Glasgow reference value; the corresponding sideforce derivatives are generally estimated with low confidence however and do not relate kinematically with $N_{\delta_{ped}}$.
- f. The \dot{x} and \dot{y} control derivatives are generally small and poorly estimated.

6.3.7 Conclusions

Six of the participating organisations in AGARD WG-18 conducted system identification on the SA-330 flight test data provided by the Royal Aerospace Establishment, UK. This report has reviewed the test data itself and the various identification methods applied by the different organisations. A six-degree-of-freedom model structure was assumed for all the work. Results have been presented including estimates of stability and control derivatives and comparison of test and reconstructed time histories for the collection of multi-step control input manoeuvres. Special consideration has been given to the RAE data consistency analysis and also a physical interpretation of the derivatives through approximations to the dynamic modes of motion. From the results presented the following observations and conclusions can be drawn.

1. Calibration factor corrections derived from a systematic output-error analysis has highlighted a variability from run to run that cannot be fully explained from the analysis. A constrained optimisation was required to achieve a realistic solution in most cases. The correction factors are generally small and readily account for integrated inertial errors that otherwise grow during the manoeuvres.
2. Many of the primary derivatives are estimated with a strong confidence by the various methods. However, the variation between results from different methods is a cause for concern. Typically, very good time history fits are achieved by two methods with widely differing (> 50%) derivative estimates.
3. Cross coupling derivatives are generally estimated with low confidence; on occasions the values are still significant which must, in turn, cast doubt on the distorted values of the associated primary derivatives.
4. An analysis of the modal behaviour through approximate formulae has proved useful in highlighting the importance or otherwise of particular combinations of derivatives. Some correlation between modal estimation has been observed, e.g. phugoid period and short period damping, Dutch roll and roll subsidence, i.e. an M_Q value appropriate to the phugoid may not be best for the pitch mode.
5. While primary responses were well matched in general, cross coupled time responses were often poorly predicted.
6. It is believed that process noise in the form of unmodelled dynamics and non-linearities contributes significantly to the variability of the results presented, inhibiting the extraction of a unique set of stability and control derivatives for the SA-330.

References

- [6.3.1] Padfield, G. D., Thorne, R.; Murray-Smith, D.; Black, C.; Caldwell, A. E.
UK Research into System Identification for Helicopter Flight Mechanics
Vertica, Vol. 11, No. 4, 1987
- [6.3.2] Turner, G. P.; Padfield, G. D.
Consistency Analysis of Helicopter Flight Test Data
RAE Technical Memorandum TM F5000, 1991
- [6.3.3] Maine, R.; Hiff, K. W.
Identification of Dynamic Systems: Theory and Formulation
NASA Reference Publication 1138, 1985
- [6.3.4] Jategaonkar, R.; Plaetschke, E.
Maximum Likelihood Parameter Estimation from Flight Test Data for General Non-Linear Systems
DVL R FB 83-14, 1983
- [6.3.5] Black, C. G.; Murray-Smith, D. J.
A Frequency-Domain System Identification Approach to Helicopter Flight Mechanics Model Validation
Vertica, Vol. 13, No. 3, 1989

- [6.3.6] Black, C. G.
A Users' Guide to the System Identification Programs OUTMOD and OFRIT
University of Glasgow, Department of Aerospace Engineering/Department of Electronics and Electrical Engineering, Report, 1989
- [6.3.7] Black, C. G.; Leith, D. J.
On the Combination of Data Sets for Helicopter System Identification
University of Glasgow, Department of Aerospace Engineering, Report No. 9016, 1990
- [6.3.8] Padfield, G. D.
On the Use of Approximate Models in Helicopter Flight Mechanics
Verton, Vol. 5, No. 3, 1981
- [6.3.9] Padfield, G. D.
The Application of System Identification to Simulation Model Validation
RAE Technical Memorandum (to be published 1991)
- [6.3.10] Padfield, G. D.; DuVal, R. W.
Applications of System Identification Methods to the Prediction of Helicopter Stability, Control, and Handling Characteristics
NASA CP-2219, 1985
- [6.3.11] Padfield, G. D.
Flight Testing for Performance and Flying Qualities
AGARD Lecture Series LS-139 'Helicopter Aeromechanics', 1985

Mass and moments of inertia		Tail rotor	
Mass	5805 kg	Diameter	3.042 m
Manufacturer's estimates based on $m = 5800$ kg		Blades	5
I_x	9638 kg m ²	Chord	0.18 m
I_y	13240 kg m ²	Airfoil	NACA 0012
I_z	25889 kg m ²	Solidity	0.19
I_{zx}	2226 kg m ²	Twist	0°
		Main/tail rotor gearing	4.82
		δ_3 angle	-45°
Main rotor		Horizontal stabilator	
Diameter	15.09 m	Span	2.11 m
Blades	4	Area	1.4 m ²
Chord	0.54 m	Incidence	-1°
Airfoil	NACA 0012		
Blade Area (from hub)	16.2 m ²	Vertical tail	
Blade Area (from cutout)	12.33 m ²	Span	1.14 m
Solidity (Thrust)	0.0317	Area	1.34 m ²
Twist	-8°	Incidence	-1.5°
Shall Angle	5°		
Nominal rotorspeed	27 rad/s		

Table 6.3.1. Physical characteristics of the RAE Research SA-330

Control	Control Input				File name	Number of runs	Recording time per run in s	Flight Conditions		
	Type	Initial displacement	Frequency content	Duration t_f or f				Mass	Airspeed	Altitude
Longitudinal	3211	Aft	$t_f \approx 7s$		3211A 080	1	30	5805 kg	80 kn	$H_p \approx 3850$ ft
Longitudinal	3211	Forward	$t_f \approx 7s$		3211F 080	1	30	5819 kg	80 kn	$H_p \approx 3800$ ft
Longitudinal	3211	Aft	$t_f \approx 7s$		F568FAC AFT	1	30	5805 kg	80 kn	$H_p \approx 3800$ ft
Longitudinal	3211	Forward	$t_f \approx 7s$		F568FAC FWD	1	30	5619 kg	80 kn	$H_p \approx 3800$ ft
Longitudinal	3211	Aft	$t_f \approx 7s$		3211A 100	1	25	5760 kg	100 kn	$H_p \approx 2000$ ft
Longitudinal	3211	Forward	$t_f \approx 7s$		3211F 100	1	40	5778 kg	100 kn	$H_p \approx 2000$ ft
Lateral	3211	Right	$t_f \approx 7s$		F568LAT RGT	1	30	5846 kg	80 kn	$H_p \approx 3800$ ft
Lateral	3211	Left	$t_f \approx 7s$		F550LAT LFT	1	40	5703 kg	80 kn	$H_p \approx 1650$ ft
Pedal	3211	Right	$t_f \approx 7s$		F576PED RGT	1	30	5781 kg	80 kn	$H_p \approx 3150$ ft
Pedal	3211	Left	$t_f \approx 7s$		F576PED LFT	1	30	5754 kg	80 kn	$H_p \approx 3200$ ft
Collective	3211	Up	$t_f \approx 7s$		F568COL UPC	1	30	5760 kg	80 kn	$H_p \approx 4150$ ft
Collective	3211	Down	$t_f \approx 7s$		F568COL DWN	1	20	5751 kg	80 kn	$H_p \approx 4100$ ft
Longitudinal	2121	AR	$t_f \approx 6s$		3211A 060	1	30	5823 kg	60 kn	$H_p \approx 1800$ ft
Longitudinal	2121	Forward	$t_f \approx 6s$		3211F 060	1	30	5782 kg	60 kn	$H_p \approx 1900$ ft
Longitudinal	Frequency sweep	—	$0.05Hz \leq f \leq 5Hz$		SWEEP 060	1	120	5737 kg	60 kn	$H_p \approx 3000$ ft
Longitudinal	Frequency sweep	—	$0.05Hz \leq f \leq 5Hz$		SWEEP 080	1	120	5737 kg	80 kn	$H_p \approx 3000$ ft
Longitudinal	Frequency sweep	—	$0.05Hz \leq f \leq 5Hz$		SWEEP 100	1	120	5737 kg	100 kn	$H_p \approx 3000$ ft

Inertias

Aircraft inertias (manufacturer's estimates) based on aircraft mass of $m \approx 5800$ kg and referred to body axes with origin in center of mass appropriate to tests flown.

$$I_x \approx 9640 \text{ kg m}^2, \quad I_y \approx 33240 \text{ kg m}^2, \quad I_z \approx 25890 \text{ kg m}^2, \quad I_{xz} \approx 2230 \text{ kg m}^2$$

Table 6.3.2. SA-330 manoeuvres flown

Group	Variables Quantity	Source	Original Sampling Rate (in Hz)
Control displacements	Forward/aft cyclic	Potentiometer	128
	Lateral Cyclic	Potentiometer	128
	Pedal	Potentiometer	128
	Collective	Potentiometer	128
Table 6.3.3. SA-330 Control Variables Data provided at a uniform sampling rate of 64 Hz.			

Group	Variables Quantity	Source	Original Sampling Rate (In Hz)
Air data	Angle of attack	Noseboom vane	128
	Angle of sideslip	Noseboom vane	128
	Airspeed	Noseboom Pitot probe	128
	Climb rate	Static pressure probe	128
Linear accelerations	Longitudinal acceleration	Accelerometer at CG and agility package	256
	Lateral acceleration	Accelerometer at CG and agility package	256
	Normal acceleration	Accelerometer at CG and agility package	256
Attitude angles (Euler angles)	Roll angle	Vertical gyro and agility package	128
	Pitch angle	Vertical gyro and agility package	128
	Yaw angle	Directional gyro	128
Angular rates	Roll rate	Rate gyro and agility package	256
	Pitch rate	Rate gyro and agility package	256
	Yaw rate	Rate gyro and agility package	256
Rotor	RPM	Tachometer	256
Table 6.3.4. SA-330 Response Variables Data provided at a uniform sampling rate of 64 Hz.			

	Attitude Pass			Velocity Pass		
Initial Conditions	$\phi(0)$ $\theta(0)$ $\psi(0)$	-0.031 (0.0029) 0.015 (0.0013) -5.867 (0.2057)		$u(0)$ $v(0)$ $w(0)$	44.507 (0.1276) 2.033 (0.1052) 0.912 (0.1484)	
Biases	p q r $\dot{\phi}$ $\dot{\theta}$ $\dot{\psi}$	0.000 (0.0001) 0.000 (0.0000) -0.007 (0.0003) 0.060 (0.0040) 0.000 (0.0023) -0.795 (0.1584)		a_x a_y a_z v β α	0.203 (0.0195) 0.336 (0.0055) -0.583 (0.0334) -0.370 (0.2324) -0.041 (0.0021) -0.048 (0.0034)	
Scale Factors	p q r $\dot{\phi}$ $\dot{\theta}$ $\dot{\psi}$	-0.440 (0.0202) -0.472 (0.0183) -0.004 (0.0102) 0.814 (0.0711) 0.842 (0.0690) -0.238 (0.0060)		a_x a_y a_z v β α	1.596 (0.1282) 1.233 (0.0573) 0.061 (0.0034) -0.071 (0.0056) -0.098 (0.0053) -2.007 (0.0063)	

Table 6.3.5. Initial condition, bias, and calibration factor estimates with free optimisation

	P	Q	R	S ₁	S ₂	S ₃	T	U	V	W	X	Y
PAC	0.000	0.000	0.000	0.000	0.000	0.000	-0.010	0.008	0.000	-0.102	-0.134	-1.944
PMD	(0.0003)	(0.0003)	(0.0003)	(0.0003)	(0.0003)	(0.0003)	(0.0029)	(0.0038)	(0.0035)	(0.0050)	(0.0055)	(0.0060)
PAC	0.000	0.000	0.000	0.000	0.000	0.000	-0.008	-0.058	0.004	-0.059	-0.672	-2.028
AFT	(0.0003)	(0.0003)	(0.0003)	(0.0003)	(0.0003)	(0.0003)	(0.0021)	(0.0009)	(0.0031)	(0.0048)	(0.0115)	(0.0117)
LAT	0.000	0.000	0.000	0.000	0.000	0.000	0.032	-0.133	0.010	-0.017	-0.122	0.000
LPT	(0.0003)	(0.0003)	(0.0003)	(0.0003)	(0.0003)	(0.0003)	(0.0065)	(0.0028)	(0.0018)	(0.0077)	(0.0134)	(0.0003)
LAT	0.000	0.000	0.000	0.000	0.000	0.000	0.002	-0.015	0.003	-0.027	-0.005	-1.999
RGT	(0.0003)	(0.0003)	(0.0003)	(0.0003)	(0.0003)	(0.0003)	(0.0013)	(0.0042)	(0.0024)	(0.0063)	(0.0065)	(0.0253)
COL	0.000	0.000	0.000	0.000	0.000	0.000	-0.024	-0.071	-0.004	-0.124	-0.023	-1.666
UPC	(0.0003)	(0.0003)	(0.0003)	(0.0003)	(0.0003)	(0.0003)	(0.0048)	(0.0023)	(0.0022)	(0.0050)	(0.0053)	(0.0120)
COL	0.000	0.000	0.000	0.000	0.000	0.000	-0.025	-0.093	-0.002	-0.183	-0.032	-1.657
DMN	(0.0003)	(0.0003)	(0.0003)	(0.0003)	(0.0003)	(0.0003)	(0.0015)	(0.0051)	(0.0002)	(0.0061)	(0.0054)	(0.0253)
PED	0.000	0.000	0.000	0.000	0.000	0.000	-0.009	-0.004	0.000	-0.086	-0.049	-1.947
PGT	(0.0003)	(0.0003)	(0.0003)	(0.0003)	(0.0003)	(0.0003)	(0.0015)	(0.0015)	(0.0002)	(0.0070)	(0.0014)	(0.0165)
PED	0.000	0.000	0.000	0.000	0.000	0.000	-0.025	-0.031	0.002	-0.062	-0.022	-2.021
PGT	(0.0003)	(0.0003)	(0.0003)	(0.0003)	(0.0003)	(0.0003)	(0.0016)	(0.0016)	(0.0025)	(0.0053)	(0.0033)	(0.0077)

Table 6.3.6. SA-330 data consistency analysis with constrained optimisation: Scale factors

	P	Q	R	S ₁	S ₂	S ₃	T	U	V	W	X	Y
PAC	-0.001	-0.001	0.004	-0.118	0.669	0.058	-0.013	-0.008	0.002	0.489	-0.071	-0.311
PMD	(0.0021)	(0.0021)	(0.0002)	(0.0072)	(0.0055)	(0.0052)	(0.0017)	(0.0026)	(0.0001)	(0.0232)	(0.0020)	(0.0027)
PAC	-0.001	0.000	-0.001	0.258	0.079	0.194	0.022	0.021	0.009	4.217	0.001	-0.570
AFT	(0.0000)	(0.0000)	(0.0001)	(0.0043)	(0.0070)	(0.0019)	(0.0013)	(0.0013)	(0.0003)	(0.1904)	(0.0012)	(0.0032)
LAT	-0.002	-0.005	0.000	-0.101	0.385	0.146	-0.019	-0.009	0.000	0.896	-0.036	0.050
LPT	(0.0033)	(0.0060)	(0.0001)	(0.0067)	(0.0077)	(0.0036)	(0.0029)	(0.0064)	(0.0003)	(0.2474)	(0.0040)	(0.0044)
LAT	-0.001	-0.001	-0.001	0.054	0.398	0.056	-0.001	0.008	0.000	-0.704	0.013	-0.072
RGT	(0.0010)	(0.0030)	(0.0000)	(0.0016)	(0.0009)	(0.0029)	(0.0003)	(0.0023)	(0.0003)	(0.1443)	(0.0027)	(0.0026)
COL	-0.001	-0.001	0.002	0.087	-0.494	0.346	0.064	0.011	0.000	0.148	-0.037	-0.089
UPC	(0.0001)	(0.0000)	(0.0001)	(0.0037)	(0.0014)	(0.0044)	(0.0023)	(0.0026)	(0.0003)	(0.2349)	(0.0029)	(0.0019)
COL	-0.001	0.002	-0.001	-0.013	-0.115	0.060	0.054	0.004	0.000	0.357	-0.016	-0.065
DMN	(0.0000)	(0.0003)	(0.0000)	(0.0055)	(0.0023)	(0.0011)	(0.0014)	(0.0021)	(0.0003)	(0.2485)	(0.0023)	(0.0014)
PED	-0.002	0.002	-0.003	-0.055	0.130	0.004	0.016	0.003	0.000	0.376	0.008	-0.039
PGT	(0.0000)	(0.0000)	(0.0000)	(0.0055)	(0.0027)	(0.0033)	(0.0013)	(0.0019)	(0.0003)	(0.2531)	(0.0046)	(0.0031)
PED	-0.003	0.006	-0.003	0.349	0.042	0.052	0.017	0.030	0.000	1.078	0.000	-0.085
PGT	(0.0000)	(0.0000)	(0.0000)	(0.0058)	(0.0014)	(0.0011)	(0.0018)	(0.0019)	(0.0003)	(0.2189)	(0.0017)	(0.0015)

() = Standard Deviation
 * = parameter constrained in algorithm

Table 6.3.7. SA-330 data consistency analysis with constrained optimisation: Biases

	$\hat{p}(0)$	$\hat{q}(0)$	$\hat{r}(0)$	$\hat{s}(0)$	$\hat{t}(0)$	$\hat{u}(0)$
P568PAC.PMD	0.015	0.016	-5.253	44.378	3.682	2.925
	(0.0019)	(0.0026)	(0.0003)	(0.1337)	(0.1113)	(0.1241)
P568PAC.AFT	-0.324	0.000	-0.446	39.538	-0.490	0.219
	(0.0014)	(0.0015)	(0.0003)	(0.1043)	(0.1528)	(0.1143)
P550LAT.LPT	0.023	0.030	-0.815	40.949	0.886	-0.951
	(0.0030)	(0.0074)	(0.0003)	(0.1070)	(0.1828)	(0.1749)
P568LAT.RGT	-0.007	0.035	-2.218	41.431	-0.997	-0.270
	(0.0003)	(0.0014)	(0.0003)	(0.1094)	(0.1149)	(0.1116)
P568COL.UPC	-0.046	0.010	-5.065	45.100	2.080	-1.649
	(0.0022)	(0.0028)	(0.0003)	(0.1036)	(0.1353)	(0.1217)
P568COL.DMN	-0.043	0.023	-5.444	41.890	0.600	0.366
	(0.0035)	(0.0023)	(0.0003)	(0.1124)	(0.1036)	(0.0755)
P576PED.LPT	0.001	0.038	-5.039	42.810	-0.793	3.172
	(0.0013)	(0.0019)	(0.0003)	(0.1912)	(0.2073)	(0.1331)
P576PED.RGT	-0.021	-0.004	-1.281	42.303	-0.271	0.877
	(0.0018)	(0.0020)	(0.0003)	(0.1057)	(0.0672)	(0.0602)

Table 6.3.8. SA-330 data consistency analysis with constrained optimisation: Initial conditions

Derivative Symbol	Unit	DLR		CERT 1		CERT 2		Glasgow Uni		NAE		NLR	
		Value	σ	Value	σ	Value	σ	Value	σ	Value	σ	Value	σ
X_u	1/s	-0.039	0.0003	-0.027	0.0018	-0.026	0.0018	-0.029	0.0079	-0.031	0.0013	-0.025	0.0007
X_v	1/s	0*	—	-0.024	0.0031	0*	—	0*	—	-0.007	0.0023	0*	—
X_w	1/s	0.069	0.0011	0.078	0.0053	0.07	0.0026	0.043	0.0164	0.042	0.0036	0.037	0.0017
X_ϕ	m/(rad s)	0*	—	-0.344	0.0942	-0.063	0.0536	0*	—	0.269	0.0866	0*	—
X_q	m/(rad s)	-2.199	0.035	0.171	0.2008	0*	—	0*	—	0.502	0.1398	0*	—
X_r	m/(rad s)	0*	—	-0.669	0.0853	-0.436	0.0533	0*	—	-0.220	0.0815	0*	—
Y_u	1/s	0*	—	0.008	0.0023	0.018	0.0024	0*	—	0.004	0.0014	0*	—
Y_v	1/s	-0.135	0.0019	-0.135	0.0037	-0.126	0.0032	-0.135	0.0263	-0.105	0.0023	-0.132	0.0015
Y_w	1/s	0*	—	-0.038	0.0059	-0.086	0.0061	0*	—	-0.031	0.0036	0*	—
Y_ϕ	m/(rad s)	1.439	0.0596	0.793	0.1124	0.530	0.1064	0.696	0.0103	0.297	0.0870	0*	—
Y_q	m/(rad s)	0*	—	0.034	0.2052	0*	—	0*	—	1.582	0.1393	0*	—
Y_r	m/(rad s)	1.27	0.0499	0.280	0.1032	0.380	0.0898	0*	—	1.358	0.0818	0.193	0.0598
Z_u	1/s	0.008	0.0029	-0.030	0.0057	0.059	0.0054	-0.0434	0.0134	-0.020	0.0029	-0.080	0.0021
Z_v	1/s	0*	—	0.029	0.0062	0.016	0.0054	0*	—	-0.024	0.0040	0*	—
Z_w	1/s	-1.025	0.0098	-0.835	0.0142	-1.041	0.0160	-1.191	0.0119	-0.841	0.0056	-0.689	0.0050
Z_ϕ	m/(rad s)	0*	—	2.323	0.1823	0.855	0.1676	0*	—	0.523	0.1441	0*	—
Z_q	m/(rad s)	0*	—	-7.07	0.3072	-7.14	0.3041	0*	—	-7.677	0.2076	0*	—
Z_r	m/(rad s)	0*	—	3.542	0.1708	1.407	0.1476	0*	—	-0.630	0.1355	0*	—

* Eliminated from model structure

 σ = Standard deviation

Table 6.3.9. SA-330 Identification Results: List of specific force derivatives with respect to flight variables

Derivative		DLR		CERT 1		CERT 2		Glasgow Uni		NAE		NLR	
Symbol	Unit	Value	σ	Value	σ	Value	σ	Value	σ	Value	σ	Value	σ
L_u	rad/(s m)	0.019	0.0005	0.012	0.0006	0.038	0.0007	0.010	0.0019	0.003	0.0002	0.006	0.0006
L_v	rad/(s m)	-0.066	0.0012	-0.055	0.0009	-0.067	0.0009	-0.064	0.0014	-0.032	0.0003	-0.044	0.0012
L_w	rad/(s m)	-0.090	0.0021	-0.035	0.0017	-0.067	0.0017	-0.027	0.0060	-0.019	0.0006	-0.020	0.0014
L_p	1/s	-2.527	0.0534	-1.195	0.0275	-1.694	0.0242	-2.012	0.0695	-0.725	0.0166	-1.090	0.0437
L_q	1/s	2.225	0.0772	-0.309	0.0633	-1.942	0.0394	0.420	0.0762	0.450	0.0266	0.283	0.0379
L_r	1/s	-0.259	0.0343	0.345	0.0234	-0.601	0.0204	0.554	0.0787	0.888	0.0156	0.540	0.0376
M_u	rad/(s m)	0.110	0.0001	0.007	0.0001	0.010	0.0002	0.013	0.0002	0.003	0.0001	0.008	0.0003
M_v	rad/(s m)	-0.170	0.0002	-0.012	0.0002	-0.013	0.0002	-0.021	0.0015	-0.006	0.0002	-0.014	0.0006
M_w	rad/(s m)	-0.004	0.0004	-0.010	0.0004	-0.018	0.0004	-0.012	0.0015	-0.006	0.0003	-0.014	0.0008
M_p	1/s	0.194	0.0090	0.110	0.0152	0.059	0.0044	-0.035	0.0237	0.173	0.0085	0.020	0.0186
M_q	1/s	-1.108	0.0171	-0.663	0.0190	-0.735	0.0164	-1.356	0.0085	-0.280	0.0142	-0.542	0.0330
M_r	1/s	0*	—	-0.039	0.0062	-0.151	0.0051	0*	—	0.383	0.0082	0*	—
N_u	rad/(s m)	0*	—	0.002	0.0003	-0.002	0.0004	0*	—	0.006	0.0002	0*	—
N_v	rad/(s m)	0.027	0.0002	0.034	0.0004	0.035	0.0004	0.029	0.0006	0.008	0.0003	0.039	0.0010
N_w	rad/(s m)	0*	—	0.013	0.0008	0.045	0.0010	0.010	0.0014	0.019	0.0003	0.010	0.0014
N_p	1/s	-0.395	0.0092	-0.031	0.0102	0.194	0.0129	-0.321	0.0106	-0.301	0.0159	0.295	0.0397
N_q	1/s	0.056	0.0075	-0.441	0.0215	-0.951	0.0232	0*	—	-1.343	0.0257	-0.526	0.0510
N_r	1/s	-0.362	0.0065	-0.475	0.01	-0.341	0.0121	-0.388	0.0348	-0.736	0.0154	-0.288	0.0295

* Eliminated from model structure

 σ = Standard deviation

Table 6.3.10. SA-330 Identification Results: List of specific moment derivatives with respect to flight variables

Derivative		DLR		CERT 1		CERT 2		Glasgow Uni		NAE		NLR	
Symbol	Unit	Value	σ	Value	σ	Value	σ	Value	σ	Value	σ	Value	σ
$X_{\delta col}$	m/(s ² %)	0*	—	0.016	0.0019	0.0127	0.0017	0.064	0.0054	0.030	0.0054	0.013	0.0012
$X_{\delta lon}$	m/(s ² %)	0.052	0.0006	0.031	0.0027	0.026	0.0021	0.012	0.0173	0.096	0.0069	0.006	0.0014
$X_{\delta lat}$	m/(s ² %)	0*	—	0*	—	0*	—	0*	—	-0.007	0.0023	0*	—
$X_{\delta ped}$	m/(s ² %)	0*	—	0*	—	0*	—	0*	—	-0.035	0.0073	0*	—
$Y_{\delta col}$	m/(s ² %)	0*	—	-0.028	0.002	-0.002	0.0020	0*	—	-0.031	0.0053	0*	—
$Y_{\delta lon}$	m/(s ² %)	0*	—	-0.001	0.0028	-0.005	0.0024	0*	—	-0.002	0.0068	0*	—
$Y_{\delta lat}$	m/(s ² %)	0.018	0.0015	0.016	0.0024	0.030	0.0024	0.018	0.0033	-0.031	0.0059	0.012	0.0020
$Y_{\delta ped}$	m/(s ² %)	-0.002	0.0017	0.006	0.0029	0.020	0.0029	-0.044	0.0274	0.157	0.0071	0.044	0.0027
$Z_{\delta col}$	m/(s ² %)	-0.223	0.0038	-0.139	0.0027	-0.202	0.0029	-0.236	0.0204	-0.031	0.0072	-0.165	0.0037
$Z_{\delta lon}$	m/(s ² %)	0.0147	0.0005	0.062	0.0034	0.103	0.0037	0.383	0.0748	0.254	0.0082	0.106*	0.0042
$Z_{\delta lat}$	m/(s ² %)	0*	—	0*	—	0*	—	0*	—	-0.031	0.0064	0*	—
$Z_{\delta ped}$	m/(s ² %)	0*	—	0*	—	0*	—	0*	—	0.157	0.0099	0*	—

* Eliminated from model structure

 σ = Standard deviation

Table 6.3.11. SA-330 Identification Results: List of specific force derivatives with respect to control variables

Derivative		DLR		CERT 1		CERT 2		Glasgow Uni		NAE		NLR	
Symbol	Unit	Value	σ	Value	σ	Value	σ	Value	σ	Value	σ	Value	σ
$L_{\delta col}$	rad/(s ² %)	-0.022	0.0009	-0.007	0.0005	-0.012	0.0005	0*	—	-0.012	0.0003	-0.015	0.0008
$L_{\delta lon}$	rad/(s ² %)	0.0147	0.005	0.062	0.0034	0.103	0.0037	0.383	0.0748	0.204	0.0382	0.0063	0.0042
$L_{\delta lat}$	rad/(s ² %)	-0.051	0.0012	-0.029	0.0008	-0.035	0.0006	-0.031	0.0017	-0.022	0.0003	-0.029	0.0009
$L_{\delta ped}$	rad/(s ² %)	0.011	0.0007	0.014	0.0005	0.001	0.00005	0.020	0.004	0.019	0.0003	0.018	0.0011
$M_{\delta col}$	rad/(s ² %)	0.010	0.0001	0.006	0.0001	0.005	0.0001	0.005	0.0004	0.005	0.0001	0.005	0.0005
$M_{\delta lon}$	rad/(s ² %)	-0.031	0.0002	-0.020	0.0003	-0.021	0.0003	-0.036	0.0008	-0.016	0.0002	-0.026	0.0006
$M_{\delta lat}$	rad/(s ² %)	0.00	0.0002	0*	—	0*	—	0*	—	0.001	0.0002	0.00	0.0005
$M_{\delta ped}$	rad/(s ² %)	0*	—	0*	—	0*	—	0*	—	0.004	0.0002	0*	—
$N_{\delta col}$	rad/(s ² %)	0*	—	0.001	0.0002	0.006	0.0002	0*	—	0.007	0.0002	0.006	0.0008
$N_{\delta lon}$	rad/(s ² %)	-0.001	0.0002	-0.009	0.0004	-0.017	0.0005	0*	—	-0.014	0.0003	-0.007	0.0010
$N_{\delta lat}$	rad/(s ² %)	-0.008	0.0002	0.00	0.0002	0.002	0.0002	-0.007	0.0004	-0.001	0.0002	0.00	0.0009
$N_{\delta ped}$	rad/(s ² %)	-0.022	0.0001	0*	—	-0.031	0.0003	-0.025	0.0008	-0.028	0.0003	-0.032	0.0011

* Eliminated from model structure

 σ = Standard deviation

Table 6.3.12. SA-330 Identification Results: List of specific moment derivatives with respect to control variables

Symbol	Delay Unit	DLR		CERT 1		CERT 2		Glasgow Uni		NAE		NLR	
		Value	σ	Value	σ	Value	σ	Value	σ	Value	σ	Value	σ
$T_{\delta\phi}$	s	0.094	—	0*	—	0.170	—	0.0095	—	0*	—	0.125	—
$T_{\delta\theta}$	s	0.125	—	0*	—	0.125	—	0.0806	—	0*	—	0.125	—
$T_{\delta\psi}$	s	0.125	—	0*	—	0.125	—	0.0099	—	0*	—	0.125	—
$T_{\delta\phi}$	s	0*	—	0*	—	0*	—	0*	—	0*	—	0.125	—

* Eliminated from model structure
 σ = Standard deviation

Table 6.3.13. SA-330 Identification Results: Equivalent control time delays

Mode of motion	AFDD	DLR	CERT		Glasgow Uni	NAE	NLR
			Without control time delays	With control time delays			
Phugoid oscillation		[-0.014, 0.261]	[-0.040, 0.270]	[-0.025, 0.265]	[0.001, 0.270]	[-0.111, 0.280]	[-0.003, 0.269]
Dutch roll oscillation	[0.250, 1.263]	[0.075, 1.375]	[0.119, 1.350]	[0.119, 1.360]	[0.147, 1.350]	[0.111, 1.304]	[0.115, 1.321]
Short period oscillation		[0.939, 1.026]	[0.065, 0.964]	[0.934, 1.200]	[0.934, 1.399]	[0.960, 0.566]	[0.741, 0.904]
Roll mode	(0.930)	(3.021)	(1.37)	(1.39)	(2.066)	(1.09)	(1.18)
Spiral mode	(0.023)	(0.048)	(-0.005)	(0.020)	(0.005)	(0.114)	(-0.062)

Shorthand notation:

s Laplace variable (in 1/s)
 $[\zeta, \omega_d]$ represents $(\zeta^2 + 2\zeta\omega_0 + \omega_0^2)$
 with ζ = damping ratio and ω_0 = undamped natural frequency (in rad/s)
 $(1/T)$ represents $(s + 1/T)$
 with T = time constant (in s)

Table 6.3.14. SA-330 Identification Results: Time constants, damping ratios and undamped natural frequencies

	Glasgow	DLR	CERT1	CERT2	RAE	NLR	Helistab
$Z_w + M_q$	-2.55	-2.133	-1.5	-1.78	-1.086	-1.34	-1.496
$-2\zeta_{sp} \omega_{sp}$	-2.64	-2.115	-1.67	-2.24	-0.921	-1.23	-1.742
$M_q Z_w + \omega_{sp}^2$	2.107	1.268	0.884	1.356	0.18	0.947	1.38
M_{olon}/M_q	1.96	1.053	0.94	1.85	0.32	0.816	1.629
Z_{ocol}/Z_w	0.0265	0.028	0.03	0.029	0.057	0.048	0.0435
M_v	0.198	0.218	0.166	0.194	0.048	0.24	0.266
	-0.012 (0.0015)	-0.004 (0.0004)	-0.01 (0.0004)	-0.018 (0.0004)	-0.002 (0.0001)	-0.014 (0.008)	-0.02

Table 6.3.15. SA-330 characteristics of short period mode

	GLASGOW	DLR	CERT1	CERT2	NAE	NLR	HELISTAB
ω_p	0.27	0.261	0.269	0.266	0.278	0.264	0.221
ω_p^*	0.268	0.282	0.255	0.274	0.211	0.24	0.195
x_u	-0.029	-0.039	-0.027	-0.026	-0.031	-0.025	-0.024
M_u	0.013	0.01	0.007	0.01	0.003	0.008	0.0074

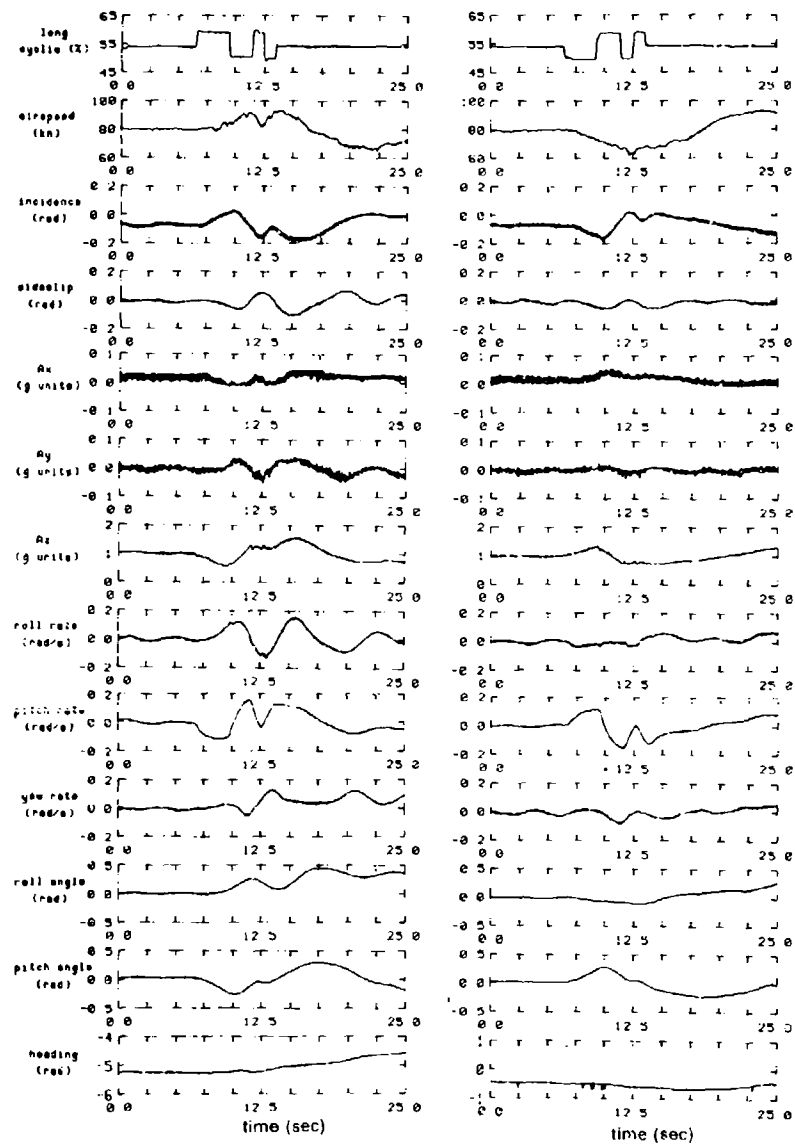
Table 6.3.16. SA-330 comparison of phugoid characteristics
 ω_p -approximation equation (6.3.30)

	GLASGOW	DLR	CERT1	CERT2	NAE	NLR	HELISTAB
$\frac{L_{\phi lat}}{L_P}$	0.0154	0.02	0.024	0.021	0.03	0.027	0.025

Table 6.3.17. SA-330 comparison of roll rate sensitivity

	Glasgow	DLR	CERT1	CERT2	NAE	NLR	Helistab
$(2\zeta_r \omega_r)^*$	0.291	0.167	0.261	0.408	0.565	0.477	0.39
$2\zeta_r \omega_r$	0.4	0.208	0.321	0.324	0.39	0.302	0.326
ω_r^*	1.34	1.36	1.43	1.23	0.865	1.24	1.19
ω_r	1.4	1.375	1.35	1.36	1.3	1.31	1.06

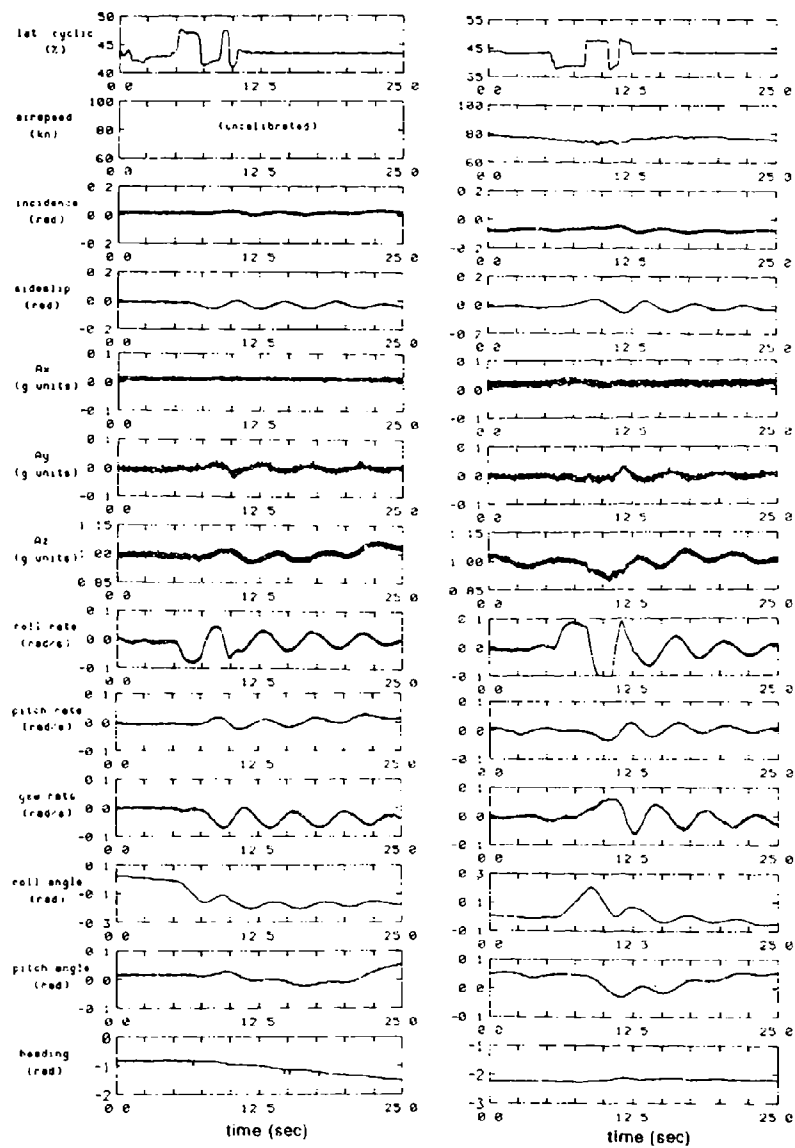
Table 6.3.18. SA-330 characteristics of Dutch roll mode



F568FAC.FWD

F568FAC.AFT

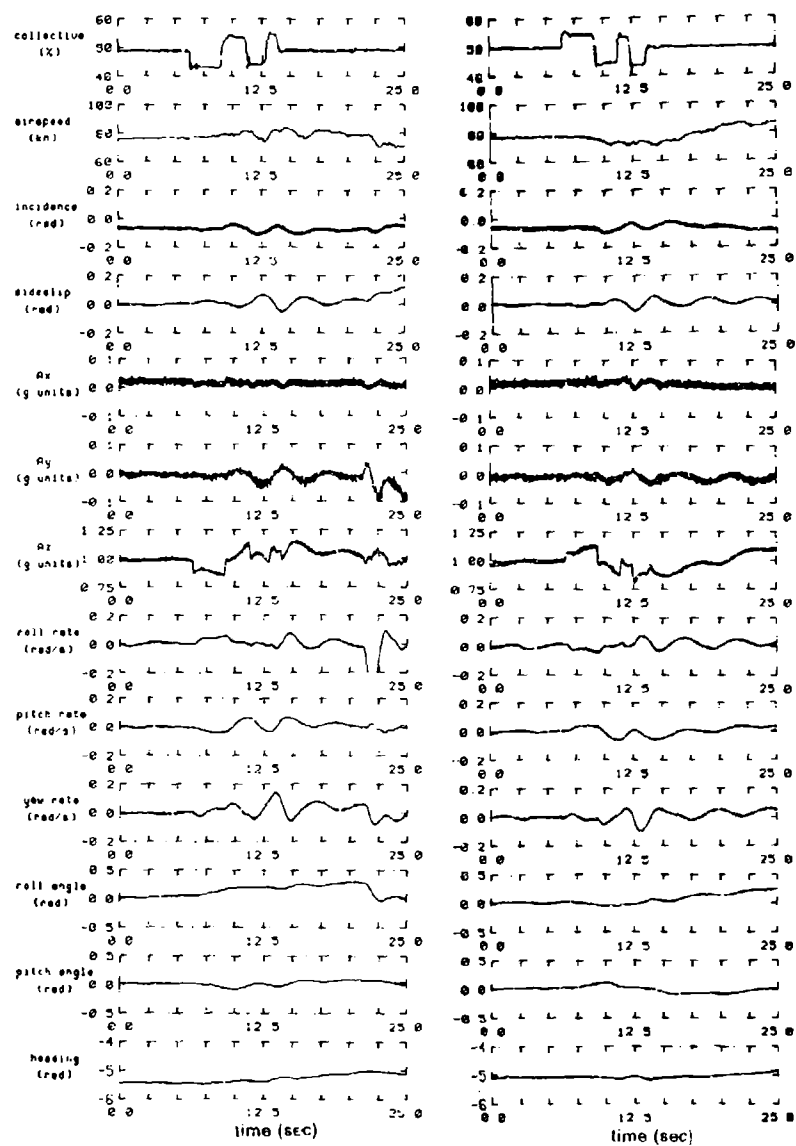
Figure 6.3.3. SA-330 database - response to 3211 longitudinal inputs



F550LAT.LFT

F568LAT.RGT

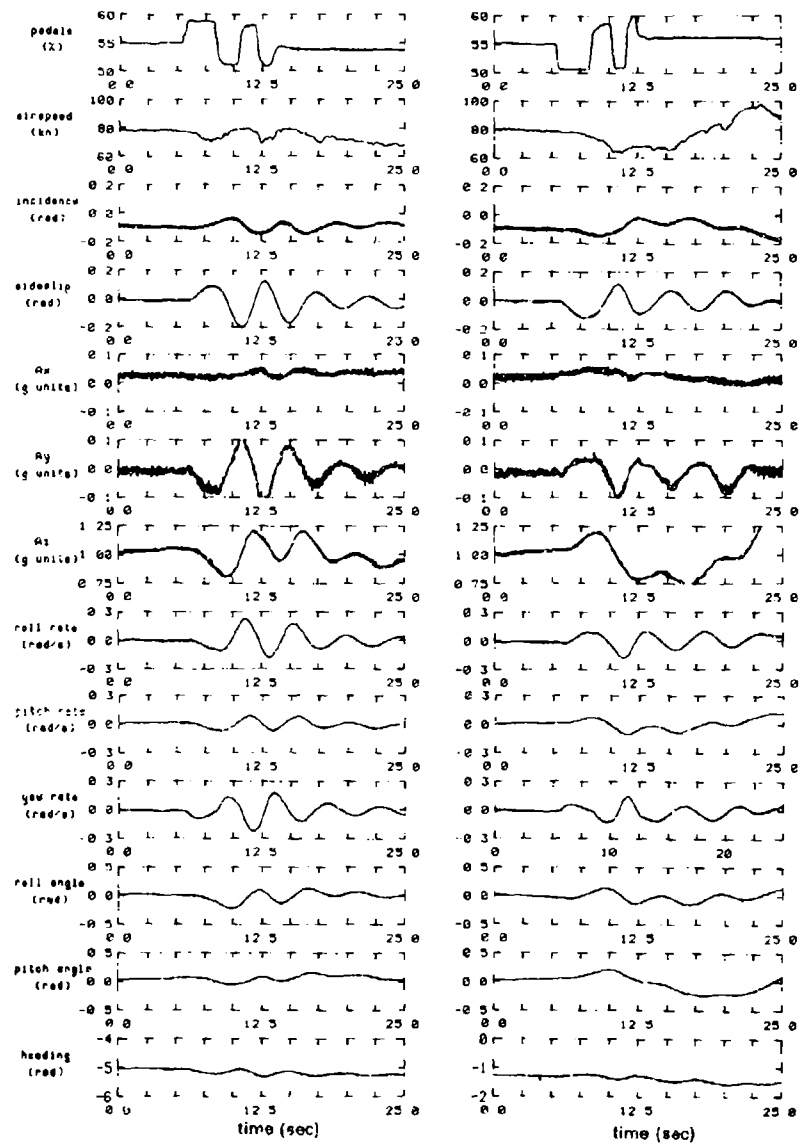
Figure 6.3.4. SA-330 database - response to 3211 lateral inputs



F568COL.UPC

F568COL.DWN

Figure 6.3.5. SA-330 database - response to 3211 collective inputs



F576PED.LFT

F576PED.RGT

Figure 6.3.6. SA-330 database - response to 3211 pedal inputs

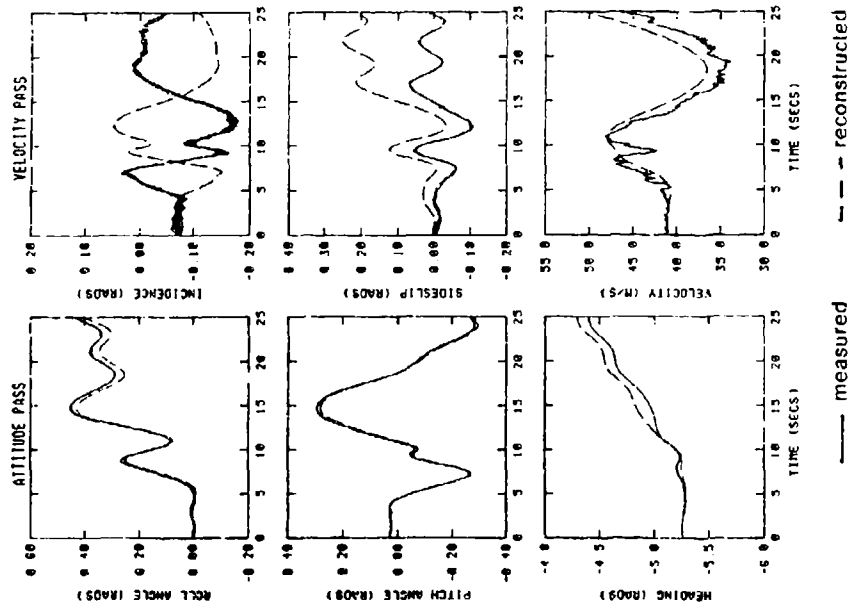


Figure 6.3.7. Comparison of measured attitudes and air data with reconstructed inertial measurements - SA-330 F568FAC.FWD

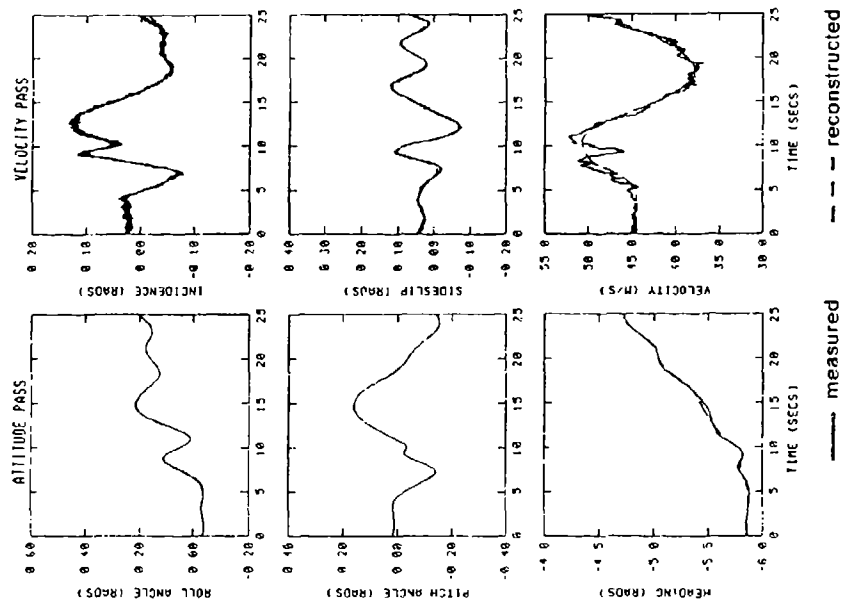


Figure 6.3.8. Comparison of measured attitudes and air data with free optimisation of reconstructed inertial measurements - SA-330 F568FAC.FWD

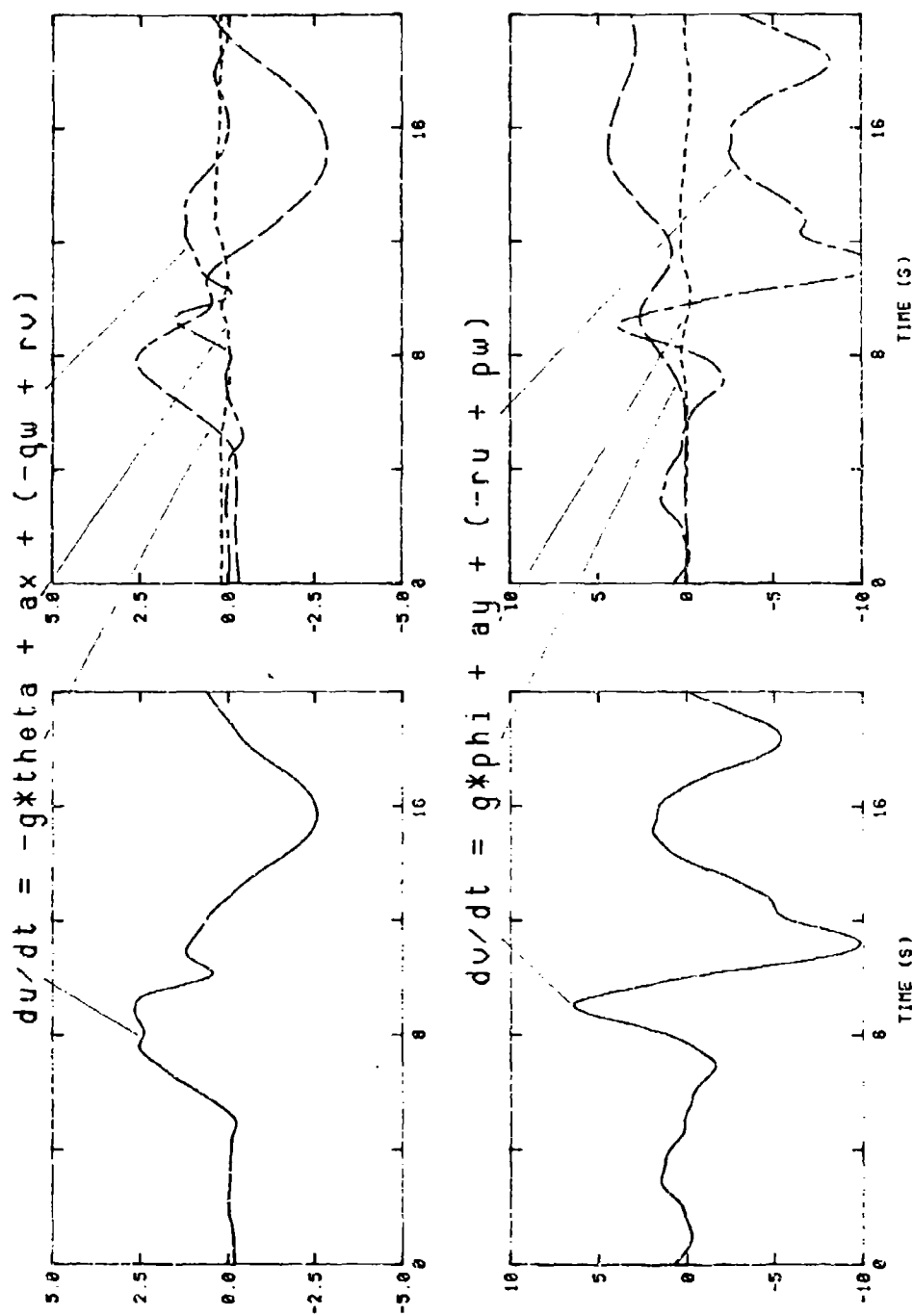


Figure 6.3.9. Components of velocity derivatives - F568FAC.FWD

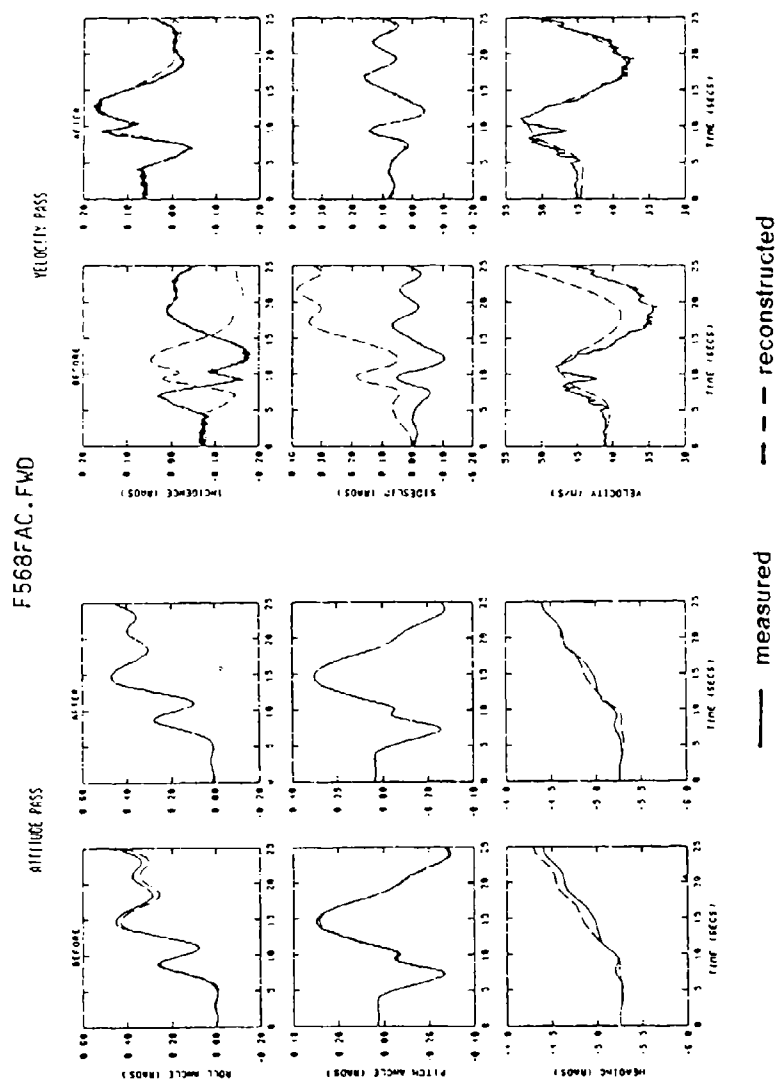


Figure 6.3.10. Comparison of measured attitudes and air data with constrained optimisation of reconstructed inertial measurements - SA-330

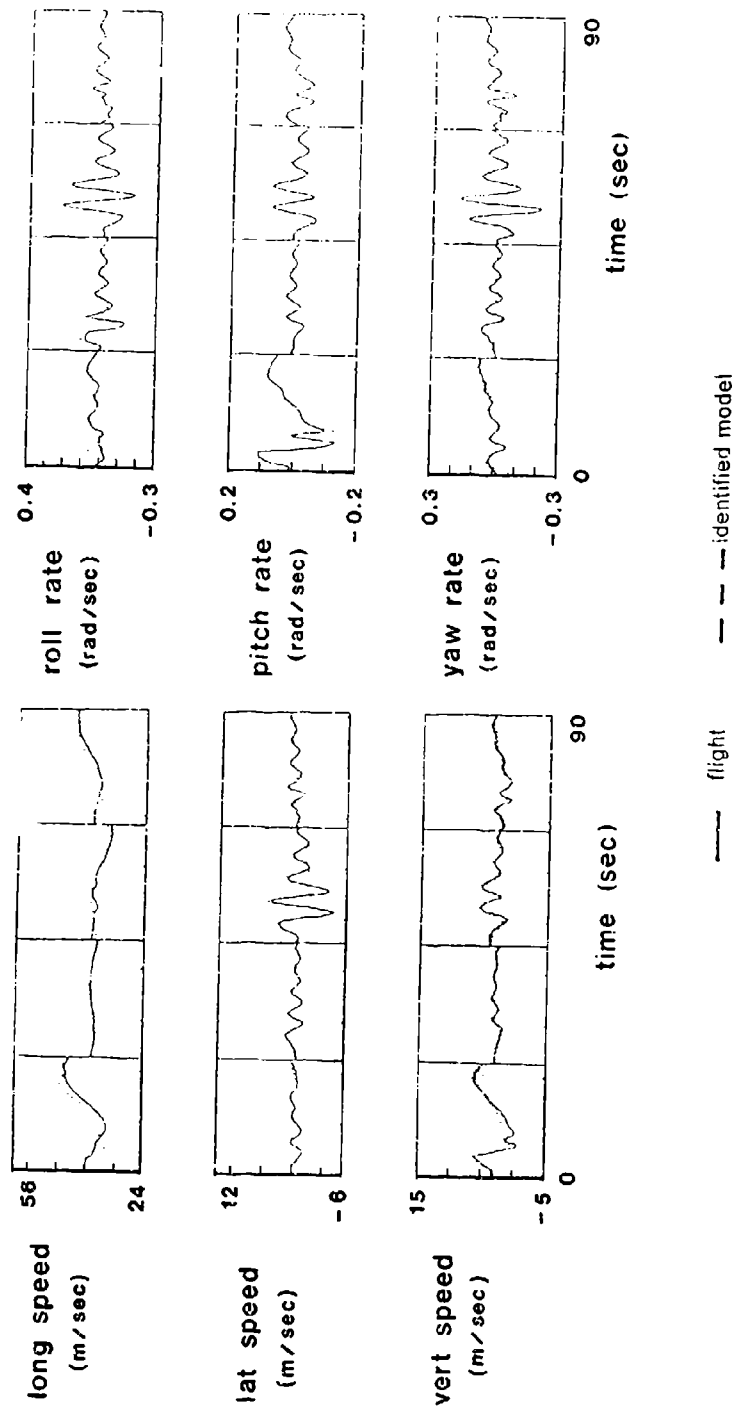


Figure 6.3.1.1. Comparison of flight and estimated times histories - Glasgow - Identification

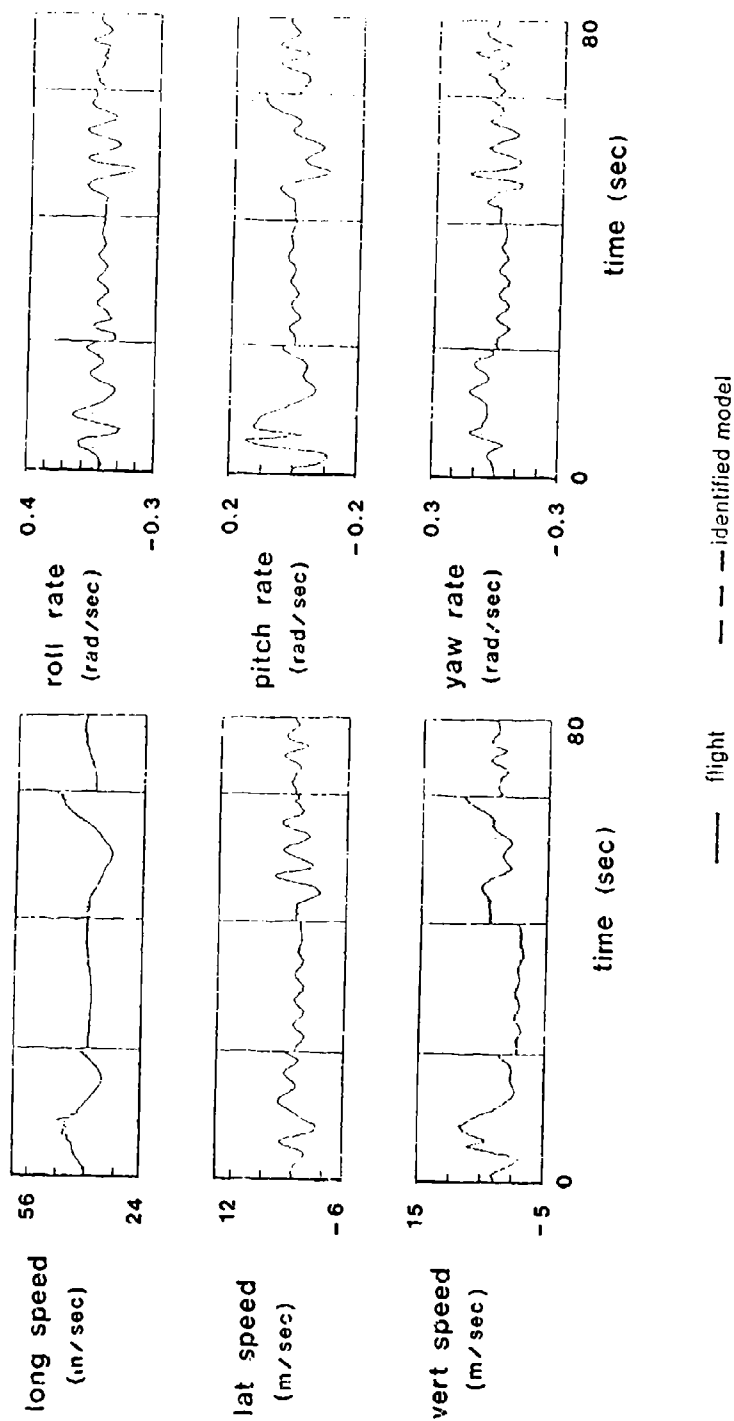


Figure 6.3.12. Comparison of flight and estimated times histories - Glasgow - Verification

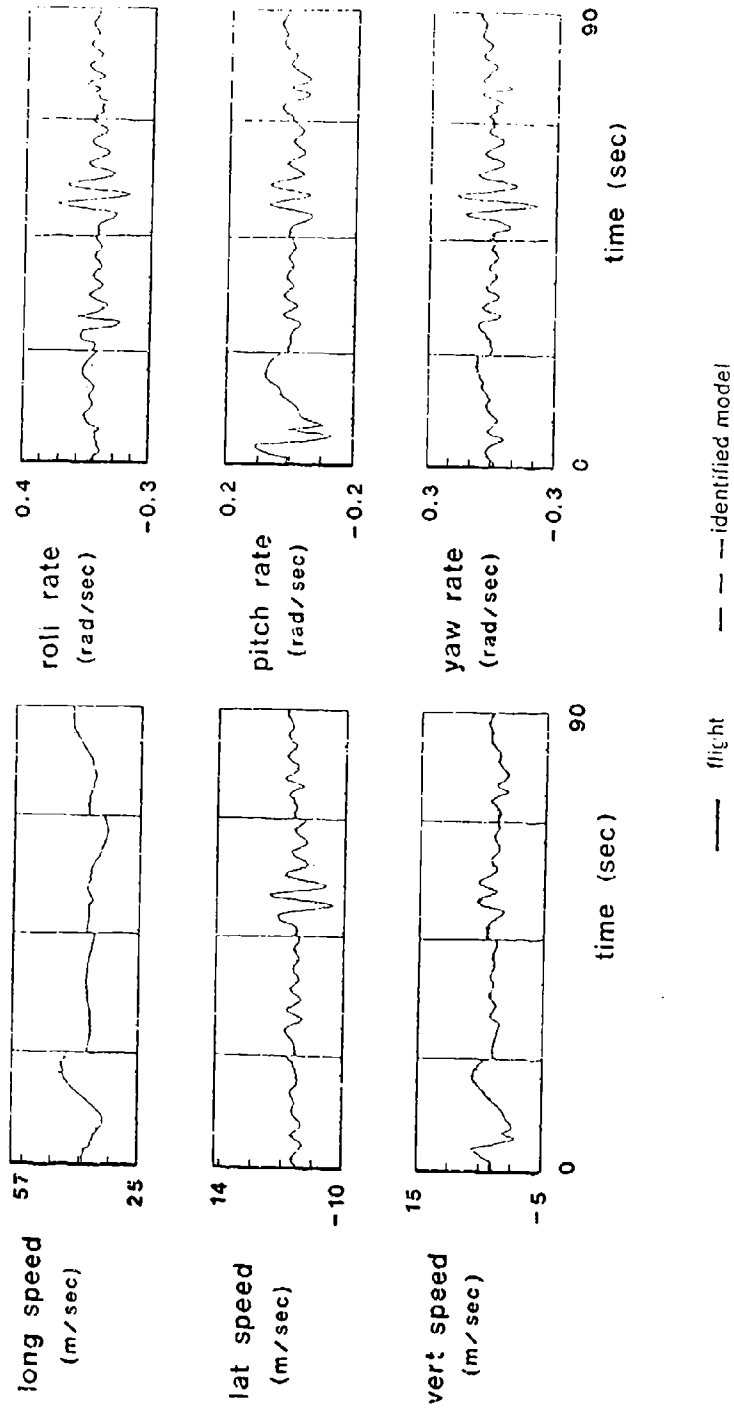


Figure 6.3.13. Comparison of flight and estimated times histories - DLR - Identification

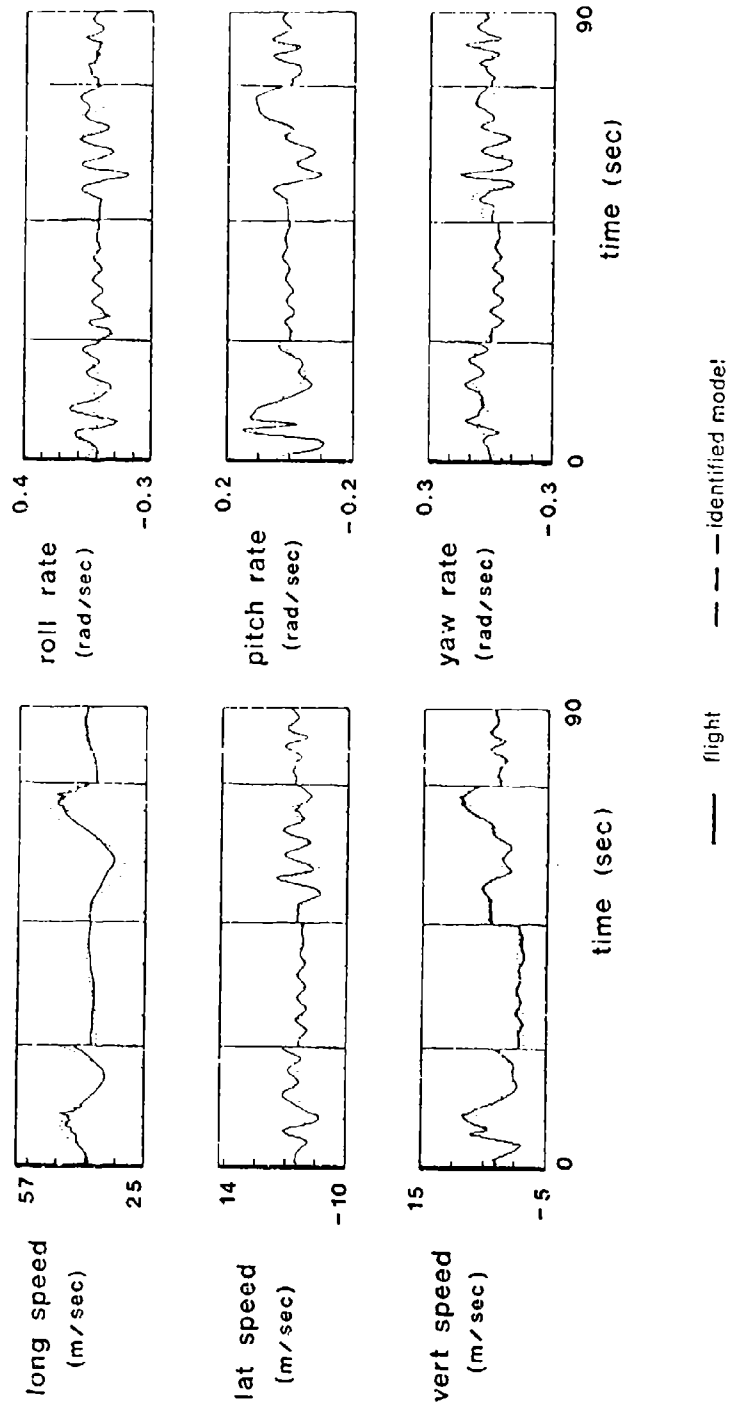


Figure 6.3.14. Comparison of flight and estimated times histories - DLR - Verification

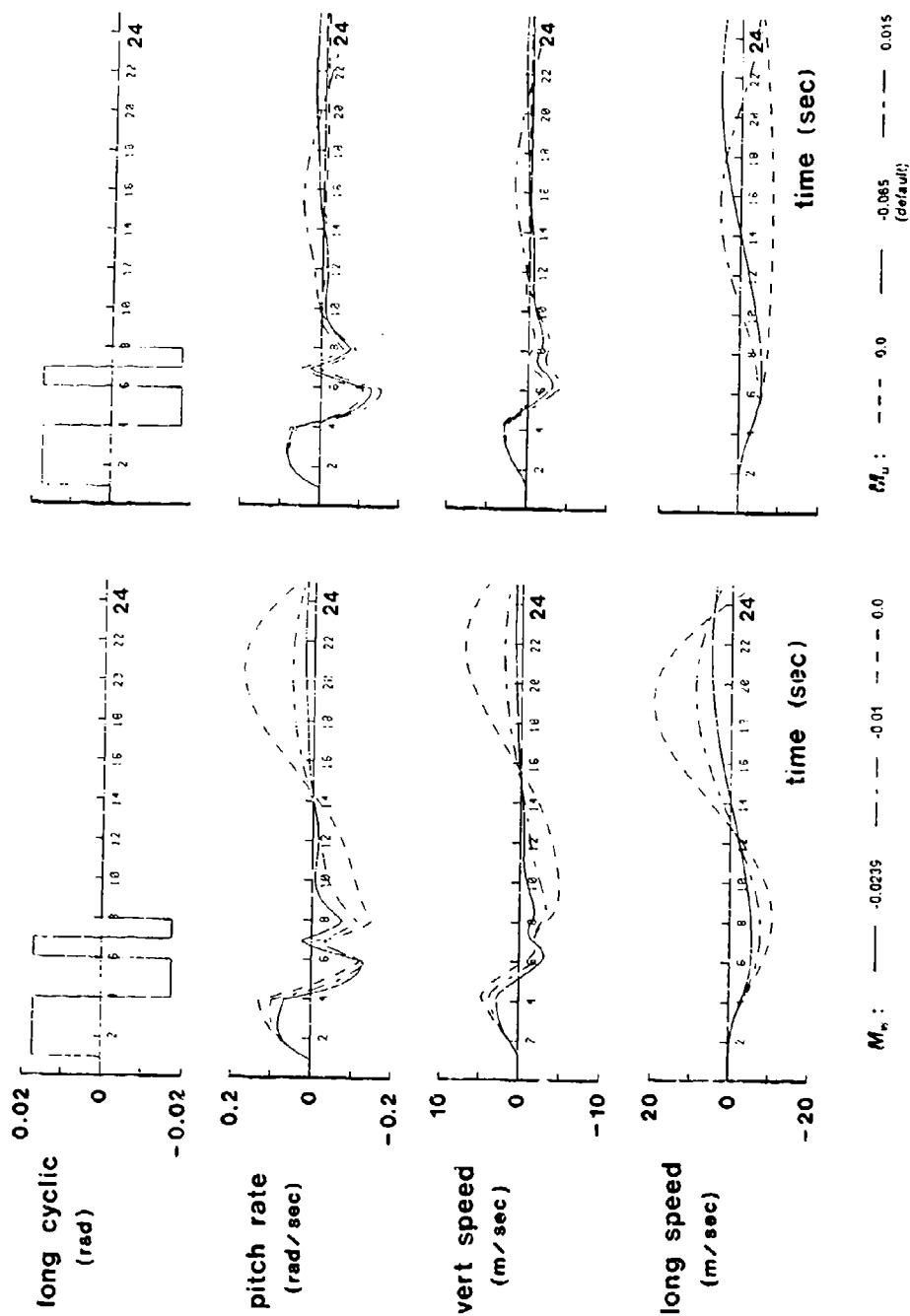


Figure 6.3.15. Helistab cyclic responses for varying M_w and M_u - SA-330 - 80 kn

7. Robustness Issues¹⁶⁾

7.1 Introduction

Successful application and adoption by the rotorcraft industry of system identification hinges on a comprehensive demonstration of robustness. While this statement is probably true in the general case, in reality, those industrial organisations that will benefit the most and the earliest are likely to be those that commit resources to understanding this enabling technology during its development. In particular, they will be in a strong position to assist in setting the standard for robustness.

Robustness issues in rotorcraft system identification may be classified conveniently as follows:

1. robustness and reliability of a-priori information required for successful system identification,
2. robustness of the identification technique used for establishing the structure of the model and estimating parameters of the model,
3. robustness (consistency and accuracy) of the identified model structure,
4. robustness (consistency and accuracy) of the estimated parameters,
5. overall robustness of the resulting mathematical model.

This section puts forward proposals for the robustness conditions and tests required in all five applications above. In some cases the proposals are tentative and the need for more substantiation work is identified. While it is clearly attractive to maximise robustness at all stages, it is also recognised that much good work has been done and insight gained with the techniques of system identification where success has been limited because of the fragility of the results i.e. lack of robustness.

7.2 A-Priori Information: Experimental Design and Data Consistency

Successful initial design of an identification experiment depends critically upon the level of uncertainty within the information available at the outset, including the accuracy of any available mathematical models of the vehicle. As discussed in section 7.5 accurate experimental design requires prior knowledge of the characteristics of the vehicle and such information is, of course, never fully available. A second concern is the accuracy and consistency of the measurements themselves: both of these issues can be discussed under the heading of a-priori information.

7.2.1 Experimental Design

Since experimental designs based on available mathematical models are unlikely to be optimal due to model uncertainties, it is important to be able to characterise some flight or model test data, if available, prior to any detailed attempts at experimental design. Such preliminary data must, of course, be representative of the flight condition for which the proposed identification tests are to be performed. Characterisation of these data sets may be carried out in terms of spectral content, amplitude probability density, maximum excursions and noise content. Measures such as these, taken together with a mathematical model of the vehicle and any other available information, provide useful insight which can have considerable influence on the design and conduct of flight experiments for system identification purposes.

Closely associated with the analysis of any preliminary flight data is a requirement for careful assessment of the instrumentation available on the aircraft to ensure that it is adequate for system identification purposes. Questions of robustness of estimates and robustness of identification methods are closely associated with the quality of the flight test data which, of course, depends ultimately on the quality of the instrumentation.

Careful attention to detail in the design and conduct of flight experiments can greatly enhance the effectiveness and value of a flight test programme. Initial conditions must be defined for each test and these conditions must be repeatable. This is possible only when there is a low turbulence level which would of course apply unless turbulence modelling is a specific objective of the flight test programme. At the analysis stage it is therefore necessary to determine the means and standard deviations of the records from all the channels prior to the

¹⁶⁾ Principal Author: D. J. Murray-Smith, University of Glasgow

application of the control input. This process allows one to check that the required initial state exists in terms of the mean values and that deviations from this mean lie below a defined threshold level.

In the design of flight experiments it is also important to make provision for repeated testing at each chosen test condition. Results from repeated tests must be examined carefully for differences. Ideally this should be done on board the aircraft or by telemetry so that further testing can be carried out if significant variations are detected.

Investigation of linearity is of great importance and at each test point inputs should be applied for different amplitudes and for different directions. The degree of nonlinearity can then be assessed qualitatively and also in a quantitative fashion in terms, for example, of the amplitude distribution function.

The frequency content of test signals is of great importance for system identification work and it is necessary to ensure that the frequency content of the test input signal used in a given application is appropriate for the modelling objectives in that particular case. Spectral analysis of the test input applied to the vehicle, coupled with similar analysis of the measured response variables, can provide valuable physical insight. For each test condition it is appropriate to carry out tests with different input signals selected to cover different parts of the frequency range. Comparisons can then be made of these data sets with a view to establishing any potential problem areas for the subsequent identification process. For example, the extent of excitation of each of the states at a given part of the frequency range can be of considerable importance. Prior knowledge of the states which are excited in a satisfactory fashion can be very helpful in guiding the user of identification software and in interpreting results.

If test input signals are to be applied by the pilot via the normal controls practical limitations of accuracy and repeatability are encountered both in terms of amplitude and timing. The difficulties of applying test signals manually restrict the range of input types which can be considered. On the other hand it may be essential in some applications, such as handling qualities studies, for the pilot to apply the test inputs.

Robustness of test inputs is an important but often neglected aspect of the input design process. As already discussed, only an approximate model of the vehicle is available prior to testing and the inputs used should be as insensitive as possible to errors in the model.

A second important point is that inputs should not contain a d.c. component since this will tend to change the operating condition of the aircraft away from the initial trim state; unless this is specifically required (e.g. classical speed - stability tests (Padfield, 1985, [7.1])).

It is possible to define cost functions, in the frequency domain, which can be used to generate optimal binary multi-step inputs. One cost function which has been used successfully has the form (Leith et al., 1989, [7.2]):

$$I = \sum_{k=1}^m a_k |F(\omega_k)|^2 \quad (7.1)$$

where $F(\omega_k)$ is the Fourier transform of a general multi-step signal for n steps.

a_k are constants, $k = 1, 2, \dots, m$

ω_k are frequencies (in rad s^{-1}), $k = 1, 2, \dots, m$

The values of the weightings a_k and the frequencies ω_k in this cost function are chosen to meet the requirements in terms of the frequencies which should or should not be excited by the input. Given the number of steps in the multi-step input the cost function is maximised in terms of the timing of these steps. Specifying a large positive coefficient a_k results in an input with a large auto-spectrum component at frequency ω_k . Conversely specifying a large negative a_k results in an input with a small auto-spectrum component at the corresponding frequency ω_k . This allows inputs to be synthesised which meet the general guidelines outlined above.

The weightings chosen for the different parts of the frequency range in this form of approach can have considerable significance in terms of robustness. Since the model of the vehicle is not known exactly the frequencies of the natural modes are not known exactly. In order to allow for uncertainties, inputs should avoid exciting a range of frequencies around the predicted position of each resonance. This should also tend to reduce the overall sensitivity to errors introduced by the pilot in applying the test inputs since errors in the auto-spectrum are then less significant in their effects.

Table 7.1 through Table 7.5 summarise the robustness conditions and tests for each aspect of the identification process. Special recommendations are included within these tables and for the experimental design aspect

(Table 7.1) these emphasise the importance of a preliminary flight test. Results from the application of an appropriate broad-band calibration input, such as a frequency sweep, should be of value in the experimental design and should provide useful information to guide the initial choice of a model structure.

7.2.2 Kinematic (Measurement) Consistency

The fact that flight data is frequently degraded by measurement and process noise and sensor calibration inaccuracies introduces a need for consistency checks on the data prior to the application of identification techniques to estimate aircraft parameters. Methods commonly used for the investigation of data consistency involve:

1. simple comparisons between redundant sensors,
2. comparisons between kinematically redundant sensors (e.g. comparisons of integrated body rotational accelerations with body angular rates), and
3. state estimation techniques such as the Kalman Filter/Smother.

Important questions of robustness arise in connection with all of these methods of consistency checking. In methods 1) and 2) biases and scale factors may be estimated using Least Squares or Maximum Likelihood techniques, but instrument modelling errors or the presence of large amounts of measurement noise can cause problems. State estimation methods may be used to reduce the uncertainty level associated with a given signal but these techniques require prior knowledge of measurement and process noise statistics which may not be readily available.

One approach to the investigation of kinematic consistency which may have some advantages, in terms of robustness, over other methods involves the use of a Bayesian estimator (see section 6.3; Black, 1989, [7.3]). For such an estimator confidence figures have to be provided for the initial values of the unknown parameters. Some physical insight can thus be incorporated within the estimation process and this may provide benefits in terms of the robustness of estimates of bias and scale factor parameters.

7.3 Identification Techniques

The robustness of a given identification technique cannot, in general, be separated from questions of experimental design, choice of model structure, and accuracy of the resulting estimates. However, in the context of the classification of robustness issues given above, the robustness, or otherwise, of a given identification technique is taken to mean the reliability of the method in terms of convergence of the optimisation procedure, susceptibility to measurement and process noise, and accuracy of initial parameter estimates.

Klein (1979, [7.4]) has provided a useful summary of the identification techniques generally applied to aircraft parameter estimation. The paper gives the theoretical properties of a number of different estimators. These properties provide useful pointers with regard to questions of robustness.

For example, in its most general form, the Maximum Likelihood method provides a means of obtaining parameters for a linearised aircraft model from flight data involving both measurement noise and process noise. On the other hand other, less general, forms of output error method are based upon an assumption that only measured outputs are corrupted by noise and that the aircraft experiences no gusts or other unmodelled disturbances. In the presence of process noise, such as atmospheric disturbances, results from output-error methods can be significantly degraded, leading to poor estimates which show large variances or high correlations. The variance of estimates obtained using equation error methods is affected not only by process noise but also by the noise level associated with all the measurements and the estimates themselves can be significantly biased using this approach even if the measurement noise and process noise components have zero mean value.

Comparisons of the robustness of different techniques can only be carried out if they involve tests in which each method is assessed using the same sets of flight data. The robustness of a given technique can, of course, be influenced considerably by the software implementations and every effort must be made to ensure that identification techniques are not being degraded by poor software design.

Other factors to be considered in making comparisons of this kind include the form of model under consideration (e.g. state space or transfer function) and the particular flight conditions included in the chosen data sets upon which the comparisons are based.

The ease of use of a method and the form of interface provided in a particular computer implementation are matters which are, in principle, quite separate from questions of robustness. However, the diagnostic tools incorporated within a particular software implementation can be of considerable importance. Robustness problems may well remain undetected unless the user is confronted with relevant evidence concerning confidence intervals, goodness of fit and cost function values. This implies a need for a well designed, flexible, user interface with extensive provision for graphical output.

The special recommendation presented in Table 7.2 for this aspect of the identification process relates to the need for identification tools to incorporate a full and well-engineered user interface which provides information concerning factors such as the goodness of fit, confidence intervals of estimates, the sensitivity to changes of model structure and the sensitivity to changes in test condition. Good graphics facilities are an essential part of this user interface.

7.4 Model Structure

Questions of robustness in terms of the estimation of model structure are, for linear six-degree-of-freedom rotorcraft identification, traditionally linked to problems associated with equation-error identification methods and to techniques for the determination of model order in transfer function models. However, the use of pseudo-control inputs (e.g. Black et al., 1989, [7.5]) or the method of successive residuals (DuVal et al., 1983, [7.6]) as a means of reducing the complexity of the parameter estimation problem also involves decisions which relate implicitly to the model structure, and may have a bearing on the accuracy of the estimates of the associated parameters.

In broader terms the model structure estimation process implies an activity in which the model may be expanded in a number of different dimensions. The number of degrees of freedom is the most obvious measure of complexity of a model structure but this aspect cannot be separated from questions of bandwidth, amplitude and helicopter components. It is vital to recognise that in the development of a model structure we can expect to see dramatic changes in effective parameters as the model is expanded.

For example, the parameters of a low-frequency reduced-order model may change significantly as additional degrees-of-freedom are introduced or the bandwidth is increased. Such changes demonstrate very clearly the weakness of reduced-order models when used outside their proper range of application.

One important indicator of problems associated with model structure is provided by the residuals which are obtained following the parameter estimation stage of the identification. Correlated residuals can often be an indicator of a possible problem associated with the model structure. The form of the residuals, when interpreted with physical understanding, may provide clues concerning the precise nature of this problem and the steps to be taken to correct the model structure. Practical difficulties can arise, however, because of the fact that large residuals may also result from the presence of correlated measurement noise in the measured flight data, or from the fact that a particular response variable is of very small amplitude, or from nonlinearities.

The step-wise regression procedures available within the Optimal Subset Regression (OSR) program (Padfield et al., 1987, [7.7]) allow the estimation of a first approximation to the parameter estimates in a class of model structures. This form of equation-error estimation provides one very convenient way of exploring the ability of different linear and nonlinear model structures to fit flight measurements. The step-wise regression procedure applies the Least Squares fit in a sequence of steps, each time adding or deleting an additional independent variable to the regression equation until a best fit is achieved. At each stage the variable chosen for entry to the regression is the one having the highest partial correlation with the residual. In this process the multiple correlation coefficient, R , is a direct measure of the accuracy of fit while the total F -ratio provides a measure of the confidence ascribed to the fit. The partial F -ratios for individual parameters provide individual confidence measures. Both R^2 and the F -ratios are tracked during the regression process in order to determine the maximum total and partial F -ratios. The regression is terminated when either R^2 reaches a pre-defined value or the individual F -ratios of remaining parameters fall below a specified critical value. An example, described by Padfield et al. (1987, [7.7]) has illustrated the value of this process for the case of a pedal doublet response in which it was found necessary to restrict the estimated model structure to simple lateral and directional motions. The relationship between the stability of the Dutch roll and the flight path angle was being investigated and, although it was found initially that the predictive capabilities of the simulation model were poor, a reduced-order upgraded model based on flight data provided greater insight concerning the mechanisms of stability loss with climb angle.

The incorporation of pure time delays within the model structure can lead to improved, and more robust estimates of derivatives within the six-degrees-of-freedom form of description in cases where these derivatives are susceptible to rotor transient effects which are not included in the assumed model structure.

In addition to bandwidth and amplitude a third important model dimension relates to the vehicle's physical components e.g. main rotor, tail rotor etc. Without the use of special load cells, however, knowledge of individual component contributions to force and moment derivatives is very difficult to extract. However, in some situations certain components dominate and in others the relationship between the components' contributions to different parts of the model structure are known and can be used to support the analysis.

It is recommended in Table 7.3 that increased emphasis should be given to establishing a valid model structure prior to the parameter estimation stage of the identification process. In order to do this more reliable techniques are needed for the estimation of model structure.

7.5 Parameter Estimates

One indicator of the robustness of parameter estimates is the value of the associated variance. It should be noted, however, that comparison of variance values obtained using different model structures is not valid.

As mentioned under the heading of model structure, checks of residuals can provide additional insight concerning questions of accuracy. If the identification process is completely accurate, both in terms of model structure and parameter estimates, the residuals will take the form of white noise. The whiteness of residuals is conventionally tested by determining the autocorrelation function of the residual sequence.

An additional measure of the robustness of parameter estimates may be provided by plots of the parameter value versus the length of the record used for the identification. The plots for each parameter should of course converge to a constant value as the record length increases. An example for the case of the Puma helicopter may be found in (Black et al., 1989, [7.5]) which includes a graph showing the dependence of estimates and the associated variances on record length for a particular flight experiment.

The sensitivity of parameter estimates to the frequency range of the data used in the estimation process can also be revealing and can provide a measure of the robustness of parameter estimates. High sensitivity to the inclusion of additional frequencies in the range used for identification is a good indicator of problems in the experimental design or model structure determination stages. Essentially the requirement, in terms of the frequency-domain, is to establish the range of frequencies over which parameter estimates are essentially constant. This process should then lead to an identified model which is valid for that frequency range. Figure 7.1 shows the results of a study (presented in section 8.3.6) of the effect of frequency range on a parameter estimate and the associated fit cost. The rapid rise in the cost function for including dynamics above 14 rad/s is due to the inability of the quasi-steady rotor modelling to characterise the coupled body/rotor nature of the true response. It has been found that the utility of quasi-steady models which approximate the rotor characteristics by an equivalent time delay can be increased if the data is band-limited to below the rotor flapping frequency (13 rad/s in this case) before the identification is carried out. Although coupled rotor/flapping instability is not represented in the resulting band-limited quasi-steady models the resulting description is still of value for estimation of control system performance.

The robustness of parameter estimates is closely associated with questions of experimental design and the spectral behaviour of the system. Plattschke et al. (1979, [7.8]) have discussed the general problem of identifiability of derivatives and have proposed the use of frequency-domain techniques for identifiability investigations. Kaletka (1979, [7.9]) has also proposed a method for isolation of significant parameters involving measures based upon time-domain quantities. Both of these approaches provide powerful tools to isolate significant terms and identifiable parameters within the model equations. Clearly, as is emphasised in Table 7.4, estimated parameters should show low sensitivity to record length in both the time domain and frequency domain.

7.6 Overall Robustness of the Model

Checks of the overall accuracy of the model resulting from the identification process can be obtained by carrying out tests on the model using data sets which were not used in the identification process. The selection of such data sets to be used for model checking can present problems in that they must be broadly similar to the sets used for the identification in terms of their spectral properties and amplitude and energy distributions. If the differences between the model responses and the corresponding measured variables are all sufficiently

small the identified model can then be accepted as a candidate model for the chosen flight condition. It will not, however, be a unique representation and it is possible that other models could give similar results.

An additional check can, of course, be provided by carrying out repeated runs at the same nominal test condition using the same experimental design. An assessment of the changes of structure and parameter estimates under these circumstances can be very revealing, especially when the extent of the model distortion is related to the error bounds of the estimated model parameters. The situation is unsatisfactory if the variations of parameters derived from tests carried out under nominally the same conditions are greater than the estimated error bounds. An example of this type of problem can be found in results obtained from the Puma helicopter using lateral cyclic test inputs where the distribution of damping appears to be different for results involving movement to the right and to the left. Excellent verification results were obtained in one case but not for the other (Figure 7.2). One of the recommendations shown in Table 7.5, is that appropriate design criteria should be established for verification inputs.

Responses obtained using other test inputs are bound to give differences in the amplitude, frequency and distribution of energy between state variables and are thus likely to give different parameter estimates. The differences may however be understandable in terms of physical reasoning and potentially useful information can sometimes be obtained by making comparisons of results from a number of test signals.

It is also very useful, when comparing parameter estimates with theoretical predictions, to examine the trend of the estimated parameters with some fundamental rotorcraft quantity defining the flight condition. Such quantities include speed, rate of climb or descent and turn rate. As pointed out by Iliff (1979, [7.10]) this simple technique can provide much valuable insight and is readily applied to aircraft where manoeuvres are small perturbations about a point in a much larger envelope.

7.7 Conclusions and Recommendations

The robustness conditions and associated tests proposed in the previous sections can be summarised in the form of Table 7.1 through Table 7.5. For each robustness condition it is possible to define one or more tests which may be of value. In some cases the proposals which have been made are very tentative and it is unlikely that any examples exist where all these robustness tests have been applied in a systematic fashion. Many cases do exist, however, in which some of the robustness tests shown in Table 7.1 through Table 7.5 have been applied and where valuable insight has been obtained from their use.

This analysis of robustness issues also highlights some of the reasons for the reluctance shown by industry in the past to adopt system identification methods for routine application.

Special recommendations are also presented in Table 7.1 through Table 7.5 for each aspect of the identification process. These provide a summary of the more detailed recommendations contained in each of the earlier sections of this chapter. It is believed that the presentation of robustness issues and corresponding tests in this way, together with these recommendations, can help to define a set of tools necessary for the successful application of system identification techniques for rotorcraft.

References

- [7.1] Padfield, G. D.
Flight Testing for Performance and Flying Qualities
AGARD Lecture Series LS-139, 1985
- [7.2] Leith, D.; Murray-Smith, D. J.
Experience with Multi-Step Test Inputs for Helicopter Parameter Identification
Vertica, Vol. 13, No.3, 1989
- [7.3] Black, C. G.
A Users' Guide to the Bayesian Nonlinear System Identification Program KINEMOD
University of Glasgow, Department of Aerospace Engineering, Internal Report, 1989
- [7.4] Klein, V.
Identification Evaluation Methods
AGARD Lecture Series LS-104, Paper 2, 1979

- [7.5] Black, C. G.; Murray-Smith, D. J.
A Frequency-Domain System Identification Approach to Helicopter Flight Mechanics Model Validation
Vertica, Vol. 13, No. 3, 1989
- [7.6] DuVal, R. W.; Wang, J. C.; Demiroz, M. Y.
A Practical Approach to Rotorcraft Systems Identification
39th AHS National Forum, St. Louis, 1983
- [7.7] Padfield, G. D.; Thorne, R.; Murray-Smith, D.; Black, C.; Caldwell, A. E.
UK Research into System Identification for Helicopter Flight Mechanics
Vertica, Vol. 11, No. 4, 1987
- [7.8] Plaetschke, E.; Schulz, G.
Practical Input Signal Design
AGARD Lecture Series LS-104, Paper 3, 1979
- [7.9] Kaleika, J.
Rotorcraft Identification Experience
AGARD Lecture Series LS-104, Paper 7, 1979
- [7.10] Iliff, K. W.
Aircraft Identification Experience
AGARD Lecture Series LS-104, Paper 6, 1979

Robustness Conditions	Robustness Tests	Special Recommendations
Precision and repeatability of initial conditions	Analysis of mean and standard deviation of all channels prior to control input	The experimental design process should incorporate a preliminary flight test to categorise the dynamic system, including sensors, actuators, control system and airframe. Results from this test should guide the design of optimal test inputs for system identification and should influence the choice of model structure.
Repeatability of selected test inputs	Repetition of flight tests and analysis of differences between responses	
Linearity	Repetition of flight tests using different amplitudes and directions of test signals Examination of amplitude distribution functions	
Low correlation between control inputs and between states	Correlation analysis of records	
Frequency content of test input in relation to modelling requirement	Spectral analysis of records	
Table 7.1. Robustness Aspect of the Experimental Design		

Robustness Conditions	Robustness Tests	Special Recommendations
Susceptibility of method to measurement noise	Examination of theoretical properties of the method Results obtained from application of method to simulated response data with added noise	Identification tools must incorporate a full and well engineered user interface exploiting maximum use of simple graphics. The tools should provide information on goodness of fit, confidence intervals, sensitivity to changes in test condition and model structure, etc.
Susceptibility of method to process noise	Examination of theoretical properties of the method Results obtained from application of method to simulated response data	

Table 7.2. Robustness Aspect of the Identification Technique

Robustness Conditions	Robustness Tests	Special Recommendations
Suitability of initial choice of model structure	Application of R^2 and F -ratio tests in stepwise regression procedure	More emphasis must be given to establishing a valid model structure before proceeding to the parameter estimation stage. Reliable tools for the assessment of model structure are required.
Suitability of model transfer function order	Examination of residuals in frequency domain	
Presence of significant unmodelled dynamics	Examination of residuals Examination of effects of introducing pure time delay	

Table 7.3. Robustness Aspect of the Identified Model Structure

Robustness Conditions	Robustness Tests	Special Recommendations
Range of parameter estimates found from different tests	Examination of variance values provided by the chosen estimation method. Examination of residuals to establish whether they show white noise properties (e.g. by autocorrelation analysis).	Estimated parameters should show low sensitivity to record length in both the frequency domain and time domain.
Dependence of estimates on record length.	Repeat estimation process for a variety of different record lengths	
Dependence of estimates on frequency range used for estimation	Repeat estimation process using frequency domain approach for a number of different frequency ranges	

Table 7.4. Robustness Aspect of the Estimated Parameters

Robustness Conditions	Robustness Tests	Special Recommendations
Overall adequacy of estimated model structure and parameters	Examination of residuals	Design criteria are needed for verification inputs to establish model properties in terms of distortion of: 1) Model responses when subjected to verification input 2) Model parameters for verification inputs
Model distortion effects when used with verification inputs	Analysis of flight test data for verification inputs	

Table 7.5. Robustness Aspect of the Resulting Mathematical Model

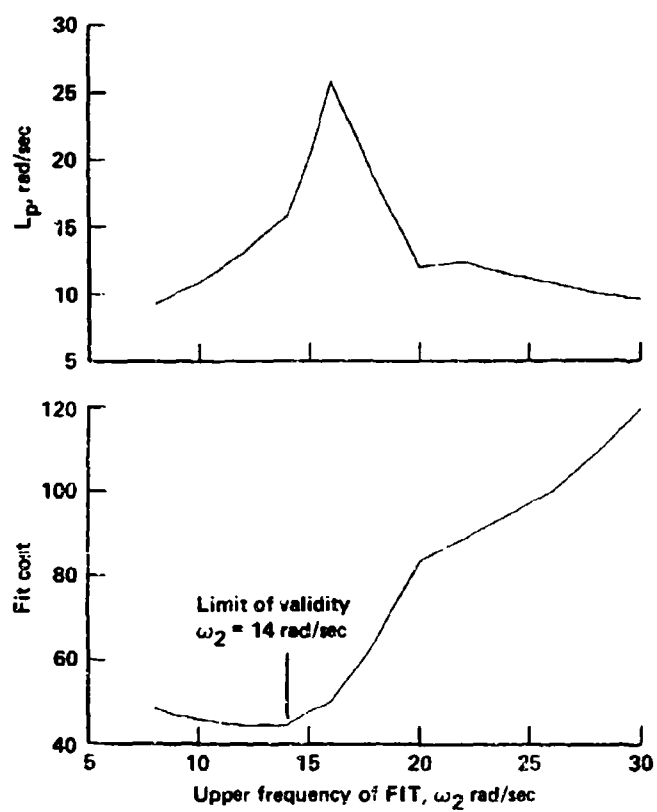


Figure 7.1. Effect of upper frequency limit on identification
Lower limit of fit is fixed, $\omega_1 = 1.0$ rad/s

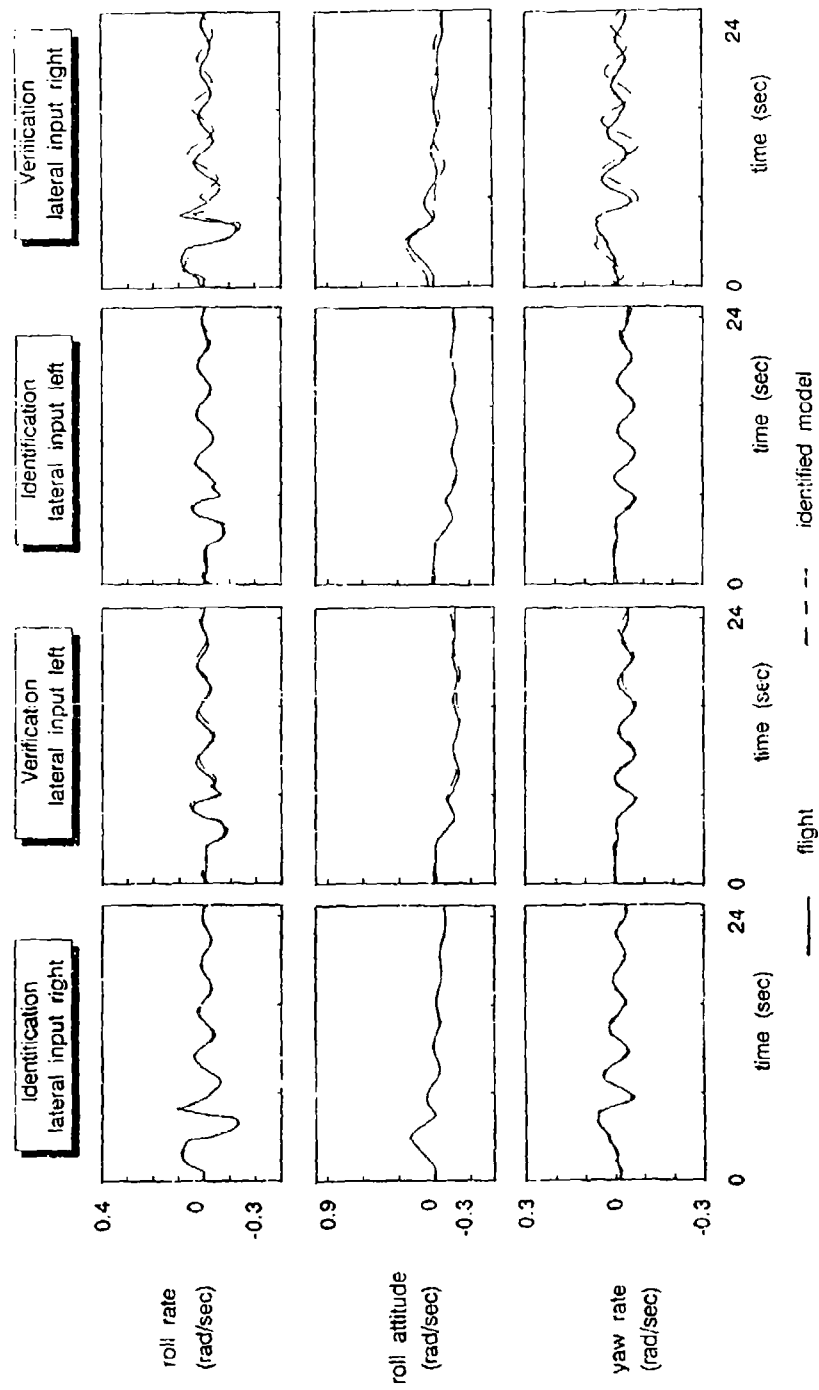


Figure 7.2. Comparison of identification and verification results

8. Application of Identification

8.1 Simulation Model Validation¹⁷⁾

8.1.1 Introduction

The potential of piloted simulation as a flight dynamics and performance support tool is considerable both in research and project applications, from design through development and certification. Some uses are listed below:

- Developing control laws for handling qualities and disturbance rejection.
- Checking compliance with flying qualities requirements for mission-task-elements and general flying tasks.
- Checking adequacy of control and stability at the edges of the flight envelope.
- Establishing control strategy following engine failure during various flight phases e.g. take-off.
- Developing functional integration of flight control with navigation, fire control, engine control systems etc.
- Development of display formats for operations in reduced usable-cue-environments.

In addition, the value of simulation in pilot training is very high both in reducing flight hours required and improving safety. Examples include procedural operations, tactical operations and emergency situations.

Confidence in the results of simulation in these applications can be directly related to the fidelity or validity of the simulation, encompassing the full range of cues to which the pilot is exposed. At a fundamental level all cues are generated by the mathematical model at the heart of a simulation and, while it is not sufficient, it is certainly necessary that a model must be a valid representation of the 'real world' to be fit for useful work. In a general sense, validation, as an activity, refers to establishing the range and accuracy of a theoretical model for predicting the behaviour of a dynamic system in response to operator (e.g. pilot) commands and external disturbances (e.g. gusts). The activity can better, and more appropriately, be described as calibration, highlighting the need for a scientific approach to the design of supporting experiments, in addition to the specialist efforts required for interpretation and analysis. The modelling range can be conveniently defined in terms of frequency and amplitude which, structurally, reflects the modal content and degree of nonlinearity. Many of the rotorcraft modelling assumptions, (e.g. for inflow distribution, blade dynamics, interference effects etc) will have a limited range of fairly precise, and a broader range of marginal, validity. In combination, the complete validity is difficult to quantify and, as in so many things, depends upon the application. But validation is also much more than calibration as an activity; making better or improving are implicit in the process of validation, and any method that defines the limits of application of a model should also be able to identify the modelling features needing further development or the areas where assumptions are breaking down.

The role of system identification in the validation activity is illustrated in Figure 8.1.1. Parameters in an identified model structure, derived from test data are compared with the same physical parameters in a theoretical model. The quality of the comparison will determine the verification effort required using different data sets and whether a model upgrade or further experiments need to be conducted. The product of this incremental and iterative exercise is a simulation model, fit for use over the range of conditions covered by the experiments; in practice, of course, use is likely to be extended beyond this range, towards conditions uncharted in the real-flight environment, often for safety reasons. The importance of validation for this special application is paramount.

8.1.2 Validation Criteria - Model Accuracy and Range

8.1.2.1 General

Scope

When discussing model range and accuracy it is important to define exactly what the model is intended to predict. In flight dynamics the three important issues are trim, stability and response. In mathematical terms, these three problem areas can be expressed as different solution forms of the general nonlinear evolutionary equations of motion (ignoring hereditary effects),

¹⁷⁾ Principal Author: G. D. Padfield, RAE

$$\frac{dx}{dt} = f(x, u, t) \quad (8.1.1)$$

where

- $x(t)$ is the state vector comprising, in general, both fuselage and rotor states;
- $f(x, u, t)$ is a general forcing function comprising contributions from inertial, gravitational and aerodynamic sources and an explicit dependence on time to allow for prescribed disturbances and nonstationary effects;
- $u(t)$ is the control vector.

The trim solution is given by

$$f(x_e, u_e) = 0 \quad (8.1.2)$$

where the subscript e refers to the equilibrium or trim values.

The stability solution is given by

$$\det \left[\lambda I - \left(\frac{\partial f}{\partial x} \right)_{x_e} \right] = 0 \quad (8.1.3)$$

where the values of λ correspond to the exponents of the small perturbation exponential transients $\exp(\lambda t)$, i.e. the eigenvalues of $(\partial f / \partial x)_{x_e}$.

The response solution is given by,

$$x(t) = \int_0^t f(x, u, t) dt \quad (8.1.4)$$

Model accuracy is therefore related to the controls u_e required to hold a state x_e , the location of the system eigenvalues λ_i and associated vectors and the time response $x(t)$ to control inputs and disturbances expressed in the time or frequency domain.

All three need to be quantified to give a comprehensive measure of model accuracy. Just how accurate the model has to be, relative to the real world, depends upon the application. For example the examination of trends during research and feasibility studies is not nearly as critical as predicting handling and control problems in a flight envelope expansion test programme. On the other hand, if the flying qualities requirements are a primary design driver in a particular area, then predicting the correct behaviour at the earliest possible stage of a project is very desirable.

Accuracy

Having argued that there can be no absolute criteria for the validity of a simulation, we can, however, propose a set of tentative target criteria for the 'all-purpose' simulation.

- Predicted trim states should match flight estimates to within 5% of full trim range for controls, attitudes and power requirements. This criterion is partly justified with the argument that at the flight envelope limits, a 10% margin in control should be available for recovery in emergencies.
- Predicted stability should match flight estimates to within 5% of the modulus of the corresponding eigenvalue (or largest system eigenvalue?).
- Predicted response, in the extended format of Mil Spec 8501 (revised, Hoh et al., 1988, [8.1.8]), or the Aeronautical Design Standard version (ADS-33C, 1989, [8.1.1]), derived from time and frequency responses to controls and disturbances, should match flight estimates to within 5% of full response range. This criterion does not include the standard time history comparison test, on the grounds that long term departures of flight and simulation responses, following initial, short-duration, control or disturbance inputs, do not generally imply poor validation; the smallest difference in initial conditions or modelling errors will always integrate to large values given enough time, and accurate piecewise comparisons of time histories after 20 or 30 seconds, for example, is an unreasonable validation test. The moving window criterion (Clark, 1989, [8.1.5]) defining the extent of acceptable time response matching, has however been used as a validation criterion for short-duration responses. The 5% bracket again seems reasonable, but its use should be limited to only the first few seconds of the response to a discrete input.

For particular applications the criteria may not need to be as stringent as above. Tischler, for example, presents criteria for the engineering validation of a nonlinear simulation model to be used for piloted investigations of helicopter accidents. For short term responses: *the peak value and 50% rise-time of the simulation and flight values shall match to within 20% of the flight values.* For long term responses, *the stability trends shall be consistent with the flight data.* For off-axes response, *the trend of the response shall have the correct signs following the on-axes input during the time period up to 100% rise-time.* To be truly valid in itself, a set of simulation validation criteria must be substantiated by pilot subjective opinion, supported by analysis quantifying the level of similarity between pilot control strategy in flight and simulation.

This is still a very immature topic, requiring fundamental research to establish rules and how they relate to the different application areas.

Range

Before discussing the application of system identification to these three problems, some definition of the range of validity is required. The natural dimensions of model range are frequency and amplitude and all three flight dynamics problems are relevant.

- Trim states are defined by the envelope of velocity (airspeed V), flight path angle (γ), sideslip angle (β) and turn rate (r_0), achievable or required, within the limits of the control ranges, power, aerodynamic or structural limits. With four controls available, only four vehicle states can be defined independently and the selection given here, although arbitrary, is a natural piloting choice of primary variables. In this case, the secondary trim variables are the body attitudes, (Ψ, Θ, Φ), rates (p, q, r), velocity components (u, v, w), torque, rotor speed and corresponding rotor flap and lag angles.
- The range over which the rotorcraft stability is to be assessed can be defined by a bounded region in the complex plane, that includes all coupled rotor/fuselage modes that impact on the flight dynamics problem under investigation. In addition to the usual linear behaviour about trim states, the stability analysis should also encompass any limit cycle behaviour through equivalent linearisation or a describing function approach where possible.
- The response problem presents the greatest challenge, with respect to the validation range. ADS-33C presents response criteria in different forms depending on the response amplitude. In general, small amplitude response is governed by the bandwidth criterion, moderate amplitude by the quickness or attack parameter, and large amplitudes by the control power.

Three features of ADS-33C are worth highlighting, however.

1. They represent minimum acceptable criteria, and therefore do not necessarily require a vehicle or simulation to be exercised across its full dynamic range.
2. They represent necessary, but not necessarily sufficient, criteria. For example, the format is single input/single output while, in practice, a simulation has to be good for situations where the pilot uses a combination of controls to manoeuvre from one trim state to another.
3. ADS-33C is a format based on a collection of one or two parameter criteria, and the method of extracting the parameters from test data is clearly defined. In particular, with one or two exceptions, the parameters are not derived from an assumed model structure so much as direct pointwise extraction from graphical data, hence system identification would appear to have little to contribute; this aspect is pursued further in the next section, and in more detail in 8.2.

While the new flying qualities format has its shortcomings, these are generally acknowledged and exist because of the inadequate database of test results available from which to construct the criteria. As a definition of response range it is certainly incomplete but is recommended here as a starting point; more work is needed to develop and expand the format to provide a comprehensive set able to exercise fully the vehicle dynamics.

8.1.2.2 Applications

System identification is, in a general sense, a sophisticated form of curve fitting and has application to all three problem areas

- trim,
- stability, and
- dynamic response.

Practically all the published work on rotorcraft system identification has been concerned with linearised models and, with some notable exceptions (Padfield (editor), 1989, [8.1.12]), with conventional six degree-of-freedom model structures. The evolutionary equations for small perturbation about a trim condition take the form,

$$\frac{dx}{dt} - Ax = Bu + g(t) \quad (8.1.5)$$

where

$$x = (u, v, w, p, q, r, \Phi, \Theta)^T,$$

$$u = (\delta_{lon}, \delta_{lat}, \delta_{ped}, \delta_{col})^T,$$

A and **B** are the state and control matrices of stability and control derivatives respectively and $g(t)$ is a general vector forcing function.

While the trim and response problems are inherently nonlinear, some useful results can be derived using the linearised form given by equation (8.1.5).

Trim

For the trim problem, system identification can be applied to the steady-state algebraic form of equation (8.1.5). Let A_a be the matrix of unknown aerodynamic derivatives and A_{ig} be the matrix of inertial and gravitational derivatives, then equation (8.1.5) can be written as

$$(A_a, B) \begin{pmatrix} x \\ u \end{pmatrix} = -A_{ig} x \quad (8.1.6)$$

In principle, a wide enough range (over small amplitudes) of new trim conditions, close to the original, can be established to enable estimates of derivatives or, in most cases, ratios of derivatives to be derived from the test data. Examples from classical stability and control testing include the speed stability derivative M_u , the rolling and yawing moments with sideslip (L_v, N_v) and pitch manoeuvre margin in steady turns.

Stability

The stability problem centres around deriving good estimates of the **A** matrix elements or a set of equivalent parameters. This application area has received by far the most attention and many of the ground rules and pitfalls are well understood. Two aspects can dominate the likelihood of success:

1. Test inputs and aircraft motion excursions should be as small as possible for the linearity assumptions to hold good and yet large enough that the noise content is small relative to the response signal. The requirements conflict and, in practice, both will be compromised.
2. Test inputs need to excite the aircraft modes, the stability of which are under investigation, in a fairly uniform manner. This requires *a-priori* knowledge of the modal distribution and usually some iteration to optimise the input shape. Doublets, multi-steps (e.g. 3211) and frequency sweeps are all in common use.

Test input design is therefore a most critical issue in deriving robust (see section 7) parameter estimates and hence stability information. Frequency domain identification has gained some favour in recent years because of the ease with which different model structures can be explored over different frequency ranges. Data derived from frequency sweep inputs, are particularly suitable to transfer function modelling, whereby the modal character, and hence model structure, is matched by polynomial fitting providing direct estimates of both system open-loop poles (eigenvalues) and closed-loop zeros.

Response

To an extent, the response problem receives partial treatment when identifying the stability characteristics. The model matching and identification is achieved on time or frequency response histories and such comparisons are often put forward as evidence that the model validation has been successful or otherwise. In reality this test or demonstration, while being convincing on one level, is never enough to ensure true validation and in many cases can be very misleading. Derivatives estimated from an identification that produces an excellent response fit can often bear little resemblance to the values of their theoretical counterparts, leaving the engineer perplexed as to what needs more validation, his theory or the system identification method. With good quality test data and careful application of a comprehensive identification analysis however, robust values of derivatives can be

estimated that can be used to glean insight into the force and moment character at small amplitude and hence support the validation of the full nonlinear model.

It has been recommended to use the ADS-33C flying qualities criteria as a format for demonstrating simulation validation. This is particularly appropriate when the simulation is being applied to establishing compliance with the requirements. A complete and substantiated flying qualities criterion should contain a specification for every effect that can impact the pilot's impression of the aircraft's ability to perform a flying task. An equivalence between simulation and flight in this sense, should then imply validation of response characteristics as far as pilot subjective opinion is concerned. No existing criterion fully complies with the CACTUS (Padfield, 1988, [8.1.13]) rules (complete, appropriate, correct, testable, unambiguous, substantiated) however, and as ADS-33C currently stands, compliance will not guarantee validation. The principal role of system identification in supporting this comparison is through equivalent system model matching. The only criterion (ADS-33C, 1989, [8.1.1]) that requires the formal use of system identification is the height response to collective (Paragraph 3.3.10.1), where a least squares fit of a delayed first order model to the response to a step input is made, to establish key handling parameters. Other criteria where parameters can be alternatively derived from identified models include pitch, roll and yaw bandwidth, lateral/directional oscillation characteristics and torque response to collective. The use of equivalent system or reduced order models for deriving such criteria is particularly appealing; considerable insight can be gained, from parameterised models, into the effects of design parameters on an aircraft's ability to meet design criteria.

The validity of a nonlinear simulation model and its theoretical foundations, in terms of its accuracy over a given range of steady state and dynamic conditions, can only be partially judged, as noted above, through comparison with small perturbation linearised approximations. The use of system identification in the validation of full nonlinear model structures has received limited attention in the aerospace community. The work of Klein et al. (1983, [8.1.10]) is a notable exception, where the authors estimate parameters associated with higher order polynomial terms (spline functions) by using different amplitude ranges in the responses. A good *a-priori* knowledge and understanding of the likely behaviour, and hence mathematical formulation, is essential for the success of this approach. Another approach to identifying nonlinear models is to work directly with the nonlinear model structure and the set of fundamental parameters, e.g. aerodynamics, structural, inertial and geometric. The parameters can be 'tuned' to minimise the error between measured and predicted responses. The approach appears attractive but the limited experience to date has exposed identifiability problems. The large number of 'adjustable' parameters precludes their simultaneous estimation and determining which parts of the simulation should be modified is a difficult task which relies mainly on engineering judgement. Therefore, the effectiveness of the parameter estimation approach depends on accurately isolating these problem areas, as parameter estimates will be affected by errors elsewhere in the simulation.

The task of identifying the problem areas in the model is hampered by the fact that the method relies on comparing response data. It is difficult to infer, from typical measured responses, the specific shortcomings in the simulation. Parameters are often embedded in approximations to component forces and moments, while the aircraft response is related to these forces and moments through coupled, nonlinear differential equations. Other disadvantages in this approach are the considerable CPU times required and potential convergence problems. To correct problems associated with matching simulated responses, techniques of inverse simulations have been proposed.

Inverse Simulation

Discussion on simulation model validation would be incomplete without reference to the relatively new developments in the field of inverse modelling, or simulation (Bradley et al., 1988, [8.1.4]; DuVal et al., 1989, [8.1.6]). This is the term given to the method whereby selected state variables are constrained to be equivalent for the test and model results and the simulation model partially inverted to determine the unconstrained motion.

A typical choice would be the aircraft velocity components (u , v , w) and heading (Ψ) or the four variables used in the trim problem (V , γ , β , r_0). Differences between the simulation and real-world will then be manifested in the behaviour of the free or unconstrained variables and controls. From this comparison a set of residual forces and moments can be computed that represent unmodelled effects. If the initial simulation gives a reasonable fit to the test result then the errors should remain small and a derivative-type linearised formulation can be used to model the residuals. In system identification terms the problem can conveniently be expressed as a combination of both equation and output-error solutions. The distinct advantage in this approach is that key state variables can be constrained, ensuring that the simulation and test stay reasonably close even in the long term. This contrasts with forward or direct simulation where even the smallest force and moment errors will integrate to large velocity and displacement errors in the long term, making comparisons of nonlinear

motions not very useful. In the method described in (DuVal et al., 1989, [8.1.6]), the fuselage degrees of freedom are disabled and the simulation driven with the measured fuselage states and controls; as noted above, this means that the simulation model is constrained to fly along the exact flight test trajectory. The aerodynamics of the simulation are then adjusted so that the predicted component loads match the measured component loads along this trajectory. If measurements of individual component loads (e.g. main, tail rotor) are available then the engineer can use system identification to refine each component model separately. Usually, however, only the overall forces and moments can be estimated from measurements of accelerations and the problems of differentiating between different component contributions remains.

8.1.3 Model Development and Upgrading

A fundamental issue woven into the validation activity concerns the identification and repair of model deficiencies. As noted in the Introduction (8.1.1), it is the collection of underlying assumptions that are being validated but, in most cases, validation will prove to be an incremental activity with the 5% accuracy margin, over the full range of application, being achieved only after considerable development and upgrading. System identification, to be truly useful as an engineering tool, must play a part in this development and be able to shed light on the physical source of a mismatch and guide the theoretical repair work. This is not an unreasonable requirement and, furthermore, it is suggested that successful interpretations of results will only be found in applications conducted by, or with direct support from, experts in flight mechanics. These points are emphasised to highlight the complex nature of the validation activity, often frustrated by the lack of a complete set of carefully measured test data, and one that requires a serious commitment of resources throughout a project life-cycle. The rules for the application of the flight mechanics knowledge on the one hand and the system identification techniques on the other are not well defined. What is clear, at least to some serious practitioners of system identification, is that the methodology provides a rational and systematic medium for comparison, interpretation and documentation in the validation activity.

In principal, there are two fundamental ways in which a simulation model can be 'wrong' or deficient:

1. Incorrect parameter set
This would include those parameters directly related to, and measurable as, physical attributes, e.g. inertias, geometry, and those derived from approximation theory as effective parameters, e.g. effective hinge offset/spring strength, aerodynamic force coefficients.
2. Incorrect model structure
This would include both model degrees of freedom and nonlinear formulations.

The two ways are connected; an effective parameter is often an approximation to a more complex effect, e.g. quasi-steady form of another degree of freedom or local linearisation of a nonlinear function. There will always be a limit to the range over which the approximation is valid and, ultimately, a breakdown in the value of an effective parameter is indicative of a model structure deficiency. It is important to understand which of the above is the culprit in a particular situation. In general, deficiencies in the second category are more difficult and time consuming to cure, although once achieved, the upgraded model will offer more opportunity to expand the application range. Unless evidence is strongly to the contrary, however, deficiencies in the first category should be exhausted before recourse to structural upgrades.

A number of general and specific points can be raised on this issue before considering some examples that will serve to highlight the role of system identification in model validation.

1. The experimental test database, from both model and full scale, needs be carefully assembled to support the validation activity. In the limit it is desirable to measure every variable that plays a part in the simulation, (e.g. individual component force and moment contributions), but in reality this is rarely achieved. It must be recognised that a limited measurement database will limit the upgrading potential.
2. An underlying principle, that brings a systematic methodology to the validation activity, is that every modelling approximation or assumption employed needs to be checked, across the range of application, through correlation with test data.
3. Derivatives estimated by a system identification method are effective parameters; for very small amplitude they are equivalent to the first order terms in a Taylor expansion of the applied forces and moments about the trim condition. Aircraft motion excursions in typical test data are generally of more moderate amplitude, however, and any nonlinearities will be embodied in the resultant derivative. It is important therefore, when comparing derivatives from flight and theory, to check for variations with motion amplitude from both sources.

4. Derivatives, predicted from a theoretical model, are themselves functions of a large number of, more fundamental, configuration and model parameters, e.g. rotor radius, lift curve slope, moments of inertia etc.. Figure 8.1.2 illustrates how, for the RAE simulation model *Helistab*, two of the pitching moment derivatives vary with three model parameters - the effective rotor flap stiffness, rotor flap inertia and centre of gravity location. There can be many more fundamental parameters than derivatives, depending on the model complexity. Model deficiencies in the first category above, i.e. incorrect parameters, can sometimes be identified through an exploration of the required fundamental parameter distortions required to match derivatives. This parameter distortion or 'fudge (kluge) factor' technique is often used in simulation validation to accommodate pilot subjective opinion. The technique is prone to considerable misuse, with a genuine source of modelling error being compensated for by distortions in an unrelated parameter. Careful applications can bear fruit, however, particularly with respect to corrections in effective parameters. Optimising the distortions to match derivatives is inherently nonlinear and multi-objective; system identification is the natural tool for such problems.
5. An understanding of the correct model structure for describing the flight behaviour of an aircraft is the key to sound validation. Two of the studies conducted under the auspices of AGARD WG-18 (sections 7 and 8.3) have recommended the use of non-parametric transfer function fitting at the initial stages to gain this understanding; this recommendation is endorsed.

With the attendant development and upgrading activities, simulation model validation based on comparison with test, is an activity that all airframe manufacturer and research laboratories have experience of. The work of Houston (1989, [8.1.9]) and Ballin and Dalang-Secrétan (1990, [8.1.2]) offer typical results from contemporary studies in UK and US Government research laboratories.

Houston's work focusses on vertical axis dynamics of an SA-330 at hover, illustrating how coning and air mass dynamics are required model elements in the prediction of body motion up to about 20 rad/s. Error in this model structure are computed as distortions in the model parameters providing some insight into the validity of assumptions associated with local momentum theory and the use of rigid blades. Measurements of blade flapping motion were essential in providing confidence in these transfer function results.

In contrast, Ballin sets out to upgrade the US Army's *GENHEL* UH-60 simulation model based on open-loop frequency and time domain flight test results. Ballin's work is an excellent example of investigative upgrading based on non-parametric frequency response models. The full flight envelope *GENHEL* incorporates a blade-element rotor with flap, lag and air mass dynamics and runs in real-time with a 6.67 ms frame on an AID-100 computer. The comparative technique proved effective in evaluating various modelling improvements, e.g. new dynamic inflow model, lag damper characteristics, and establishing a model which is 'fully adequate for real-time handling qualities', up to 10 rad/s.

8.1.4 Example

The following example provides some insight into how the results of system identification can be used systematically in the validation process.

8.1.4.1 General

The framework for simulation model validation and the application areas of system identification have been set out in the previous two sections. Establishing criteria for model range and accuracy and highlighting the required model development were the two specific areas addressed. The WG-18 test databases are insufficient to cover the full range of issues included in the trim, stability and response problems. All three aircraft databases are, however, typical of those used to support simulation model validation and a number of useful examples can be derived from them, one of which will be detailed here.

The primary simulation model used in this case study is the RAE *Helistab* model (Padfield, 1981, [8.1.14]; (Padfield, 1989, [8.1.15])). This model is intrinsically nonlinear and can be trimmed in a general condition of sideslipping, turning, descending flight. Coning and first harmonic flap and rotor speed/engine governor degrees of freedom complement the fuselage states. Current developments include three degree-of-freedom rotor lag and inflow dynamics. Rotor aerodynamics are derived from linear blade element/momentum theory and the rigid blade/centre hinge-spring analogue is used to model both hingeless and small-offset articulated rotors. Fuselage and tail surface aerodynamics are nonlinear functions of incidence, sideslip and rotor downwash. The quasi-steady, six degree-of-freedom version is used for the comparisons discussed here. Figure 8.1.3 and Figure 8.1.4 show the three translational and three rotational velocities for the four SA-330 test runs. Fundamental questions that can be asked of the system identification approach are:

1. Can a comparison of flight-estimated and theoretically-predicted aerodynamic derivatives shed light on the model strengths and weaknesses?
2. Can the stability characteristics of aircraft dynamic modes be correctly estimated?

These two questions and their answers are closely related. Often, approximations for mode frequency and damping can be derived from simplifying assumptions and expressed in terms of a limited number of parameters. Comparisons of the equivalent modal parameters from flight and theory and their constituent parts can be effective at highlighting areas of overall simulation model deficiency. In section 8.1.4.2 below, this approach will be explored for the Dutch roll motion. Before this, a number of relevant observations can be made from an examination of the comparisons in Figure 8.1.3 and Figure 8.1.4.

1. Pedal Response (Figure 8.1.3)

- a. speed changes are greater in flight (~ 5 m/s).
- b. initial yaw, roll and sideslip response are distinctly greater in the simulation.
- c. the Dutch roll mode appears more damped and of lower frequency in the simulation.
- d. the pitch and heave responses appear considerably smaller in the simulation.

2. Lateral Cyclic Response (Figure 8.1.3)

- a. roll response appears sharper in the simulation.
- b. the Dutch roll response in roll and yaw is greater in flight.
- c. the pitch and heave responses are smaller in the simulation.
- d. speed changes are small during the manoeuvre (~ 2.5 m/s).

3. Collective (Figure 8.1.4)

Relatively unsteady initial conditions on this run obscure the comparisons to an extent, but these are by far the poorest of the four axes.

- a. initial pitch and roll response are similar in character but the free response of the flight results contains considerably more Dutch roll content.
- b. the yaw and sideslip responses in flight are considerably greater than the simulation initially, following the collective input, and during the free response.
- c. airspeed changes are moderately large ($\sim 5 \dots 10$ m/s), but poorly predicted by simulation.

4. Longitudinal Cyclic (Figure 8.1.4)

- a. pitch and heave responses appear sharper and less damped in the simulation.
- b. the Dutch roll response in roll and yaw is substantially greater in the simulation.
- c. speed changes are fairly well predicted (~ 10 m/s).

Some of these observations will be reviewed in the light of the system identification analysis in section 8.1.4.2.

The complete set of *Helistab* stability and control derivatives and corresponding eigenvalues are contained in Table 8.1.1 for the 80 kn flight condition. Data is also included on aircraft configuration and the magnitude of the perturbations used to generate the derivatives numerically.

8.1.4.2 Lateral-Directional Motion

The dominant motion throughout the responses shown in Figure 8.1.3 is the weakly damped Dutch roll mode. The lateral-directional dynamics of the SA-330 at the 80 kn flight condition appear to be classical with a roll subsidence and spiral motion completing the modal set. It is of interest to explore whether the mismatch in the Dutch roll response between flight and simulation illustrated can be explained through the estimated derivatives. Table 8.1.2 compares the primary lateral/directional derivatives from flight and simulation, the former taken from the DLR and University of Glasgow analyses. Numbers in parentheses are standard deviations of the parameter estimates; as a rough rule of thumb, values below 10% to 15% of the parameter itself are considered to imply a high confidence level. The Dutch roll eigenvalues are also included in the Table and show that the fourth-order lateral sub-system provides a reasonably good approximation in all three cases. This is a significant result in itself, indicating that although the pitch and heave motions are appreciable, they do not have a first order effect on frequency and damping at this flight condition. Lower order approximations to the Dutch roll mode can be derived for a range of different cases, the simplest being when the motion is pure yaw. This is clearly inappropriate in the present case with the roll/yaw ratio approximately unity (see Figure 8.1.3). A more general and useful approximation can be derived by isolating the spiral dynamics with the sideways-velocity degree of freedom.

$$v_0 = v + V\Psi$$

(8.1.7)

The lateral equations can then be written in the alternate form (Padfield et al., 1982, [8.1.7]),

$$\frac{d}{dt} \begin{bmatrix} \dot{v}_0 \\ v \\ \dot{\psi} \\ \rho \end{bmatrix} - \begin{bmatrix} 0 & 0 & Y_v & g \\ 0 & 0 & 1 & 0 \\ -N_r & -VN_v & N_r + Y_v & g - VN_p \\ L_r/V & L_v & -L_r/V & L_p \end{bmatrix} \begin{bmatrix} \dot{v}_0 \\ v \\ \dot{\psi} \\ \rho \end{bmatrix} = 0 \quad (8.1.8)$$

The partitioning shown divides the dynamics into the three modes of increasing modulus:

- spiral,
- Dutch roll, and
- roll subsidence.

If the conditions for 'weak coupling' between the partitioned degrees of freedom are met (Milne, 1965, [8.1.11]), then the approximation for the Dutch roll eigenvalue can be written,

$$\lambda^2 + 2\zeta\omega_n\lambda + \omega_n^2 = 0 \quad (8.1.9)$$

where

$$2\zeta\omega_n = - \frac{N_r + Y_v + \sigma \left(\frac{L_r}{V} - \frac{L_v}{L_p} \right)}{1 + \sigma \frac{L_r}{VL_p}} \quad (8.1.10)$$

$$\omega_n^2 = \frac{VN_v + \sigma L_v}{1 + \sigma \frac{L_r}{VL_p}} \quad (8.1.11)$$

$$\sigma = \frac{g - VN_p}{L_p} \quad (8.1.12)$$

This approximation shows how the Dutch roll damping is affected by the derivatives L_v , N_p and L_r in addition to the yaw damping N_r . Likewise, the frequency is modified by L_v in addition to the primary stiffness N_v . The approximate eigenvalues for all three cases are shown in Table 8.1.2 ($\lambda^{(3)}$) along with the coefficient of (8.1.9). In general there is excellent agreement with the Dutch roll eigenvalues for each case. The *Helistab* damping prediction is double the flight estimate, confirming the observation made in section 8.1.4.1, and the frequency is 20% lower in the simulation. Comparing the make-up of the Dutch roll characteristics from equation (8.1.9) the following points can be made:

1. *Helistab* over-estimates the basic yaw damping (estimated from flight) by 66%.
2. *Helistab* underestimates the principal roll derivatives by 20%.
3. Flight estimate of N_p is more than double the *Helistab* value.
4. Flight estimate of N_v is 20% higher than *Helistab*.
5. L_r from flight is negative, from theory positive; the flight values are estimated with low confidence.
6. Yaw control derivative $N_{\delta_{ped}}$ from flight is nearly half the *Helistab* value.

On the basis of these observations, assuming that the flight derivatives estimated are 'correct', a set of corresponding, tentative, hypotheses can be made concerning the simulation model validation.

1. The yaw damping and control sensitivity are dominated by the tail rotor; the simple tail rotor model (with fin blockage) adopted in *Helistab* needs refinement.
2. The uniform increase in primary roll derivatives (L_v , L_p , $L_{\delta_{lat}}$) suggests an incorrect roll moment of inertia I_y or rotor Lock number, the latter possibly reflecting the effects of unmodelled dynamic inflow.
3. The derivative N_p has a strong destabilising effect on the Dutch roll mode accounting for about 65% of the damping decrement (additional term). The larger flight value could be explained by an incorrect pro-

duct of inertia I_{zx} in the simulation. More subtle aerodynamic effects are difficult to accommodate within the simple rotor model structure in *Helistab*.

4. The directional stability is clearly underpredicted by *Helistab*. This is unlikely to be a tail rotor effect in view of (1) above; in fact, the evidence suggests that N_y due to the tail rotor should actually be less than predicted. The fuselage and empennage contributions to N_y in *Helistab* are derived from wind tunnel data and an obvious conclusion is that these do not relate directly to the flight situation.
5. The positive L_r from *Helistab* comes entirely from the tail rotor, is stabilising, but is not significant in the Dutch roll damping. The negative and higher DLR value is not insignificant, but is perplexing as no well understood mechanism gives rise to such an effect. The relatively high value of the standard deviation for this derivative suggests a low confidence factor.
6. In addition to the above effects, the absence of a rotor wake/tail rotor/empennage model in the simulation must have a significant impact on the results, particularly the yawing derivatives.

Such hypotheses form the starting point for a second phase of the validation exercise; some appear plausible and consistent but others are more dubious. All will need checking against other conditions, e.g. damping/control sensitivity from step inputs, dihedral and weathercock stability from sideslip tests, before the simulation is modified. In any case, more detailed component measurements (e.g. main/tail rotor thrust/moment) may be required before a simulation deficiency is fully understood and rectified. It should be remembered that derivatives encapsulate any nonlinear effects when derived from experimental data and tests at varying amplitudes will be required to establish the presence and importance of such effects. Nevertheless, as a starting point, the flight estimates have enabled considerably more systematic validation evidence to be gathered, compared with any speculation derived from the observations in section 8.1.4.1. There remains the question, of course, as to the validity of the flight estimated derivatives. The time history comparisons of the DLR lateral sub-system and flight data are presented in Figure 8.1.5; the fit is not as good as the fully coupled response shown in Figure 8.1.6. The coupling effects clearly contribute to the response, even though the damping and frequency are not affected significantly; the simplified approximation cannot shed any new light on the nature of the lateral to longitudinal coupling in the Dutch roll.

The Glasgow derivatives, shown in Table 8.1.2, show reasonable consistency with the DLR results with two notable exceptions - L_r and $L_{\phi lat}$. The large positive value of L_r accounts for the greater stability of the Dutch roll mode according to the Glasgow estimates ($t_{1/2} \sim 4$ s compared with 8 s for DLR). The lower roll control sensitivity and damping from the Glasgow analysis correlates with lower estimate for effective time delay shown in Table 8.1.2 (Black, 1987, [8.1.3]), highlighting the fact that these are strictly equivalent parameters; the effects of higher order dynamics have been ignored as such but encompassed within the effective time delay. The 'true' value of some stability and control derivatives cannot therefore be estimated with any certainty. The Dutch roll approximations do show, however, that useful insight into modelling accuracy can be gained from such combined parameters.

Table 8.1.3 shows a comparison of Dutch roll eigenvalues for the BO 105 (DLR Model 3) and AH-64 derived from the DLR flight estimated derivatives with the corresponding approximations derived from equation (8.1.9) on page 255. The comparisons are very good, apart from the BO 105 frequency estimate, adding support to the value of the approximation across different aircraft types. As a concluding note to this section, Figure 8.1.7 illustrates the current Dutch roll handling qualities criterion of ADS-33C. The criterion is expressed in terms of handling qualities level boundaries for damping and frequency for different Mission Task Elements (MTE). The data points correspond to flight estimates and theoretical predictions for all three aircraft; the SA-330 theoretical part is derived from the *Helistab* case discussed, the BO 105 point from the DLR blade-element model, and the AH-64 result from the MDHC Flyrt nonlinear rotor-map model. It is interesting to note that for all three aircraft, theory predicts about twice the damping measured in flight. Moreover, on the criterion diagram the data points lie on either side of the Level 1/2, Level 2/3 boundaries, depending on the aircraft role (i.e. MTE). Considering the aircraft types under consideration, the Level 2/3 boundary is probably appropriate for both. A conclusion that can be drawn is that none of the simulation models (which are state-of-the-art for disc, blade element and rotor-map models respectively) is capable of predicting Dutch roll damping adequately for compliance demonstration. This is considered to be a reflection on simulation modelling in general and the detailed analysis of the SA-330 data has provided insight into how, for this aircraft, *Helistab* is deficient.

8.1.5 Conclusions and Recommendations

A number of conclusions and recommendations can be drawn from the discussions presented:

1. Validation as an activity can be considered in two stages:

- firstly, establishing the range and accuracy of the simulation model and,
- secondly, establishing the modelling deficiencies and required upgrades.

This section has proposed a framework for the application of system identification in these two stages.

2. Accuracy and range can be defined in terms of three flight mechanics problem areas:

- trim,
- stability and
- response.

System identification can play a role in all three problem areas.

Range can conveniently be defined in term of the frequency and amplitude scope of intended operation. Accuracy requirements depend on the application, but a 5% bracket is proposed as an all-purpose criterion; some applications may require even better comparison, some less.

3. The use of system identification in model upgrading has to be complemented with a good understanding of the underlying physical assumptions and mathematical approximations.
4. Full account needs to be taken of the existing Industrial practices, skills, and expertise when making recommendations for the use of system identification in model validation.
5. The example chosen to highlight the value of system identification in simulation validation has been the Dutch roll motion of the SA-330. A simple approximation for Dutch roll damping and frequency has highlighted the likely origins of modelling deficiencies. Current simulation models are poor at predicting cross coupling effects. Of perhaps greater significance is the overestimation of Dutch roll damping by current simulation models leading to a more favourable compliance with ADS-33C, i.e. Level 2 rather than Level 3 handling qualities.

References

- [8.1.1] AVSCOM
Aeronautical Design Standard - ADS-33C; Handling Qualities Requirements for Military Rotorcraft
US AVSCOM, St. Louis, MO, 1989
- [8.1.2] Ballin, M. B.; Dalang-Secretan, M.-A.
Validation of the Dynamic Response of a Blade element UH-60 Simulation Model in Hovering Flight
Proceedings of the 46th Annual Forum of the American Helicopter Society, Washington DC, 1990
- [8.1.3] Black, C. G.
Consideration of Trends in Stability and Control Derivatives from Helicopter System Identification
Proceedings of the 13th European Rotorcraft Forum (Paper 7.8), Arles, France, 1987
- [8.1.4] Bradley, R.; Thomson, D. G.
Validation of Helicopter Mathematical Models by Comparison of Data from Nap-of-the-Earth Flight Tests and Inverse Simulation
14th European Rotorcraft Forum, Milano, Italy, 1988
- [8.1.5] Clark, M. J.
Demonstrating the Validity of Gas Turbine Engine Models for Use in Real-Time Applications
Proceedings of 2nd Institute of Measurement and Control 'Model Validation' Conference, London, 1989
- [8.1.6] DuVal, R. W. et al.
Flight Simulation Model Validation Procedure, a Systematic Approach
Vertica, Vol. 13, No. 3, 1989
- [8.1.7] Padfield, G. D.; DuVal, R. W.
Applications of System Identification Methods to the Prediction of Helicopter Stability Control and Handling Characteristics
In 'Helicopter Handling Qualities', NASA CP-2219, 1982
- [8.1.8] Hoh, R. H.; Key, D. L.
Proposed Specification for Handling Qualities of Military Rotorcraft, Volume 1 - Requirements
USA AVSCOM Technical Report 87-A-4, 1988

- [8.1.9] Houston, S. S.
Identification of a Coupled Body/coning/inflow Model of Puma Vertical Response in the Hover
Vertica, Vol. 13, No. 3, 1989
- [8.1.10] Klein, V.; Patterson, J. G.
Determination of Aeroplane Model Structure from Flight Data Using Splines and Stepwise Regression
NASA TP-2126, 1983
- [8.1.11] Milne, R. D.
The Analysis of Weakly Coupled Dynamical Systems
International Journal of Control, Vol. 2, No. 2, 1965
- [8.1.12] Padfield, G. D. (Editor)
Applications of System Identification in Rotorcraft Flight Dynamics
Vertica 'Special Edition', Vol. 13, No. 3, 1989
- [8.1.13] Padfield, G. D.
Helicopter Handling Qualities and Control: Is the Helicopter Community Prepared for Change?
Conference Overview Paper, R.Ae.Soc. International Conference 'Helicopter Handling Qualities and Control',
London, 1988
- [8.1.14] Padfield, G. D.
A Theoretical Model of Helicopter Flight Mechanics for Application to Piloted Simulation
RAE Technical Report 81048, 1981
- [8.1.15] Padfield, G. D.
Theoretical Modelling for Helicopter Flight Dynamics: Development and Validation
Proceedings of ICAS 88, Jerusalem, 1988, (RAE Technical Memorandum FM 25, 1989)

<u>Stability derivatives</u>						
	u	w	q	v	p	r
X	-0.02413	0.00218	0.7411	0.0073	0.3303	0.00
Z	-0.0482	-0.7302	41.0772	0.0255	0.5669	0.00
M	0.00736	-0.0199	-0.7661	-0.00493	-0.2211	0.00
Y	-0.00438	-0.0203	0.3207	-0.1248	-0.7510	-40.897
L	-0.00582	-0.0525	0.7583	-0.0549	-1.6771	0.142
N	0.0098	0.0326	-0.1643	0.0216	-0.1741	-0.5697

<u>Control derivatives</u>				
	θ_o	θ_{ls}	θ_{lc}	θ_{tr}
X	-2.0546	-9.546	0.4862	0.00
Z	-96.795	-27.7184	0.00	0.00
M	1.5626	6.4123	-0.3238	0.00
Y	-2.4806	-0.2069	9.6746	4.1414
L	-6.4913	-0.6815	22.8395	2.059
N	-5.9196	1.4955	2.5202	-8.220

<u>Mode</u>	<u>Eigenvalue</u>	<u>Perturbation magnitude for derivative computation</u>
roll substance	-1.6833	u, v, w - 1.5 m/s
pitch short period	-0.871 \pm 0.9332i	p, q, r - 0.05 rad/s
Dutch roll	-0.163 \pm 1.0171i	
phugoid	-0.0104 \pm 0.2214i	$\theta, \phi, - 0.05$ rad
spiral	-0.11985	$\theta_o, \theta_{ls}, \theta_{lc}, \theta_{tr} - 0.005$ rad

<u>Puma flight and configuration data</u>	
V = 80 kn , $\rho = 1.0978$ kg/m ³ , M = 5805 kg , $I_{xx} = 9638$ kg m ² ,	
$I_{yy} = 33240$ kg m ² , $I_{zz} = 25889$ kg m ² , $I_{xz} = 2222$ kg m ² ,	
$X_{cg} = 37.5$ mm fwd	

Table 8.1.1. Helistab Data

	DLR	Glasgow	Helistab
Y_v	-0.135 (0.0019)	-0.135 (0.02630)	-0.125
L_v	-0.066 (0.0012)	-0.0642 (0.00149)	-0.055
N_v	0.027 (0.0002)	0.029 (0.00069)	0.0216
L_p	-2.527 (0.0534)	-2.012 (0.0695)	-1.677
N_p	-0.395 (0.0092)	-0.3216 (0.0106)	-0.174
L_r	-0.259 (0.0343)	0.554 (0.0787)	0.142
N_r	-0.362 (0.0065)	-0.3887 (0.0348)	-0.57
$L_{\delta lat}$	-0.051 (0.0012)	-0.0317 (0.0017)	-0.043
$N_{\delta lat}$	-0.008 (0.0002)	-0.00738 (0.00047)	-0.0047
$L_{\delta ped}$	0.011 (0.0007)	0.0209 (0.004)	0.0109
$N_{\delta ped}$	-0.022 (0.0001)	-0.0254 (0.00086)	-0.0436
$r_{\delta lat}$	0.125	0.01 (0.0150)	0.00
$r_{\delta ped}$	0.00	0.00	0.00
$\lambda^{(1)}$	-0.104 \pm 1.37i	-0.2 \pm 1.35i	-0.163 \pm 1.017i
$\lambda^{(2)}$	-0.089 \pm 1.27i	-0.154 \pm 1.329i	-0.166 \pm 1.08i
$2\zeta\omega_o$	0.1674	0.291	0.390
ω_o^2	1.842	1.79i	1.417
$\lambda^{(3)}$	-0.081 \pm 1.34i	-0.157 \pm 1.39i	-0.199 \pm 1.199i
	$\lambda^{(1)}$ - Dutch roll (fully coupled model)		
	$\lambda^{(2)}$ - Dutch roll (lateral subset)		
	$\lambda^{(3)}$ - Dutch roll (2nd order roll/yaw approximation)		

Table 8.1.2. Comparison of SA-330 lateral/directional characteristics

	SA-330	BO-105	APACHE
Full eqns	-0.104 \pm 1.37i	-0.35 \pm 2.5i	-0.17 \pm 1.726i
Approx	-0.081 \pm 1.34i	-0.33 \pm 3.21i	-0.171 \pm 1.843i
Theory	-0.163 \pm 1.017i [*]	-0.65 \pm 2.61i ⁺	-0.407 \pm 1.857i

Table 8.1.3. Dutch roll mode eigenvalues - Comparison of flight estimates (DLR) with theory

(* = RAF Helistab, + = DLR theory, # = MDHC flyt)

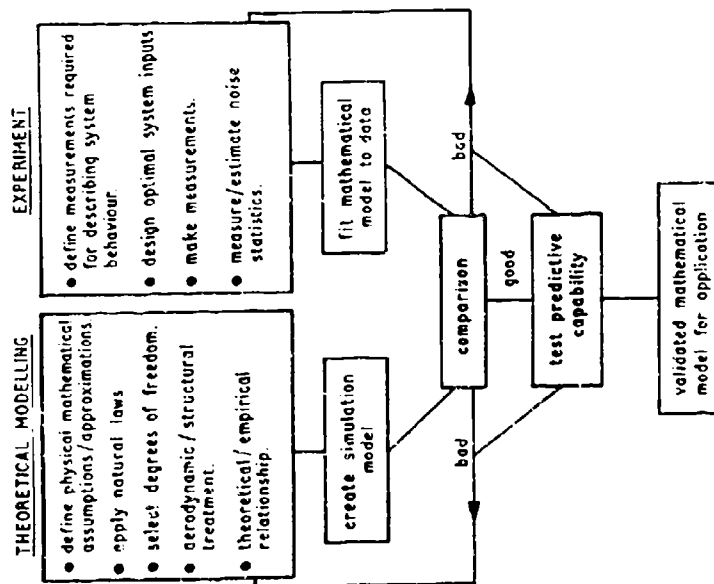


Figure 8.1.1. System identification

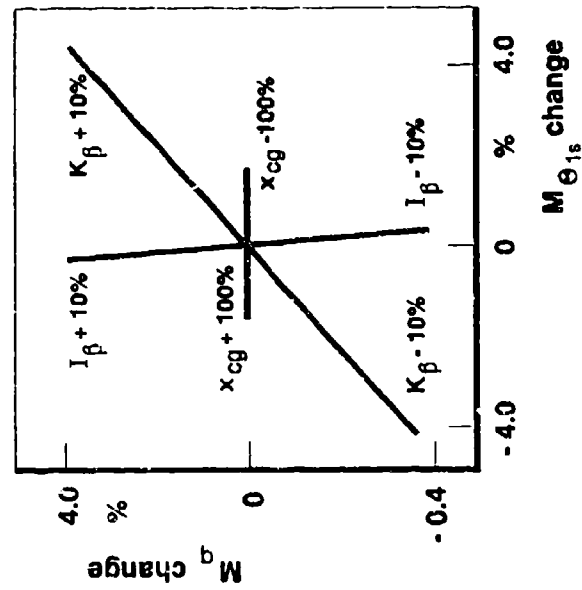


Figure 8.1.2. Derivative changes with design parameters (Helistab SA-330 - 80 kn)

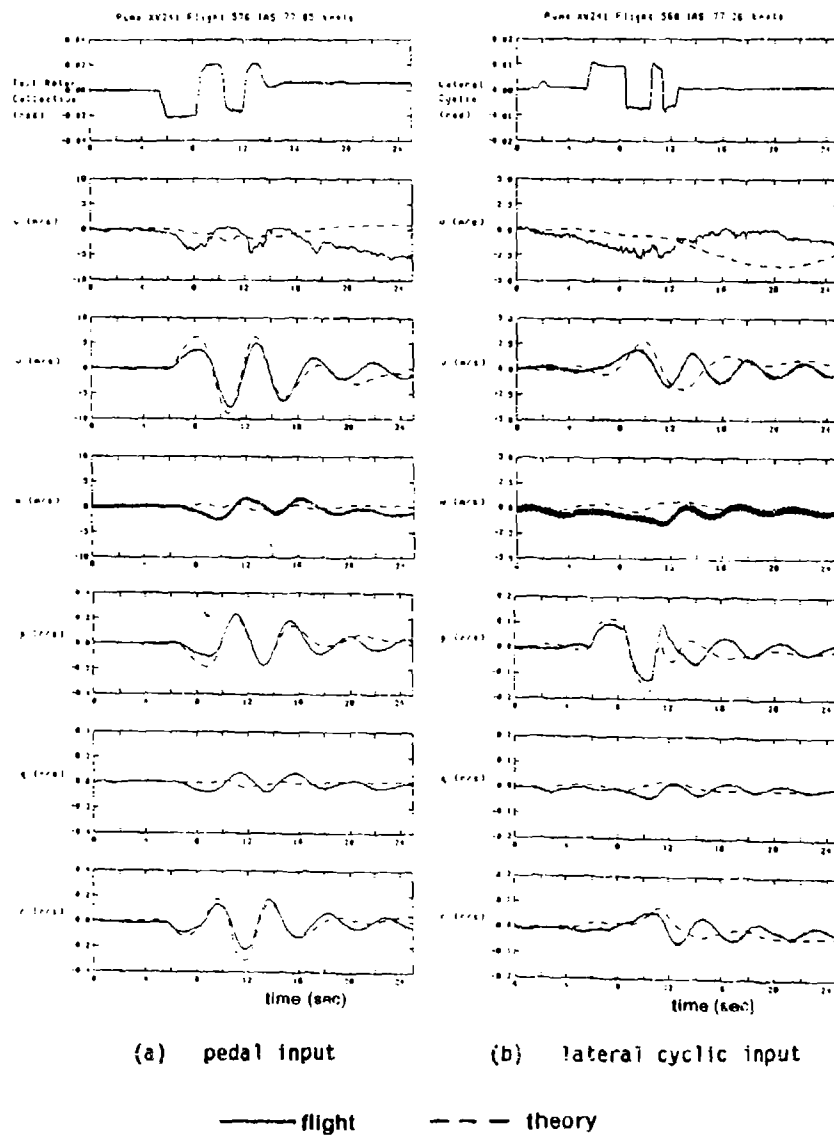


Figure 8.1.3. Comparison of flight and Helistab control response (pedal and lateral cyclic input)

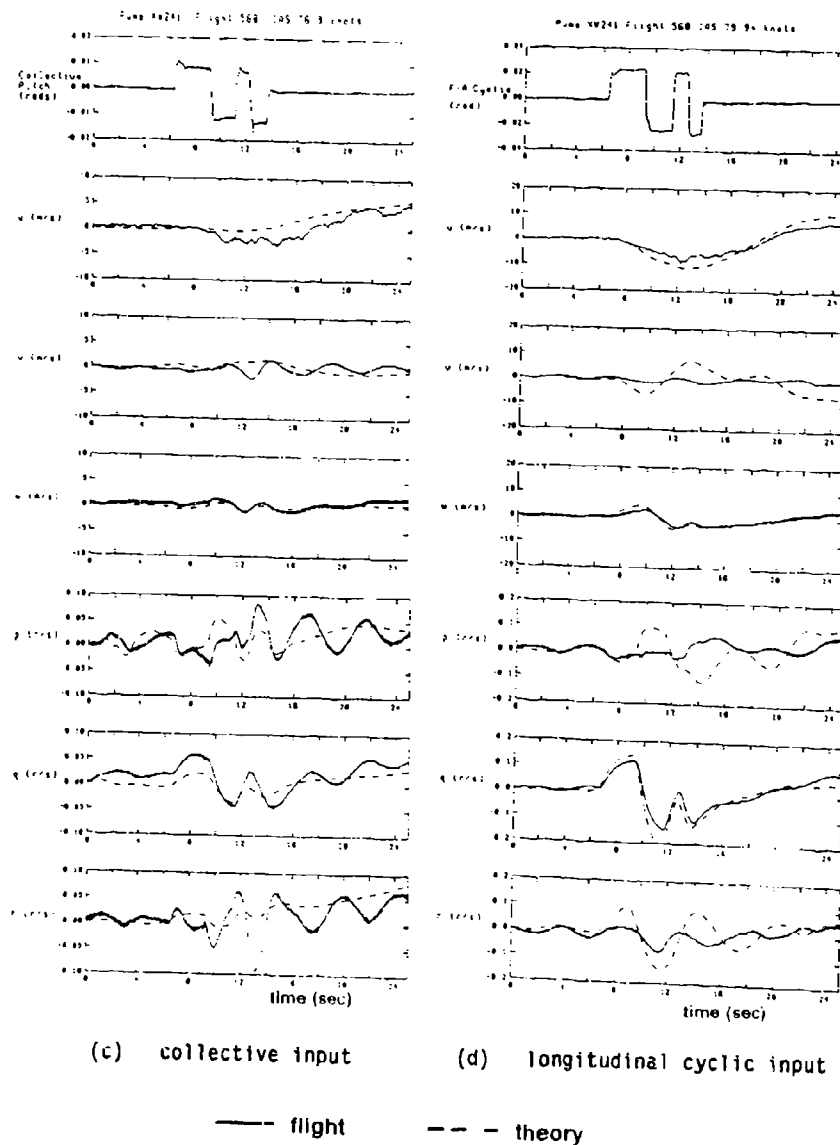


Figure 8.1.4. Comparison of flight and Helistab control response (collective and longitudinal cyclic input)

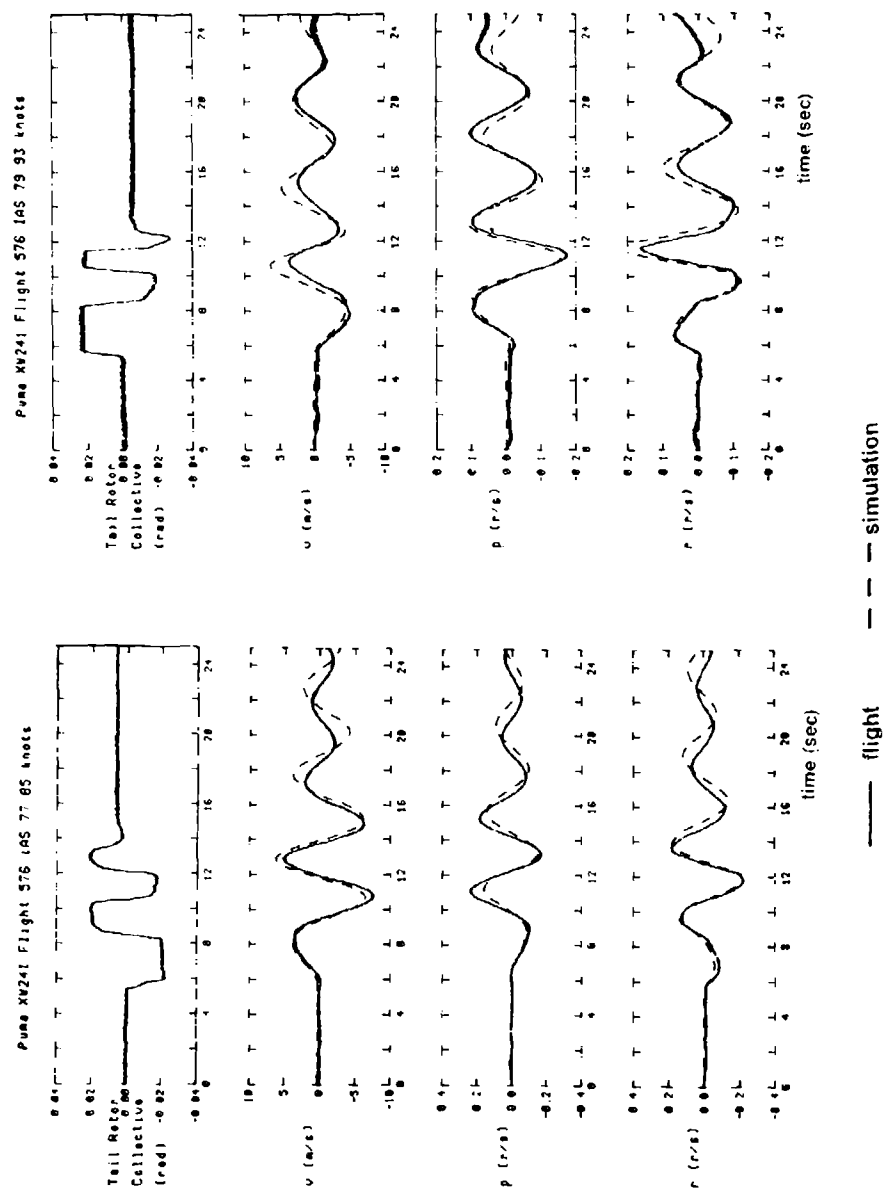


Figure 8.1.5. Comparison of flight and 3 DoF simulation (DLR estimates)

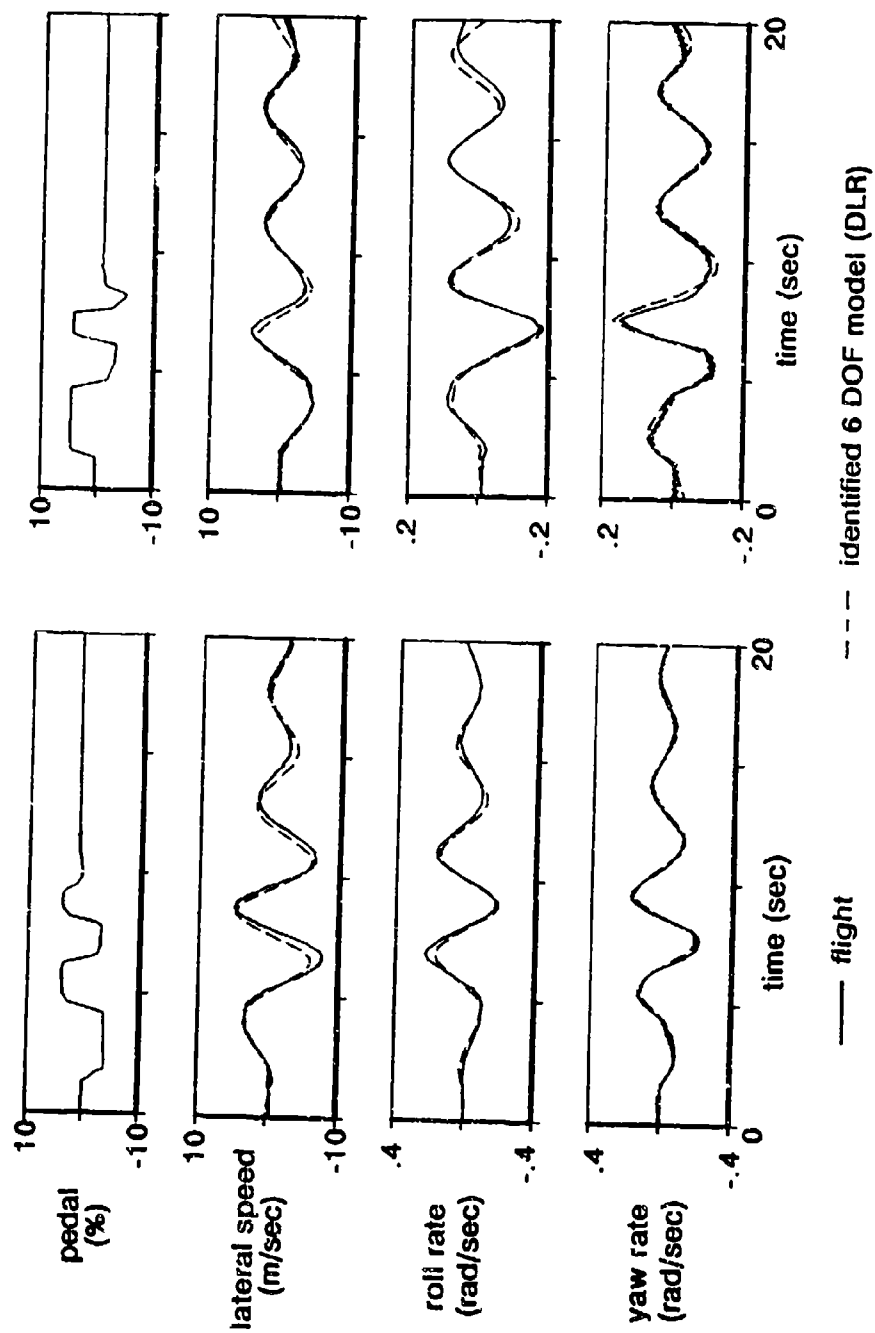


Figure 8.1.6. Comparison of flight and 6 DoF simulation (DLR estimates)

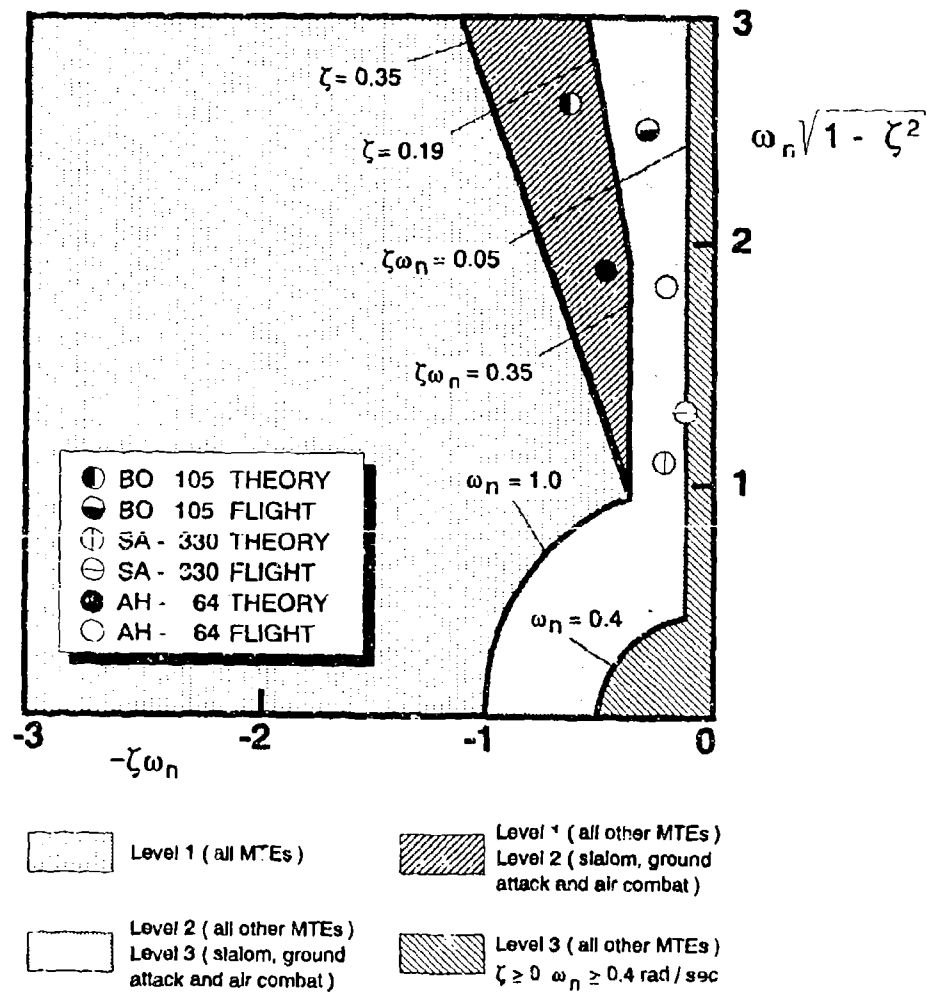


Figure 8.1.7. Comparison of flight and simulation estimates of Dutch roll stability characteristics with ADS 33C criteria

8.2 Handling Qualities¹⁸⁾

8.2.1 Introduction

System identification techniques have seen wide application in the fixed-wing and rotary-wing handling-qualities communities for characterizing the dynamics of air vehicles and piloted simulations. The extracted models are commonly used in closed-loop analyses of the pilot/vehicle system (Figure 8.2.1) to expose potential handling-qualities deficiencies and to check vehicle compliance against design specifications (Wilhelm et al., 1991, [8.2.1], Anon., 1988, [8.2.2]). A key factor that has been responsible for the broad and successful application of system identification techniques in the handling-qualities community is probably the relative simplicity of the models which are desired for pilot-in-the-loop analyses as compared to the full six or more degrees-of-freedom models required for most other applications. Generally, these analyses consider only the on-axis, single input/single-output response of the pilot/vehicle system. The extracted vehicle model may be non-parametric, such as frequency-response, or a low-order parametric model, such as a transfer function, or a simplified-decoupled state-space representation. Both time-domain and frequency-domain methods have been widely used for these applications.

This paper discusses system identification methods for rotorcraft handling-qualities studies. The requirements for flight testing, data analyses, and modeling for handling-qualities applications of system identification are contrasted with the requirements for extracting multi-input/multi-output state-space models for flight mechanics purposes. Typical handling-qualities analysis results are illustrated using the WG18 databases for the BO 105 and AH-64 helicopters.

8.2.2 Basic Handling-Qualities Concepts

Pilot/vehicle interaction in closed-loop control tasks is commonly analyzed by first modeling the pilot as a low-order compensator, and then analyzing the pilot/vehicle feedback system as a servomechanism (Figure 8.2.1). This section uses *classical control theory* to analyze the pilot/vehicle servomechanism and to illustrate basic handling-qualities concepts, although state-space based optimal methods are also available in the literature and have been used successfully (Anon., 1988, [8.2.2]).

In attitude tracking tasks, the pilot attempts to null the error e between the commanded aircraft attitude r and the actual aircraft attitude c through suitable motion of the aircraft stick, δ (Figure 8.2.1). The rate of pilot stick inputs $d\delta/dt$ is characterized by the cross-over frequency ω_c , a fundamental handling-qualities parameter, defined as the frequency at which the compensated open-loop magnitude response of c/e is 0 dB. Higher cross-over frequencies allow tighter closed-loop tracking, but imply higher stick deflection rates, and thus higher workload. The cross-over frequency is selected by the pilot to achieve the task performance requirements in the presence of noise or disturbances. A large body of test data (Anon., 1988, [8.2.2]) indicates that the cross-over frequency for attitude tracking tasks is typically in the range of $1 \text{ rad/s} \leq \omega_c \leq 3 \text{ rad/s}$.

Classical servomechanism theory can be used to show that good closed-loop characteristics (e.g. stability margins and command tracking) require that the overall compensated open-loop response c/e displays an average K/s characteristic (-20 dB/decade magnitude slope) in the cross-over frequency region. While the pilot ($Y_p = \delta/e$) can compensate for poor rotorcraft characteristics ($Y_c = c/\delta$) to achieve the desired overall cross-over characteristics ($c/e = Y_p Y_c$), this leads to increased pilot workload and resulting poor handling-qualities ratings. The minimum workload is achieved when the pilot can act as a pure gain regulator through a neuromuscular delay (Anon., 1988, [8.2.2]):

$$Y_p = K_p \exp(-\tau s) \quad (8.2.1)$$

where typical values of time delay are $0.2 \text{ s} < \tau < 0.4 \text{ s}$.

Simplified pilot/vehicle analyses (Anon., 1988, [8.2.2]) assume that the pilot acts as a pure gain regulator (ignoring the time delay τ), and selects the maximum cross-over frequency ω_c that can be achieved while maintaining acceptable stability margins (e.g. phase margin = 45° , gain margin = 6 dB). This maximum achievable pure-gain pilot cross-over frequency is termed the "bandwidth frequency" (ω_{bw}) in the handling-qualities community, and can be determined by inspection of the attitude response of the helicopter alone (Y_c) as obtained from system identification (Figure 8.2.2). The bandwidth frequency can also be considered as the inverse closed-loop time constant ($1/T_c$), since:

¹⁸⁾ Principal Author: Mark B. Tischler, AFDD

$$\frac{c}{r} \approx \frac{\omega_c}{s + \omega_c} \quad (8.2.2)$$

thus,

$$\frac{1}{T_c} = \omega_c = \omega_{bw}$$

High-bandwidth responses, and thus associated short rise times, are desirable for aggressive closed-loop piloting tasks, such as air-to-air tracking and air refueling. Lower bandwidth responses (and associated longer rise times) are acceptable for less aggressive tasks such as up-and-away cruise flight and maneuvering.

Task requirements for increased piloting aggressiveness lead to the need for higher cross-over frequencies than can be achieved by the simple pure gain piloting technique of equation (8.2.1). The increased phase lag (i.e. deteriorating phase margin) associated with higher cross-over frequencies must be offset by pilot-supplied lead, i.e. control anticipation. These requirements for pilot lead cause an increase in pilot workload and a degradation in perceived handling qualities. A measure of the rate of deterioration in the aircraft phase margin and, therefore, the requirement for pilot-supplied lead is obtained from a handling-qualities metric referred to as phase delay τ_p :

$$\tau_p = - \frac{\Phi_{2\omega_{180}} + 180^\circ}{57.3 \times 2\omega_{180}} \quad (8.2.3)$$

High values of phase delay indicate that when the pilot attempts to rapidly increase the cross-over frequency, there will be large demands for pilot lead. This, in turn, leads to poor handling-qualities and increased probability of pilot induced oscillations (Anon., 1988, [8.2.2]). Tasks which can be considered as "low gain" require lower cross-over frequencies and are, therefore, not as sensitive to large phase delays. The current *US Handling-Qualities Requirements for Military Rotorcraft ADS-33C* (Anon., 1988, [8.2.3]) specify desirable levels of bandwidth and phase delay for on-axis attitude responses (e.g. $c/\delta = \Phi/\delta_{lat}$ in Figure 8.2.1) appropriate to a variety of piloting tasks. Desirable (Level 1) handling-qualities for the roll response to lateral stick inputs are shown in Figure 8.2.3 for:

- (a) high gain (target acquisition and tracking) tasks and
- (b) all other piloting tasks.

Compliance with these specifications must be demonstrated for the flight vehicle (and/or simulation) using non-parametric frequency-response identification techniques.

Non-parametric models identified in the frequency-domain are very useful for these handling-qualities analyses because:

1. They are rapidly obtained from flight tests.
2. They contain no inherent assumptions of model structure or order.
3. The handling-qualities metrics (ω_{bw} , τ_p) are determined directly from inspection.

Frequency-response testing and analysis techniques initially developed and demonstrated for helicopters using the XV-15 (Tischler et al., 1983, [8.2.4]) and the Bell 214-ST aircraft (Tischler et al., 1987, [8.2.5]) have become a standard part of the rotorcraft specification compliance testing procedure.

Parametric models are needed in handling-qualities studies which use parametric analysis tools such as root locus, and state-space based methods (Anon., 1988, [8.2.2]). Also, the correlation of subjective handling-qualities ratings with vehicle-based aerodynamic characteristics (e.g. roll damping and roll control sensitivity) is often used in the development of handling-qualities design criteria. Parametric models used for this purpose are generally low-order, decoupled single-input/single-output transfer-function representations of the "effective" aircraft response characteristics important in the pilot cross-over frequency range. For example, in the fixed-wing handling-qualities specification, a second-order model must be identified to allow characterization of the short-period response of aircraft pitch attitude to longitudinal inputs and demonstrate compliance with the design criteria. The ADS-33C specification for rotorcraft gives desirable characteristics of the vertical velocity response to collective inputs in terms of a first-order transfer-function model \dot{h}/δ_{col} . An excellent review and analysis of helicopter handling-qualities using parametric system identification of low-order models is given by Houston and Horton (1987, [8.2.6]) based on SA-330 and Lynx flight test and simulation data. Both frequency-domain and time-domain methods are employed in the handling-qualities communities for parametric system identification.

The following sections demonstrate the application of both non-parametric and parametric system identification methods for handling-qualities studies.

8.2.3 Non-parametric Model Identification for Handling-Qualities Studies

This section discusses special requirements for identification of non-parametric (frequency-response) models and presents an illustrative example using the BO 105 data base.

Non-parametric models used in the evaluation of handling-qualities based on bandwidth and phase delay metrics must be accurate in the frequency range of the data used in the calculation (e.g. equation (8.2.3) for τ_p):

$$0.5 \omega_{bw} < \omega < 2.5 \omega_{180} \quad (8.2.4)$$

As seen in Figure 8.2.3, the range of acceptable bandwidth frequencies in the pitch and roll axis is roughly $1 \text{ rad/s} - 4 \text{ rad/s}$. Based on equation (8.2.4), and assuming a simple second-order closed-loop attitude response characteristic, the required range of accurate identification is roughly 0.5 rad/s to 15 rad/s . Clearly the very low frequency behavior of the phugoid (and spiral) dynamics are not as important for handling-quality applications as they are to the requirements for identifying a complete 6 DoF flight mechanics model.

The frequency-sweep input is particularly well suited for achieving accurate non-parametric (frequency-response) identification because it produces an even distribution of spectral content across the desired frequency range. The range of excitation is determined by selecting the period of the lowest frequency input and the cycle rate of the highest frequency input. At least two complete frequency sweeps are concatenated to increase the amount of data used in the spectral analyses and thus reduce the variance in the spectral estimates. Three frequency sweeps are executed consecutively in each of the primary axes to ensure that two good runs are obtained. Instrumentation requirements for identifying handling-qualities models are essentially the same as those required for identifying the more complete flight mechanics. The instrumentation characteristics must be carefully selected to minimize their influence on the aircraft response characteristics being identified. Further, the characteristics of the sensors and filters must be well known so that their effect can be incorporated in the analyses and not cause the extracted response characteristics to be biased by the instrumentation dynamics. Finally, the flight tests must be conducted during periods of minimum ambient wind and turbulence to reduce the random errors in the identification.

Flight-test inputs for flight-mechanics model identification are typically difficult to execute for the hover flight condition. However, the reduced identification frequency-range needed for handling-qualities applications allows much shorter record lengths and higher minimum excitation frequencies, thus reducing difficulty of achieving acceptable excitation even in hover. Furthermore most handling-qualities applications are concerned with the augmented (i.e. stability control augmentation system engaged) vehicle response characteristics, for which the aircraft dynamics are generally more stable and more nearly decoupled than the bare airframe.

Attitude response identification (e.g. Φ / δ_{lat}) in the mid- and high-frequency range is best achieved using the angular-rate signals (ρ / δ_{lat}) which have better frequency content compared to the attitude measurement variables. Then, the required response is obtained by applying numerically a $1/s$ correction

$$\frac{\Phi}{\delta_{lat}} = \frac{1}{s} \frac{\rho}{\delta_{lat}}$$

in the frequency domain.

Figure 8.2.4 shows an example of the Φ / δ_{lat} response for the BO 105 obtained from the AGARD WG18 frequency sweep data at 80 kn (events 44, 45, 46). The bandwidth and phase delay metrics are readily obtained from the figure and equation (8.2.3) to yield:

$$\begin{aligned} \omega_{bw} &= 5.72 \text{ rad/s} \\ \tau_p &= 0.062 \text{ s} \end{aligned} \quad (8.2.5)$$

These values are then spotted on the ADS-33C specifications in Figure 8.2.3. The BO 105 characteristics are seen to be in the desirable range even for the most demanding piloting tasks. This is a reflection of the high effective hinge offset of the BO 105 hingeless rotor, and the lack of additional time delays in this unaugmented aircraft. Much larger effective time delays are usually associated with flight control system augmentation in advanced rotorcraft (Tischler, 1987, [8.2.7]).

The presence of the lead-lag dynamics causes a dip in the phase curve near the $2\omega_{180}$ frequency as indicated in Figure 8.2.4. This causes the phase characteristics to be a nonlinear function of frequency and makes the

phase delay calculation extremely sensitive to the identified value of $2\omega_{180}$. In such circumstances, the phase delay parameter should be determined by a least-squares fit to the phase data in the piloted cross-over region (ADS-33C) as illustrated in Figure 8.2.5. The results show that for the present case, the least-squares calculation produces essentially the same phase delay value as was obtained directly from the two point approximation in Figure 8.2.4.

8.2.4 Parametric Model Identification for Handling-Qualities Analyses

Handling-qualities analyses based on parametric models of the pilot/aircraft system of Figure 8.2.1 must be accurate in the region encompassing the pilot cross-over, ω_c . As a rule of thumb, the frequency range of validity should encompass:

$$0.3 \omega_c \leq \omega \leq 3.0 \omega_c \quad (8.2.6)$$

The pilot's feedback loop suppresses the dynamics at lower frequencies, while the natural roll-off behavior of system response reduces the importance of the high-frequency dynamics. Thus, closed-loop pilot/vehicle characteristics are dominated by the open-loop response c/e in the frequency range of equation (8.2.6).

Parametric system identification methods for application to handling-qualities must be tailored to be most accurate in the frequency range of equation (8.2.6), with considerably reduced accuracy being acceptable outside of this frequency range. This suggests that handling-qualities models for attitude task analyses ($1 \text{ rad/s} \leq \omega_c \leq 3 \text{ rad/s}$) should be accurate in the frequency range of 0.3 rad/s to 9 rad/s . WG18 identification results indicate that a quasi-steady model formulation will be quite acceptable for characterizing helicopter dynamics in this frequency range. Furthermore, as discussed earlier, parametric handling-qualities models are generally assumed to have a very simple decoupled, first or second order structure to expose the dominant characteristics of concern to the pilot. This is especially true for analyzing handling-qualities of augmented vehicle dynamics, since augmentation tends to suppress most of the coupled and secondary open-loop vehicle dynamics. Clearly, model structures for handling-qualities analyses applications are significantly simpler than the 6 DoF flight mechanics models identified by WG18. The rudimentary models adopted to represent the pilot (e.g. equation (8.2.1)) make a more accurate modeling of the rotorcraft dynamics inappropriate.

The simple parametric model structures adopted for handling-qualities analyses allow considerable relaxation of the input design requirements and computational algorithms needed for parametric system identification. The main requirement is to acquire data with record lengths on the order of 2 to 3 time constants of the modes included in the model. For example, a typical heave damping constant ($Z_w = -0.5/\text{s}$) implies a time constant of 2 seconds. Thus, desirable record lengths to identify this parameter from flight data would be of the order of 4 to 6 seconds. These record lengths are considerably shorter than necessary to identify the coupled and lower frequency behavior for a full 6 DoF flight mechanics model. Rapid identification algorithms based in both frequency-domain (Tischler et al., 1983, [8.2.5]; Tischler et al., 1987, [8.2.6]) and time domain (Anon., 1988, [8.2.3]) are available for this application. The following two examples based on the WG18 AH-64 data-base illustrate the use of time-domain and frequency-domain system identification methods to extract lower-order parametric handling-qualities models.

8.2.4.1 Time-Domain Identification Example

The ADS-33C specification requires the identification of the first-order model of vertical response to collective:

$$\frac{\dot{h}}{\delta_{cc}} = \frac{K \exp(-t\tau)}{T_h s + 1} \quad (8.2.7)$$

based on a simplified time-domain output-error technique. The required analysis assumes that the input is a pure step. This yields the simple closed-form solution for the vertical rate response:

$$\dot{h}_{est}(t) = K \left[1 - \exp\left(-\frac{t-\tau}{T_h}\right) \right] \quad \text{for } t > \tau \quad (8.2.8)$$

$$\dot{h}_{est}(t) = 0 \quad \text{for } t \leq \tau \quad (8.2.9)$$

Although not contained in the current specification, the constraint of equation (8.2.9) is necessary to yield a causal model response (Howitt, 1990, [8.2.8]). In practice, the starting time ($t = 0$) is assumed to be at the mid point of the control input, since a finite time will always be required to achieve the full input during flight.

testing. The parameters of equation (8.2.7) are to be obtained by a non-linear optimization search to minimize the squared-error (ϵ^2) between the model output and flight test data:

$$\epsilon^2 = (\dot{h}_{\text{est}} - \dot{h}_{\text{data}})^2 \quad (8.2.10)$$

Table 8.2.1 on page 274 presents the ADS-33C specifications of the parameter values for desirable handling-qualities (Level 1).

The collective step response of the AH-64 for the 130 kn flight condition shown in Figure 8.2.6 was obtained by using the first portion of the doublet record (flight 883, event 10). The input is assumed to begin at $t = 1.2$ s, which corresponds to the mid-point of the initial collective step. The end-of-record is taken at $t = 4.51$ s, which corresponds to the point of collective control reversal. Therefore, the total record length used in the identification procedure is $t = 3.31$ s. Considering an approximate heave damping value ($Z_w = -0.5 \text{ s}^{-1}$) based on the AH-64 results obtained by the DLR (section 6.1), the system time constant is about 2 seconds, thus indicating that the record length is marginally acceptable for the current identification problem.

The transfer-function parameters identified using the data of Figure 8.2.6 are:

$$\begin{aligned} K &= -1.60 \text{ ft s}^{-2}/\% = -0.488 \text{ m s}^{-2}/\% \\ \tau &= 0.192 \text{ s} \\ T_h &= 1.86 \text{ s} \end{aligned} \quad (8.2.11)$$

The model response as estimated from equations (8.2.8), (8.2.9), and (8.2.11) is shown in Figure 8.2.6. The correlation coefficient r^2 is a measure of the accuracy with which the identified model satisfactorily characterizes the flight test data:

$$r^2 = \frac{\sum_{i=1}^n (\dot{h}_{\text{est}} - \bar{\dot{h}}_{\text{data}})^2}{\sum_{i=1}^n (\dot{h}_{\text{data}} - \bar{\dot{h}}_{\text{data}})^2} \quad (8.2.12)$$

where $\bar{\dot{h}}$ denotes the mean value of \dot{h} . For the results of Figure 8.2.6 is:

$$r^2 = 1.017 \quad (8.2.13)$$

The specification requires a correlation coefficient in the range of 0.97 to 1.03. Therefore, while there are significant deviations between the model predictions and the flight test data, the fit is considered to be satisfactory for handling-qualities applications. Comparison of the equation (8.2.10) parameters with the specification (Table 8.2.1) indicates that the AH-64 achieves desirable (Level 1) handling-qualities characteristics for the vertical response.

When a helicopter is operating with the automatic flight control system disengaged, as in the present case, the parameters of equation (8.2.10) correspond to the bare airframe stability and control derivatives:

$$\begin{aligned} Z_{\delta \text{col}} &= K = -0.488 \text{ m s}^{-2}/\% \\ Z_w &= -\frac{1}{T_h} = -0.54 \text{ s}^{-1} \\ \tau &= \text{rotor delay} = 0.192 \text{ s} \end{aligned} \quad (8.2.14)$$

The DLR results for these parameters as obtained from the full 6 DoF model identification are repeated for comparison with equation (8.2.14):

$$\begin{aligned} Z_{\delta \text{col}} &= -0.264 \text{ m s}^{-2}/\% \\ Z_w &= -0.547 \text{ s}^{-1} \\ \tau &= 0.117 \text{ s} \end{aligned} \quad (8.2.15)$$

The rather crude identification technique of equation (8.2.8) yields an accurate identification of heave damping (Z_w). The normal sensitivity ($Z_{\delta \text{col}}$) and time delay (τ) are somewhat overestimated, and may be correlated - trading off one against the other in the simple identification scheme. The Level 1 specification is achieved even for the overestimated time delay of equation (8.2.14), although the pilot opinion of the model of equation (8.2.15) would probably more accurately reflect the true aircraft behavior.

8.2.4.2 Frequency-Domain Identification Example

Frequency-domain methods provide a reliable approach for extracting physically meaningful low-order handling-qualities models because:

1. model structure can be selected based on a visual inspection of the non-parametric frequency-response identification results and
2. the frequency range of fit can be restricted to the model's range of applicability (Chen et al., 1987, [8.2.9]).

This approach is illustrated using the WG18 frequency sweep data for the AH-64.

The frequency response of pitch rate due to longitudinal actuator inputs was obtained (from flight 883 events 3 and 5) using the frequency-response identification techniques of section 5.5 and is presented in Figure 8.2.7. Good coherence is achieved in the frequency range from 0.6 rad/s (corresponding to the starting frequency of the automated sweep) to 10 rad/s. The coherence function of nearly unity indicates excellent identification accuracy and response linearity in this range. Visual inspection of the frequency response of Figure 8.2.7 indicates a fundamental first order characteristic. Attempts to fit the pitch rate response with a second-order model, or a simultaneous fit of the pitch rate and normal acceleration responses with the short period model proposed by RAE (Houston et al., 1987, [8.2.6]) resulted in overparameterization. The second-order pitch rate transfer function reduced to a first order form, thus indicating a very weak coupling between pitch rate and vertical responses. This finding is further supported by the very small identified values of the M_w coupling derivative determined by the DLR ($M_w = 0.013$) and the NAE and MDHC ($M_w = 0.00513$). The following decoupled pitch rate response was obtained from a 20 point match over the frequency range of from 0.6 rad/s to 10 rad/s:

$$\begin{aligned} \frac{q}{\delta_{lon}} &= \frac{M_{\delta lon} \exp(-r_{lon}s)}{s - M_q} \\ M_{\delta lon} &= 0.0274 \text{ s}^{-2}/\% \\ M_q &= -0.7754 \text{ s}^{-1} \\ r_{lon} &= 0.0993 \text{ s} \end{aligned} \quad (8.2.16)$$

The frequency response comparison between the low-order transfer function model (equation (8.2.16)) and flight test data is excellent over the frequency range of the fit as shown in Figure 8.2.7. For comparison with the above simple model results, the parameters obtained by the DLR for the full 6 DoF model (Section 6.1) are repeated below:

$$\begin{aligned} M_{\delta lon} &= 0.0275 \text{ s}^{-2}/\% \\ M_q &= -0.7741 \text{ s}^{-1} \\ r_{lon} &= 0.100 \text{ s} \end{aligned} \quad (8.2.17)$$

The agreement between the first order, 1 DoF, handling-qualities model and the full 6 DoF results is remarkable (compare equations (8.2.16) and (8.2.17)), substantiating the use of the simplified model in the limited frequency range of applicability.

The utility of the simplified transfer function model was checked using time domain verification for a doublet input. As seen in Figure 8.2.8, the predicted and measured responses of pitch rate and pitch attitude are nearly identical for the 8 seconds record length shown in the figure. This 8 seconds record corresponds to about 6 time constants of the identified pitch rate mode. Clearly, the transient pitch rate response characteristics of the AH-64 that are of interest to handling-qualities are satisfactorily captured by this very simple first-order transfer-function model.

As seen in Figure 8.2.7, the poor coherence at low frequency is not satisfactory for allowing an extraction of the bandwidth and phase delay parameters from the identified frequency-response. However, these parameters can be obtained by extrapolating the transfer function model response into the needed frequency range:

$$\begin{aligned} \omega_{bw} &= 0.678 \text{ rad/s} \\ \tau_p &= 0.074 \text{ s} \end{aligned} \quad (8.2.18)$$

Comparison of these values with the AHS-33C specifications (Figure 8.2.3) indicates Level 2 handling-qualities for the unaugmented AH-64 in the nonaggressive piloting tasks. Level 2 handling-qualities for a failed (or disengaged) AFCS condition is generally considered acceptable.

8.2.5 Summary

Key considerations in the application of system identification techniques to handling-qualities studies that were highlighted in this section are:

1. Requirements on flight testing, models structure, and identification algorithms are substantially eased because of
 - a. the rather restricted frequency range of applicability needed for analyzing pilot-in-the-loop handling-qualities; and
 - b. the desire for simple handling-qualities models which capture the inherent dynamic characteristics using a few number of parameters.
2. Non-parametric models are very useful for handling-qualities and are easily obtained in the frequency domain from frequency-sweep flight test data.
3. Simple parametric models are useful for characterizing the dominant vehicle characteristics in the frequency range of interest to handling-qualities and for establishing handling-qualities design guidelines.
4. Examples of frequency and time domain identification techniques applied to the BO 105 and AH-64 databases illustrate that rather simple modeling and identification methods can reliably be used to support rotorcraft handling-qualities studies.

References

- [8.2.1] Wilhelm, K.; Nieuwpoort, T.
Handling Qualities Evaluation Techniques
To be published in: AGARD AR-279, 1991
- [8.2.2] Anon.
Advances in Flying Qualities
AGARD Lecture Series LS-157, 1988
- [8.2.3] Anon.
Handling Qualities Requirements for Military Rotorcraft
AGARD Lecture Series LS-157, 1988
- [8.2.4] Tischler, M. B.; Leung, J. G. M.; Dugan, D. C.
Frequency-Domain Identification of XV-15 Tilt-Rotor Aircraft Dynamics in Hovering Flight
AIAA/AHS 2nd Flight Testing Conference, Las Vegas, 1983
- [8.2.5] Tischler, M. B.; Fletcher, J. W.; Diekmann, V. L.; Williams, R. A.; Cason, R. W.
Demonstration of Frequency-Sweep Testing Technique Using a Bell 214-ST Helicopter
NASA TM-89422, 1987
- [8.2.6] Houston, S. S.; Horton, R. I.
The Identification of Reduced Order Models of Helicopter Behaviour for Handling Qualities Studies
13th European Rotorcraft Forum, Arles, France, 1987
- [8.2.7] Tischler, M. B.
Digital Control of Highly Augmented Combat Rotorcraft
NASA TM-88346, 1987
- [8.2.8] Howitt, J.
Comments on the Proposed MIL-H-8501 Update Criterion on Height Rate Response Characteristics
RAE Working Paper WP FM 041, 1990
- [8.2.9] Chen, R. T. N.; Tischler, M. B.
The Role of Modeling and Flight Testing in Rotorcraft Parameter Identification
Vertica, Vol. 11, No. 4, 1987

LEVEL	T_h (in seconds)	τ (in seconds)
1	5.0	0.20
2	∞	0.30

Table 8.2.1. ADS-33C Specifications for Height Response Handling-Qualities

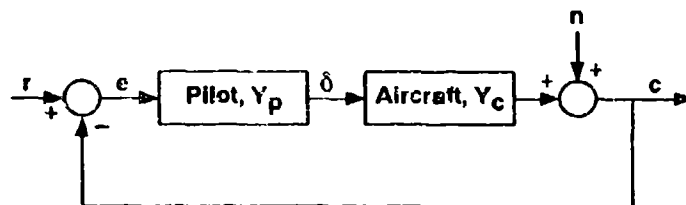


Figure 8.2.1. Pilot/vehicle system block diagram

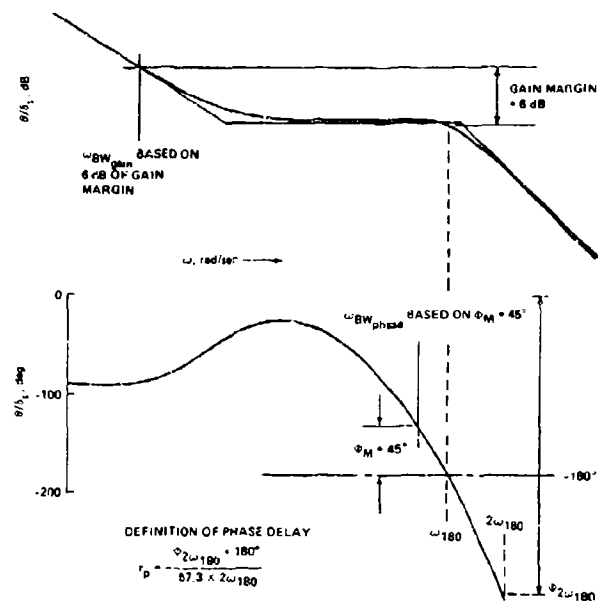
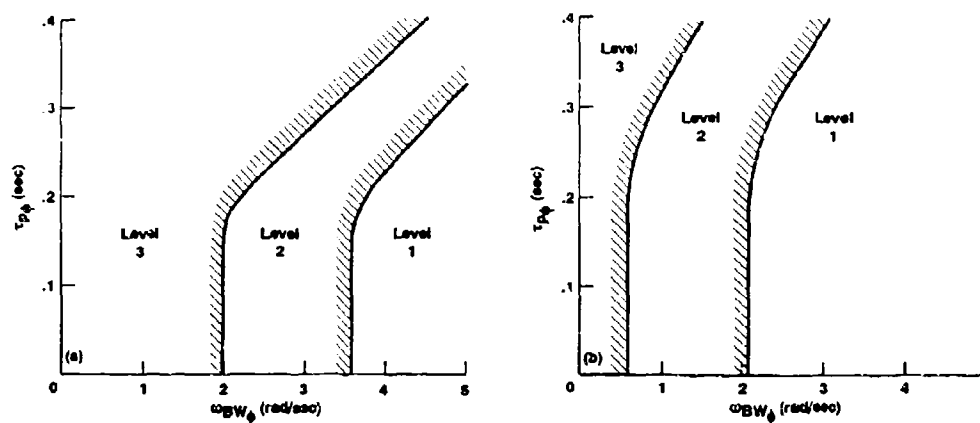


Figure 8.2.2. Determination of bandwidth and phase delay criteria

Figure 8.2.3. Requirements for roll response to lateral stick inputs
(a) high gain tasks; (b) all other piloting tasks

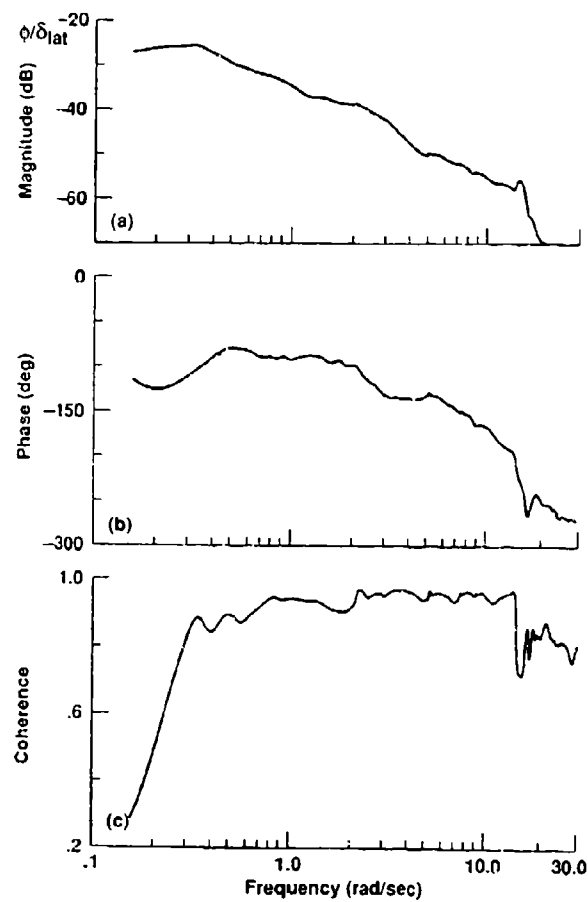


Figure 8.2.4. Roll attitude response to lateral stick (ϕ/δ_{lat}) identified from BO 105 frequency-sweep data

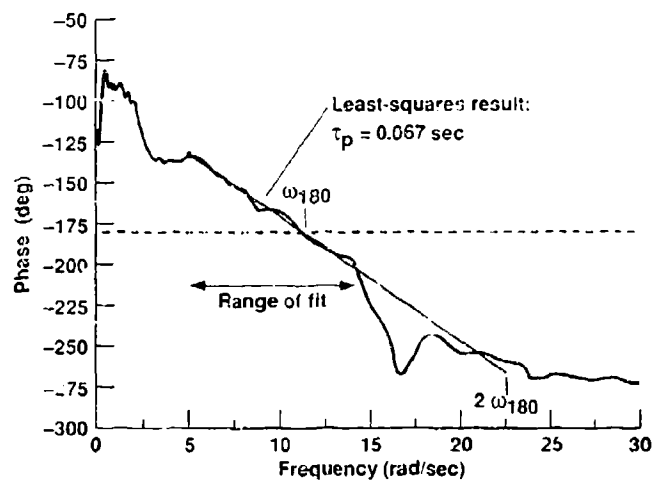


Figure 8.2.5. Determination of phase delay using least squares fitting procedure

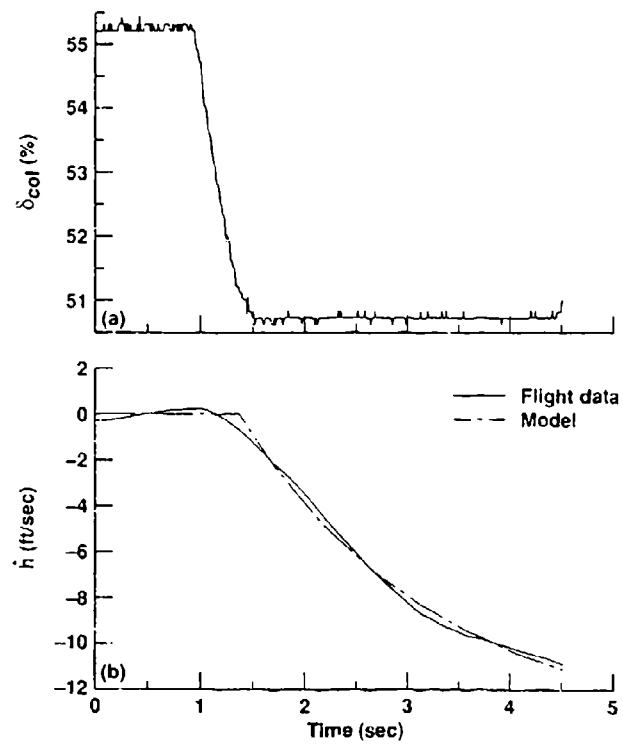


Figure 8.2.6. Flight data and handling-qualities model identification, equation (8.2.8), for vertical rate response

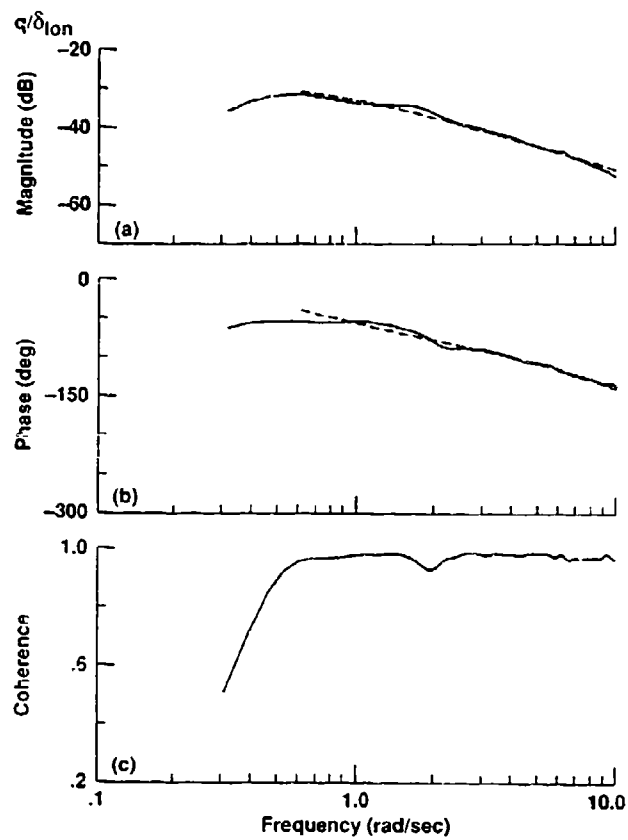


Figure 8.2.7. Pitch attitude response to longitudinal cyclic identified from AH-64 frequency-sweep data.

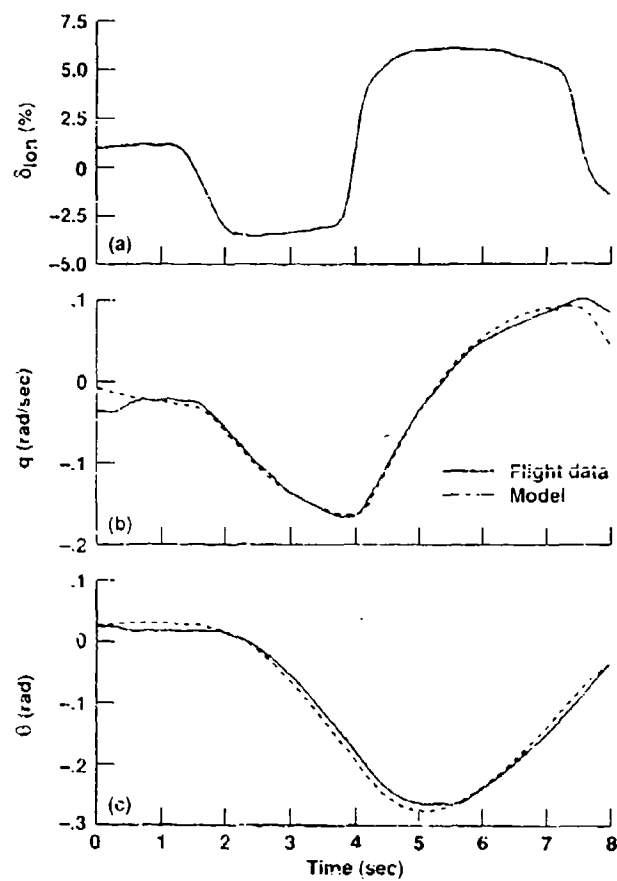


Figure 8.2.8. Time-domain verification of first-order pitch model, equation (8.2.16), of the A11-64.

8.3 System Identification Requirements for High-Bandwidth Rotorcraft Flight Control System Design¹⁹⁾

8.3.1 Introduction

System identification procedures provide an excellent tool for improving mathematical models used for rotorcraft flight control system design. Dedicated flight tests of a prototype helicopter can be conducted to update the flight mechanics to update the flight mechanics models and optimize control system gains early in the development process. Such an approach has already been taken by Kaletka and von Grünhagen (1989, [8.3.1]) in the development of a fly-by-wire BO 105, and by Bosworth and West (1986, [8.3.2]) in the development of the X-29A.

The identification of models for use in flight control system design involves requirements that are considerably different from those encountered in other applications such as piloted simulation and wind tunnel model validation. Models identified for use in simulation and wind tunnel validation must be generally accurate over a wide spectrum of frequencies from trim (zero frequency) and phugoid (low frequency) to the dominant transient responses of the longitudinal short-period and roll-subsidence modes (mid/high frequency). Therefore, in terms of stability and control derivatives, the low-frequency parameters such as the speed derivatives may be just as important to a pilot's perception of simulation fidelity as an accurate value of roll damping.

Practical flight control system design requires models that are:

1. highly accurate in the crossover frequency range-to exploit the maximum achievable performance from the helicopter; and,
2. robust in the crossover range with respect to flight condition, and input form and size-to ensure that closed-loop stability/performance is maintained. The control system design can be made sufficiently robust to compensate for poor model robustness, but at the expense of performance.

These requirements are especially difficult for advanced high-bandwidth control systems where the crossover range occurs at frequencies near the limit of current identification capabilities.

This paper examines in detail these requirements for system identification application to high-bandwidth flight control design. Much of this paper discusses the need in control system design for higher-order models that include rotor dynamics. It is interesting to note that the inclusion of rotor flapping dynamics in an optimal control system design methodology was investigated by Hall and Bryson (1973, [8.3.3]) many years ago.

The roll response of the BO 105 helicopter (Figure 8.3.1) at a trim condition of 40 m/s is used throughout to illustrate the points of the analysis. The high-bandwidth/highly-coupled rotor system of the BO 105 presents a difficult system designer with a "most difficult case" scenario. Flight data presented in this paper was obtained from the DLR Institute for Flight Mechanics as part of the AGARD WG18 on Rotorcraft System Identification.

8.3.2 Simple Model-Following Control System

Figure 8.3.2 shows a simple design of the roll channel for control system based on an explicit model-following concept. An attitude-command/attitude-hold configuration is shown, with only roll angle feedback for the present. The error signal is formed from the difference between the actual roll angle response and that of the desired command model.

The control law design problem for this simple system involves the selection of the stabilization loop gain K , and an appropriate command model. Design requirements based on the U.S. military handling qualities specification (Hoh et al., 1988, [8.3.4]) are for an overall closed-loop roll attitude bandwidth Φ/Φ_c (based on 45° phase margin) in the range of $2 \text{ rad/s} \leq \omega_{bw} \leq 4 \text{ rad/s}$. The desired stabilization loop bandwidth $(\omega_{bw})_{stab}$ of Φ/Φ_m is selected as twice this range $4 \text{ rad/s} \leq (\omega_{bw})_{stab} \leq 8 \text{ rad/s}$ to achieve good model-following and gust rejection (Fischler, 1987 [8.3.5]). This implies a stabilization loop crossover frequency (of Φ/Φ_c) in the same range, with associated satisfactory phase and gain margins. The following section addresses the identification and modeling aspects for achieving these desired stabilization loop characteristics Φ/Φ_m . Command model selection Φ_m/Φ_c is not addressed herein, because it is not an identification issue.

¹⁹⁾ Principal Author: Mark B. Titchler, AFDD

8.3.3 Identification Models for Control System Design

Identification models for use in control system design can be categorized as non-parametric (e.g., frequency-response) or parametric (e.g., transfer-functions and state-space models). Both types of models are discussed in this section.

8.3.3.1 Nonparametric Frequency-Response Model

Nonparametric identification models are highly useful as starting points for control system design because they contain no inherent assumptions on model order or structure. The frequency response is complete and accurate (within the frequency-range of good coherence), and provides the fundamental open-loop characteristics needed for both classical and modern frequency-domain based design methods. The identified frequency-response is a describing function model of locally linearized nonlinear behavior. The severity of this assumption can be checked by comparing extracted describing functions for different input amplitudes.

A robust control system design requires a model that is accurate over a frequency range that spans the intended crossover region. However, the helicopter's dynamics and thus the achievable crossover frequency are unknown at this stage. Thus a nonparametric model that is accurate over a broad frequency range is desirable. Pilot generated frequency-sweeps are especially well suited for this purpose (Chen et al., 1986, [8.3.6]; Tischler et al., 1987, [8.3.7]). Piloted frequency-sweeps of the BO 105 were conducted over a range of frequencies from 0.1 Hz to 5 Hz (corresponding to angular frequencies of 0.63 rad/s to 31.4 rad/s) to excite all the dynamic modes of concern (Figure 8.3.3).

The identified open-loop (Φ/δ_{lat}) frequency response of the BO 105 body/rotor/actuator system for the 40 m/s flight condition shown in Figure 8.3.4 was obtained using the spectral analysis techniques of reference (Tischler, 1987, [8.3.8]). The spectral analysis was optimized for accuracy in the frequency-range of $1 \text{ rad/s} \leq \omega \leq 30 \text{ rad/s}$, which covers all modes of concern near the crossover range. The associated coherence (Figure 8.3.4 part c) indicates accurate identification in this frequency range. The Bode plot of Figure 8.3.4 shows that with roll attitude feedback only, a maximum crossover frequency (Φ/Φ_c of $\omega_c = 5.72 \text{ rad/s}$) can be achieved for phase and gain margins of 45° and 6 dB, respectively. These characteristics meet the design specifications for this simple system. However, roll rate feedback will be necessary to offset additional lags in a practical design implementation (Tischler, 1987, [8.3.5]).

8.3.3.2 Parametric Model

A parametric model of the roll response is useful to facilitate detailed control design studies. The fundamental considerations in deriving such a parametric model are:

1. Frequency-range of validity

The frequency-range of model validity should extend substantially on either side of the crossover frequency. As a rule of thumb, dynamics modes with frequencies of 0.3 to 3.0 times the crossover frequency will contribute substantially to the closed-loop response. In the present case, this indicates that the parametric model should be valid in the frequency range of 2 rad/s to 10 rad/s, which includes all of the classical attitude response modes (short period, dutch roll, and roll subsidence) and the regressing rotor modes (flapping and 1-lag), and dynamic inflow (for lower speed conditions). Accurate characterization outside of this frequency range is not important to control system design for the design bandwidth selected here. Closed-loop control suppresses all low frequency open-loop response, so that accurate knowledge of the speed derivatives (phugoid and spiral dynamics) is of little importance.

2. Model Order

The model order must be high enough to capture the important dynamic characteristics in the frequency-range of model validity. In the frequency-domain, this means a sufficient number of states to achieve a "good fit" of the nonparametric response of Figure 8.3.4 is needed in the desired frequency range. However, if the model order is excessive, model parameters will exhibit large variability to small changes in flight condition, input form, and input size which will compromise robustness (Taylor, 1974, [8.3.9]).

3. Estimate of Model Accuracy

Flight control design requires an estimate of the accuracy of the aerodynamic parameters. Modern Multiple-Input-Multiple-Output (MIMO) methods that feedback all outputs to all controls require a consistent level of accuracy in the characterization of all of the on- and off-axis responses. Metrics such as the

Cramer-Rao lower bound, multi-run scatter, and frequency-response errors are useful for assessing model accuracy.

4. Model Robustness

Models must be robust with respect to flight condition, input form, and input size. Model structure determination methods are useful in reducing parameter insensitivity and correlation, which in turn improves model robustness. Also model verification with alternative input forms, and magnitudes are useful in this regard.

8.3.4 A High-Order Model for Roll Response

A 7th-order model is selected as the "baseline model" that captures the key dynamics in the frequency-range of concern (2 rad/s to 18 rad/s):

1. coupled roll/rotor flapping dynamics (2nd order),
2. lead-lag/air resonance (2nd order),
3. dutch roll dynamics (2nd order),
4. roll angle integration (1st order),
5. actuator dynamics (equivalent time delay).

Dynamic inflow modes are not explicitly included in the above list, because of their small influence at this forward flight speed (40 m/s). (Implicit effects of inflow on the rotor modes are captured in matching the frequency-response data.) The roll angle response to lateral stick transfer-function for the baseline model is then 4th-order numerator and 7th-order denominator. The model parameters shown in Table 8.3.1 were obtained from a frequency response fit of Figure 8.3.4 from 1 rad/s to 30 rad/s using 50 points. The frequency-response comparison with the data is seen in Figure 8.3.5 to characterize the dynamics accurately in the range of concern, thus indicating that model is of sufficiently high order. The mismatch near the lead-lag mode (13 rad/s) reflects the reduced accuracy (lower coherence) of the flight data in this frequency range (Figure 8.3.4). The 45° phase margin crossover frequency for the baseline model is taken from Figure 8.3.5 as $\omega_c = 5.32$ rad/s which is within 7% of the data, and the baseline gain margin and the frequency for closed-loop instability (ω_u) matches the data (Table 8.3.2).

The transfer function model indicates a highly coupled body-roll/rotor-flapping mode ($\zeta = 0.51$, $\omega = 13.7$ rad/s) as is expected for the hingeless rotor system (high effective hinge offset) of the BO 105 Helicopters with low effective hinge offset rotors (or equivalently low flapping stiffness), such as some articulated systems, will generally exhibit two essentially decoupled first order modes:

1. body angular damping (L_p , M_q),
2. 1st order rotor regressing

The decoupled rotor mode is often modelled by an effective time delay. The degree of body/rotor coupling is determined by the flapping stiffness as illustrated in Figure 8.3.6 from Hefley et al (1986, [8.3.10]). The lead-lag mode is very lightly damped ($\zeta = 0.0421$) due only to structural damping of the hingeless rotor and the low aerodynamic damping. The total modal damping ($\sigma = -\zeta\omega = 0.668 \text{ s}^{-1}$) agrees very well with previously published experimental data (Warmbrodt et al., 1984, [8.3.11]). Significant roll/yaw coupling is apparent from the separation of the complex pole/zero combination of the dutch roll mode. Finally, the equivalent time delay corresponds well to known control system hydraulics and linkage lags.

Figure 8.3.7 shows the root locus for variation in the roll angle gain K_ϕ (of Figure 8.3.2). The pole at the origin moves to the crossover range, and the dutch roll mode is driven into the neighboring zero in a stable manner. The lead-lag mode is also driven toward the neighboring complex zero, and is slightly stabilized ($\zeta = 0.0440$) for the nominal crossover frequency ($\omega_c = 5.32$). The attitude feedback gain K_ϕ is limited by the destabilization of the rotor/flapping mode. Added time delay to account for unmodelled dynamics does not change these results significantly.

The closed-loop frequency response of Φ/Φ_m (from Figure 8.3.2) shown in Figure 8.3.8 for $K_\phi = 322.9 \text{ %/rad}$ indicates that good model-following will be achieved out to the desired stabilization-loop bandwidth frequency (4 rad/s to 8 rad/s). The closed-loop data curve also shown in the figure was generated by calculating $KG/(1 + KG)$ for each frequency, using the open-loop data curve of Figure 8.3.4. The good agreement between the closed-loop baseline model response and the (calculated) data over the broad frequency range (1 rad/s to 30 rad/s) further demonstrates the validity of the 7th-order model for predicting high-bandwidth flight control system performance.

Two important quantitative metrics of closed-loop performance (Φ/Φ_m) are bandwidth (ω_{bw}) and phase delay (τ_D). Closed-loop bandwidth ω_{bw} is defined in the handling-qualities community (Hoh et al., 1988, [8.3.4]) as the frequency at which phase margin of the closed-loop response, Φ/Φ_m in this case, is 45° . (This definition applies for attitude command systems as in the present study.) The phase delay is a measure of the phase rolloff near the bandwidth frequency and reflects the total effective time delay of the high frequency dynamic elements (rotor and actuator in this simple case). The phase delay is defined as (Hoh et al., 1988, [8.3.4]):

$$\tau_D = -\frac{\Phi_{2\omega_{180}} + 180^\circ}{57.3 \times 2\omega_{180}} \quad (8.3.1)$$

where

ω_{180} = frequency where the phase of (Φ/Φ_m) = -180°

$\Phi_{2\omega_{180}}$ = phase angle at a frequency of $2\omega_{180}$.

The bandwidth and phase delay metrics are well predicted by the higher-order model as shown in Table 8.3.2.

An additional feedback of roll-rate will be required in the control system to offset lags and time delays associated with practical design implementation. Figure 8.3.9 shows a root locus for variation of roll-rate feedback gain K_p . For no additional time delay, rotor/flapping mode stability remains the limitation on rate feedback gain, although the lead-lag mode damping is clearly reduced for moderate gain levels. When 50 ms of additional time delay is included to account for filters and computational delay in a practical digital control system implementation (Tischler, 1987, [8.3.5]), the lead-lag mode becomes rapidly destabilized and sets the limit on rate feedback. (A lag and a pure delay have the same effect on destabilizing the lead-lag mode for this case.) This result illustrates the need for accurate knowledge of the lead-lag dynamics in high-bandwidth control system design. Analytical studies by Diftler (1988, [8.3.12]), Miller and White (1987, [8.3.13]), and Curtiss (1986, [8.3.14]) have made the same conclusions. A flight test investigation by Chen and Hindson (1986, [8.3.15]) using a variable-stability CH47 helicopter demonstrated the importance of rotor dynamics and control system lags in determining feedback gain bandwidth limits.

8.3.5 Lower-Order Models for Broad-Band Roll Response

Two levels of approximation that are commonly made in formulating models for identification are considered in this section:

1. Omit lead-lag dynamics (5th order)

A 5th-order roll-attitude response model was obtained by refitting the frequency response data without the lead-lag mode (Table 8.3.1 and Table 8.3.2). The transfer function result is consistent with 7th-order model, with only slight variations in the remaining parameters. This indicates that the lead-lag/air-resonance mode can be modelled as a one-way-coupled (parasitic mode), similar in nature to an aircraft structural mode. Thus, the lead-lag transfer functions (quadratic dipoles) could be appended onto a 8 DOF identification model (flapping dynamics only). This approach has been successfully applied in the state-model identification of BO 105 dynamics (Tischler et al., 1990, [8.3.16]).

The frequency-response matches of the 5th-order model matches the high-order model very well (Figure 8.3.16), except of course for the omission of the lead-lag mode. The fitting error shown in Table 8.3.1 indicates only a slight degradation relative to the 7th-order model. The roll-angle gain is again limited by destabilization of the coupled roll/flapping mode. Of course, roll-rate limitations due to lead-lag instability will not be detected by this model. Comparison of the closed-loop response (Φ/Φ_m) of the 5th-order and 7th-order model (Figure 8.3.11) shows that the reduced-order model is very accurate except for the lead-lag mode omission. The quantitative metrics match the baseline model results (Table 8.3.2).

2. Quasi-steady rotor dynamics (4th order).

A 4th-order model is obtained by adopting a quasi-steady assumption for the roll dynamics and treating the rotor as an equivalent time delay. The resulting transfer function model fit is given in Table 8.3.1. The time delay of 0.0743 s now accounts for 0.023 s from the hydraulics/ actuator system and 0.051 s from the effective rotor delay. The quasi-steady roll damping mode is estimated at $L_p = -9.87$ rad/s. The dutch roll pole/zero quadratic has been de-tuned for this single axis fit. (This could be improved by considering a simultaneous match of β/δ_r , which will enforce the correct dutch roll location (Tischler, 1987, [8.3.8]). The frequency-response of this model is seen in Figure 8.3.10 to be a poor approximation, especially at higher-frequency, as expected by the adoption of a crude rotor flapping approximation. This

is further emphasized by the threefold increase in the fitting cost relative to the 5th-order model (Table 8.3.1). The 45° phase margin crossover frequency is under-predicted by 20 % relative to the baseline model, while the gain margin is overpredicted by 57 % (Table 8.3.2).

The root locus versus attitude gain for this model (Figure 8.3.12) indicates that the gain limitation is due to the destabilization of a coupled 2nd-order pure rigid body mode. Thus, the quasi-steady model fails to capture key dynamics of the coupled roll/flapping mode. Finally, the closed-loop bandwidth is underestimated by 26 % as indicated in Figure 8.3.11 and Table 8.3.2. Overall, the use of the 4th order model to match the full frequency range (1 rad/s to 30 rad/s) is seen to be inappropriate.

8.3.6 Quasi-Steady Models for Low-Frequency Roll Response

The utility of the quasi-steady approximation in characterizing the lower-frequency dynamics was investigated. For this study, the dutch roll dynamics were omitted.

Figure 8.3.13 shows the variation in L_p and the fitting cost for changes in the upper fitting frequency $8 \text{ rad/s} \leq \omega_2 \leq 30 \text{ rad/s}$. The roll damping rises from $L_p = -9.3$ for $\omega_2 = 8 \text{ rad/s}$ to $L_p = 20.4$ for $\omega_2 = 15 \text{ rad/s}$; however, the cost function remains fairly constant in this range. For $\omega_2 > 14 \text{ rad/s}$, the cost function rises dramatically, indicating a poor characterization of the dynamic response. Note that for the $\omega_2 = 30 \text{ rad/s}$, the roll damping drops to $L_p = -9.6$, which closely corresponds to the 4th-order model of Table 8.3.1. The extreme sensitivity in the model parameters and cost function for $\omega_2 > 14 \text{ rad/s}$, shows that this frequency is the limit of the validity of the quasi-steady assumption. For $\omega_2 < 14 \text{ rad/s}$, the cost function remains fairly constant at $CF = 45$, which roughly corresponds with the 5th order fitting error, the higher-order model being more accurate as expected. The variability in L_p seen even for $7 \text{ rad/s} \leq \omega_2 \leq 13 \text{ rad/s}$ will be limited by the simultaneous fit of multiple responses in the full model identification (Tischler et al., 1990, [8.3.8]).

The Φ/δ_{lat} frequency-response for the $\omega_2 = 13 \text{ rad/s}$ case is shown in Figure 8.3.14 to have comparable accuracy as the baseline model in the range of 1 rad/s to 13 rad/s (except for the omission of the dutch roll mode). The estimated crossover frequency is nearly identical to the high-order baseline model. Also, the closed-loop performance metrics are much closer to the baseline model than was the 4th-order model (Table 8.3.2). The first order model for $\omega_2 = 30 \text{ rad/s}$, also shown in Figure 8.3.14, is seen to poorly characterize the response at both low and high frequency. The frequency range of the fit is clearly inappropriate for the quasi-steady model structure. A similar analysis conducted on the pitch response indicates a useful bandwidth for the quasi-steady assumption of 13 rad/s. Thus, the overall useful bandwidth of the quasi-steady model structure is 13 rad/s.

This analysis indicates that improved utility of the quasi-steady models can be achieved if the data is band-limited to below the rotor flapping frequency (13 rad/s in this case) before the identification is completed. This band-limitation easily accomplished in frequency-domain identification methods, since the fitting range is an explicit function of frequency (Tischler et al., 1990, [8.3.16]; Tischler, 1988, [8.3.17]). In time-domain methods, the data should be filtered to eliminate the high-frequency dynamics (Chen et al., 1986, [8.3.6]). Although the coupled rotor/flapping instability can still not be replicated with such band-limited quasi-steady models, the nominal control system performance may be adequately estimated.

8.3.7 Conclusions

1. An accurate model for helicopter control system studies requires coupled body/rotor flapping and lead-lag dynamics. The lead-lag response may be treated as a one-way coupled parasitic mode for the case study evaluated herein.
2. For a single-rotor hingeless helicopter, the coupled body/rotor-flapping mode limits the gain on attitude feedback, while the lead-lag mode limits the gain on attitude-rate feedback.
3. Quasi-steady models that approximate the rotor response by an equivalent delay are useful for estimating nominal control system performance if the data used in the identification is band-limited to frequencies below the coupled body/rotor response.

References

- [8.3.1] Kaletka, J.; von Grnhausen, W.
Identification of Mathematical Derivative Models for the Design of a Model Following Control System
 45th Annual National Forum of the American Helicopter Society, Boston, MA, 1989

- [8.3.2] Boaworth, J. T.; West, J. C.
Real-Time Open-Loop Frequency Response Analysis of Flight Test Data
AIAA Paper 86-9738, 3rd AIAA Flight Testing Conference, Las Vegas, 1986
- [8.3.3] Hall, W. E. Jr.; Bryson, A. E. Jr.
Inclusion of Rotor Dynamics in Controller Design for Helicopters
Journal of Aircraft, Vol. 10, No. 4, 1973
- [8.3.4] Hoh, R. H.; Mitchell, D. G.; Aponso, B. L.; Key, D. L.; Blanken, C. L.
Proposed Specification for Handling Qualities of Military Rotorcraft. Vol. 1: Requirements
USAAVSCOM Tech. Report 87-A-4, 1988
- [8.3.5] Tischler, M. B.
Digital Control of Highly Augmented Combat Rotorcraft
NASA TM-88346, 1987
- [8.3.6] Chen, R. T. N.; Tischler, M. B.
The Role of Modeling and Flight Testing in Rotorcraft Parameter Identification
42nd Annual National Forum of the American Helicopter Society, System Identification Session, Washington, DC, 1986
- [8.3.7] Tischler, M. B.; Fletcher, J. W.; Diekmann, V. L.; Williams, R. A.; Cason, R. W.
Demonstration of Frequency-Sweep Testing Technique Using a Bell 214-ST Helicopter
NASA TM-89422, 1987
- [8.3.8] Tischler, M. B.
Frequency-Response Identification of XV-15 Tilt-Rotor Aircraft Dynamics
NASA TM-89428, 1987
- [8.3.9] Taylor, L. W. Jr.
Application of a New Criterion for Modeling Systems
AGARD CP-172, 1974
- [8.3.10] Heffley, R. K.; Bourne, S. M.; Curtiss, H. C. Jr.; Hess, R. A.
Study of Helicopter Roll Control Effectiveness Criteria
NASA CR-177404, 1986
- [8.3.11] Warmbrodt, W.; Peterson, R. L.
Hover Test of a Full-Scale Hingeless Rotor
NASA TM-85990, 1984
- [8.3.12] DiNler, M. A.
UH-60A Helicopter Stability Augmentation Study
14th European Rotorcraft Forum (Paper No. 74), Milano, Italy, 1988
- [8.3.13] Miller, D. G.; White, F.
A Treatment of the Impact of Rotor-Fuselage Coupling on Helicopter Handling Qualities
43rd Annual Forum of the American Helicopter Society, 1987
- [8.3.14] Curtiss, H. C. Jr.
Stability and Control Modeling
12th European Rotorcraft Forum (Paper No. 41), Garmisch-Partenkirchen, FRG, 1986
- [8.3.15] Chen, R. T. N.; Hindson, W. S.
Influence of High-Order Dynamics on Helicopter Flight-Control System Bandwidth
Journal of Guidance, Control, and Dynamics, Vol. 9, No. 2, 1986
- [8.3.16] Tischler, M. B.; Cauffman, M. G.
Frequency-Response Method for Rotorcraft System Identification with Applications to the BO 105 Helicopter
46th Forum, American Helicopter Society, Dynamics I-Session, Washington, DC, 1990
- [8.3.17] Tischler, M. B.
Advancements in Frequency-Domain Methods for Rotorcraft System Identification
2nd International Conference on Basic Rotorcraft Research, University of Maryland, College Park, MD, 1988

Model	Fitting range (in rad/s)	Transfer function	Fit cost
Baseline Model 7th order	1 ... 30	$\frac{2.62 [0.413, 3.07] [0.0696, 16.2] e^{-0.0225s}}{(0) [0.277, 2.75] [0.0421, 15.8] [0.509, 13.7]}$	12.1
Coupled body/rotor 5th order	1 ... 30	$\frac{2.47 [0.499, 3.11] e^{-0.0216s}}{(0) [0.319, 2.71] [0.413, 13.5]}$	26.8
Broad-band quasi-steady 4th order	1 ... 30	$\frac{0.200 [0.283, 2.04] e^{-0.0743s}}{(0) [0.214, 2.13] (9.87)}$	102.3
13 rad/s band-limited quasi-steady 2nd order	1 ... 13	$\frac{0.300 e^{-0.0836s}}{(0) (14.6)}$	44.2

Table 8.3.1. Roll response models, Φ / δ_a

Numerators and denominators of the transfer functions are decomposed into products of functions of the variable s .

$[\zeta, \omega_n]$ represents the second order polynomial $s^2 + 2\zeta\omega_n s + \omega_n^2$, with undamped natural angular frequency ω_n and the damping ratio ζ of modulus $|\zeta| \leq 1$.

$(1/T)$ represents the first order polynomial $s + 1/T$, where T = time constant.

Model	Open-loop metrics Φ/Φ_0			Closed-loop metrics Φ/Φ_m	
	ω_c (in rad/s)	GM (in dB)	ω_u (in rad/s)	ω_{bw} (in rad/s)	τ_p (in s)
Data	5.72	6.39	11.4	8.58	0.0658
Baseline model	5.32	6.51	11.3	9.46	0.0659
Coupled body/rotor	5.33	5.70	11.5	9.62	0.0682
Broad-band quasi-steady	4.28	10.2	10.2	6.98	0.0545
13 rad/s band-limited	5.26	7.96	11.1	8.33	0.0600

Table 8.3.2. Comparison of performance estimates

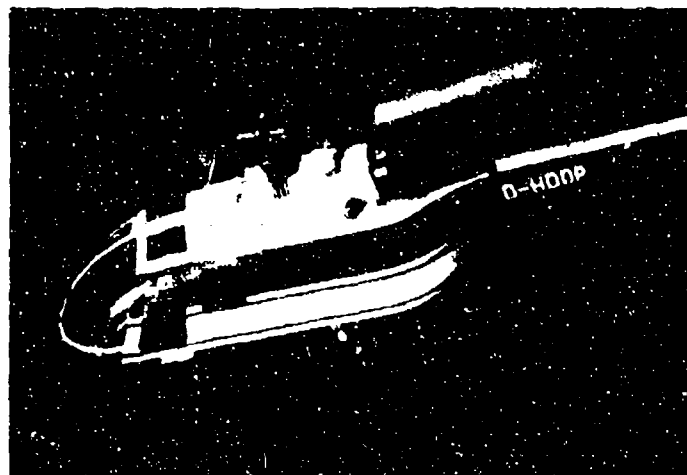


Figure 8.3.1. BO 105 case study helicopter

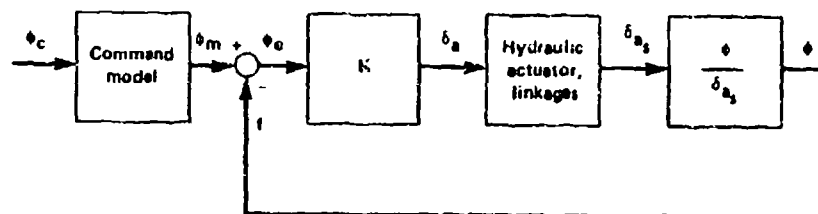


Figure 8.3.2. Simple explicit model-following control system

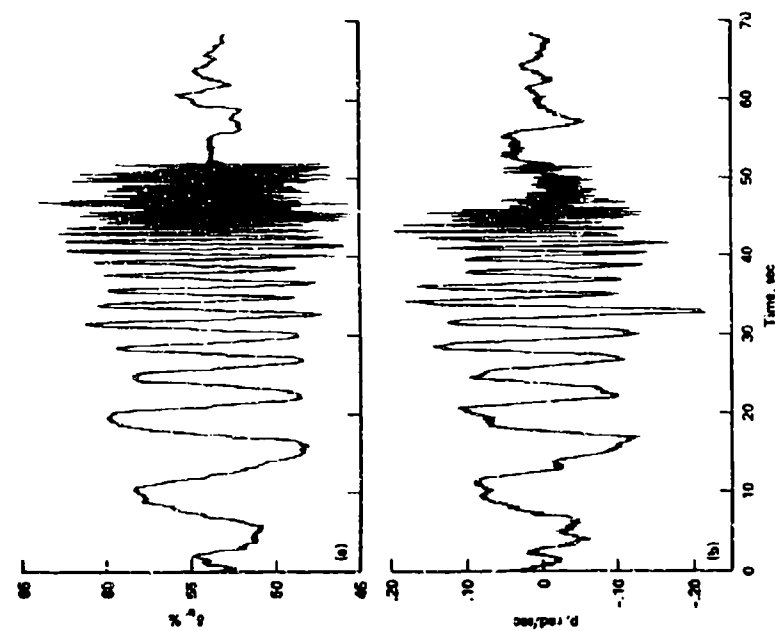


Figure 8.3.3. Flight data of roll axis frequency-sweep

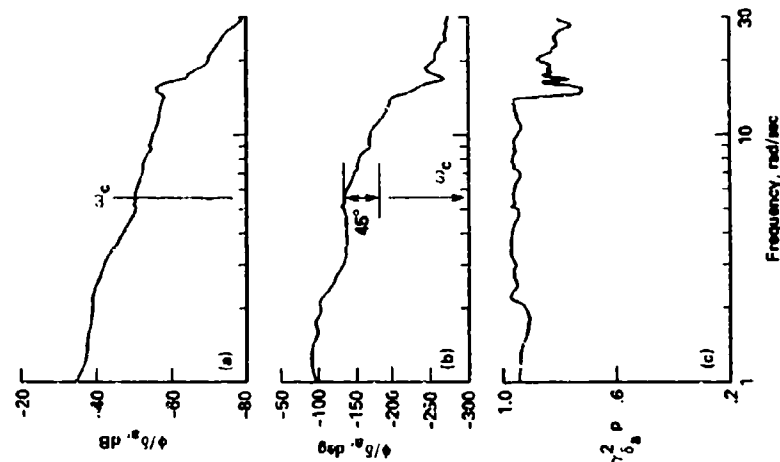


Figure 8.3.4. Frequency-response identification
a) Pilot lateral stick input, δ_{lat}
b) roll rate, p

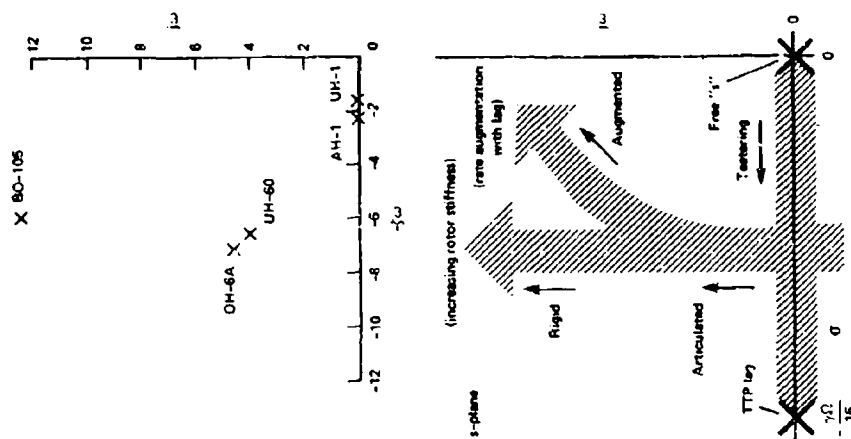


Figure 8.3.6. Short-term eigenvalue locations as a function of flapping stiffness

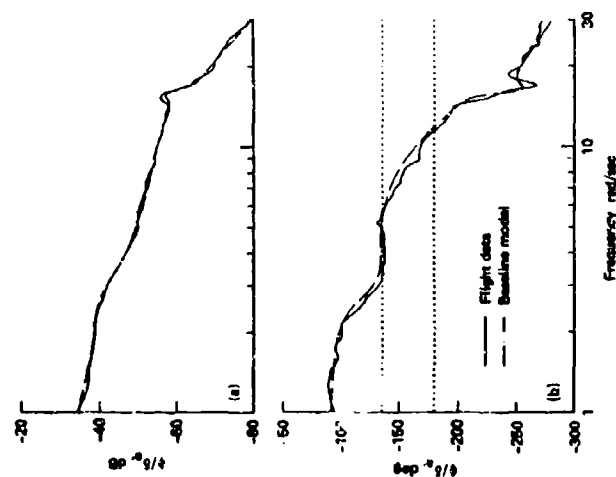


Figure 8.3.5. Comparison of baseline model (7th order) and flight data

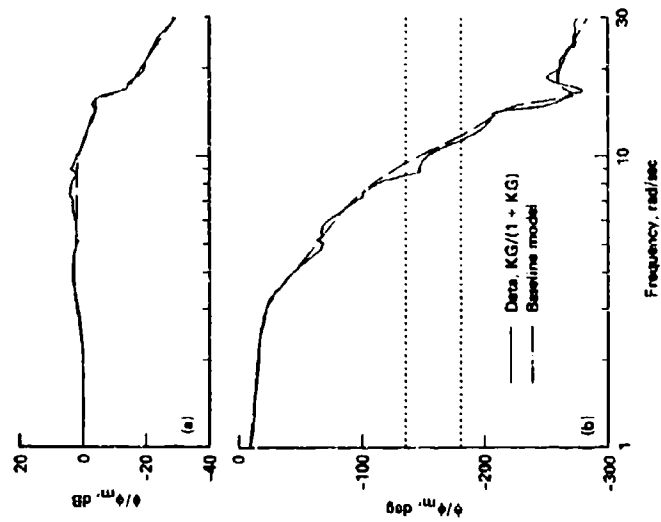


Figure 8.3.8. Comparison of closed loop response, ϕ/ϕ_m of baseline model vs. data

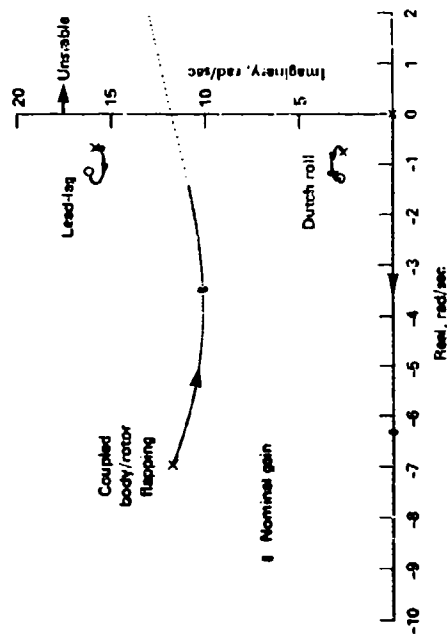


Figure 8.3.7. Stabilization loop root locus, varying roll attitude feedback gain K_ϕ

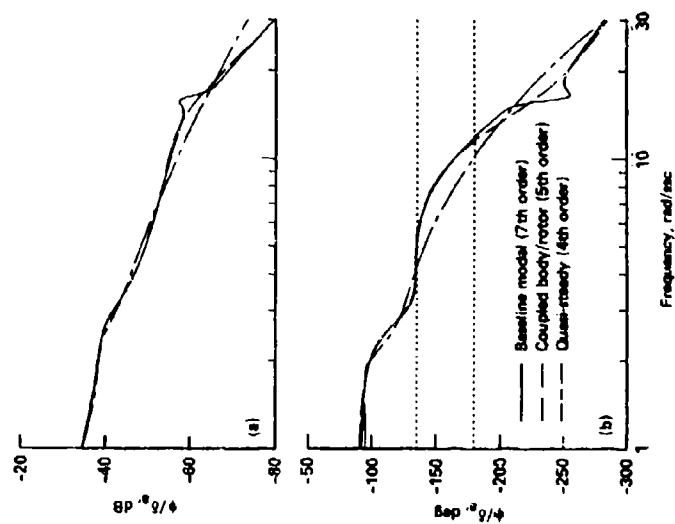
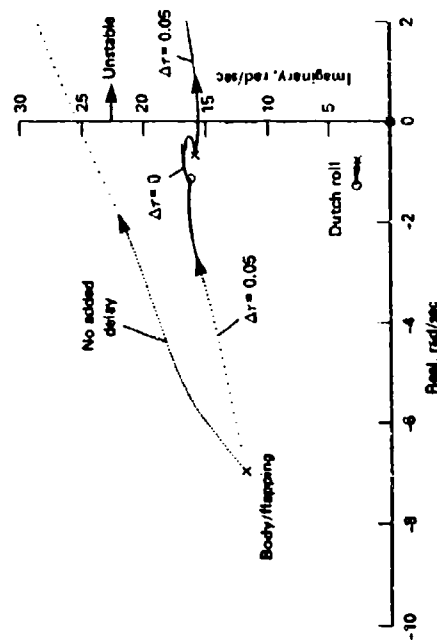


Figure 8.3.10. Lower-order broad-band models

Figure 8.3.9. Stabilization-loop root locus, varying roll-rate gain K_p

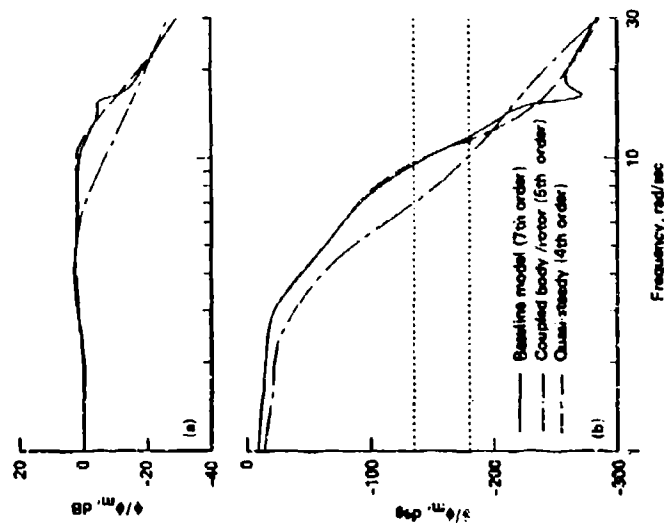


Figure 8.3.11. Closed loop responses of lower-order broad-band models

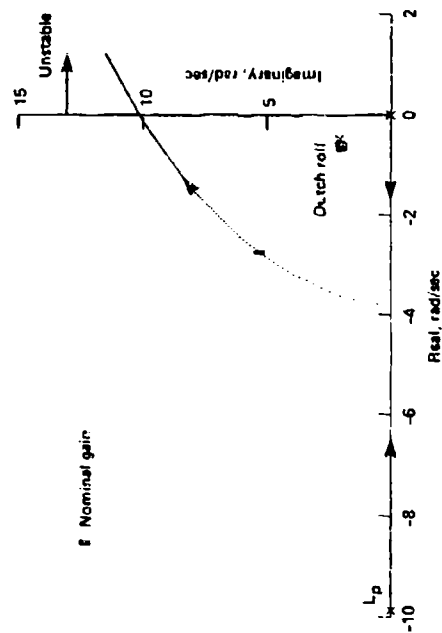


Figure 8.3.12. Stabilization-loop root locus for 5th order (quasi-steady) model varying attitude gain

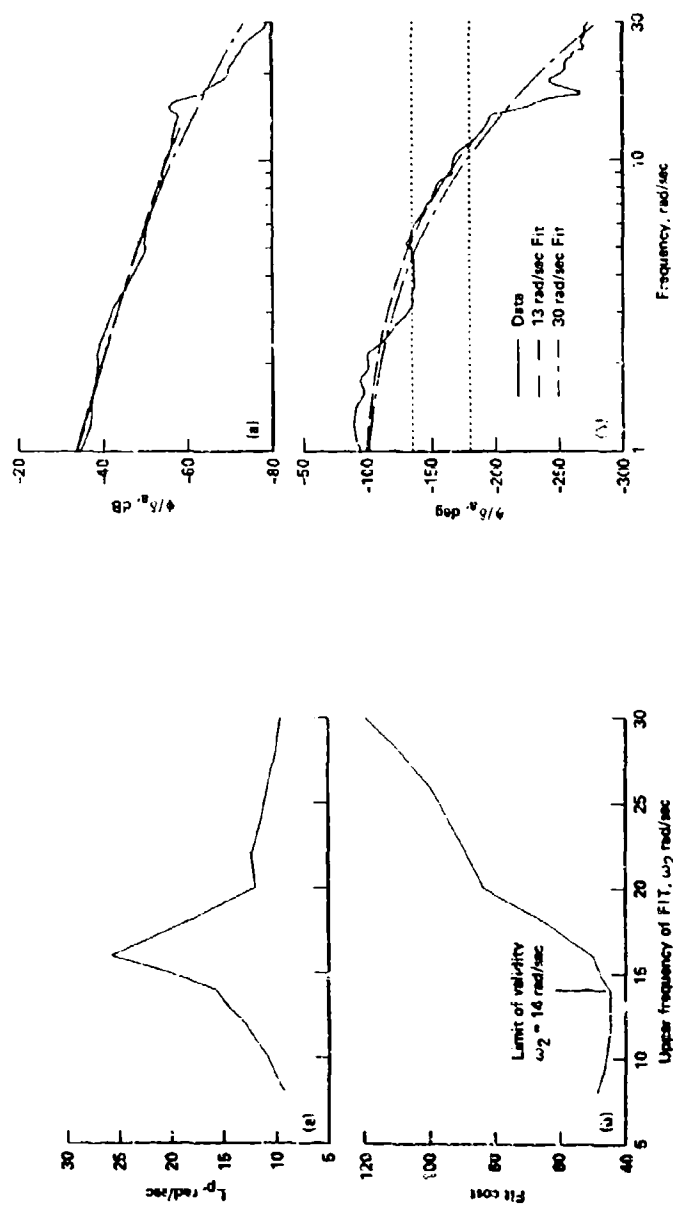


Figure 8.3.13. Effect of upper frequency limit ω_2 on quasi-steady identification
Lower limit of $\hat{\omega}_1$ is fixed, $\omega_1 = 1.0 \text{ rad/s}$

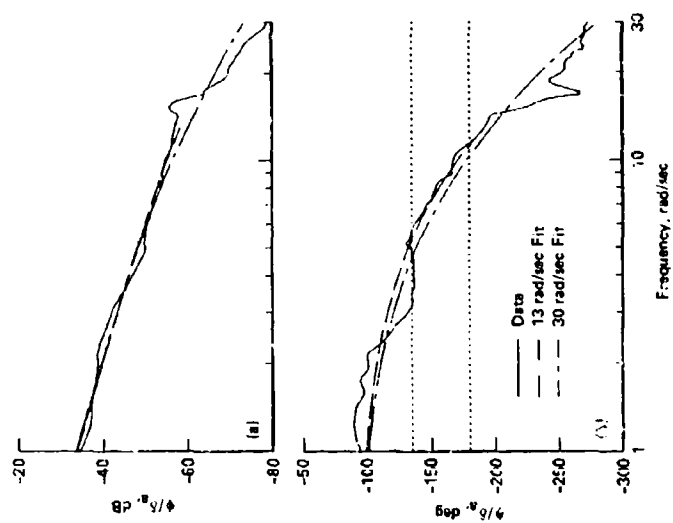


Figure 8.3.14. Rand-limited and broad-band quasi-steady models

9. Conclusions and Recommendations

This Report has documented the activities and accomplishments of the AGARD Working Group WG-18 on *Rotorcraft System Identification*. First, recent system identification activities were reviewed. Following this, the technical work carried out by the Working Group was presented: the common flight test data bases provided to the Group were described and the applied identification methodologies characterised. Results obtained from data quality investigations and identification and verification analyses were presented in detail in the form of case studies. Robustness issues were addressed. Finally, examples drawn from the main application areas for system identification approaches were illustrated. In most of the individual sections, summaries or conclusions and recommendations were included. In this section, the main conclusions are drawn together and some general recommendations of the application of system identification approaches are given.

The following conclusions were obtained:

1. The review of recent system identification activities has clearly shown that the development and application of identification techniques is concentrated in research organisations whereas the application in Industry is still sporadic and tentative. For example, in areas like model validation and trouble shooting during development flight tests, a strong reliance is placed on experience and engineering judgement in the interpretation of discrepancies between simulation and flight test data. Here, time history comparisons are the most common practice. However, Industry responses indicated a need for more effective comparative and diagnostic tools and an increasing interest in the application of identification techniques. Main concerns were related to the maturity level and the limitations of present methods. The responses have also emphasised the craft-like nature of modelling rotorcraft flight dynamics and the need for system identification tools to be compatible with this approach. An evaluation of the problem areas highlighted by Industry has shown that many of the flight dynamics problems could potentially have been solved using system identification.
2. Flight test data obtained from the AH-64, BO 105, and SA-330 were provided to the Working Group. In section 4 on *AGARD Working Group Data Base*, it was shown that each data base provided more measurements than required for system identification, although the AH-64 flight test were generated for other purposes. It can be stated that modern flight test instrumentations usually include the measurements needed for the identification of 6 degrees-of-freedom rigid body models. Special emphasis, however, should be placed on the design and conduct of suitable flight test manoeuvres and the need for a careful check of the accuracy of the measured data.
3. From the evaluation of the three case studies the main conclusions are:
 - The flight test data must provide as much information as possible on vehicle dynamics within the frequency range of interest.
 For example, the AH-64 flight test manoeuvres, which were not generated for identification purposes, were only about 10 seconds long and could not give sufficient low-frequency information. Specific input signals should be used to excite the aircraft modes of interest. Here, both, multi-step 3211 input signals and frequency sweeps are appropriate, with the distinction that the 3211 signal seems to be more suited for time-domain identification techniques whereas frequency sweep data were preferred for a frequency-domain approach.
 - Flight test manoeuvres should be repeated for redundancy. In addition to the tests designed for the identification, flight tests with other input signals, e.g. doublets, should be flown to be used for the verification of the identified models.
 - Significant effort was spent in the Working Group to evaluate the data reliability. Redundant measurements were used to detect scale factor errors and measurement offsets. Various techniques were applied ranging from Least Squares methods to extended Kalman Filter methods. The obtained results were generally in good agreement, although the more complex methods provided a higher flexibility in detecting and isolating error sources and in generating reconstructed time histories. A detailed study was conducted with the SA-330 PUMA flight test data, where a systematic analysis highlighted a variability in the scale factor estimation from run to run that could not fully be explained from the analysis. The study demonstrated the considerable effort necessary for the reconstruction of reliable data and illustrated the need for an immediate data quality check during the flight test phase. The flight test data from all three data bases have also shown that the measurement of the helicopter airspeed components is still significantly less accurate than inertial measurements.

- Identification results provided by the Working Group Members showed considerable variations between different methods. This is particularly true for cross-coupling derivatives but also for some primary derivatives. This fact is cause for a concern inasmuch as the time history fits for both identification and verification results do not show significant differences. Certainly, typical helicopter characteristics, like more or less significant coupling between degrees of freedom and high correlation between control and damping derivatives, play a role. There is, however, also some serious concern and doubts about the suitability of rigid body models, where rotor dynamics are neglected or approximated by equivalent time delays. From the BO 105 case study it can be concluded that so-called more advanced identification methods, like Maximum Likelihood, seem to be best suited for the extraction of physically reliable models. The comparison of the BO 105 results from such techniques (ranging from time-domain Maximum Likelihood approaches to a frequency-domain method) showed good agreements for the identified derivatives and the identification and verification plots in both time-domain and frequency-domain formats. The SA-330 derivatives were compared using approximate formulas for the aircraft modes of motion. This method has highlighted how the different derivatives contribute to the modes but could not entirely resolve the variations in the estimates obtained from the different methods.
4. For the application of system identification, three main areas were addressed: Simulation model validation, handling qualities, and rotorcraft flight control system design. It was demonstrated that system identification can play a major role in these areas.
 - In simulation model validation, identification results are particularly needed for the determination of simulation model deficiencies and to support the model upgrading. Differences between theoretically predicted and flight derived derivative estimates can point the way in these areas. The SA-330 Dutch roll behaviour was explored in this context.
 - Handling qualities can often be obtained from relatively simple non-parametric or parametric models which describe only the dominant aircraft characteristics. Such models can be obtained relatively easily from system identification and are useful for establishing handling-qualities design guidelines. Several examples were presented including the criterion for vertical response to collective control input using the AH-64 data.
 - In contrast to the handling qualities application, which usually addresses the lower frequency range of vehicle dynamics, the design of high-bandwidth flight control systems requires accurate rotorcraft models extending to the higher frequency range. Here, often models are needed that include rotor degrees of freedom with coupled body/rotor flapping and lead/lag dynamics. First identification results derived using the BO 105 database are motivating and promising and certainly show the direction for further research work. However, these approaches were beyond the scope of detailed study by the Working Group.

Based on the discussions and the results generated in the Working Group some recommendations with respect to the application of system identification in Industry and the further improvement of the approaches can be summarized:

1. It is felt that system identification techniques (and in particular the more advanced methods) have reached a maturity level that makes them a useful and powerful tool to support Industry activities in model validation, handling qualities evaluations, control system design, and rotorcraft system design. They can potentially provide a major contribution in risk and cost reduction during the rotorcraft development phase.
2. To fully realise this potential it is desirable to establish a closer contact between research organisations, who have developed and applied system identification techniques, and Industry. The extensive knowledge available in the research organisations and the design experience in Industry are major prerequisites for a successful common and practical application of identification approaches. This potential should be utilized as early as possible in order to make use of these tools in an optimal way.
3. To support interdisciplinary activities it is also highly recommended to establish teams of representatives from research organisations and Industry to make use of the individual experiences and to define future needs, where the available techniques can help to meet the requirements in the field of rotorcraft system developments (like the NATO NH 90). In addition, a major application area is seen in the support of simulator improvements needed for development and training purposes. The planned AGARD Lecture Series LS 178 on *Rotorcraft System Identification* will be used as a spur to stimulate the formation of such support teams.

4. One of the main obstacles for the comparative application of system identification to helicopters is the lack of standards or other agreements on special concepts, quantities and symbols in the domain of rotorcraft flight dynamics. This lack makes it very difficult if not impossible to establish a common conceptual basis for the investigations and the comparisons. As, however, such standards exist for aircraft in general and cover many areas of rotorcraft flight dynamics ([9.1]), it is recommended to use these for helicopters wherever possible. This not only would facilitate the comparisons but would also eliminate possible error sources.
5. It is further recommended to intensify the contact between research organisations working in the field of rotorcraft identification. Further research work should particularly concentrate on the development of reliable approaches for model structure determination to make the estimation processes computationally faster and more efficient. Control input design is a second critical research topic requiring more attention. A further objective is the development and identification of extended rotorcraft models that are valid in a wide frequency range and the determination of significant nonlinearities to be included in the models to extend their validity beyond small perturbation assumptions.
6. To date, practically all rotorcraft identification work has been related to level flight conditions in the medium or higher speed range and to small amplitude manoeuvres. The work of WGI-18 has demonstrated the challenge involved with such manoeuvres, yet they can be considered relatively easy compared with other manoeuvres within the flight envelope, e.g. hover manoeuvres, turning manoeuvres, flight in turbulence, where coupling or measurement uncertainties can be much greater. Research activities need to spread into these more complex areas in order that the new problems can be faced and solution methods developed. There is scope for simulation test data to be used initially to guide test input / manoeuvre design and the development and refinement of identification methods. Research organisations need to lead the way in the important development.
7. Finally it is recommended that the helicopter manufacturers, particularly, make a determined effort to assimilate the results of this AGARD Working Group and feedback within their own Nations their continuing concerns and aspirations.

References

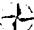
- [9.1] Anon
Flight dynamics - Concepts quantities and symbols
 Part 1: Aircraft motion relative to the air
 Part 2: Motions of the aircraft and the atmosphere relative to the Earth
 Part 3: Derivatives of forces, moments and their coefficients
 Part 4: Parameters used in the study of aircraft stability
 Part 5: Quantities used in measurements
 Part 6: Aircraft geometry
 Part 7: Flight points and flight envelopes
 ISO Standard 1151-1 to 1151-7

REPORT DOCUMENTATION PAGE

1. Recipient's Reference	2. Originator's Reference	3. Further Reference	4. Security Classification of Document
	AGARD-AR-280	ISBN 92-835-0632-4	UNCLASSIFIED
5. Originator	Advisory Group for Aerospace Research and Development North Atlantic Treaty Organization 7 rue Ancelle, 92200 Neuilly sur Seine, France		
6. Title	ROTORCRAFT SYSTEM IDENTIFICATION		
7. Presented at			
8. Author(s)/Editor(s)	Various		9. Date September 1991
10. Author's/Editor's Address	Various		11. Pages 292
12. Distribution Statement	This document is distributed in accordance with AGARD policies and regulations, which are outlined on the back covers of all AGARD publications.		
13. Keywords/Descriptors			
<input checked="" type="checkbox"/> Rotorcraft <input checked="" type="checkbox"/> Helicopter <input checked="" type="checkbox"/> Flight tests <input checked="" type="checkbox"/> System Identification <input checked="" type="checkbox"/> Data validation <input checked="" type="checkbox"/> Derivative models <input checked="" type="checkbox"/> Model verification <input checked="" type="checkbox"/> Identification application <input checked="" type="checkbox"/> Case studies			
14. Abstract			
<p>For fixed wing aircraft, system identification methods to determine stability and control derivatives from flight test data are used with confidence. The application of the same techniques to rotorcraft is not so far advanced mainly because of the helicopter aeromechanical complexity. Only a few specialists, mostly in research organisations, have concentrated on this field and the application in industry is still sporadic.</p> <p>To coordinate these activities within the AGARD nations a Working Group was constituted to focus on the applicational aspects of the various individual approaches and to evaluate the strengths and weaknesses of the different methods. Members of the Working Group applied their individual identification approaches to three common flight test data sets (AH-64, BO 105, and SA-330) that were provided to the Group by MDHC, DLR, and RAE.</p> <p>The Report contains the findings of the Working Group including a documentation of the data bases, the applied identification methodologies, and major application areas. For each of the three helicopters, comparisons of the obtained results are discussed in the format of case studies, covering data quality evaluations, identification, and the verification of the obtained models. 25</p> <p>This report was prepared by the Working Group WG 18 sponsored by the Flight Mechanics Panel of AGARD.</p>			

<p>AGARD Advisory Report 280 Advisory Group for Aerospace Research and Development, NATO ROTORCRAFT SYSTEM IDENTIFICATION Published September 1991 292 pages</p> <p>For fixed wing aircraft, system identification methods to determine stability and control derivatives from flight test data are used with confidence. The application of the same techniques to rotorcraft is not so far advanced mainly because of the helicopter aeromechanical complexity. Only a few specialists, mostly in research organisations, have concentrated on this field and the application in industry is still sporadic.</p> <p style="text-align: right;">P.T.O.</p>	<p>AGARD-AR-280</p> <p>Rotorcraft Helicopter Flight tests System identification Data validation Derivative models Model verification Identification application</p>	<p>AGARD Advisory Report 280 Advisory Group for Aerospace Research and Development, NATO ROTORCRAFT SYSTEM IDENTIFICATION Published September 1991 292 pages</p> <p>For fixed wing aircraft, system identification methods to determine stability and control derivatives from flight test data are used with confidence. The application of the same techniques to rotorcraft is not so far advanced mainly because of the helicopter aeromechanical complexity. Only a few specialists, mostly in research organisations, have concentrated on this field and the application in industry is still sporadic.</p> <p style="text-align: right;">P.T.O.</p>	<p>AGARD-AR-280</p> <p>Rotorcraft Helicopter Flight tests System identification Data validation Derivative models Model verification Identification application</p>
<p>AGARD Advisory Report 280 Advisory Group for Aerospace Research and Development, NATO ROTORCRAFT SYSTEM IDENTIFICATION Published September 1991 292 pages</p> <p>For fixed wing aircraft, system identification methods to determine stability and control derivatives from flight test data are used with confidence. The application of the same techniques to rotorcraft is not so far advanced mainly because of the helicopter aeromechanical complexity. Only a few specialists, mostly in research organisations, have concentrated on this field and the application in industry is still sporadic.</p> <p style="text-align: right;">P.T.O.</p>	<p>AGARD-AR-280</p> <p>Rotorcraft Helicopter Flight tests System identification Data validation Derivative models Model verification Identification application</p>	<p>AGARD Advisory Report 280 Advisory Group for Aerospace Research and Development, NATO ROTORCRAFT SYSTEM IDENTIFICATION Published September 1991 292 pages</p> <p>For fixed wing aircraft, system identification methods to determine stability and control derivatives from flight test data are used with confidence. The application of the same techniques to rotorcraft is not so far advanced mainly because of the helicopter aeromechanical complexity. Only a few specialists, mostly in research organisations, have concentrated on this field and the application in industry is still sporadic.</p> <p style="text-align: right;">P.T.O.</p>	<p>AGARD-AR-280</p> <p>Rotorcraft Helicopter Flight tests System identification Data validation Derivative models Model verification Identification application</p>

<p>To coordinate these activities within the AGARD nations a Working Group was constituted to focus on the applicational aspects of the various individual approaches and to evaluate the strengths and weaknesses of the different methods. Members of the Working Group applied their individual identification approaches to three common flight test data sets (AH-64, BO 105, and SA-330) that were provided to the Group by MDHC, DLR, and PAE.</p> <p>The Report contains the findings of the Working Group including a documentation of the data bases, the applied identification methodologies, and major application areas. For each of the three helicopters, comparisons of the obtained results are discussed in the format of case studies, covering data quality evaluations, identification, and the verification of the obtained models.</p> <p>This report was prepared by the Working Group WG 18 sponsored by the Flight Mechanics Panel of AGARD.</p> <p>ISBN 92-835-0632-4</p>	<p>To coordinate these activities within the AGARD nations a Working Group was constituted to focus on the applicational aspects of the various individual approaches and to evaluate the strengths and weaknesses of the different methods. Members of the Working Group applied their individual identification approaches to three common flight test data sets (AH-64, BO 105, and SA-330) that were provided to the Group by MDHC, DLR, and RAE.</p> <p>The Report contains the findings of the Working Group including a documentation of the data bases, the applied identification methodologies, and major application areas. For each of the three helicopters, comparisons of the obtained results are discussed in the format of case studies, covering data quality evaluations, identification, and the verification of the obtained models.</p> <p>This report was prepared by the Working Group WG 18 sponsored by the Flight Mechanics Panel of AGARD.</p> <p>ISBN 92-835-0632-4</p>
<p>To coordinate these activities within the AGARD nations a Working Group was constituted to focus on the applicational aspects of the various individual approaches and to evaluate the strengths and weaknesses of the different methods. Members of the Working Group applied their individual identification approaches to three common flight test data sets (AH-64, BO 105, and SA-330) that were provided to the Group by MDHC, DLR, and RAE.</p> <p>The Report contains the findings of the Working Group including a documentation of the data bases, the applied identification methodologies, and major application areas. For each of the three helicopters, comparisons of the obtained results are discussed in the format of case studies, covering data quality evaluations, identification, and the verification of the obtained models.</p> <p>This report was prepared by the Working Group WG 18 sponsored by the Flight Mechanics Panel of AGARD.</p> <p>ISBN 92-835-0632-4</p>	<p>To coordinate these activities within the AGARD nations a Working Group was constituted to focus on the applicational aspects of the various individual approaches and to evaluate the strengths and weaknesses of the different methods. Members of the Working Group applied their individual identification approaches to three common flight test data sets (AH-64, BO 105, and SA-330) that were provided to the Group by MDHC, DLR, and RAE.</p> <p>The Report contains the findings of the Working Group including a documentation of the data bases, the applied identification methodologies, and major application areas. For each of the three helicopters, comparisons of the obtained results are discussed in the format of case studies, covering data quality evaluations, identification, and the verification of the obtained models.</p> <p>This report was prepared by the Working Group WG 18 sponsored by the Flight Mechanics Panel of AGARD.</p> <p>ISBN 92-835-0632-4</p>

NATO  OTAN

7 RUE ANCELLE · 92200 NEUILLY-SUR-SEINE

FRANCE

Telephone (1)47 38.57.00 · Telex 610 176

Telecopie (1)47 38.57.99

DIFFUSION DES PUBLICATIONS

AGARD NON CLASSIFIEES

L'AGARD ne detient pas de stocks de ses publications, dans un but de distribution generale a l'adresse ci-dessus. La diffusion initiale des publications de l'AGARD est effectuee aupres des pays membres de cette organisation par l'intermediaire des Centres Nationaux de Distribution suivants. A l'exception des Etats-Unis, ces centres disposent parfois d'exemplaires additionnels; dans les cas contraire, on peut se procurer ces exemplaires sous forme de microfiches ou de microcopies aupres des Agences de Vente dont la liste suit.

CENTRES DE DIFFUSION NATIONAUX

ALLEMAGNE

Fachinformationszentrum,
Karlsruhe
D-7514 Eggenstein-Leopoldshafen 2

BELGIQUE

Coordonnateur AGARD-VSL
Etat-Major de la Force Aerienne
Quartier Reine Elisabeth
Rue d'Evere, 1140 Bruxelles

CANADA

Directeur du Service des Renseignements Scientifiques
Ministere de la Defense Nationale
Ottawa, Ontario K1A 0K2

DANEMARK

Danish Defence Research Board
Ved Idrætsparken 4
2100 Copenhagen Ø

ESPAGNE

INIA (AGARD Publications)
Pintor Rosales 34
28008 Madrid

ETATS-UNIS

National Aeronautics and Space Administration
Langley Research Center
M/S 180
Hampton, Virginia 23665

FRANCE

O.N.E.R.A. (Direction)
29, Avenue de la Division Leclerc
92320, Châtillon sous Bagneux

GRECE

Hellenic Air Force
Air War College
Scientific and Technical Library
Dekelia Air Force Base
Dekelia, Athens TGA 1010

ISLANDE

Director of Aviation
c/o Flugrad
Reykjavik

ITALIE

Aeronautica Militare
Ufficio del Delegato Nazionale all'AGARD
Aeroporto Pratica di Mare
00040 Pomezia (Roma)

LUXEMBOURG

Libr. Belgique

NORVEGE

Norwegian Defence Research Establishment
Ann. Biblioteket
P.O. Box 25
N-2007 Kjeller

PAYS-BAS

Netherlands Delegation to AGARD
National Aerospace Laboratory NLR
Kluyverweg 1
2629 HS Delft

PORTUGAL

Portuguese National Coordinator to AGARD
Gabinete de Estudos e Programas
CUAFA
Base de Alfragide
Alfragide
2700 Amadora

ROYAUME-UNI

Defence Research Information Centre
Kentigern House
65 Brown Street
Glasgow G2 8EX

TURQUIE

Milli Savunma Başkanlığı (MSB)
ARGE Daire Başkanlığı (ARGE)
Ankara

LE CENTRE NATIONAL DE DISTRIBUTION DES ETATS-UNIS (NASA) NE DETIENT PAS DE STOCKS DES PUBLICATIONS AGARD ET LES DEMANDES D'EXEMPLAIRES DOIVENT ETRE ADRESSEES DIRECTEMENT AU SERVICE NATIONAL TECHNIQUE DE L'INFORMATION (NTIS) DONT L'ADRESSE SUIT.

AGENTS DE VENTE

National Technical Information Service
(NTIS)
5285 Port Royal Road
Springfield, Virginia 22161
Etats-Unis

ESA Information Retrieval Service
European Space Agency
10, rue Mario Nikis
75015 Paris
France

The British Library
Document Supply Division
Boston Spa, Wetherby
West Yorkshire LS23 7BQ
Royaume Uni

Les demandes de microfiches ou de photocopies de documents AGARD (y compris les demandes faites auprès du NTIS) doivent comporter la dénomination AGARD, ainsi que le numéro de série de l'AGARD (par exemple AGARD-AG-315). Des informations analogues, telles que le titre et la date de publication sont souhaitables. Veuillez noter qu'il y a lieu de spécifier AGARD-R-nnn et AGARD-AR-nnn lors de la commande de rapports AGARD et des rapports consultatifs AGARD respectivement. Des références bibliographiques complètes ainsi que des résumés des publications AGARD figurent dans les journaux suivants:

Scientific and Technical Aerospace Reports (STAR)
publié par la NASA Scientific and Technical
Information Division
NASA Headquarters (NTI)
Washington D.C. 20546
Etats-Unis

Government Reports Announcements and Index (GRA&I)
publié par le National Technical Information Service
Springfield
Virginia 22161
Etats-Unis

(accessible également en mode interactif dans la base de données bibliographiques en ligne du NTIS, et sur CD-ROM)



Imprimé par Specialised Printing Services Limited
40 Chigwell Lane, Loughton, Essex IG10 3TZ